SOUTH COAST AIR QUALITY MANAGEMENT DISTRICT

Appendix V

Modeling and Attainment Demonstration

2016 AIR QUALITY MANAGEMENT PLAN

March 2017

FINAL 2016 AQMP
APPENDIX V

MODELING AND ATTAINMENT DEMONSTRATIONS

MARCH 2017

SOUTH COAST AIR QUALITY MANAGEMENT DISTRICT
GOVERNING BOARD

Chairman: DR. WILLIAM A. BURKE
Speaker of the Assembly Appointee

Vice Chairman: BEN BENOIT
Mayor Pro Tem, Wildomar
Cities of Riverside County

MEMBERS:

MARION ASHLEY
Supervisor, Fifth District
County of Riverside

JOE BUSCAINO
Councilmember, 15th District
City of Los Angeles Representative

MICHAEL A. CACCIOTTI
Mayor, South Pasadena
Cities of Los Angeles County/Eastern Region

JOSEPH K. LYOU, Ph. D.
Governor's Appointee

SHEILA KUEHL
Supervisor, Third District
County of Los Angeles

LARRY MCCALLON
Mayor Pro Tem, Highland
Cities of San Bernardino County

JUDITH MITCHELL
Councilmember, Rolling Hills Estates
Cities of Los Angeles County/Western Region

SHAWN NELSON
Supervisor, Fourth District
County of Orange

DR. CLARK E. PARKER, SR.
Senate Rules Committee Appointee

DWIGHT ROBINSON
Councilmember, Lake Forest
Cities of Orange County

JANICE RUTHERFORD
Supervisor, Second District
County of San Bernardino

EXECUTIVE OFFICER:

WAYNE NASTRI

CONTRIBUTORS

South Coast Air Quality Management District

Wayne Nastri
Executive Officer

Jill Whynot
Chief Operating Officer

Philip Fine, Ph.D.
Deputy Executive Officer
Planning, Rule Development, & Area Sources

Joseph Cassmassi (Retired)
Planning and Rules Director
Planning, Rule Development, & Area Sources

Michael Krause
Planning and Rules Manager
Planning, Rule Development, & Area Sources

Authors

Sang-Mi Lee, Ph.D., Program Supervisor
Xinqiu Zhang, Ph.D., Air Quality Specialist
Scott Epstein, Ph.D., Air Quality Specialist
Kalam Cheung, Ph.D., Air Quality Specialist
Salvatore Farina, Temporary Air Quality Specialist
Marc Carreras Sospedra, Ph.D., Air Quality Specialist
Susan Yan, Air Quality Specialist

Contributors

SCAQMD Planning, Rule, Development & Area Sources

Mia Camacho, Student Intern
Ryan Kean, Student Intern

Reviewer

Barbara Baird, J.D., Chief Deputy Counsel

TABLE OF CONTENTS

CHAPTER 1

MODELING OVERVIEW

Introduction

Air quality modeling to demonstrate future attainment of air quality standards is an integral part of the planning process to achieve clean air. Modeling provides the means to relate emission reductions from pollution sources to the resulting air quality improvements. The attainment demonstrations provided in the 2016 AQMP reflect updated emissions estimates, new technical information, enhanced air quality modeling techniques, updated attainment demonstration methodology, and the control strategies provided in Chapter 4. While the primary target of the 2016 AQMP is to demonstrate progress toward the 2008 8-hour ozone standard of 75 ppb by 2031, efforts to meet other air quality standards and the corresponding analyses are included in the 2016 AQMP and presented in this appendix. Both the revoked 1997 8-hour standard (80 ppb) and the revoked 1979 1-hour standard (120 ppb) are included in the analysis with attainment years of 2023 and 2022, respectively. This Appendix also provides detailed attainment demonstrations of the annual and 24-hour PM2.5 standards (12 and 35 $\mu g/m^3$).

The District's goal is to develop a control strategy and corresponding attainment demonstration that: 1) ensures that ambient air quality standards for all criteria pollutants are met by the established deadlines in the federal Clean Air Act (CAA) and 2) achieves an expeditious rate of progress towards attaining the air quality standards. The overall control strategy is designed such that efforts to achieve the standard for one criteria pollutant complement efforts to meet standards for other pollutants.

Background

The South Coast Air Basin is classified as an "extreme" nonattainment area for ozone. The 2016 AQMP addresses three ozone standards: the 2008 8-hour standard of 75 ppb, the revoked 1997 8-hour standard of 80 ppb, and the revoked 1-hour standard of 120 ppb. The attainment deadline years are 2031, 2023 and 2022, respectively. The emissions inventory and meteorological conditions were developed for 2012 base year.

The Basin is currently a "serious" nonattainment area for 24-hour PM2.5 and "moderate" nonattainment for annual PM2.5. The 2012 AQMP addressed attainment of the 2006 24-hour standard of 35 $\mu g/m^3$ by 2014; however, the unforeseen drought that occurred in the 2011-2014 time period inhibited the projected progress towards attainment. The District requested a voluntary bump-up from "moderate" status to "serious" nonattainment status in the "Supplement to the 24-Hour PM2.5 State Implementation Plan for the South Coast Air Basin" submitted to U.S. EPA in 2015 and subsequently approved in 2016. For "moderate" nonattainment areas, the attainment deadline was 2015 based on CAA *Title 1, Part D, Subpart 4, Section 188(c)(l),* which establishes that attainment must be reached by the end of the 6th calendar year after the effective date of designation. The year 2019 is the new attainment deadline for "serious" nonattainment areas for the 24-hour PM2.5 standard.

The Basin was designated a "moderate" nonattainment area for the 2012 annual PM2.5 standard of 12 $\mu g/m^3$ on April 15, 2015. This designation sets an attainment deadline of December 31, 2021. Despite the recent drought, the Basin shows continued improvement in annual PM2.5 design values. The base year annual PM2.5 design values at Mira Loma are lower than the previous 1997 standard of 15 $\mu g/m^3$, but do

not yet meet the new 2012 standard of 12 µg/m^3 (Figure 5-11), indicating that additional reductions may be needed to meet the more stringent standard. Acknowledging the challenges in meeting the standard, including the feasibility of proposed measures, uncertainties in drought conditions, and the potential inability to credit all ozone strategy reductions towards PM2.5 attainment if approved under CAA Section 182(e)(5), SCAQMD will request a voluntary bump-up to the "serious" classification, with a new attainment date of 2025. Future year attainment was analyzed for 2021, the original target for "moderate" nonattainment, and 2025, the revised attainment date for the requested "serious" status. This AQMP includes all the milestone years significant to future PM2.5 attainment status: 2019 (24-hour PM2.5 attainment date), 2021 (annual PM2.5 attainment date for "moderate" nonattainment status) and 2025 (annual PM2.5 attainment date for "serious" nonattainment status). In addition, 2023 was included in the analysis to evaluate co-benefits of the ozone strategy on PM attainment and to assess the practicability of an earlier PM2.5 attainment date.

Model Selection

The numerical platform employed in AQMP attainment demonstrations has been updated continually to reflect the state-of-the-science available at the time of plan development throughout the past decades.

During the development of the 2003 Plan, the District convened a panel of seven experts to independently review the regional air quality modeling conducted for ozone and PM10. The consensus of the panel was for the District to move to more current state-of-the-art dispersion platforms and chemistry modules.

At that time, the model selected for the 2007 AQMP ozone attainment demonstrations was the Comprehensive Air Quality Model with Extensions (CAMx) [Environ, 2002], using SAPRC99 chemistry. For PM2.5, the 2007 AQMP used the CAMx "one atmosphere" approach which coupled CB-IV gas-phase chemistry and a static two-mode particle size aerosol module as the particulate modeling platform. The CAMx "one atmosphere" chemistry approach better preserved mass consistency taking advantage of an advanced dispersion platform.

In the 2007 AQMP, CAMx coupled with the SAPRC99 chemistry was used to demonstrate attainment of the federal ozone standard. A total of 36 days were simulated, covering 6 ozone episode periods from which 19 days meeting performance criteria were selected for inclusion in the attainment demonstration. Future year ozone projections were developed using the CAMx/SAPRC99 couple supported by MM5 meteorological data fields and day specific emissions inventories.

The 2007 AQMP PM2.5 attainment demonstration incorporated the CAMx/CB-IV chemistry and aerosol modules together with the MM5 meteorological fields. The PM2.5 analyses relied on average week day and weekend day emissions profiles that were adjusted for monthly averaged temperature and humidity. The annual and episodic PM2.5 demonstrations were based on 365 days of particulate simulation. It is important to note that PM2.5 and ozone attainment demonstrations were run independently due to differences in the computational requirements resulting from separate modeling domains and definitions of vertical structure.

In keeping with the recommendations of the expert panel as well as the Scientific Technical Peer Modeling Review Committee, the 2012 AQMP continued to move forward in the incorporation of state-of-the-art modeling platforms to conduct regional modeling analyses in support of the PM2.5 attainment demonstrations and ozone updates. The 2012 AQMP PM2.5 attainment demonstration was developed using the U.S. EPA supported Community Multiscale Air Quality (CMAQ) (version 4.7.1) air quality modeling platform with SAPRC99 chemistry, and the Weather Research and Forecasting model (WRF) (version 3.3) meteorological fields. Supporting PM2.5 and ozone simulations were also conducted using the most current, publicly available version of CAMx (Environ, Inc, version 5.3) which also used SAPRC99 chemistry and WRF meteorology. The model analyses were conducted on an expanded domain, with increased resolution in the vertical structure and a 4 x 4 km horizontal grid size.

The 2016 AQMP ozone and PM2.5 attainment demonstration has been developed using the U.S. EPA recommended CMAQ (version 5.0.2) modeling platform with SAPRC07 chemistry, and the Weather Research and Forecasting Model (WRF) (version 3.6) meteorological fields. (Comprehensive descriptions of the CMAQ modeling system are provided by U.S. EPA at their SCRAM website: http://www.epa.gov/scram001/. Additional descriptions of the SAPRC99 chemistry module are provided at the UCR website: http://www.engr.ucr.edu/~carter/SAPRC/. Documentation of the NCAR WRF model is available from UCAR website: http://www.wrf-model.org/).

Modeling Methodology

Design Values

U.S. EPA guidance recommends the use of multiple year averages of design values, where appropriate, to dampen the effects of single year anomalies to the air quality trend due to factors such as adverse or favorable meteorology or radical changes in the local emissions profile. The trend of Basin ozone design values is presented in Figure V-1-1. The 8-hour design values have averaged a reduction of approximately 2 ppb per year over the 14-year period while the 1-hour design values have decreased 2.3 ppb per year on average. The most recent 8-hour design value (102 ppb) continues to exceed the 1997 8-hour ozone standard (80 ppb) by 28 percent and the 2006 ozone standard by 36 percent (75 ppb). In addition, the most recent 1-hour design value of 135 ppb exceeds the 1979 1-hour ozone standard (120 ppb) by 13 percent. In each case, the trend in ozone levels is steadily moving in the direction of air quality improvement.

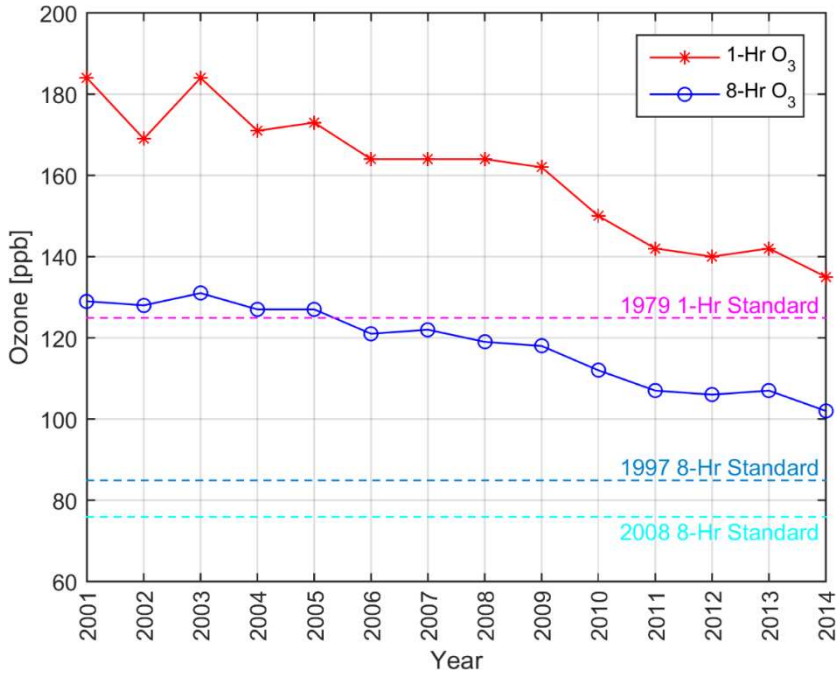

FIGURE V-1-1

South Coast Air Basin Ozone Design Values
Note: Each value represents the 3-year average of the 4th highest 8-Hour Average Ozone concentration. 1-hour Ozone design value was determined as the 4th highest value within a three year period.

The trend in the Basin 24-hour PM2.5 design values, determined from routinely monitored Federal Reference Methods (FRM) monitoring, from 1999 through 2014 (Figure V-1-2) depicts sharp reductions in concentrations over the period. However, the rate of decrease in both annual and 24-hour design values has slowed in recent years. The 24-hour PM2.5 design value for 2001 was 76 µg/m^3 while the 2014 design value (based on data from 2012, 2013 and 2014) is 38 µg/m^3. The annual PM2.5 design value has demonstrated a reduction of 15.2 µg/m^3 over the period from 2001 through 2014. The apparent slowing in the rate of PM2.5 reduction in recent years is largely due the reduced convection and wet deposition from the multi-year drought affecting the region. In the absence of this severe drought, it is anticipated that the Basin would be closer to attaining both the annual and 24-hour PM2.5 standards.

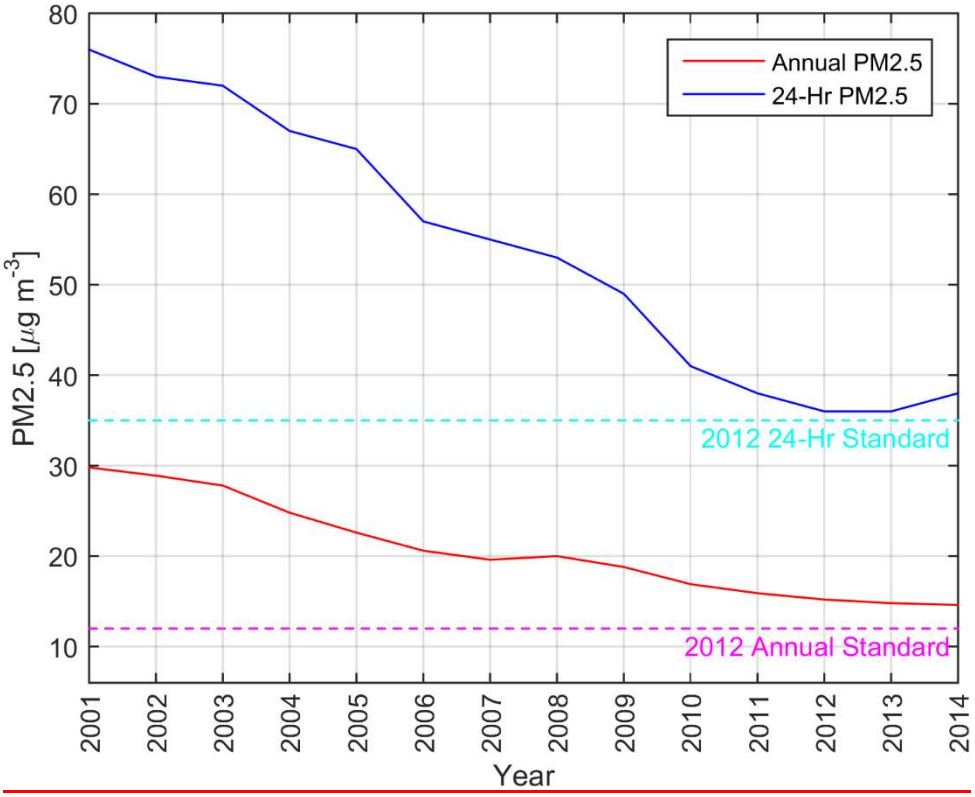

FIGURE V-1-2

South Coast Air Basin Annual PM2.5 and 24-Hour Average Design Values
Note: Each value represents the 3-year average of the highest annual average PM2.5 concentration

In its modeling guidance, U.S. EPA has recommended that a multiple year weighted design value be used in the attainment demonstrations. The 2012 AQMP relied on a set of 5-years of monitored particulate data centered on 2008, the base year selected for the emissions inventory development and the anchor year for the future year PM2.5 projections. The 2016 AQMP relies on a set of 5-years of monitored ozone and PM2.5 data centered on 2012, the base year of the analysis.

Regional Modeling

The 2012 AQMP employs the CMAQ air quality modeling platform with SAPRC07 chemistry and WRF meteorology as the primary tool used to demonstrate future year attainment of the ozone and PM standards. As in the 2012 AQMP attainment demonstrations, PM2.5 and ozone were modeled jointly with the same model configuration. Ozone simulations focused on the ozone season (May 1st to September 30th) and PM2.5 simulations were conducted for 366 days. Predicted daily maximum values of 24-hour PM2.5 and 8-hour ozone were calculated from the respective running 24-hour and 8-hour average simulated concentrations. In addition, daily-maximum 1-hour ozone values were calculated from the ozone simulations and annual average PM2.5 values were calculated from the PM2.5 simulations.

As in the 2012 AQMP, the 2016 AQMP simulations were conducted using a Lambert Conformal grid projection where the western boundary of the domain is at 084 UTM, over 100 miles west of the ports of

Los Angeles and Long Beach. The eastern boundary extends beyond the Colorado River, while the northern and southern boundaries of the domain extend to the San Joaquin Valley and the Northern portions of Mexico (3543 UTM). The grid size is 4 x 4 kilometers with a vertical resolution of 18 layers. Figure V-1-3 depicts the modeling domain which includes a grid of 154 cells from west to east and 102 cells from south to north.

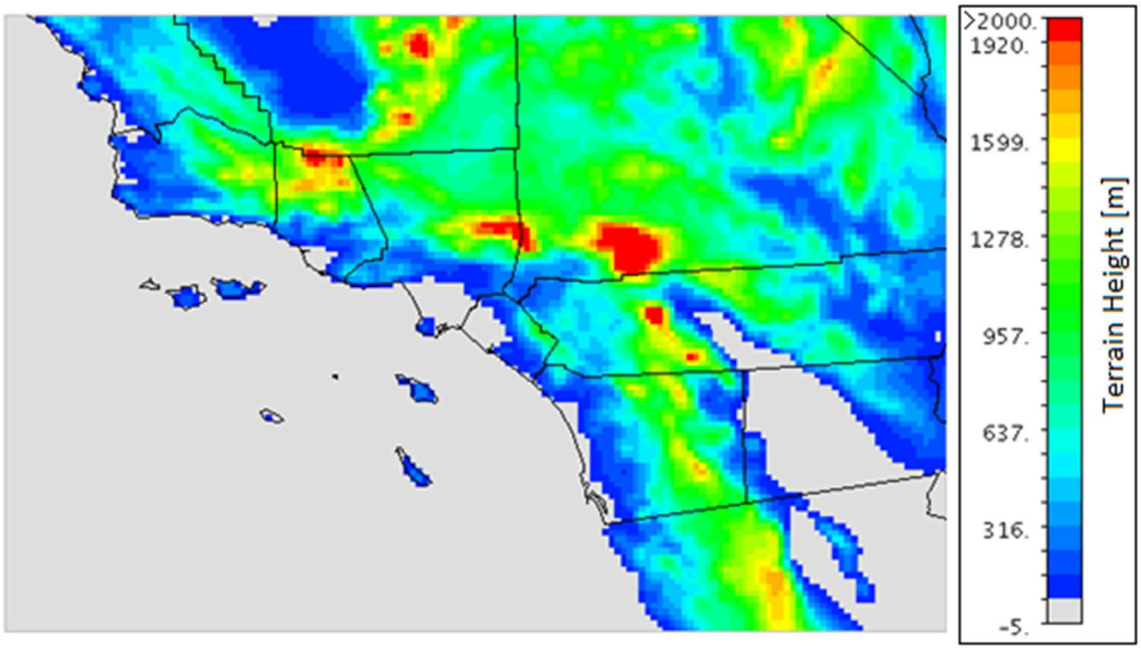

FIGURE V-1-3

2016 AQMP Regional Modeling Domain

For the 2016 AQMP, WRF was updated with the most recent version (version 3.6) available at the time of this protocol preparation and was evaluated with a set of input data, which include land-use classification and sea-surface temperature initialization fields. The WRF simulations were initialized from National Centers for Environmental Prediction (NCEP) analyses data and run for 4-day increments with the option for four dimensional data assimilation (FDDA). NCEP analysis data refers to the set of model predictions assimilated with available measurements in a retrospective mode.

The atmospheric chemistry package used in the CMAQ simulations relied on SAPRC07 gas phase chemistry with version "c" toluene updates with the AERO6 aerosol mechanism, the Euler Backward Iterative solver, the Yamo horizontal advection scheme, the WRF vertical advection scheme, the multiscale CMAQ horizontal diffusion scheme, the ACM2 vertical diffusion scheme, in-line photolysis calculations, and clean homogeneous initial values.

Relative Response Factors and Future Year Design Values

To bridge the gap between air quality model output evaluation and applicability to the health based air quality standards, EPA guidance has proposed the use of relative response factors (RRF). The RRF concept was first used in the 2007 AQMP modeling attainment demonstrations. The RRF is simply a ratio of future year predicted air quality with the control strategy fully implemented to the simulated air quality in the base year. The procedure for the attainment demonstration are pollutant and averaging period specific. For 8-hour ozone simulations, the top 10 days in the base-year and the corresponding days in the future year are used to determine the RRF. This is different from the methodology used in the 2012 AQMP where the aggregated response of several episode days to the implementation of the control strategy are used to develop an averaged RRF for projecting a future year design value. To demonstrate attainment of 1-hour ozone, the top three days in the base year and the corresponding days in the future year are used to determine the RRF. This provides a more objective and accurate analysis that they episode-based strategy in previous AQMPs. For 24-hour PM2.5, the top 10 percentile of modeled concentrations in each quarter of the simulation year are used to determine the quarterly RRF. For the annual average PM2.5, the quarterly average RRFs are used for the future year projections.

The future year design value is estimated by multiplying the non-dimensional RRF to the measured base year design value. Thus, the simulated improvement in air quality, based on multiple meteorological episodes, is translated to a simple metric that directly determines compliance of the standard. Equations V-1 and V-2 summarize the calculation.

Equation V-1.

RRF = (Future-Year Model Prediction) / (Base-Year Model Prediction)

Equation V-2.

To demonstrate attainment: RRF x Measured Base Year Design Value ≤ Air Quality Standard

The modeling analyses described above use the RRF and design value approach to demonstrate future year attainment of the standards. The RRF approach aims to minimize the effects of biases in the model simulations, thus providing more accurate projections of future air quality.

Weight of Evidence

Modeling guidance strongly recommends the use of corroborating evidence to support the future year attainment demonstration. The weight of evidence demonstration for the 2016 AQMP includes a sensitivity analysis where area-source emissions were spatially perturbed and a model performance evaluation of two different approaches for modeling on-road emissions. A multi-variable regression model was also developed to forecast 24-hour and annual PM2.5 design values as a function of emissions and meteorological conditions.

Uncertainties Associated with the Technical Analysis

As with any attainment plan, there are uncertainties associated with the technical analysis. The following paragraphs describe the primary contributors to such uncertainties as well as some of the safeguards built in to the air quality planning process to manage and control such uncertainties.

Demographic and Growth Projections

Uncertainties exist in the demographic and growth projections for future years. As projections are made to longer periods (i.e., over ten or more years), the uncertainty of the projections become greater. Examples of activities that may contribute to these types of uncertainties include the rate and the type of new sources locating in the Basin and their geographic distribution, future year residential construction, military base reuse and their air quality impact, and economic conditions.

Emissions Inventory

While significant improvements have been realized in mobile source emissions models, uncertainties continue to exist in the mobile source emissions inventory estimates. EMFAC2014 on-road mobile source emission estimates have improved with each new EMFAC release. On-road mobile source emissions have inherent uncertainties with the current methodologies used to estimate vehicle miles traveled and the impacts of fuel additives such as ethanol. Stationary (or point) source emission estimates have less associated uncertainties compared to area source emission estimates. Major stationary sources report emissions annually whereas minor stationary and area source emissions are, in general, estimated based on a top down approach that relies on production, usage or activity information. Area source emissions including paved road dust and fugitive dust have significant uncertainties in the estimation of particulate ($PM_{2.5}$) emissions due to the methodologies used for estimation, temporal loading and weather impacts.

Ambient Air Quality Monitoring Data

Generally, ambient air quality measurements are accurate to within plus or minus half of a unit of measurement (e.g., for ozone usually reported in units of parts-per-hundred million (pphm) would be accurate to within ±0.5 pphm or ±5 ppb). Due to rounding conventions, the Basin's 8-hour attainment status based on ambient monitoring data would be achieved if all ozone monitors reported ozone concentration levels less than or equal to 84.9 ppb. Similar uncertainty is observed in particulate data measurements and laboratory analysis. For example, PM2.5 is comprised of six primary constituents ($NH4^+$, NO3, $SO4^-$, OC, EC and crustal), as well as bonded water and total mass. Each of the primary species has individual uncertainty associated with the laboratory analysis procedure and the type of filter media to collect the sample. The total mass collected can be affected by minor changes in the volumetric flow that fall within the approved instrument calibration range. As a consequence, the sum of the total species may not add up to or may exceed the filter measured mass.

Air Quality and Meteorological Models

The air quality models used for ozone and particulate air quality analysis are state-of-the-art, comprehensive 3-dimensional models that utilize 3-dimensional meteorological models, complex chemical mechanisms that accurately simulate ambient reactions of pollutants, and sophisticated numerical methods to solve complex mathematical equations that lead to the prediction of ambient air quality concentrations. While air quality models progressively became more sophisticated in employing improved chemical reaction modules that more accurately simulate the complex ambient chemical reaction mechanisms of the various pollutants, such improved modules are still based on limited experimental data that carry associated uncertainties. In order to predict ambient air quality concentrations, air quality models rely on the application of sophisticated numerical methods to solve complex mathematical equations that govern the highly complex physical and chemical processes that also have associated uncertainties. Layer averaging of model output reduces the sensitivity of the model to changing patterns in the vertical structure.

Safeguards against Uncertainties

While completely eliminating uncertainties is an impossible task, there are a number of features and practices built into the air quality planning process that manage and control such uncertainties and preserve the integrity of an air quality management plan.

The concerns regarding future year uncertainties in the technical analysis are reduced with future AQMP revisions. Each AQMP revision employs the best available technical information. Under state law, AQMP revision is a dynamic process with revisions occurring every three years. AQMP revision represents a "snapshot in time" providing the progress achieved since the previous AQMP revision and efforts still needed in order to attain air quality standards.

Under the federal Clean Air Act, a state implementation plan (SIP) is prepared for each criteria pollutant. The SIP is not required to be updated on a routine basis under the federal Clean Air Act. However, the federal Clean Air Act recognizes that uncertainties do exist and provides a safeguard if a nonattainment area does not meet an applicable milestone or attain federal air quality standards by their applicable dates. Contingency (or backstop) measures are required in the AQMP and must be developed into regulations such that they will take effect if a nonattainment area does not meet an applicable milestone or attainment date. In addition, federal sanctions may be imposed until an area meets applicable milestone or attainment targets.

In December 2014, U.S. EPA released an updated draft guidance document (U.S. EPA 2014) on the use of modeled results to demonstrate attainment of the federal ozone, PM2.5 and regional haze air quality standards. The guidance document recognized that there will be uncertainties with the modeling analysis and recommends supplemental analysis or a weight of evidence discussion that corroborates the modeling attainment analysis where attainment is likely, even if the modeled results are inconclusive. Where possible, the U.S. EPA recommends that at least one "mid-course" review of air quality, emissions and modeled data be conducted. A second review, shortly before the attainment date, should be

conducted also. Statistical trend analyses of monitored data can also provide support for assessing the likelihood for future year attainment. The District will undertake such actions at the appropriate times.

Document Organization

This document provides the federal attainment demonstration for ozone and updates for annual and 24-hour PM2.5 attainment. Chapter 2 provides the Modeling Protocol which summarizes the key elements that have been revised relative to the 2012 AQMP Modeling protocol. Chapter 3 provides a discussion of the meteorological modeling including a comprehensive model performance evaluation. Chapter 4 provides a brief summary of the modeling emissions, including characterization of the daily/diurnal emissions profiles and OGV emissions. Chapter 5 provides the 8-hour ozone attainment demonstration meeting the 2023 and 2031 attainment dates. The ozone analysis includes discussions of the representativeness of the 2012 meteorological year, base-year modeling performance, and projections of future year concentrations for baseline emissions as well as the implementation of the short-term control strategy. The ozone analysis will also provide updated isopleth analyses and a discussion of future year carrying capacities for the current and proposed ozone standards. Carrying capacity plots for the 8-hour Ozone attainment target years are provided in Attachment 5 and 6 of this report. As with the particulate analyses, weight of evidence discussions for ozone will be incorporated in Chapter 5. Chapter 6 provides an update to projected annual PM2.5 concentrations for the different future year emissions scenarios. The chapter includes a characterization of the particulate species profile, discussion of the revised attainment demonstration methodology, and selected future year particulate impacts. Similarly, Chapter 7 will provide an update to the future year 24-hour PM2.5 attainment demonstration. Chapter 8 updates the 1-hour ozone attainment demonstration presented in the 2012 AQMP. 1-hour ozone isopleths to estimate carrying capacity were updated and provided in Attachment 6 of this report. Chapter 9 provides a brief summary of the analysis. Table V-1-2 lists the Attachments to this document.

TABLE V-1-2

Attachments

Number	Description
Attachment-1	WRF Graphical Performance Statistics
Attachment-2	CMAQ Model Performance Figures
Attachment-3	CEPA Source Level Emissions Reduction Summary
Attachment-4	8-hour Ozone Isopleths for 2031
Attachment-5	8-hour Ozone Isopleths for 2023
Attachment-6	1-hour Ozone Isopleths for 2022
Attachment-7	Annual Unmonitored Area Analysis Supplement
Attachment-8	24-hour Unmonitored Area Analysis Supplement

References

U.S. EPA (2014) Draft Modeling Guidance for Demonstrating Attainment of Air Quality Goals for Ozone, PM2s, and Regional Haze

CHAPTER 2

MODELING PROTOCOL

Background

One of the basic requirements of a modeling attainment demonstration is the development of a comprehensive modeling protocol that defines the scope of the regional modeling analyses including the attainment demonstration methodology, meteorological and chemical transport platforms, gridded and speciated emission inventories, and geographical characteristics of the modeling domains. The protocol also defines the methodology to assess model performance and the selection of the simulation periods. The 2012 AQMP provided a comprehensive discussion of the modeling protocol used for the development of the PM2.5 and ozone attainment demonstrations. The 2012 AQMP Modeling Protocol, presented in the Chapter 2 of Appendix V, served as the prototype of the 2016 AQMP modeling protocol.

The 2016 AQMP demonstrates attainment of ozone and PM2.5 standards in 12 future landmark years. (See Table V-2-1) The future attainment years are identified based on nonattainment designation, pollutant standards, and geographical area. 2012 was chosen as the base year to maintain consistency with the base year employed in the SCAG's Regional Transportation Plan/Sustainable Communities Strategy (RTP/SCS).

TABLE V-2-1

Modeling Years for 2016 AQMP

Modeling Year	Plan	NAAQS	Areas
2012	Base Year	Modeling Base Year	
2017	2008 8-hour ozone	75 ppb	Imperial, San Diego
2018	1997 8-hour ozone	80 ppb	Coachella, W. Mojave Desert
2019	2006 24-hour PM2.5	35 µg/m3	South Coast
2020	2008 8-hour ozone	75 ppb	Ventura
2021	Annual PM2.5	12 µg/m3	South Coast
2022	1-hour ozone	120 ppb	South Coast
2023	1997 8-hour ozone	80 ppb	South Coast
	Annual PM2.5	12 µg/m3	South Coast
2025	Annual PM2.5	12 µg/m3	South Coast
2026	2008 ozone	75 ppb	Coachella, W. Mojave Desert
2031	2008 ozone	75 ppb	South Coast
2037	2015 ozone	70 ppb	South Coast

Attainment Demonstration

8-hour Ozone

The methodology used to demonstrate attainment depends on the pollutant of interest. The 8-hour attainment demonstration was performed based on the U.S. EPA guidance document, "Draft Modeling Guidance for Demonstrating Attainment of Air Quality Goals for Ozone, PM2s, and Regional Haze", issued on Dec 3rd, 2014. Compared to the previous guidance, US EPA (2007), the ozone attainment demonstration has been significantly updated. The new guidance requires that a maximum concentration be determined among 9 grids around a monitoring station and that the specific grid location be carried to a future year modeling scenario when calculating relative response factors (RRF). This 3 X 3 grid is recommended for all model grid resolutions, differing from the previous guidance, which recommended a 7 X 7 grid for a 4 km grid resolution simulation—the grid resolution used in this modeling. Another major difference is the number of days accounted for in the attainment demonstration. In the 2012 and earlier AQMPs, all days that met the selection criteria were used to calculate future year design values. The specific criteria used in the last AQMP required that the predicted daily max was within 20 % of the site-specific design value, the unpaired daily-max prediction error was less than 20%, and the prediction was higher than the federal standard, for inclusion. In the new guidance, the number of days accounted for in the RRF calculation is limited to the top 10 days of base year simulated concentrations. In the past, the uniquely high ozone concentrations in the Basin led to the inclusion of more than ten days in the RRF calculation. For example, the Crestline site, a design site in the 2012 AQMP, typically would have over 50 days or more included in the RRF calculation. On the other hand, a focus on the top ten days meeting the selection criteria in the new methodology produces future-year design values that are more responsive to emission reductions.

Annual PM2.5

The Final 2016 AQMP annual PM2.5 modeling employs the same approach to estimate the future year annual PM2.5 levels as was described in the 2012 and 2007 AQMP attainment demonstrations, except for the changes described in the 2014 U.S. EPA guidance document (U.S. EPA, 2014). The site- and species-specific RRF approach is consistent with the previous AQMPs. Four SASS sites and Mira Loma, the design site of the Basin, were used in the analysis. Quarterly averaged speciation fractions from the 2012 SASS measurements and quarterly-mean PM2.5 concentrations from corresponding FRM monitors (5 years and 20 quarters) were used to determine quarterly averaged concentrations of nitrate ion (NO3), ammonium ion (NH4), sulfate ion (SO4), elemental carbon (EC), organic carbon (OC), sea salt, and other primary PM2.5 material. The modeling platform developed for the ozone attainment demonstration was extended to the entire year to acquire quarterly average RRFs for each of the seven relevant species. Component-specific RRF values were applied to the base-year species concentrations to forecast future year component-specific concentrations. Particle bound water is then calculated using U.S. EPAs regression model approximation of the AIM model based on simulated concentrations of the ammonium, nitrate, and sulfate ions. (EPA, 2006). All species concentrations, along with a "blank" concentration, are summed for each quarter to produce quarterly averaged future total PM2.5 concentrations. A 5-year weighted

average of the annual mean concentrations is then calculated to produce a future-year 5-year weighted design value.

24-hour PM2.5

FRM mass and species-specific mass were calculated using an approach similar to the one followed for the annual design value, except that the 8 highest days from each quarter were included in the calculation. This is based on the assumption that the 98th percentile value can occur in any quarter and the 8th highest is the 98th percentile of 365 samples. Then, 32 sets of FRM mass and corresponding species fractions were retrieved per year, for the five-year period from 2010 to 2014. A set of species-specific RRFs were generated for each future year simulation from the top 10% of modelled PM2.5 days. RRFs were generated for the ammonium ion (NH4), nitrate ion (NO3), sulfate ion (SO4), organic carbon (OC), elemental carbon (EC), sea salt (Salt) and a combined grouping of other primary PM2.5 material (Other). A total of 7 species-specific RRFs were generated per quarter. Then future year concentrations of the seven component species were calculated by applying the model generated quarterly RRFs to the speciated 160 base year design values (8 days per quarter, 4 quarters per year and 5 year period). Particle bound water was determined using U.S. EPAs regression model approximation of the AIM model based on simulated concentrations of the ammonium, nitrate and sulfate ions (EPA, 2006). A blank mass of 0.5 µg/m3 was added to each base and future year simulation. The 32 days in each year (8 per quarter) were then re-ranked based on the sum of all predicted PM species to establish a new 98th percentile concentration. A weighted average of the resulting future year 98th percentile concentrations for each of the five years was used to calculate future design values for the attainment demonstration.

1-hour Ozone

For 1-hour ozone, no recent modeling guidance has been developed since the standard has been revoked.

The 1997 AQMP and 2003 AQMP 1-hour ozone attainment demonstrations relied on direct output from model simulations to project future year air quality and design values. This “deterministic” approach was based on the premise that future year projected baseline inventories were accurate and the impacts of implementing the control program were well simulated. In addition, the form of the 1-hour ozone standard was directed at the fourth highest concentration in a three year period for a given air monitoring station. In essence, the analysis looked at the 2nd highest concentration in a given year, typically occurring during the worst-case meteorological scenario.

The 2012 AQMP attainment demonstration relied primarily on the “deterministic approach”, but included the RRF methodology as weight of evidence discussion. Similar to the 2012 AQMP, the current AQMP utilized both “deterministic” and RRF approaches, given the fact that there is no official guidance for 1-hour ozone and both approaches have their limitations and strengths. The deterministic method relies on accurate modeling and the proper selection of a meteorological episode while the RRF approach tends to place less reliance on individual day model performance since the factor is based on an average of several events having similar meteorological profiles. However, basing the RRF on multiple days may mask the meteorological profile characteristics of an extreme event such as an annual second maximum concentration.

However, even if the RRF approach similar to the 8-hour demonstration was employed, the number of days included in the RRF calculation was re-evaluated. This was intended to accommodate the definition of the 1-hour ozone design value in contrast to that of the 8-hour. The 8-hour ozone standards takes the 4th highest readings of a year averaged over a three-year period. However, the 1-hour standard allows one exceedance a year, resulting in a design value based on the 4th highest value in a three-year period. In other words, the 1-hour standard focuses on the 1st or the 2nd highest day of the year, while the 8-hour accounts for the 4th highest day. Therefore, the optimal number of days for inclusion in the RRF calculation was determined to be three days after carefully examining CMAQ performance to capture episode days in 2012.

Numerical Models Employed for the 2016 AQMP

Table V-2-2 provides a side-by-side comparison of the 2007, 2012 and the current 2016 AQMP modeling protocols. The modelling protocol was significantly updated from the 2007 to the 2012 AQMP; however, changes between the 2012 and 2016 AQMP were minimal. In general, changes have occurred in the following categories: emissions inventories, future-year simulations, the level of the non-attainment designation and the attainment demonstration methodology. As such, these changes are expected to occur with each subsequent modeling update.

TABLE V-2-2

Numerical Modeling Platforms and Domains for 2016 and previous AQMPs

	2007 AQMP	2012 AQMP	2016 AQMP
Modeling Base Year	2005 Ozone: episode based PM: Annual	2008 Ozone: June – Aug PM: Annual	2012 Ozone: May – Sep PM: Annual
Chemical Transport Model	CAMx	CMAQ as primary tool CAMx as weight of evidence	CMAQ
Meteorological Model	MM5 version 3 Non-Hydrostaic model Hybrid of MM5/CALMET as weight of evidence	WRF version 3.3 with Updated Land Use	WRF version 3.6 with Updated Land Use
Emission: On-Road Off-Road	EMFAC 2007 CARB OFFROAD Model	EMFAC 2011 EMFAC-LDV EMFAC-HD EMFAC-SG Category Specific Calculation	EMFAC 2014 Single package Category Specific Calculation
Modeling Domain	Separate domains for O3 and PM modeling O3: 550 km by 370 km in E-W and N-S PM: 325 km by 200 km	624 km by 408 km	624 km by 408 km
Grid Resolution	5km by 5km grid	4km by 4 km grid	4km by 4km grid
Vertical Layer	O3: 16 layers up to 5km above the ground level (agl) PM: 8 layers	18 layers with 14 layer below 2000 m agl and 50 hPa as top boundary	18 layers with 14 layer below 2000 m agl and 50 hPa as top boundary

An entire year from January to December was simulated for the PM attainment demonstration – both 24-hour and annual averages. Five consecutive months starting from May 1st until September 30th were modeled for the ozone analysis. While this approach is similar to the approach used in the 2012 AQMP, it differs from the 2007 AQMP and prior AQMPs, which focused on selected high ozone episodes.

As in the 2012 AQMP, CMAQ was selected as the primary chemical transport modeling platform in the 2016 AQMP. CMAQ is a community model readily available in the public domain, allowing for the incorporation of the most recent algorithms and parameterizations as compared to models maintained by the private sector. For example, CMAQ has been recently equipped with the newest chemical mechanism, SAPRC07, however, CAMx still uses the older version of SAPRC99. In addition, as demonstrated in the 2012 AQMP, CMAQ performed comparatively or better than CAMx when simulating photochemistry within the Basin. Note that CAMx was employed for a weight of evidence analysis in the 2012 AQMP and as the primary dispersion platform in the 2007 AQMP. The CMAQ version used for 2016 AQMP included a modification in the subroutine "rdbcon.F", which reads lateral boundary values from the boundary conditions file. The original "rdbcon.F" repeatedly accesses boundary files at every chemical sync step, even though the boundary values stay constant during an hour window. The updated version reads the boundary values only once in every hour, which is the frequency interval of both the MCIP meteorological input file and the boundary conditions file. This modification reduces CPU time substantially by decreasing the input read time, while results do not change because the boundary values read by CMAQ are the same. The update was reported to Community Modeling and Analysis System (CMAS) center who is in charge of CMAQ update and maintenance. An additional modification was included in the AERO_DATA.F subroutine to by-pass the reading of PH2O emissions. Emissions of PH2O is not included in the AQMP inventory. The default AERO6 subroutine in CMAQ requires PH2O emission, and if these species are not present in the emission files, CMAQ does not run. This subroutine was modified so that these species are no longer required to continue with the simulation. Details of the CMAQ configuration are given in Table V-2.3.

TABLE V-2-3

Chemical Transport Modeling Platform for the 2016 and 2012 AQMPs

Options	2012 AQMP	2016 AQMP
Numerical Model	CMAQ version 4.7.1 as primary CAMx as Weight of Evidence	CMAQ version 5.0.2
Modeling Grid	156 by 102 grids with 4 km grid distance	Same
Gas Phase Chemical Mechanism	SAPRC99	SAPRC07 with version "c" toluene updates
Aerosol Mechanism	AERO5	AERO6
Chemical Solver	Euler Backward Iterative solver (EBI)	Same
Horizontal Advection	Piecewise Parabolic Method. (PPM)	Yamo
Vertical Advection	PPM	WRF
Horizontal Diffusion	Multiscale CMAQ scheme	Same
Vertical Diffusion	ACM2	Same
Photolysis	Lookup table	In-line Calculation
Initial Values	Clean Homogeneous Condition	Same
Boundary Values	Model for OZone and Related chemical Tracers (MOZART)	Same

The Weather Research and Forecast (WRF) model remains as the primary tool for meteorological modeling. For the 2016 AQMP, WRF was updated with the most recent version (version 3.6) available at this time and was evaluated with a set of input data, which include land-use classification and sea-surface temperature initialization fields (Table V-2-4).

TABLE V-2-4

Meteorological Modeling Platform for 2016 and 2012 AQMPs

Options	2012 AQMP	2016 AQMP
Numerical Model	WRF version 3.3	WRF Version 3.6.1
Nesting	Same	Same
Vertical Layers	30 layers with the lowest layer at 20 m above ground level	Same
Simulation Length	4 day with 24 hour spin-up	Same
Initial & Boundary Value	NAM Analysis field	NAM analysis field NARR analysis field
Landuse	Modified USGS landuse with 24 categories	Modified USGS landuse with 24 categories MODIS satellite retrieved landuse
Sea Surface Temperature	NAM surface analysis field	NAM surface analysis field Global Ocean Data Assimilation Experiment (GODAE) SST
Surface Layer Scheme	Slab Thermal Diffusion scheme	Slab Thermal Diffusion scheme NOAH scheme
Planetary Boundary Layer (PBL) scheme	YSU	Same
Date Assimilation	Analysis nudging at every 6 hours for the outermost domain only No temperature and moisture nudging for the PBL	Same

WRF simulations were conducted with three nested domains with grid resolutions of 36, 12 and 4 km (Figure V-2-1). The innermost domain spans 652 km by 460 km in the east–west and north–south directions, respectively, which includes the greater Los Angeles area, its surrounding mountains, and ocean waters off the coast of the Basin (Figure. V-2-2). A Lambert conformal map projection was used with reference latitudes of 30° and 60° N and the center of the modeling domain positioned at 37° N and 120° 30 ′ W.

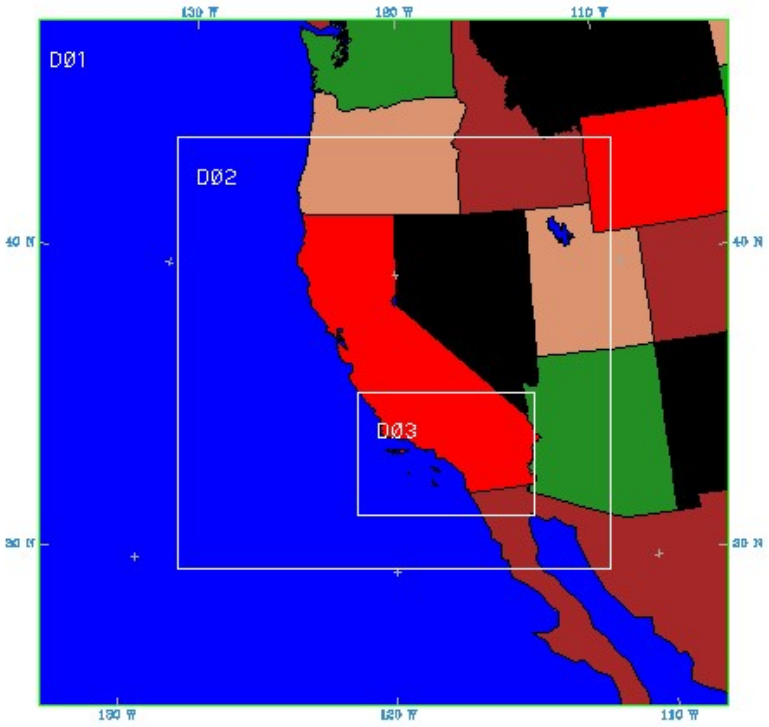

FIGURE V-2-1

Three nested domains used in WRF simulation

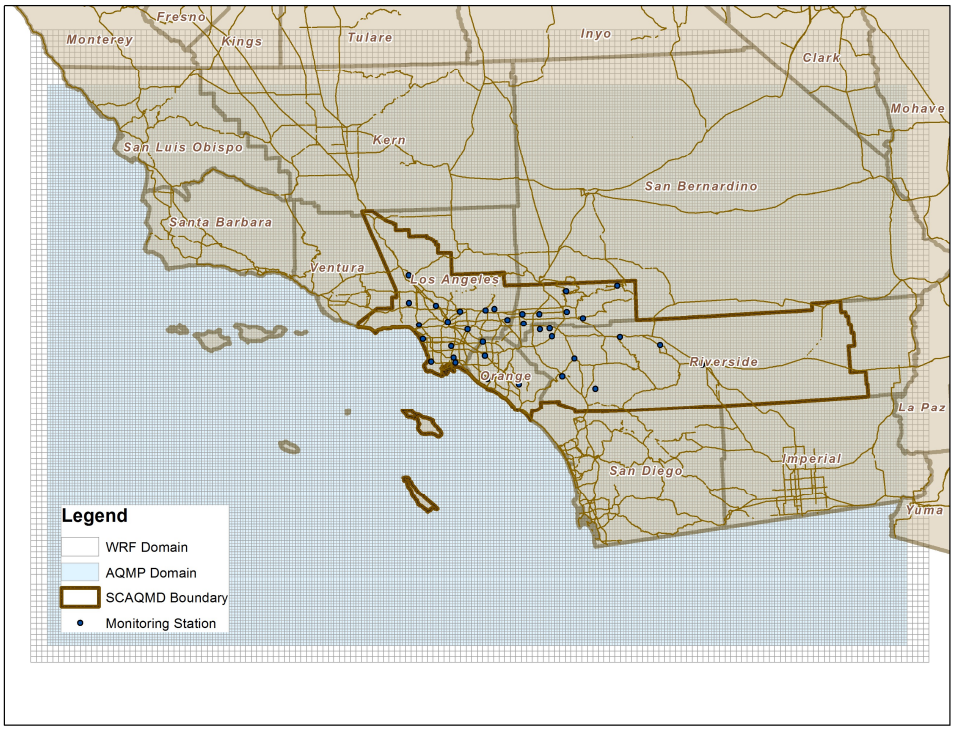

FIGURE V-2-2

The relative locations of the inner most WRF domain compared to the CMAQ domain. The boundary of South Coast AQMD boundary and air monitoring locations are overlaid by a thick solid line and black dots, respectively.

The model employed 30 vertical layers, with the lowest computational layer centered approximately at 20 m above ground level (agl) and a top layer centered at 50 hPa. Note that the WRF layers given in the Table V-2-5 are layer interfaces, meaning that actual computational volume is defined as the space between layer interfaces. The National Center for Environmental Prediction (NCEP) North American Model (NAM) model output (grid 212, 40 km grid spacing) together with vertical soundings and surface measurements, were used to compile initial and boundary values for the outermost domain as well as for the Four Dimensional Data Assimilation (FDDA) to WRF. The YSU planetary boundary layer scheme, WSM 3-class simple ice microphysics scheme, RRTM longwave radiation, Dudhia shortwave radiation were chosen as the default methods for the AQMP simulations after carefully considering various options available for WRF. Kain–Fritsch cumulus schemes were employed for the outer two domains, while no cumulus parameterization was used for the innermost domain. The thermal diffusion land-surface scheme was employed after evaluating the NOAH and Pleim-Xu schemes extensively.

TABLE V-2-5

Vertical Computational Layer Interfaces for 2016 AQMP modeling

Layer Index	Eta Level for WRF	Eta Level for CMAQ
31	0.0000	0.0000
30	0.0232	
29	0.0493	
28	0.0788	0.0788
27	0.1120	
26	0.1495	
25	0.1917	
24	0.2394	
23	0.2930	0.2930
22	0.3536	
21	0.4218	
20	0.4954	
19	0.5635	
18	0.6254	0.6254
17	0.6809	
16	0.7301	
15	0.7733	0.7733
14	0.8107	0.8107
13	0.8431	0.8431
12	0.8709	0.8709
11	0.8946	0.8946
10	0.9148	0.9148
9	0.9319	0.9319
8	0.9463	0.9463
7	0.9585	0.9585
6	0.9688	0.9688
5	0.9774	0.9774
4	0.9846	0.9846
3	0.9907	0.9907
2	0.9958	0.9958
1	1.0000	1.0000

Emissions Processing

On-Road mobile source emissions were calculated based on EMFAC 2014 and the 2016 Regional Transportation Plan/Sustainable Communities Strategy (RTP/SCS). Temporal and spatial allocation of on-road emissions were improved to accurately represent continuous measurements from in-road traffic sensors. Traditionally, on-road vehicle count is specified at five distinctive time zones of the day: morning peak (7-9AM), mid-day (10am-3pm), afternoon peak (4-7pm), evening peak (8-9pm) and night (10pm-6am). This profile was used to simulate a typical weekday traffic pattern in the Basin. The traffic count was then scaled to reflect changes in volume during each day of week based on an adjustment factor from CARB. However, this approach does not account for variations in traffic patterns due to seasonal changes, holidays, cultural activities or weather since it simulates a 'typical weekday' traffic flow. In an attempt to reflect such seasonal and cultural effects on on-road emissions, new temporal allocation profiles were constructed from traffic measurements available through the California Department of Transportation Performance Measurement System (PeMS). The PeMS network collects traffic data at over 9000 sensor locations within the Basin on a real-time basis at 5-minute time resolution, providing an actual real world traffic allocation that reflects social events, responses to weather conditions, and cultural behavior. This new PeMS-based methodology reallocates emissions temporally and spatially but does not affect the total amount of emissions from on-road mobile sources.

Off-Road emissions reflect updated speciation profiles and spatial surrogate factors for the following categories: construction equipment, recreational boats, composting, dairy cattle count, prescribed burning in future years, agricultural burning, architectural coatings, aircraft emissions, and military ordinance and vehicles on the San Clemente Naval Station. Gasoline dispensing facilities and oil and gas operations are subject to changes based on revised CARB and U.S. EPA emission calculation methodologies, respectively. Table V-2-6 summarizes changes in emission processing methodology between the 2012 and 2016 AQMP. The list of categories adjusted for day specific weather and activity is given in Table V-2-7.

TABLE V-2-6

Summary of Emission Processing for 2012 and 2016 AQMPs

Options	2012 AQMP	2016 AQMP
On-Road Emissions	EMFAC 2011 ○ 3 modules Light Duty Vehicles (LDV), Heavy Duty vehicles (HD) and Scenario Generating module (SG). ○ Modified DTIM Temporal Allocation using CARB/Caltrans Adjustment Factors	EMFAC 2014 ○ Single package integrated all the three components of the previous version ○ Emissions mode to get total amount of emissions in Tons per Day ○ Emissions rate to estimate grams per emissions of specific vehicle category, activity, etc Temporal Allocation using Caltrans real-time traffic data
Vehicle Miles Traveled	2012 Regional Transportation Plan/Sustainable Communities Strategy (RTP/SCS)	2016 Regional Transportation Plan/Sustainable Communities Strategy (RTP/SCS)
Off-Road Emissions	Category Specific Calculation	Same
Mexico Emissions	Revised Mexican emissions profile	Same

TABLE V-2-7

List of Emissions Categories with Day-Specific Adjustments

Day-Specific Emission Categories
• Ocean-going vessels • Agricultural burning • Wildfires • Prescribed burns • Residential wood combustion (curtailment programs) • Facilities that have closed since 2012 • Facilities that have had large upsets • Paved road dust • Unpaved road dust • Windblown dust • Livestock dust • Biogenic and On-Road motor vehicle emissions are adjusted using day/hour-specific meteorological data.

Computational Resources

The main computation platform employs Linux-based parallel processing computers. New servers, compiled to enhance computational capability, were configured with Red-Hat version 6.4 O/S and 64 bit operating systems. The Fortran and C compilers were transitioned to Intel group compilers for the current AQMP, while Portland Group Compilers were used in the default configuration for the 2012 AQMP. The shift to the Intel compilers was initiated to provide a 10-20% improvement in computational speed. Details of the computing resources are summarized in Table V-2-8.

TABLE V-2-8

Details of Computational Resources used in the 2007, 2012 and 2016 AQMPs.

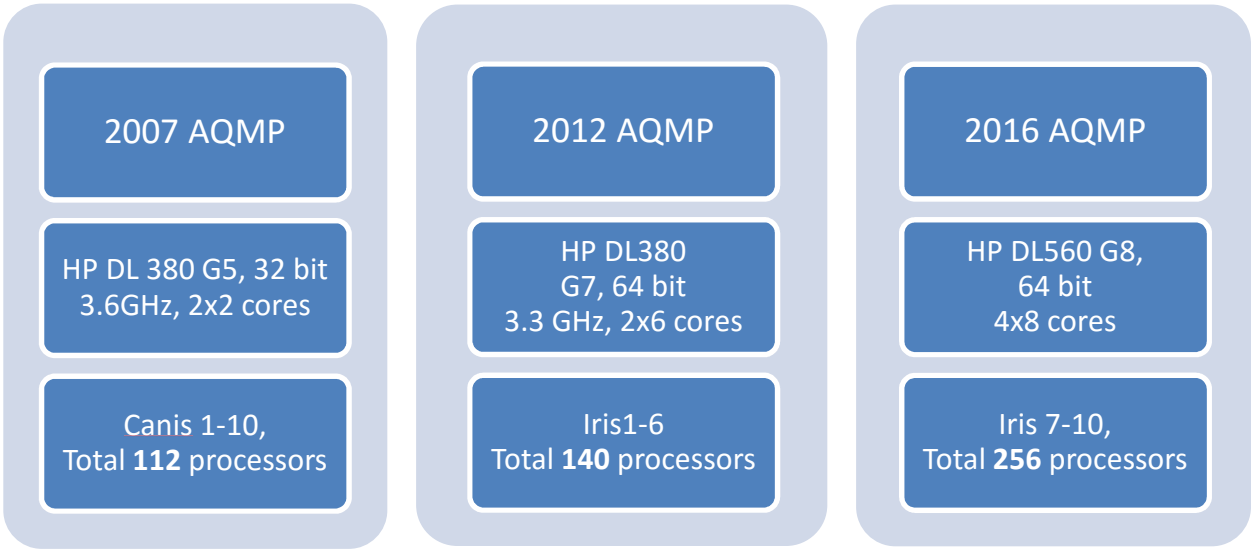

References

US EPA (2007) Guidance on the Use of Models and Other Analyses for Demonstrating Attainment of Air Quality Goals for Ozone, PM2.5, and Regional Haze, EPA -454/B-07-002

US EPA (2011) Memorandum on "Update to the 24 Hour PM2.5 NAAQS Modeled Attainment Test"

US EPA (2014) Draft Modeling Guidance for Demonstrating Attainment of Air Quality Goals for Ozone, PM2s, and Regional Haze

CHAPTER 3

METEOROLOGICAL MODELING AND SENSITIVITY ANALYSES

Overview

This chapter provides a description of the meteorological modeling that serves as the foundation of the 2016 AQMP modeling analysis. During the 2012 AQMP, SCAQMD conducted extensive tests on the performance of WRF compared with the previously used MM5 model and showed that WRF performs as well as or even better than MM5. Based on the discussions with the District's science and technology advisory groups during the 2012 AQMP, WRF was selected as the primary numerical platform for the generation of meteorological fields. Therefore, WRF-derived meteorology was used for chemical transport modeling in the 2012 AQMP and presently, the 2016 AQMP. WRF is a mesoscale meteorological forecast model used by the National Weather Service, academic institutes and the scientific community. It is under continual review and updates, under the administration of National Center for Atmospheric Research (NCAR), to reflect state-of-art modeling knowledge. This chapter describes the numerical configuration, sensitivity tests on key parameterizations, the input database, and initial and boundary values used in the ozone and PM2.5 attainment demonstration.

Meteorological Modeling Configuration

WRF is one of the most widely used meteorological models. It has been applied to a wide variety of phenomena and a wide spectrum of geographical and climatological situations. It is also listed in EPA's Support Center for Regulatory Atmospheric Modeling (SCRAM) site, a numerical-model clearinghouse. The WRF Non-hydrostatic Mesoscale Model (NMM) core is also used as a platform for official weather forecast by National Weather Service (NWS). One of the most significant advantages of using WRF arises from its large user community; the model is regularly applied to simulate various phenomena on a wide variety of computational machines. This enables robust tests of the model physics and numerics and provides a unique opportunity to fix any errors and incorporate the state-of-the science in a short time period.

WRF is a 3-D prognostic model that solves the Navier-Stokes' equation, accounts for thermodynamics, conserves mass, and incorporates radiative energy transfer. WRF has been applied to a wide range of phenomena, such as regional climate, monsoons, cyclones, mesoscale fronts, land-sea breezes and mountain-valley circulations. There are two platforms within the WRF framework: Advanced Research WRF (ARW) and Non-hydrostatic Mesoscale Model (NMM). The ARW configuration was chosen for the current modeling analyses.

WRF simulations were conducted with three nested domains at grid resolutions of 36, 12 and 4 km. The innermost domain has 163 by 115 grid points in abscissa and ordinate, respectively, which spans 652 km by 460 km in east-west and north-south directions, respectively. Geographically, the domain encompasses the greater Los Angeles and suburban areas, its surrounding mountains, and seas off the coast of the Basin as shown in Figure V-3-1. The figure also shows the relative locations and sizes of the three nested grids. The innermost domain, excluding first three boundary columns and rows, served as the CMAQ chemical transport modeling domain. The relative locations of the WRF, CMAQ, and SCAQMD's jurisdiction are presented in Figure V-3-2.

The model employed 30 layers vertically with the lowest computational layer being approximately 20 m above ground level (agl) and the top layer at 50 hPa. Four Dimensional Data Assimilation (FDDA) was conducted using grid analysis data that was enhanced with available surface and vertical sounding data. The Yon-Sei University (YSU) (Hong, 1996) scheme was used to model the planetary boundary layer (PBL). Cloud radiation and simple ice cloud physics were chosen for simulations after carefully considering various available options in WRF. Kain-Fritsch cumulus schemes were employed to the outer two domains, while no cumulus parameterization was used for the innermost domain. The selections of LSM scheme, initial and boundary values, and the use of land use and sea surface temperature data are discussed further in the next section.

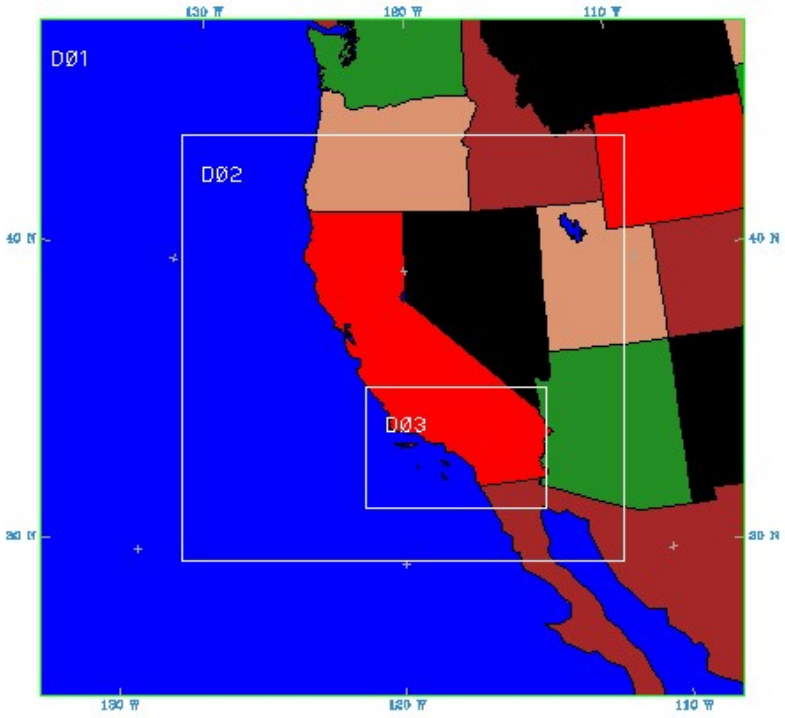

FIGURE V-3-1

Three nested modeling domains employed in the WRF simulations

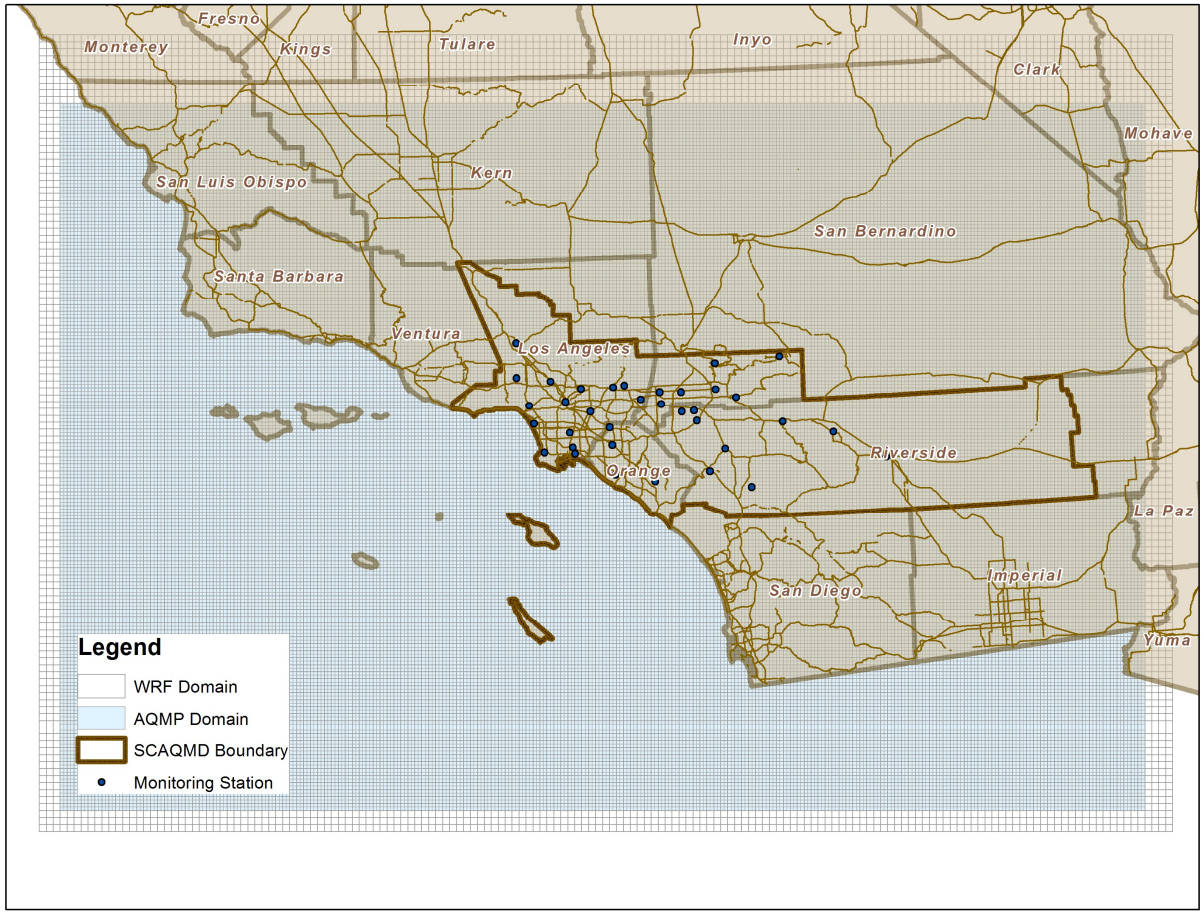

FIGURE V-3-2

The inner most WRF domain and CMAQ modeling domain with respect to the SCAQMD jurisdiction boundary.

Table V-3-1 below provides a summary of the WRF configuration used in the 2016 AQMP in comparison with the 2012 AQMP. Major parameters finalized for the 2016 AQMP are similar to those used in the 2012 AQMP, except sea surface temperature. A list of physics options and parameters that were evaluated extensively as a part of the 2016 AQMP is provided in Table V-3-2. Those that were identified as critical to describe air pollution episodes are presented.

TABLE V-3-1

Overview of WRF configuration for 2016 AQMP in comparison with 2012 AQMP

Options	2012 AQMP	2016 AQMP
Numerical Model	version 3.3	Version 3.6.1
Nesting	Three nested Domains	
Vertical Layers	30 Layers with the lowest layer at 18 m agl	
Simulation Length	4 day with 24 hour spin-up	
Planetary Boundary Layer (PBL) scheme	Yon-Sei University (YSU) scheme	
Data Assimilation	Analysis nudging at every 6 hours for the outermost domain only No temperature and moisture nudging within the PBL	
Initial & Boundary Value	NAM Analysis field	
Landuse Database	Modified USGS Landuse with 24 categories	
Sea Surface Temperature	NAM surface analysis field	Global Ocean Data Assimilation Experiment High Resolution Sea Surface Temperature (GHR SST) Data
Surface Layer Scheme	Thermal Diffusion scheme	

TABLE V-3-2

The list of WRF Sensitivity Test Categories and elements tested in each category

Testing Categories	Database
Initial Guess Field	– North American Model (NAM) Analysis Field – North American Regional Re-analysis (NARR) Field
Land Surface Scheme	– Thermal Diffusion scheme – NOAH Land Surface scheme – Pleim-Xu scheme
Land Use Database	– USGS 2001 vs. 2011 database – SCAQMD modified Sub-Urban category – MODIS satellite driven dataset
Sea Surface Temperature	– Global Ocean Data Assimilation Experiment High Resolution Sea Surface Temperature (GHR SST)Data 6hourly, about 9 km spatial resolution

Sensitivity Tests for Numerical Parameterizations

WRF offers multiple user options for numerical parameterizations, initial and boundary values, values of various coefficients, the level of observational data assimilation, etc. While these options provide an opportunity to optimize the model for a specific application, an ill-suited configuration can lead to less accurate results. In this context, atmospheric physics and parameters closely related with air quality were screened and the options with the most representative results were incorporated into subsequent numerical experiments. The categories given in Table V-3-1 and Table V-3-2 have been thoroughly vetted to determine the best model options.

Initial Guess Field

WRF, as any mesoscale-meteorological model, reads in an initial 3-D field of prognostic meteorological variables. These initial fields are usually an output of a larger-scale model such as global scale model or mesoscale model covering a larger domain. The North American Model (NAM) analysis product, a National Weather Service (NWS) operational forecast product, was employed in the WRF simulations for the 2012 AQMP. NAM is a real-time forecast product enhanced with available surface and atmospheric vertical sounding data in a retrospective fashion. The NAM analysis output is widely used and readily available through the National Center for Atmospheric Research (NCAR) science data repository. While NAM is the default analysis product used for the Basin simulations, other data sets such as the Global Forecast System (GFS) forecast and the North American Regional Reanalysis (NARR) data are alternatives known to produce synoptic activities in the Pacific Northwest reasonably well. Angevine (2011) suggested that the

European Center for Medium-range Weather Forecast model (ECMWF) and the GFS data were superior in simulating the marine boundary layer along the Southern California coast. However, ECMWF data is not readily available free-of-charge since it is a European product. In addition, the GFS has a coarser grid resolution that may affect its capability to regenerate high resolution topographic features that are critical to re-produce orography induced thermal circulation pattern in the Basin. The GFS products are available from 28 to 70 km resolution. The National Center for Environmental Prediction (NCEP) NARR products are on the Eta 221 grid at 29 pressure levels. They were produced using the Eta 32 km model with 45 vertical layers. The input data includes all observations used in the NCEP/NCAR Global Reanalysis project, and additional precipitation data, TOVS 1B radiances, profiler data, land surface and moisture data, etc. The output analyses are presented every third hour with an additional 9 variables in the 3-hour forecasts to reflect accumulations or averages. Like the NAM analysis product, the NARR data is readily available free-of-charge through the NCAR science data repository. In addition, CARB uses NARR as their default initial and boundary values for their WRF simulation. The NAM analysis data was produced for Grid 212 with 40 km grid spacing.

The initial data field was used to drive lateral boundary values of the outermost domain, after it was nudged with available measurements to further reduce potential errors in the input data field. Therefore, the information embedded in those data fields impact not only the initial time step but also the entire simulation.

The differences in the NAM and NARR dataset were rather significant especially for water vapor mixing ratio and surface wind speed. Temperature followed each other closely. Figure V-3-3 shows the time series of daily max temperature, water vapor mixing ratio and wind speed retrieved from NAM, NARR and corresponding observations for the period of May 1st to September 30th, 2012 in Riverside. NAM data followed the observed water vapor trend closely, but showed substantial under-bias for wind speed. On the contrary, NARR generated a relatively dry atmosphere, but represented measured wind speed better than NAM. Note the data in Figure V-3-3 is WRF input data taken directly from NAM and NARR rather than WRF output.

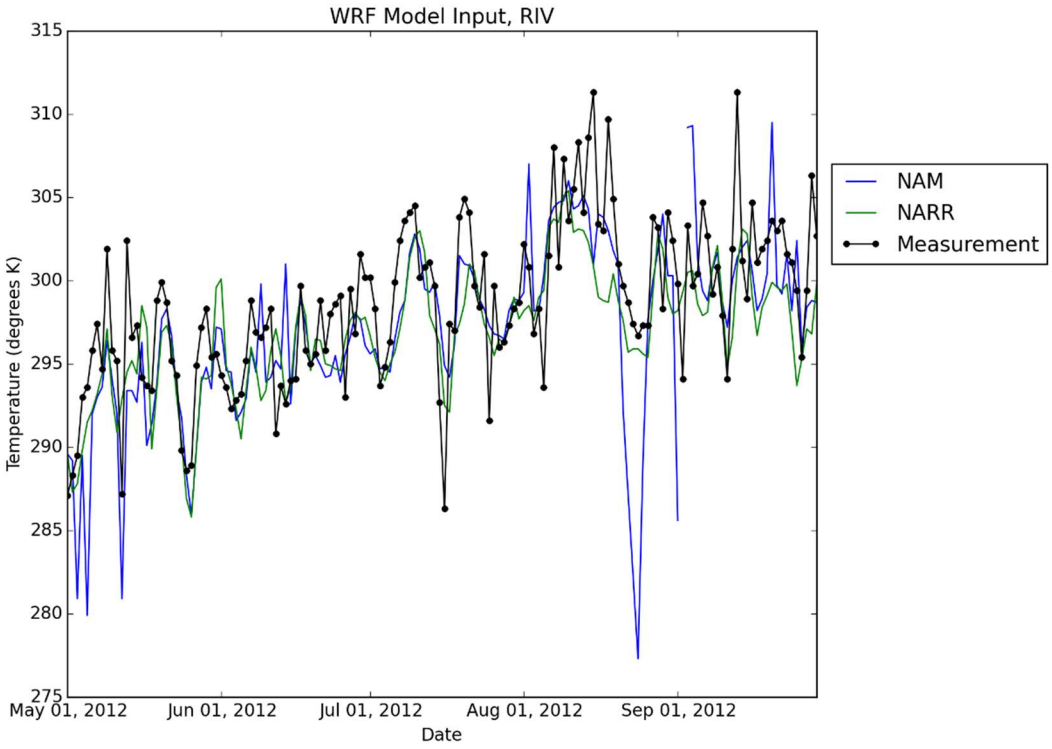
WRF Model Input, RIV
Temperature (degrees K)
315
310
305
300
295
290
285
280
275
May 01, 2012
Jun 01, 2012
Jul 01, 2012
Aug 01, 2012
Sep 01, 2012
Date
NAM
NARR
Measurement

(a)

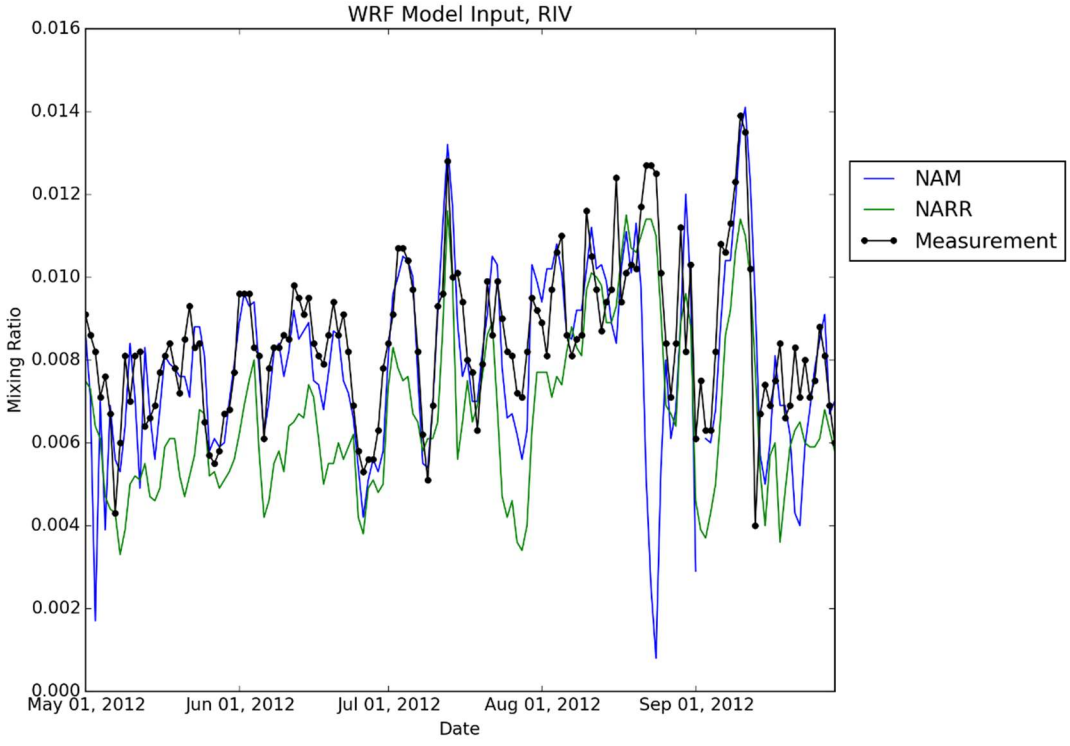
WRF Model Input, RIV
Mixing Ratio
0.016
0.014
0.012
0.010
0.008
0.006
0.004
0.002
0.000
May 01, 2012
Jun 01, 2012
Jul 01, 2012
Aug 01, 2012
Sep 01, 2012
Date
NAM
NARR
Measurement

(b)

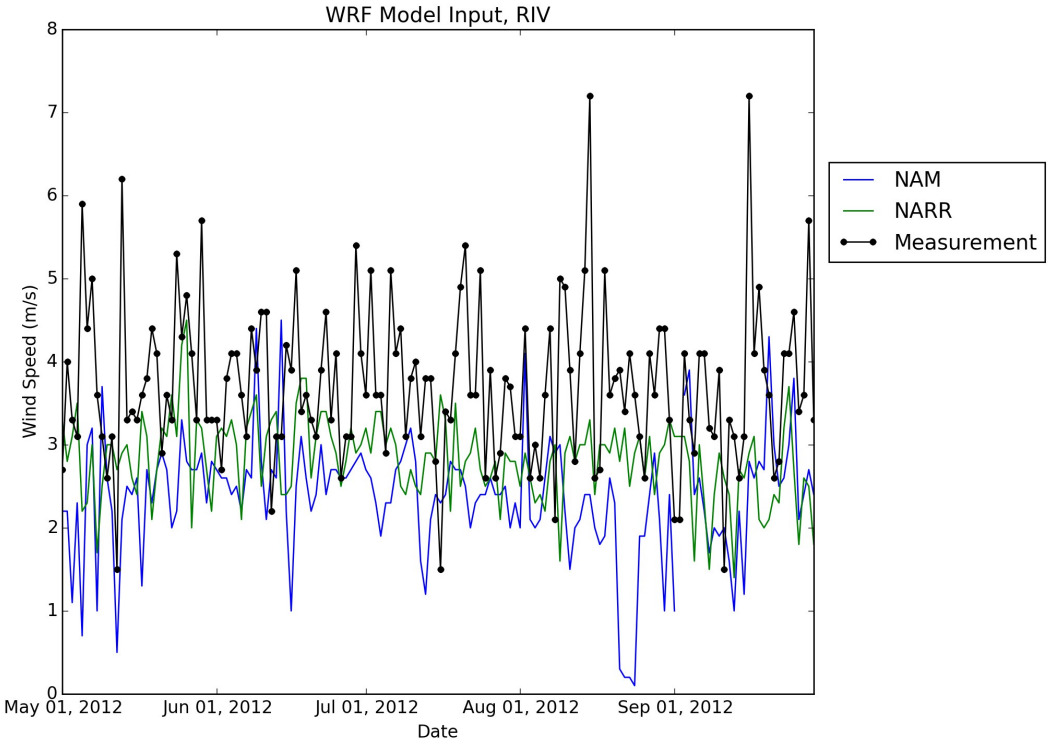

(c)

FIGURE V-3-3

Time series of (a) Temperature, (b) Water Vapor Mixing Ratio and (c) Wind Speed retrieved from NAM and NARR and measurements taken at Riverside March Air Force Base.

The input fields create noticeable differences in the WRF prediction, as shown in Figure V-3-4. While temperature fields were well predicted by both of the initial datasets, the moisture field simulated with the NARR was drier than NAM. This dry bias appears to be carried over from the input data fields to the output data fields presented in Figure V-3-4.

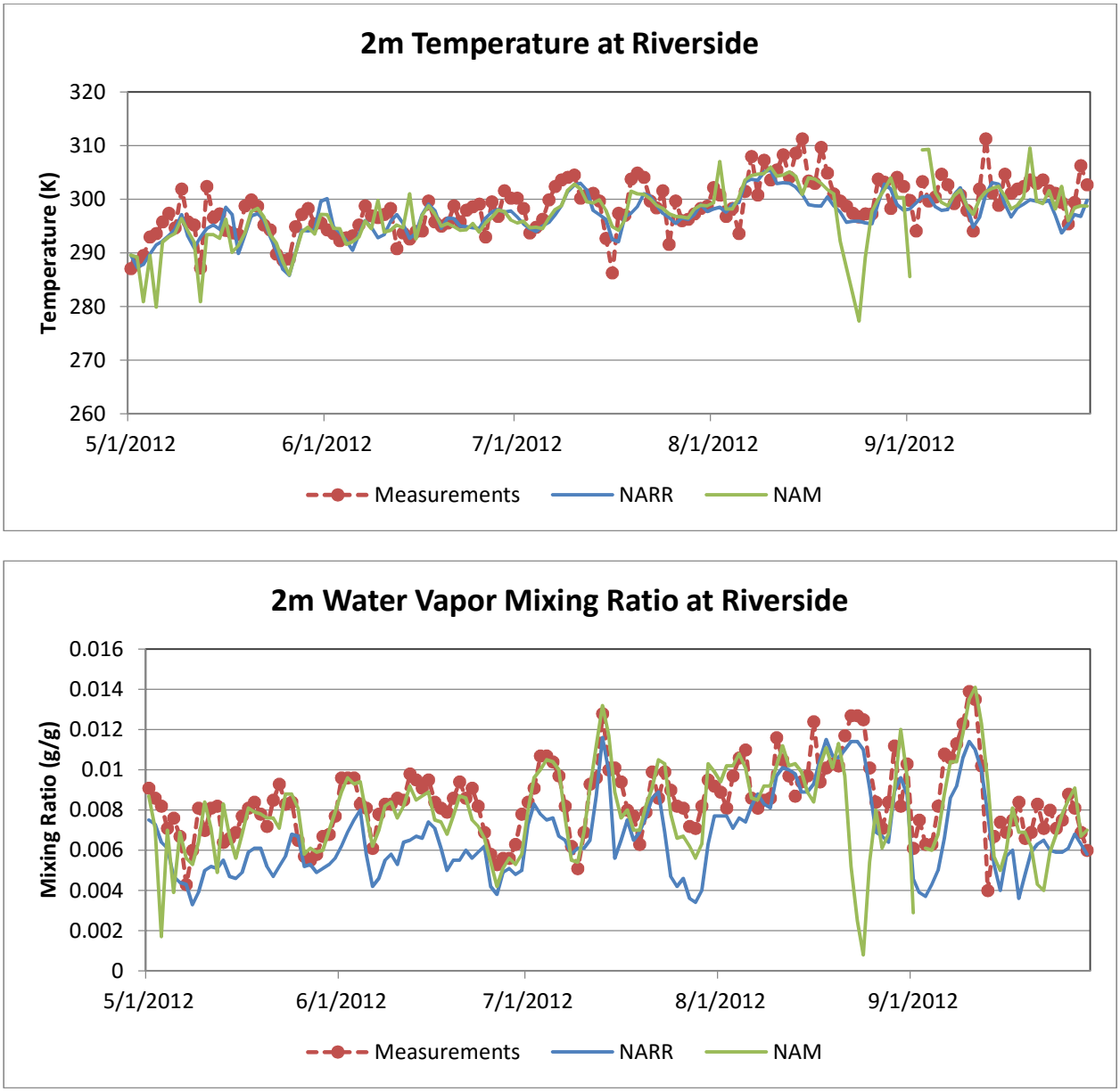

FIGURE V-3-4

Time Series of Measurements and WRF predicted Temperature (top), and Water Vapor Mixing Ratio (bottom) at Riverside. NARR (blue solid line) and NAM (green solid line), respectively, used as initial and boundary values.

Land Surface Scheme

The three land surface models (LSM) considered for WRF performance tests were the five-layer thermal diffusion scheme, the NOAH, and Pleim-Xiu (P-X) schemes. Similar tests were conducted during the 2012 AQMP attainment demonstration, but model output is especially sensitive to the choice of land surface scheme. Since a new series of input data fields including Sea Surface Temperature (SST) and land use was introduced for WRF modeling, it was necessary to re-visit the performance of the widely available schemes and re-optimize the performance.

The thermal diffusion scheme is the simplest and least computationally expensive among the three schemes. It calculates soil temperature as a result of thermal diffusion between layers, which are defined at the depths of 0.01, 0.02, 0.04, 0.08, and 0.16 m with the deepest layer being a fixed substrate. The NOAH scheme predicts the soil temperature and moisture prognostically in four layers (Chen and Dudhia, 2001). The P-X LSM (Pleim and Xiu, 1995; Xiu and Pleim, 2001), originally based on the ISBA model of Noilhan and Planton (1989), includes a 2-layer force-restore soil temperature and moisture model. The top layer is taken to be 1 cm thick, and the lower layer is 99 cm. Grid aggregate vegetation and soil parameters are derived from fractional coverages of land use categories and soil texture types. There are two indirect nudging schemes using soil moisture and deep soil temperature (Pleim and Xiu, 2003).

The three schemes provided notably different predictions (Figure V-3-5, Figure V-3-6 and Figure V-3-7). First, wind speed was stronger with the Thermal-diffusion scheme both for the convective and the nocturnal periods. While the NOAH and P-X schemes produced approximately similar wind speeds, the P-X showed the lightest wind during the convective period (Figure V-3-6). The PBL heights were dramatically different in all three schemes. The NOAH scheme predicted the deepest mixing, which in-turn, triggered momentum transfer from the upper atmosphere to the surface level, contributing to stronger winds near the surface level. The Thermal-diffusion scheme showed the least amount of vertical mixing, indicating a lower extent of ventilation, which is the product of vertical mixing and horizontal advection wind. As expected, the Thermal-diffusion scheme was the most successful in simulating high ozone concentrations observed during the summer ozone season. The overall performance of the three schemes are summarized in Table V-3-3, which will be discussed in the following section.

(a)

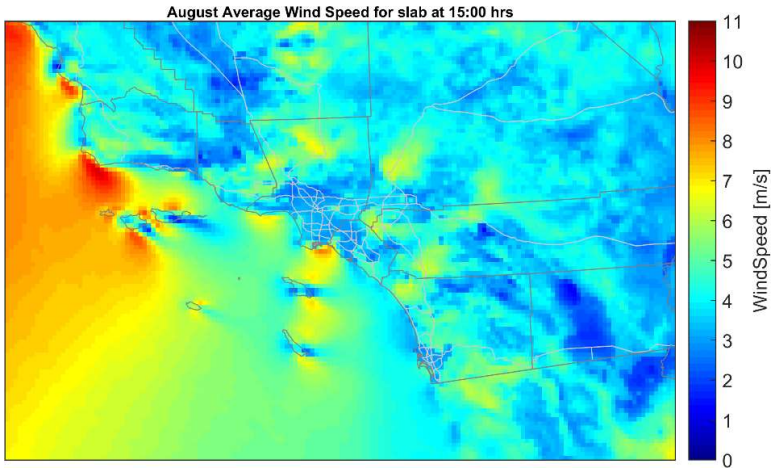

(b)

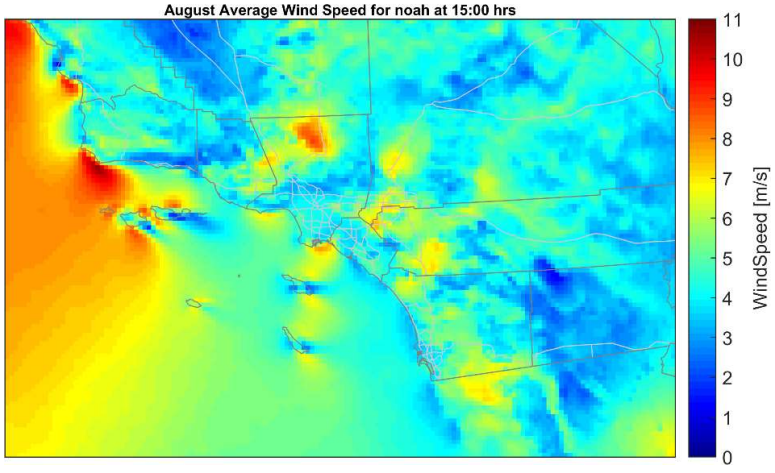

(c)

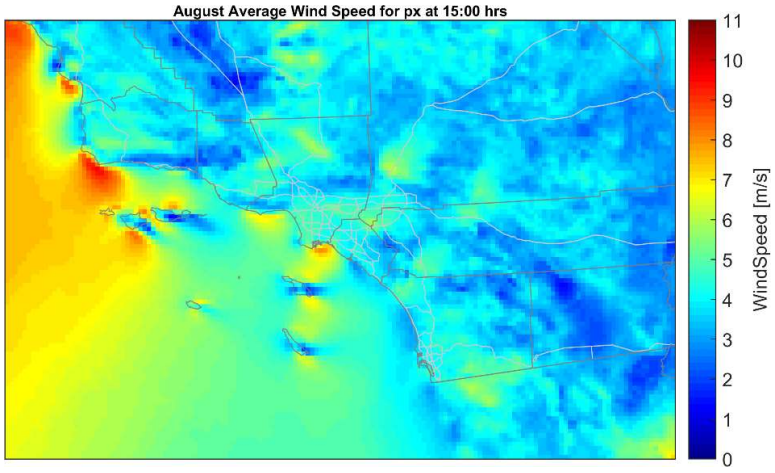

FIGURE V-3-5

Horizontal distribution of wind speed at 1500 PST predicted with (a) Thermal Diffusion, (b) NOAH, and (c) Pleim-Xiu Land Surface Scheme. The winds are composited for the month of August.

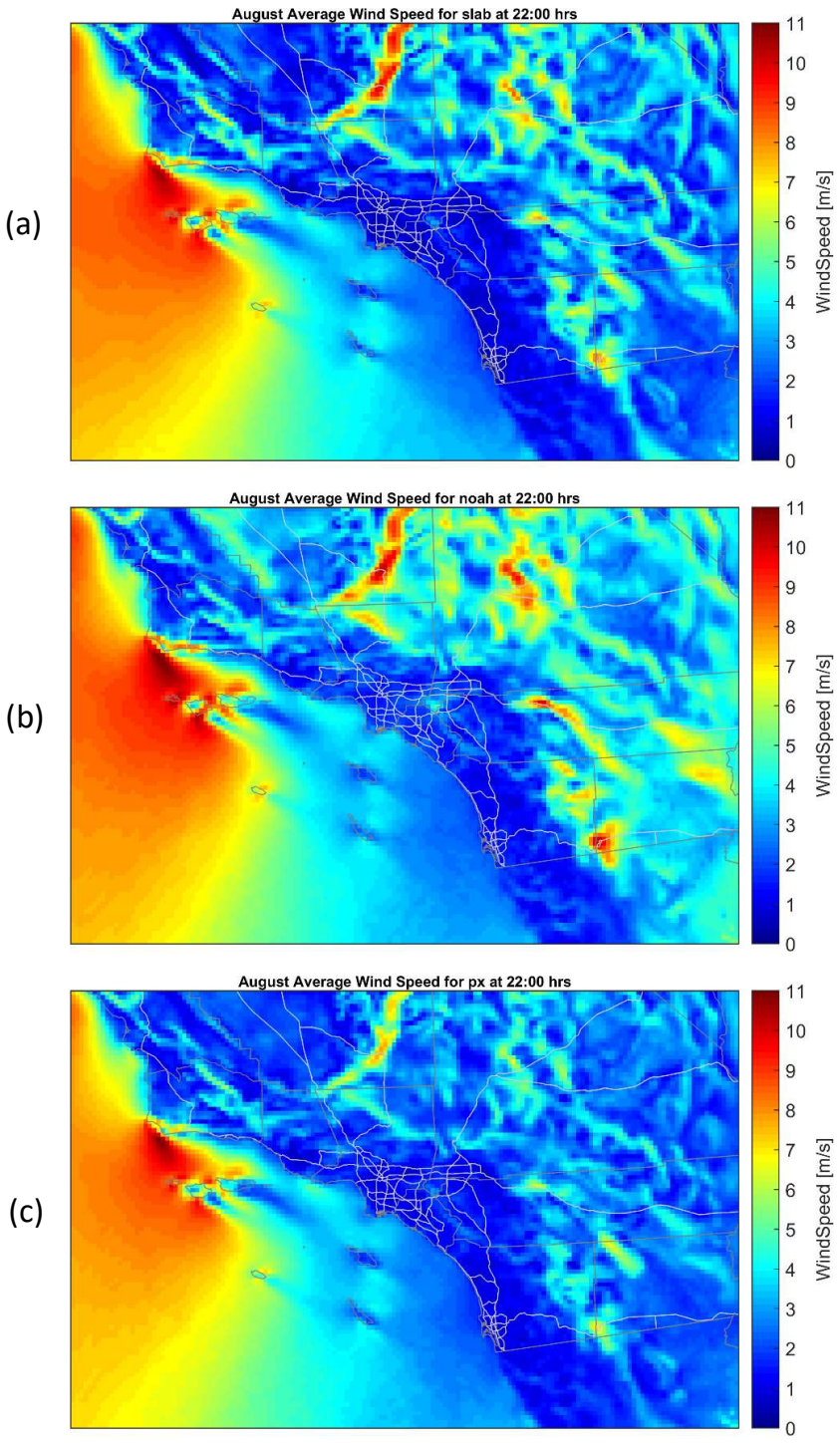

FIGURE V-3-6

Horizontal distribution of wind speed at 2200 PST predicted with (a) Thermal Diffusion, (b) NOAH, and (c) Pleim-Xiu Land Surface Scheme. The winds are composited for the month of August.

(a)

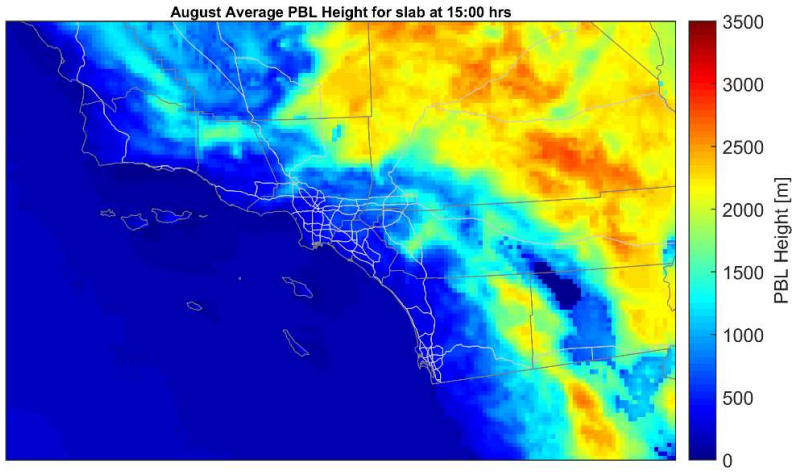

(b)

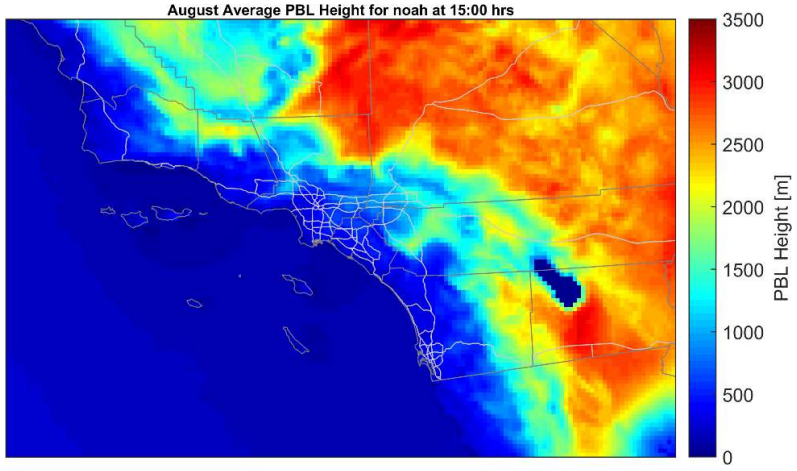

(c)

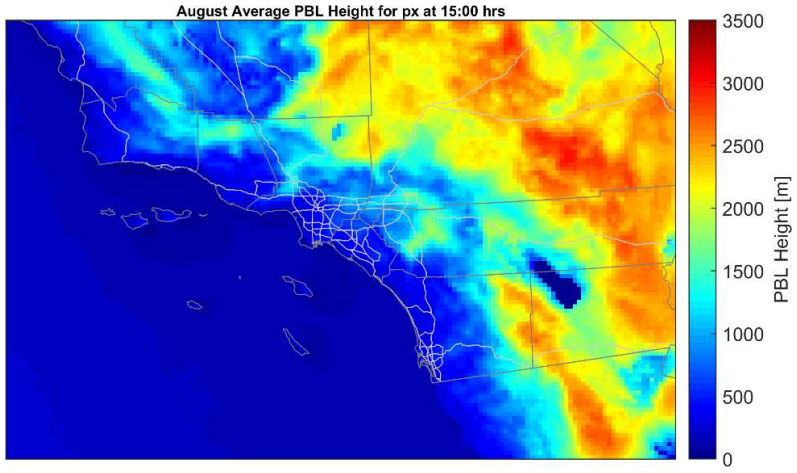

FIGURE V-3-7

Planetary Boundary Layer depth predicted for 1500 PST in August. (a) Thermal Diffusion, (b) NOAH, and (c) Pleim-Xiu Land Surface Schemes were used respectively.

The performance of each scheme was compared against measurements taken from NWS weather stations. Figures V-3-8 through Figure V-3-11 show seasonal average biases of surface wind speed predicted by the Thermal Diffusion and NOAH land surface schemes. During morning hours, both the Thermal Diffusion and the NOAH schemes under-predict surface wind speeds. This negative bias occurred at most of the locations within the Basin, while coastal stations showed a larger degree of under-prediction than inland locations. The under-prediction continues to prevail for the convective period (Figure V-3-10 and Figure V-3-11), yet the degree of negative bias was enhanced in the Thermal Diffusion scheme, indicating that the Thermal Diffusion scheme tended to simulate weak winds that lead to the accumulation of air contaminant concentrations. This is well represented by the ventilation index, defined as horizontal advection multiplied by vertical mixing layer depth (Figure V-3-12). As expected from the surface wind and PBL depth, the Thermal Diffusion scheme ("slab") showed less ventilation than the NOAH scheme, leading to the highest pollutant concentration. Accordingly, the Thermal Diffusion scheme excelled in predicting high ozone concentrations observed during episode periods in the Basin compared to the other schemes and therefore, it was selected as the default land surface scheme for this attainment demonstration. The amount of ventilation is sensitive to geographical location since the PBL depth and horizontal wind speed depends on geography and its associated thermal and dynamic forcing. Deeper mixing in the inland sites, such as Ontario and Riverside resulted in a greater amount of ventilation (Figure V-3-12).

While the PBL depth is one of key elements to predict pollutant concentrations, no conventional measurements are available to validate the PBL predictions. The closest National Weather Service Radiosonde site is located in San Diego, which is over 150 miles away from LA, representing different weather and climate. Staff conducted a preliminary study to retrieve PBL depths from a radiometer and Radar wind profilers/Radio Acoustic Sounding System (RASS) placed at the Los Angeles airport, Ontario airport, Riverside and Irvine. Even though the results from the wind profilers/RASS appear to be good for qualitative assessments of diurnal and seasonal variation, the degree of uncertainties involved in the measurements and data retrieval pose challenges in drawing quantitative information to evaluate model predictions. Still, the PBL heights predicted by the NOAH scheme appeared to be significantly deeper than previous measurements reported in the area for similar climatological conditions. A radiometer provides little more reasonable PBL depth than the RASS, but the measurements are limited to the Los Angeles airport site. All three land surface schemes showed large deviations from the radiometer data, indicating challenges to simulate the marine boundary layer correctly.

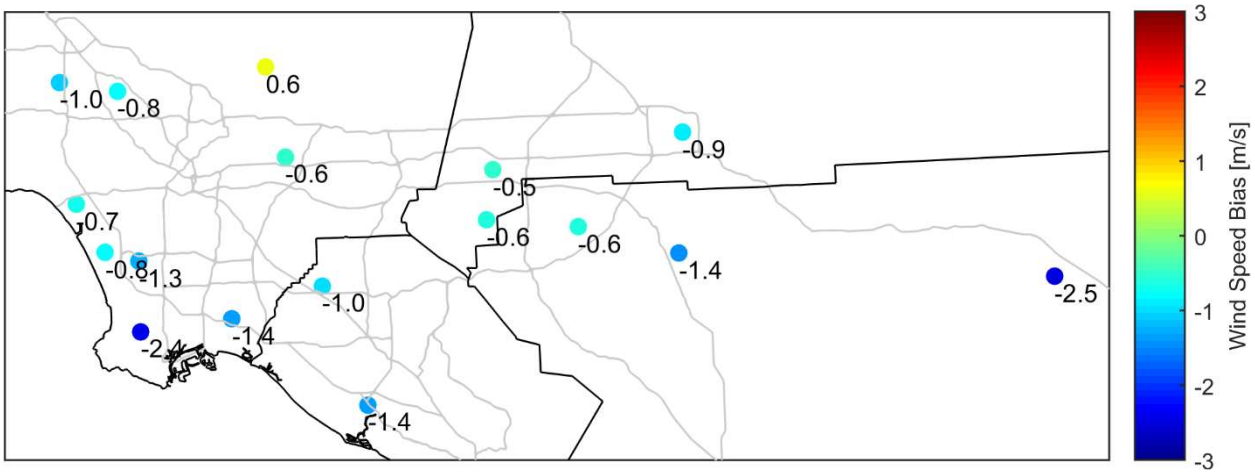

FIGURE V-3-8

August average bias of surface wind speed predicted with the Thermal Diffusion Land Surface Scheme. The bias corresponds to 0800 PST.

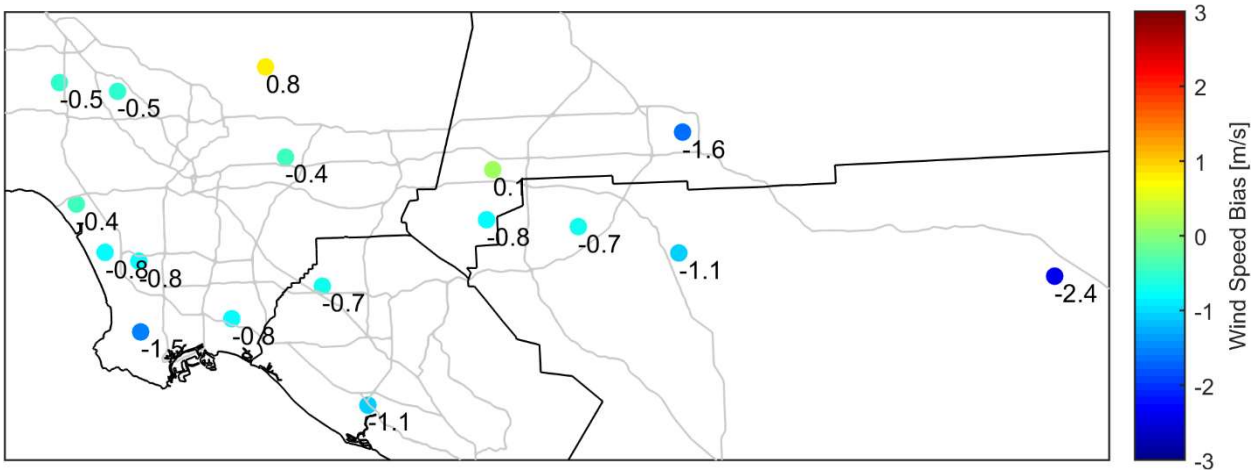

FIGURE V-3-9

August average bias of surface wind speed predicted with the NOAH Land Surface Scheme. The bias corresponds to 0800 PST.

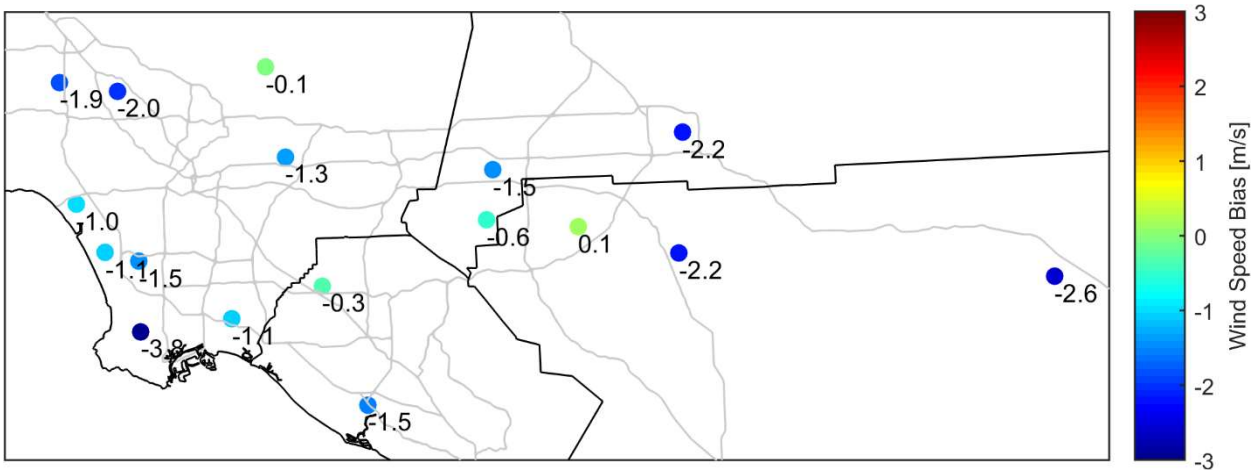

FIGURE V-3-10

August average bias of surface wind speed predicted with the Thermal Diffusion Land Surface Scheme. The bias corresponds to 1700 PST.

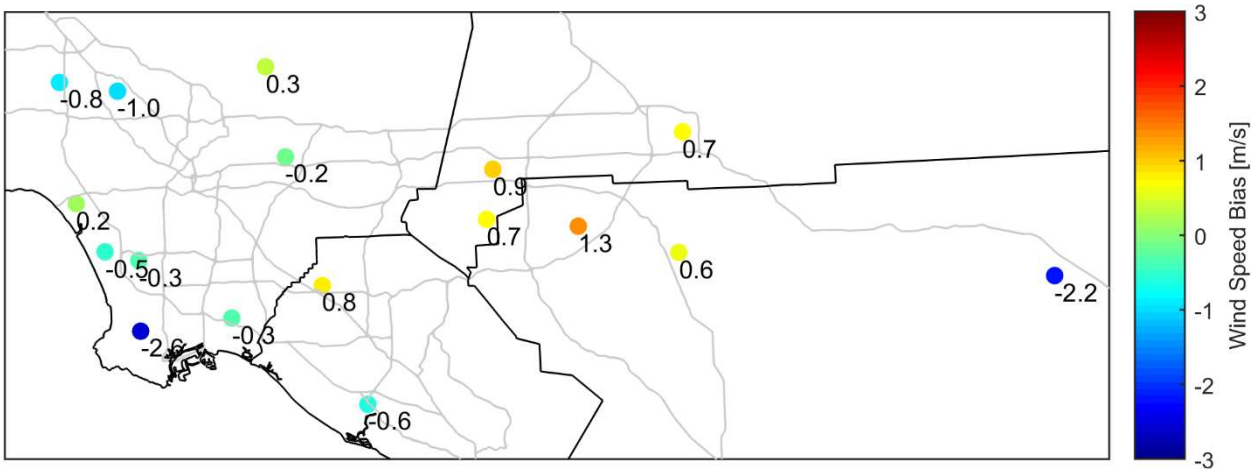

FIGURE V-3-11

August average bias of surface wind speed predicted with the NOAH Land Surface Scheme. The bias corresponds to 1700 PST.

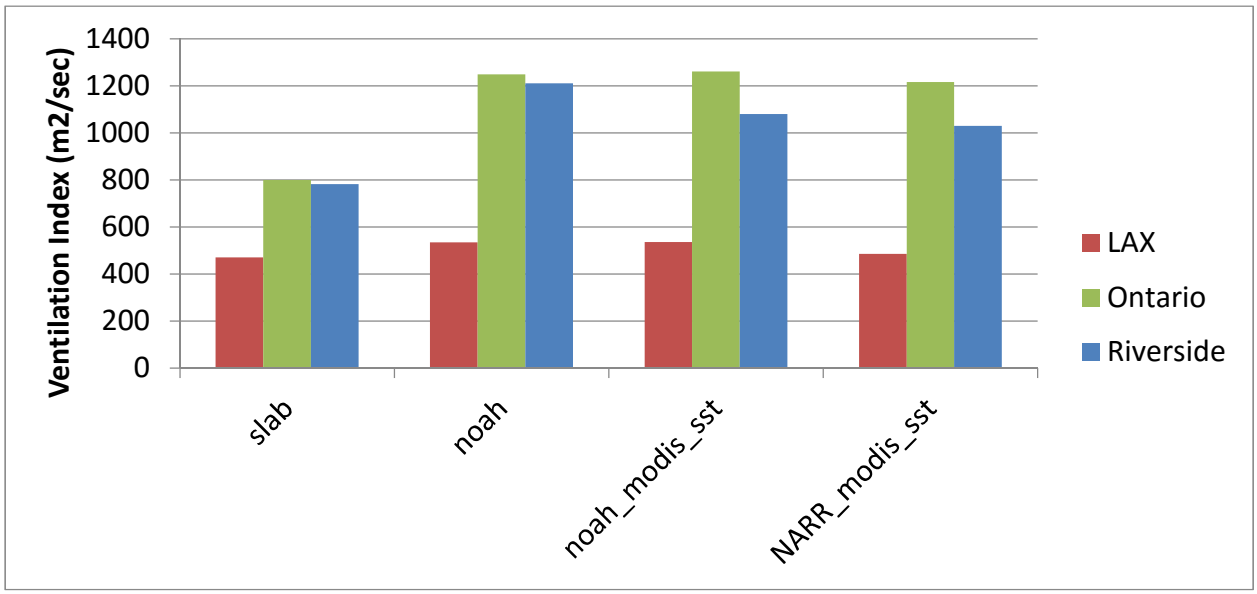

FIGURE V-3-12

Seasonal Average Ventilation Index (calculated as PBL height multiplied by surface wind speed) for the period from May through September

Land Use Representation

The U.S. Geological Society (USGS) default land use database and the Moderate Resolution Imaging Spectroradiometer (MODIS) satellite-based dataset (NASA, 2012) are both available to represent land use in WRF. The USGS dataset has been the default dataset for mesoscale modeling for WRF. While it is a ready-to-use off-the-shelf database, some data representations are several-decades old and consequently do not reflect changes in the areas that have experienced rapid development in recent years. The South Coast Air Basin, especially in parts of Riverside, San Bernardino and the San Fernando Valley areas, have experienced rapid development in the last decade that turned shrub and grassland into suburban housing units and impervious land cover. Accordingly, the location and extent of urban representation in the USGA dataset is often inaccurate for the Basin. During the 2012 AQMP, SCAQMD staff developed new land use categories ready for the use in WRF simulation. The new dataset was based on the USGS database, but contains a new category defined as 'sub-urban', which represents low-density residential neighborhoods with single and/or double story houses. The new category was introduced mostly in the inland Riverside, San Bernardino and San Fernando valleys where rapid growth occurred in early 2000's. Land use retrieved by the MODIS satellite shows a large degree of development, for which extent and location agrees well with the modified USGS category in Figure V-3-13a. While the MODIS land use is expected to capture concurrent land use adequately, it is compatible only with NOAH land surface scheme, thus cannot be used with the Thermal Diffusion nor PX schemes. On the contrary, the USGS can be used universally in all the land surface schemes. In this context, this modified USGS land use with the added sub-urban category is used for the current modeling simulations (Figure V-3-13).

The USGS updates Land Use Land Cover (LULC) periodically. The latest version, updated in 2011, was compared with 2001, which was approximately when the recent rapid development in the Basin started (Figure V-3-14). The red shading represents urbanized areas. While the expansion of urban areas is evident from the first two figures, the difference of the two shown in Figure V-3-14c emphasizes the location and size of the expansion.

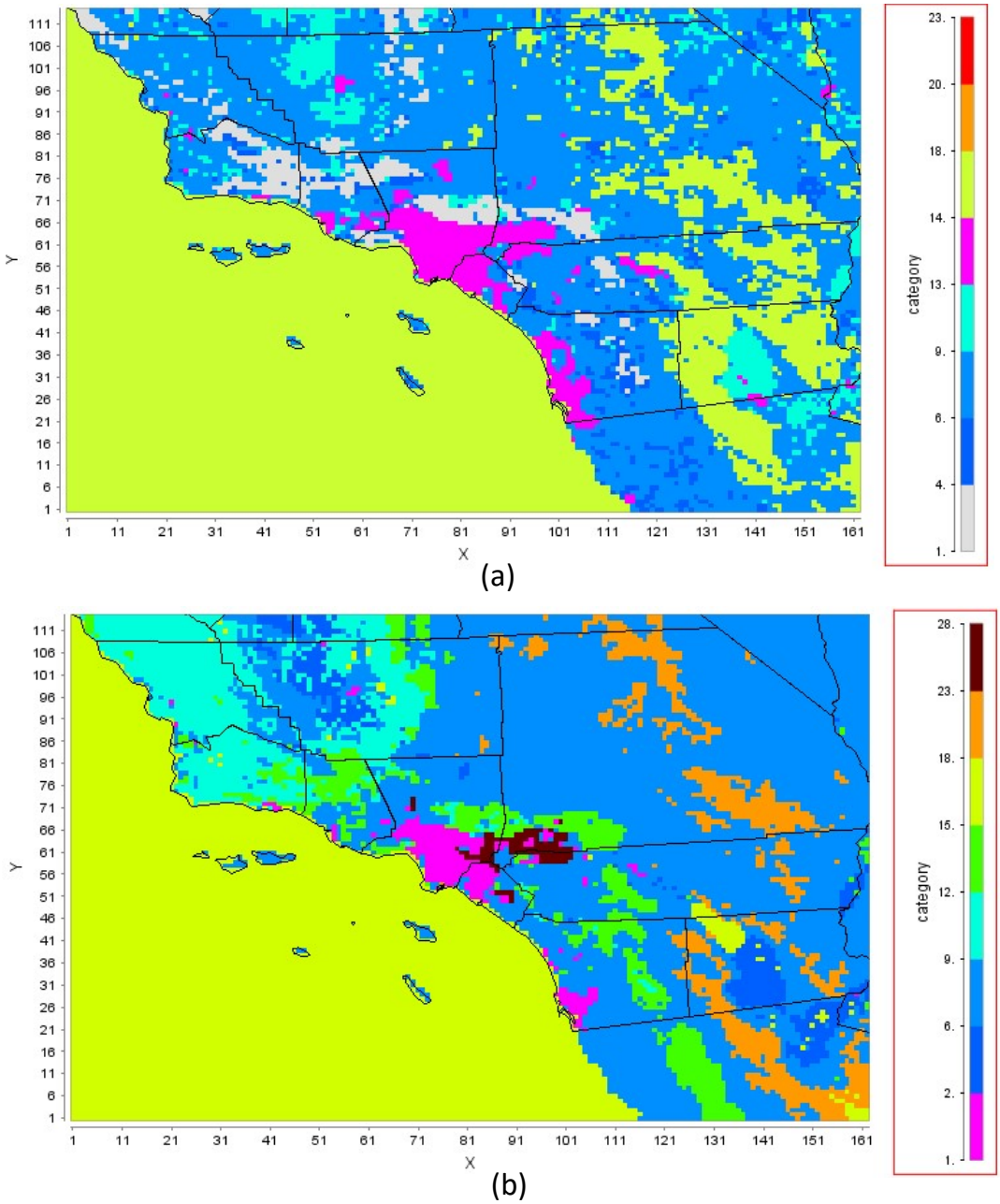

FIGURE V-3-13

Land Use categories for the WRF innermost domain. They are retrieved from (a) MODIS satellite based 20 categories, and (b) USGS land use with added Suburban category. The dark brown color represents the suburban category.

(a)

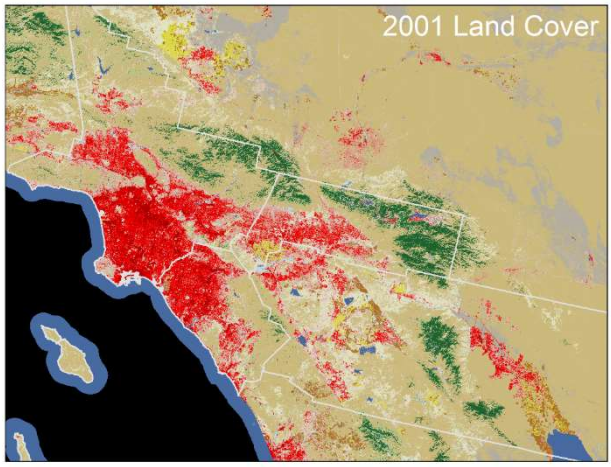

(b)

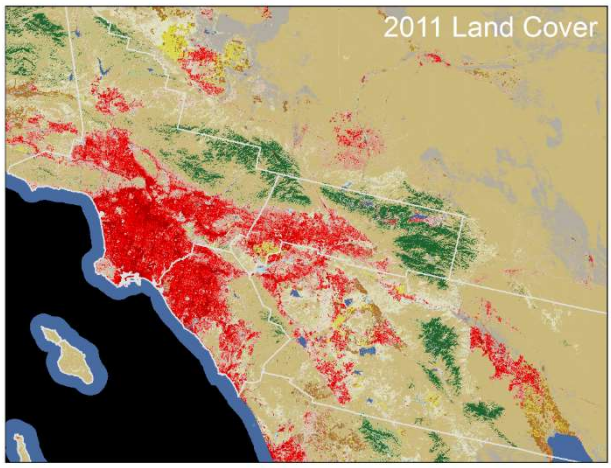

(c)

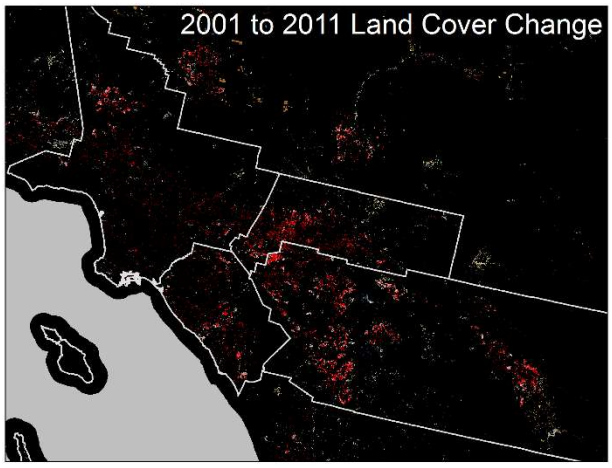

FIGURE V-3-14

Land Use Land Cover data for the South Coast Air Basin compiled for (a) 2001, (b) 2011, and (c) the difference between the two.

Sea Surface Temperature

Sea Surface Temperature (SST) is another critical factor that drives the land-sea breeze and up-slope/down-slope flow. The NAM analysis field, the initial guess field used for the current project, includes skin temperature, but not SST. The skin temperature is defined as the temperature of the interface between soil and the atmosphere that establishes radiative equilibrium. The skin temperature is identical to the SST over the sea. While the default approach in the NAM analysis field uses the skin temperature as SST, the satellite based SST is available in a high resolution real-time based format. The Global Data Assimilation Experiment (GODAE) provides 4-5 km grid resolution SST data as a part of High Resolution Sea Surface Temperature Pilot Project (GHRSST-PP). It was initiated to develop an operational system to produce a climate quality SST data product to serve the needs of GODAE and the wider scientific community. Every 6-hour SST data was acquired through GODAE FTP data hub. The SST was averaged for the month of August and compared with the skin temperature from the NAM analysis data. The SST shows large degree of variability in the domain (Figure V-3-15). But, in general the GODAE SST indicates warmer ocean waters south of Point Conception and colder waters along the shore of Ventura, Los Angeles, Orange and northern San Diego counties. The colder ocean during the daytime can result in an enhanced sea breeze. A grid cell near Catalina Island was treated as land in the NAM field, resulting in the hot spot near the Island. Note that SST is incorporated only for the ocean grid points; therefore, values over land were discarded.

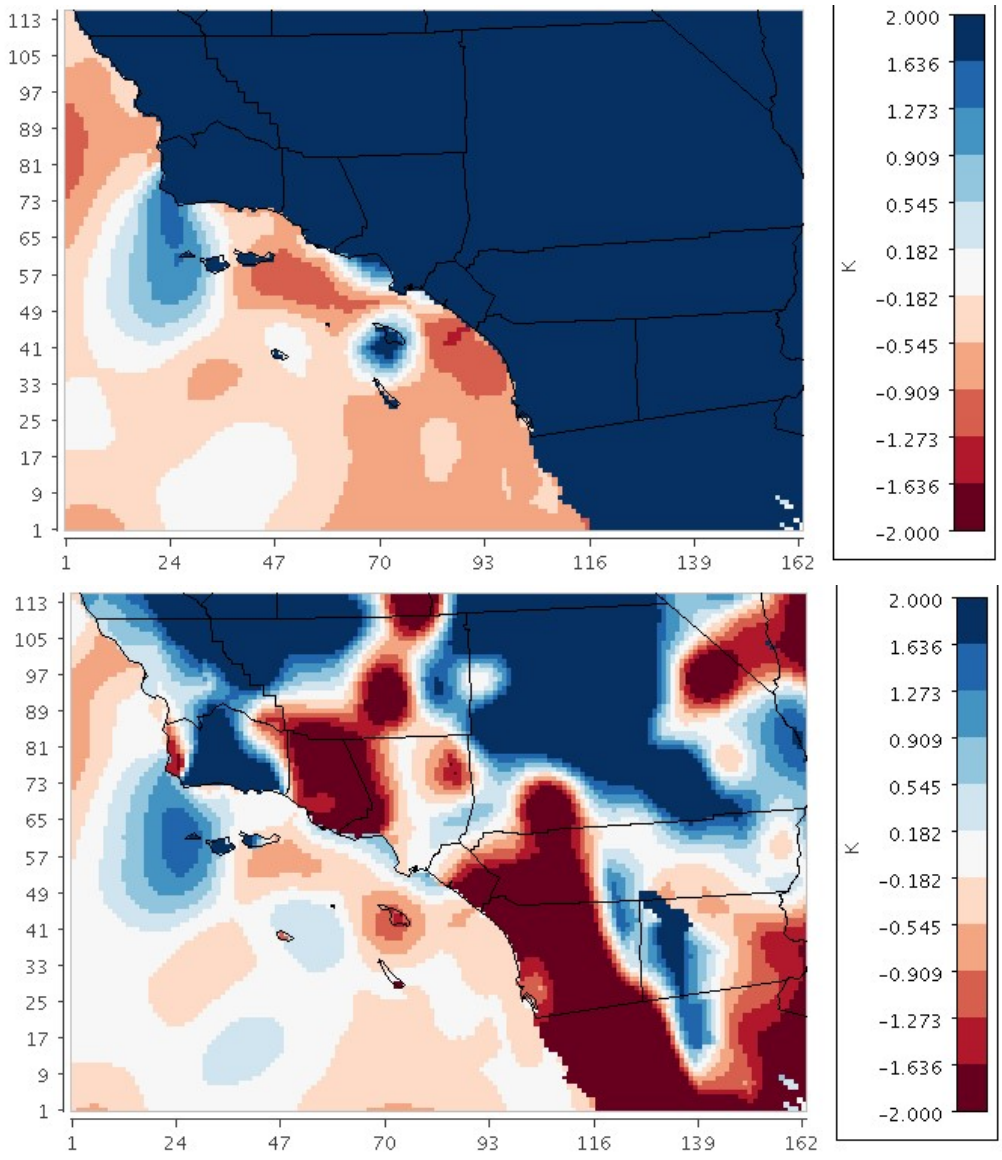

FIGURE V-3-15

The differences of Skin Temperature and Sea Surface Temperature (Skin Temperature – Sea Surface Temperature) composited for the month of August. The 0000 UTC and 1200 UTC fields are presented in the upper and lower panel, respectively.

Statistical Evaluation of the Sensitivity Tests

The sensitivity tests discussed above were evaluated using statistical measures to determine the optimum configuration for the Basin. The measurements used in this statistical evaluation were taken from NWS stations which were predominately located at airports. This is due to the assumption that an airport site

appropriately represents prevailing weather conditions with minimum interference of local obstructions. The stations used in the evaluation and their geographical locations are marked in Figure V-3-16. The 2 m temperature, water vapor mixing ratio and 10 m wind speed were selected for the evaluation based on the importance in simulated chemical reactions and transportation pattern. The following statistical measures were used in the evaluation:

Bias Error (B): calculated as the mean difference in prediction (*P*)-observation (*O*) pairings with valid data within a given analysis region and for a given time period (hourly or daily):

$$B = \frac{1}{IJ}\sum_{j=1}^{J}\sum_{i=1}^{I}\left(P_j^i - O_j^i\right)$$

Gross Error (E): calculated as the mean absolute difference in prediction-observation pairings with valid data within a given analysis region and for a given time period (hourly or daily):

$$E = \frac{1}{IJ}\sum_{j=1}^{J}\sum_{i=1}^{I}\left|P_j^i - O_j^i\right|$$

Root Mean Square Error (RMSE): calculated as the square root of the mean squared difference in prediction-observation pairings with valid data within a given analysis region and for a given time period (hourly or daily):

$$RMSE = \left[\frac{1}{IJ}\sum_{j=1}^{J}\sum_{i=1}^{I}\left(P_j^i - O_j^i\right)^2\right]^{1/2}.$$

The graphical presentation of the WRF performance evaluation for the ozone season, May 1st to September 30th 2012 is provided in Figures V-3-17 through Figure V-3-19. Four sets of simulations included in the comparison are 1) Thermal diffusion LSM with modified USGS land use, 2) NOAH LSM with default USGS land use, 3) NOAH with MODIS land use and GODAE SST, and lastly 4) NOAH with NARR initial guess field, MODIS land use and GODAE SST. All four simulations showed distinctive geographical dependency. Inland locations such as Riverside and San Bernardino show a larger degree of error than coastal stations. This appeared to be consistent with temperature, water vapor and wind predictions. NOAH LSM with MODIS land use and GODAE SST showed the least amount of errors in all the variables and locations. Between NAM and NARR, NAM best represented temperature, but predictions of wind speed were comparable between the two methods. The updated SST resulted in a better prediction of temperature, but not water vapor nor wind speed. The temperature gradient between sea and land drives local thermal circulation. However, while, the improved temperature fields were expected to lead to a better land-sea breeze wind prediction, improved performance was not evident in the simulations. This reflects the fact that wind is driven not only by thermal gradients but also other factors such as pressure gradients, Coriolis force, friction, and turbulent mixing. Therefore, temperature itself is not enough to improve the wind predictions. The sensitivity tests are summarized in Table V-3-3 as well. The table

includes all the three major LSMs – Thermal Diffusion, NOAH and PX schemes, sensitivity tests on land use and SST. While all the three LSMs showed advantages in a specific variable, the overall performance was similar. The MODIS land use did not show any improvement over the default USGS land use. However, the updated SST fields improved all four variables – wind speed, direction, temperature and water vapor in the Basin.

The sensitivity tests were extended to CMAQ in order to evaluate their impacts on chemical transport. Table V-3-4 summarizes the ozone statistics simulated with three different WRF fields (Thermal Diffusion, NOAH and P-X land surface schemes). The Thermal Diffusion scheme showed a tendency to over-predict ozone in the coastal areas and slightly under-predict ozone in the inland downstream areas. On the contrary, NOAH yielded smaller biases in the coastal regions but a larger degree of biases in the receptor areas. The performance of the PX scheme was in between the NOAH and Thermal Diffusion schemes. While all the schemes appeared to have strengths and weakness in certain geographical area, design sites are typically in the inland receptor region. Consequently, accurate predictions in the inland receptor region are more imperative than performance in the coastal or central LA basin. Therefore, the Thermal Diffusion scheme with the updated SST and modified USGS was selected as a default configuration.

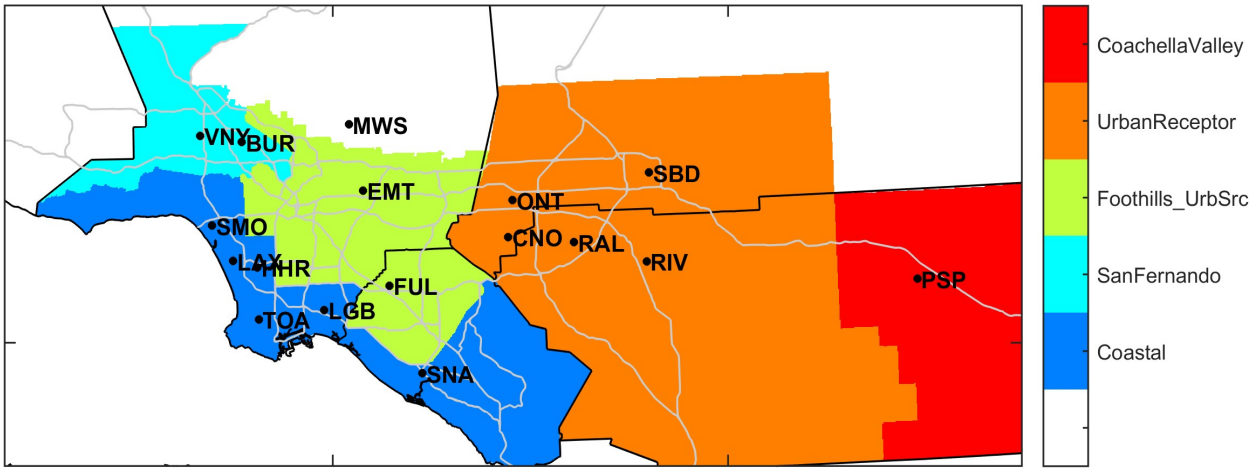

FIGURE V-3-16

Location of NWS stations used in the model performance evaluation and geographical zones

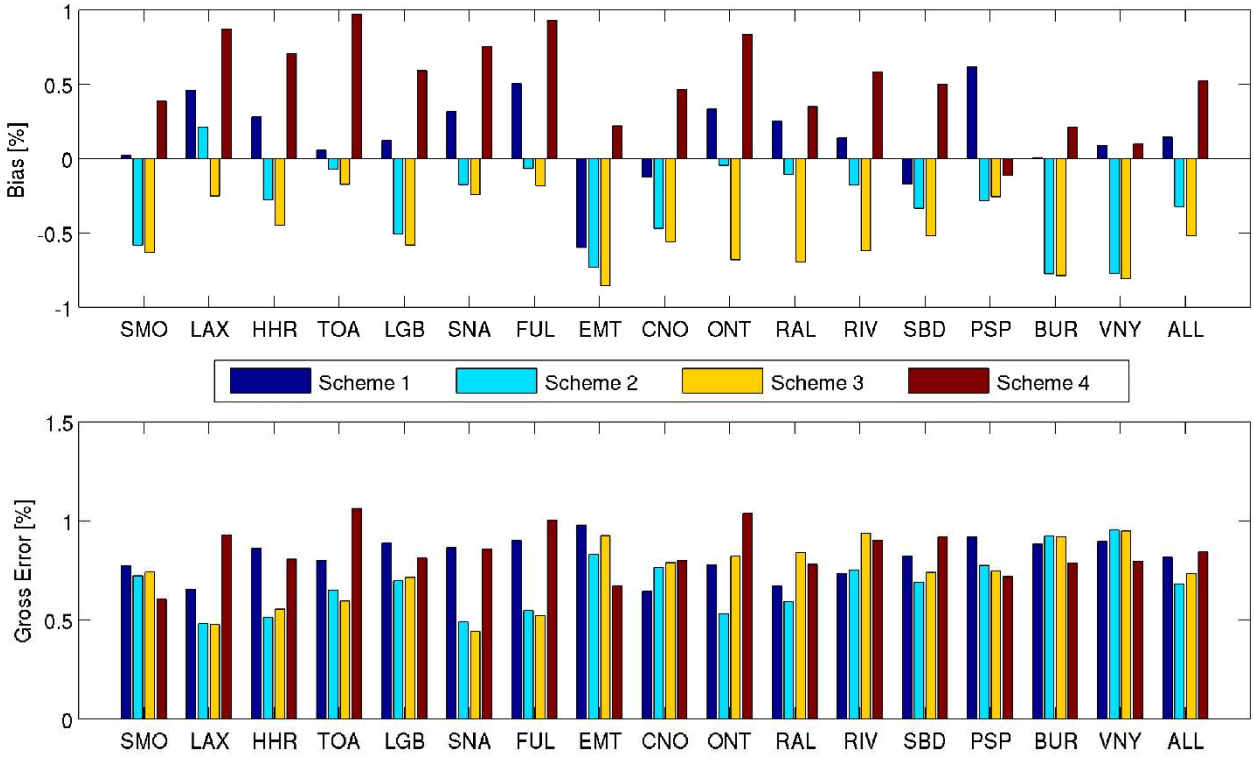

FIGURE V-3-17

Normalized Bias Error (upper panel) and Normalized Gross Error (lower panel) of temperature predictions at NWS airport monitor locations. They are averaged over the period of May 1st to September 30th, 2012. Scheme 1) Thermal diffusion LSM with modified USGS land use. Scheme 2) NOAH LSM with default USGS land use. Scheme 3) NOAH with MODIS land use and GODAE SST. Scheme 4) NOAH with NARR initial guess field, MODIS land use and GODAE SST.

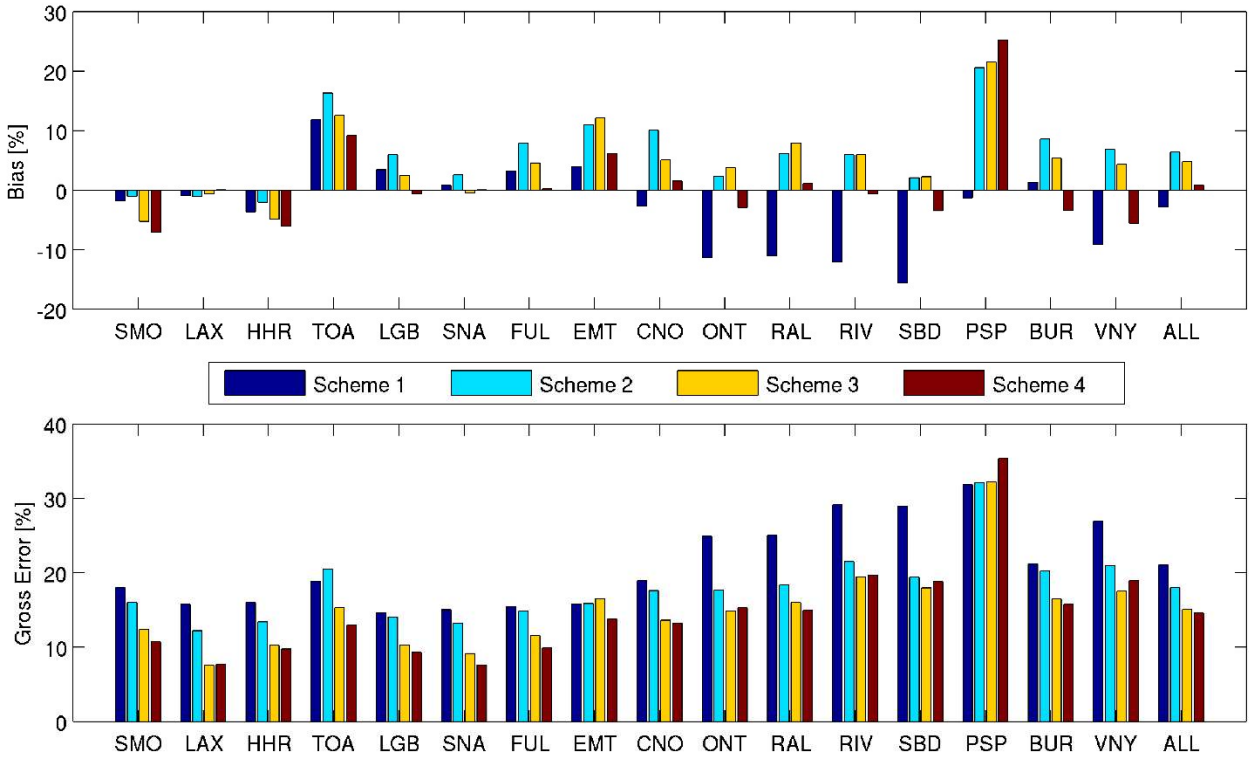

FIGURE V-3-18

Normalized Bias Error (upper panel) and Normalized Gross Error (lower panel) of water vapor mixing ratio predictions at NWS airport monitor locations. They are averaged over the period of May 1st to September 30th, 2012. Scheme 1) Thermal diffusion LSM with modified USGS land use. Scheme 2) NOAH LSM with default USGS land use. Scheme 3) NOAH with MODIS land use and GODAE SST. Scheme 4) NOAH with NARR initial guess field, MODIS land use and GODAE SST.

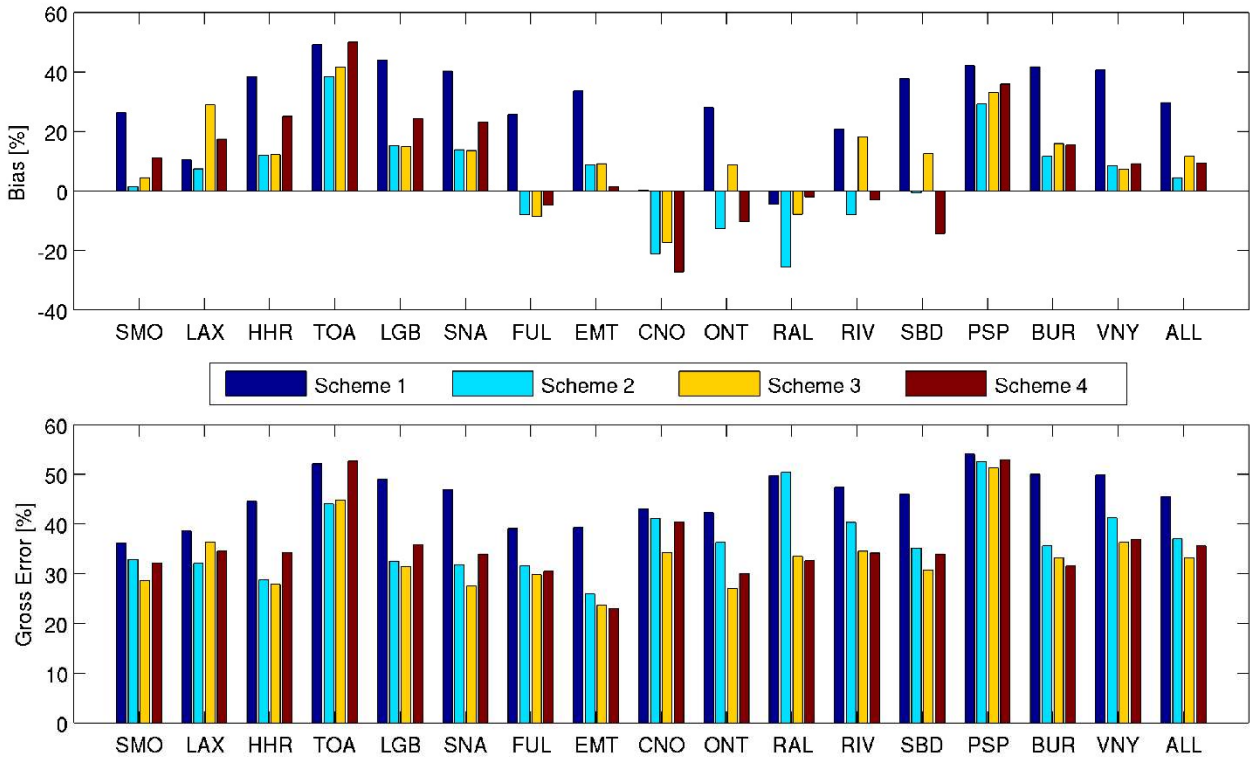

FIGURE V-3-19

Normalized Bias Error (upper panel) and Normalized Gross Error (lower panel) of surface wind speed predictions at NWS airport monitor locations. They are averaged over the period of May 1st to September 30th, 2012. Scheme 1) Thermal diffusion LSM with modified USGS land use. Scheme 2) NOAH LSM with default USGS land use. Scheme 3) NOAH with MODIS land use and GODAE SST. Scheme 4) NOAH with NARR initial guess field, MODIS land use and GODAE SST.

TABLE V-3-3

WRF performance statistics analyzed for the month of August 2012. Land Surface Schemes and Land use dataset and Sea Surface Temperature were included in the evaluation.

		Thermal Diffusion	NOAH	PX	NOAH_MODIS	NOAH_MODIS_SST	Thermal Diffusion_SST
Wind Speed [m/s]	Mean OBS	3.4	3.4	3.4	3.4	3.4	3.4
	Mean PRD	1.6	2.5	2.1	2.3	2.3	2.0
	Bias	1.3	0.4	0.8	0.6	0.6	1.0
	Gross Error	1.5	1.0	1.2	1.1	1.1	1.2
	RMSE	1.8	1.4	1.5	1.5	1.5	1.6
Temperature [K]	Mean OBS	299.2	299.2	299.2	299.2	299.2	299.2
	Mean PRD	299.0	299.6	298.9	300.1	300.3	298.9
	Bias	-0.2	-0.7	0	-1.2	-1.3	-0.1
	Gross Error	2.1	1.6	1.8	1.8	1.9	1.8
	RMSE	2.7	2.2	2.3	2.4	2.4	2.3
Humidity [kg/kg]	Mean OBS	10.9	10.9	10.9	10.9	10.9	10.9
	Mean PRD	11.7	10.6	11.6	10.5	10.8	12.1
	Bias	-0.7	0.4	-0.7	0.4	0.2	-1.2
	Gross Error	1.6	1.3	1.5	1.3	1.3	1.7
	RMSE	2.1	1.8	2.0	1.7	1.8	2.2

TABLE V-3-4

CMAQ simulated 1-hour ozone concentrations and Root Mean Square Errors using Thermal-Diffusion, NOAH and PX Land Surface Schemes. The statistics were analyzed for the month of August, 2012.

Stations	1-hour O3 Measurements	Thermal Diffusion		NOAH		PX	
		Average	RMSE	Average	RMSE	Average	RMSE
WSLA	51.1	69.5	25.8	63.4	19.0	67.3	24.4
LAXH	47.0	62.5	23.3	57.3	16.9	60.1	20.1
LGBH	45.9	63.8	25.5	55.6	15.5	61.1	21.8
CELA	58.2	68.0	20.0	61.2	12.4	66.6	17.9
CMPT	50.8	66.8	22.6	59.1	13.8	63.9	19.7
PICO	67.2	71.2	16.0	63.9	12.5	70.1	14.3
LAHB	61.6	73.9	19.7	66.3	11.0	72.1	17.2
POMA	85.2	83.0	17.0	74.4	17.2	80.5	15.6
PASA	76.9	73.7	15.6	66.8	16.5	74.0	15.5
BURK	81.3	75.5	18.8	69.9	19.6	74.5	20.0
RESE	83.1	78.0	16.1	72.4	19.4	75.8	19.5
SCLA	99.4	82.5	23.9	76.7	28.1	80.7	26.2
AZUS	84.4	79.4	17.7	70.5	20.4	78.0	15.9
GLEN	97.6	82.4	24.0	73.1	29.0	79.8	23.9
CSTA	46.6	63.7	24.6	56.5	14.8	60.8	20.1
ANAH	52.0	70.1	24.3	61.6	14.9	67.1	21.5
MSVJ	61.7	73.6	20.4	64.1	14.4	71.1	18.6
RIVR	94.3	89.2	18.3	82.1	20.2	86.7	16.8
MRLM	92.2	89.5	17.4	81.7	19.5	88.4	15.0
PERI	85.9	79.9	20.4	82.5	14.4	83.3	16.2
ELSI	77.0	77.9	13.7	78.3	14.2	81.7	12.8
UPLA	99.9	86.0	23.5	75.6	29.5	82.2	24.0
FONT	102.6	88.5	24.2	78.2	30.2	85.2	23.5
SNBO	96.8	90.2	17.3	80.1	21.6	83.2	19.3
RDLD	97.6	85.4	19.4	80.5	22.8	82.5	21.1
CRES	98.3	90.1	18.4	79.8	22.7	83.9	20.3
BNAP	80.2	72.2	18.0	71.7	13.7	70.7	16.4
PLSP	74.2	61.8	16.5	64.6	14.5	62.9	16.4
INDI	59.5	61.5	8.6	60.6	8.4	61.8	9.5

Overall Performance Evaluation

The overall performance of WRF simulations used as transport fields for the CMAQ modelling is provided in Figure V-3-20 through Figure V-3-22. The Basin is divided into five zones based on geographical location and emission source-receptor characteristics (Figure V-3-16). They are listed below:

- Coastal zone including inland Orange County
- Foothills and Urban Source zone that covers heavy traffic urban center and its surrounding foothill areas
- Urban Receptor zone that covers most of inland Riverside and San Bernardino areas
- San Fernando Valley
- Coachella Valley

Performance was evaluated for each month in each zone for the entire year of 2012. Temperature, water vapor mixing ratio, and wind speed were evaluated in terms of Normalized Gross Bias and Normalized Gross Error. Temperature and water vapor predictions are more accurate in the summer season than the winter months. Wind speed deviations did not show a strong seasonal variation. Geographically, winds are predicted most accurately at the inland urban receptor sites. Accurate wind predictions in this region of elevated ozone concentrations is one of the most critical factors to simulate chemical transport. Hourly predictions compared against measurements at two selected locations are provided in Figure V-3-23 and Figure V-3-24. Diurnal variation of temperature, humidity and surface wind are well represented by WRF.

Overall, the daily WRF simulation for 2012 provided representative meteorological fields that well characterized the observed conditions. These fields were used directly in the CMAQ joint particulate and ozone simulations.

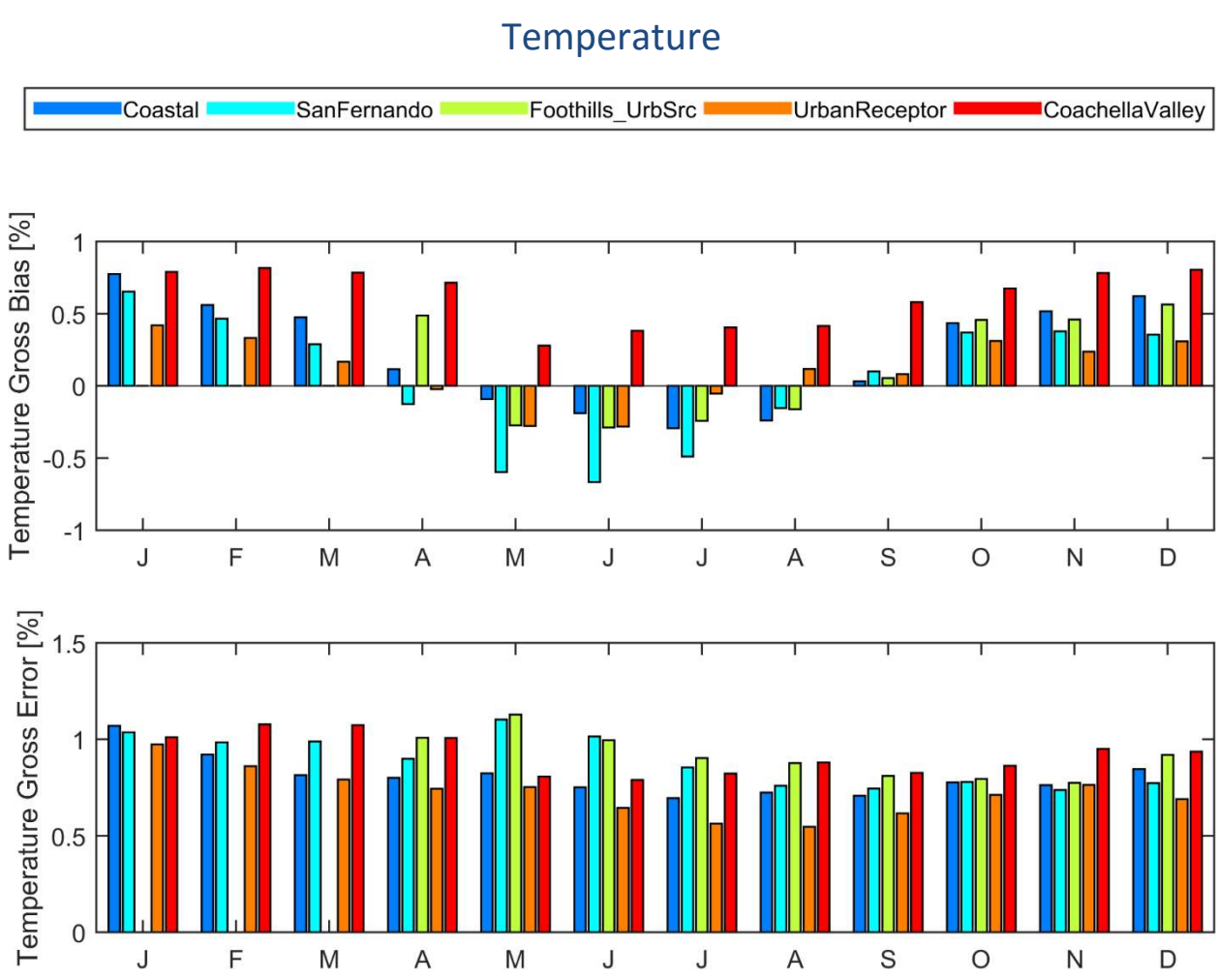

FIGURE V-3-20

Monthly Averaged Normalized Gross Bias and Normalized Gross Error of WRF predicted temperatures at each geographical zone. Missing regional monthly data indicate that more than 50percent of the measurements are not available.

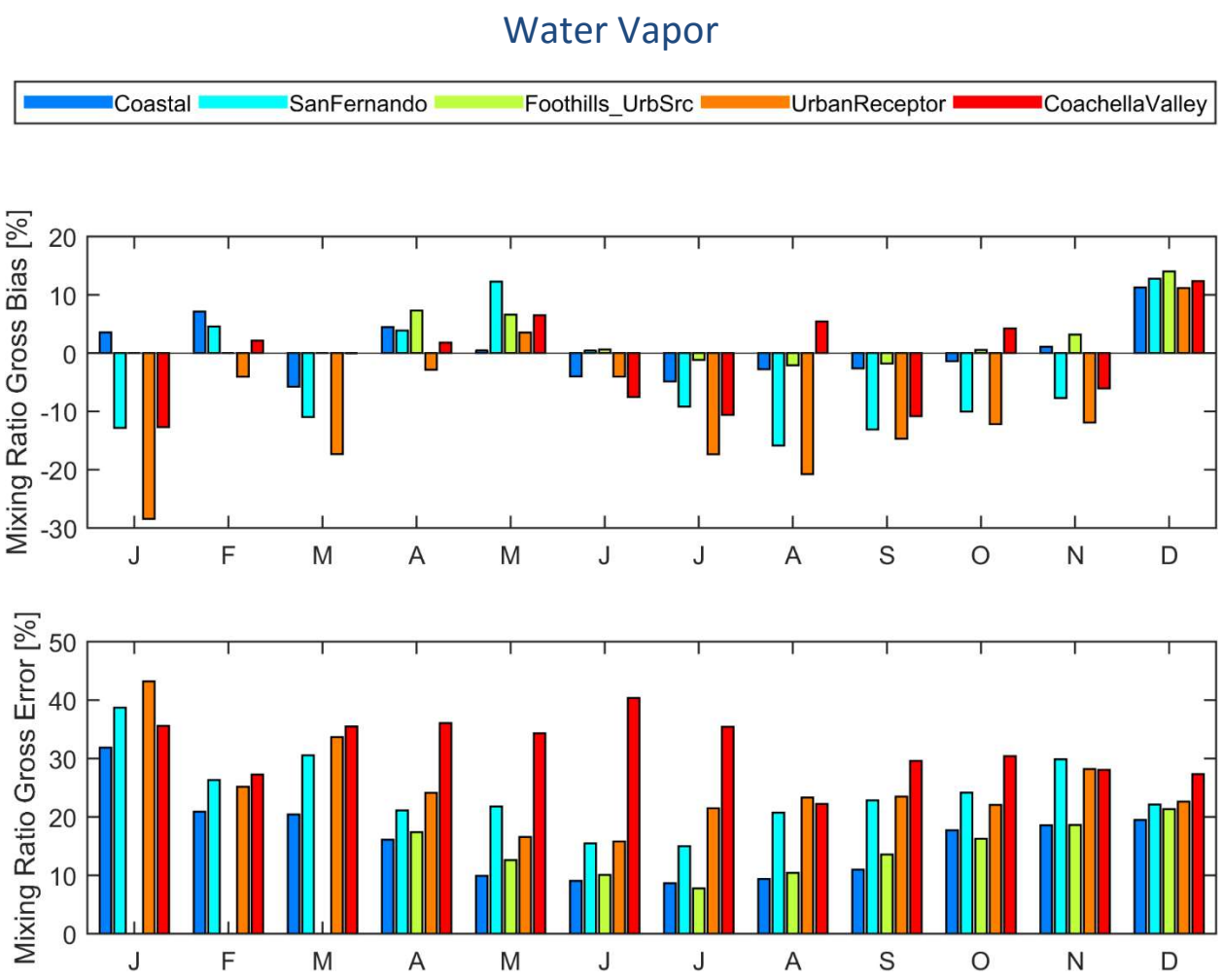

FIGURE V-3-21

Monthly Averaged Normalized Gross Bias and Normalized Gross Error of WRF predicted water vapor mixing ratio at each geographical zone. Missing regional monthly data indicate that more than 50percent of the measurements are not available.

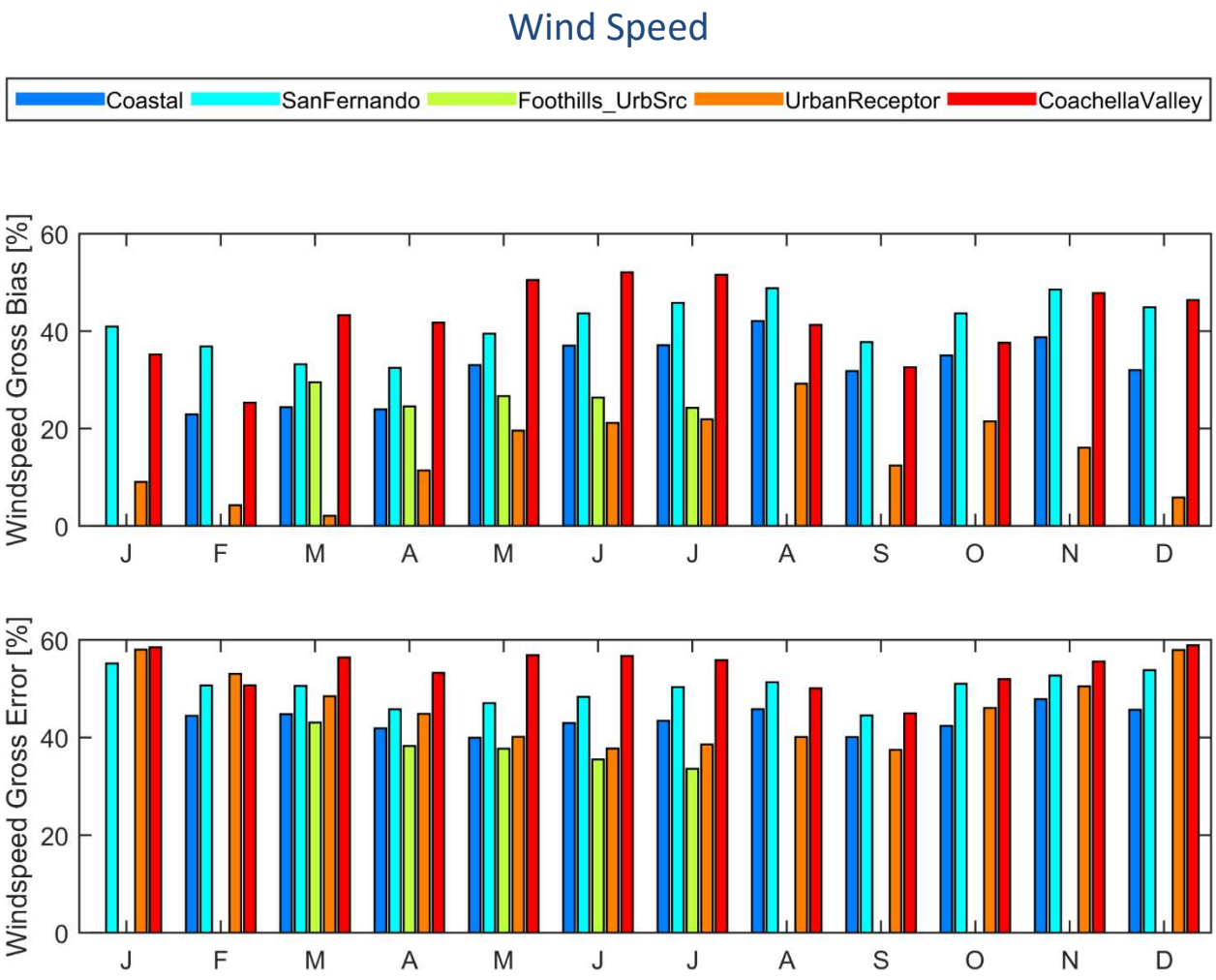

FIGURE V-3-22

Monthly Averaged Normalized Gross Bias and Normalized Gross Error of WRF predicted wind speed at each geographical zone. Missing regional monthly data indicate that more than 50percent of the measurements are not available.

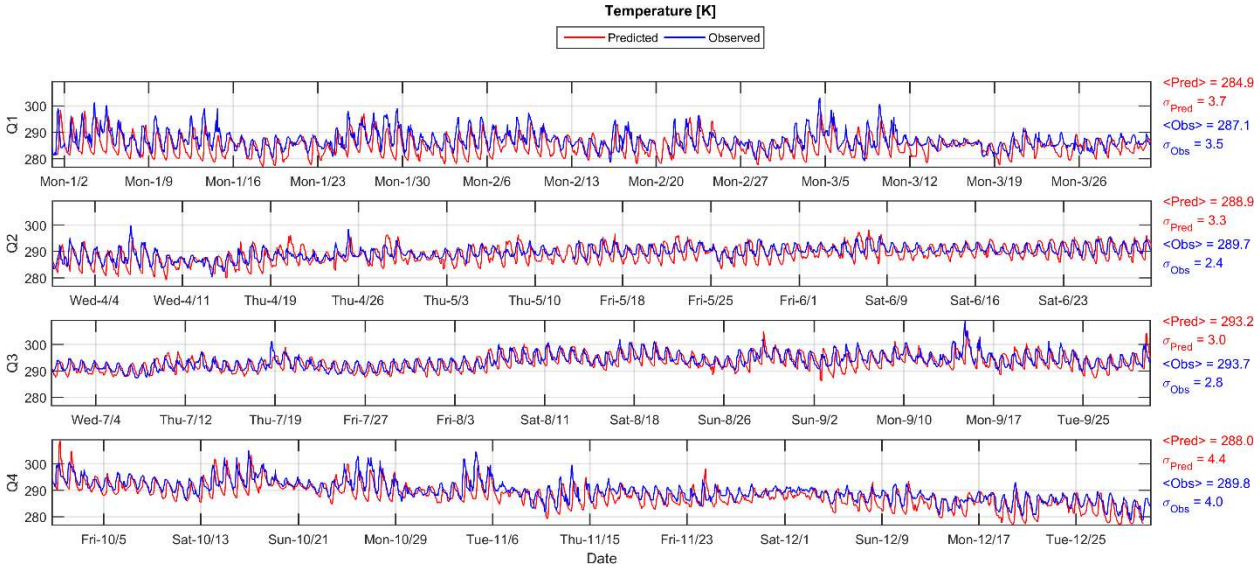
Temperature [K]
Predicted
Observed
Q1
Q2
Q3
Q4
300
290
280
<Pred> = 284.9
σPred = 3.7
<Obs> = 287.1
σObs = 3.5
<Pred> = 288.9
σPred = 3.3
<Obs> = 289.7
σObs = 2.4
<Pred> = 293.2
σPred = 3.0
<Obs> = 293.7
σObs = 2.8
<Pred> = 288.0
σPred = 4.4
<Obs> = 289.8
σObs = 4.0
Mon-1/2
Mon-1/9
Mon-1/16
Mon-1/23
Mon-1/30
Mon-2/6
Mon-2/13
Mon-2/20
Mon-2/27
Mon-3/5
Mon-3/12
Mon-3/19
Mon-3/26
Wed-4/4
Wed-4/11
Thu-4/19
Thu-4/26
Thu-5/3
Thu-5/10
Fri-5/18
Fri-5/25
Fri-6/1
Sat-6/9
Sat-6/16
Sat-6/23
Wed-7/4
Thu-7/12
Thu-7/19
Fri-7/27
Fri-8/3
Sat-8/11
Sat-8/18
Sun-8/26
Sun-9/2
Mon-9/10
Mon-9/17
Tue-9/25
Fri-10/5
Sat-10/13
Sun-10/21
Mon-10/29
Tue-11/6
Thu-11/15
Fri-11/23
Sat-12/1
Sun-12/9
Mon-12/17
Tue-12/25
Date

(a)


Mixing Ratio [g/kg]
Predicted
Observed
Q1
Q2
Q3
Q4
15
10
5
<Pred> = 5.7
σPred = 1.7
<Obs> = 5.9
σObs = 1.9
<Pred> = 8.8
σPred = 1.8
<Obs> = 8.9
σObs = 1.6
<Pred> = 12.0
σPred = 1.2
<Obs> = 11.7
σObs = 1.2
<Pred> = 7.9
σPred = 2.7
<Obs> = 8.5
σObs = 2.8
Mon-1/2
Mon-1/9
Mon-1/16
Mon-1/23
Mon-1/30
Mon-2/6
Mon-2/13
Mon-2/20
Mon-2/27
Mon-3/5
Mon-3/12
Mon-3/19
Mon-3/26
Wed-4/4
Wed-4/11
Thu-4/19
Thu-4/26
Thu-5/3
Thu-5/10
Fri-5/18
Fri-5/25
Fri-6/1
Sat-6/9
Sat-6/16
Sat-6/23
Wed-7/4
Thu-7/12
Thu-7/19
Fri-7/27
Fri-8/3
Sat-8/11
Sat-8/18
Sun-8/26
Sun-9/2
Mon-9/10
Mon-9/17
Tue-9/25
Fri-10/5
Sat-10/13
Sun-10/21
Mon-10/29
Tue-11/6
Thu-11/15
Fri-11/23
Sat-12/1
Sun-12/9
Mon-12/17
Tue-12/25
Date

(b)

(c)

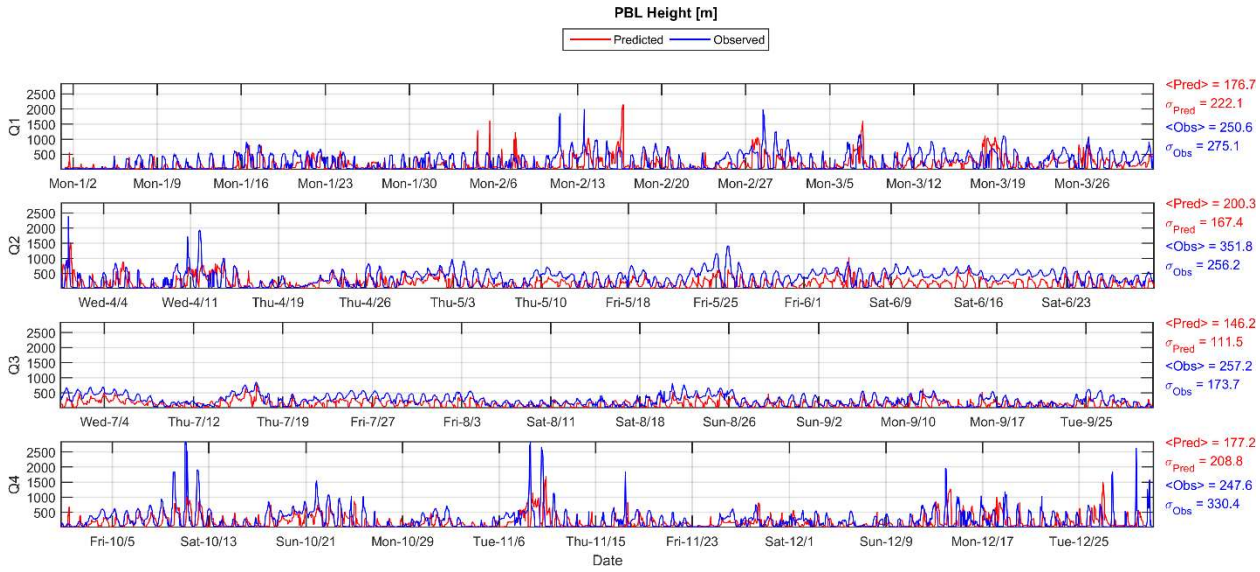

(d)

FIGURE V-3-23

Times Series of Measured and WRF simulated (a) Temperature, (b) Water Vapor Mixing Ratio, (c) Wind Speed and (d) PBL depth at Los Angeles international airport for the period of Jan 1st to December 31st, 2012. Measurements are presented in blue and Model predictions are in red.

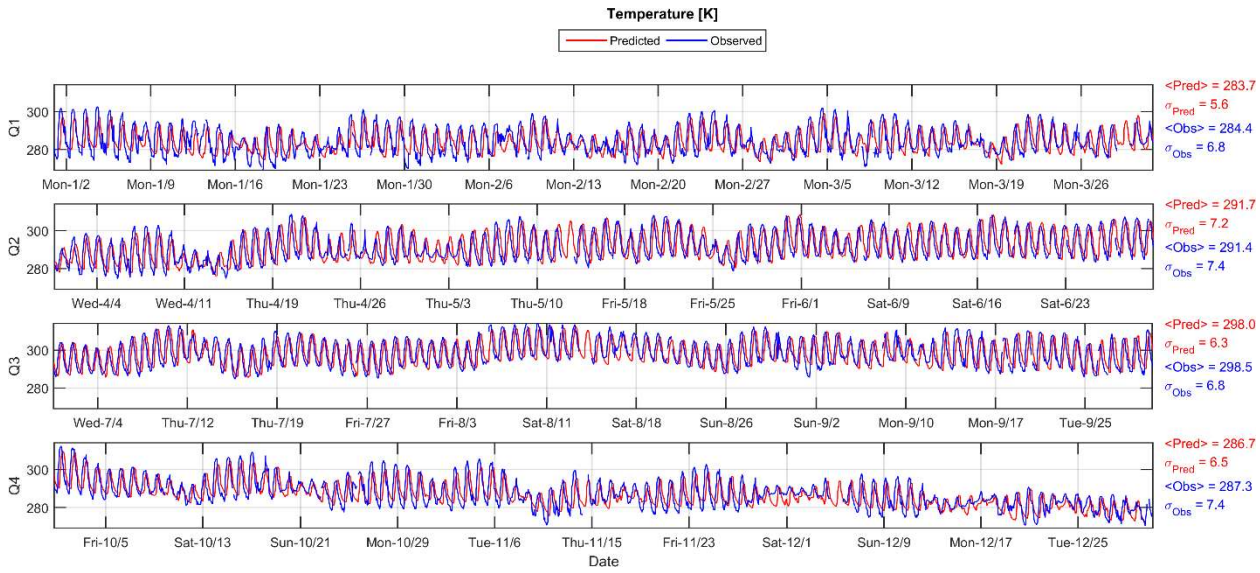
Temperature [K]
Predicted
Observed
Q1
Q2
Q3
Q4
300
280
<Pred> = 283.7
σPred = 5.6
<Obs> = 284.4
σObs = 6.8
<Pred> = 291.7
σPred = 7.2
<Obs> = 291.4
σObs = 7.4
<Pred> = 298.0
σPred = 6.3
<Obs> = 298.5
σObs = 6.8
<Pred> = 286.7
σPred = 6.5
<Obs> = 287.3
σObs = 7.4
Mon-1/2
Mon-1/9
Mon-1/16
Mon-1/23
Mon-1/30
Mon-2/6
Mon-2/13
Mon-2/20
Mon-2/27
Mon-3/5
Mon-3/12
Mon-3/19
Mon-3/26
Wed-4/4
Wed-4/11
Thu-4/19
Thu-4/26
Thu-5/3
Thu-5/10
Fri-5/18
Fri-5/25
Fri-6/1
Sat-6/9
Sat-6/16
Sat-6/23
Wed-7/4
Thu-7/12
Thu-7/19
Fri-7/27
Fri-8/3
Sat-8/11
Sat-8/18
Sun-8/26
Sun-9/2
Mon-9/10
Mon-9/17
Tue-9/25
Fri-10/5
Sat-10/13
Sun-10/21
Mon-10/29
Tue-11/6
Thu-11/15
Fri-11/23
Sat-12/1
Sun-12/9
Mon-12/17
Tue-12/25
Date

(a)

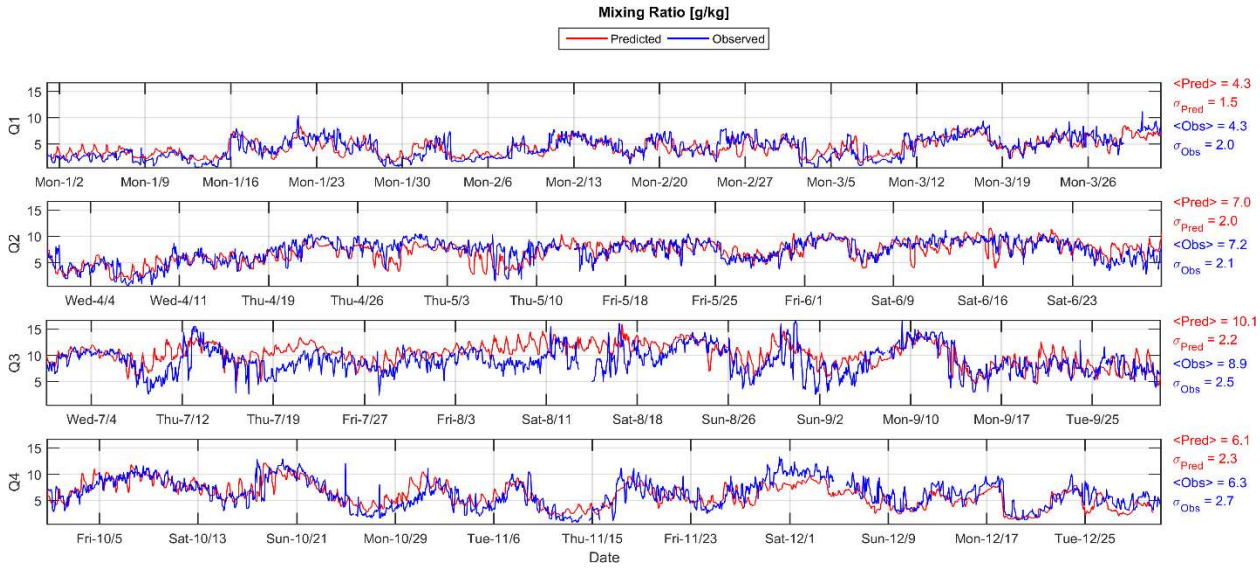
Mixing Ratio [g/kg]
Predicted
Observed
Q1
Q2
Q3
Q4
15
10
5
<Pred> = 4.3
σPred = 1.5
<Obs> = 4.3
σObs = 2.0
<Pred> = 7.0
σPred = 2.0
<Obs> = 7.2
σObs = 2.1
<Pred> = 10.1
σPred = 2.2
<Obs> = 8.9
σObs = 2.5
<Pred> = 6.1
σPred = 2.3
<Obs> = 6.3
σObs = 2.7
Mon-1/2
Mon-1/9
Mon-1/16
Mon-1/23
Mon-1/30
Mon-2/6
Mon-2/13
Mon-2/20
Mon-2/27
Mon-3/5
Mon-3/12
Mon-3/19
Mon-3/26
Wed-4/4
Wed-4/11
Thu-4/19
Thu-4/26
Thu-5/3
Thu-5/10
Fri-5/18
Fri-5/25
Fri-6/1
Sat-6/9
Sat-6/16
Sat-6/23
Wed-7/4
Thu-7/12
Thu-7/19
Fri-7/27
Fri-8/3
Sat-8/11
Sat-8/18
Sun-8/26
Sun-9/2
Mon-9/10
Mon-9/17
Tue-9/25
Fri-10/5
Sat-10/13
Sun-10/21
Mon-10/29
Tue-11/6
Thu-11/15
Fri-11/23
Sat-12/1
Sun-12/9
Mon-12/17
Tue-12/25
Date

(b)

(c)

FIGURE V-3-24

Times Series of Measured and WRF simulated (a) Temperature, (b) Water Vapor Mixing Ratio, and (c) Wind Speed at March Air Force Base for the period of Jan 1st to December 31st, 2012. Measurements are presented in blue and Model predictions are in red.

References

Angevine, W.M., L. Eddington, K. Durkee, C. Fairall, L. Bianco and J. Brioude, 2012: Meteorological Model Evaluation for CalNex 2010, Monthly Weather Review, 140, 3885-3906

Noilan, J., and S. Planton, 1989: A simple parameterization of land surface processes for meteorological models. Mon. Wea. Rev., 117, 536-549.

Pleim, J. E., and A. Xiu, 1995: Development and testing of a surface flux and planetary boundary layer model for application in mesoscale models. J. Appl. Meteor., 34, 16-32.

Xiu, Aijun, and J. E. Pleim, 2001: Development of a Land Surface Model. Part I: Application in a Mesoscale Meteorological Model. J. Appl. Meteor., 40, 192–209.

Pleim, J. E., and A. Xiu, 2003: Development of a land surface model. Part II: Data assimilation. J. Appl. Meteor., 42, 1811-1822.

CHAPTER 4

MODELING EMISSIONS, BOUNDARY CONDITIONS, AND INITIAL CONDITIONS

Modeling Emissions Inventory

Table V-4-1 provides the baseline and controlled modeling emissions inventories used in the attainment demonstration and alternative analyses. The CMAQ simulations were based on the annual average inventory, with adjustments made for source-specific temporal profiles and daily temperature variations. A brief characterization of the annual day emissions used for the modeling analysis follows. An extensive discussion of the overall emissions inventory is summarized in Appendix III.

Inventory Profile

Baseline modeling inventories for the historical year 2012 and the future years 2017, 2018, 2019, 2020, 2021, 2022, 2023, 2025, 2026, 2031 and 2037 are discussed in this section. The baseline emissions projection assumes no emission controls beyond already adopted measures and rules. These projections reflect the emissions resulting from increases in population and vehicle miles traveled (VMT), as well as the implementation of all adopted rules and regulations. The cut-off date for the District's regulations is December 2015 and for CARB's regulations is November 2015. The controlled emission projections reflect the benefits of implementation of the 2016 AQMP control measures relative to future baseline emissions. Detailed descriptions of the control measures are provided in Chapter 4 and Appendix IV of the 2016 AQMP.

Appendix III contains emission summary reports by source category for the historical base year and future baseline scenarios used in this modeling analysis. Attachments 2 and 3 of this appendix contain the Controlled Emission Projection Algorithm (CEPA) emissions summary report by source category for the future (2022, 2023, 2025 and 2031) controlled scenarios. Day specific point, mobile and area emissions inventories were generated for each day in the 2012 base year. On-road mobile source emissions were generated based on information from SCAG transportation modeling, ARB EMFAC2014 emissions rates, observed daily traffic variations and modeled daily temperatures. A more detailed description on generating on-road modeling emissions follows. County-wide area source and off-road source emissions were gridded using the spatial emissions surrogate profiles developed for the 2016 AQMP.

TABLE V-4-1

Annual Average Day and Planning Anthropogenic Emissions Inventory (tons/day)

	Annual Average						Summer Planning		Winter Planning	
Year	VOC	NOX	CO	SOX	PM2.5	NH3	PVOC	PNOX	PCO	PNO2
(a) Baseline										
2012	470	540	2123	18	66	81	500	522	2053	530
2017	392	398	1590	17	64	76	416	390	1532	390
2018	382	373	1506	17	64	75	405	366	1450	366
2019	376	353	1447	17	64	74	398	347	1392	347
2020	370	330	1394	17	64	73	391	325	1339	324
2021	365	309	1357	17	64	73	386	305	1303	304
2022	362	290	1325	17	64	73	383	287	1271	286
2023	359	257	1298	17	64	72	379	255	1245	253
2025	353	241	1247	17	64	72	372	239	1194	237
2026	352	234	1232	17	64	72	370	233	1180	231
2031	345	214	1188	18	65	73	362	214	1139	211
(b) Controlled[1]										
2022	352	268	1238	17	62	73	371	265	1189	263
2023	307	143	822	17	64	72	319	141	807	143
2025	341	214	1136	17	64	72	358	213	1089	211
2031	284	96	666	18	62	73	294	96	651	95

[1]Reflecting SCAG's 2016 RTP/SCS

Gridded day-specific on-road emissions

On-road mobile sources are responsible for a large fraction of the total VOC, NOx, and CO emissions in the modeling domain. These emission sources are highly dependent on time and location with variations up to a factor of 8 between overnight and peak traffic hours at a specific location. On-road mobile emission patterns vary significantly throughout the week and year. This variation may also be location-dependent as emissions are a function of the proximity to high-employment areas, sporting events, or seasonal activities.

In past AQMPs, the temporal variation of on-road mobile emissions was purely a function of the day of the week. The total emissions in each grid cell was determined with SCAG transportation modeling outputs on traffic volumes and speeds along with EMFAC emission rates. Traffic emissions were apportioned hourly by a day-of-week throughput profile consisting of a Sunday, Monday, Tuesday-Thursday, Friday, and Saturday schedule. A light-duty and heavy-duty vehicle throughput profile was used to apportion emissions for each vehicle class independently. The same day-of-week throughput profiles were applied to each grid cell in each county in the modelling domain. The peak emissions occur mid-week (Tuesday through Thursday) while emissions on Saturday and Sunday decreased by about 30 percent, primarily due to a reduction in truck traffic during the weekend.

For the 2016 AQMP modelling, real-time traffic flow measurements from 2012 were used to apportion traffic volumes on an hourly basis throughout the five counties, Ventura, Los Angeles, Orange, Riverside and San Bernardino, in the center of the modelling domain. Light- and heavy-duty vehicle flow data is location dependent and accounts for special events, holidays, seasonality, and meteorologically-driven traffic profiles. Due to of the sparsity of monitoring data in the five outlying counties, San Luis Obispo, Santa Barbara, Kern, Imperial and San Diego, grid-based on-road emissions in those counties were created with the traditional approach.

Methodology

The CalTrans Performance Measurement System (PeMS) data was used to simulate light-duty vehicle emissions from 2012. Data from over 9,000 traffic monitoring stations were processed to generate traffic profiles for each hour of 2012 as a function of location. FIGURE V-4-1 details the location of each PeMS monitoring station. Vehicle flow measurements were normalized by the annual average traffic flow at that particular location.

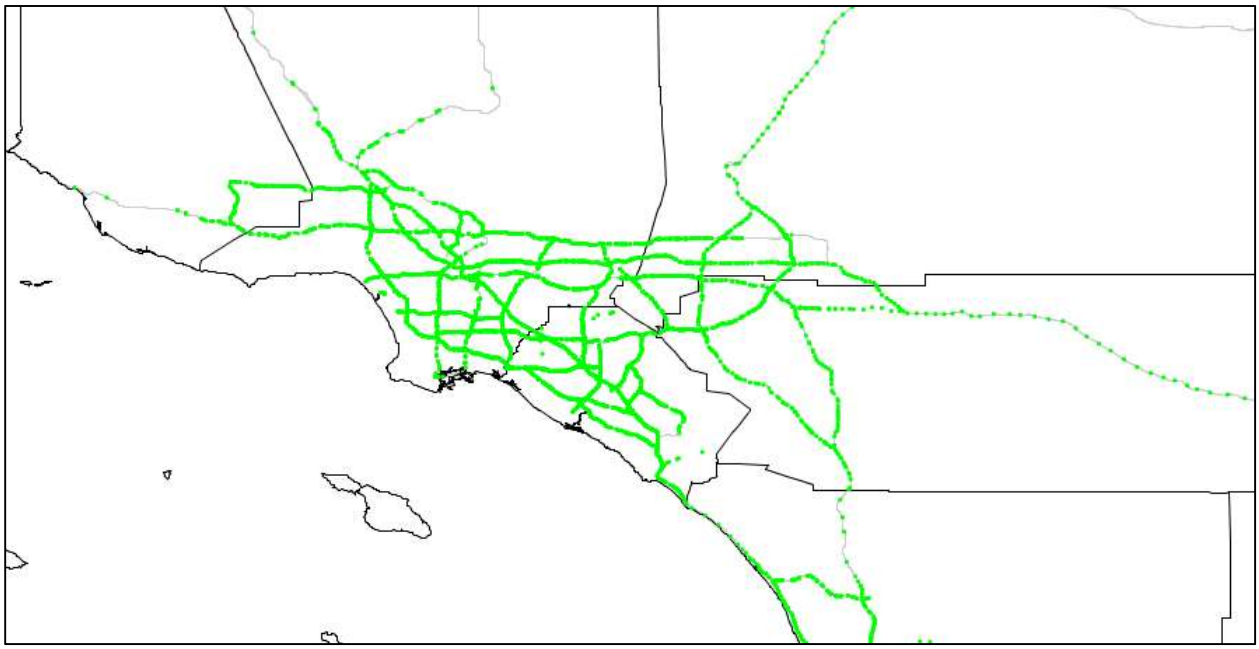

FIGURE V-4-1

Location of PeMS traffic monitoring station. Each monitoring station is noted with a green dot. Monitoring stations typically had sensors in each lane of traffic travelling in one direction.

Caltrans PeMS Weight-In-Motion (WIM) data was used to model the flow profiles of heavy-duty vehicles. While it was only possible to use 11 WIM stations in the modelling domain, heavy-duty vehicles tend to make longer distance trips than light-duty vehicles, allowing for reasonable projections of flow profiles over longer distances. Since heavy-duty vehicles are classified by weight, the WIM data could partitioned between heavy-heavy-duty, medium-heavy-duty, and light-heavy-duty vehicle flow. These flow profiles are extrapolated along routes that were expected to share similar characteristics such as direction of travel and/or proximity to shipping hubs. Figure V-4-2 illustrates the locations of each of the 11 WIM stations and the routes assumed to share the same flow characteristics. Flow profiles at each WIM station were normalized by the yearly average vehicle flow.

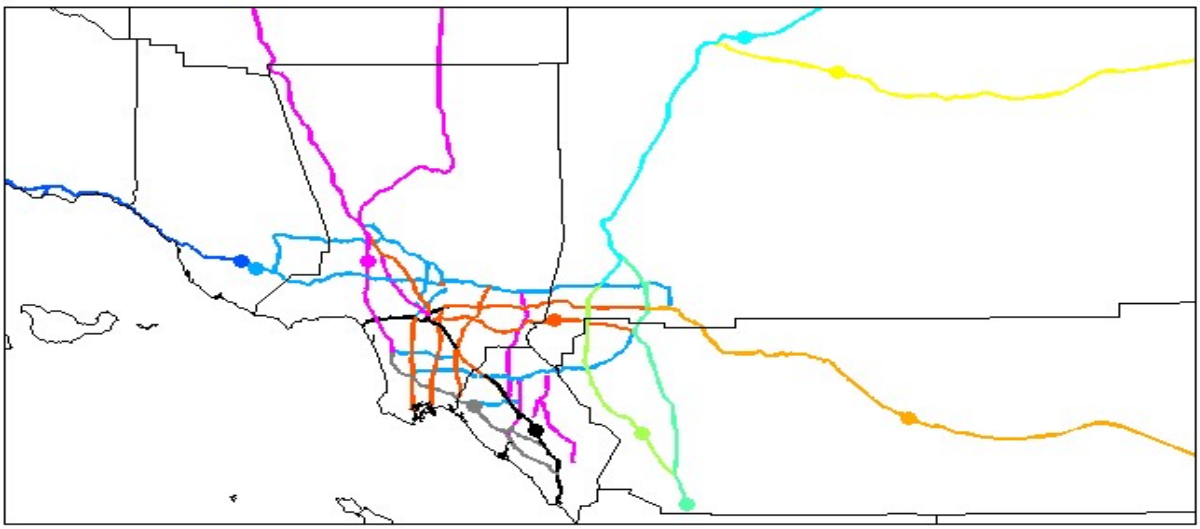

FIGURE V-4- 2

Locations of WIM sensors and corresponding routes assumed to share flow characteristics. Sensors are illustrated with colored dots. Major freeways are colored to indicate the WIM sensor used to represent their heavy-duty vehicle flow profile.

Normalized light- and heavy-duty (light-heavy-duty, medium-heavy-duty, and heavy-heavy-duty) traffic profiles were gridded into the 4km x 4km modelling grid. An inverse-distance-squared weighted interpolation was used to fill in grid cells without traffic sensors. FIGURE V-4-3 and Figure V-4-4 show the spatial dependence of normalized traffic profiles at two specific times in 2012: Wednesday July 4th (a holiday) at 5:00 PM and Wednesday July 11th at 5:00 PM, respectively. 2012 traffic links were assigned a yearly flow profile based on the grid cell that the center of the link occupies. The yearly flow profile determined from 2012 measurement data was applied to projected link locations in future years as well.

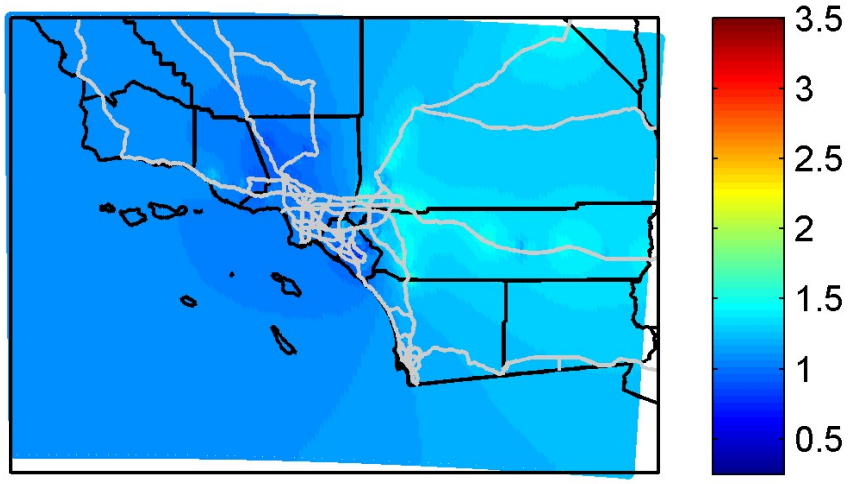

FIGURE V-4-3

Normalized light-duty vehicle flow on Wednesday, July 4th 2012 at 5:00 PM

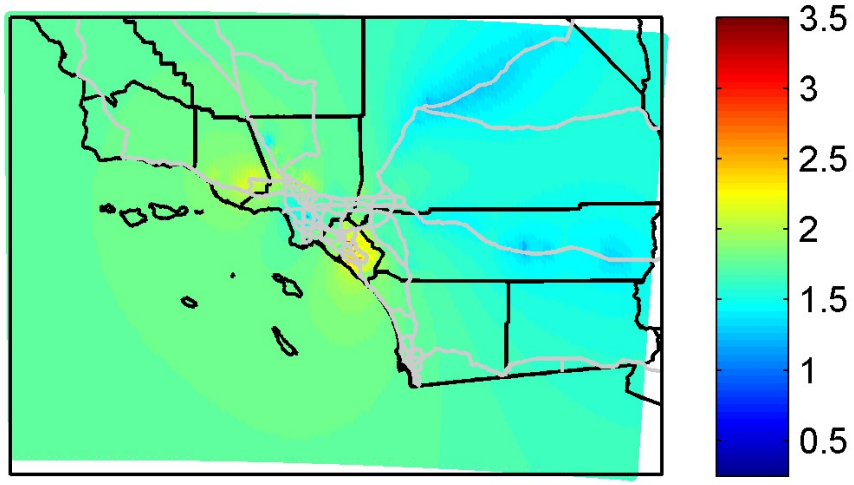

FIGURE V-4-4

Normalized light-duty vehicle flow on Wednesday, July 11th 2012 at 5:00 PM

As shown in Figure V-4-5, the resulting daily total SCAB on-road emissions vary significantly. The variations are primarily due to day of week and major holidays. The daily changes in atmospheric conditions and traffic volumes in addition to day of week also affected the emissions. The seasonal changes in fuel blends also contributed to lower levels of NOx emissions in summer, especially in on-road mobile section.

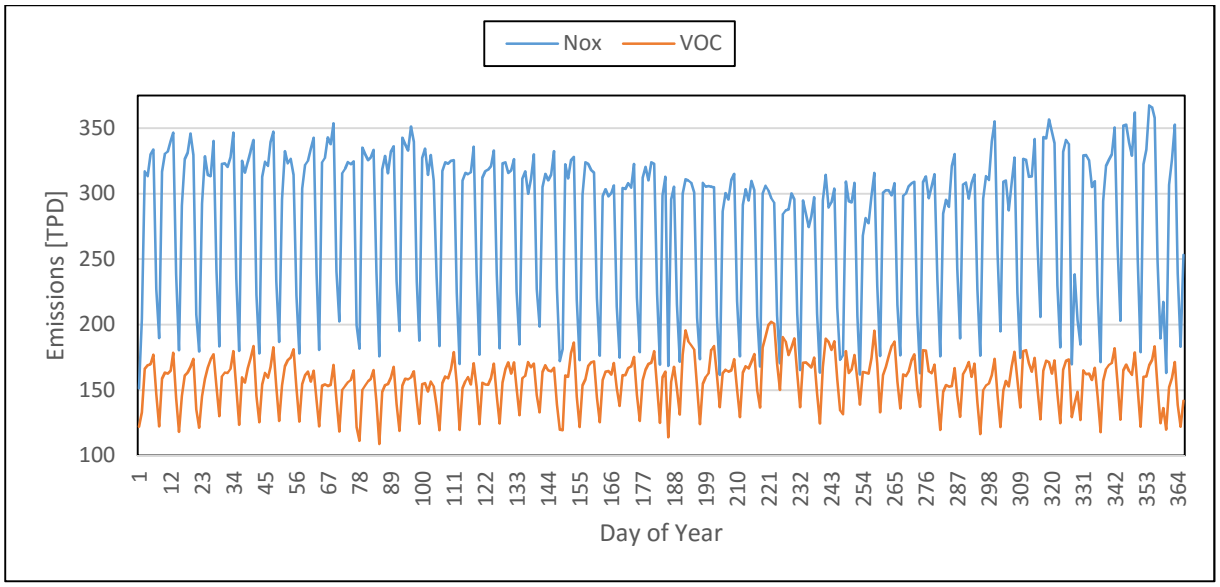

FIGURE V-4-5

2012 daily On-Road NOx and VOC emissions in the SCAB.

Annual Emissions Profiles

Day specific emissions were generated for all days in 2012. Figure V-4-6 illustrates the total CO and NOx emissions contained in the modeling domain for each day in 2012. CO emissions are indicative of the on-road mobile source inventory while NOx further incorporates signatures of stationary and off-road emissions. Note that the emissions totals in tons per day are roughly double the totals presented in Table V-4-1. This is because the values in Table V-4-1 represent basin-wide total emissions while those in Figure V-4-6 comprise totals from the entire modeling domain. The profile clearly depicts a changing emissions pattern with two distinct cycles represented: a weekly cycle, illustrated by Sunday through Saturday peaks and valleys, and day-to-day variations in emissions within the weekly cycle. Although not included in Figure V-4-6, spatially and temporally resolved emissions from wild and prescribed fires were also included in the emissions in the modeling domain.

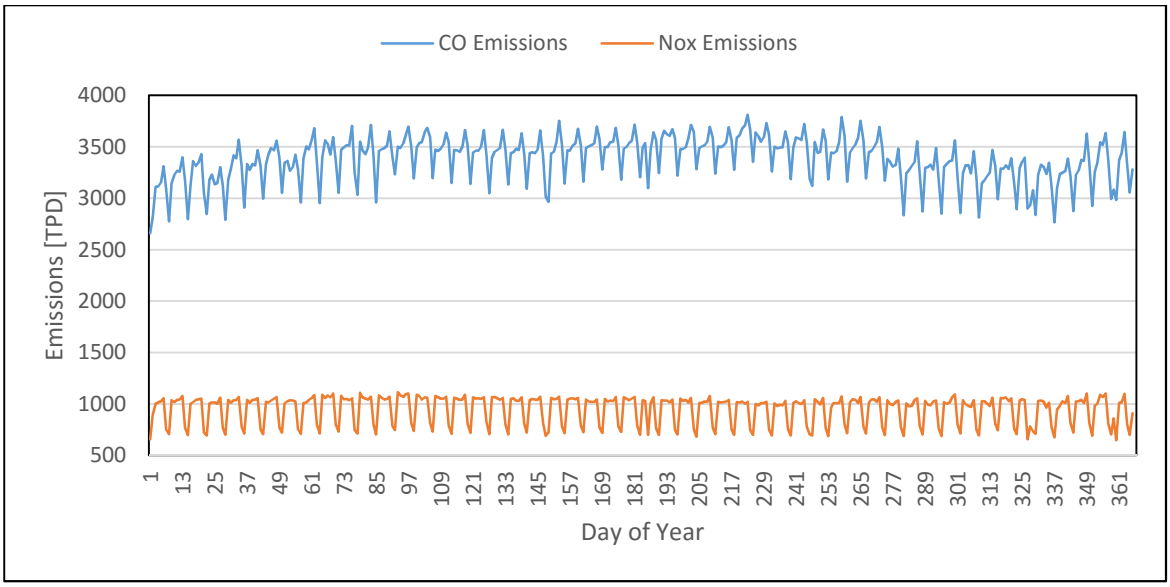

FIGURE V-4-6

2012 daily CO and NOx emissions in the modeling domain.

Diurnal Emissions Profiles

Where applicable, point, area and off-road mobile sources were adjusted to a day-of-week throughput profile consisting of a Monday-Friday, Saturday and Sunday schedule. Figure V-4-7 depicts the day-of-week and hour-of-day NOx emissions patterns for stationary, on-road, and off-road sources with ocean going vessels (OGVs) independently represented. The peak emissions occur mid-week (Tuesday through Thursday) while emissions on Saturday and Sunday decrease by about 30 percent. Based on CALTRANS data, NOx emissions from heavy-duty vehicles are reduced by more than 60 percent on Saturdays with further reductions occurring on Sundays. Increases in off-road mobile source activities (e.g. pleasure craft and recreational vehicles) account for the bulk of the VOC increase on both Saturdays and Sundays.

Monday and Friday are transitional days with on-road emissions slightly lower than mid-week with slightly modified diurnal profiles. Off-road emissions are relatively consistent throughout the week whereby weekend reductions in some off-road categories (e.g. construction) are replaced by weekend activity emissions (e.g. recreational vehicles and boats). In general, OGV emissions are constant with shipping activities ongoing as a function of arrivals and departures. The largest stationary source contributions (e.g. refineries, power generation and residential combustion) represent daily usage and do not vary much over the course of the week.

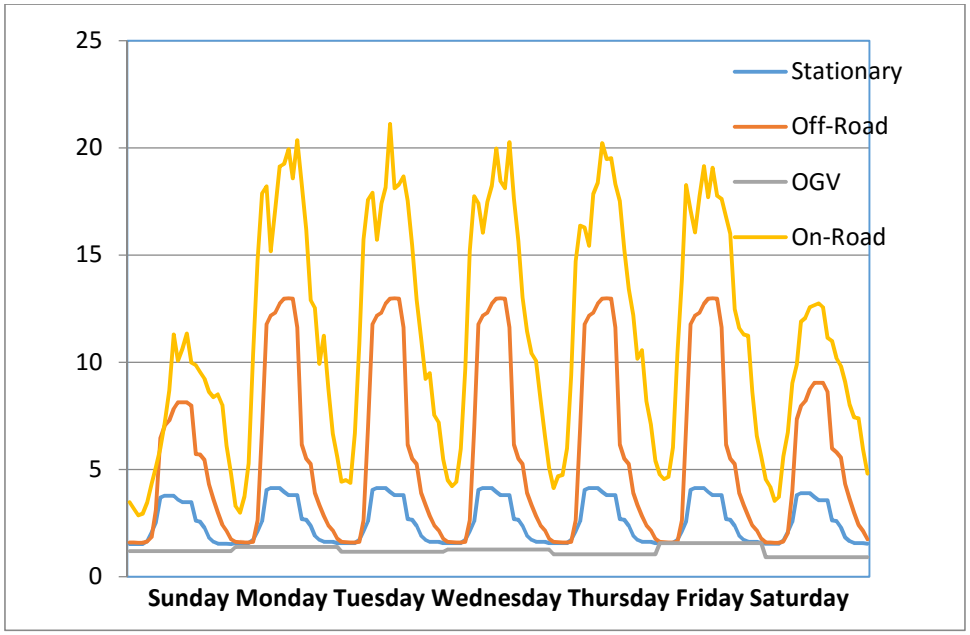

FIGURE V-4-7

Diurnal NOx emissions (tons per hour) in the SCAB: Sunday - Saturday.

Spatial Distribution

Figures V-4-8 through V-4-11 provide the spatial distribution of NOx emissions for the stationary (including area sources), OGV, off-road, on-road and total anthropogenic categories. Area and off-road sources in the modeling domain are typically assigned to a surrogate distribution profile (maintained by CARB) to allocate the daily emissions. Area source NOx emissions are included in the stationary source projection depicted in Figure V-4-8.

Over 90 spatial gridding surrogates were used in distributing area and off-road source emissions. The surrogates were developed and accumulated over the last twenty years and undergo some revisions during each AQMP development process. As in past AQMPs base and future year socioeconomic data, information such as population, employment and housing, developed by SCAG during its 2016 RTP/SCS process, were incorporated in the surrogates. Notable revisions in gridding surrogates during this AQMP include changes in surrogates for recreational boats and off-road equipment.

Paved and Unpaved Road Dust Emissions

U.S. EPA recently revised its AP-42 methodology to estimate paved road dust whereby the new method removed the factor addressing tire and brake wear (to address potential double counting) but retained a California usage profile and adjustments for rain and silt loading (CARB, 2013).

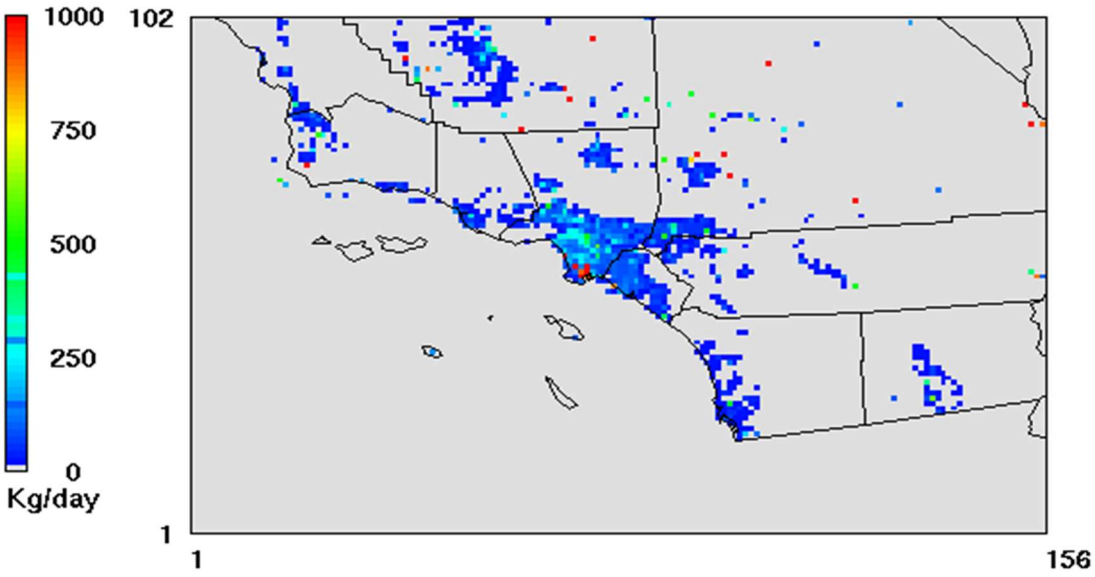

FIGURE V-4-8

Stationary source NOx emissions (Kg per day) in the modeling domain

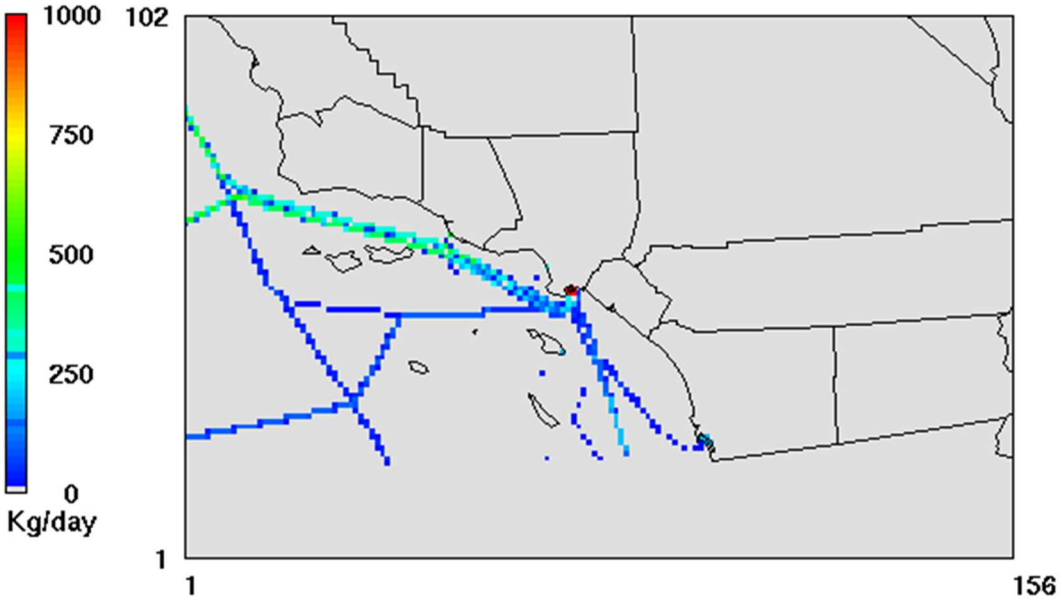

FIGURE V-4-9

OGV NOx emissions (Kg per day) in the modeling domain

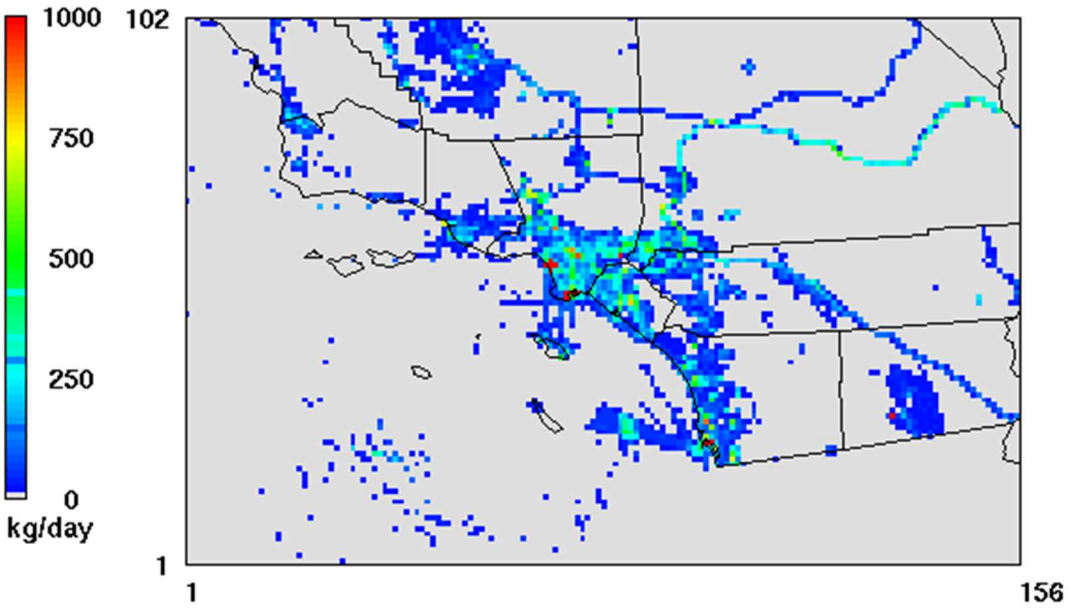

FIGURE V-4-10

Off-Road NOx emissions (Kg per day) in the modeling domain

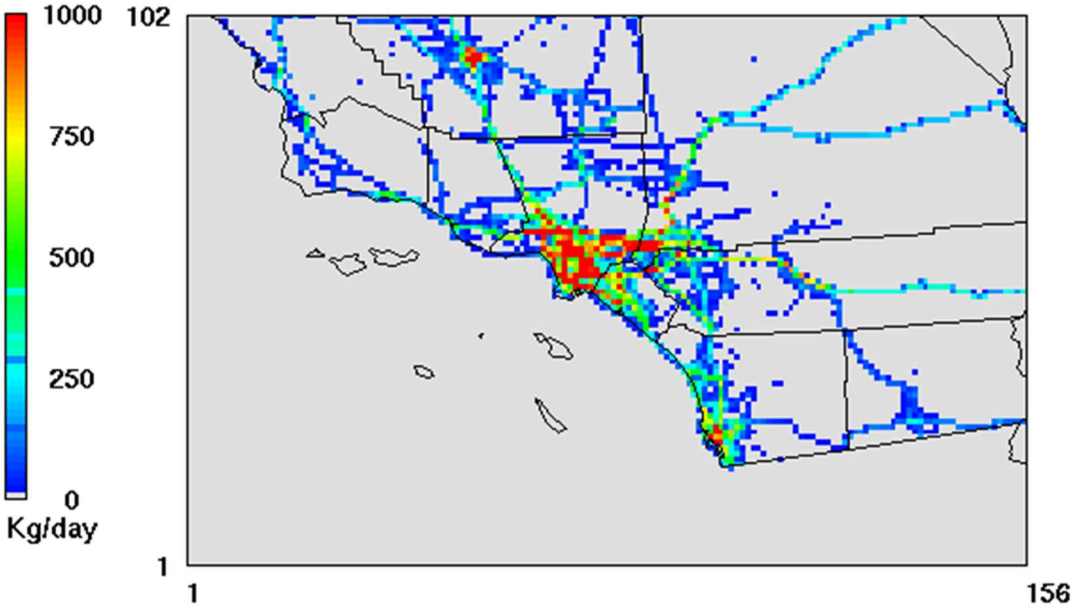

FIGURE V-4-11

On-Road NOx emissions (Kg per day) in the modeling domain

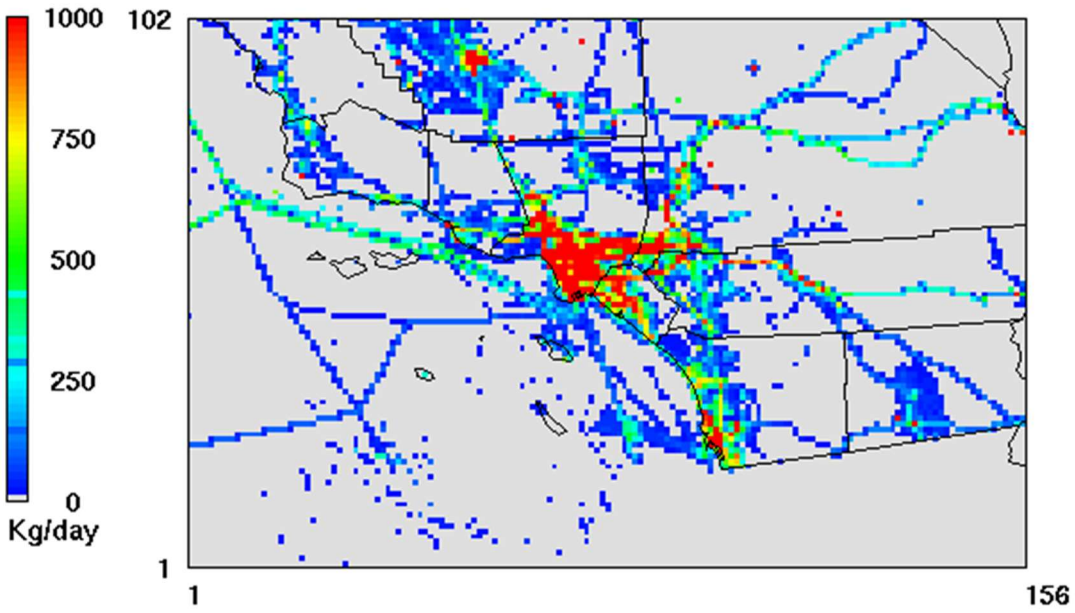

FIGURE V-4-12

Total Anthropogenic NOx emissions (Kg per day) in the modeling domain

In addition, the base year paved road dust emissions are a function of VMT. In the four preceding AQMPs, paved road dust emissions were adjusted to reflect a cap on emissions growth for high VMT road types in future years. The adjustment was made by leaving paved road dust constant on freeways unless there was a change in centerline miles. The US EPA expressed a preference in using the same methodology when calculating base and future emissions. For the current AQMP analysis, future year road dust emissions were projected based on SCAG future year VMT. Daily road dust emissions were adjusted according to countywide precipitation in 2012. Unpaved road dust was allocated based on GIS land use profiles.

Ammonia Inventory Adjustments

Selected revisions were made to the spatial distribution and emissions categories for the ammonia inventory. In general, the total ammonia in the inventory was reduced from 119 TPD in the 2007 AQMP inventory, 109 TPD in the 2012 AQMP to the 81 TPD in current AQMP. The reduction of ammonia emissions was primarily due to the continuation of decreasing livestock operations in the SCAB. Table V-4-2 provides a summary comparison of the 2002, 2008 and 2012 ammonia inventories from the 2007 AQMP, the 2012 AQMP and the current 2016 AQMP.

TABLE V-4-2

Annual average day ammonia emissions inventory (tons/day)

Source Category	2007 AQMP	Final 2012 AQMP	2016 AQMP
	2002 Inventory	2008 Inventory	2012 Inventory
Livestock	26	18.6	12.7
Soil*	1.4	1.8	1.8
Domestic	25.1	25.1	25.1
Landfill	1.1	3.6	3.8
Composting	9.7	17.8	1.0
Fertilizer	6.1	1.5	1.4
Sewage Treatment	0.1	0.2	0.2
Wood Combustion		0.1	0.2
Industrial	13.2	20.2	18.9
On-Road Mobile	36.1	19.9	18.1
Off-Road Mobile		0.1	0.1
Total	118.8	108.9	82.9

*Not anthropogenic

Biogenic Emissions

Daily biogenic VOC emissions inventories were developed by CARB using the Model of Emissions of Gases and Aerosols from Nature (MEGAN) emissions model. The biogenic inventories were calibrated based on spatially resolved hourly temperature from WRF modeling. Figure V-4-13 provides the daily total emissions of biogenic VOC, in TPD, in the SCAB. The trend shows higher emissions for the spring and summer months with several peaks occurring in May, July and August when temperatures were elevated.

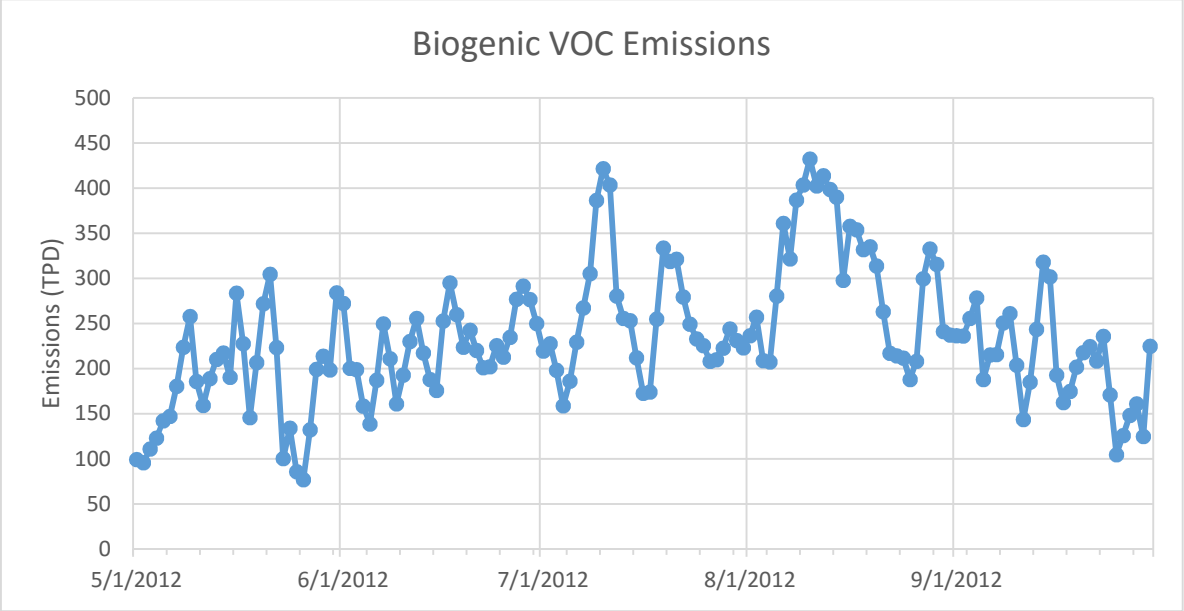

FIGURE V-4-13

2012 daily biogenic VOC emissions in the Basin.

Ocean Going Vessels

The information on daily vessel arrivals and departures was provided by the ports of Long Beach and Los Angeles. Factors were developed to capture the day-to-day variation in emissions. Figure V-4-14 depicts the vessel weighted adjustment factors throughout 2012. The factor ranges from 0.73 to 1.33. The daily OGV emissions were obtained by applying the adjustment factor to the annual average day OGV emissions. Although the adjustment factors were developed based on the information from the ports of Los Angeles and Long Beach, the factors were applied to OGV emissions throughout the modeling domain.

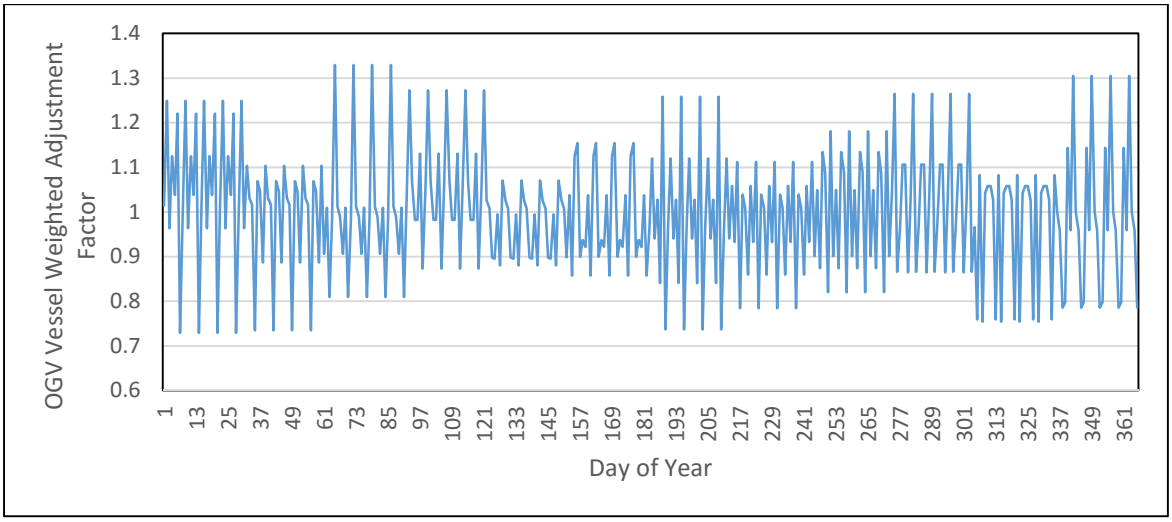

FIGURE V-4-14

2012 daily vessel weighted OGV SOx emissions in the modeling domain

Recreational Boats

Recreational boat emissions were assigned spatially to lakes and coastal waters and temporally to weekends and weekdays based on an analysis of 173 images of harbors and lakes throughout the SoCAB. In total, approximately 2500 boats were counted, measured, and categorized from high-resolution aerial images. Approximately 1000 boats were counted from aerial lower-resolution images. 20 lakes and 7 coastal areas were investigated. Only images captured after 2001 were used for the analysis. Spatial surrogates were developed from these data to allocate recreational boat emissions to coastal waters or lakes in Los Angeles County and Orange County.

Boundary and Initial Conditions

The initial condition for the CMAQ simulations was generated using the default profile available from the CMAQ standard package. Then, a five day spin-up period was introduced to offset the homogeneity in initial values. This method is consistent with the strategy implemented in the 2007 and 2012 AQMP's.

The 2012 AQMP addressed the impact of lateral boundary conditions on simulation predictions. Lateral boundaries investigated include the U.S. EPA's clean boundary, a global chemistry model driven boundary (Model for OZone and Related chemical Tracers, MOZART) and a hybrid approach using the clean boundary and field measurements. Sensitivity tests concluded that the MOZART driven boundary values performed best, therefore it served as the primary platform for boundary values.

As in the 2012 AQMP, MOZART (Emmons et al., 2010) was used to define the boundary conditions (BCs) for the outer 12 km statewide CMAQ domain, while boundary conditions for the inner South Coast 4 km domain were derived from the 12 km output. MOZART is a comprehensive global model used to simulate atmospheric composition including both gases and bulk aerosols (Emmons et al., 2010). It was developed by the National Center for Atmospheric Research, the Max-Planck-Institute for Meteorology (Germany), and the Geophysical Fluid Dynamics Laboratory of the National Oceanic and Atmospheric Administration, and is widely used in the scientific community for both global atmospheric chemistry studies and for providing the dynamic boundary conditions needed for regional air quality modeling. Boundary conditions were extracted for inorganic gases and VOCs along with aerosol species such as elemental carbon, organic matter, sulfate, soil and nitrate. MOZART4-GEOS5 simulations by Dr. Louisa Emmons (NCAR) for the year 2012 were used to represent the boundary conditions in the 2012 AQMP. These simulations are publically available and can be downloaded at http://www.acom.ucar.edu/wrf-chem/mozart.shtml. These simulations are similar to those of Emmons et al. (2010), but with updated meteorological fields. Boundary condition data was extracted from the MOZART-4 output and processed into CMAQ model ready format using the computer program "mozart2camx" developed by the Ramboll-Environ Corporation (available at http://www.camx.com/download/support-software.aspx). The final MOZART derived BCs for the statewide domain represent day-specific mixing ratios, which vary in both space (horizontal and vertical) and time (every hour).

Figures V-4-15 and V-4-16 show surface ozone concentrations averaged along the four domain boundaries. Typically, the western boundary, located west of the Basin over the Pacific Ocean, shows the lowest concentrations followed by the southern boundary. The average ozone concentration over the entire ozone season at the western boundary is approximately 35 ppb, whereas the seasonally averaged concentration on the southern boundary is approximately 42 ppb. The general circulation in Southern California is from west to east, and as a result, the eastern boundary is affected by the upwind emissions in the domain, which results in a higher boundary value over the eastern boundary. The average ozone concentration along the eastern boundary is approximately 50 ppb. Finally, the northern boundary is affected by emissions from central California and present the highest average concentration of ozone, approximately 55 ppb.

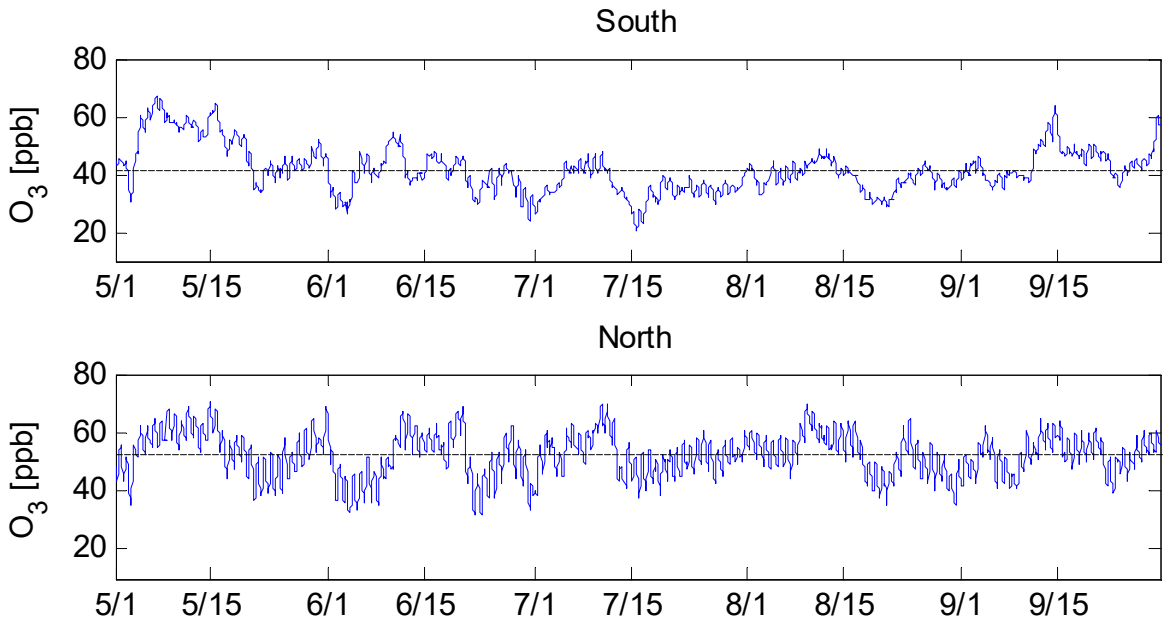

FIGURE V-4-15

Surface ozone concentration at the South and North boundary

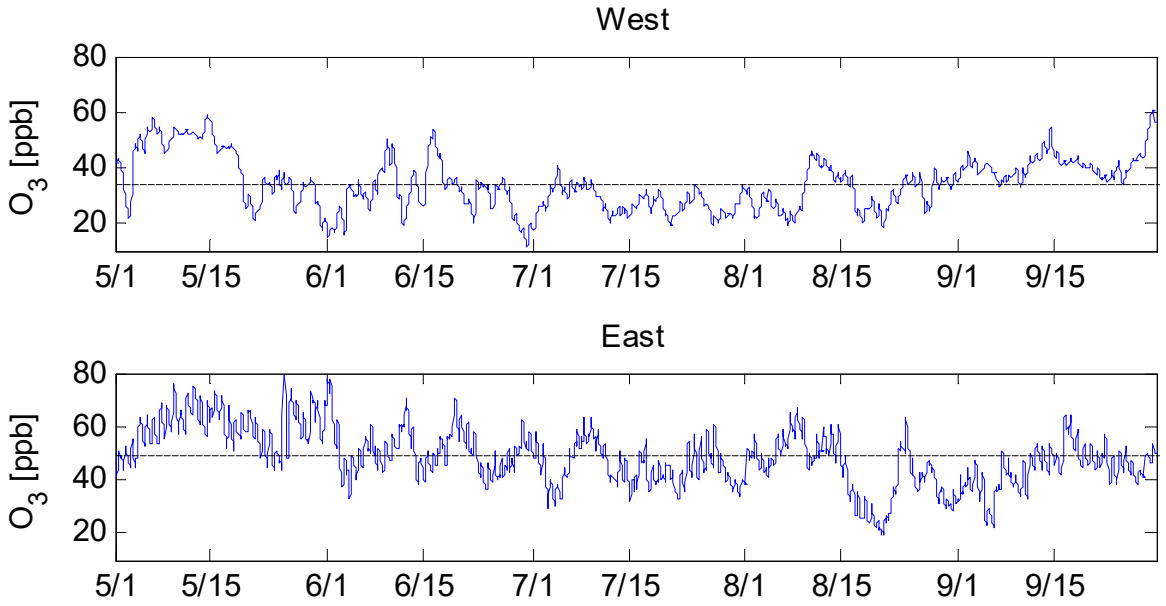

FIGURE V-4-16

Surface ozone concentration at the West and East boundary

Figures V-4-17 through V-4-20 present the monthly ozone vertical profiles averaged long the southern and northern boundaries, respectively, at two hours of the day. In general, ozone concentrations tend to be higher in the upper layers, especially along the cleaner boundaries. The difference between concentrations at the surface and concentrations aloft is larger along the cleaner boundaries. In particular, ozone concentrations along the western boundary exhibit the most contrast between ground level and upper levels. On the contrary, the northern and eastern boundary, which have higher ozone concentrations due to the influence of central and Southern California emissions, present a flatter vertical profile throughout the ozone season.

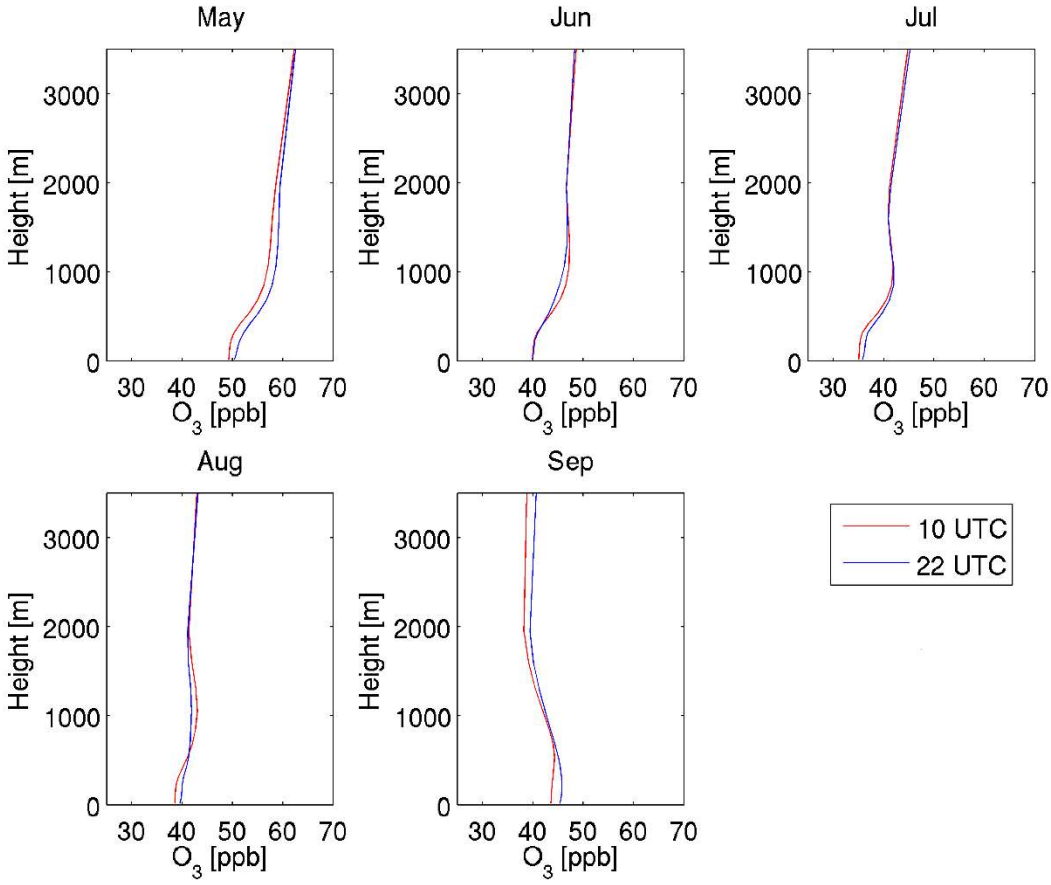

FIGURE V-4-17

Ozone vertical profile in the South boundary

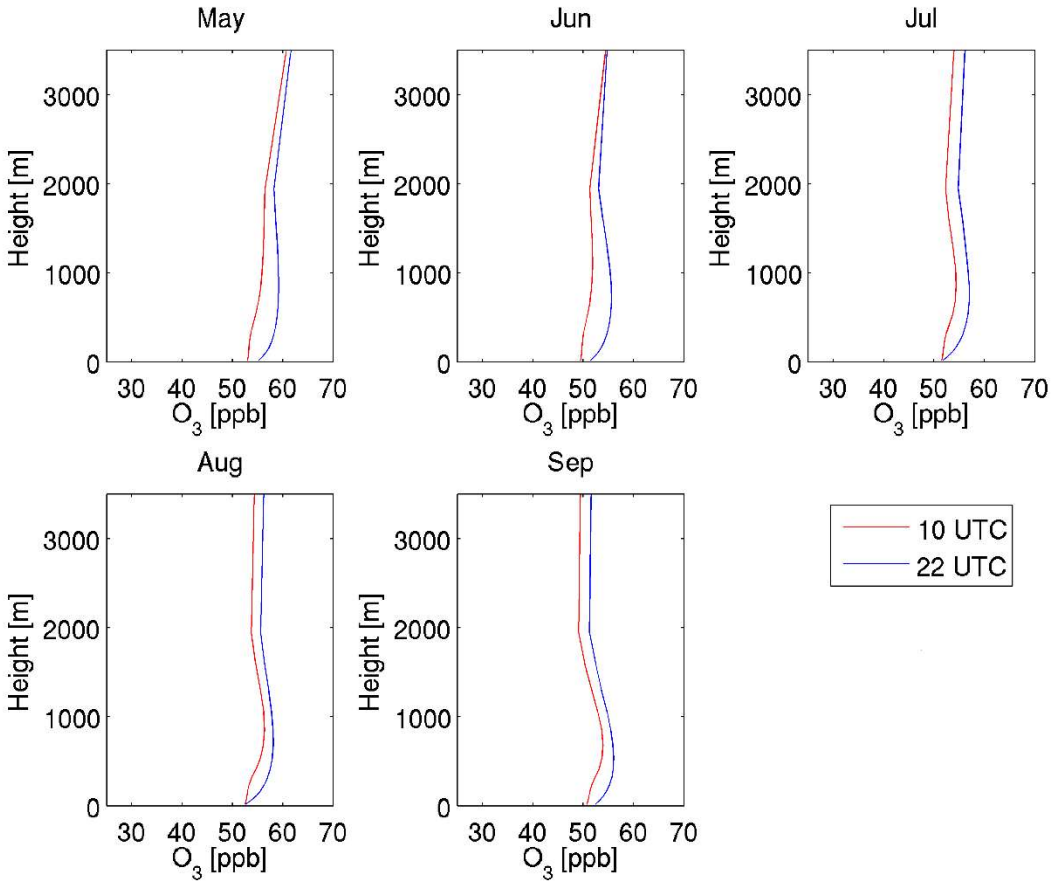

FIGURE V-4-18

Ozone vertical profile in the North boundary

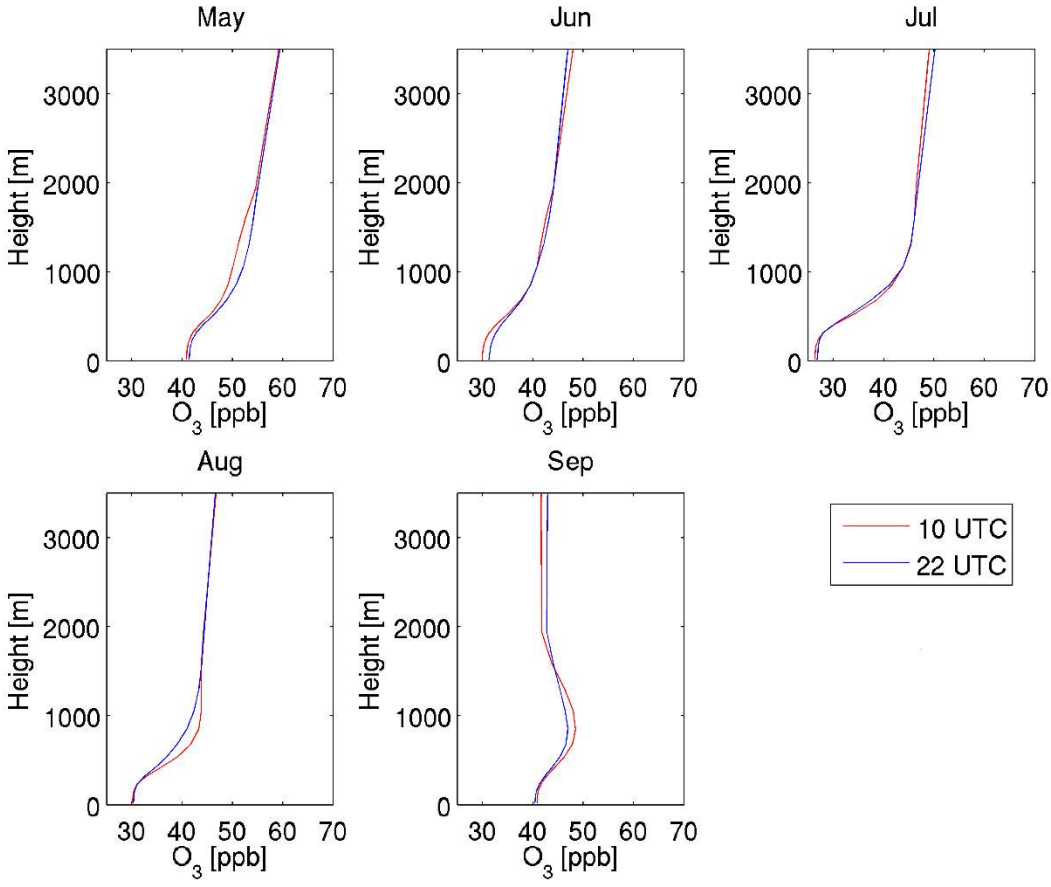

FIGURE V-4-19

Ozone vertical profile in the West boundary

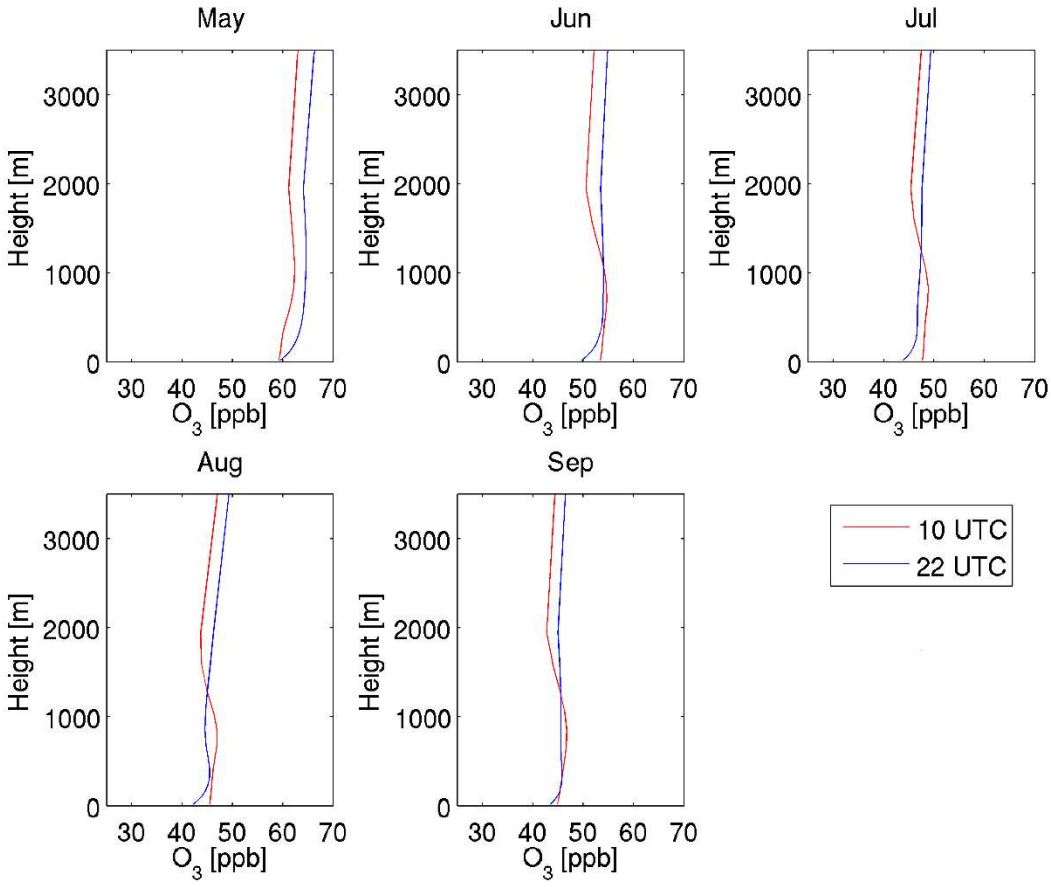

FIGURE V-4-20

Ozone vertical profile in the East boundary

The boundary values used in future year simulations were retrieved from the same approach as the base year (2012), except that anthropogenic emissions were adjusted based on the projected future emission levels in the State. In this approach, the emissions from out of state and out of continent were not adjusted due to the lack of accurate information, but the impact of state-wide emission reductions was considered.

References

Emmons, L. K., Walters, S., Hess, P. G., Lamarque, J.-F., Pfister, G. G., Fillmore, D., Granier, C., Guenther, A., Kinnison, D., Laepple, T., Orlando, J., Tie, X., Tyndall, G., Wiedinmyer, C., Baughcum, S. L., and Kloster, S.: Description and evaluation of the Model for Ozone and Related chemical Tracers, version 4 (MOZART-4), Geosci. Model Dev., 3, 43-67, doi:10.5194/gmd-3-43-2010, 2010.

CHAPTER 5

8-HOUR OZONE ATTAINMENT DEMONSTRATION

Introduction

The 2016 AQMP demonstrates attainment of two 8-hour ozone standards: the 2008 standard of 75 ppb and currently revoked 1997 standard of 80 ppb.

The 2012 AQMP provided a comprehensive 8-hour ozone analysis that demonstrated future year attainment of the 1997 federal ozone standard (80 ppb) by 2023 with implementation of short-term measures and CAA Section 182(e)(5) long term emissions reductions. The analysis concluded that NOx emissions of approximately 65 percent from the 2023 baseline were necessary to demonstrate attainment. The 2023 baseline summer planning emissions inventories included 438 and 319 TPD of VOC and NOx, respectively.

As presented in Chapter 3 of the 2016 AQMP, 2023 baseline emissions of both precursor pollutants are estimated to be lower than th3 2023 baseline emissions established in the 2012 AQMP. The 2016 AQMP baseline VOC and NOx summer planning emissions for 2023 have been revised to 379 and 255 TPD, respectively. The emissions revision incorporated changes made by federal and California regulations adopted post-2010, changes resulting from updates in the emission calculation methodologies for selected sources, and changes resulting from updated socio-economic factors.

The 2016 AQMP attainment demonstrations rely on air quality measurements collected during the 5-year period centered on 2012, which is the base year selected for the emissions inventory development, the WRF meteorological simulation, and the anchor year for the future year ozone and PM2.5 projections. The attainment demonstration methodology, established in the updated U.S. EPA guidance, was used to demonstrate attainment with a revised Relative Response Factor (RRF) approach.

Ozone Representativeness

The CMAQ modeling provided Basin-wide ozone air quality simulations for each hour in 2012. It includes 153 days from May 1st to September 30th of 2012.

The 2007 AQMP ozone attainment demonstrations evaluated a set of days characterized by restrictive meteorology or episodes occurring during concurrent intensive field programs. These episode periods were rated based on how representative they were relative to the ozone standard being evaluated. For the now revoked 1-hour ozone standard, the attainment demonstration focused on a limited number of days closely matching the annual design value. Typically, the analysis addressed 5 episodes of each last a few days. The 2007 AQMP was the first to address the 8-hour ozone standard and the use of RRFs in the future year ozone projection. The analysis included 36 days in the simulation to provide a robust characterization of the RRFs for use in the attainment demonstration. The ozone modeling guidance recommended that a minimum of 5-days of simulations meeting modeling acceptance criteria were used in a future year RRF calculation, but also recommended incorporating as many days as possible to fully

capture both the meteorological variations in the ozone season and the response to different daily emissions profiles.

The 2012 AQMP used a different approach. Instead of the episode-based limited simulation days, it included season-long comprehensive CMAQ simulations. The ozone season was assumed to be June through August. It analyzed 92 simulation days and chose the days where the predicted daily max is within the 20 % error of the site-specific design value, the unpaired daily-max prediction error is less than 20%, and the prediction is higher than the federal standard. The number of days used in the RRF calculation differed from station to station. Approximately 50 days met the criteria at Crestline—more than half of the entire simulation period.

The approach used in the current AQMP is similar to the approach of the 2012 AQMP with the following exceptions per the U.S. EPA guidance (U.S. EPA, 2014). The ozone season was expanded from May to September (153 simulation days) in order to capture exceedances that occurred in early and late summer. Only the top 10 days are used to calculate the RRF. Some stations employ less than 10 days as daily maximum 8-hr values must exceed 60 ppb for inclusion into the analysis. In the 2012 AQMP, the maximum modelled grid cell in the 3x3 grid centered at each station was retrieved from the base and future simulations. In the current AQMP, the maximum modelled value in the 3x3 grid surrounding each station is compared to the corresponding grid position in the future year.

Basin-wide ozone air quality simulations were conducted for each hour in the 2012 ozone season (May 1st to September 30th). Figure V-5-1 depicts the time series of the daily Basin 8-hour maximum and the daily maximum 8-hour ozone air quality at Crestline (the past Basin design station) and Redlands (the current Basin design station) during the 2012 ozone season. All station days meeting the acceptance criteria—the predicted daily max is within the 20 % error of the site-specific design value and the prediction is higher than the federal standard of 75 ppb— were included in the RRF calculation. During this period, several well defined multiday ozone episodes occurred in the Basin with 107 total days having daily Basin-wide maximum concentrations of 75 ppb or higher. Several locations in the San Bernardino and Riverside Valleys exhibit similar transport and daily patterns of ozone formation as Crestline and Redlands. Typically, Crestline shows the highest concentration in the Basin and has been the design site in the previous AQMPs. Crestline exhibits the highest daily maximum 8-hr ozone in the Basin of 112 ppb in 2012.

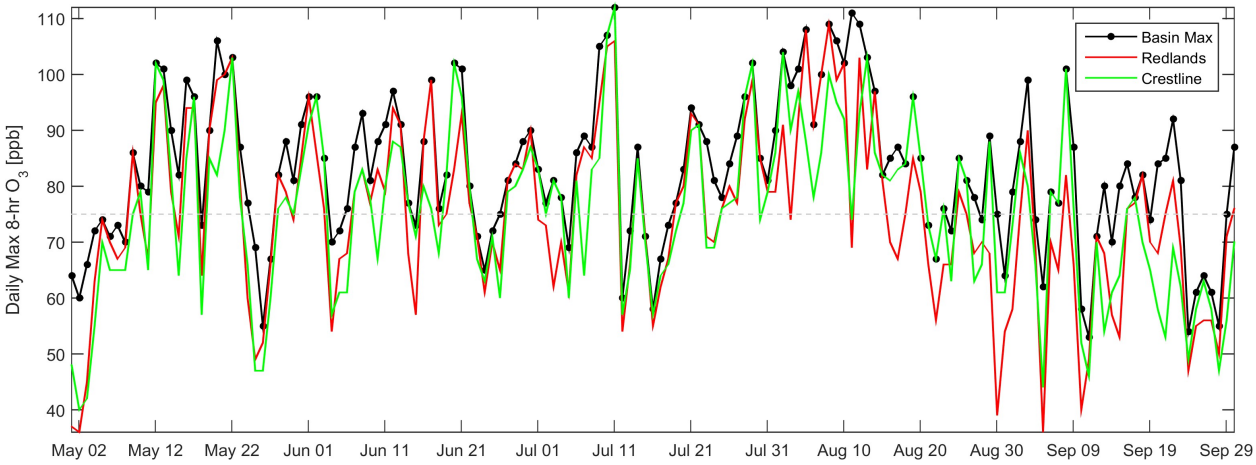

FIGURE V-5-1

Observed Basin, Redlands, and Crestline Daily Maximum 8-Hr Average Ozone Concentrations: May 1 through Sept 30, 2012.

However, Redlands is the new design site with a 5-year weighted design value of 104.7 ppb for the period of 2010 to 2014. This reflects changes in the emission characteristics and associated changes in the chemical reactions instrumental for ozone production. Crestline is the second highest site with design value of 103.0 ppb. Note that the 5-year weighted design value for the attainment demonstration should be rounded to the nearest tenth of a ppb, while the conventional design value for a three-year period should be truncated to the integer value. Table V-5-1 lists the 2010 to 2014 5-year weighted design values used in the future year ozone projections. Stations are color coded according to their performance evaluation zone defined in the Model Performance Evaluation section below.

TABLE V-5-1

2010–2012 Weighted 8-hr Ozone Design Values

Station	2010–2014 8-hr Design Value	2012 Weekend Days > 75 ppb	2012 Weekday Days > 75 ppb	Performance Evaluation Zone
Costa Mesa	63.2	1	0	Coastal
LAX	61.0	1	0	Coastal
Long Beach	56.0	0	0	Coastal
Mission Viejo	72.0	0	1	Coastal
West Los Angeles	64.7	0	0	Coastal
Burbank	78.3*	6	3	SanFernando
Reseda	89.0	11	17	SanFernando
Santa Clarita	97.3	30	32	SanFernando
Azusa	79.3	9	2	Foothills
Glendora	92.7	29	18	Foothills

TABLE V-5-1 (CONCLUDED)

2010–2012 Weighted 8-hr Ozone Design Values

Station	2010–2014 8-hr Design Value	2012 Weekend Days > 75 ppb	2012 Weekday Days > 75 ppb	Performance Evaluation Zone
Pasadena	76.7*	7	5	Foothills
Anaheim	65.0	0	0	UrbanSource
Central Los Angeles	64.0	1	0	UrbanSource
La Habra	69.3	2	0	UrbanSource
Pico Rivera	67.7	2	0	UrbanSource
Pomona	84.3	12	5	UrbanSource
Banning	95.3	21	45	UrbanReceptor
Crestline	103.0	30	59	UrbanReceptor
Fontana	101.0	35	30	UrbanReceptor
Lake Elsinore	85.3	6	11	UrbanReceptor
Mira Loma	92.7	24	29	UrbanReceptor
Perris	91.0	17	32	UrbanReceptor
Redlands	104.7	35	50	UrbanReceptor
Rubidoux	96.3	24	29	UrbanReceptor
San Bernardino	98.0	29	28	UrbanReceptor
Upland	96.7	25	24	UrbanReceptor
Indio	84.3	7	23	CoachellaValley
Palm Springs	91.7	14	43	CoachellaValley

* NOTE: Burbank and Pasadena are each missing one three-year design value due to the inability to satisfy the completeness criteria. Therefore, the design values at these sites are estimated from the remaining years.

Ozone Modeling Configuration

In the 2007 AQMP, Comprehensive Air Quality Model with extensions (CAMx) was used as the primary chemical transport modeling platform. CAMx, including its predecessor, the Urban Airshed Model (UAM) (EPA, 1990) has been applied to many air pollution episodes in California and has demonstrated its capability as a tool for the attainment demonstration. While the District has a long history and significant expertise with the use of CAMx, the Community Multi-scale Air Quality (CMAQ) model has been widely applied to various locations and episodes and is actively updated by a large users' community, including the U.S. EPA. Therefore, the 2012 AQMP used CMAQ as the primary modeling tool and CAMx to provide weight of evidence. CMAQ version 5.0.2, used in the current AQMP, has an updated aerosol chemical mechanism, updated numerical solvers for mass consistent advection scheme, updated in-line plume rise calculation, updated in-line photolysis calculation, and an updated adjustment for nocturnal diffusion parameters when compared to version 4.7.1 used in the 2012 AQMP. SAPRC07 with version "c" toluene

updates, Euler Backward Iterative (EBI) chemical solver, aero6 aerosol module, Yamo horizontal advection scheme, WRF vertical advection, and Asymmetric Convective Model version-2 (ACM2) vertical diffusion scheme were used in CMAQ. See Chapter 2 of Appendix 5 for the details of the modeling protocol associated with the chemical transport modeling.

The inner-most modeling domain of the WRF simulation overlaps the CMAQ modeling domain, except that the WRF domain contains an extra 3 grid cells along the western, southern, and eastern boundary and an extra 9 grid cells along the northern boundary. The CMAQ domain contains 156 cells in the east/west direction and 102 cells in the N-S direction. The vertical coordinate and each computational layer definition are identical to those of the WRF. However, layers in the middle and upper troposphere are combined to maximize computational efficiency, resulting in fewer number of layers. Impacts of vertical layer collapsing and the configuration employed to minimize artificial errors associated with this approximation have been evaluated intensively during the 2012 AQMP; the configuration developed in the previous AQMP was employed in the current simulations. In total, 18 layers were included in the CMAQ simulations with approximately 14 layers located below 2000 m above the ground level.

Base-Year Ozone Model Performance Evaluation

For the CMAQ performance evaluation, the modeling domain is separated into several sub-regions or zones. Figure V-5-2 depicts the sub-regional zones used for base-year simulation performance. The different zones present unique air quality profiles. Previous AQMP's employed nine zones that represented the Basin and portions of Ventura County, the Mojave Desert and the Coachella Valley. However, based on recent measurement findings, current analysis re-defined the analysis zone into six areas: "Coastal" zone representing monitoring areas 2-4 and 18-21, "SanFernando" zone representing monitoring areas 6,7, and 13 within the San Fernando Valley, "Foothills" zone representing monitoring areas 8 and 9, "UrbanSource" zone representing monitoring areas 1, 5, 10-12, 16, and 17, "UrbanReceptor" zone representing monitoring areas 22-29 and 33-38, and "CoachellaValley" zone representing monitoring areas 30 and 31. Of the six areas, the "UrbanReceptor" region represents the Basin maximum ozone concentrations and the primary downwind impact zone. Table V-5-2 contains additional information regarding each station used in the analysis.

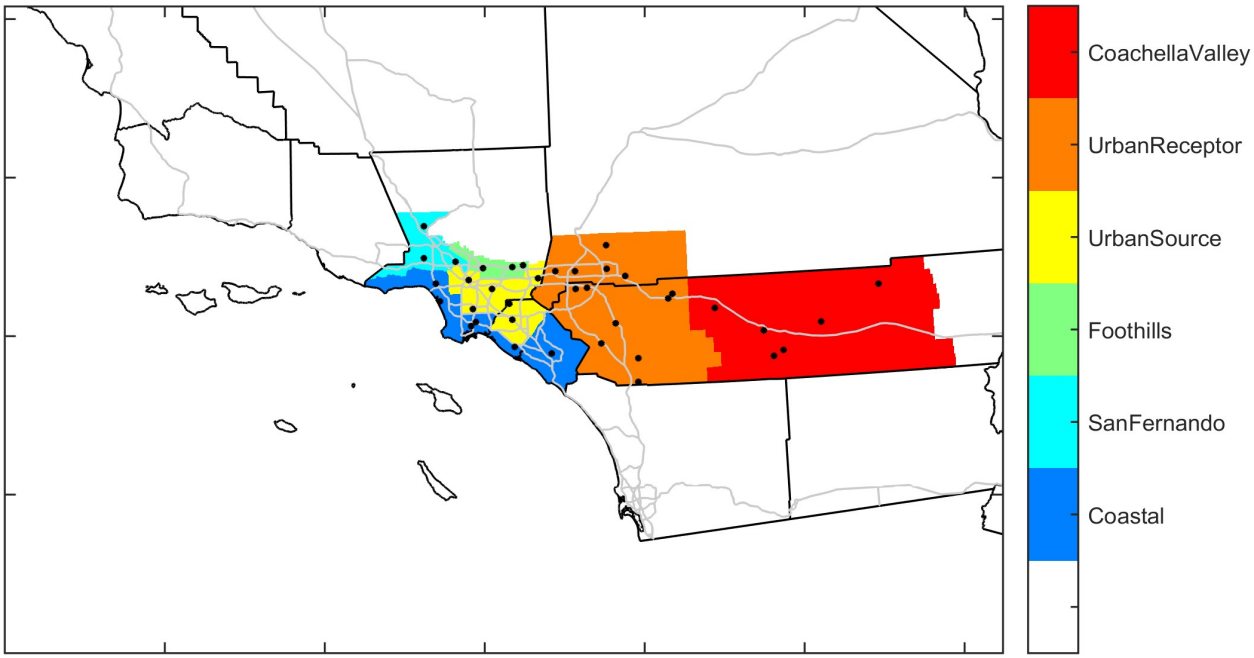

FIGURE V-5-2

Performance Evaluation Zones

TABLE V-5-2

Station Information

Location	Abbreviation	County	EPA Site Number	Monitoring Area	Performance Evaluation Zone
Costa Mesa	CSTA	Orange	1003	18	Coastal
LAX	LAXH	Los Angeles	5005	3	Coastal
Long Beach	LGBH	Los Angeles	4002	4	Coastal
Long Beach Hudson	HDSN	Los Angeles	4006	4	Coastal
Mission Viejo	MSVJ	Orange	2022	19	Coastal
West Los Angeles	WSLA	Los Angeles	113	2	Coastal
Burbank	BURK	Los Angeles	1002	7	SanFernando
Reseda	RESE	Los Angeles	1201	6	SanFernando
Santa Clarita	SCLR	Los Angeles	6012	13	SanFernando
Azusa	AZUS	Los Angeles	2	9	Foothills
Glendora	GLEN	Los Angeles	16	9	Foothills
Pasadena	PASA	Los Angeles	2005	8	Foothills
Anaheim	ANAH	Orange	7	17	UrbanSource
Central Los Angeles	CELA	Los Angeles	1103	1	UrbanSource
Compton	CMPT	Los Angeles	1302	12	UrbanSource
La Habra	LAHB	Orange	5001	16	UrbanSource

TABLE V-5-2 (CONCLUDED)

Station Information

Location	Abbreviation	County	EPA Site Number	Monitoring Area	Performance Evaluation Zone
Pico Rivera	PICO	Los Angeles	1602	11	UrbanSource
Pomona	POMA	Los Angeles	1701	10	UrbanSource
Banning	BNAP	Riverside	12/1016	29	UrbanReceptor
Crestline	CRES	San Bernardino	5	37	UrbanReceptor
Fontana	FONT	San Bernardino	2002	34	UrbanReceptor
Lake Elsinore	ELSI	Riverside	9001	25	UrbanReceptor
Mira Loma	MRLM	Riverside	8005	23	UrbanReceptor
Perris	PERI	Riverside	6001	24	UrbanReceptor
Redlands	RDLD	San Bernardino	4003	35	UrbanReceptor
Riverside	RIVR	Riverside	8001	23	UrbanReceptor
San Bernardino	SNBO	San Bernardino	9004	34	UrbanReceptor
Temecula	TMCA	Riverside	9	26	UrbanReceptor
Upland	UPLA	San Bernardino	1004	32	UrbanReceptor
Indio	INDI	Riverside	1999/2002	30	CoachellaValley
Palm Springs	PLSP	Riverside	5001	30	CoachellaValley

Statistical Evaluation

The statistics used to evaluate 8-hour average CMAQ ozone performance include the following:

Statistic for O_3	Definition
Daily-Max Bias Error Unpaired	Average of the differences in observed and predicted daily maximum values. Negative values indicate under-prediction. $BiasError = \frac{1}{N}\sum(Obs - Pred)$
Daily-Max Bias Error Paired	Average of the differences in daily maximum observed value and the corresponding predicted concentration at the hour that the observational maximum was reached. Negative values indicate under-prediction. $BiasError = \frac{1}{N}\sum(Obs - Pred)$

Daily-Max Gross Error Unpaired	Average of the absolute differences in observed and predicted daily maximum values $GrossError = \frac{1}{N}\sum\lvert Obs - Pred\rvert$
Daily-Max Gross Error Paired	Average of the absolute differences in daily maximum observed value and the corresponding predicted concentration at the hour that the observational maximum was reached. $GrossError = \frac{1}{N}\sum\lvert Obs - Pred\rvert$
Normalized Daily-Max Bias Error Unpaired	Average of the quantity: difference in observed and predicted daily maximum values normalized by the observed daily maximum values. Negative values indicate under-prediction. $NormBiasError = \frac{1}{N}\sum\left(\frac{Obs-Pred}{Obs}\right)\cdot 100$
Normalized Daily-Max Bias Error Paired	Average of the quantity: difference in daily maximum observed value and the corresponding predicted concentration at the hour that the observational maximum was reached normalized by the observed daily maximum concentration. Negative values indicate under-prediction. $NormBiasError = \frac{1}{N}\sum\left(\frac{Obs-Pred}{Obs}\right)\cdot 100$
Normalized Daily-Max Gross Error Unpaired	Average of the quantity: absolute difference in observed and predicted daily maximum values normalized by the observed daily maximum concentration $NormGrossError = \frac{1}{N}\sum\left\lvert\frac{Obs-Pred}{Obs}\right\rvert\cdot 100$
Normalized Daily-Max Gross Error Paired	Average of the quantity: absolute difference in daily maximum observed value and the corresponding predicted concentration at the hour that the observational maximum was reached normalized by the observed daily maximum concentration $NormGrossError = \frac{1}{N}\sum\left\lvert\frac{Obs-Pred}{Obs}\right\rvert\cdot 100$

Peak Prediction Accuracy Unpaired	Difference in the maximum of the observed daily maximum and the maximum of the predicted daily maximum normalized by the maximum of the observed daily maximum $PPA = \frac{(maximum(Pred) - \text{maximum}(Obs))}{\text{maximum}(Pred)}$

Predicted concentrations are extracted from model output in the grid cell that each monitoring station resides.

The base year average regional model performance for May through September 2012 for each of the six zones are presented in Tables V-5-3 to V-5-8 for days when Basin maximum 8-hour ozone levels were at least 60 ppb. Only stations with more than 75% of the hourly measurements during each month of the ozone season were included in the analysis.

In general, the model over-predicts 8-hr daily-maximum ozone concentrations in the "Coastal" and "UrbanSource" regions. Conversely, the model under-predicts 8-hr daily-maximum ozone concentrations in the "SanFernando", "Foothills", and "UrbanReceptor" regions.

U.S. EPA guidance (2014) describes four types of analysis as model performance evaluation. They are operational, diagnostic, dynamic and probabilistic approaches. The operational evaluation techniques include statistical and graphical analyses aimed at determining whether the modeled simulated variables are comparable to measurements and the diagnostic evaluation focuses on process-oriented analyses that determine whether the individual processes and components of the model system are working correctly, both independently and in combination. The statistical evaluation and series of sensitivity tests discussed in the 'Weight of Evidence and Stress Test' section were focused on these two types of evaluation. While the Dynamic evaluation assesses the ability of the air quality model to predict changes in air quality given changes in source emissions or meteorology, the principal forces that drive the air quality model, the U.S. EPA guidance recommends a test as a part of the dynamic evaluation. That is to look at operational performance under varying conditions, e.g., by day of the week, by season, and regionally The mix of pollutants vary by day of the week and from city to city so when a model shows good operational performance across these different chemical environments, this supports the assertion that it will respond appropriately to changes in emissions. The AQMP attainment modeling includes a five-month period starting from May to September, which includes various meteorological conditions, emission variability, seasonal changes, etc. Modeling results exhibit a robust model performance across these different chemical environments, thus supporting the assertion that the modeling set-up responds appropriately to changes in emissions. Lastly, the probabilistic evaluation attempts to assess the level of confidence in the model predictions through techniques such as ensemble model simulations. As an attempt to an ensemble analysis or, at least evaluation over multiple the modeling platforms, CAMx model was tested extensively within the AQMP modeling framework as well as Multiple Air Toxics Exposure studies (MATES). CAMx fundamentally yielded results comparable to CMAQ for the modeling cases (not presented) so that CMAQ was selected as the primary modeling platform. In all, the 2012 AQMP covers

all the four types of model performance evaluation methods that the U.S. EPA guidance (2014) recommends.

TABLE V-5-3

2012 Base Year 8-Hour Average Ozone Performance for Days When Regional 8-Hour Maximum ≥ 60 ppb in the "Coastal" region

Month	Mean Pred. [ppb]	Mean Obs. [ppb]	Number of Daily Max > 60 ppb	Daily-Max Mean Pred. Unpaired [ppb]	Daily-Max Mean Pred. Paired [ppb]	Daily-Max Mean Obs. [ppb]	Daily-Max Bias Err. Unpaired [ppb]	Daily-Max Bias Err. Paired [ppb]	Daily-Max Gross Err. Unpaired [ppb]	Daily-Max Gross Err. Paired [ppb]	Norm Daily-Max Bias Err. Unpaired [%]	Norm Daily-Max Bias Err. Paired [%]	Norm Daily-Max Gross Err. Unpaired [%]	Norm Daily-Max Gross Err. Paired [%]	Peak Prediction Accuracy Unpaired [ppb]
May	41.5	37.7	145	56.8	53.4	48.4	8.4	5	9.5	8.4	13.6	6.5	16.3	16.1	21.4
Jun	34.8	34.5	150	50.5	47.1	43.7	6.9	3.4	8.5	7.9	12.1	2.8	16.5	18.6	12.8
Jul	29.9	30.1	145	44	41.8	41.3	2.7	0.5	6.5	6.9	3.2	-4.2	15.7	19.1	11.7
Aug	33.4	28.6	155	50.1	48.9	41.5	8.6	7.4	10.7	10.1	13.9	11.5	19.8	19.1	21.6
Sep	36.4	30.7	130	53.4	51.9	48.1	5.3	3.8	9.2	8.9	7.4	3.5	17.1	18	10.3

TABLE V-5-4

2012 Base Year 8-Hour Average Ozone Performance for Days When Regional 8-Hour Maximum ≥ 60 ppb in the "SanFernando" region

Month	Mean Pred. [ppb]	Mean Obs. [ppb]	Number of Daily Max > 60 ppb	Daily-Max Mean Pred. Unpaired [ppb]	Daily-Max Mean Pred. Paired [ppb]	Daily-Max Mean Obs. [ppb]	Daily-Max Bias Err. Unpaired [ppb]	Daily-Max Bias Err. Paired [ppb]	Daily-Max Gross Err. Unpaired [ppb]	Daily-Max Gross Err. Paired [ppb]	Norm Daily-Max Bias Err. Unpaired [%]	Norm Daily-Max Bias Err. Paired [%]	Norm Daily-Max Gross Err. Unpaired [%]	Norm Daily-Max Gross Err. Paired [%]	Peak Prediction Accuracy Unpaired [ppb]
May	46.1	38.5	87	62.3	60.9	62.9	-0.7	-2	7	6.9	-1.5	-4.1	11.5	11.8	-10.5
Jun	40.7	39	90	60.3	59.3	62.4	-2.2	-3.1	6.9	6.9	-5.1	-6.8	12.4	12.8	0.4
Jul	35.5	38.2	87	56.7	56	65.7	-9.1	-9.8	10.6	10.9	-17.5	-19.1	20.1	21	-28.6
Aug	41.3	37.4	93	63	62.1	68.5	-5.5	-6.4	9.3	9.7	-10.4	-12.1	15.9	16.9	-14.5
Sep	39	33.3	78	56.7	55.7	63.3	-6.6	-7.6	10.9	11.4	-15.7	-18.5	22.3	24.6	-18.8

TABLE V-5-5

2012 Base Year 8-Hour Average Ozone Performance for Days When Regional 8-Hour Maximum ≥ 60 ppb in the "Foothills" region

Month	Mean Pred. [ppb]	Mean Obs. [ppb]	Number of Daily Max > 60 ppb	Daily-Max Mean Pred. Unpaired [ppb]	Daily-Max Mean Pred. Paired [ppb]	Daily-Max Mean Obs. [ppb]	Daily-Max Bias Err. Unpaired [ppb]	Daily-Max Bias Err. Paired [ppb]	Daily-Max Gross Err. Unpaired [ppb]	Daily-Max Gross Err. Paired [ppb]	Norm Daily-Max Bias Err. Unpaired [%]	Norm Daily-Max Bias Err. Paired [%]	Norm Daily-Max Gross Err. Unpaired [%]	Norm Daily-Max Gross Err. Paired [%]	Peak Prediction Accuracy Unpaired [ppb]
May	45.5	34.5	87	61.7	60.9	56.9	4.8	4	7.8	7.4	7.8	6.6	12.6	12	-13.2
Jun	39.5	34.6	90	58.2	57.4	56.7	1.5	0.7	7	6.9	1.7	0.2	12.1	12.3	-20.9
Jul	33.2	31.8	87	52.2	51.4	59.6	-7.4	-8.2	9.9	9.8	-17.5	-19.3	21.8	22.2	-8.9
Aug	39.1	32	93	59.6	58.4	63.8	-4.2	-5.4	9.1	10	-10.1	-13.1	17	19.6	-14.9
Sep	39.2	32.5	78	54.4	52.6	62.2	-7.7	-9.5	12.3	12.7	-18	-23.3	25.2	28.6	-14.3

TABLE V-5-6

2012 Base Year 8-Hour Average Ozone Performance for Days When Regional 8-Hour Maximum ≥ 60 ppb in the "UrbanSource" region

Month	Mean Pred. [ppb]	Mean Obs. [ppb]	Number of Daily Max > 60 ppb	Daily-Max Mean Pred. Unpaired [ppb]	Daily-Max Mean Pred. Paired [ppb]	Daily-Max Mean Obs. [ppb]	Daily-Max Bias Err. Unpaired [ppb]	Daily-Max Bias Err. Paired [ppb]	Daily-Max Gross Err. Unpaired [ppb]	Daily-Max Gross Err. Paired [ppb]	Norm Daily-Max Bias Err. Unpaired [%]	Norm Daily-Max Bias Err. Paired [%]	Norm Daily-Max Gross Err. Unpaired [%]	Norm Daily-Max Gross Err. Paired [%]	Peak Prediction Accuracy Unpaired [ppb]
May	41.2	34.1	174	59.1	57.6	49.9	9.2	7.7	9.9	8.8	15.1	12.6	16.3	14.7	3.7
Jun	35	32.4	180	54.2	52.7	47.5	6.7	5.2	8.3	7.2	11.2	8.6	14.7	13.4	2.5
Jul	29.6	28.6	170	47.7	45.6	46.6	0.7	-0.4	7	6.6	-1.2	-4.1	15.9	16.3	4.4
Aug	33.8	26.8	186	54.7	53.9	48.3	6.4	5.6	9.8	9.5	9.1	7.4	17.3	17.3	8.3
Sep	34.5	27.3	156	53.7	52.7	52.6	1.1	0.1	9.3	9.2	-0.4	-3.2	18.2	19	-13.5

TABLE V-5-7

2012 Base Year 8-Hour Average Ozone Performance for Days When Regional 8-Hour Maximum ≥ 60 ppb in the "UrbanReceptor" region

Month	Mean Pred. [ppb]	Mean Obs. [ppb]	Number of Daily Max > 60 ppb	Daily-Max Mean Pred. Unpaired [ppb]	Daily-Max Mean Pred. Paired [ppb]	Daily-Max Mean Obs. [ppb]	Daily-Max Bias Err. Unpaired [ppb]	Daily-Max Bias Err. Paired [ppb]	Daily-Max Gross Err. Unpaired [ppb]	Daily-Max Gross Err. Paired [ppb]	Norm Daily-Max Bias Err. Unpaired [%]	Norm Daily-Max Bias Err. Paired [%]	Norm Daily-Max Gross Err. Unpaired [%]	Norm Daily-Max Gross Err. Paired [%]	Peak Prediction Accuracy Unpaired [ppb]
May	54.7	45.5	258	71.5	69.7	68.8	2.6	1.4	8.9	8.3	3.8	2.2	12.5	11.9	-6.9
Jun	49.6	44.1	267	68.9	67.1	68.8	0.3	-1	9.5	9.4	-0.7	-2.6	14.3	14.8	-0.8
Jul	44	43.5	257	64.1	62.9	71.2	-6.7	-7.7	11.6	12.1	-13	-15.6	20.4	22.2	-11.1
Aug	47.9	43.5	279	69.6	68.6	74	-4.4	-5.3	10.4	10.7	-8.5	-10.3	16.2	17.2	-0.7
Sep	44.7	38.7	234	60.5	59	65.5	-5	-6.5	11.5	11.5	-11.2	-14.3	20.9	21.7	-7.2

TABLE V-5-8

2012 Base Year 8-Hour Average Ozone Performance for Days When Regional 8-Hour Maximum ≥ 60 ppb in the "CoachellaValley" region

Month	Mean Pred. [ppb]	Mean Obs. [ppb]	Number of Daily Max > 60 ppb	Daily-Max Mean Pred. Unpaired [ppb]	Daily-Max Mean Pred. Paired [ppb]	Daily-Max Mean Obs. [ppb]	Daily-Max Bias Err. Unpaired [ppb]	Daily-Max Bias Err. Paired [ppb]	Daily-Max Gross Err. Unpaired [ppb]	Daily-Max Gross Err. Paired [ppb]	Norm Daily-Max Bias Err. Unpaired [%]	Norm Daily-Max Bias Err. Paired [%]	Norm Daily-Max Gross Err. Unpaired [%]	Norm Daily-Max Gross Err. Paired [%]	Peak Prediction Accuracy Unpaired [ppb]
May	61.5	59.8	116	69.4	67.9	70.9	-1.4	-2.9	6.7	7	-2.5	-4.8	9.6	10.6	-6.5
Jun	54.3	55.8	120	63.3	60.7	66.8	-3.6	-6.1	9	9.5	-7.1	-11.5	15.1	16.8	-2.5
Jul	46.4	47.5	114	54.1	51.1	57.4	-3.1	-6.1	8.7	9.2	-6.9	-13.2	16.8	18.8	-10.4
Aug	47.1	43.3	124	55.6	51.7	54.3	1.2	-2.6	8.4	8.3	1.8	-6.4	15.4	16.9	-21.5
Sep	46.4	38.7	104	54.2	52	50.9	3.3	1.1	8.6	8.4	5.4	0.4	15.8	16.6	-1

Model performance can be evaluated graphically with scatter plots. Figure V-5-3 compares the measured and modelled maximum 8-hr ozone concentrations for 2012 in each region. Figure V-5-4 compares the measured and modelled 8-hr ozone concentrations for every hour in each region.

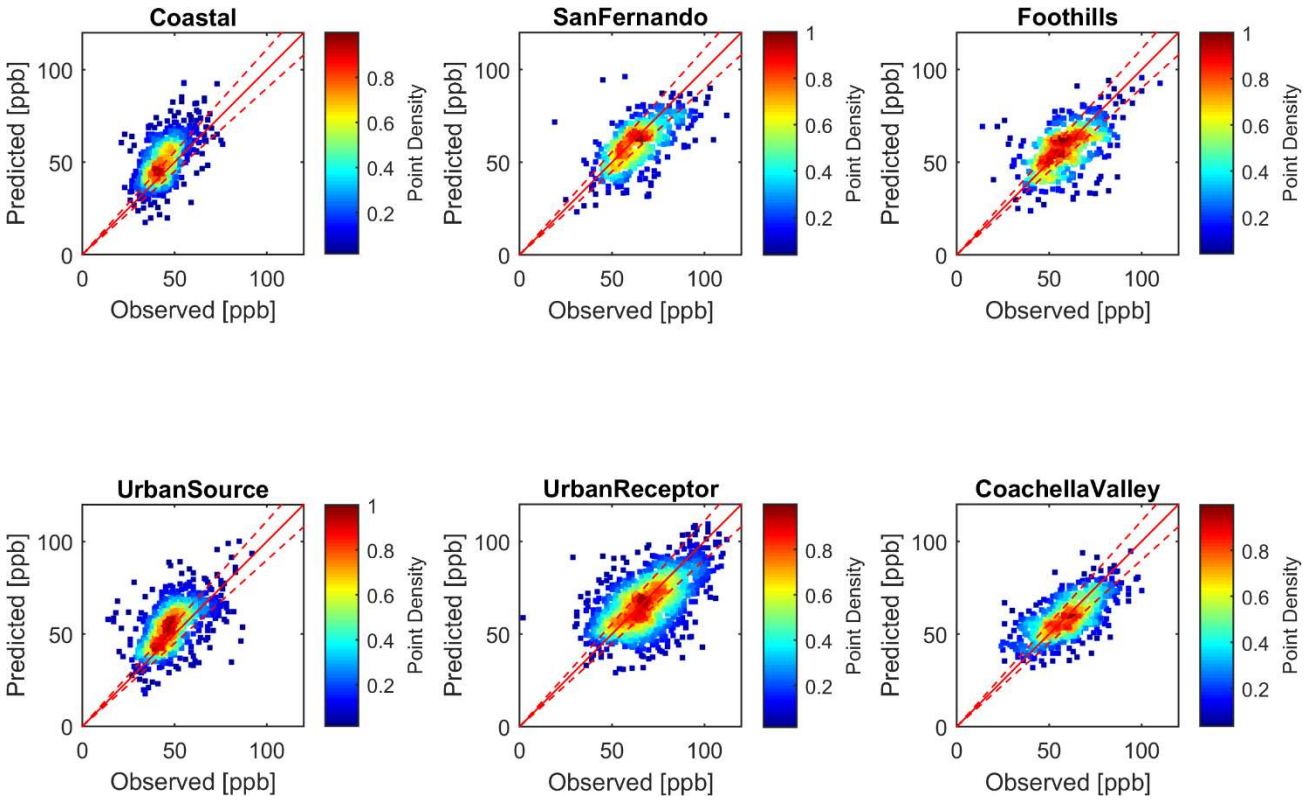

FIGURE V-5-3

Observed Vs.Predicted 8-Hour Ozone Maximums. Dashed lines Indicate 10% Error Bounds.

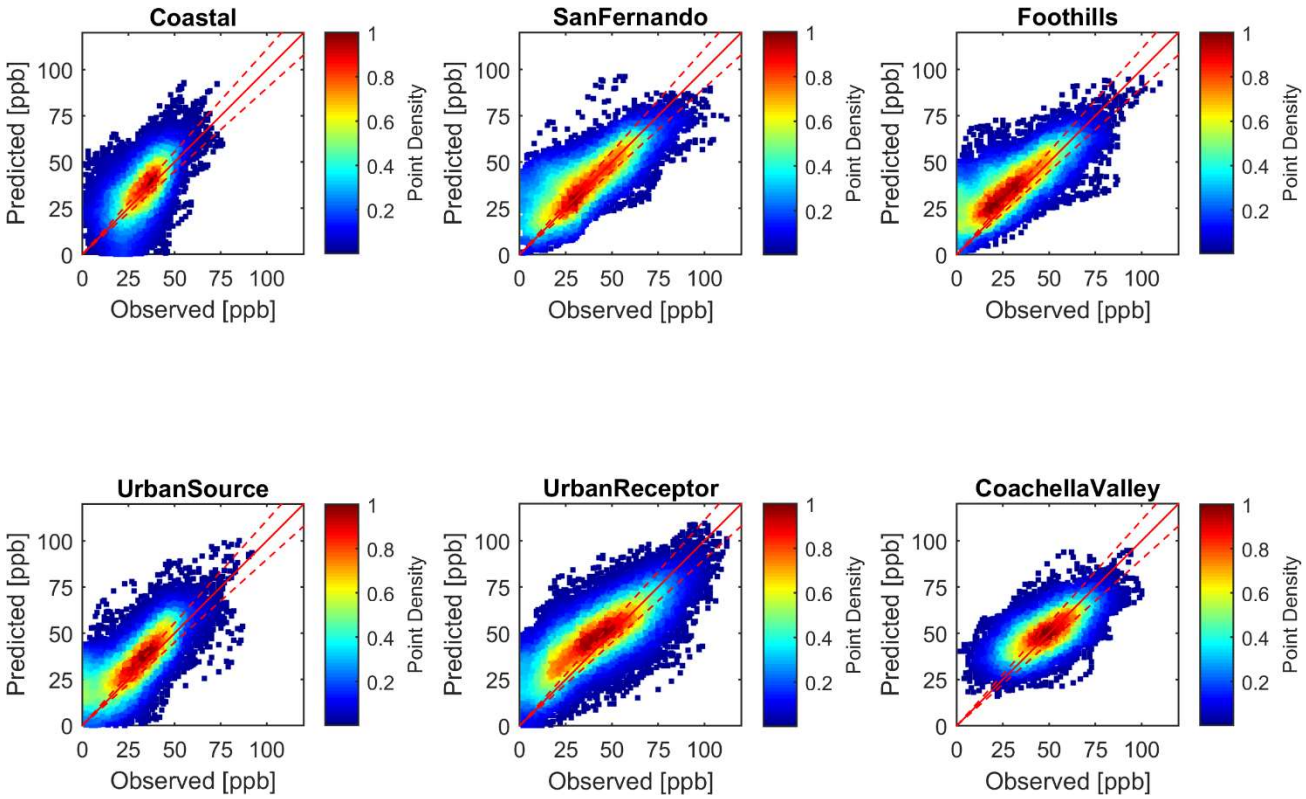

FIGURE V-5-4

Density Scatter Plot of Observed Vs.Predicted 8-Hour Regional Ozone Hourly Values. Dashed lines Indicate 10% Error Bounds.

The scatter and density scatter plots show consistent results: low bias in the high concentration cases and high bias in the low concentration regime with larger deviations at low concentrations. Geographical bias is also evident, with over-prediction in the coastal zone and under-prediction in the 'San Fernando', and 'Foothills' zones. Still, predictions in the 'UrbanReceptor' zone, in where the design site and most of traditional receptor stations are located, agrees reasonably well with the measurements. While the model deviation is more noticeable at low concentrations, the latest U.S. EPA guidance (U.S. EPA, 2014) requires the use of only the top 10 days in the RRF calculation, indicating that the modeling capability to predict high concentrations is more important than the prediction of low concentrations.

Time Series of Observed and Predicted Ozone

Figures V-5-5 through V-5-10 show the diurnal trends of observed and predicted 8-hour ozone for the each day from May 1st through September 30th, 2012 for six stations following a transport route from the coastal area of the Basin to inland Crestline and Redlands. Supplemental diurnal observed and predicted 8-hour ozone for all remaining air quality sites are provided as Attachment 7 to this appendix. The geographical bias is clearly present in the time series – over-prediction in West Los Angeles, and under-prediction in the inland area. However, the under-prediction of peak concentration is not rare in photochemical modeling. In fact, the District has successfully demonstrated its capability to predict episodic events better than other agencies

in the nation, including the National Oceanic and Atmospheric Administration (NOAA)/EPA, the official air quality forecast agency.

Overall, it is important to note that the effects of prediction biases or errors are mitigated by the use of relative response factors for the attainment analysis.

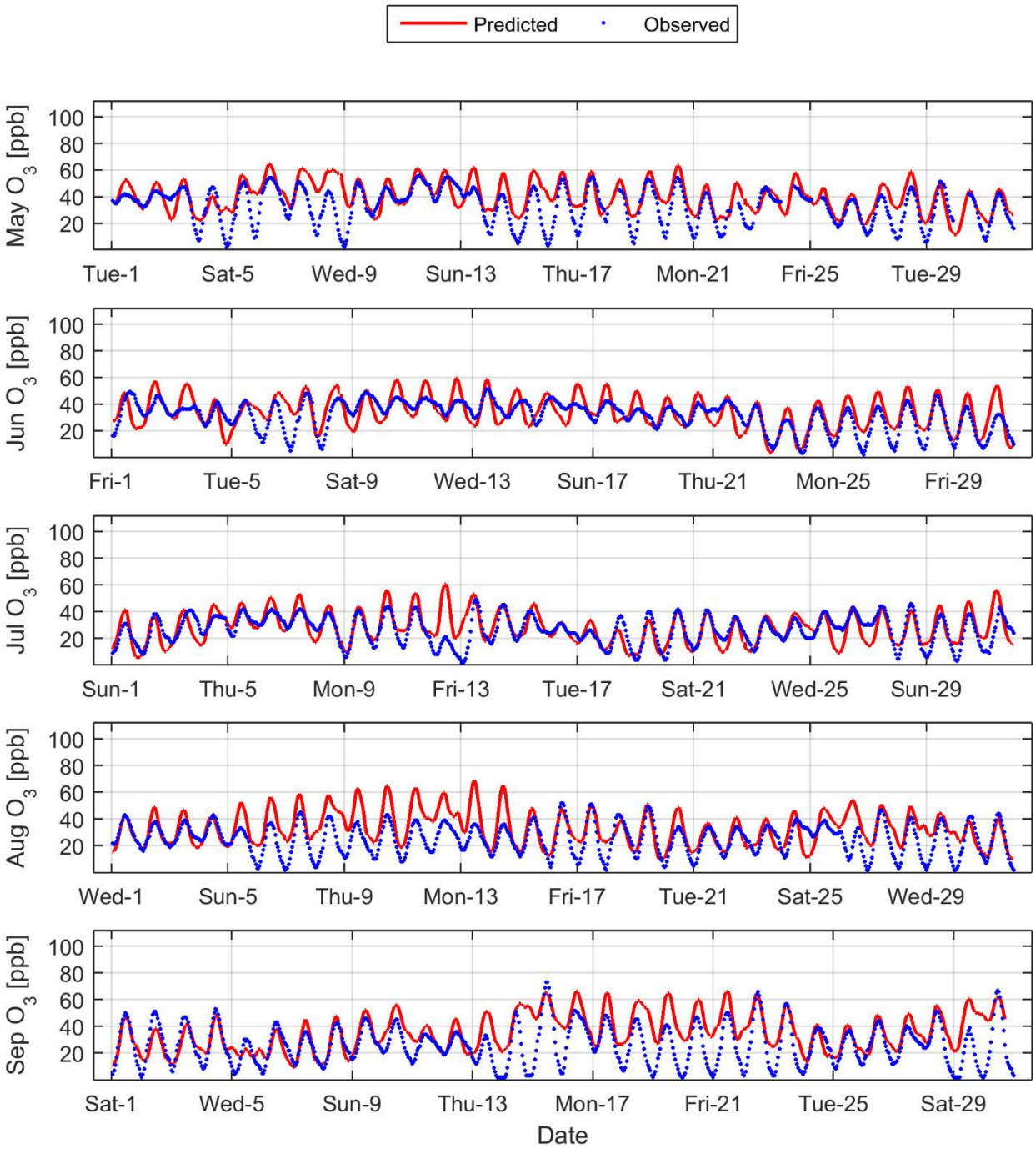

FIGURE V-5-5

Time Series of Observed Vs.Predicted 8-Hour West Los Angeles Ozone

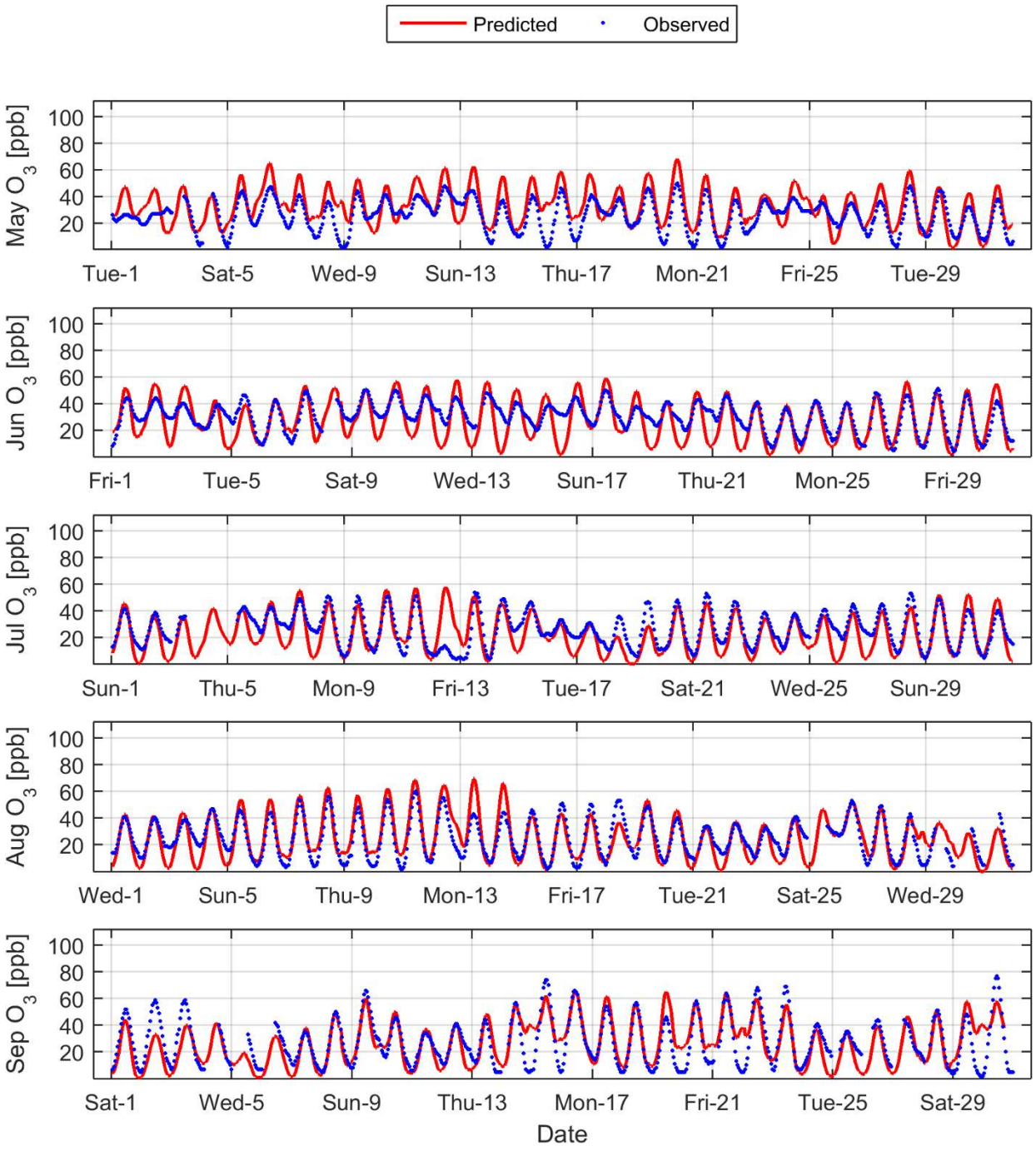

FIGURE V-5-6

Time Series of Observed Vs.Predicted 8-Hour Central Los Angeles Ozone

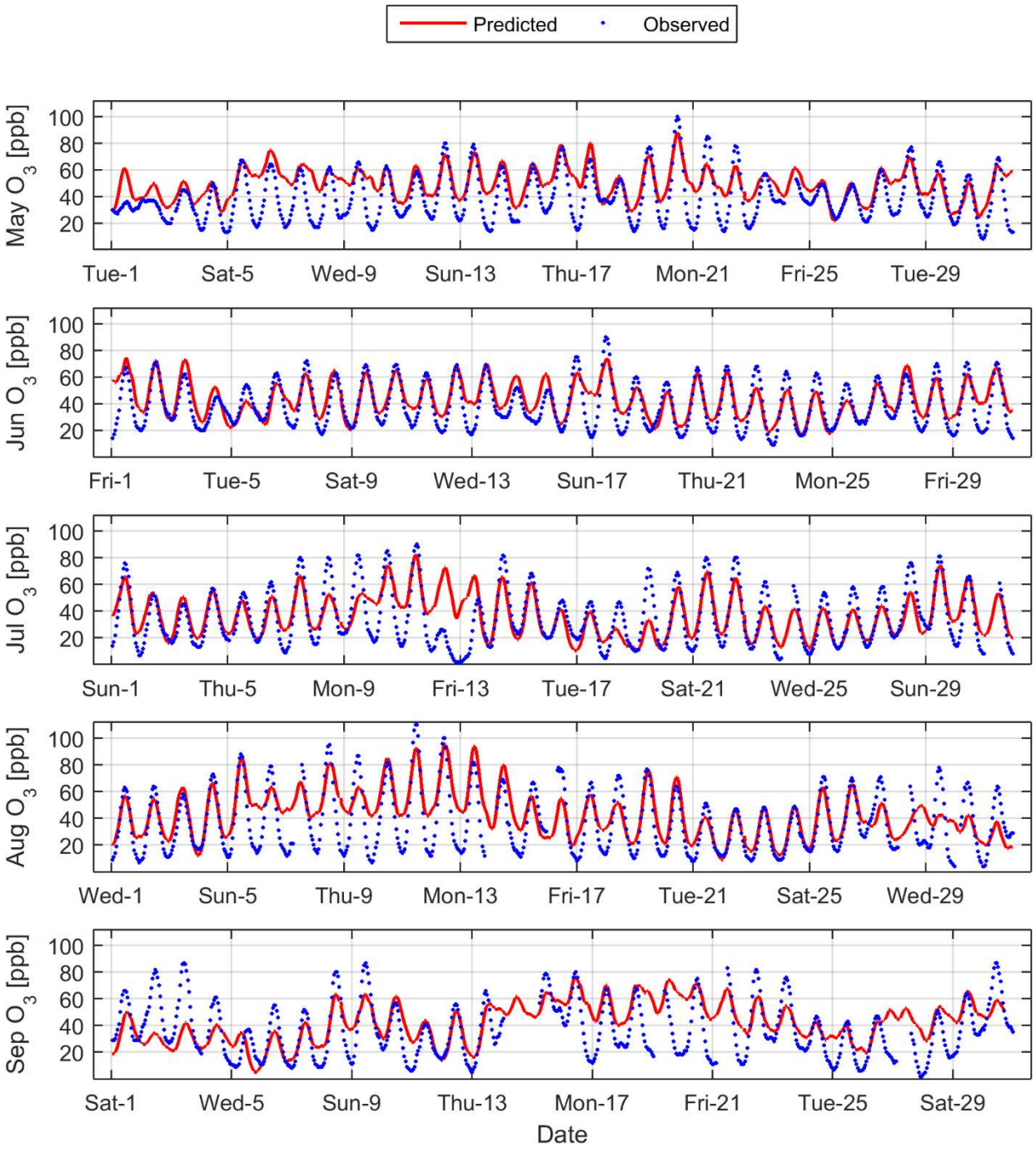

FIGURE V-5-7

Time Series of Observed Vs. Predicted 8-Hour Glendora Ozone

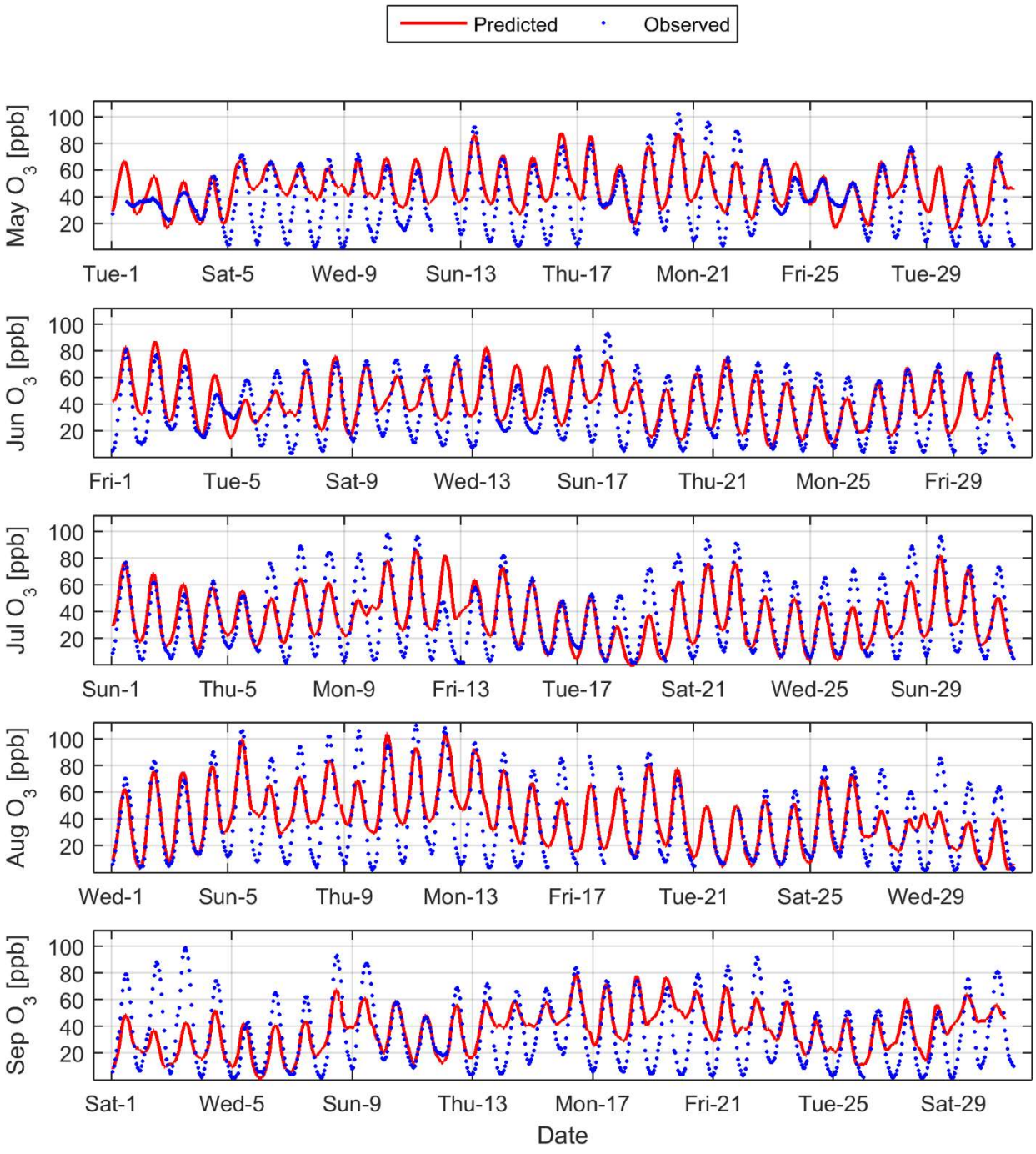

FIGURE V-5-8

Time Series of Observed Vs. Predicted 8-Hour Fontana Ozone

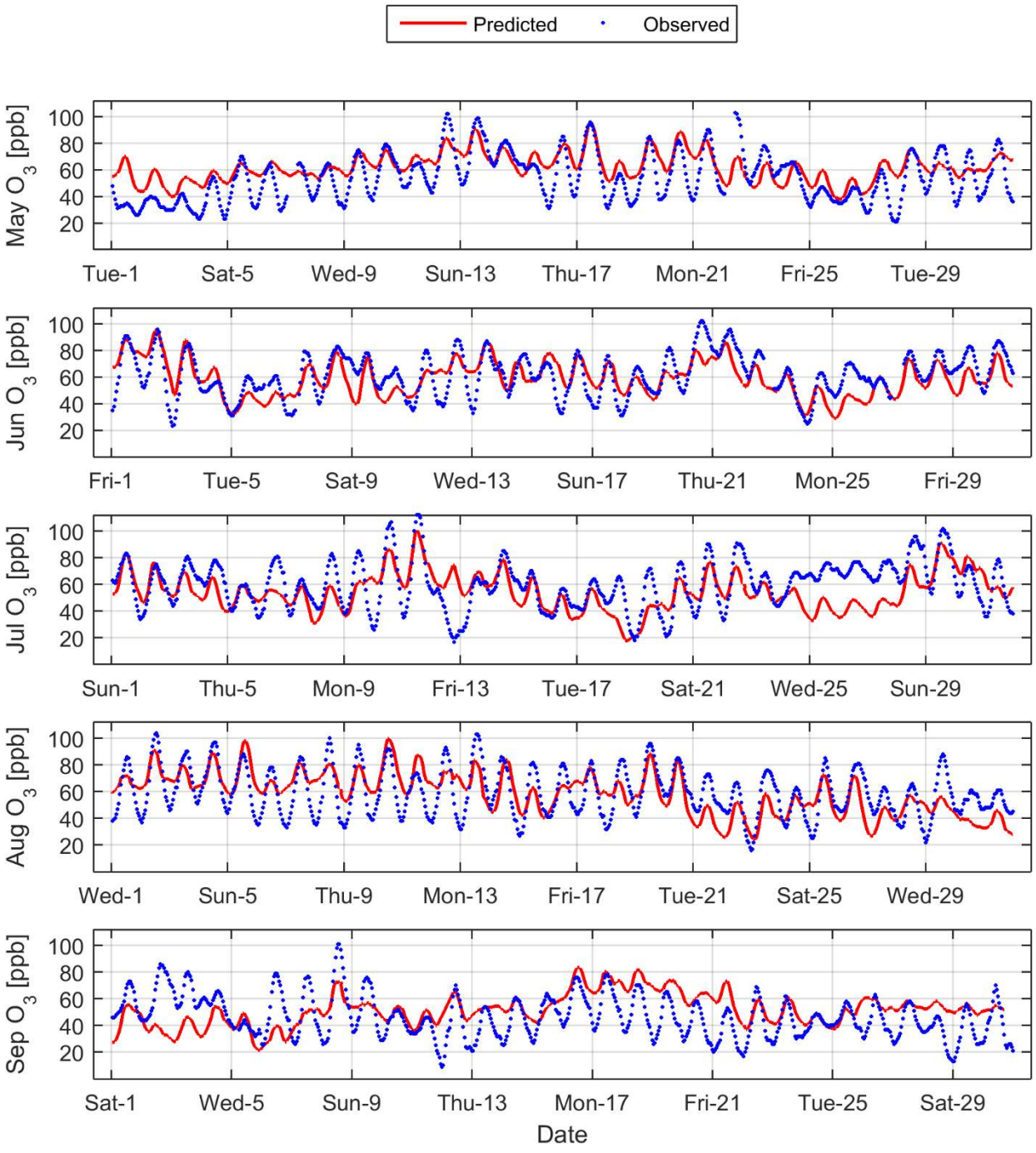

FIGURE V-5-9

Time Series of Observed Vs. Predicted 8-Hour Crestline Ozone

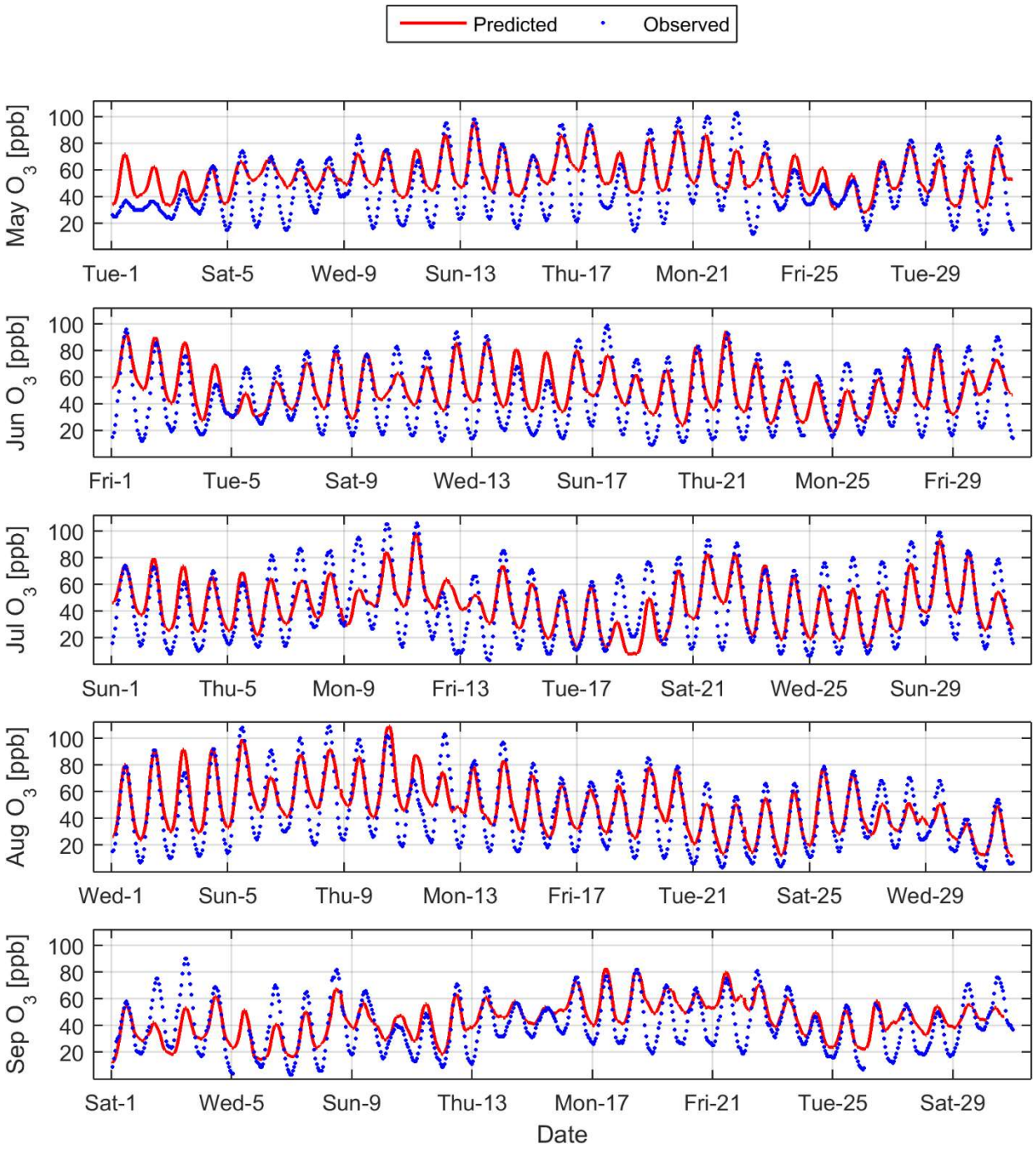

FIGURE V-5-10

Time Series of Observed Vs.Predicted 8-Hour Redlands Ozone

Ozone Modeling Approach

The set of 153 days from May 1st through September 30th, 2012 was simulated and analyzed to determine daily 8-hour average maximum ozone for the 2012, 2023, and 2031 emissions inventories. A set of simulations with incremental VOC and NOx emissions reductions from 2023 and 2031 baseline emissions was generated to create ozone isopleths for each station in the Basin. The ozone isopleths provide updated guidance for the formulation of the future control strategies.

Ozone RRFs were calculated using the ratio methodology described in the EPA modelling guidance (U.S. EPA, 2014). The RRF calculation has been changed significantly from the previous guidance. The guidance released in 2007 provided the framework for the 2012 AQMP (U.S. EPA, 2007). One of the biggest differences is the number of days accounted for in the RRF calculation. The 2007 guidance calls for all the days that meet the selection criteria to be included in the RRF calculation. The criteria required that the un-paired peak error was less than 20% ((Pred – Obs) /Pred ≤ 0.2), the predicted daily max was within 20 % of the site specific design value ((Pred – DV)/DV) ≤ 0.2), and the prediction was higher than the federal standard of 75 ppb. The new approach recommended by the EPA (2014) recommends that only the top 10 days are included in the RRF. The model performance criteria requiring that the unpaired peak error is less than 20% is still employed along with requiring that all values included in the RRF have predictions greater than or equal to 60 ppb. The RRF is undefined at sites with less than 5 days that meet this criteria. The number of days that meet the selection criteria are different from station to station, depending on model prediction accuracy and air quality characteristics. In the case of Crestline, the number of days that qualified for the RRF in the 2007 guidance was approximately 50 days, more than half of the entire simulation period, whereas the new approach uses only 10 days.

In the 2012 AQMP, the maximum modelled grid cell in the 3x3 grid centered at each station was retrieved from the base and future simulations. In the current AQMP, the maximum modelled value in the 3x3 grid surrounding each station is compared to the corresponding grid position in the future year. In addition, the definition of a neighboring grid is fixed to 3X3, regardless of the grid resolution. For example, the 2007 guidance required a 7X7 grid surrounding each station for the default AQMP 4 km grid resolution. Overall, the new guidance promotes control strategies to be focused on high episode days rather than the average high days of a season.

Future Ozone Air Quality

The 2016 AQMP addresses both the 2007 standard of 75 ppb and the 1997 standard of 80 ppb, of which attainment dates are 2031 and 2023, respectively. Table V-5-9 summarizes the results of the updated ozone simulations. Included in the table are the 2023 ozone baseline and 2023 controlled ozone projections from the 2012 AQMP ozone attainment demonstration submitted to U.S. EPA as part of the SIP. The 2012 AQMP concluded that NOx emission must be reduced by more than 70% of baseline emissions to meet the 80 ppb standard by 2023.

The Final 2016 AQMP baseline ozone simulations reflect the changes made to the 2023 and 2031 baseline inventories. The Final 2016 AQMP summer planning inventory for 2023 has a similar VOC/NOx emissions

ratio, (1.49 vs. 1.37) although total tonnages of both precursor emissions are lower than presented in the 2012 AQMP. Reduced 2023 baseline VOC and NOx emissions in the 2016 AQMP relative to the 2012 AQMP reflects the impact of rules and regulations adopted after the 2012 AQMP, updated methodologies to estimate emissions, and revised growth projections.

Both 2023 and 2031 baseline scenarios without any additional reduction beyond already adopted measures do not lead to attainment, indicating additional emission reductions are necessary to meet the standards. NOx must be reduced by 45% and 60% beyond the 2023 and 2031 baseline, respectively. With proposed controls in place, the updated analysis demonstrates that all stations in the Basin will meet the 1997 federal 8-hour ozone standard by 2023 and the 2007 standard by 2031. The proposed reduction is significantly less than the estimates presented in the 2012 AQMP. Several factors contributed to this change. First, year-to-year, design values are declining, indicating improvements in air quality. This is partly due to the Great Recession, which reduced emissions during 2010 to 2014, the period used in the 5-year weighted design value. The decline in design values are also an indication of the efficacy of control strategies proposed and implemented in Basin. Secondly, the unforeseen economic downturn lowered the baseline inventory substantially; therefore, even though the carrying capacity is somewhat similar, the percentage reduction is higher. Thirdly, the new attainment demonstration focuses on high days, as discussed in the RRF calculation. The high days are assumed to be caused by local emission sources rather than transport from out-of-state or from higher altitudes. Therefore, the controls on local emission sources are more effective as the model is more responsive to reductions.

Note that the implementation thresholds are 84.9 ppb for the 1997 standard and 75.9 ppb for the 2008 standard. This is due to the unit (0.08 ppm) and the number of decimal points written in the CAA when referencing the 1997 standard along with the truncation approach associated with the 2008 standard.

TABLE V-5-9

Model-Predicted 8-Hour Ozone Design Values (ppb)

Station	2012 AQMP		2016 AQMP			
	2023 Baseline	2023 Controlled Scenario	2023 Baseline	2023 Controlled Scenario	2031 Baseline	2031 Controlled Scenario
Azusa	95	77	77	70	75	62
Banning	94	73	89	78	85	71
Crestline	107	81	93	81	89	72
Fontana	104	81	96	84	92	75
Glendora	107	84	93	83	90	74
Lake Elsinore	85	66	74	65	70	58
Perris	88	66	80	70	76	62
Pomona	100	80	83	75	81	67
Redlands	103	77	95	82	90	73
Reseda	90	73	79	71	75	64
Riverside	100	77	89	78	86	69
San Bernardino	108	83	90	78	86	70
Santa Clarita	94	73	84	76	80	68
Upland	106	83	92	82	89	73

**Burbank and Pasadena do not have 2012 base-year design values due incomplete measurement data in one or multiple years between 2010 and 2014.

Spatial Projections of 8-Hour Ozone Design Values

The spatial distribution of ozone design values for the 2012 base year is shown in Figure V-5-11. Future year ozone air quality projections for 2023 and 2031 with and without implementation of all proposed control measures are presented in Figures V-5-12 through V-5-15. The predicted ozone concentrations will be significantly reduced in the future years in all parts of the Basin with the implementation of proposed control measures in the South Coast Air Basin. Future design values are predicted from model RRFs and measured base-year design values. Future design values are then interpolated using a natural neighbor interpolation to generate the interpolated fields.

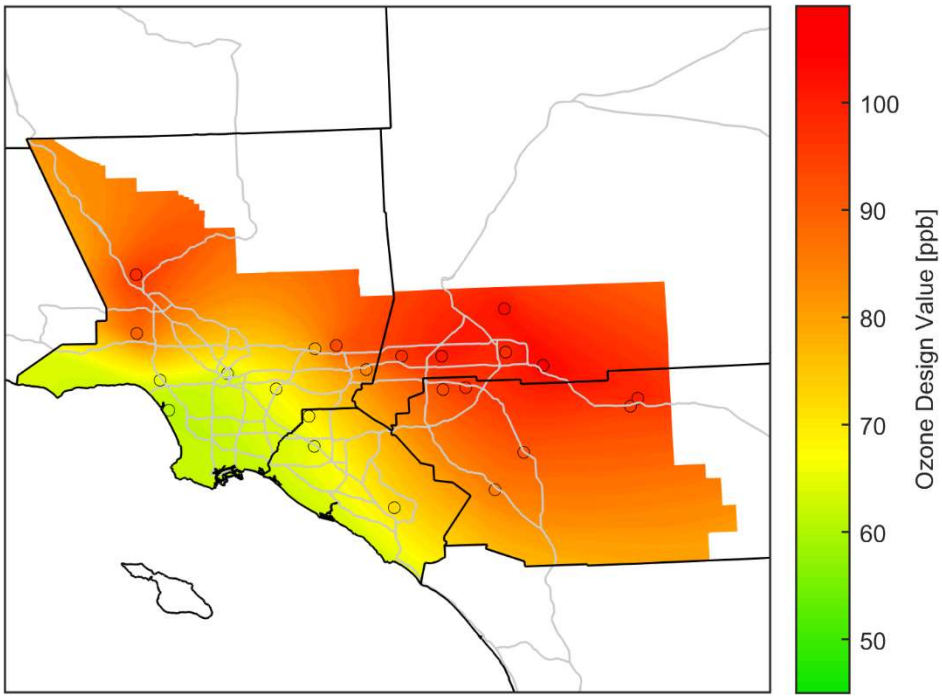

FIGURE V-5-11

Interpolated 2012 8-Hour Ozone Design Values (ppb). The Circles Indicate Air Monitoring Stations.

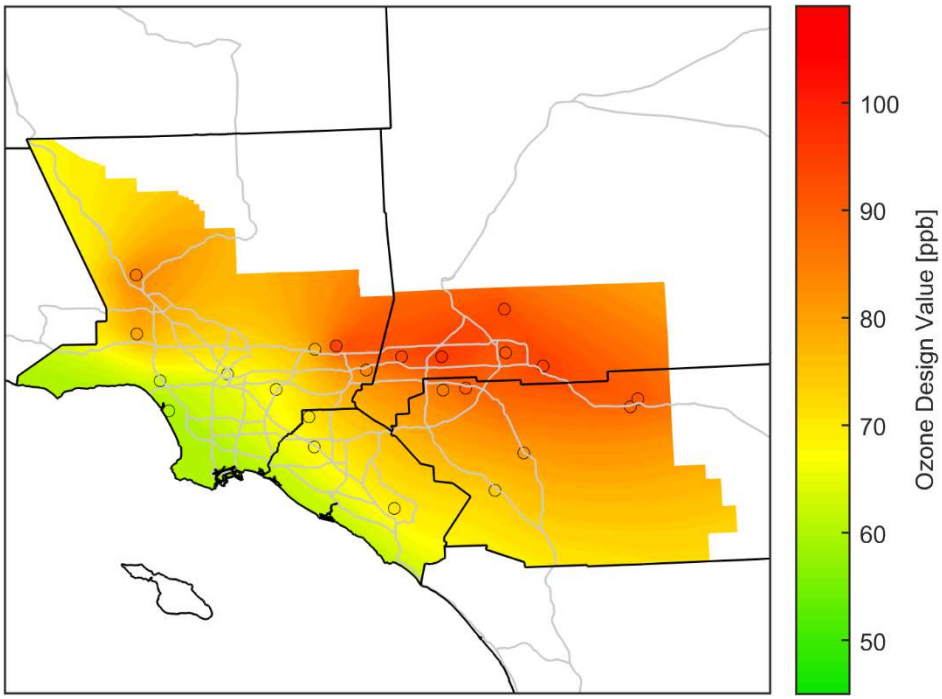

FIGURE V-5-12

Interpolated 2023 Baseline 8-Hour Ozone Concentrations (ppb)

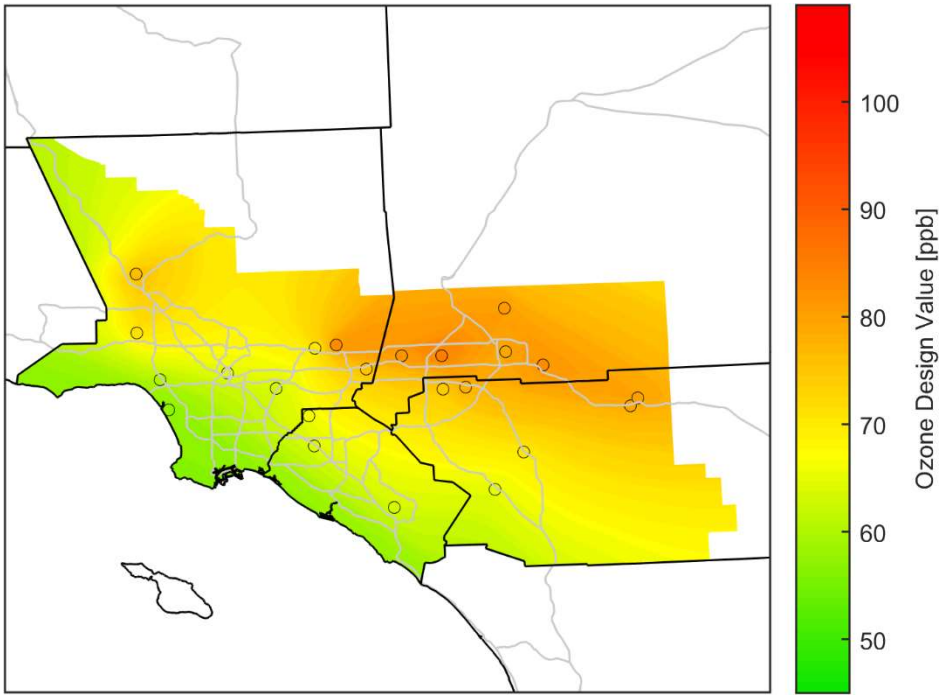

FIGURE V-5-13

Interpolated 2023 Controlled 8-Hour Ozone Concentrations (ppb)

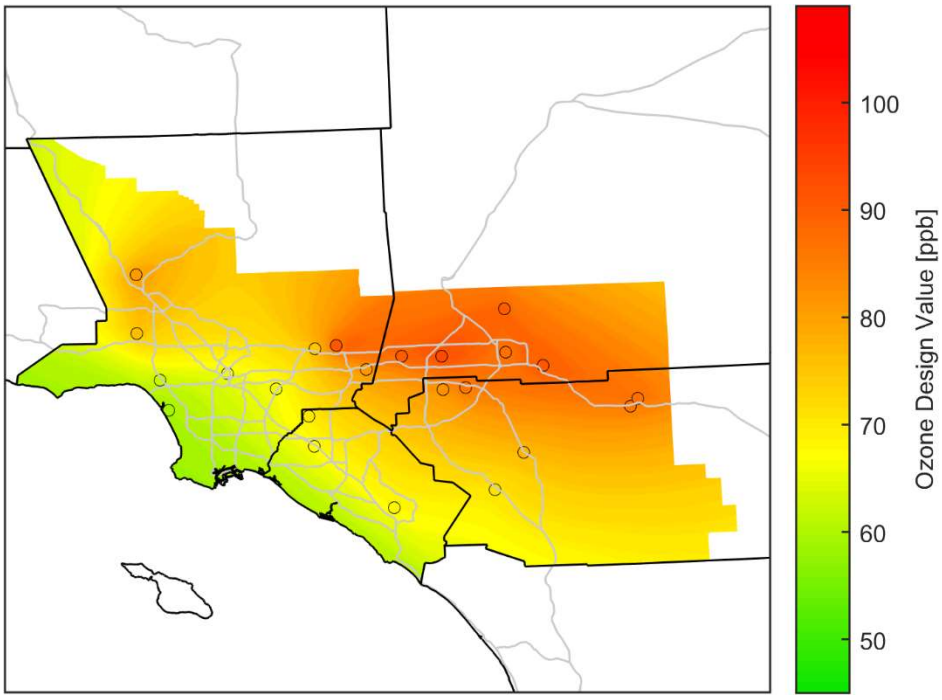

FIGURE V-5-14

Interpolated 2031 Baseline 8-Hour Ozone Concentrations (ppb)

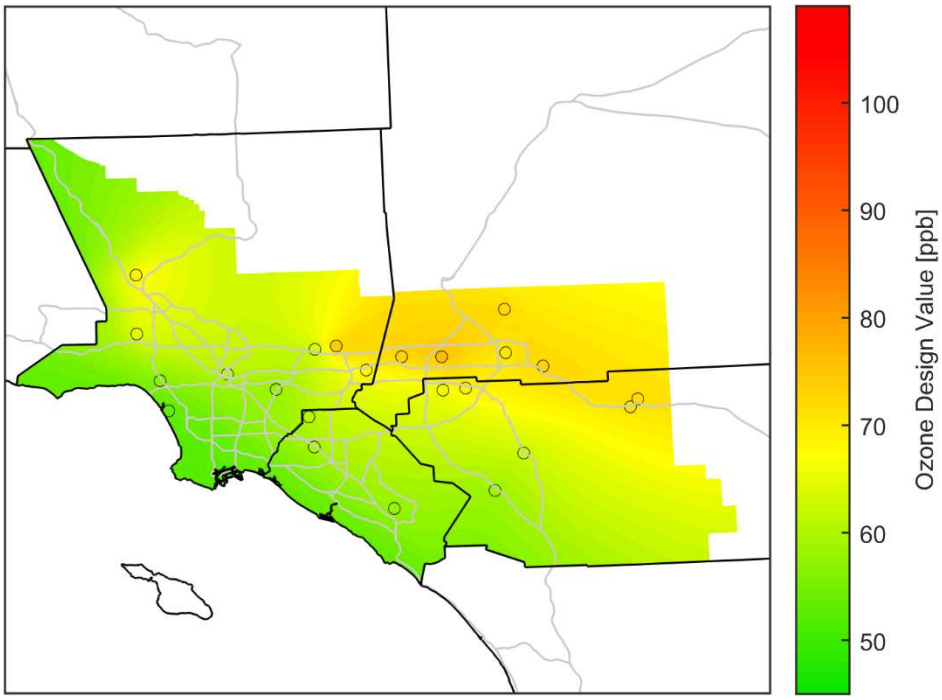

FIGURE V-5-15

Interpolated 2031 Controlled 8-Hour Ozone Concentrations (ppb)

Coachella Valley

The Coachella Valley is currently a nonattainment area for the 2008 8-hour ozone NAAQS (0.075 ppm). With an attainment due date of July 20, 2027, emission reductions required to meet the standard need to be in place by the end of 2026 and the modeling demonstration must show attainment in 2026. The 2026 baseline future projection, with no additional emissions controls beyond rules and regulations already adopted, still exceed the 2008 standard at Palm Springs (0.079 ppm), but not at Indio (0.075 ppm). However, further control measures applied to upwind South Coast Air Basin emission reductions will be in place by 2023, as described in Chapter 4, in order for the Basin to meet the 1997 ozone NAAQS (0.08 ppm). With these additional Basin reductions, the Coachella Valley is projected to be below the 2008 NAAQS in 2023, three years before the 2026 deadline, with all Coachella Valley design values predicted to be below 0.075 ppm. Thus, attainment of the 2008 8-hour ozone NAAQS in the Coachella Valley is ensured by the anticipated NOx reductions from the Basin's control strategy designed to meet the 1997 ozone standard in the Basin.

Unmonitored Area Analysis

An unmonitored area analysis was conducted to estimate the design values at unmonitored locations. This analysis uses both the measurement design values and the modelled ozone profiles throughout the modelling domain to estimate 8-hour daily max ozone design values at unmonitored locations.

Five-year weighted design values were calculated for all monitoring stations within and in the vicinity of the modelling domain for the 2010 to 2014 period. These measured design values were then interpolated spatially using a natural-neighbor interpolation based on a Voronoi tessellation. Figure V-5-16 and Figure V-5-17 illustrates the spatial distribution of 8-hr Ozone 5-year weighted design values. Only stations that meet the data completeness requirement for each of the 5 years were included in the analysis.

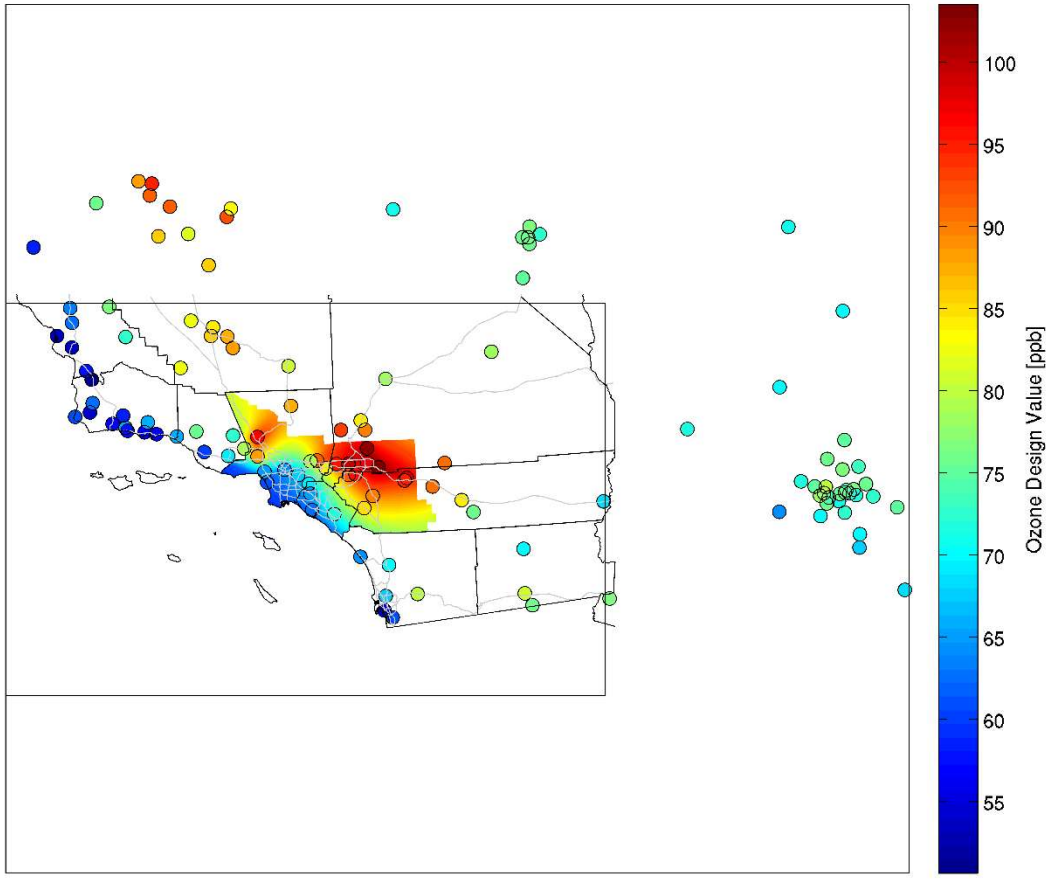

FIGURE V-5-16

8-hr Daily Maximum Ozone Design Values in 2012. Interpolated Fields and Monitor Data.

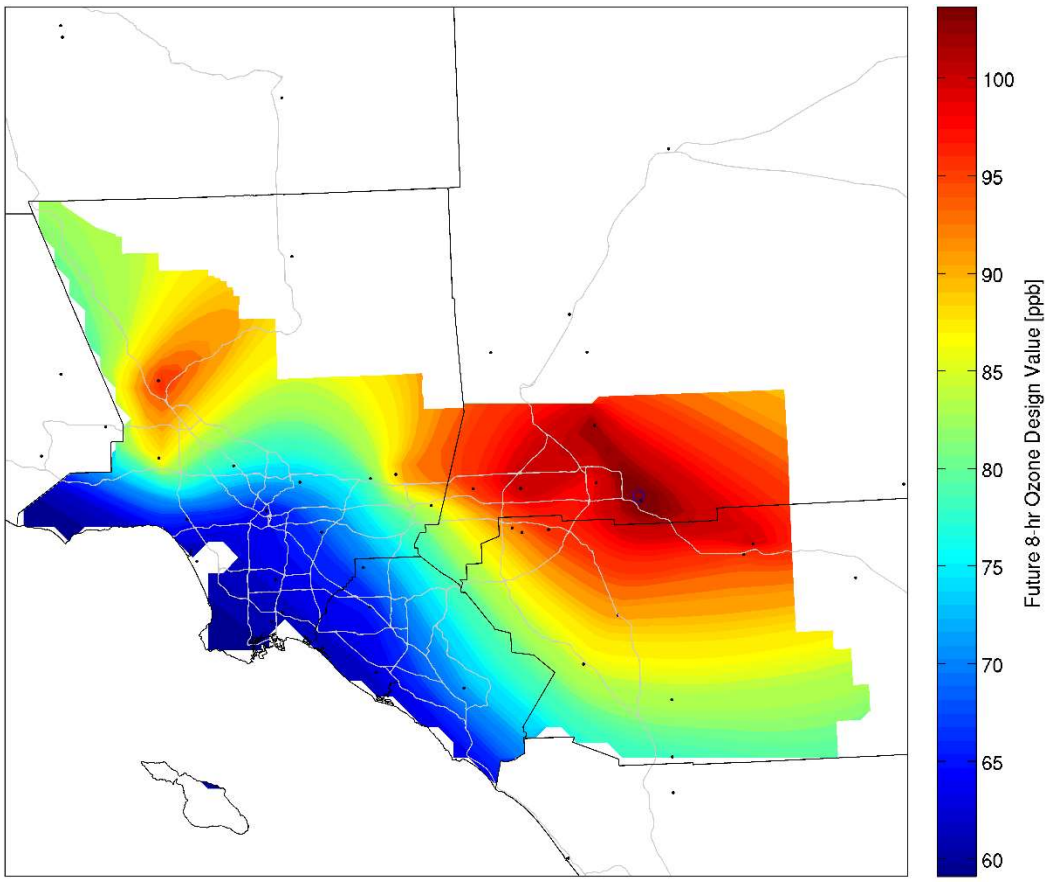

FIGURE V-5-17

Interpolated 8-hr Daily Maximum Ozone Design Values in 2012.

Domain-wide relative response factors (RRFs) can be calculated to forecast ozone design values in future years. The top 10 highest daily-maximum 8 hour concentrations in the model data are averaged in the base and future years. The RRF is the quotient of this average in the future year and this average in the base year. Only top ten daily-maximum 8-hour concentrations that are greater or equal to 60 ppb are used in the RRF. RRFs are still calculated if at least 5 daily measurements in the top ten values are greater or equal to 60 ppb. However, the RRF cannot be calculated if there are less than 5 daily measurements exceeding 60 ppb in either the base or future years. The domain-wide RRF for the 2023 model simulation and the 2031 model simulation are presented in Figure V-5-18 and Figure V-5-19, respectively.

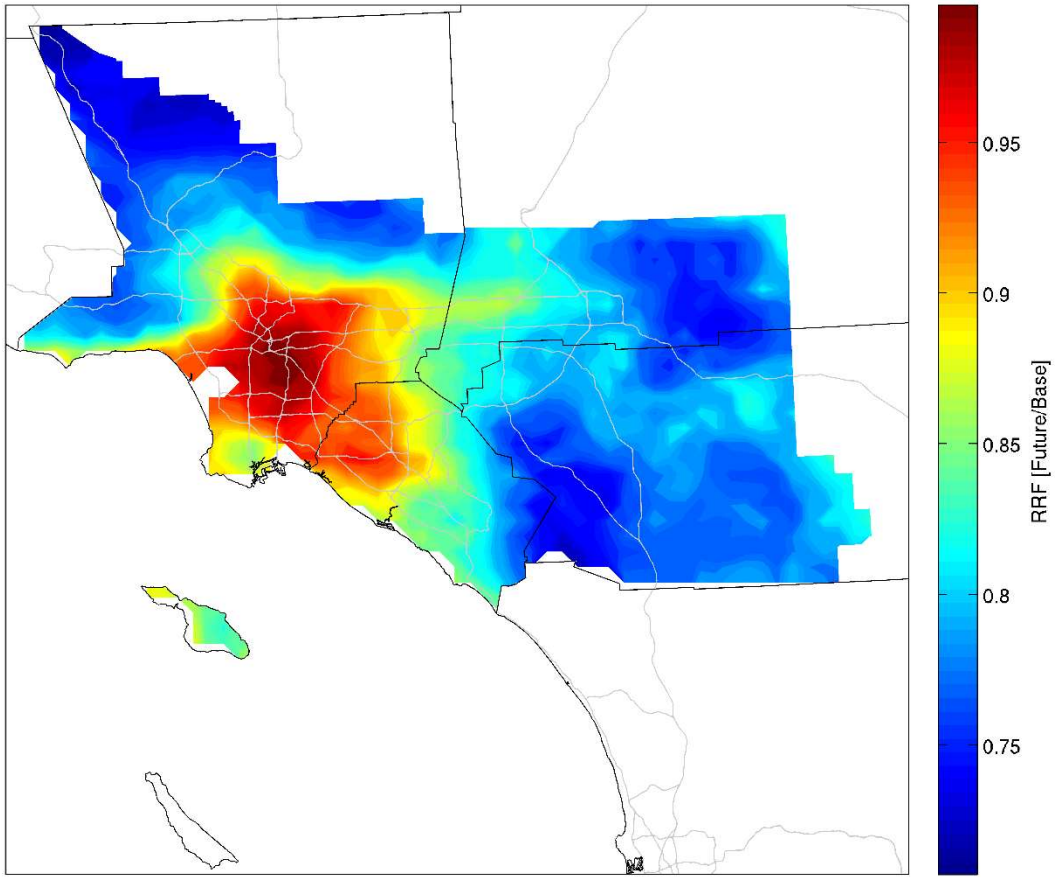

FIGURE V-5-18

2023 RRF Fields. White Areas within the Basin Indicate that There Are Not Enough Measurements Greater Than or Equal to 60 ppb to Calculate a RRF.

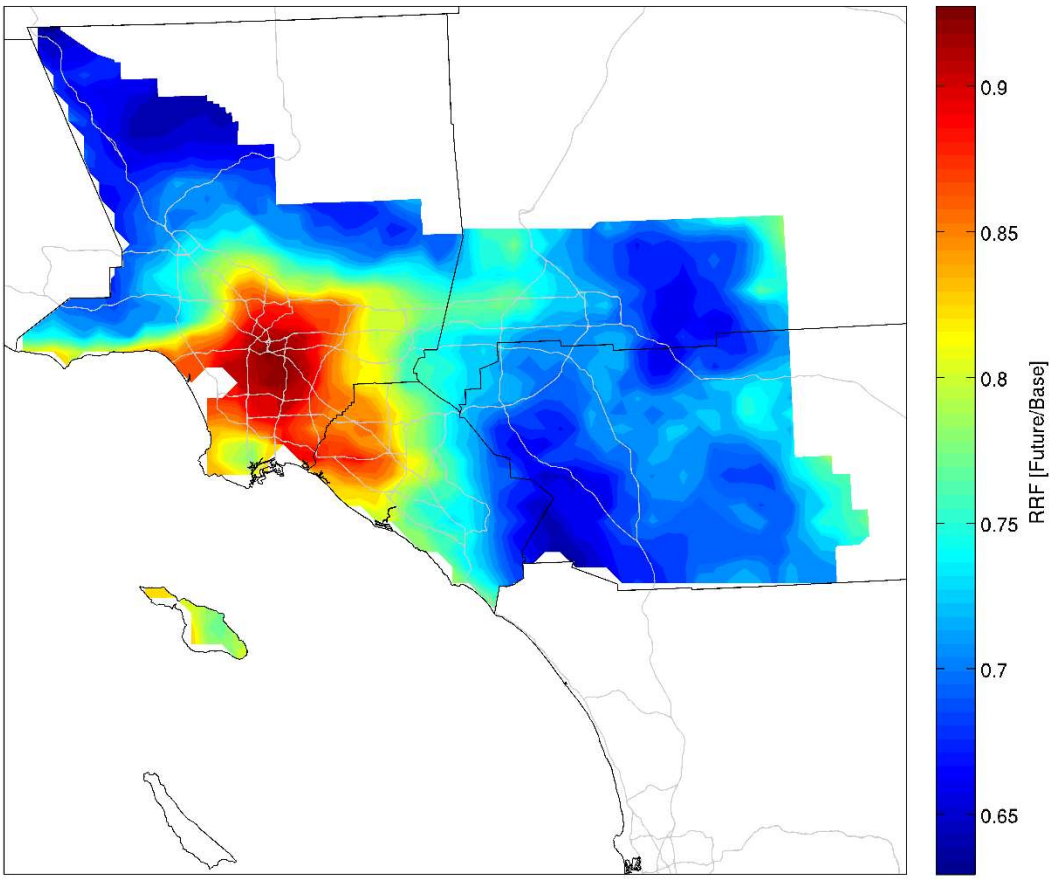

FIGURE V-5-19

2031 RRF Fields. White Areas within the Basin Indicate that There Are Not Enough Measurements Greater Than or Equal to 60 ppb to Calculate a RRF.

The calculated RRF fields are then used to project the interpolated measurement field to simulate future year concentrations. Plots illustrating the future ozone predictions for 2023 and 2031 control scenarios are presented below in Figures V-5-20 and V-5-21.

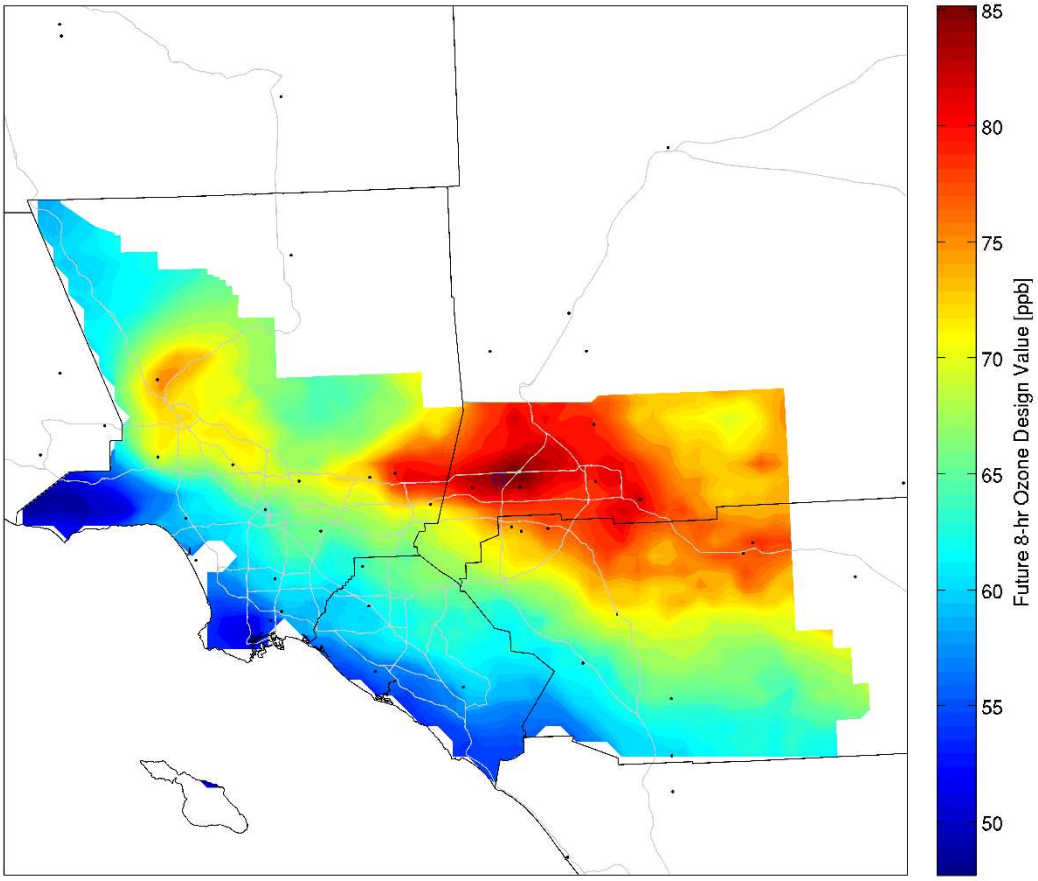

FIGURE V-5-20

2023 Controlled Ozone Predictions throughout the Modelling Domain. The Basin Maximum Concentration is 85.7 ppb. The Blue Circle Indicates the Cell with the Highest Projected Ozone Concentration.

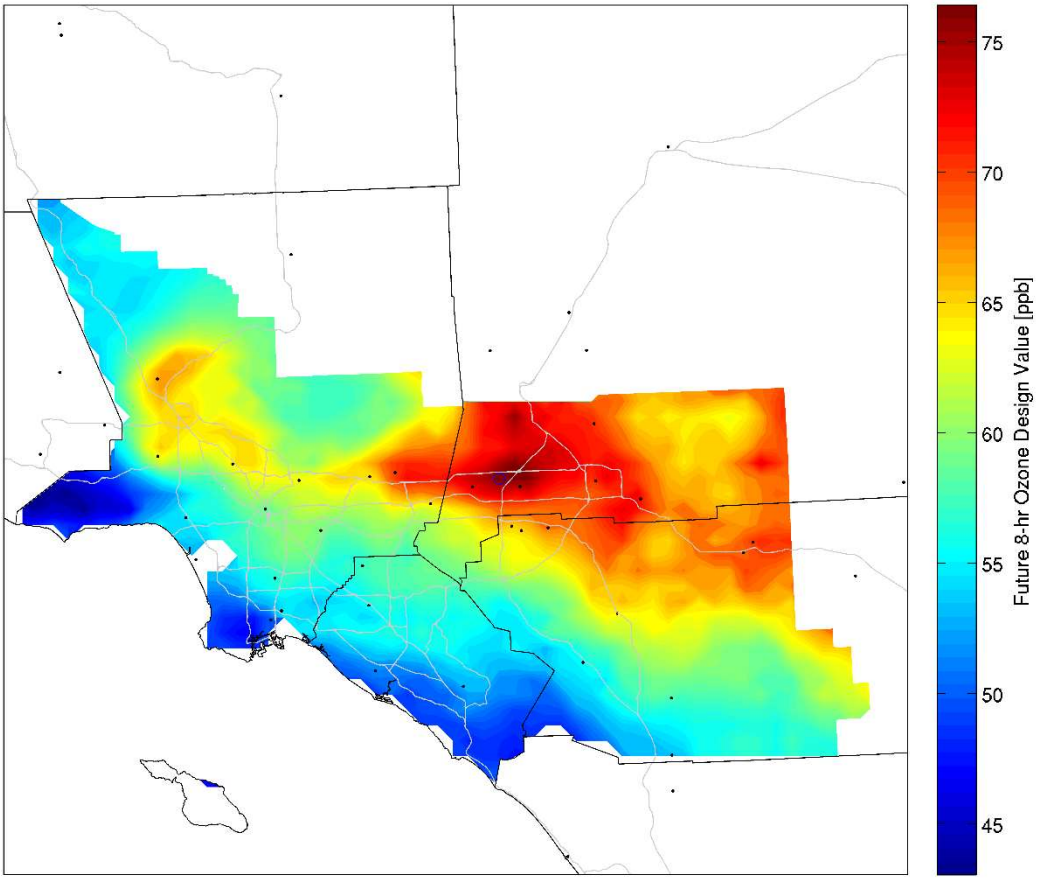

FIGURE V-5-21

2031 Controlled Ozone Predictions throughout the Modelling Domain. The Basin Maximum Concentration is 76.9 ppb. The Blue Circle Indicates the Cell with the Highest Projected Ozone Concentration.

Controls do not reduce ozone concentrations uniformly and therefore, the location with the largest Ozone concentration shifts in future years. Redlands has the highest 2012 5-year weighted design value. In 2023 and 2031, the unmonitored area analysis predicts that the Fontana area will have the largest design value in the Basin. This is consistent with the attainment demonstration, which focuses solely on monitor design values.

The most significant uncertainty in the unmonitored area analysis arises from the choice of interpolation scheme. Measured design values were interpolated using different interpolation methods. They are natural-neighbor interpolation based on a Voronoi tessellation, a nearest-neighbor interpolation scheme, a linear interpolation scheme, "1/R" inverse distance weighting interpolation schemes using several different number of neighbors, and "$1/R^2$" inverse distance weighting interpolation schemes using several different number of neighbors. The performance of each interpolation scheme was evaluated by performing the interpolation with all stations except one and comparing the predicted value in the location of the missing station and the actual design value at that site. This procedure was repeated for each station and interpolation scheme. The

natural-neighbor interpolation produced the lowest residual sum suggesting that it best represents the design values in the modelling domain.

A more comprehensive unmonitored area analysis was conducted using the EPA MATS software. The same procedure as above was repeated in MATS using the default inverse distance weights interpolation to project future design values. A gradient adjusted approach was also performed by adjusting measured 5-year design values by the modelled spatial gradient and interpolating to create a gradient adjusted baseline concentration field. Spatially dependent RRFs were then used to forecast future design values. Forecasted future ozone design values were similar to concentrations predicted with our initial analysis. In 2023 and 2031, Rancho Cucamonga was predicted to have the highest ozone design values at 85.7 and 76.9 ppb, respectively. See Table V-5-10. The differences between the in-house post-processing analysis and the MATS approach were mostly resulted from the spatial interpolation scheme. The in-house post-processor used the Voronoi tessellation per the EPA guidance, while the MATS used inverse-distance weighting scheme since the Voronoi tessellation is not available.

TABLE V-5-10

Comparison of Highest Basin Design Values for Unmonitored Area Analysis. In-House Analysis Summarizes the Results Shown in Previous Figures. Using the MATS Software, this Analysis was Repeated (Left Column) and Enhanced (Right Column).

	In-House Analysis	MATS Software	
Simulation	**Max DV in Basin (ppb)**	**Max DV in Basin (ppb)**	**Max DV in Basin (ppb) gradient adjusted value**
Base Year	104.3 (Redlands)	102.7 (Redlands)	107.6 (Yucaipa/Oak Glen)
2023 Control	85.7 (Rancho Cucamonga)	88.3 (Rancho Cucamonga)	85.6 (Fontana)
2031 Control	76.9 (Rancho Cucamonga)	79.7 (Yucca Valley)	76.9 (Rancho Cucamonga)

Looking Beyond 2031

In 2015, the U.S. EPA lowered the federal 8-hour ozone standard to 70 ppb. Recent 8-hour ozone rule implementation guidance requires that a SIP revision with an updated attainment demonstration and control strategy be submitted to U.S. EPA no later than four years after designation. The Basin will likely be designated as an “extreme” nonattainment area for the new standard in 2017, consistent with the classification of the 75 ppb standard. Thus, the deadline for attainment of the 70 ppb standard is 20 years after designation (likely 2037)—6 years after the attainment deadline for the 75 ppb federal standard. It is critical to conduct a preliminary analyses to assess the need for potential adjustments to the overall control strategy when considering this new standard and deadline. The preliminary projections, based upon ozone “isopleths” developed for the 2031 emission scenarios indicate that the 2037 Basin NOx carrying capacity to meet the 70 ppb standard could be as low as 75 TPD (Figure V-5-22). This is an additional 62 percent of NOx reduction

beyond the projected 2037 baseline and approximately 21 TPD of additional NOx emission reductions between 2031 and 2037. 8-hour ozone isopleths for all Basin sites exceeding the standard are provided in Attachment 4.

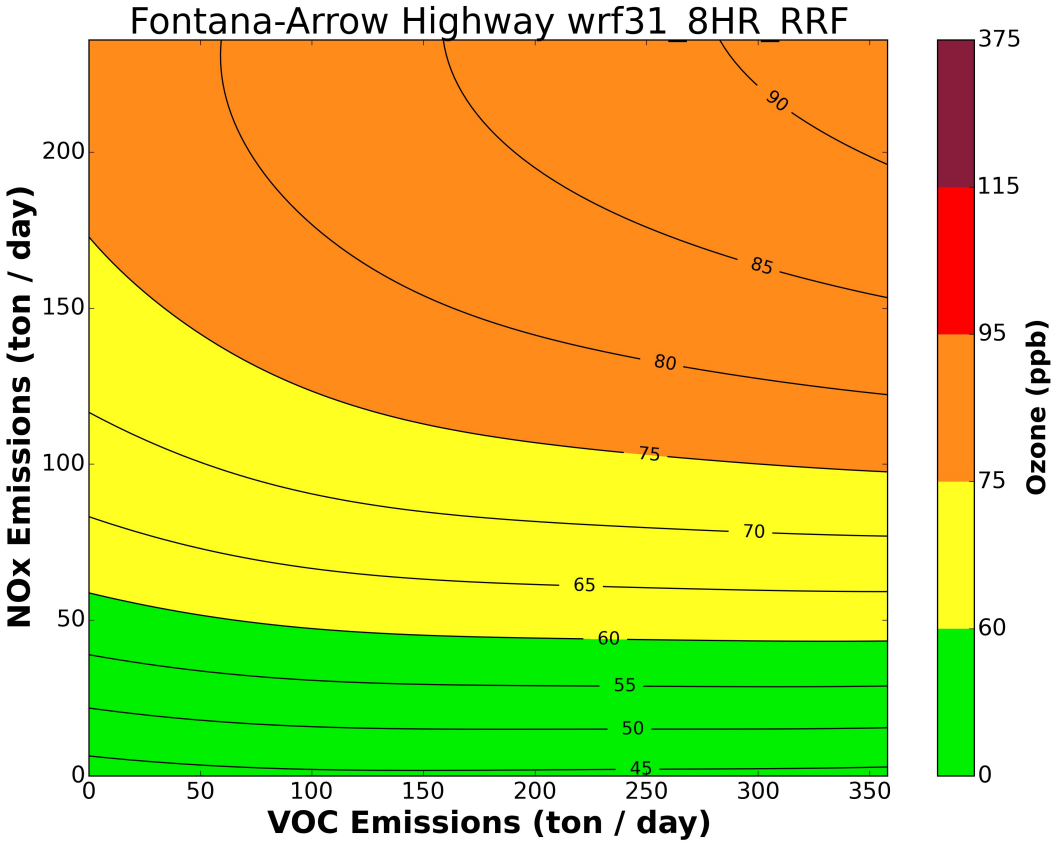

FIGURE V-5-22

2031 Fontana 8-Hour Ozone Isopleth

Weight of Evidence Analysis & Stress Tests

Spatial Perturbation of Emissions

Two emissions scenarios were investigated to evaluate the sensitivity of the spatial distribution of emissions on the resulting air quality. The location of emissions from area sources were shifted from the base configuration using two methods: Case 1) area source emissions were shifted five cells west and five cells south in the modelling domain—a total of 20 km in each direction and Case 2) area source emissions were randomly shuffled by one grid cell at a time along the east-west axis and the north-south axis. The dual axis shuffle is executed a total of 8 times, with the restriction that the max distance moved is 10 cells in any direction. The result is a distribution of emissions relocated from zero to 10 cells in any direction. Figure V-

5-23 displays the number of cells that travel a specified distance along the east-west and north-south direction.

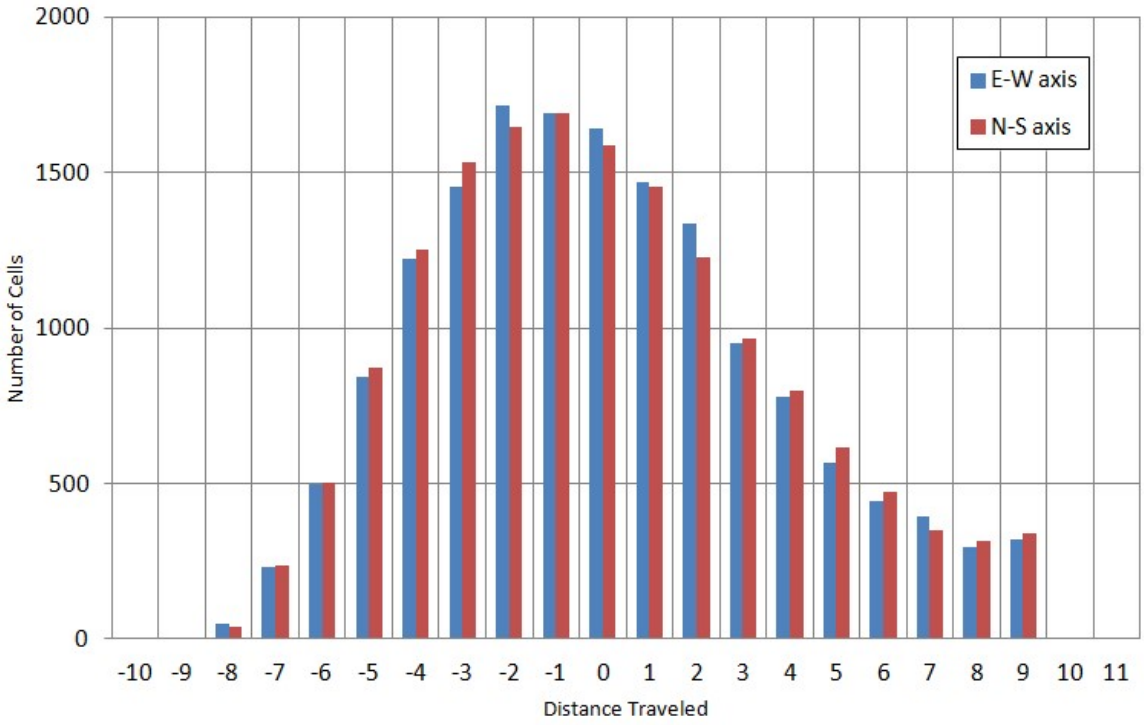

FIGURE V-5-23

Distance Traveled in the "Case 2" Spatial Emissions Perturbation

CMAQ was then used to predict base-year ozone concentrations resulting from these perturbed emission fields. Differences between ozone predicted with unperturbed emissions and perturbed emissions depend on location. At some monitoring stations, differences are significant. Table V-5-11 displays the magnitude of changes in model-output predicted fourth-highest daily maximum ozone values for Case 1 and Case 2.

TABLE V-5-11

Percent Difference in Model Predicted 4th Highest Daily Maximum Ozone Values in the Base Year

Station	Case 1 [%]	Case 2 [%]
Anaheim	0.8	6.8
Azusa	14.3	16.0
Banning	6.3	0.0
Burbank	15.8	13.5
Los Angeles	11.7	11.7
Compton	8.8	9.6
Crestline	-0.1	0.1
Costa Mesa	-1.1	7.2
Lake Elsinore	4.6	1.8
Fontana	5.7	2.4
Glendora	9.7	11.2
Long Beach Hudson	8.9	9.9
La Habra	3.7	6.0
LAX	8.7	7.6
Long Beach Hudson	9.9	12.5
Mira Loma	3.2	2.3
Mission Viejo	0.9	6.8
Pasadena	13.0	10.6
Perris	3.6	1.1
Pico Rivera	6.7	8.9
Pomona	4.1	3.6
Redlands	1.8	3.7
Reseda	5.2	4.4
Riverside	3.4	1.4
Santa Clarita	1.3	3.3
San Bernardino	0.2	0.5
Temecula	7.3	2.6
Upland	5.9	2.3
West Los Angeles	9.0	8.7

Large changes in model predictions throughout the Basin underscore the importance of spatially allocating area source emissions where they are generated. A subsequent analysis can be used to estimate changes in future design values (Table V-5-12) that would result from each perturbed emission scenario.

TABLE V-5-12

Estimated Difference in Future Design Values (Emissions Perturbation – Unperturbed Emissions)

Station	Case 1 2023 [ppb]	Case 1 2031 [ppb]	Case 2 2023 [ppb]	Case 2 2031 [ppb]
Anaheim	1.3	1.3	-0.2	-0.2
Azusa	2.5	2.4	-3.0	-3.0
Banning	0.4	0.4	-1.1	-1.0
Burbank	-0.7	-0.7	0.0	0.0
Compton	0.0	0.0	0.0	0.0
Crestline	-0.5	-0.5	1.1	1.1
Elsinore	0.3	0.3	0.1	0.1
Fontana	-4.6	-4.5	-3.1	-3.0
Glendora	-1.7	-1.7	-3.8	-3.7
La Habra	1.2	1.2	1.5	1.5
LAX	-0.6	-0.6	-0.1	-0.1
Mira Loma	-0.9	-0.9	-0.7	-0.7
Mission Viejo	1.9	1.8	-0.2	-0.2
Pasadena	0.0	0.0	0.0	0.0
Perris	-1.3	-1.3	-0.3	-0.3
Pico Rivera	-1.9	-1.8	-2.2	-2.2
Pomona	-0.5	-0.5	3.6	3.5
Redlands	-0.1	-0.1	-1.6	-1.5
Reseda	1.5	1.4	0.0	0.0
Riverside	0.0	0.0	-1.2	-1.1
Santa Clarita	3.2	3.0	0.5	0.4
San Bernardino	-0.8	-0.8	-2.1	-2.0
Temecula	0.0	0.0	0.0	0.0
Upland	-3.4	-3.3	-2.5	-2.4
West Los Angeles	-2.1	-2.1	-0.5	-0.5

At some locations, estimated 2023 and 2031 design values exhibit significant changes from the unperturbed emission scenario. The Case 1 perturbation leads to overestimates of up to 3 ppb and underestimates of up to 5 ppb in 2023 and 2031. Similarly, the Case 2 perturbation leads to overestimates of up to 4 ppb and underestimates of up to 4 ppb in 2023 and 2031. This analysis further asserts the importance of accurately spatially allocating emissions throughout the modelling domain.

Comparison of 2012 and 2016 On-Road Emissions

For the 2016 AQMP modelling, real-time traffic flow measurements during 2012 were used to apportion emissions on an hourly basis throughout the modelling domain. Light- and heavy-duty vehicle flow data is

location dependent and accounts for special events, holidays, seasonality, and meteorologically-driven traffic profiles. Chapter 4 of Appendix 3 details this revised methodology.

CMAQ simulations of the 2012 base-year were conducted with the traditional on-road emissions framework and the modified (PeMS & WIM) on-road emissions framework. Each simulation used an identical emissions inventory, however, the time and location of on-road emissions was modified. Note that the emissions inventory used for this sensitivity analysis differs from the final emission inventory for the 2016 AQMP. Figure V-5-24 illustrates the model bias, gross error, and RMSE when comparing the "Traditional" and "PEMS & WIM" 8-hour ozone predictions to the measurement data.

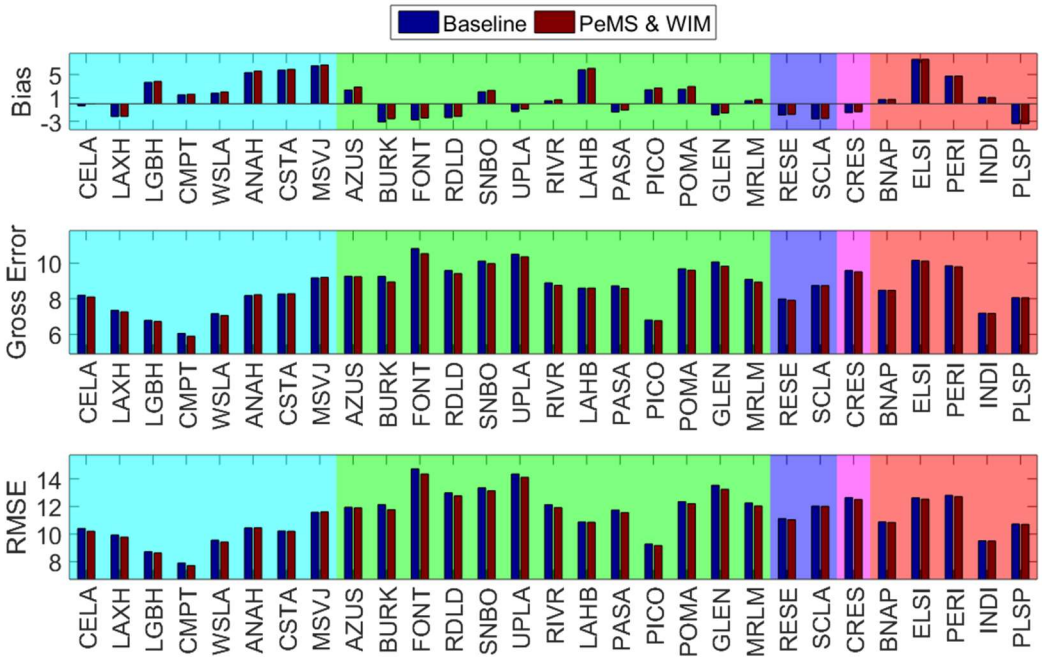

FIGURE V-5-24

Comparison of Bias, Gross Error, and Root-mean-square Error Using the "Traditional" and "PeMS & WIM" On-road Emissions Profiles. Monitoring Stations Are Color-coded Based on the Region of the Basin That They Reside. (Coastal Inland, Inland Urban, San Fernando Valley, Mountain, Inland Desert)

The "PeMS & WIM" on-road emissions profiles predicts slightly higher 8-hour ozone concentrations at most stations in the Basin. However, the gross error and root-mean-squared error has improved in almost all locations over the traditional case. While the model performance is similar on average, some daily maximum 1-hour and 8-hour ozone predictions can differ significantly, up to 10 ppb. The maximum extent of model prediction differences is illustrated with error-bars in Figure V-5-25.

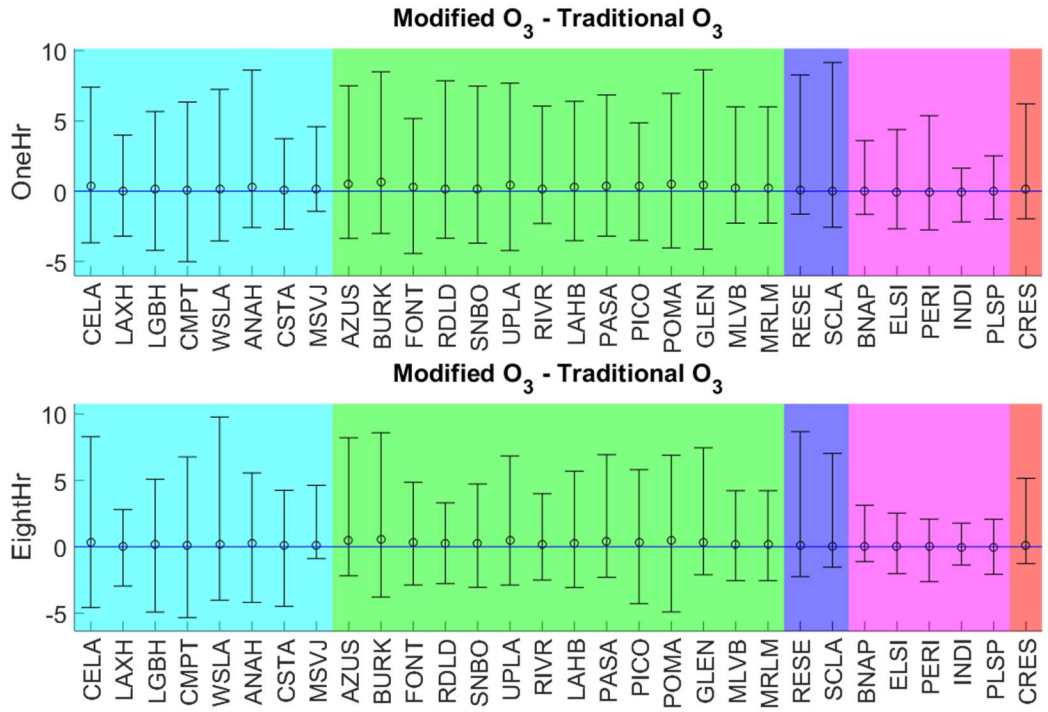

FIGURE V-5-25

Differences in Max-daily 8-hour and 1-hour Ozone Prediction in ppb between "Modified" (PeMS & WIM) and "Traditional" On-road Emissions Profiles. Error Bars Indicate the Maximum and Minimum Extent of Differences in the Predicted Values. Circles Indicate the Average Difference at Each Location. Monitoring Stations Are Color-coded Based on the Region of the Basin That They Reside. (Coastal Inland, Inland Urban, San Fernando Valley, Inland Desert, Mountain)

Significant differences are concentrated on weekends in the inland urban portions of the Basin. Figure V-5-26 shows the daily max 1-hour ozone differences for each station on each day of 2012. The warmest colors typically occur on weekend days, indicating larger daily max 1-hour ozone predictions with the PeMS & WIM profiles. Differences are somewhat seasonal, illustrating the ability of the PeMS & WIM profiles to capture seasonal variations in traffic patterns.

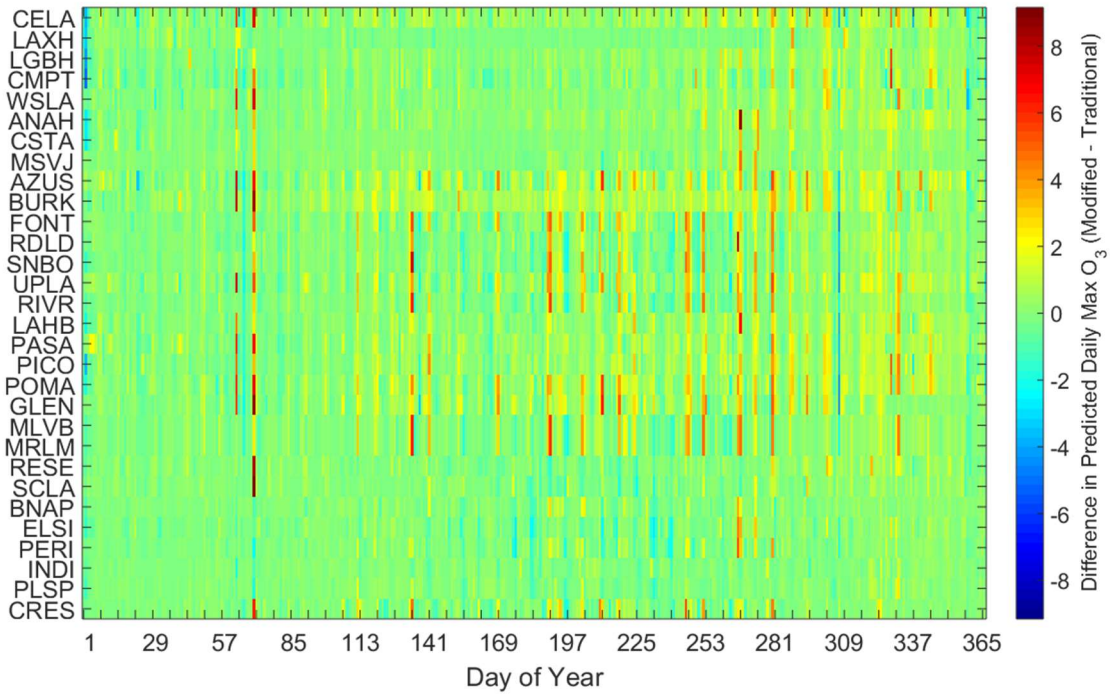

FIGURE V-5-26

Differences in Predicted Daily Max 1-hour Ozone (PeMS & WIM "Modified" – "Traditional")

Projections of Ozone without International Emissions

Section 179(B) of the Clean Air Act states that a state implementation plan shall be approved if the State can establish, to the approval of U.S. EPA that an implementation plan will attain and maintain ambient air quality standards by the attainment date "but for emissions emanating from outside of the United States." Modelling guidance specifying how to evaluate the contribution of emissions emanating from outside the US towards the ozone design values is not available. In light of this, we have done a sensitivity analysis model simulation to probe the contribution of international emissions towards attainment.

The global chemical transport model, MOZART, and CMAQ on a state-wide domain is used to generate boundary conditions of all relevant species for the modelling domain used for the attainment demonstration. To evaluate the contribution of foreign emissions on ozone design values, the contribution of emissions emanating from outside the US should be removed from the boundary conditions allowing CMAQ to forecast ozone concentrations in this hypothetical scenario. Two major problems arise when attempting to quantify this scenario. It is unclear what "emissions emanating from outside the US" entail. One could imagine the situation where all lands outside the US are represented by a desert without biogenic or anthropogenic emissions. However, background concentrations of ozone entering the modeling domain would still be present. The stratospheric ozone layer would likely still be present in the absence of foreign emissions. Stratospheric/tropospheric exchange of ozone would then contribute to background ozone

concentrations in the troposphere. In addition, the contribution of ozone and its precursors from the US would also contribute to the background ozone concentrations entering the modeling domain. The second major problem is operational in nature. The SCAQMD does not currently operate a global model, which is necessary to quantify the regional modeling domain boundary conditions for this hypothetical situation.

In light of these uncertainties and limitations, a sensitivity analysis was conducted to bound the forecasted future design values under various model domain boundary conditions. A relative response factor (RRF) approach was used to forecast 2031 uncontrolled design values. The predicted 2031 design values ($\boldsymbol{DV_{2031\_zeroBV}}$) are a function of the base-year measured design values ($\boldsymbol{DV_{2012\_meas.}}$) and a RRF, which compares the future simulated ozone concentrations ($\boldsymbol{CMAQ_{2031\_zeroBV}}$) with the revised boundary conditions and the 2012 base-year simulations with standard boundary conditions ($\boldsymbol{CMAQ_{2012\_baselineBV}}$):

$$\boldsymbol{DV_{2031\_zeroBV} = DV_{2012\_meas.} * \left(\frac{CMAQ_{2031\_zeroBV}}{CMAQ_{2012\_baselineBV}}\right)} \qquad \text{Eq. 1}$$

The RRF, denoted with the terms in parenthesis is calculated according to the standard methodology, which includes the top 10 days > 60 ppb at each monitoring location meeting the performance criteria from the base year and the corresponding days in the future year. One can derive this equation by framing the analysis in two steps, starting with the derivation of a hypothetical base-year design value that is predicted in the absence of foreign emissions ($\boldsymbol{DV_{2012\_zeroBV}}$).

$$\boldsymbol{DV_{2012\_zeroBV} = DV_{2012\_meas.} * \left(\frac{CMAQ_{2012\_zeroBV}}{CMAQ_{2012\_baselineBV}}\right)} \qquad \text{Eq. 2a}$$

To calculate the future 2031 design values under the revised boundary conditions, the revised base-year design value could then be scaled by a RRF comparing the 2031 ozone concentrations and the 2012 ozone concentrations both predicted in the absence of foreign emissions.

$$\boldsymbol{DV_{2031\_zeroBV} = DV_{2012\_zeroBC} * \left(\frac{CMAQ_{2031\_zeroBV}}{CMAQ_{2012\_baselineBV}}\right)} \qquad \text{Eq. 2b}$$

Combination of Eq. 2a and Eq. 2b yields Eq. 1. A simulation was investigated to evaluate the sensitivity of background ozone concentrations on uncontrolled 2031 design values. An extreme bounding case was design with zero for all the species along the western and southern boundaries. This is an extreme bounding case, given that even pre-industrial ozone level would be approximately 10 ppb (Volz and Kley, 1988). Moreover, in reality, the western and southern boundary conditions would be affected by US emissions and stratospheric/tropospheric transport. This 2031 uncontrolled simulation was run without Mexican emissions.

Future design values were simulated and are summarized in Table V-5-13. The highest values was still expected to occur along the San Bernardino foothill areas, confirming in-Basin emissions and subsequent photochemical reactions are primarily responsible for high design values in the Basin. However, the values in the table need to be interpreted with caution, since this represents unrealistic extreme scenario. Currently, there is no guidance to show the influence of emissions emanating outside the U.S. in the attainment demonstration. While boundary values are close proxy for emissions originating outside a modeling domain, intensity and chemical speciation of emissions cannot be represented via boundary values. A global chemical transport model is the best way to evaluate this influence quantitatively.

TABLE V-5-13

Design Values Calculated for Extreme Bounding Values, Which Has Zero Concentrations along Western and Southern Boundaries

Year	2012				2031	
Boundary Values	Realistic Boundary Value		Zero Boundary Value		Zero Boundary Value	
Station	CMAQ Prediction	Design Value (Measurements)	CMAQ Prediction	Adjusted Design Value with zero Transport through boundary	CMAQ Prediction	Design Value with zero transport through boundary
Azusa	82.9	79.3	65.9	63.0	66.3	63.4
Glendora	88.7	92.7	69.8	72.9	73.2	76.5
West Los Angeles	64.7	64.7	41.6	41.6	42.3	42.3
Los Angeles	63.4	64.0	48.6	49.1	52.3	52.8
Reseda	83.2	89.0	69.9	74.8	60.0	64.2
Pico Rivera	72.3	67.7	58.7	54.9	59.7	55.8
Pomona	83.3	84.3	66.1	66.9	68.6	69.4
LAX	64.2	61.0	30.7	29.1	32.9	31.3
Santa Clarita	89.1	97.3	74.6	81.5	61.6	67.2
Anaheim	65.8	65.0	48.6	48.1	53.1	52.5
Mission Viejo	72.8	72.0	55.5	55.0	55.2	54.6
La Habra	71.4	69.3	53.4	51.9	56.8	55.1
Banning	88.4	95.3	72.8	78.5	67.6	72.9
Indio	79.4	84.3	63.8	67.7	55.4	58.8
Palm Springs	84.9	91.7	73.6	79.5	62.2	67.1
Perris	91.9	91.0	76.3	75.6	67.8	67.2
Riverside	97.3	96.3	78.4	77.7	75.0	74.3
Mira Loma	96.5	92.7	76.6	73.6	72.3	69.4
Elsinore	88.5	85.3	76.0	73.3	63.8	61.5
Crestline	97.6	103.0	78.8	83.1	73.3	77.4
Upland	90.7	96.7	72.2	77.0	71.9	76.7
Fontana	94.0	101.0	76.8	82.5	74.3	79.9
Redlands	98.6	104.7	80.9	85.9	74.8	79.4
San Bernardino	95.5	98.0	78.7	80.8	71.8	73.7

Long-term Trends in Ozone Background Levels

Between 1980 and 2003, energy consumption more than doubled in Asia leading to a significant increase in Asian emissions. Black carbon, organic carbon, carbon monoxide, non-methane VOCs, SO_2, and NOx have all increased significantly (Ohara, Akimoto et al. 2007). Rapid growth of emissions in Asia along with natural variations in stratospheric/tropospheric exchange (Verstraeten, Neu et al. 2015) affects surface ozone levels in the United States. Moreover, transport of ozone and its precursors to surface locations in the U.S. is strongest in the spring (Brown-Steiner and Hess 2011). Surface measurements and aircraft campaigns over the eastern North Pacific find that background ozone concentrations in the spring have increased by approximately 10 ppb from 1985 to 2003 (Jaffe 2003).

Ground-based background ozone measurements in Southern California are not available. Therefore, we have analyzed long-term height-resolved satellite measurements of ozone to investigate the trend in background concentrations entering the Basin from 2005 to 2013.

Methodology

Satellite-based height resolved ozone measurements were obtained from the Ozone Monitoring Instrument (OMI) aboard the National Aeronautics and Space Administration Aura satellite (Levelt, van den Oord et al. 2006). The OMI is an ultraviolet-visible spectrometer on a sun-synchronous orbit providing once-daily measurements of ozone in the troposphere and stratosphere. Measurements have a spatial resolution of 13km x 24km with 18 height layers, with the center of the lowest layer between the surface and 700 hPa.

Tropospheric data was compared to a network of ozonesondes maintained by NOAA Earth System Research Laboratory (National Oceanic and Atmospheric Administration and Global Monitoring Division 2014). Ozonesonde measurements have a high degree of accuracy compared to tropospheric satellite measurements. Ozonesonde measurements, available at intervals ranging from five to 30 days at six locations (Figure V-5-27), were used to validate and adjust tropospheric ozone satellite measurements. Ozonesonde and satellite measurements during and outside the ozone season at each location were compared as a function of height in Figure V-5-28 and Figure V-5-29, respectively. Measurement locations were considered coincident when the center of a satellite measurement was captured within 0.5 degrees latitude and longitude of the ozonesonde location. In order to detect any systematic biases and calibrate the satellite measurements, corresponding satellite and ozonesonde measurements taken with two hours of each other were identified and plotted on opposite axes. This ozonesonde/satellite comparison in the troposphere for each of the six ozonesonde stations with corresponding data acquired from 2004 to 2014 is presented in Figure V-5-30.

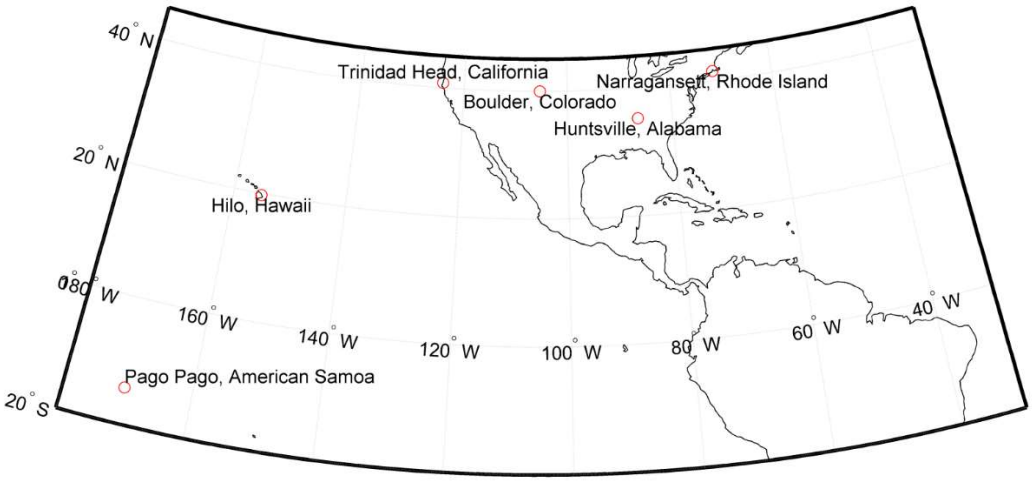

FIGURE V-5-27

Location of Ozonesondes Used to Validate and Calibrate Satellite Data

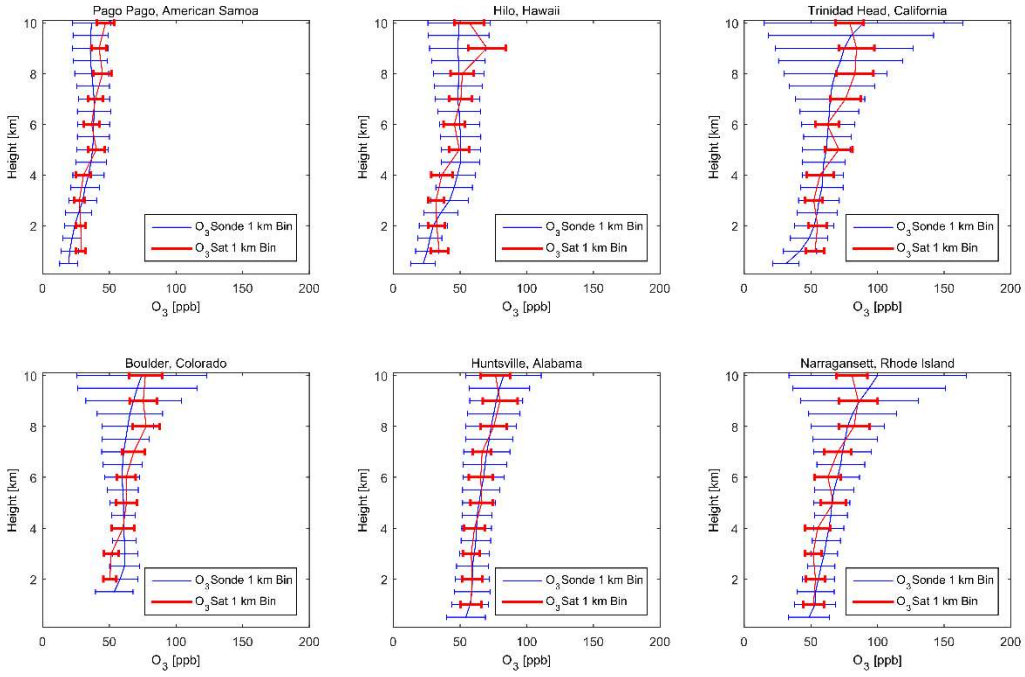

FIGURE V-5-28

Comparison of Ozonesonde and Satellite Data at Six Locations during the Ozone Season. Ozonesonde Data is Binned at a Resolution of 500 m. Satellite Data is Binned at a Resolution of 1 km. The Extent of the Horizontal Bars Represents the Standard Deviation of All Measurements in the Corresponding Height Bin.

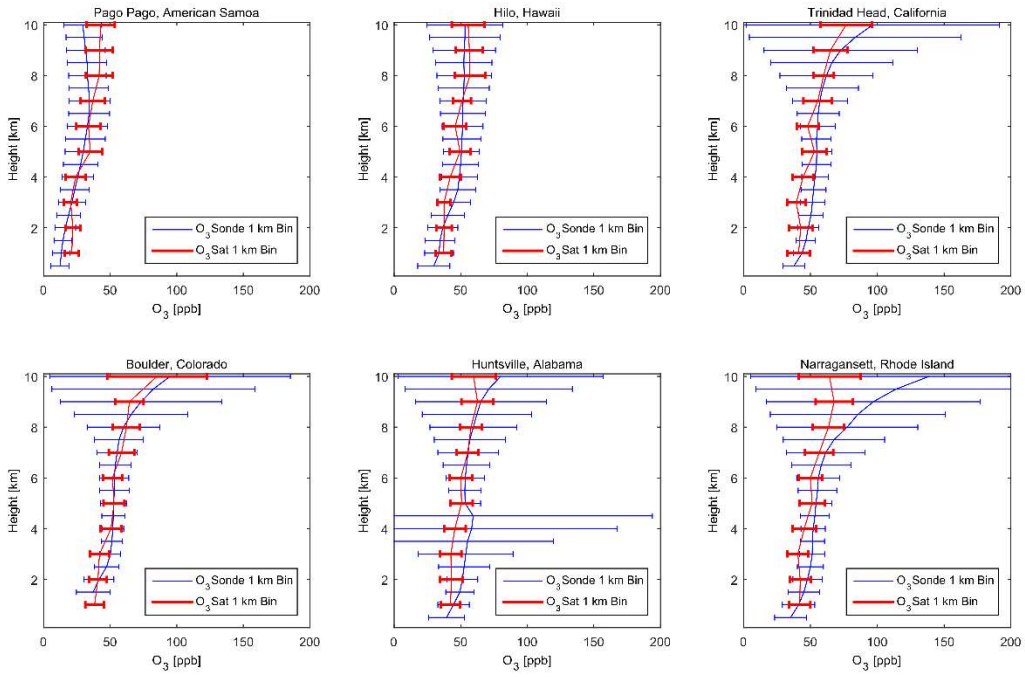

FIGURE V-5-29

Comparison of Ozonesonde and Satellite Data at Six Locations outside the Ozone Season. Ozonesonde Data is Binned at a Resolution of 500 m. Satellite Data is Binned at a Resolution of 1 km. The Extent of the Horizontal Bars Represents the Standard Deviation of All Measurements in the Corresponding Height Bin.

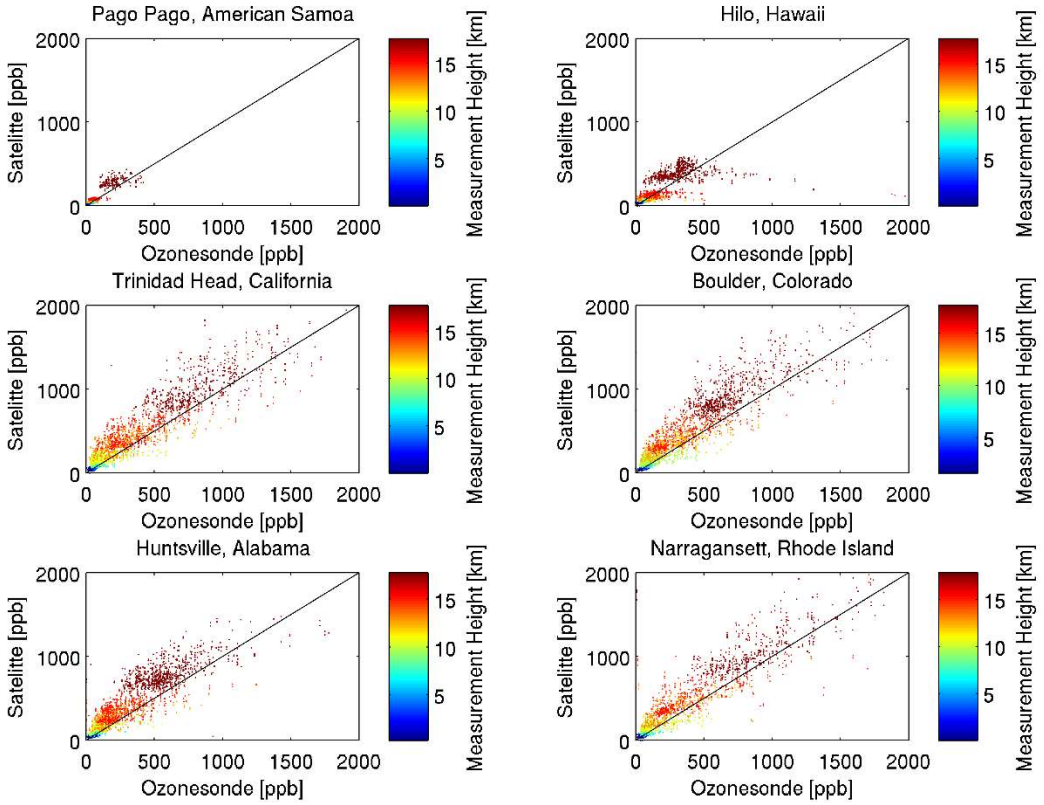

Figure V-5-30

Comparison of Ozonesonde and Satellite Data Taken at Corresponding Locations and Times

Satellite measurements were averaged within three geographical regions (Figure V-5-31). All samples with centers of their 13km x 24km resolution measurements lying inside each of the three geographical regions were considered. "Western Background" and "Eastern Background" comprise two large areas southwest of San Nicolas Island over the Pacific Ocean. Prevailing winds with a large westerly component entering the Basin minimize the influence from SoCAB emissions within the "Western Background" and "Eastern Background" regions. A similar yearly trend in ozone levels within each of these regions further asserts that concentrations are not appreciably influenced from local sources. A third region covering the SoCAB termed "Polluted" was also investigated to further validate the methodology. This region should not be compared to measurements at monitoring stations as many of the satellite measurements sample areas in remote regions of the SoCAB.

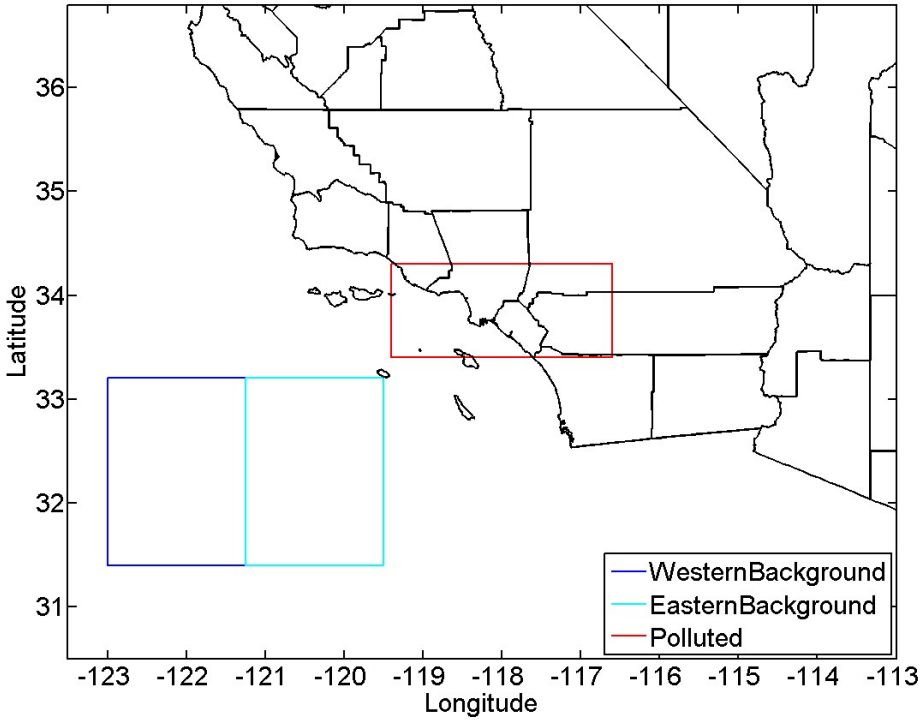

Figure V-5-31

Geographical Regions Investigated to Observe Multi-year Trends in Satellite-based Tropospheric Ozone Levels

Results

Satellite ozone measurements, calibrated with ozonesonde measurements, within each of the three regions investigated were averaged on a yearly basis (Figure V-5-32). Only data from the lowest height bin was used. One should exercise caution in drawing conclusions from the quantitative surface ozone measurements, however, we are confident that long-term trends in the data are grounded in reality. The satellite measurements in the lowest bin are not technically surface measurements as the top of the lowest bin can be on the order of 3000 m in altitude.

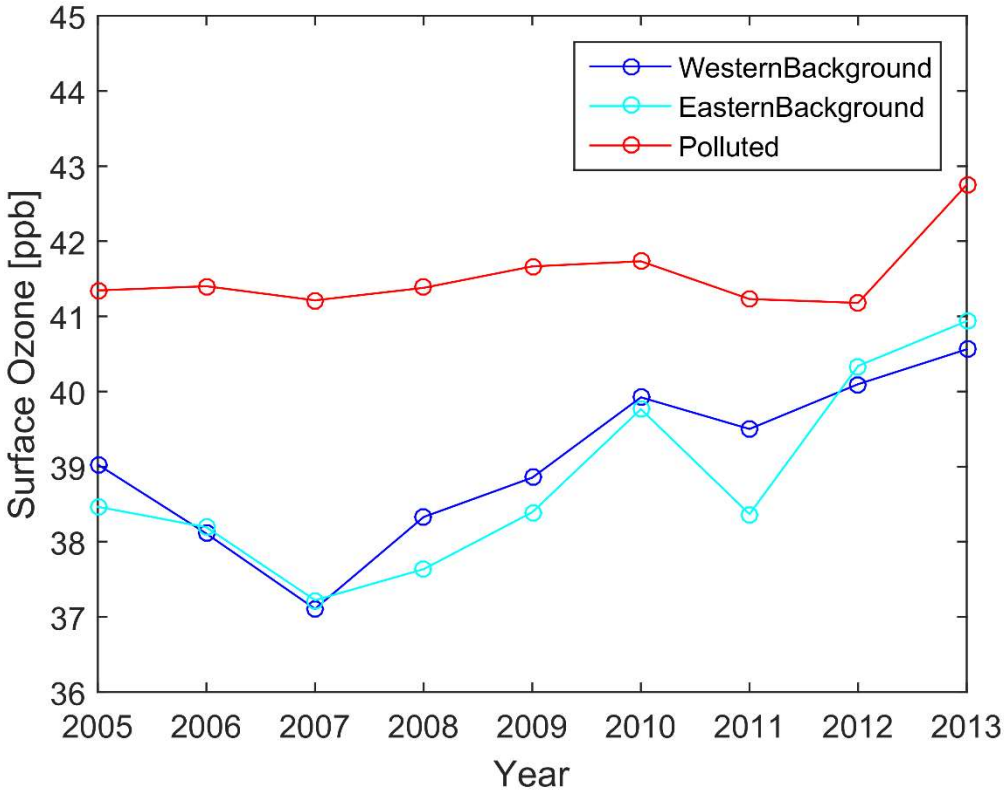

Figure V-5-32

Yearly Averaged Satellite Ozone Measurements within the Lowest Layer

Background ozone concentrations entering the SoCAB have increased between 2005 and 2013 at an average rate of approximately 0.25 ppb per year. As is expected, concentrations over polluted regions are larger than the concentrations in the background regions.

This long-term increase in background concentrations is also evident in the surface measurement station data. Basin design values have decreased significantly since 1980 (Figure V-5-33).

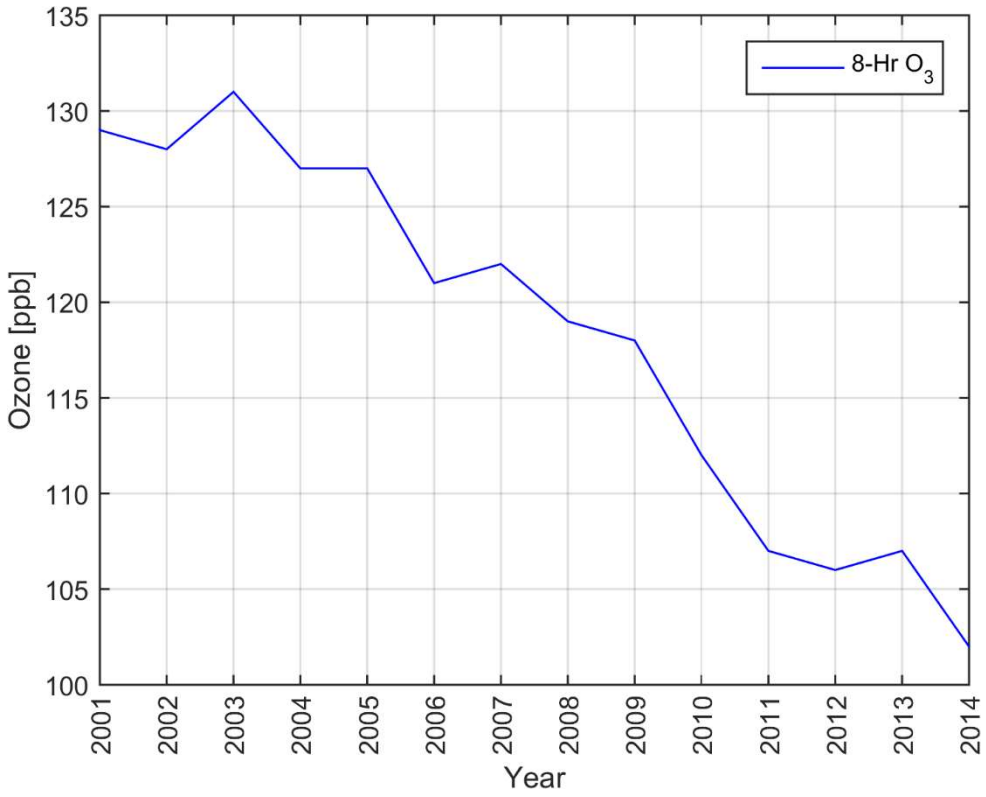

Figure V-5-33

Trend in 3-year Averaged 8-hr Ozone Basin Design Value

However, investigation of histograms (Figure V-5-34) detailing half-decadal changes in average daily maximum 8-hr ozone distributions reveals that concentrations have not decreased uniformly on all days. Figure V-5-34Figure reveals that the percent of days exceeding the 2008 NAAQS 8-hr Federal Standard of 75 ppb has decreased significantly since 1980 when looking at all surface measurement stations in the SoCAB. On the other hand, the frequency of extremely clean days has decreased in the past few decades, further suggesting that background concentrations have increased. An identical trend is observed when separating the measurements into western basin, central basin, and eastern basin categories.

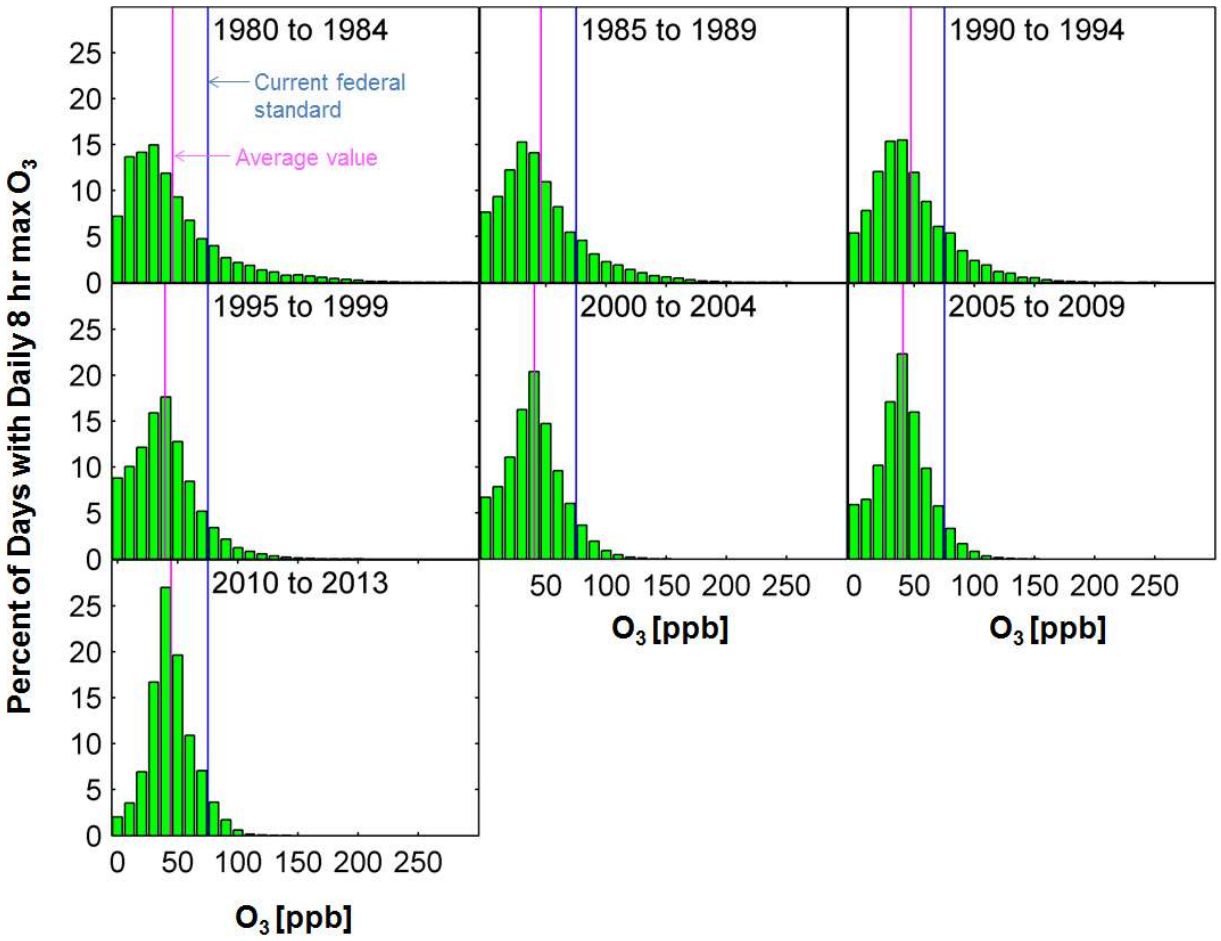

Figure V-5-34

Half-decadal Histograms Detailing the Percent of Days with Each Specific 8-hour Maximum Daily Ozone Value

References

Brown-Steiner, B. and P. Hess (2011). "Asian influence on surface ozone in the United States: A comparison of chemistry, seasonality, and transport mechanisms." Journal of Geophysical Research **116**(D17).

Jaffe, D. (2003). "Increasing background ozone during spring on the west coast of North America." Geophysical Research Letters **30**(12).

Levelt, P. F., G. H. J. van den Oord, M. R. Dobber, A. Malkki, V. Huib, J. de Vries, P. Stammes, J. O. V. Lundell and H. Saari (2006). "The ozone monitoring instrument." Geoscience and Remote Sensing, IEEE Transactions on **44**(5): 1093-1101.

National Oceanic and Atmospheric Administration, U. S. D. o. C. and E. S. R. L. Global Monitoring Division (2014). Ozone Sonde Vertical Profile Data. Boulder, CO.

Ohara, T., H. Akimoto, J. Kurokawa, N. Horii, K. Yamaji, X. Yan and T. Hayasaka (2007). "An Asian emission inventory of anthropogenic emission sources for the period 1980-2020." Atmos. Chem. Phys. **7**(16): 4419-4444.

Verstraeten, W. W., J. L. Neu, J. E. Williams, K. W. Bowman, J. R. Worden and K. F. Boersma (2015). "Rapid increases in tropospheric ozone production and export from China." Nature Geosci **8**(9): 690-695.

Volz A., Kley D. (1988) Evaluation of the Montsouris series of ozone measurements made in the nineteenth century, Nature, 332, 240-242

US EPA, Guidance on the Use of Models and Other Analyses for Demonstrating Attainment of Air Quality Goals for Ozone, PM2.5, and Regional Haze, EPA -454/B-07-002 April 2007

US EPA, Draft Modeling Guidance for Demonstrating Attainment of Air Quality Goals for Ozone, PM2.5, and Regional Haze, EPA December 2014

CHAPTER 6

ANNUAL PM2.5 ATTAINMENT DEMONSTRATION

Introduction

On April 15, 2015, the South Coast Air Basin was designated a 'moderate' non-attainment area for the 2012 annual PM2.5 standard of 12 µg/m3. This designation sets an attainment deadline of December 31, 2021, based on CAA subpart 4, which establishes that attainment must be reached by the end of the 6th calendar year after the effective date of designation. Acknowledging the challenges in meeting the standard, including the feasibility of proposed measures, uncertainties in drought conditions, and the potential inability to credit all ozone strategy reductions towards PM2.5 attainment if approved under CAA Section 182(e)(5), SCAQMD will request a voluntary bump-up to the "serious" classification, with a new attainment date of 2025. Future year attainment was analyzed for 2021, the original target for "moderate" nonattainment, and 2025, the revised attainment date for the requested "serious" status.

The 2012 AQMP demonstrated attainment of the 15 µg/m3 1997 standard as well as the 24-hour standard of 35 µg/m3. As a part of a multi-pollutant integrated plan, the 2016 AQMP demonstrates attainment of the federal annual PM2.5 standard of 12 µg/m3 using the new modeling platform and emissions inventory. This demonstration shows that the 2016 AQMP control strategy will continue to move air quality levels expeditiously towards attainment of the federal standards.

PM2.5 FRM Sampling

The SCAQMD maintains a sampling network of Federal Reference Method (FRM) PM2.5 monitors at 20 sites throughout the Basin and Coachella Valley. This network is supplemented by Federal Equivalent Method (FEM) continuous PM2.5 monitors at a subset of these locations to report real-time data to the public and to feed for forecasting algorithms. The FRM samplers are designated as the primary data to determine attainment status, therefore, FRM data is used for design value calculations and the attainment demonstration. U.S. EPA has granted SCAQMD a waiver from using the continuous PM2.5 monitors for regulatory/attainment determination purposes, since they do not meet the accuracy requirements to be considered federal equivalent method (FEM) measurements.

Speciated PM2.5 Sampling

The District adopted a Multi-Channel Fine Particulate (MCFP) sampling system for the PTEP monitoring program in 1995, and the TEP 2000 program in 1998-1999. New PM samplers, speciated air sampling system (SASS) samplers, were deployed at four sites in the Basin. The SASS sampler collects PM2.5 particles on 47mm quartz and Teflon filters simultaneously within the same sampler continuously for 24-hours for subsequent laboratory chemical analysis. Samples were originally collected one out of every six days.

PM2.5 speciation data, measured as individual species at the four sites in the District air-monitoring network during 2012, provided the PM2.5 chemical characterization for evaluation and validation of the CMAQ annual and episodic modeling. The four sites include Riverside-Rubidoux, Fontana, Anaheim and Central Los Angeles (Figure V-6-1). These four sites represent each county that the monitor is located in. The Riverside-Rubidoux used to have the highest concentration in the Basin until the Mira Loma site established in 2006 showed higher PM concentrations. Mira Loma does not include speciation sampling, but its proximity to Rubidoux and common airflow and transport patterns enables the use of the Rubidoux speciation data to represent particulate speciation at Mira Loma. Both sites are directly downwind of the dairy production areas of Chino and the warehouse distribution centers located in the northwestern corner of Riverside County. PM2.5 mass, ions, organic and elemental carbon, and metals, for a total of 43 chemical species, were analyzed from a one-in-six day sampling schedule at the 4 sites.

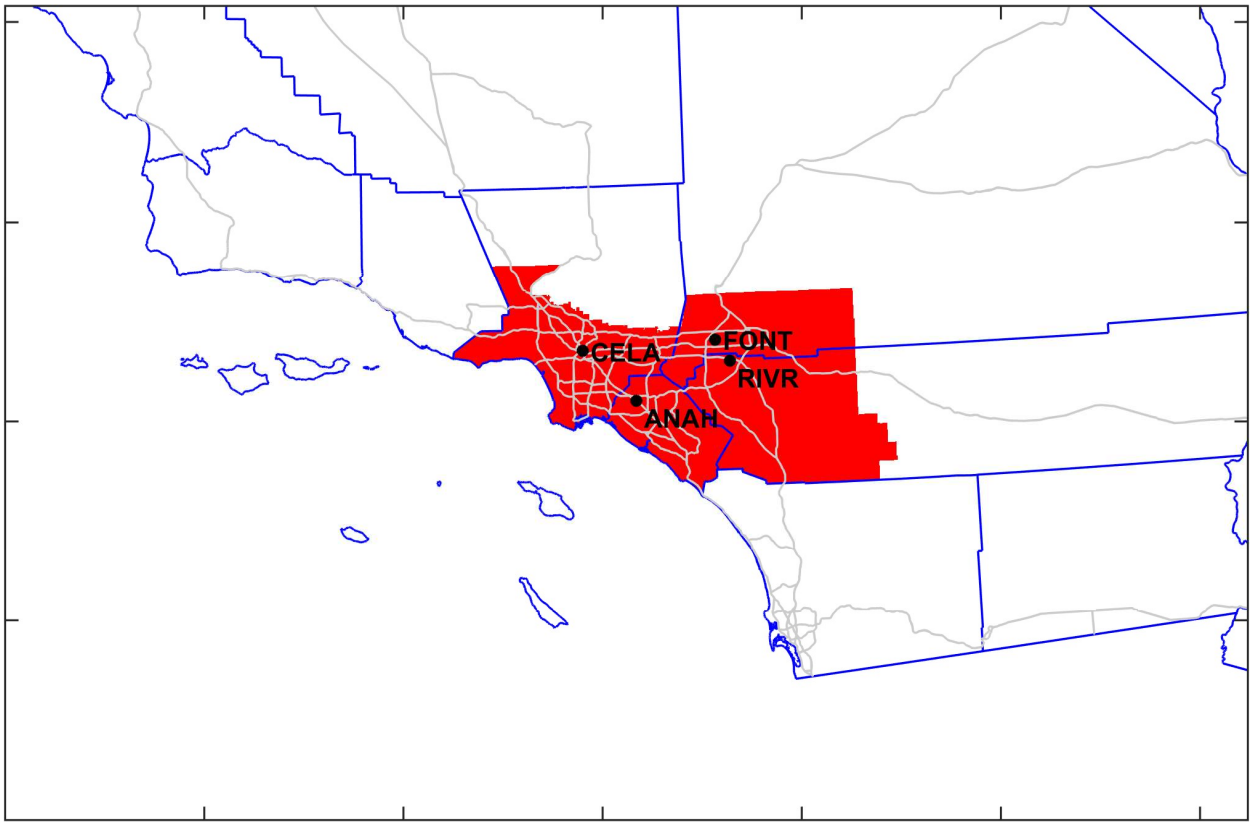

FIGURE V-6-1

SASS Sampling Sites in the Basin

PM2.5 speciation data measured by the SASS samplers are used to derive the species fractions required for the PM2.5 attainment demonstration methodology. U.S. EPA's PM2.5 modeling guidance recommends calculating future year PM2.5 design values by multiplying quarterly, species specific RRFs with the base year speciated design values for each quarter for each monitoring site. Base year design values are determined from the FRM mass data, however the FRM filters are not chemically speciated. Therefore, the guidance document recommends multiplying the species fractions that are measured in a speciation sampler such as the SASS to the FRM mass data to derive chemically speciated design values for the FRM data. In the following sections, 24-hour and annual average species concentrations measured by the SASS sampler are summarized and the chemically speciated FRM data are derived for the future year design value calculations.

Annual PM2.5 Modeling Approach

The Final 2016 AQMP annual PM2.5 modeling employs the same approach to estimate the future year annual PM2.5 levels as was described in the 2012 and 2007 AQMP attainment demonstrations, except for the introduction of minor updates recommended in the 2014 U.S. EPA guidance document (U.S. EPA, 2014). The site and species specific RRF approach is consistent to the previous AQMPs. A five-year weighted quarterly average from the 2010 to 2014 period was established as the 2012 design value. Four SASS sites and Mira Loma, the design site of the Basin, were used in the analysis.

The modeling platform developed for the ozone attainment demonstration was extended to the entire year to acquire quarterly average RRFs. A day-specific emissions inventory was developed to reflect the temperature and relative humidity dependency of mobile sources and biogenic emissions. Also, seasonal fuel switching and the resulting emission rates were incorporated in the modeling inventory.

In addition to the base year (2012), future milestone years simulated under this plan were 2021 and 2025, with the former being the target attainment year for a 'moderate' non-attainment area and the latter for a 'serious' non-attainment area. Both baseline and control scenarios were simulated for each of the future years. CMAQ output was averaged over the 3X3 grid around each monitoring station per the latest EPA guidance, differing from the single-cell strategy used in the 2012 AQMP. In contrast, the 24-hour PM2.5 attainment demonstration requires a single cell retrieval.

The five-year design values based on the FRM method are listed in Table V-6-1. These are calculated according to the following steps; 1) quarterly average of the FRM mass, 2) annual average from the quarterly averages, 3) average of a three-year period centered at 2011, 2012 and 2013, respectively, and lastly 4) average of the three, overlapping three-year periods.

The future year design values reflect the weighted quarterly average concentration calculated from the projections of five years of days. Once site- and species-specific RRFs are calculated from CMAQ simulations, they are applied to the quarterly average design values which are averaged for the period of 2010 to 2014 using the 5-year weighted average approach. The average of the quarterly species-specific projections is the future design value.

TABLE V-6-1

Five-Year Weighted Annual PM2.5 Design Values for 2012 (µg/m^3)

Monitoring Site	Annual
Anaheim	10.6
Los Angeles	12.4
Fontana	12.6
Mira Loma	14.9
Rubidoux	13.2

Performance Evaluation

EPA guidance assesses model performance on the ability to predict both PM2.5 component species concentrations and the total mass. No specific performance criteria thresholds are recommended in EPA's modeling guidance document. This is because the model uses relative response factors rather than direct predictions to forecast future concentrations. Performance is evaluated by examining key statistics and graphical representations of differences between model-predicted concentrations and observations. The statistics examine model bias and error, while graphical representations of model prediction as a function of time and concentration scatter plots supplement the model performance evaluation. The CMAQ modeling results presented for each station are based on the same "1-cell" basis, as recommended by the guidance.

For the CMAQ performance evaluation, the modeling domain is separated into several sub-regions or zones. Figure V-6-2 depicts the sub-regional zones used for base-year simulation performance. The different zones present unique air quality profiles. The Basin is represented by six zones: "Coastal" zone representing Source Receptor Area (SRA) 2-4 and 18-21, "San Fernando" zone representing SRA 6,7, and 13 within the San Fernando Valley, "Foothills" zone representing SRA 8 and 9, "Urban Source" zone representing SRA 1, 5, 10-12, 16, and 17, "Urban Receptor" zone representing SRA 22-29 and 33-38, and "Coachella Valley" zone representing SRA 30 and 31. The "Urban Receptor" region typically has the highest PM2.5 concentrations in the Basin. Table V-6-2 explicitly lists the station location and their assigned performance evaluation zone.

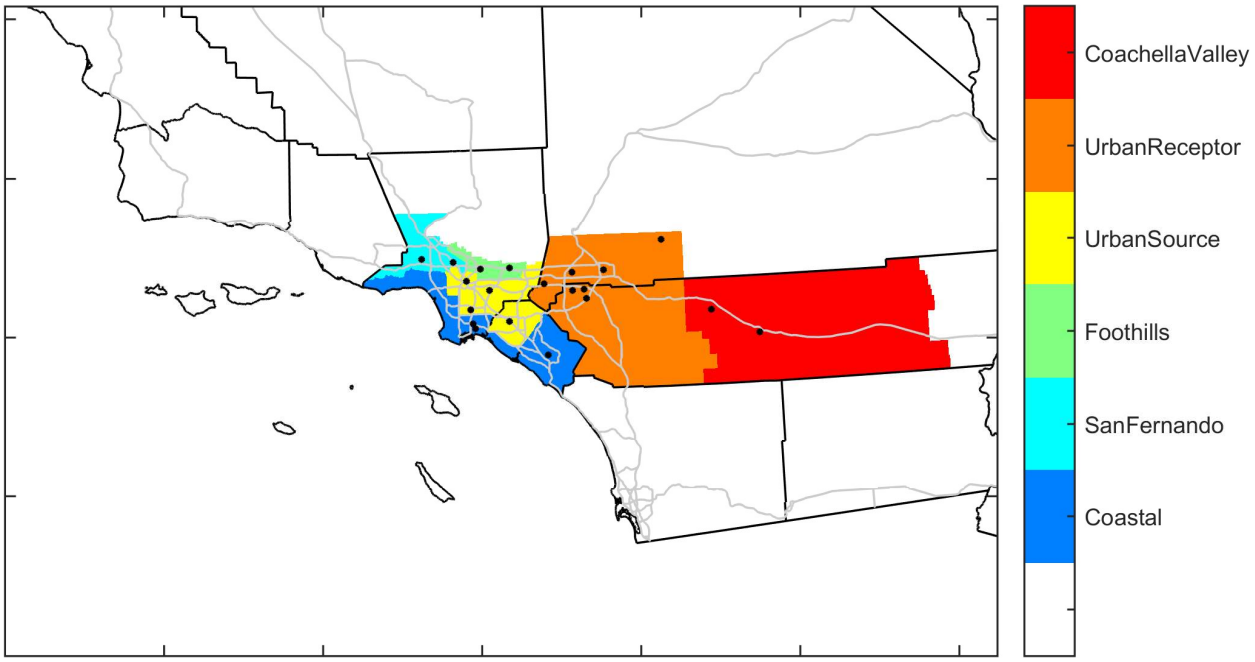

FIGURE V-6-2

Performance Evaluation Zones. Black Dots Indicate the Location of FRM Stations.

Daily predicted and observed PM2.5 concentrations at CELA, ANAH, FONT, MRLM, and RIVR are presented in Figures V-6-3 through V-6-7. While absolute concentrations may differ, the model simulates trends in PM2.5 reasonably well. Both modelled and observed PM2.5 concentrations are more episodic in the 1st and 4th quarter. Concentrations have less day-to-day variation in the 2nd and 3rd quarters at all the 4 sites. This behavior is likely due to differences in meteorology throughout the year. Weather patterns during the first quarter and the second half of the 4th quarter are typically highly variable; precipitation days, cold, high-winds and unstable conditions associated with synoptic scale storms are all commonly experienced during the winter months. On the contrary, spring and summer weather patterns are dominated by high pressure systems, leading to less day-to-day variation in boundary layer heights and wind speeds.

TABLE V-6-2

FRM Stations in the South Coast Air Basin

Station Location	Station Abbreviation	Source Receptor Area (SRA)	Performance Evaluation Zone
Long Beach	LGBH	4	Coastal
Mission Viejo	MSVJ	19	Coastal
South Long Beach	SLBH	4	Coastal
Azusa	AZUS	9	Foothills
Pasadena	PASA	8	Foothills
Burbank	BURK	7	San Fernando
Reseda	RESE	6	San Fernando
Big Bear	BGBR	38	Urban Receptor
Fontana	FONT	34	Urban Receptor
Mira Loma	MRLM	23	Urban Receptor
Ontario	ONFS	33	Urban Receptor
Riverside	RIVR	23	Urban Receptor
Riverside Magnolia	RIVM	23	Urban Receptor
San Bernardino	SNBO	34	Urban Receptor
Anaheim	ANAH	17	Urban Source
Compton	CMPT	12	Urban Source
Los Angeles	CELA	1	Urban Source
Pico Rivera	PICO	11	Urban Source
Indio	INDI	30	Coachella Valley
Palm Springs	PLSP	30	Coachella Valley

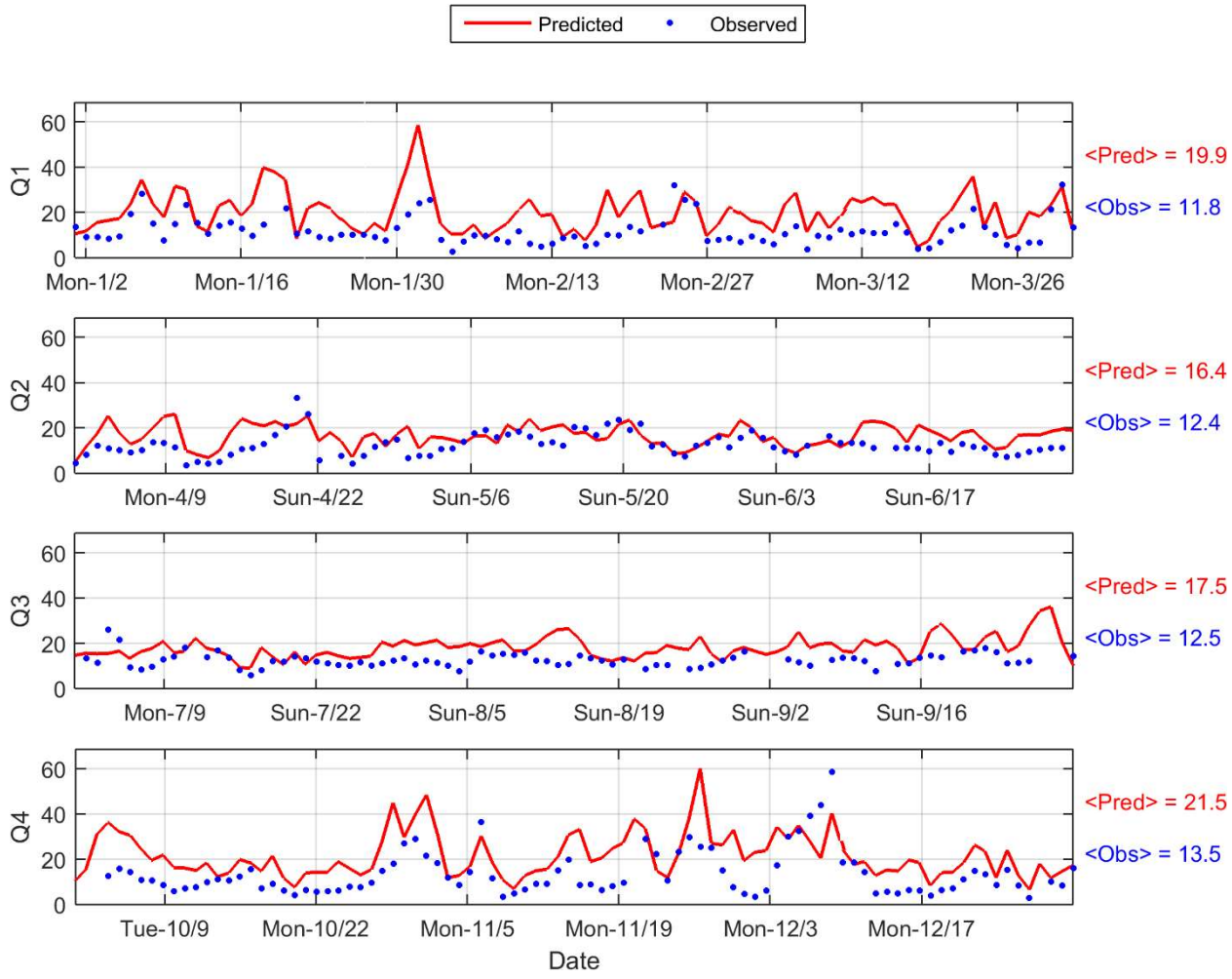

FIGURE V-6-3

2012 Modelled and Measured 24-hour Average PM2.5 Concentrations in Los Angeles

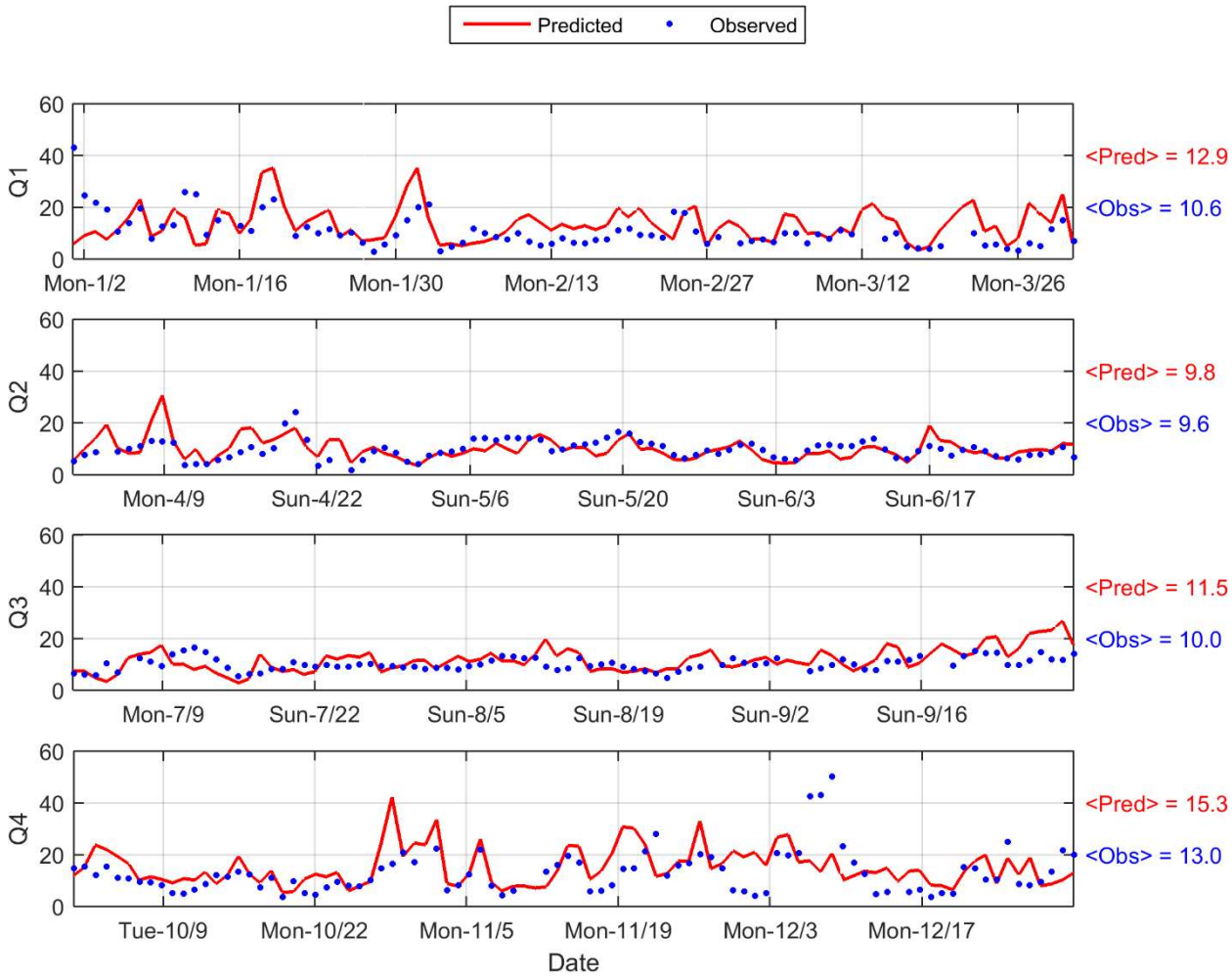

FIGURE V-6-4

2012 Modelled and Measured 24-hour Average PM2.5 Concentrations in Anaheim

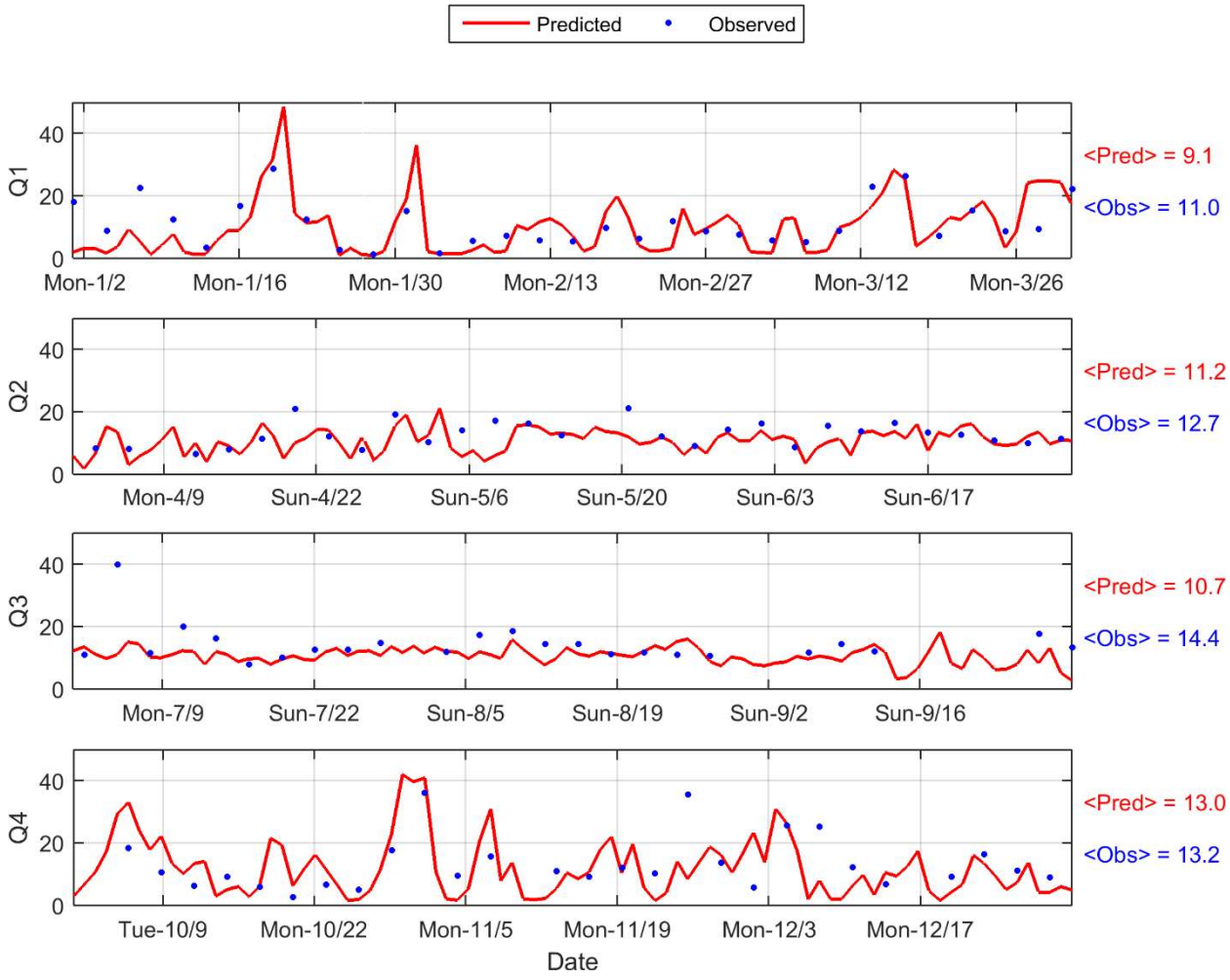

FIGURE V-6-5

2012 Modelled and Measured 24-hour Average PM2.5 Concentrations in Fontana

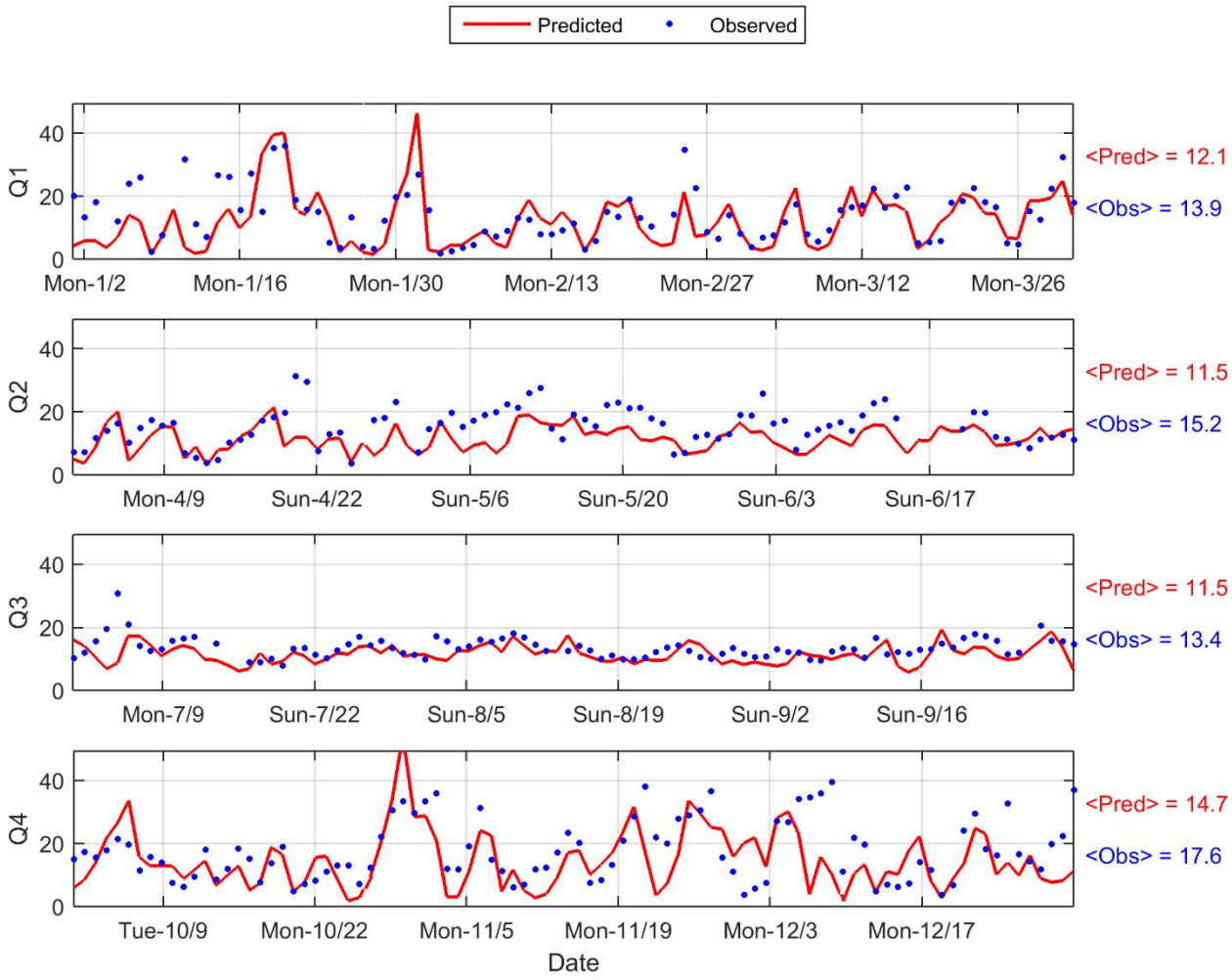

FIGURE V-6-6

2012 Modelled and Measured 24-hour Average PM2.5 Concentrations in Mira Loma

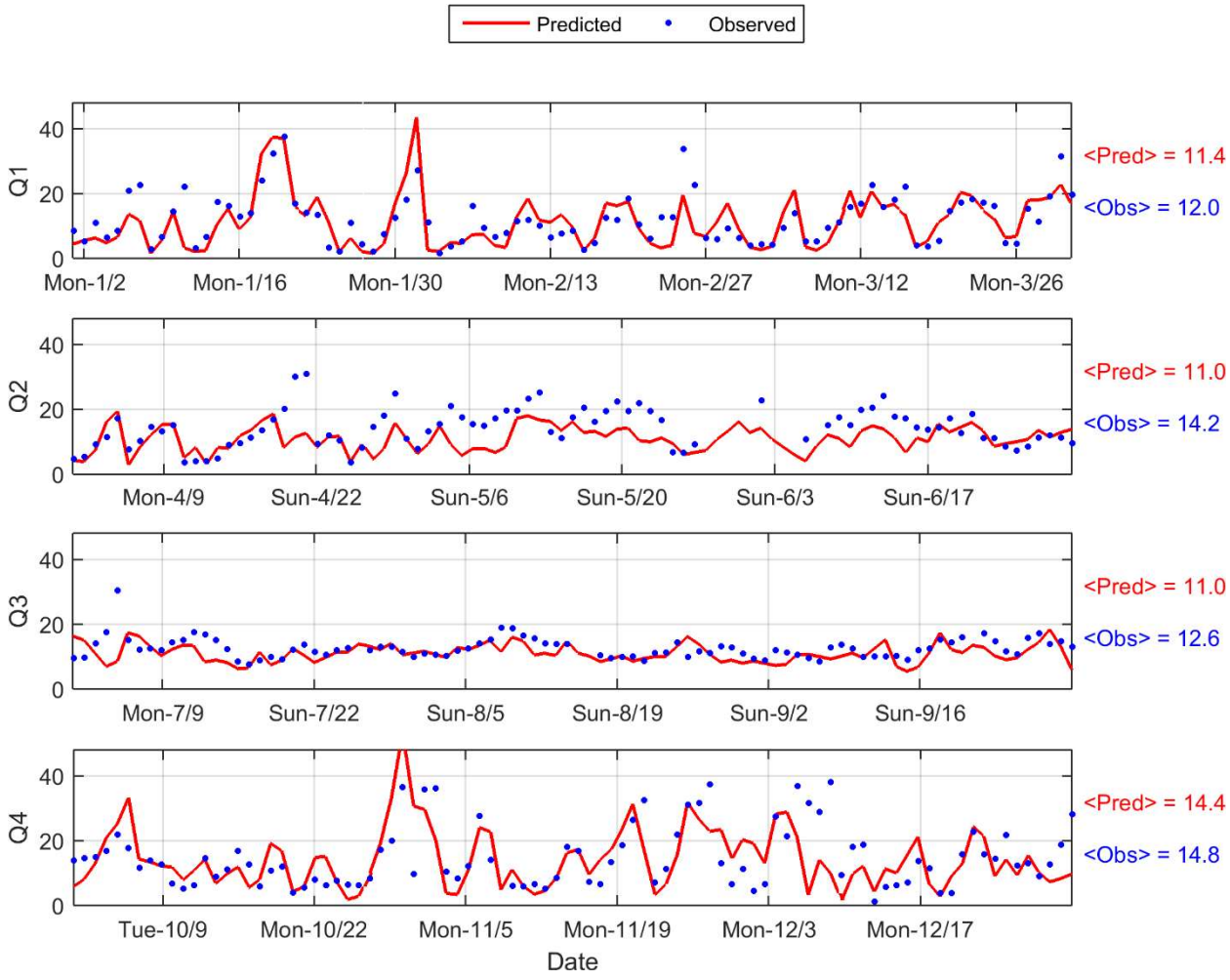

FIGURE V-6-7

2012 Modelled and Measured 24-hour Average PM2.5 Concentrations in Riverside

Scatter plots comparing daily FRM observations and corresponding model predictions for each region are presented in Figure V-6-8.

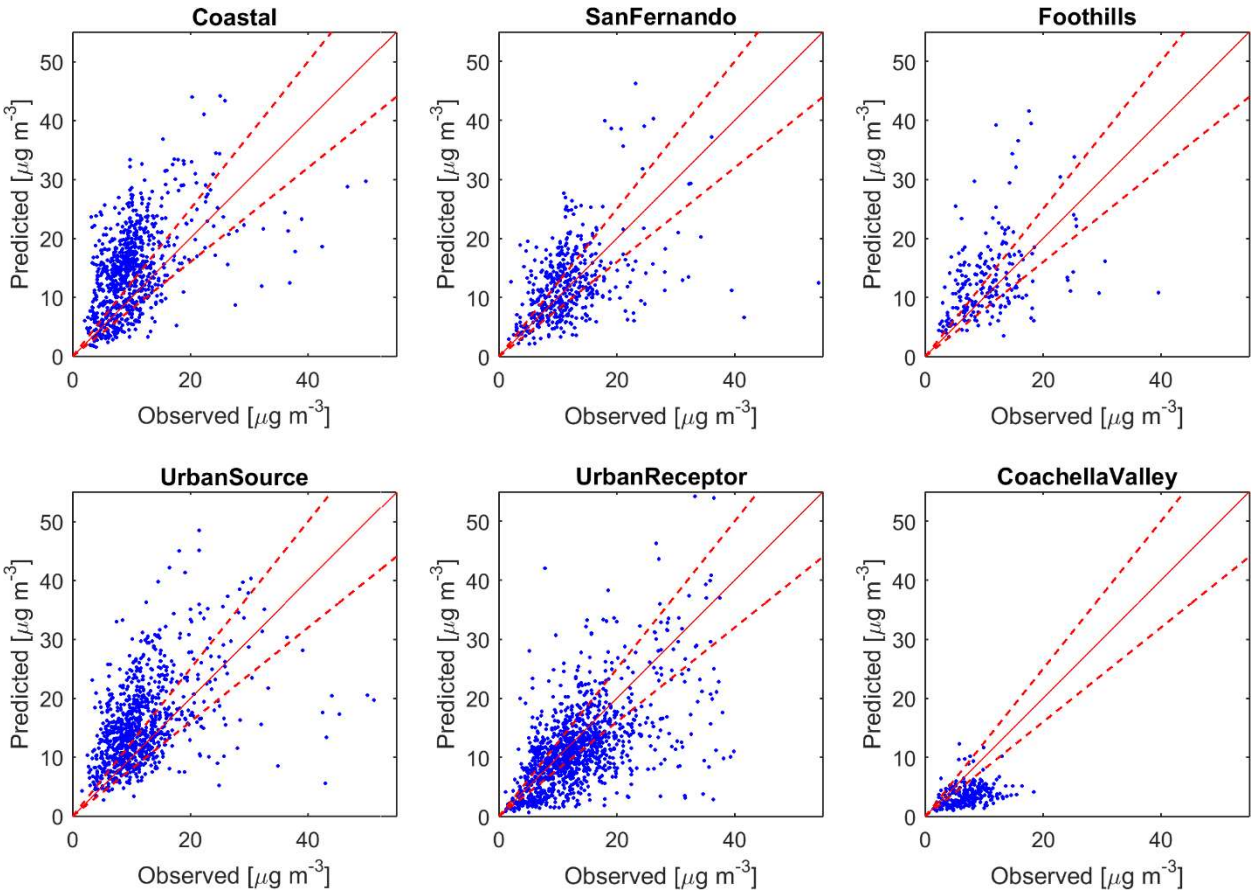

FIGURE V-6-8

2012 Modelled and FRM Measured PM2.5 Comparison for Each Region. Dashed Lines Indicate Agreement within 20 percent.

Statistical Evaluation of Total PM2.5 mass

CMAQ over-predicts total PM2.5 mass in the "Coastal", "Foothills" and "Urban Source" regions. Conversely, PM2.5 concentrations are under-predicted in the "Coachella Valley" region. The "San Fernando", "Urban Receptor" regions, are well represented by CMAQ in the base year. The "Urban Receptor" region typically contains the highest PM2.5 concentrations in the Basin. Statistical measures to evaluate the modeling performance in each geographical zone are provided in Table V-6-3.

The statistics used to evaluate the daily CMAQ PM2.5 performance include the following:

Statistic for PM2.5	Definition
Bias Error	Average of the differences in observed and predicted daily values. Negative values indicate under-prediction. $$BiasError = \frac{1}{N}\sum(Obs - Pred)$$ where "N" is the number of values.
Normalized Bias Error	Average of the quantity: absolute difference in observed and predicted daily values normalized by the observed daily concentration $$NormBiasError = \frac{1}{N}\sum\left(\frac{Obs-Pred}{Obs}\right)\cdot 100$$
Gross Error	Average of the absolute differences in observed and predicted daily values $$GrossError = \frac{1}{N}\sum\lvert Obs - Pred\rvert$$
Normalized Gross Error	Average of the quantity: absolute difference in observed and predicted daily values normalized by the observed daily concentration $$NormGrossError = \frac{1}{N}\sum\left\lvert\frac{Obs-Pred}{Obs}\right\rvert\cdot 100$$

TABLE V-6-3

Quarterly Statistical Analysis of Total PM2.5 Mass for Each of the Six Analysis Zones

Region	Timeframe	Mean Pred. [µg/m^3]	Mean Obs. [µg/m^3]	Bias Error [µg/m^3]	Norm Bias Error [%]	Gross Error [µg/m^3]	Norm Gross Error [%]
Coachella Valley	Q1	3.8	5.3	2	34.8	2.3	40.8
Coachella Valley	Q2	3.1	8.1	5	59.4	5	59.6
Coachella Valley	Q3	3.8	8.9	5.1	55.9	5.1	55.9
Coachella Valley	Q4	4.4	5.9	1.4	16.6	2.3	38
Coachella Valley	**Annual**	**3.8**	**7.1**	**3.4**	**42.1**	**3.7**	**48.7**
Coastal	Q1	14.8	9.9	-6.9	-83.3	8.1	93.6
Coastal	Q2	10.5	9.3	-2.5	-35.7	4.5	54
Coastal	Q3	12.2	9.6	-3.9	-44.1	5.1	56.5
Coastal	Q4	15	11.5	-5.1	-84.9	7.5	95.7
Coastal	**Annual**	**13.1**	**10.1**	**-4.6**	**-61.5**	**6.3**	**74.5**
Foothills	Q1	14	9.4	-4.2	-63	5.8	73
Foothills	Q2	11.7	11.1	-0.9	-21.1	3.8	39
Foothills	Q3	11.8	12.8	1.2	1.7	4.2	30.7
Foothills	Q4	14.6	9.5	-5.2	-71.6	6.8	81.6
Foothills	**Annual**	**13**	**10.7**	**-2.2**	**-37.3**	**5.1**	**55**
SanFernando	Q1	11.5	11.6	-0.3	-12.9	5.3	45.2
SanFernando	Q2	10.5	10.8	-0.5	-12.1	3.6	34.6
SanFernando	Q3	11.4	11.4	-0.6	-9.6	3.2	30.1
SanFernando	Q4	13.2	13.3	-0.4	-28.1	6.6	60.6
SanFernando	**Annual**	**11.6**	**11.7**	**-0.5**	**-15.4**	**4.6**	**42.3**
UrbanReceptor	Q1	10.6	12	0.8	0.3	4.7	41.8
UrbanReceptor	Q2	9.4	13.3	2.6	13.3	4.1	30.2
UrbanReceptor	Q3	9.5	12.8	2.2	13.9	3.2	23.5
UrbanReceptor	Q4	12.5	14.6	0.7	-12.4	6.5	53
UrbanReceptor	**Annual**	**10.5**	**13.2**	**1.6**	**3.5**	**4.6**	**37.4**
UrbanSource	Q1	17.4	11.5	-5.1	-63.2	7.1	72.4
UrbanSource	Q2	12.9	10.9	-2.1	-27.9	3.8	41.1
UrbanSource	Q3	13.9	11	-3	-31	4.4	42.4
UrbanSource	Q4	18.6	13.4	-5.1	-71.5	8	81.6
UrbanSource	**Annual**	**15.7**	**11.7**	**-3.8**	**-48.5**	**5.9**	**59.5**

Model performance in the "Urban Receptor" region consistently outperforms the five other regions exhibiting the smallest normalized bias and normalized gross error for the annual analysis. Model performance in the "Urban Receptor" region is also strong when evaluating statistics on a quarterly basis. It is important to model this region accurately, as it contains the stations with the highest PM2.5 concentrations in the Basin.

Model Performance of Speciated PM2.5 Predictions

Figures V-6-9 through V-6-12 compare predicted and observed particulate sulfate, nitrate, elemental carbon, and organic carbon concentrations for the four stations where speciation data are available (ANAH, CELA, FONT, and RIVR).

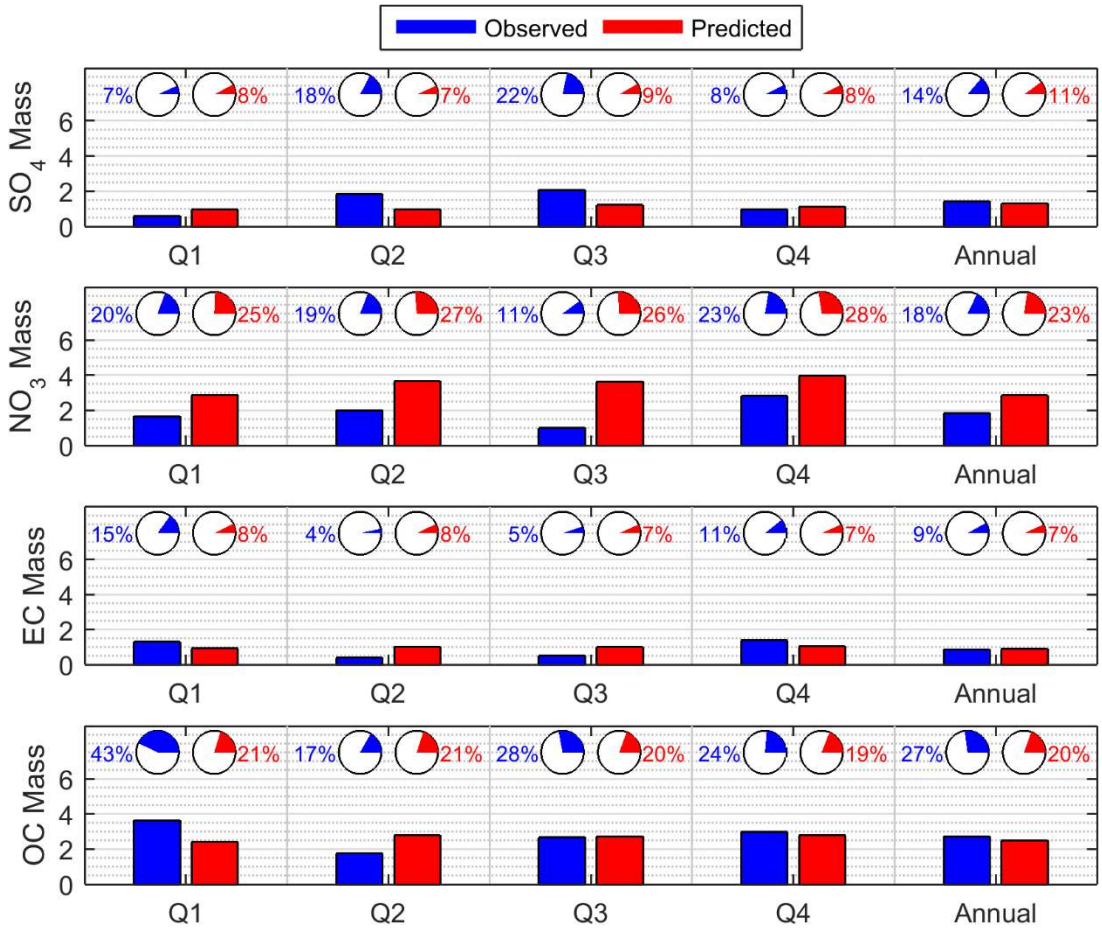

FIGURE V-6-9

2012 Modelled and Measured PM2.5 Speciation in Anaheim. Bars Indicate the Absolute PM2.5 Concentration of Each Species in µg/m^3. Pie Charts Represent the Species Fraction.

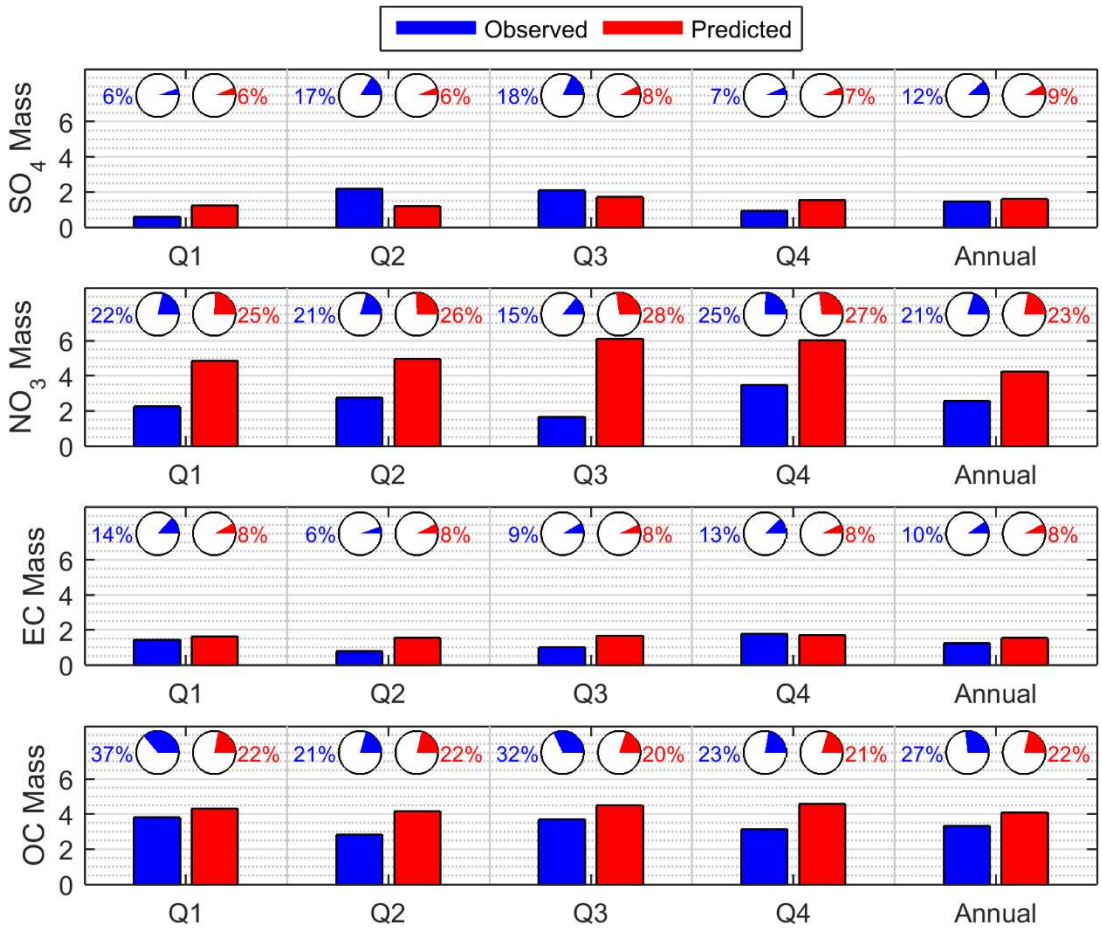

FIGURE V-6-10

2012 Modelled and Measured PM2.5 Speciation in Los Angeles. Bars Indicate the Absolute PM2.5 Concentration of Each Species in µg/m^3. Pie Charts Represent the Species Fraction.

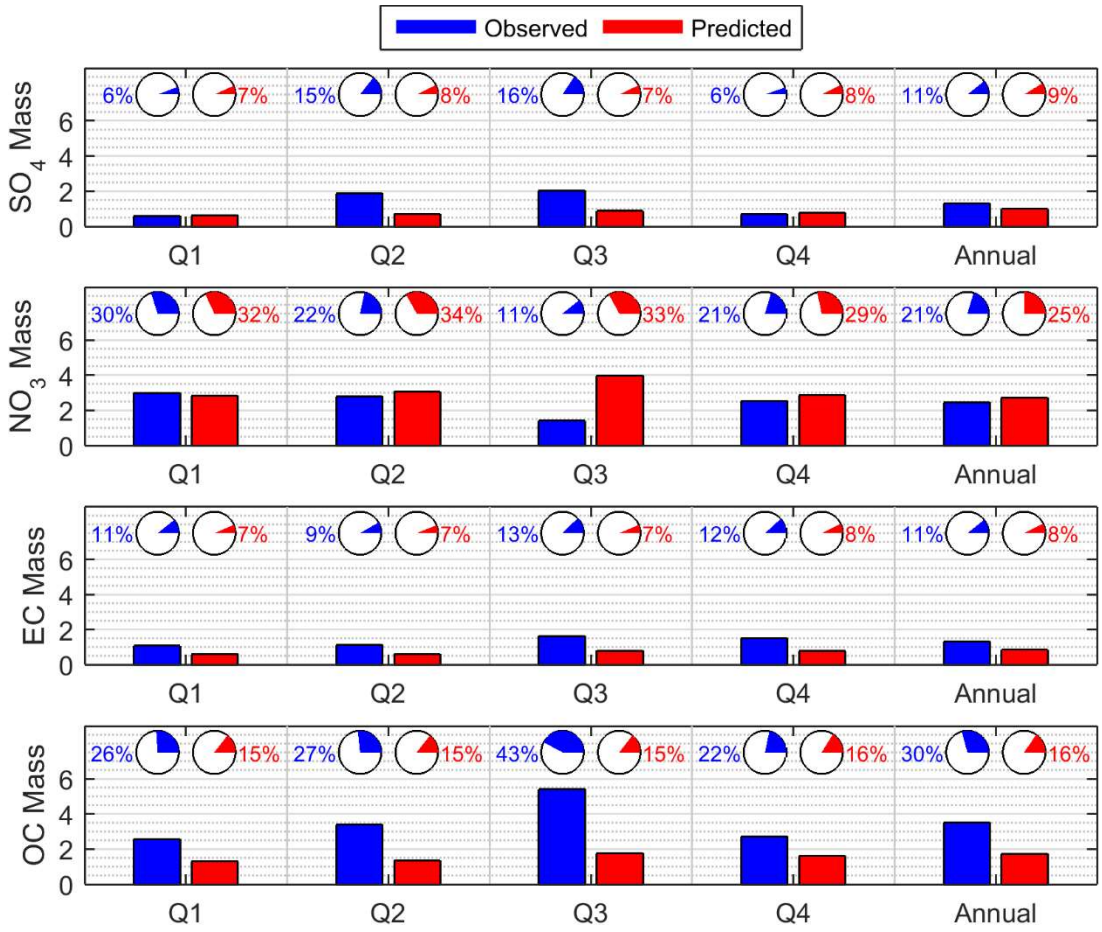

FIGURE V-6-11

2012 Modelled and Measured PM2.5 Speciation in Fontana. Bars Indicate the Absolute PM2.5 Concentration of Each Species in µg/m^3. Pie Charts Represent the Species Fraction.

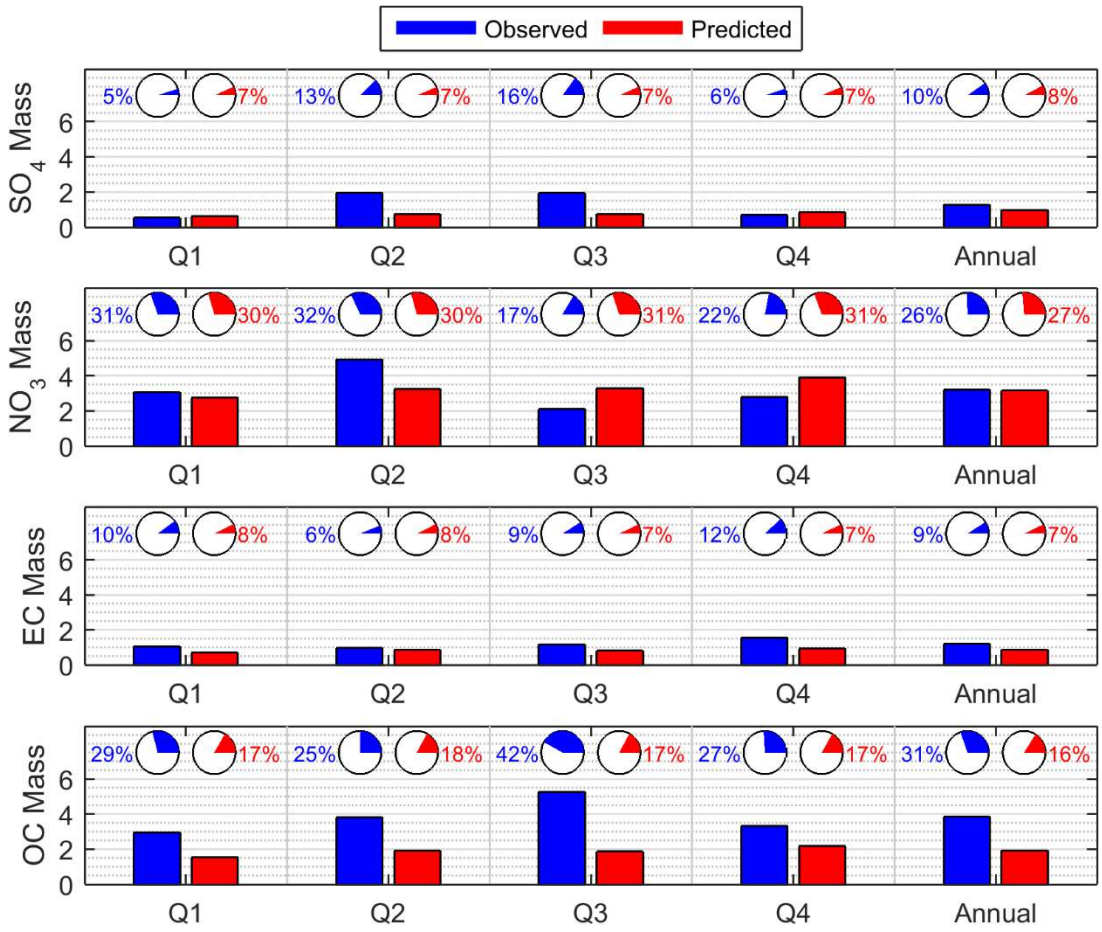

FIGURE V-6-12

2012 Modelled and Measured PM2.5 Speciation in Riverside. Bars Indicate the Absolute PM2.5 Concentration of Each Species in µg/m^3. Pie Charts Represent the Species Fraction.

Nitrate fractions and total nitrate are in general, slightly overestimated by the model. Large differences are exhibited in the third and fourth quarters of the year. One of the largest model uncertainties results from the prediction of boundary layer heights. Inaccuracies in boundary layer height predictions can lead to significant over or under-predictions of concentration. However, comparison of nitrate fraction removes this uncertainty as nitrate concentrations are normalized by the total PM2.5 concentration.

CMAQ predicts EC fractions well, with only slight differences in predicted and observed fractions. Unlike nitrate and sulfate fractions, there is no discernable temporal variation in accuracy.

Both the fraction of sulfate in the particulate mass and the total sulfate mass are represented well in the first and fourth quarters of the year at all stations. However, the model fails to accurately represent the increased sulfate fraction and elevated concentrations typically experienced in the second and third quarters. Figure V-6-13 shows daily differences in modelled and observed sulfate concentrations for each of the monitoring stations with speciation data. Larger under-predictions occur during the spring and summer at each location.

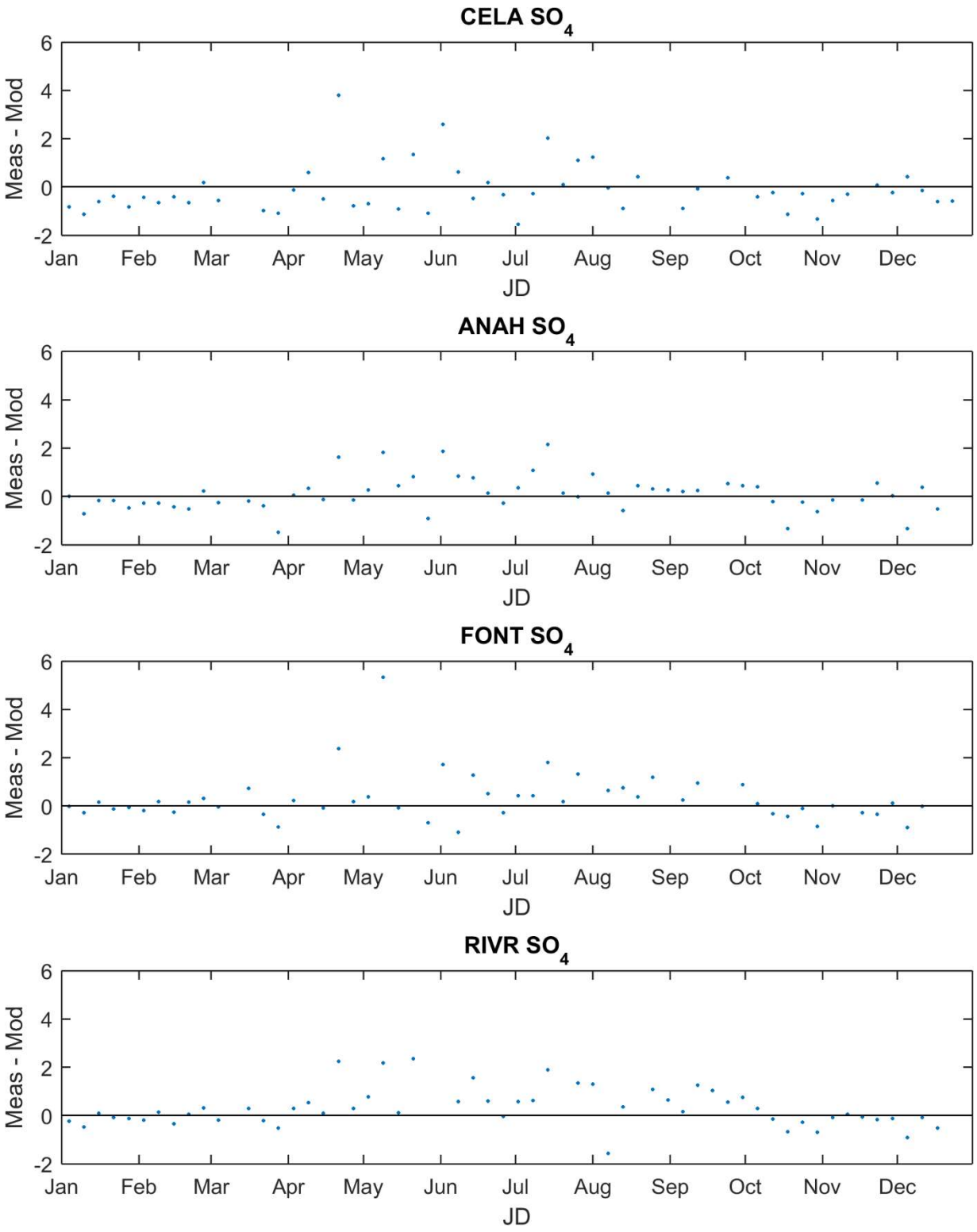

FIGURE V-6-13

2012 Differences in Modelled and Measured SO4 Mass.

Particulate sulfate formation is driven by hydroxyl radical concentrations and aqueous chemistry. The variation of hydroxyl radical concentration with season is well-characterized. Therefore, the modelled and observed dependence of sulfate fraction on water vapor mixing ratio was compared. Figures V-6-14 through V-6-17 illustrate the dependence of water mixing ratio on the sulfate fraction at each of the four measurement stations with speciation measurements.

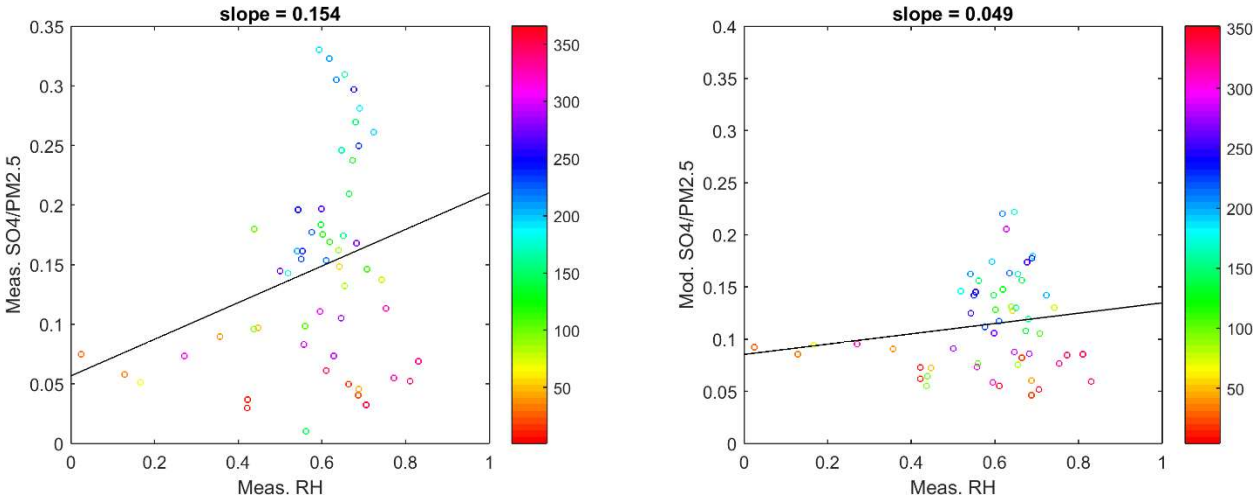

FIGURE V-6-14

2012 modelled and measured sulfate fraction dependence on water mixing ratio. Sulfate fractions are observed/modelled in Anaheim (ANAH). Water mixing ratios are observed/modelled at a nearby meteorological station in Fullerton (FUL). Modelled data points correspond to the days that measurements were available.

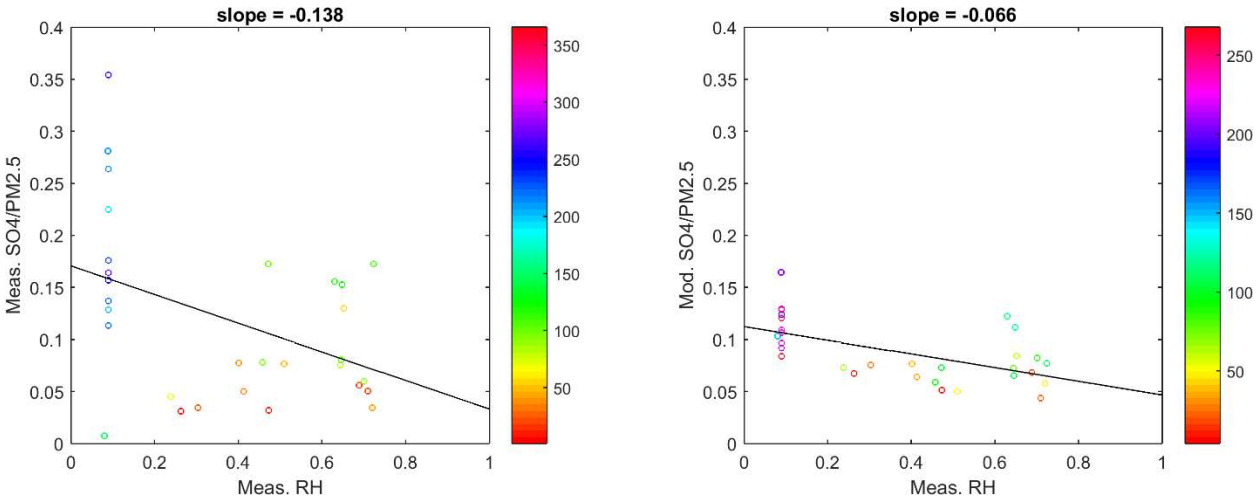

FIGURE V-6-15

2012 modelled and measured sulfate fraction dependence on water mixing ratio. Sulfate fractions are observed/modelled in Los Angeles (CELA). Water mixing ratios are observed/modelled at a representative meteorological station in Fullerton (FUL). Modelled data points correspond to the days that measurements were available.

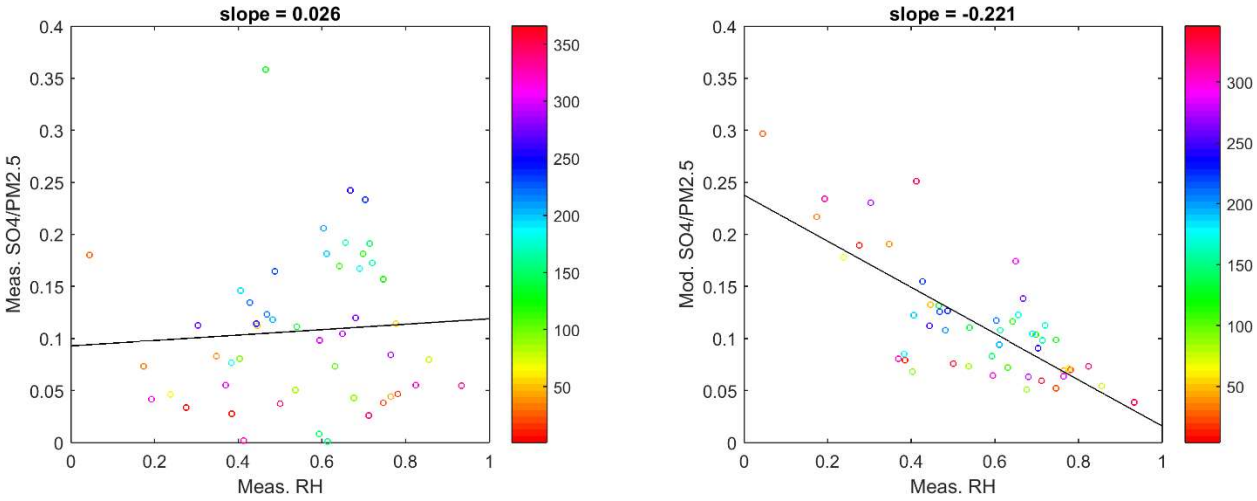

FIGURE V-6-16

2012 modelled and measured sulfate fraction dependence on water mixing ratio. Sulfate fractions are observed/modelled in Fontana (FONT). Water mixing ratios are observed/modelled at a nearby meteorological station in Ontario (ONT). Modelled data points correspond to the days that measurements were available.

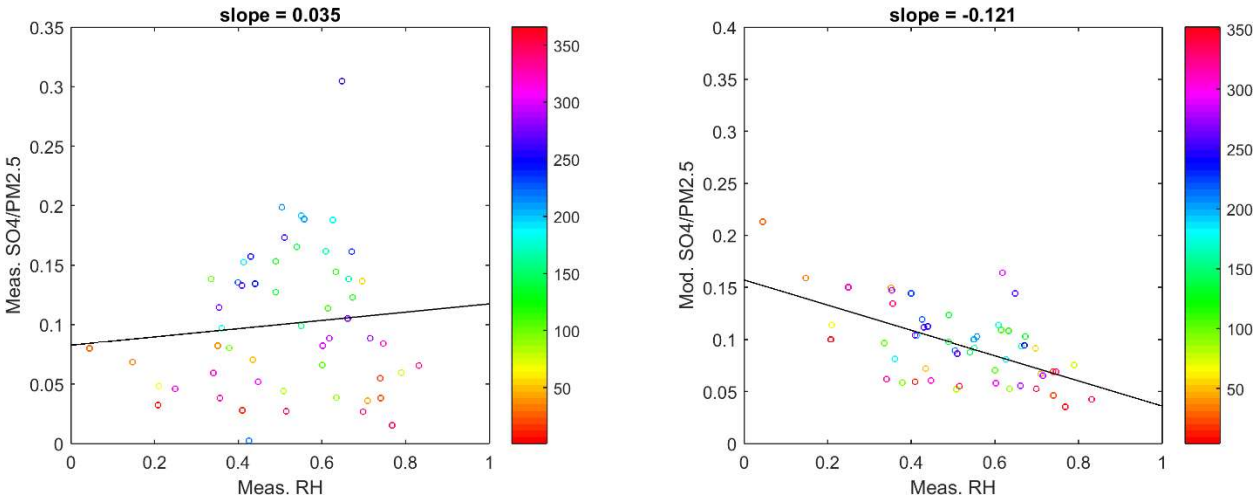

FIGURE V-6-17

2012 modelled and measured sulfate fraction dependence on water mixing ratio. Sulfate fractions are observed/modelled in Riverside (RIVR). Water mixing ratios are observed/modelled at a nearby meteorological station in Riverside (RAL). Modelled data points correspond to the days that measurements were available.

According to the observations, sulfate fraction is a strong function of the water mixing ratio at all four stations with slopes ranging from 0.014 to 0.021 kg g-1. However, modelled values exhibit a much weaker dependence. Since higher water mixing ratios occur in the spring and summer months, the model underestimates sulfate fraction during the second and third quarter. A comparison of modeled sulfate fractions and measured water mixing ratio also exhibits a weak dependence (not pictured). Therefore sulfate underestimation may be in part due to an inadequate capture of aqueous sulfate formation processes and not uncertainties in water mixing ratio predictions.

The absence of dimethyl sulfide emissions, a large source of biogenic sulfur, in our modelling analysis (DMS) may also contribute to this underestimation. DMS is produced by marine organisms. Transfer across the sea-air interface is dependent on ambient temperature, wind speed, and ambient concentrations of DMS. Once in the atmosphere, DMS is oxidized to form SO2. This process is the most important source of SO2 in the marine atmosphere. SO2 is then oxidized in gaseous or aqueous environments leading to the formation of particulate sulfate. Surface oceanic DMS concentrations are typically higher in spring in summer months when biological productivity is highest. Transport across the sea-air interface and into the atmosphere is also expected to be highest in the spring and summer months when on-shore winds are typically strongest. This unaccounted-for source of sulfate, which is more significant in the spring and summer months, could also explain model underestimation of particulate sulfate during the 2nd and 3rd quarter of the year.

Figure V-6-18 illustrates how sulfate model performance correlates with wind speed, wind direction, and ambient temperature. This figure is consistent with the hypothesis that the absence of oceanic DMS emissions in the model leads to an under-prediction of sulfate. This under-prediction is more significant during periods of strong onshore winds and higher temperatures.

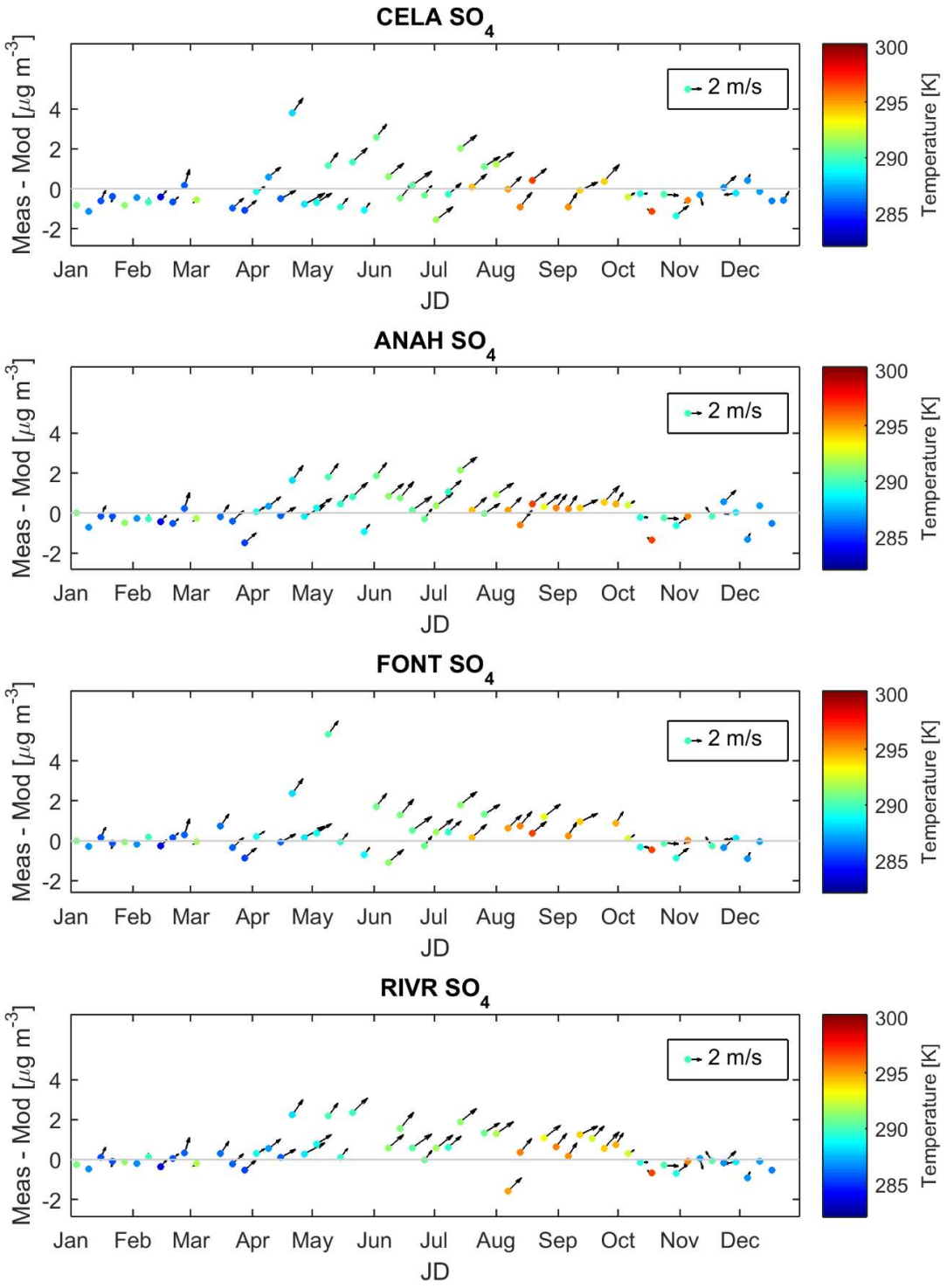

FIGURE V-6-18

PM2.5 sulfate model performance as a function of daily averaged wind speed, wind direction, and temperature at the closest corresponding airport station. Wind vectors indicate the direction that the wind blows from. The legend details the scale of the wind vectors. Colored dots indicate the average daily temperature.

Modelled sulfate is underestimated when the winds are relatively strong and originating from the west-south-west. This is consistent with the hypothesis that DMS from oceanic sources (west-south-west of the Basin) is a significant source of PM2.5 sulfate that is not captured sufficiently in the model.

The organic carbon fraction is underestimated in CMAQ. This underestimation is more significant in the inland locations of Fontana and Riverside, especially during the summer months, potentially due to the increased significance of photo-oxidation during transport from urban source regions. Model comparisons with speciation measurements must be evaluated in light of two main caveats: there is uncertainty of the measured organic fraction (calculated from a mass balance approach) that arises from the SANDWICH technique (Frank 2006) and the observed OC concentrations represent the organic compounds that remain on the FRM filter whereas the modeled OC concentrations represent ambient OC. OC typically contains a large semi-volatile fraction, which may evaporate or condense in response to variations in atmospheric conditions. An in-depth analysis of the sources of OC in the SoCAB and Secondary Organic Aerosol (SOA) formation mechanisms are needed to explain the significant model underestimations.

The average speciation profile at the four SASS stations over all quarters indicates that 34 percent of total PM2.5 mass is organic (Figure V-6-19). This organic fraction is consistent with measurements from other researchers using different instruments. This organic mass is comprised of primary organic aerosol (POA) and secondary organic aerosol (SOA). SOA is a significant fraction of the total organic aerosol; 63 percent of the total organic mass in Pasadena during the CalNex campaign was secondary (Hayes, Ortega et al. 2013; See Figure V-6-20) (Parrish 2014). Note that these measurements were of non-refractory PM1 and may differ slightly for PM2.5. However, less than 20 percent of the total OA mass is larger than 1 µm, indicating that the SOA/POA ratio should be similar for PM2.5 and PM1. This indicates that approximately 21 percent of the total PM2.5 mass in the Basin is SOA and approximately 13 percent is POA.

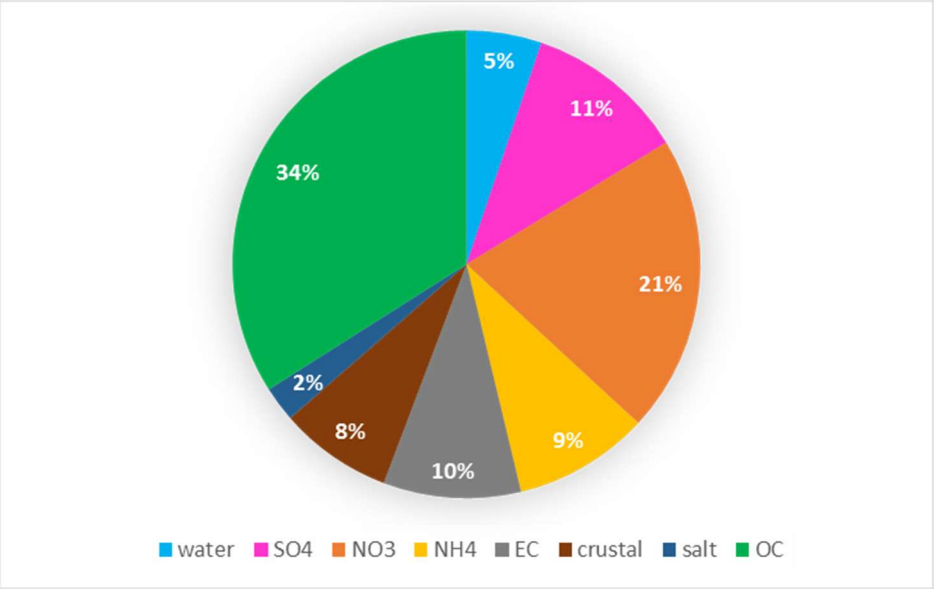

FIGURE V-6-19

Average Speciation Profile of $PM_{2.5}$

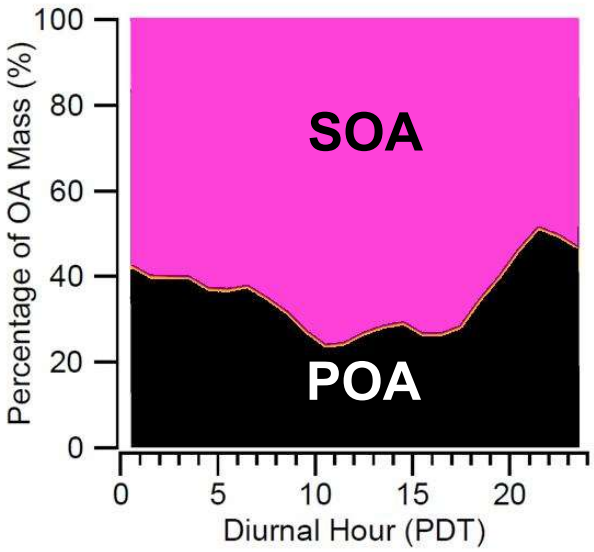

FIGURE V-6-20

Relative contribution of SOA and POA towards total organic aerosol mass in Pasadena in the summer of 2010. Adapted from (Hayes, Ortega et al. 2013)

The recent literature indicates that CMAQ underestimates observed SOA mass in the SoCAB by large factors—in some cases, up to a factor of 25 (Baker, Carlton et al. 2015, Hayes, Carlton et al. 2015). This

severe underestimation can distort prioritization of the most important precursors. While even the most current version of CMAQ does not close this gap, one should be cognizant of the reasons why CMAQ fails to accurately capture both total and secondary organic aerosol mass.

CMAQ SOA Mass Simulation

SOA underestimation may be due to the following factors (Baker, Carlton et al. 2015):

- missing VOC mass in the emission inventory
- poor model characterization of oxidants
- underestimation of SOA formation yields
- missing intermediate volatility organic compound (IVOC) emissions

Recent research has determined that IVOC emissions are an extremely important source of SOA (Figure V-6-21), yet the SOA from these emissions is not captured in CMAQ (Zhao, Hennigan et al. 2014). Certain emission categories are large IVOC sources, suggesting that reduced SOA formation (and lower PM2.5) could be an important co-benefit of controlling these sources.

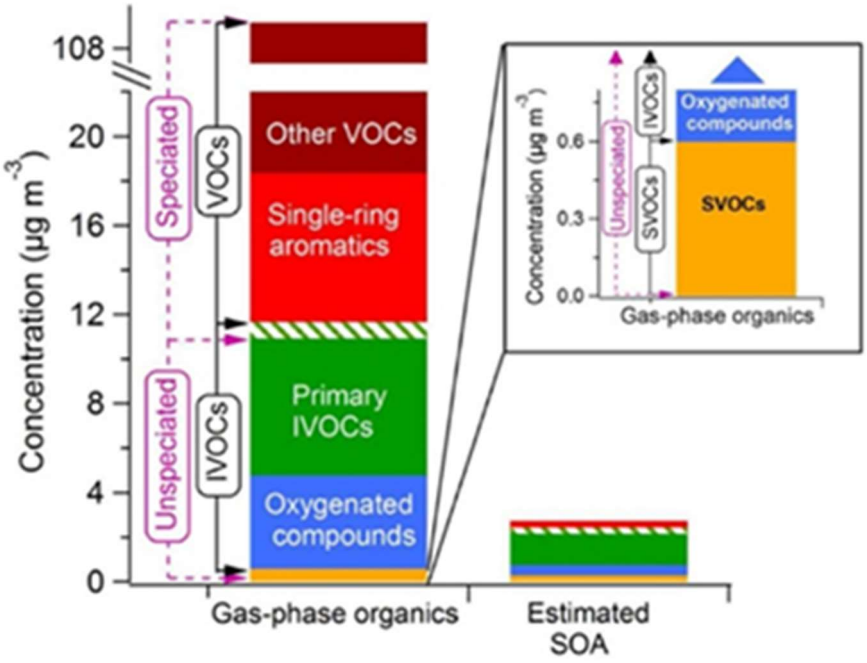

FIGURE V-6-21

Average concentrations of VOCs, IVOCs, and SVOCs and their estimated contribution towards SOA concentrations during CalNex. Total IVOC and Semi-volatile organic compounds (SVOC) are lower estimates. Note the discontinuous y-axis. Adapted from Zhao et al. 2014.

How IVOCs Lead to SOA Emissions

Many combustion sources emit a large set of organic compounds with different volatilities. The least volatile compounds condense soon after they are emitted and cool, forming POA. The most volatile compounds are VOCs, which ultimately may lead to ozone and possibly SOA as they are oxidized in the atmosphere. These VOCs are relatively easy to measure, and their chemistry is captured well with CMAQ. The largest uncertainty arises from the compounds that are less volatile than VOCs, making them difficult measure, but do not have volatilities that are low enough to lead to condensation as POA in the exhaust. These IVOCs and to a lesser extent, semi-volatile organic compounds (SVOCs), are very effective SOA precursors and their chemical reactions and emissions are largely not included in CMAQ. VOC and SVOC evaporation from ambient temperature application such as consumer products could also be an important SOA contributor assuming that there is ample time for evaporation

While these findings are relatively new, laboratory measurements are straightforward. The exhaust from a combustion source is put into a “smog chamber” equipped with UV lights where atmospherically relevant oxidant concentrations are added to simulate atmospheric processing. The SOA emission factor

for some sources may be significantly higher than the POA emission factor. Figure V-6-22 shows the results of experiments designed to measure POA, SOA, and VOC emission factors from gasoline vehicles, diesel vehicles, and biomass combustion. Gasoline vehicles on average can produce 50 times more SOA than POA. Moreover, on the timescale of a few hours, many direct PM combustion sources will also form a significant amount of secondary PM—potentially more than direct PM emissions—after they get oxidized in the atmosphere. The fractional contribution of several SOA sources in Pasadena calculated with a box model is shown in Figure V-6-23. Aerosol composition measurements were used as inputs to the model. The SOA from cooking emissions is a first-order estimate, as experiments designed to quantify these emission factors are still in progress.

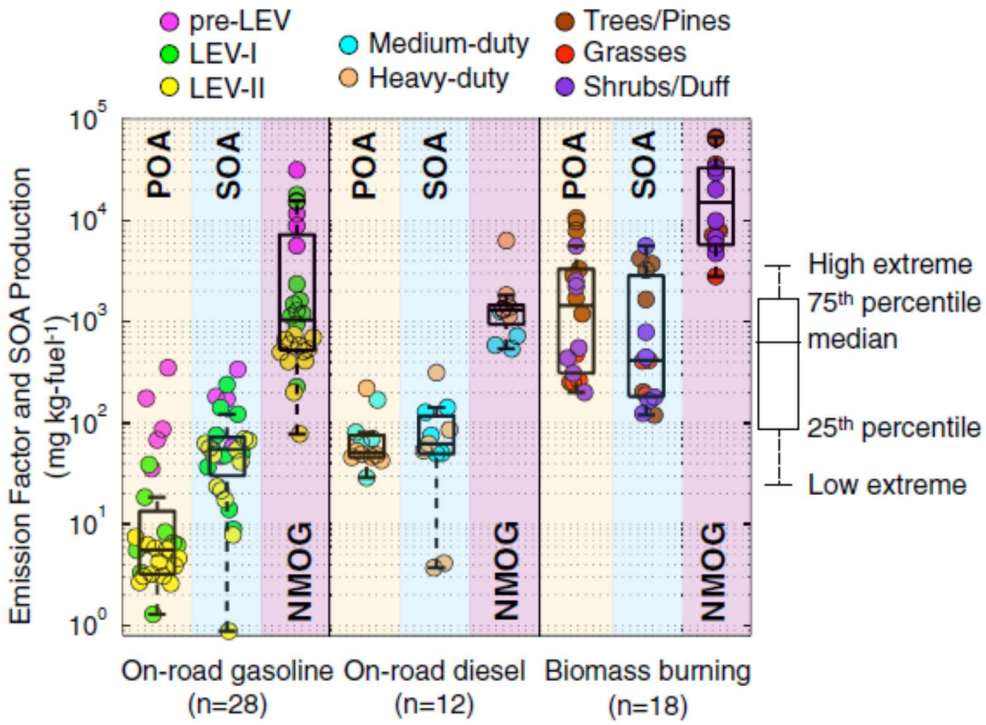

FIGURE V-6-22

Measured smog chamber emission factors of POA, SOA, and NMOG (VOCs) for three combustion sources. SOA emission factors are greater than or equal to POA emission factors for each source. These experiments represent only a few hours of photochemical aging. Diesel vehicles are not equipped with DPF. Figure from: (Jathar, Gordon et al. 2014)

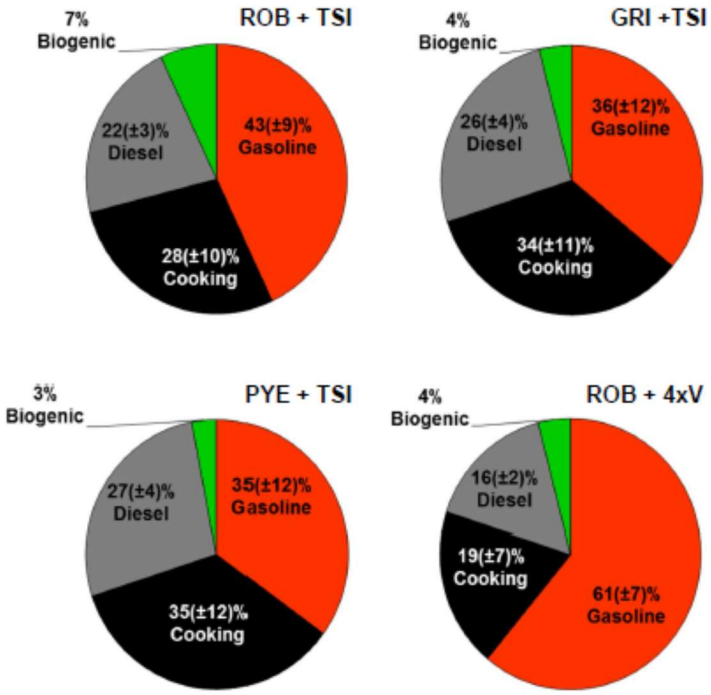

FIGURE V-6-23

Fractional contribution of SOA sources in Pasadena during CalNex 2010 calculated with four parameterizations. Figure from (Hayes, Carlton et al. 2015)

Annual PM2.5

Annual average PM2.5 species concentrations at the four SASS sites are shown in Figure V-6-24. Among the four stations, the lowest annual average PM2.5 concentration was observed at Anaheim and the highest annual average concentration was observed at Rubidoux. The highest sulfate concentration was observed in central Los Angeles, while the highest concentration of ammonium and nitrate occurred in Rubidoux. Annual average concentrations also show that OC is the most abundant component, being approximately equivalent to a third of the total PM2.5 concentration. As measured by the SASS sampler, OC concentrations are believed to be the most uncertain as explained in the 24-hour PM2.5 attainment demonstration chapter of this appendix.

Quarterly Average Data

Quarterly average PM2.5 species concentrations at the four SASS sites are shown in Figure V-6-25 through Figure V-6-28. In general, the sites in the western half of the Basin: Los Angeles and Anaheim, tend to have the highest average levels in the fourth quarter. Rubidoux also presents the highest concentration in the fourth quarter, whereas Fontana experiences the highest concentration in the third quarter. All stations tend to have the lowest concentrations in the first or second quarter. Typically, spring storms and favorable atmospheric dispersion drive PM2.5 concentrations down in the second quarter. Los Angeles and Anaheim presented the lowest concentrations during the second quarter, whereas Rubidoux and Fontana had the lowest value in the first quarter.

On average, secondary ammonium, nitrate and sulfate comprise about 40 percent of the total PM2.5 concentration and show strong seasonal variability. High nitrate concentrations in the fall or winter are caused by the favorable formation of ammonium nitrate under cool temperatures, high humidity and frequent nocturnal inversions. On the contrary, high summertime temperatures reduce concentrations of ammonium nitrate—a relatively volatile species. The higher values of sulfate typically occur under conditions of strong-elevated inversions and strong sea breeze transport toward inland areas, which is the characteristic of late spring and summer. In addition, heterogeneous formation of sulfate is favored by higher temperatures occurring in the summer. Higher temperatures with abundant afternoon sunlight and the persistence of morning fog and low clouds trigger both homogeneous and heterogeneous sulfate formation reactions to produce secondary sulfate.

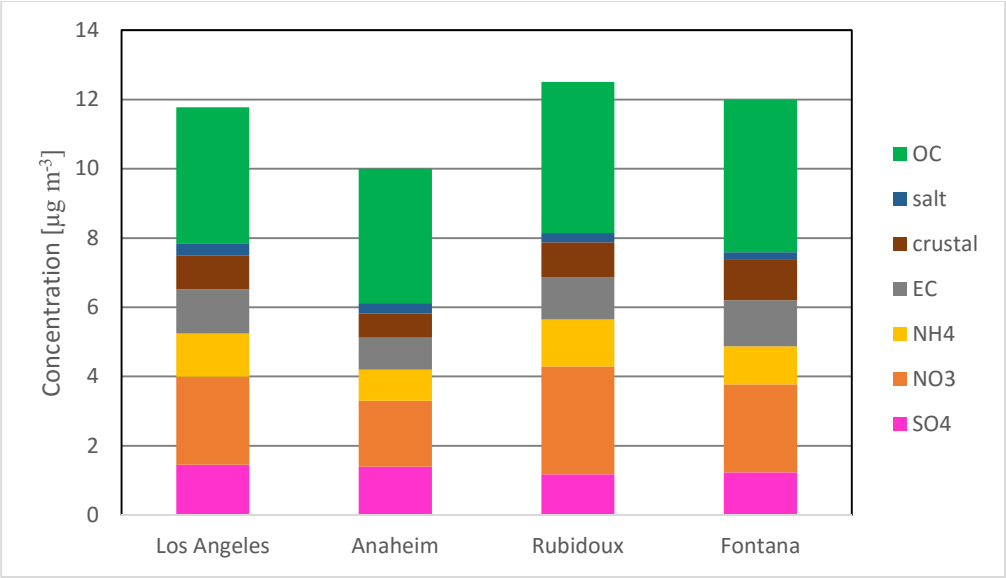

FIGURE V-6-24

Annual Average PM2.5 Species Concentrations at 4 SASS Sites (µg/m^3)

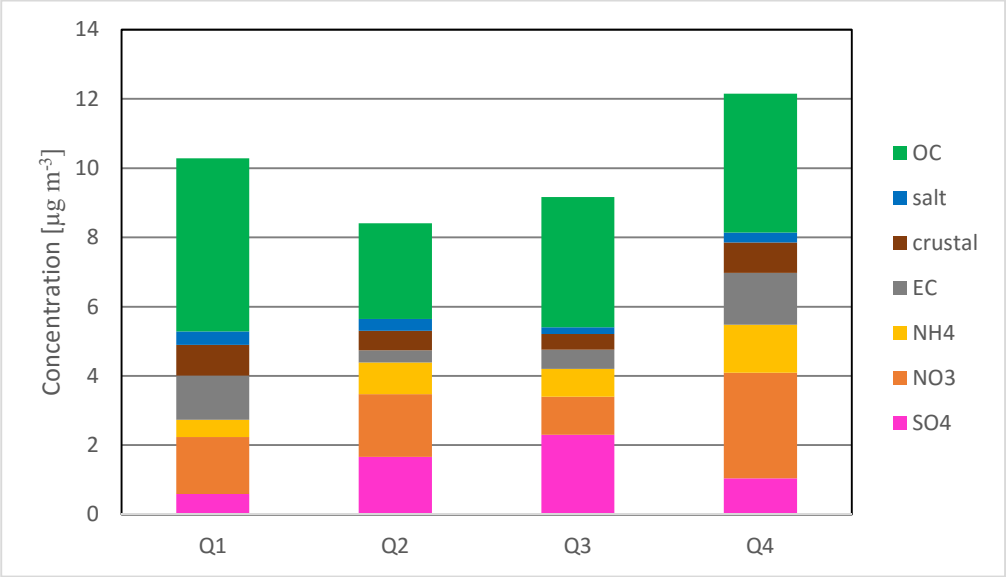

FIGURE V-6-25

PM2.5 Quarterly Average Species Concentrations (µg/m^3) at Anaheim

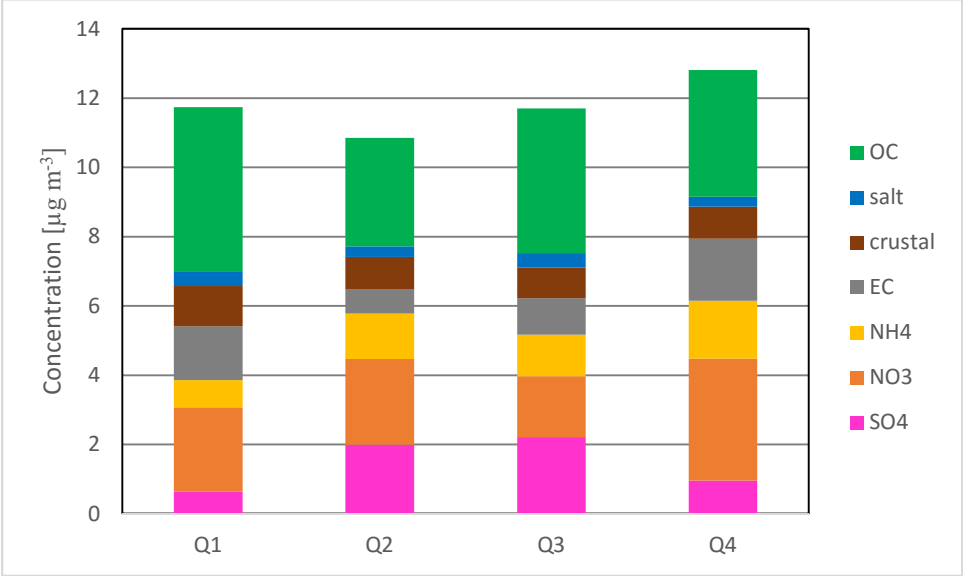

FIGURE V-6-26

PM2.5 Quarterly Average Species Concentrations (µg/m^3) at Downtown Los Angeles

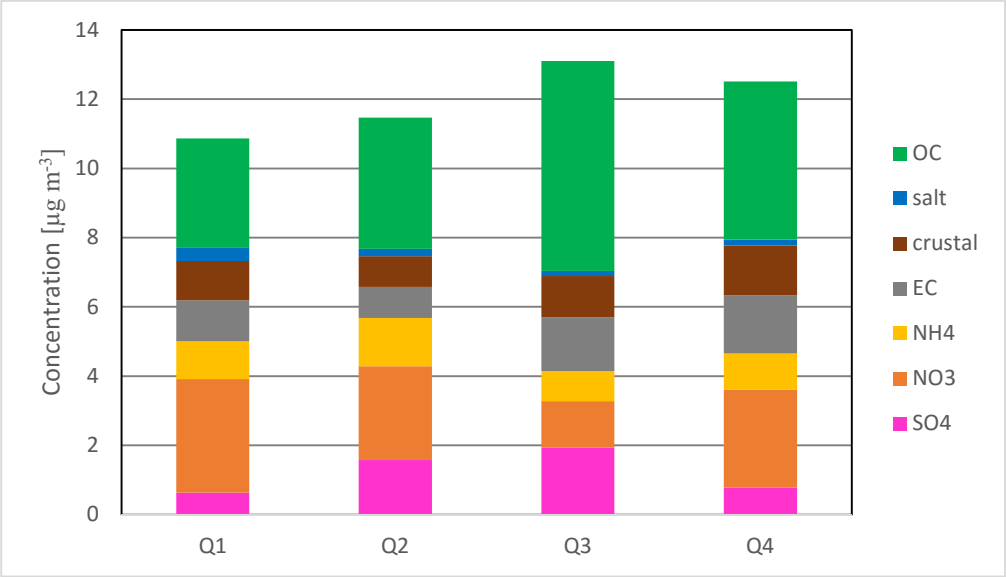

FIGURE V-6-27

PM2.5 Quarterly Average Species Concentrations (µg/m^3) at Fontana

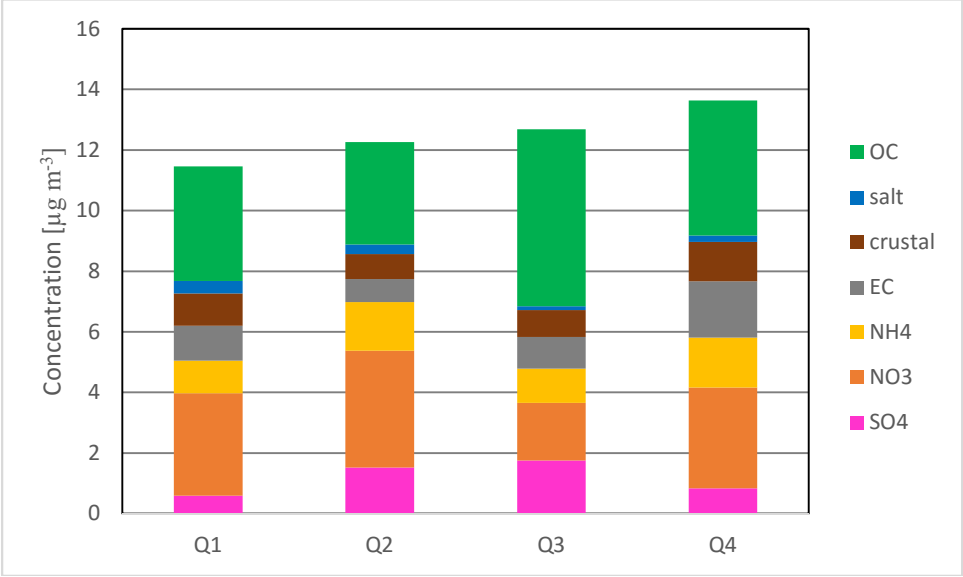

FIGURE V-6-28

PM2.5 Quarterly Average Species Concentrations (µg/m^3) at Rubidoux

OC and nitrate are the two most common species with OC comprising between 25 percent and 43 percent of the total PM2.5 mass, depending on season and location. OC in general tends to be higher during the 3rd quarter. Higher temperatures and abundant sunlight increase evaporative emissions of Secondary Organic Aerosol (SOA) precursors, and increase photochemical processing of those precursors. However, OC concentrations measured with the SASS sampler are believed to be highly uncertain and as a consequence are subject to the "Sulfate, Adjusted Nitrate, Derived Water, Inferred Carbon Hybrid (SANDWICH)" method correction for component mass reconciliation. Roughly 11 percent to 30 percent of the total PM2.5 mass is nitrate. Figures V-6-29 through V-6-32 provide the corrected species fractions for each site and each quarter.

Table V-6-4 lists annual and 5-year weighted quarterly average design values at each of the four SASS sites covering the period 2010 through 2014. Table V-6-5 lists the SANDWICH applied 5-year weighted quarterly speciation FRM data for each station. As expected, the annual fractional contributions to the quarterly mass at each site differed from those on the 24-hour standard design days.

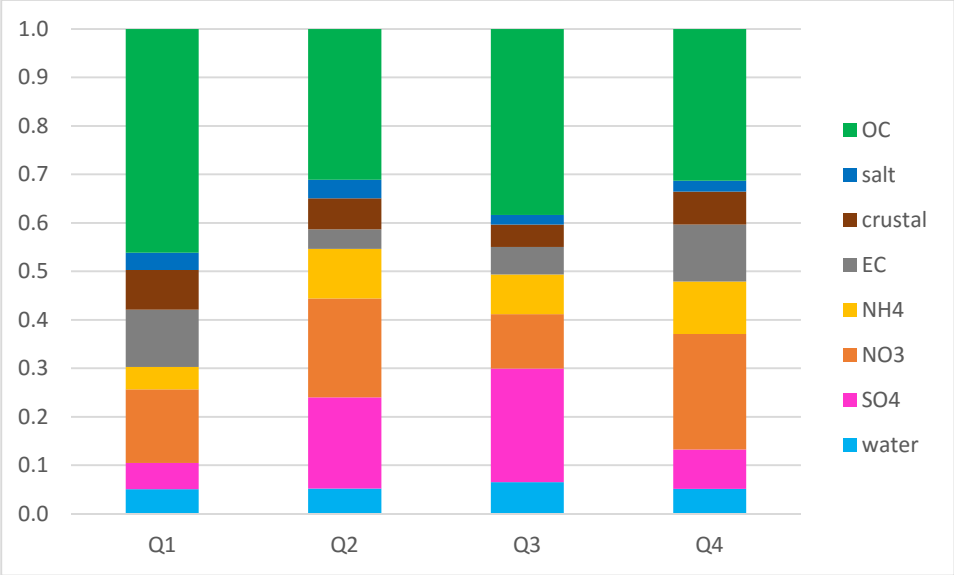

FIGURE V-6-29

2012 Anaheim quarterly PM2.5 species fractional splits after the SANDWICH correction

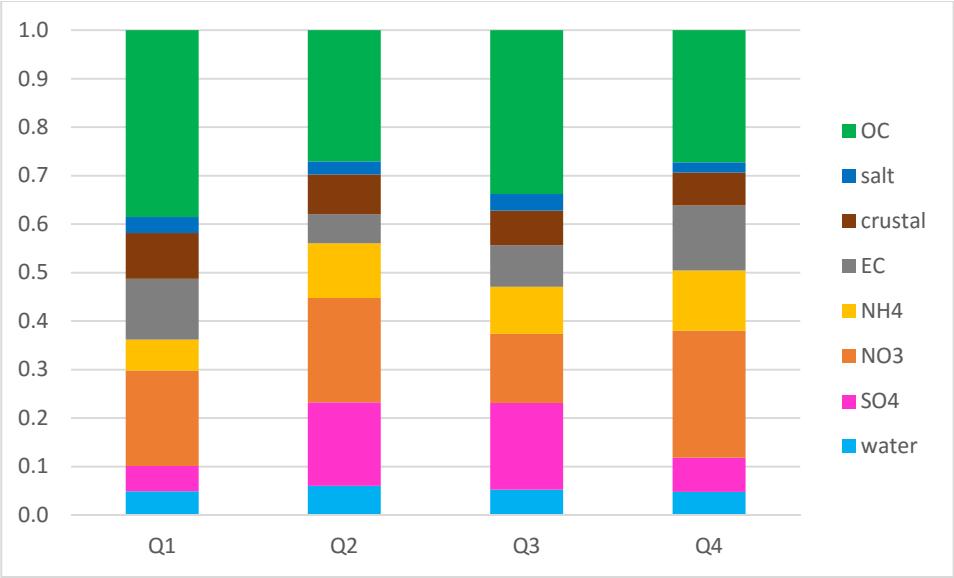

FIGURE V-6-30

2012 Los Angeles quarterly PM2.5 species fractional splits after the SANDWICH correction

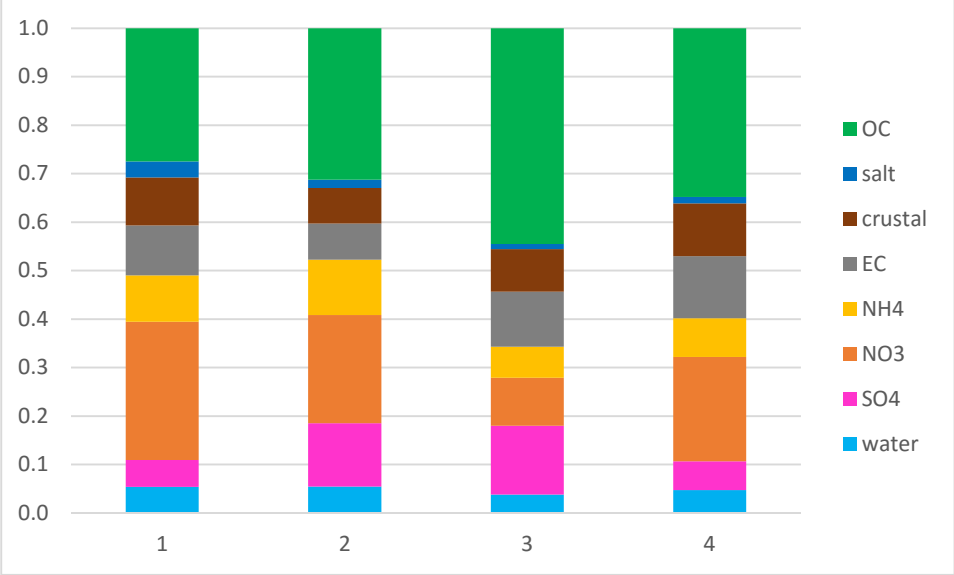

FIGURE V-6-31

2012 Fontana quarterly PM2.5 species fractional splits after the SANDWICH correction

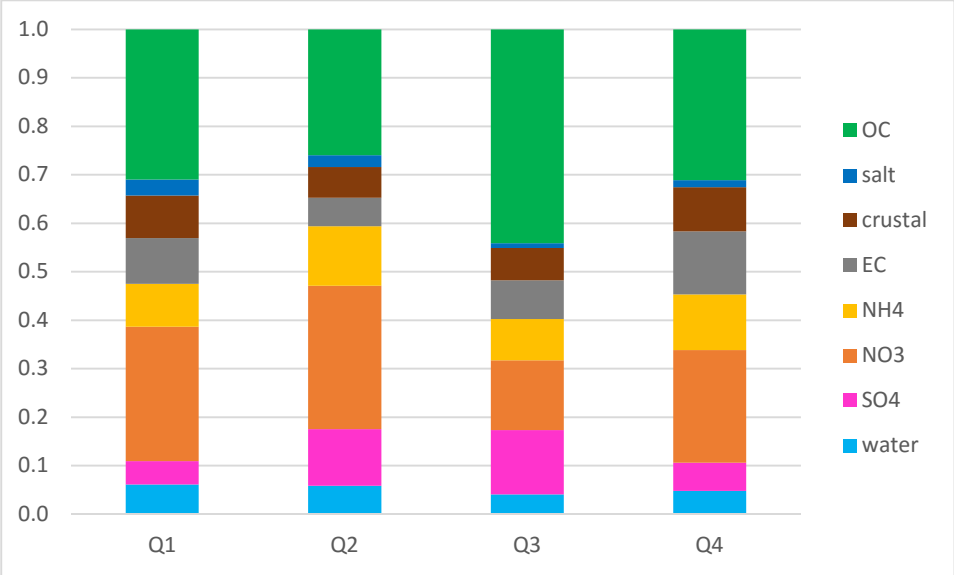

FIGURE V-6-32

2012 Rubidoux quarterly PM2.5 species fractional splits after the SANDWICH correction

TABLE V-6-4

5-Year Weighted Annual and Quarterly PM2.5 Design Values (2010–2014)

Monitoring Site	Quarter 1 (µg/m^3)	Quarter 2 (µg/m^3)	Quarter 3 (µg/m^3)	Quarter 4 (µg/m^3)	Annual (µg/m^3)
Anaheim	10.83	8.87	9.81	12.81	10.58
Los Angeles	12.35	11.55	12.35	13.45	12.43
Fontana	11.48	12.13	13.62	13.13	12.59
Mira Loma	14.50	14.10	13.91	16.94	14.86
Rubidoux	12.20	13.03	13.22	14.32	13.19

TABLE V-6-5

SANDWICH Applied Quarterly Speciated FRM Data

Site		Mass	OC	EC	NH4	NO3	SO4	Crustal	Salt	Water	Blank
Los Angeles	1q	12.350	4.567	1.487	0.760	2.329	0.616	1.114	0.393	0.584	0.500
Los Angeles	2q	11.550	2.991	0.666	1.250	2.374	1.903	0.901	0.297	0.669	0.500
Los Angeles	3q	12.350	4.005	1.018	1.145	1.690	2.122	0.846	0.404	0.620	0.500
Los Angeles	4q	13.450	3.524	1.729	1.612	3.388	0.919	0.884	0.276	0.616	0.500
Anaheim	1q	10.830	4.766	1.219	0.478	1.567	0.561	0.846	0.372	0.521	0.500
Anaheim	2q	8.870	2.603	0.336	0.859	1.710	1.570	0.531	0.323	0.437	0.500
Anaheim	3q	9.810	3.573	0.532	0.762	1.042	2.182	0.429	0.182	0.608	0.500
Anaheim	4q	12.810	3.849	1.445	1.333	2.930	1.000	0.841	0.278	0.634	0.500
Rubidoux	1q	12.200	3.622	1.109	1.035	3.241	0.565	1.020	0.392	0.715	0.500
Rubidoux	2q	13.030	3.252	0.732	1.536	3.710	1.462	0.796	0.308	0.734	0.500
Rubidoux	3q	13.220	5.615	1.014	1.084	1.828	1.688	0.847	0.125	0.520	0.500
Rubidoux	4q	14.320	4.299	1.791	1.588	3.215	0.802	1.262	0.202	0.662	0.500
Fontana	1q	11.480	3.017	1.133	1.047	3.133	0.609	1.085	0.366	0.590	0.500
Fontana	2q	12.130	3.631	0.864	1.332	2.597	1.514	0.849	0.207	0.636	0.500
Fontana	3q	13.620	5.837	1.493	0.836	1.295	1.866	1.153	0.140	0.499	0.500
Fontana	4q	13.130	4.395	1.618	1.005	2.715	0.755	1.377	0.171	0.594	0.500

Figures V-6-33 through V-6-36 present the ratio of the 24-hour to annual PM2.5 fractional species contributions for the four SASS sites. These plots provide insight into the contribution of PM2.5 components during episodic concentration peaks, relative to their contribution to the PM2.5 annual average. In general, the 24-hour PM2.5 “other” category is consistently a smaller percentage than the annual PM2.5 “other” for all seasons. In the inland locations of Fontana and Rubidoux, where secondary PM dominates, ammonium and nitrate have generally higher fractions for the episodic 24-hour PM2.5. On the contrary, EC presents lower fractions for the episodic 24-hour PM2.5. EC is generally a primary pollutant and is generated by sources such as traffic that do not present significant seasonal variability, and therefore contributes consistently to the annual average. OC, which has both primary and secondary contributions, also presents lower fractions in inland locations. This indicates that episodic PM2.5 in inland locations is generally dominated by the formation of ammonium nitrate, which originates predominately from photochemical reactions of NOx emitted at upwind locations. In Los Angeles and

Anaheim, where PM concentrations are dominated by primary emissions, ammonium and nitrate do not have as high of a fraction as compared to the fraction at inland stations. In Los Angeles, sulfate fractions remain fairly constant near unity during the first three quarters, indicating that the influence of sulfate sources like the Long Beach and Los Angeles Port complex and heavy duty vehicle traffic remain constant during those periods.

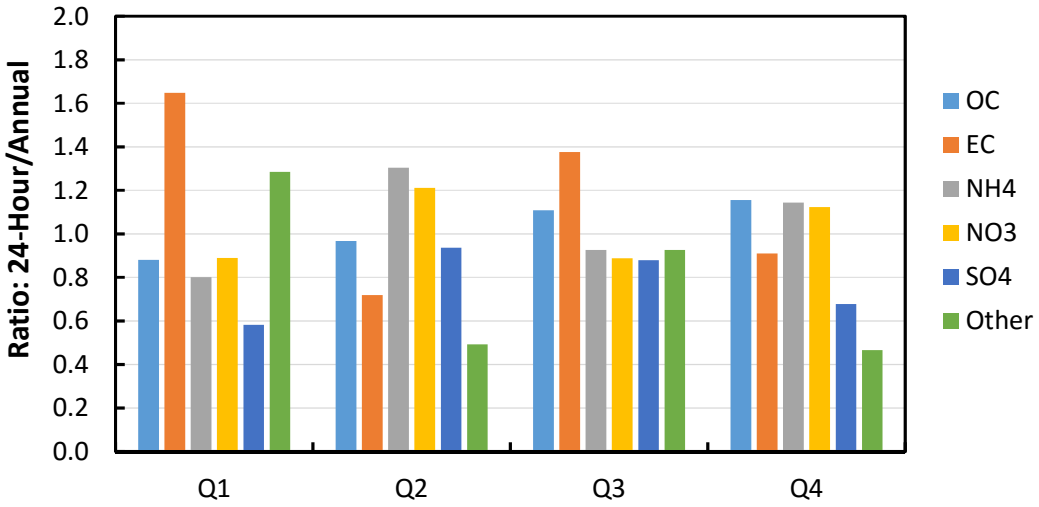

FIGURE V-6-33

2012 average quarterly ratio of 24-hour to annual species fractional contributions to PM2.5 after the SANDWICH correction for Anaheim

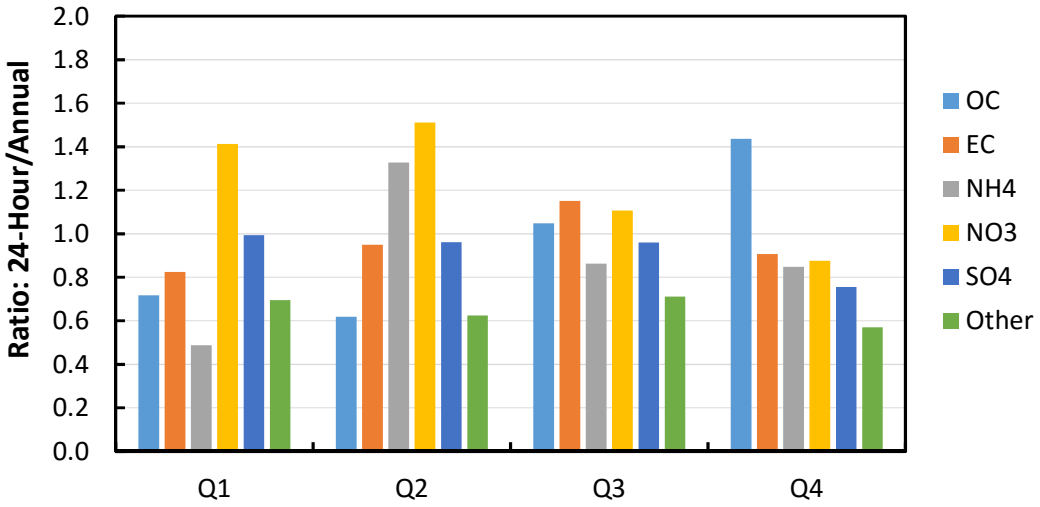

FIGURE V-6-34

2012 average quarterly ratio of 24-hour to annual species fractional contributions to PM2.5 after the SANDWICH correction for Los Angeles

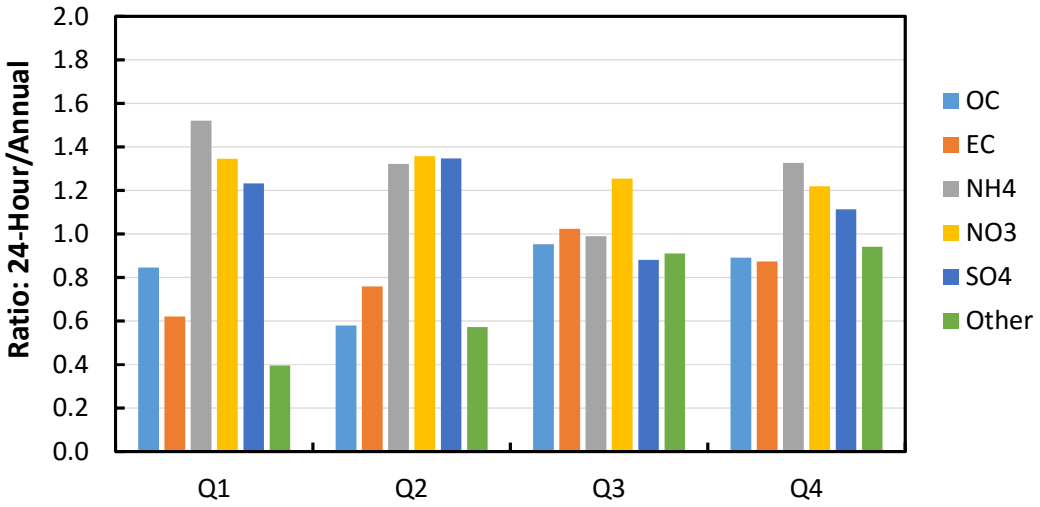

FIGURE V-6-35

2012 average quarterly ratio of 24-hour to annual species fractional contributions to PM2.5 after the SANDWICH correction for Fontana

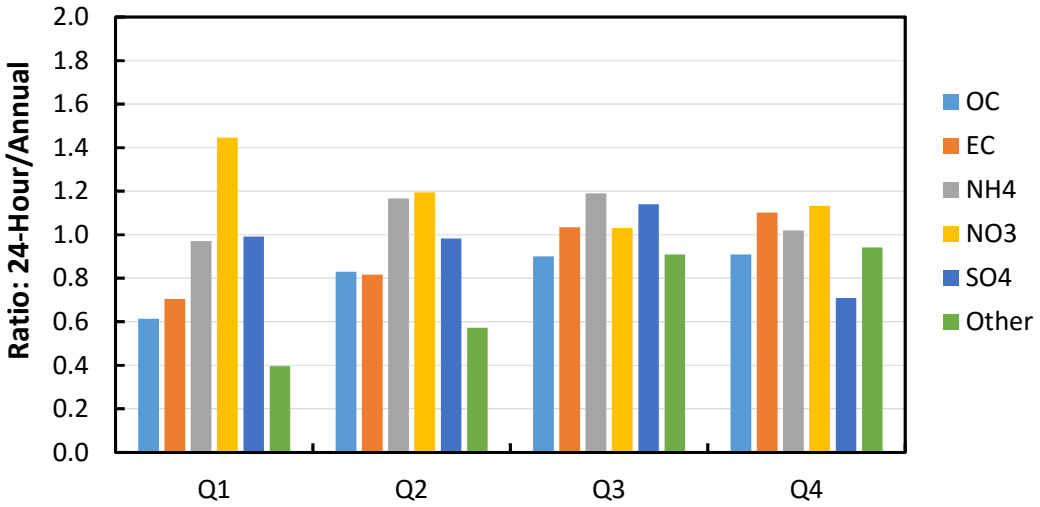

FIGURE V-6-36

2012 average quarterly ratio of 24-hour to annual species fractional contributions to PM2.5 after the SANDWICH correction for Rubidoux

Future Annual PM2.5 air quality

PM2.5 annual concentrations projected for milestone years under different control scenarios are shown in Figure V-6-37. Mira Loma is projected to remain the most polluted station in 2021 and 2025. All areas will be in attainment of the federal annual standard (12 µg/m3) by 2025 in the presence of directly emitted PM controls. However, Mira Loma will not attain the annual standard in 2021, even in the presence of controls. Impacts of the ozone control strategy on future PM2.5 design values were also investigated. The ozone control strategy will lead to attainment of the annual PM2.5 standard by 2023. Due to the limitation that emission reductions approved under CAA Section 182(2)(5) cannot apply toward the PM2.5 attainment demonstration, reductions associated with non 182(e)(5) measures were simulated for 2025 (the column marked in orange in Figure V-6-37). This was projected to be sufficient to reach attainment, indicating that the ozone strategy leading to 2023 attainment is critical for annual PM2.5 attainment. Tables V-6-6 through V-6-9 provide the projected future year PM2.5 annual design values by component species for 2021 and 2025 with proposed controls implemented.

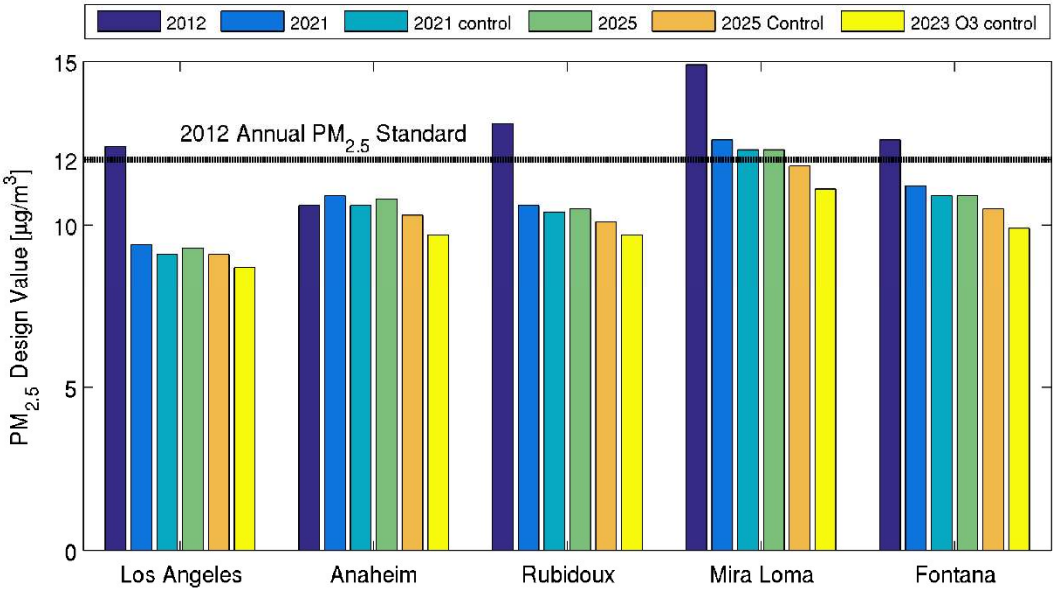

FIGURE V-6-37

Annual Average PM2.5 Concentrations. Federal Standard in Denoted with Horizontal Grey Line.

TABLE V-6-6

CMAQ Predicted 2021 Annual Concentrations (µg/m^3) with Directly Emitted PM Control

Locations	NH4	NO3	SO4	OC	EC	Others	Water	Blank	Salt	Mass
Anaheim	0.6	1.3	1.2	3.4	0.6	0.7	0.5	0.5	0.3	9.1
Fontana	0.7	1.5	1.1	3.8	0.8	1.2	0.5	0.5	0.2	10.4
Los Angeles	0.9	1.9	1.3	3.4	0.8	1.0	0.5	0.5	0.3	10.6
Mira Loma	1.0	2.2	1.2	4.4	0.9	1.3	0.6	0.5	0.3	12.3
Rubidoux	0.8	1.9	1.1	4.0	0.8	1.1	0.5	0.5	0.2	10.9

TABLE V-6-7

CMAQ Predicted 2025 Annual Concentrations (µg/m^3)

Locations	NH4	NO3	SO4	OC	EC	Others	Water	Blank	Salt	Mass
Anaheim	0.6	1.2	1.2	3.7	0.6	0.8	0.5	0.5	0.3	9.3
Fontana	0.6	1.4	1.2	4.1	0.8	1.3	0.5	0.5	0.2	10.5
Los Angeles	0.9	1.8	1.3	3.7	0.8	1.0	0.5	0.5	0.3	10.8
Mira Loma	0.9	2.0	1.2	4.8	0.9	1.3	0.6	0.5	0.3	12.3
Rubidoux	0.7	1.7	1.1	4.3	0.8	1.1	0.5	0.5	0.3	10.9

TABLE V-6-8

CMAQ Predicted 2023 PM Annual Concentration (µg/m^3)
with the Control Strategy to Attain 8-hour Ozone Standard in 2023

Locations	NH4	NO3	SO4	OC	EC	Others	Water	Blank	Salt	Mass
Anaheim	0.4	0.7	1.2	3.7	0.6	0.8	0.7	0.5	0.2	8.7
Fontana	0.4	0.8	1.2	4.1	0.8	1.3	0.5	0.5	0.2	9.7
Los Angeles	0.6	1.0	1.3	3.7	0.8	1.0	0.5	0.5	0.3	9.7
Mira Loma	0.5	1.1	1.2	4.8	0.9	1.2	0.6	0.5	0.3	11.1
Rubidoux	0.5	0.9	1.1	4.3	0.8	1.1	0.5	0.5	0.2	9.9

TABLE V-6-9

CMAQ Predicted 2025 Annual Concentrations (µg/m^3) Emission Reductions Associated with non-182(e)(5) Measures.

Locations	NH4	NO3	SO4	OC	EC	Others	Water	Blank	Salt	Mass
Anaheim	0.5	1.0	1.2	3.7	0.6	0.8	0.6	0.5	0.3	9.0
Fontana	0.5	1.1	1.2	4.1	0.8	1.3	0.5	0.5	0.2	10.1
Los Angeles	0.8	1.5	1.3	3.7	0.8	1.0	0.5	0.5	0.3	10.3
Mira Loma	0.7	1.6	1.2	4.8	0.9	1.3	0.6	0.5	0.3	11.8
Rubidoux	0.6	1.4	1.1	4.3	0.8	1.1	0.5	0.5	0.2	10.5

Spatial Projections of Annual PM2.5 Design Values

Figure V-6-38 provides a perspective of the Basin-wide spatial extent of annual PM2.5 design values in the base year, 2012. Figures V-6-39 and V-6-40 provide the Basin-wide spatial extent of annual PM2.5 projected for 2021 baseline and controlled scenario. With and without additional controls, by 2021, the number of grid cells with concentrations exceeding the federal standard is restricted to a small region around the Mira Loma monitoring station in northwestern Riverside County. Figure V-6-41 shows the projected PM2.5 concentrations in 2023 with the full implementation of the ozone control strategy, but no additional control on directly emitted PM. The 2025 baseline case does not lead to attainment of the standard (Figure V-6-42), but NOx and VOC reductions from non-182(e)(5) control measures are expected to lead to attainment as all the monitoring stations within the Basin exhibit annual PM2.5 levels below the federal standard of 12 µg/m^3. (Figure V-6-43).

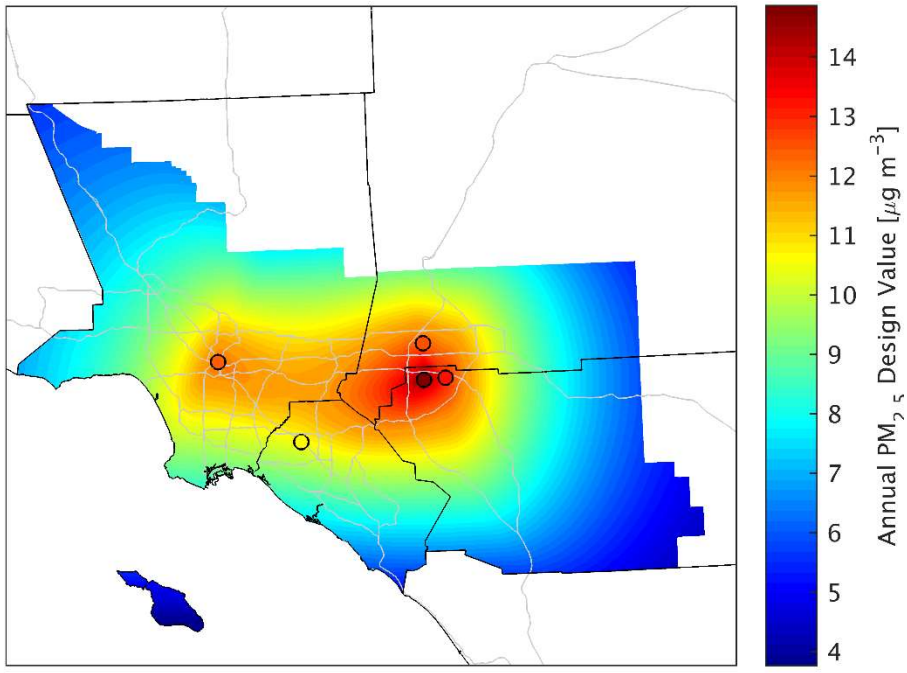

FIGURE V-6-38

2012 Annual PM2.5 Design Value (µg/m^3)

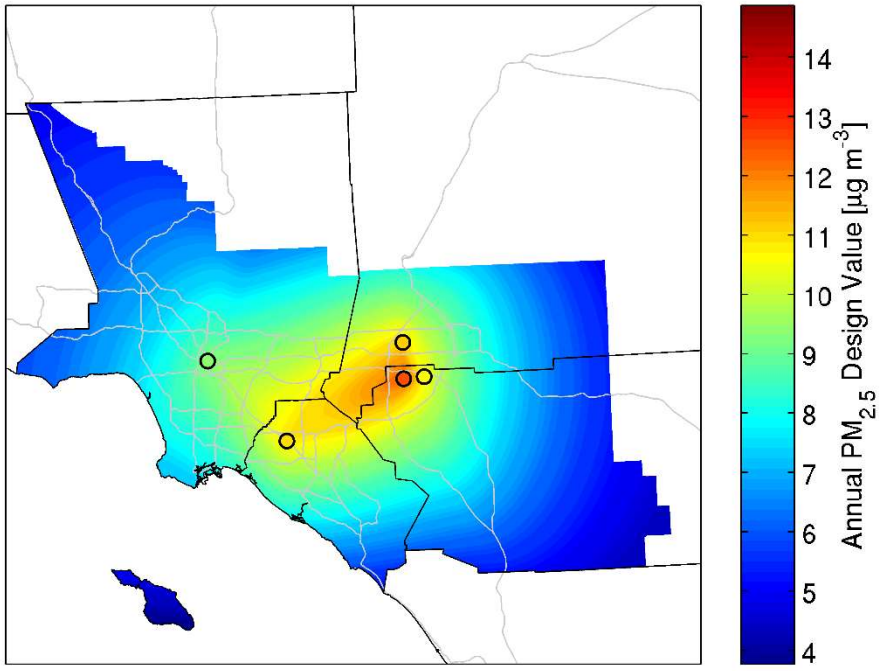

FIGURE V-6-39

2021 Baseline Annual PM2.5 Concentrations (µg/m^3)

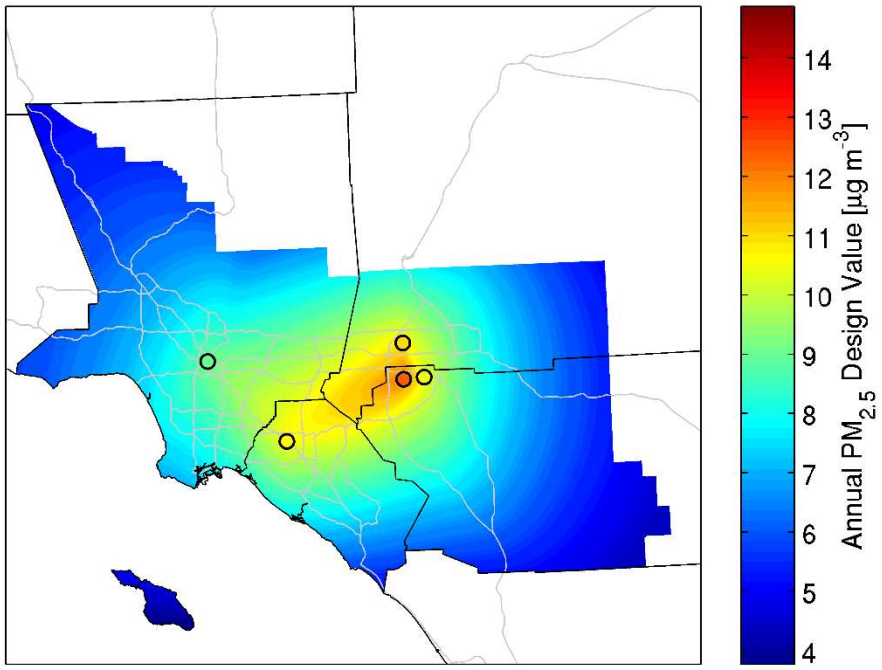

FIGURE V-6-40

2021 Annual PM2.5 Concentrations with Directly Emitted PM Control (µg/m^3)

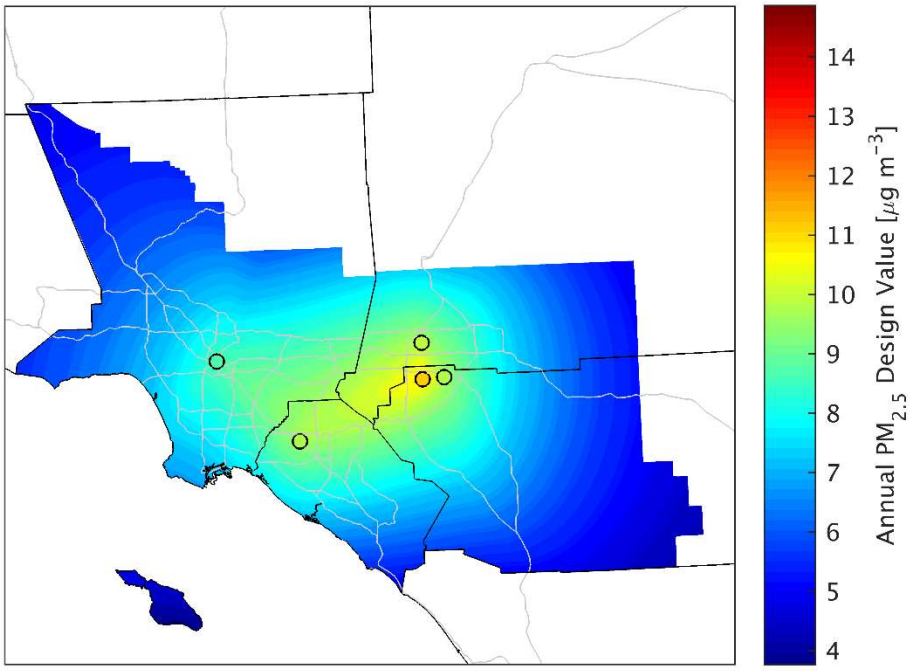

FIGURE V-6-41

2023 Annual PM2.5 Concentration (µg/m^3) with the Control Strategy to attain 8-hour Ozone Standard.

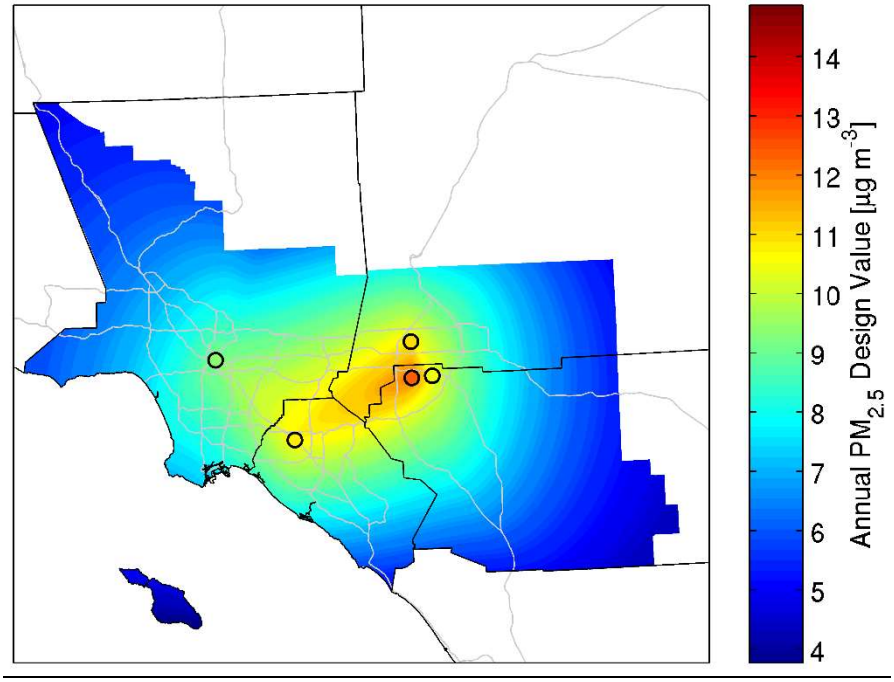

FIGURE V-6-42

2025 Baseline Annual PM2.5 Concentrations (µg/m^3)

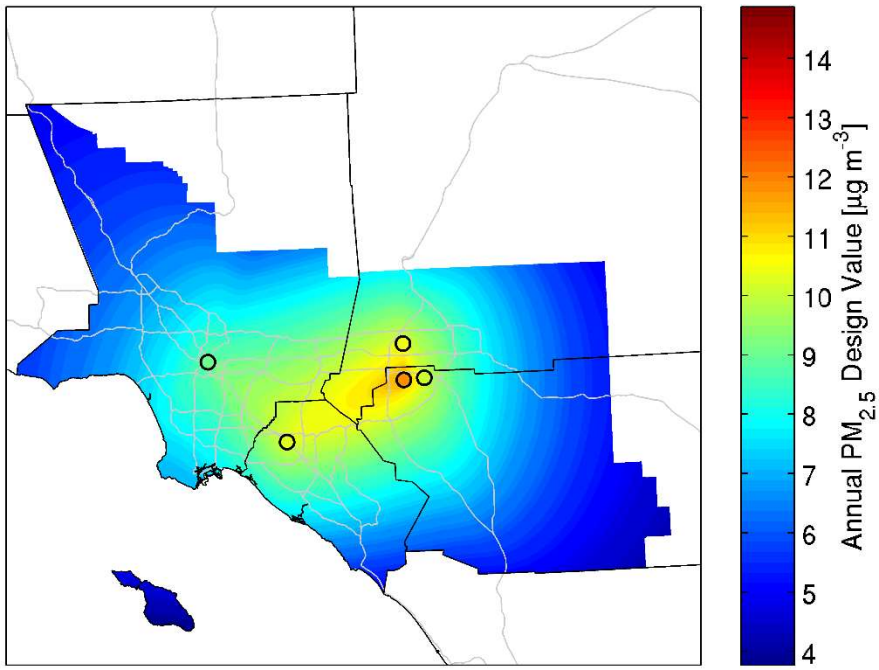

FIGURE V-6-43

2025 Annual PM2.5 Concentration (µg/m^3) with Emission Reductions Associated with non-182(e)(5) measures.

Unmonitored Area Analysis

U.S. EPA modeling guidance requires that the attainment demonstration include an analysis that confirms that all grid cells in the modeling domain meet the federal standard. This "unmonitored area analysis" is essential since speciation monitoring is conducted at a limited number of sites in the modeling domain. Variability in the species profiles at selected locations coupled with the differing responses to emissions control scenarios are expected to result in spatially variable impacts to PM2.5 air quality in any grid cell. As described earlier in this chapter, speciation profiles from SASS sites in adjacent or collocated grid cells are used in the formal attainment demonstration for Mira Loma. With interpolation of the SASS speciation profiles, attainment demonstrations can be directly conducted for the remaining grid cells where FRM mass data has been collected over the 5-year period (2010–2014).

The methodology used to assess the unmonitored grid cell impact is as follows. The speciation fractions throughout the Basin for each relevant species except particle bound water were estimated with a natural neighbor interpolation for each quarter of 2012. While the four SASS speciation stations encompass all areas of high PM concentrations in the Basin, it was necessary to create "pseudo stations" at the corners

of the modelling domain to aid in extrapolation. The speciation fractions at these pseudo stations were assigned as the average speciation fraction measured at all four stations. The speciation fractions in areas of the Basin which are expected to have high PM concentrations were not appreciably affected by the choice of "pseudo station" speciation as the areas of interest are much closer to the SASS stations than the "pseudo stations." A natural neighbor interpolation based on a Voronoi tessellation has been shown to reproduce ozone concentration profiles in the Basin more accurately than an inverse distance weighting, inverse distance weight squared, nearest neighbor, or linear interpolation scheme (See Appendix 5, Chapter 5). Figure V-6-44 details the interpolated nitrate species fractions in quarters 1-4. The interpolated species fractions for all relevant species are presented in Attachment 7.

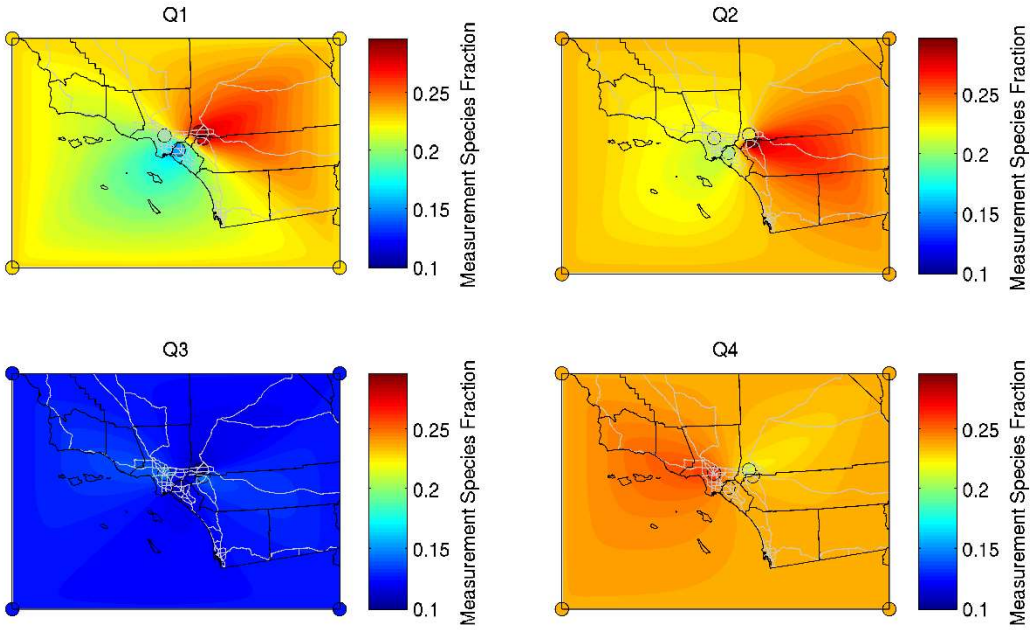

FIGURE V-6-44

2012 Interpolated Annual Measurement Species Fractions for Nitrate. FRM locations are illustrated with black dots. SASS speciation stations and "pseudo stations" are illustrated with circles.

In the unmonitored area analysis, five-year weighted annual PM2.5 design values were calculated for all Federal Reference Method (FRM) monitoring stations within the modelling domain for the 2010 to 2014 period for each quarter. Only quarters that meet the completeness criteria established by the EPA were used in the analysis. While some stations did not have a complete 5-year data record, we still choose to include them in the analysis if they contained more than 6 out of 9 values for the weighted-average. Years 2010 and 2014 were weighed once, years 2011 and 2013 were weighed twice, and 2012 was weighed thrice. Figures V-6-45 through V-6-48 illustrate the number of weighted values for each station for quarters 1-4. Stations that were not used in the analysis are marked with an "x".

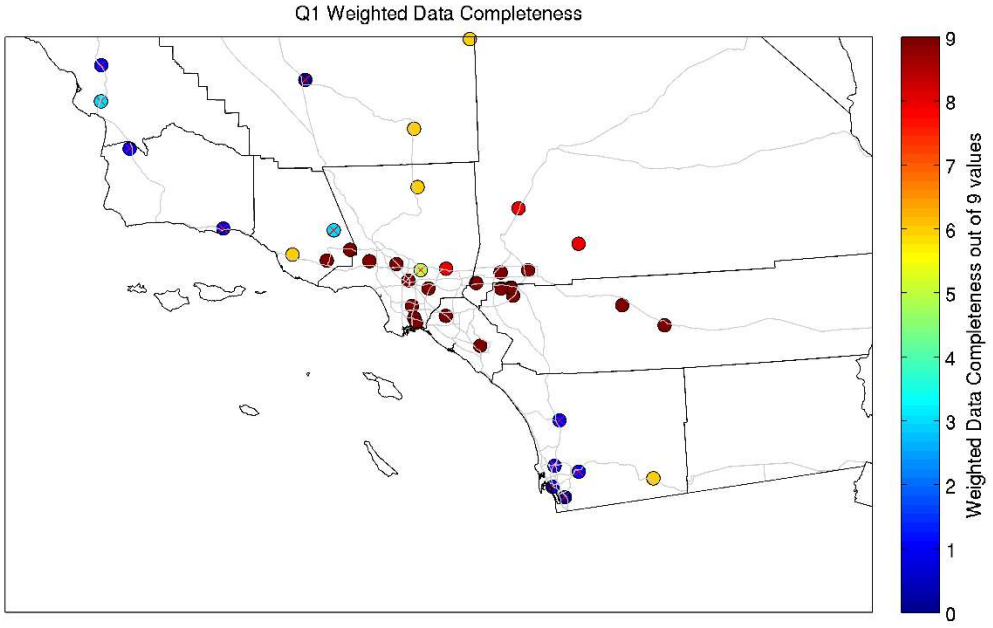

FIGURE V-6-45

Weighted data completeness for quarter 1 (2010–2014)

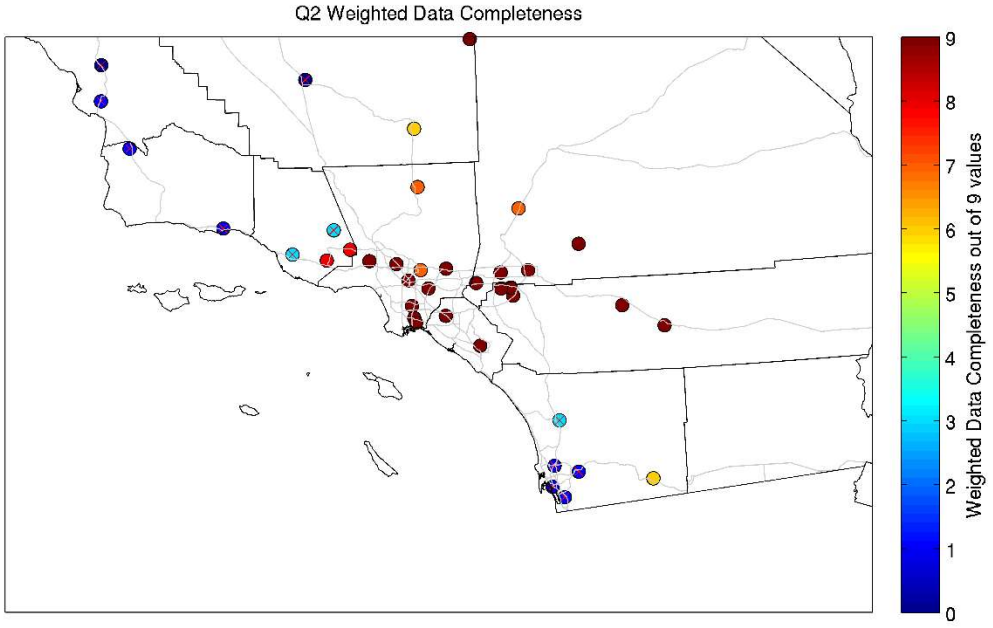

FIGURE V-6-46

Weighted data completeness for quarter 2 (2010–2014)

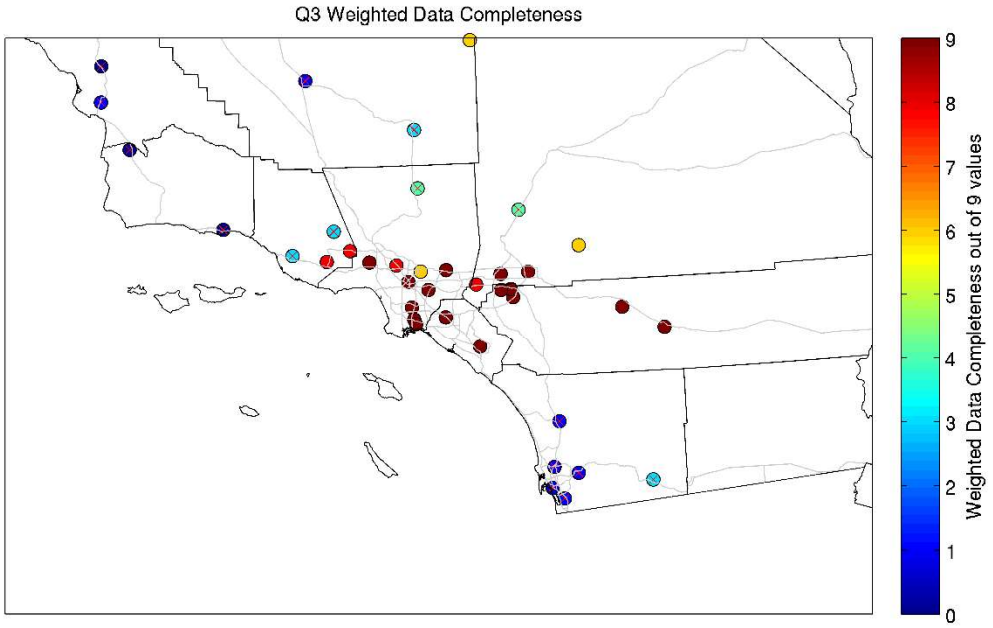

FIGURE V-6-47

Weighted data completeness for quarter 3 (2010–2014)

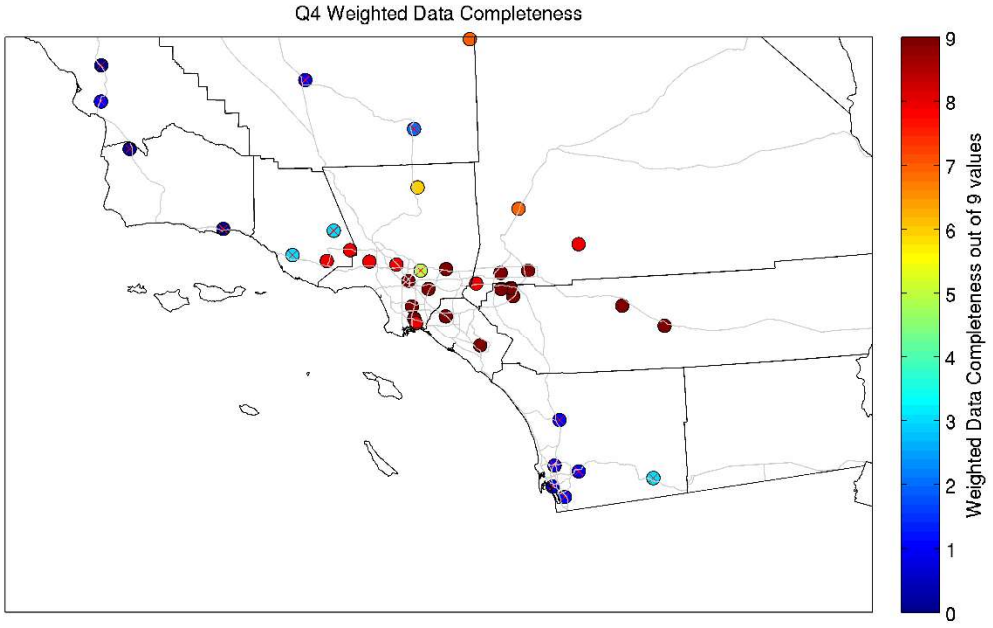

FIGURE V-6-48

Weighted data completeness for quarter 4 (2010–2014)

Quarterly design values were interpolated using a natural neighbor interpolation based on a Voronoi tessellation using only the stations identified to meet the established data completeness requirements. The concentration fields were not extrapolated outside existing stations. Figure V-6-49 presents the interpolated FRM total PM2.5 mass fields for each quarter. The product of the interpolated total PM2.5 mass from the FRM monitors and the interpolated speciation fractions from the SASS monitors yields spatial distributions of speciated mass in each quarter. Figure V-6-50 presents the nitrate mass fields for quarter 1-4. Mass fields for all other species are presented in Attachment 7.

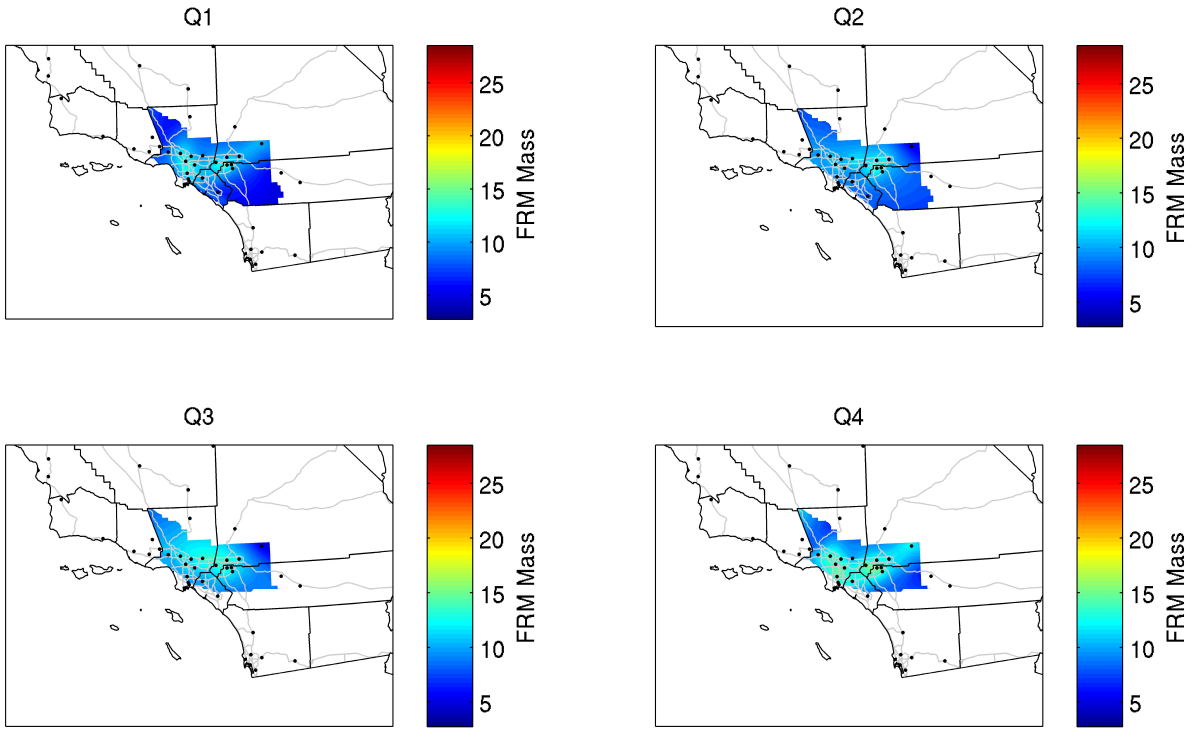

FIGURE V-6-49

Interpolated FRM data from all stations meeting data completeness requirements (2010–2014 weighted average)

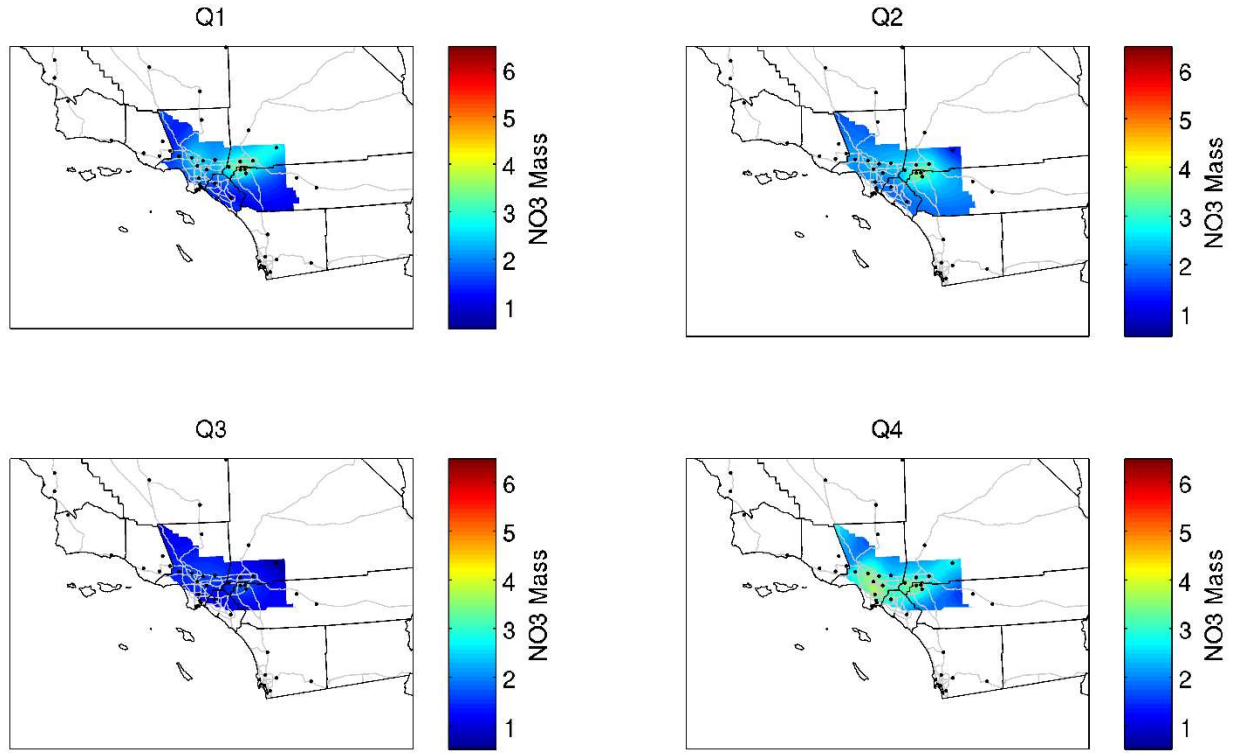

FIGURE V-6-50

Annual quarterly-averaged nitrate mass (2010–2014 weighted average)

In order to maintain consistency with the attainment demonstration at individual stations, base and future year species concentrations at each grid cell were replaced with the average value of the 3x3 grid encompassing the selected grid cell. Model derived base and future-year quarterly-averaged species concentrations were used to calculate RRFs for each species except water. RRFs were multiplied by quarterly-averaged species concentrations (e.g. Figure V-6-51) to project future species concentrations. Particle-bound water was then calculated using a polynomial regression of the Aerosol Inorganic Model (AIM) and summed along with a "blank" concentration to calculate the quarterly-averaged PM2.5 future-year design values. Quarterly PM2.5 concentrations were averaged to produce future-year design values throughout the Basin (See Attachment 7). 2021 design values from uncontrolled and controlled emission scenarios are presented in Figures V-6-51 and V-6-52, respectively. 2023 design values resulting from the ozone control strategy are presented in Figure V-6-53. 2025 design values are presented in Figure V-6-54 (uncontrolled), Figure V-6-54 (controlled), and Figure V-6-56 (controlled with non-182(e)(5) measures).

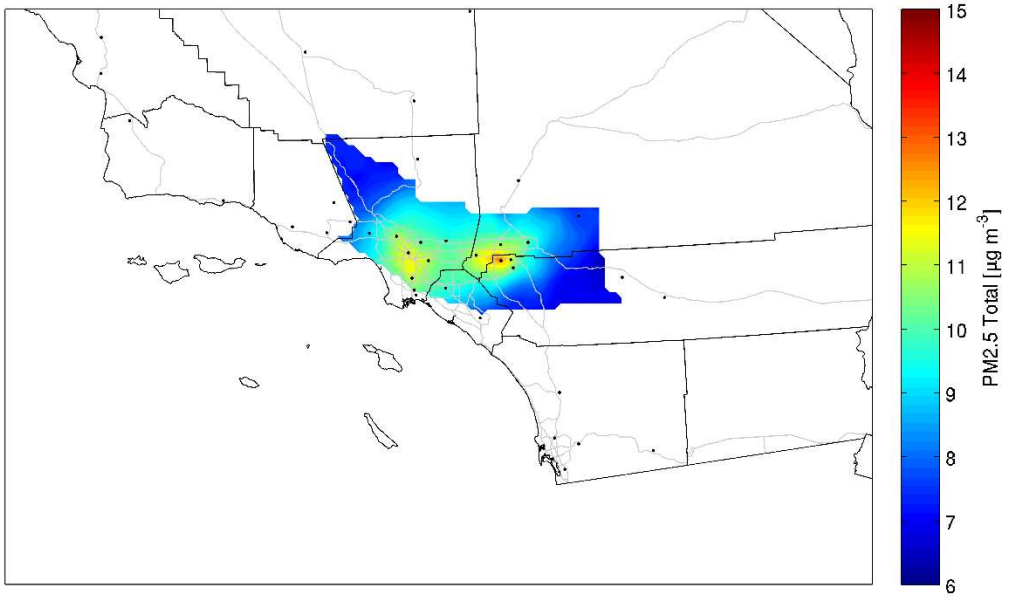

FIGURE V-6-51

2021 Baseline Annual PM2.5 Projection

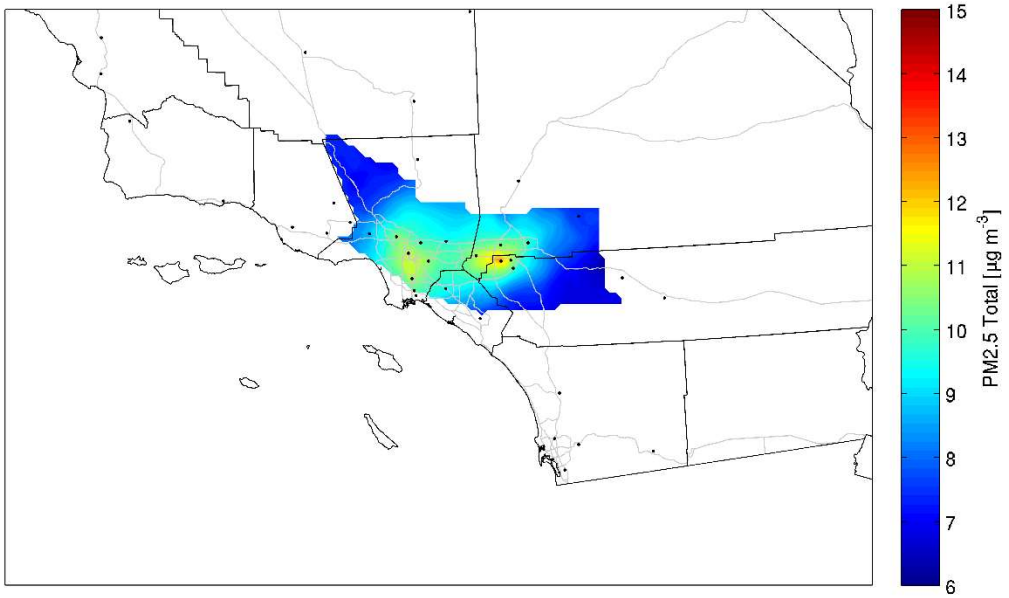

FIGURE V-6-52

2021 Annual PM2.5 Projection with PM control

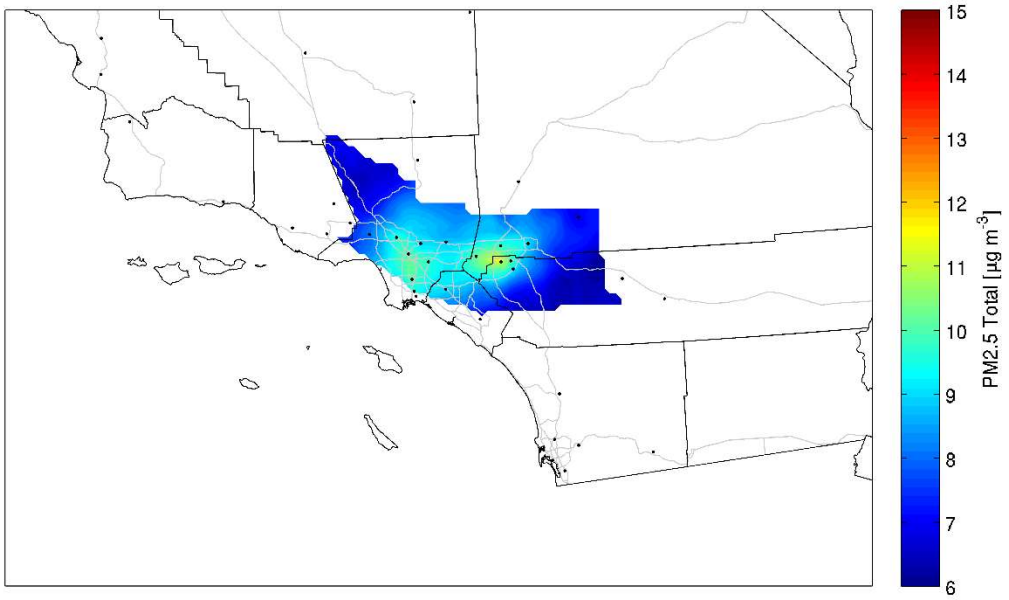

FIGURE V-6-53

2023 Annual PM2.5 Projection with 8-hour Ozone Attainment Scenario

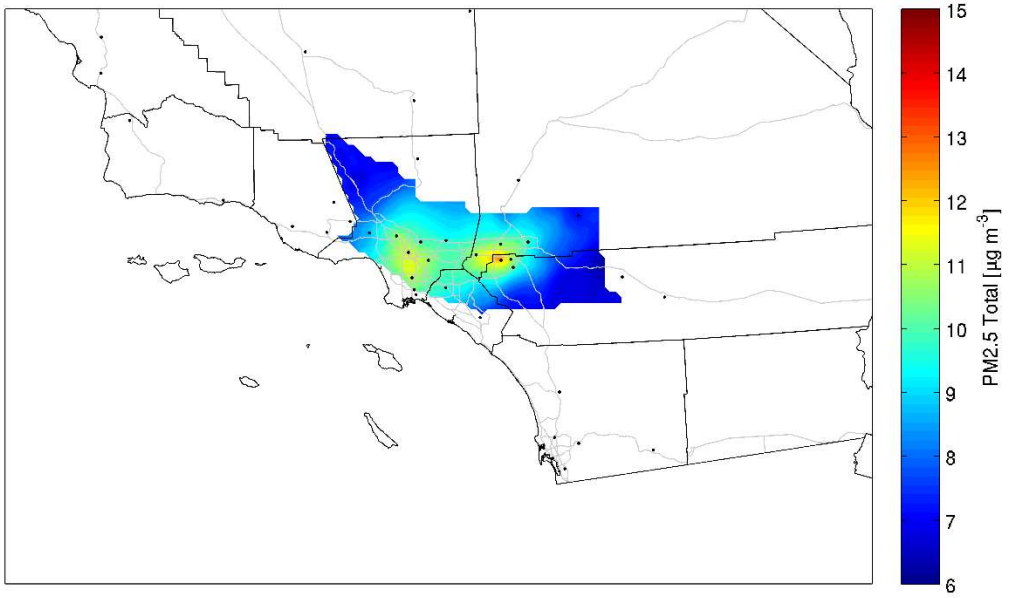

FIGURE V-6-54

2025 Baseline Annual PM2.5 Projection

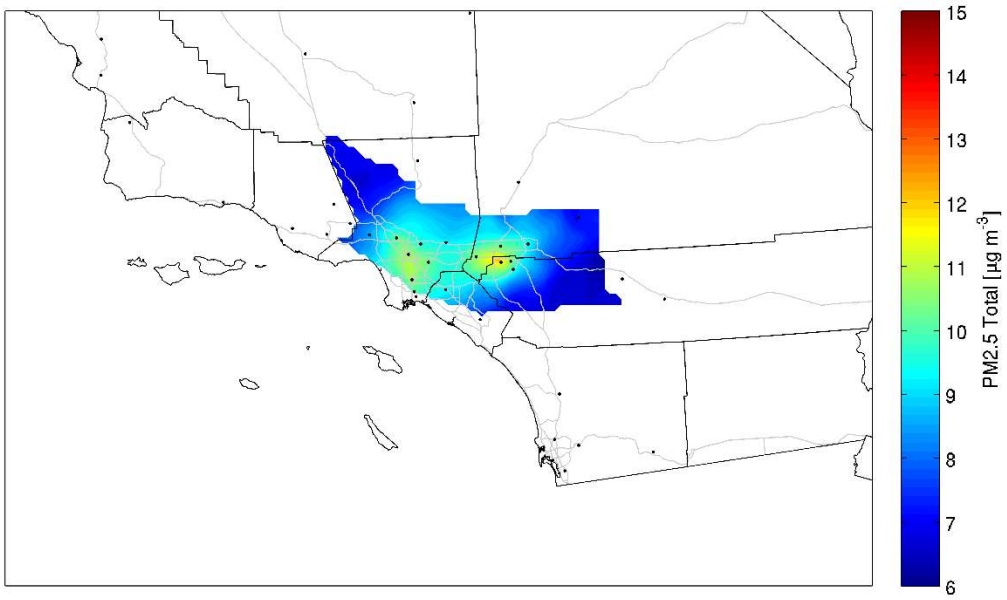

FIGURE V-6-55

2025 Annual PM2.5 Projection with Emission Reductions Associated with non-182(e)(5) Measures.

TABLE V-6-10

Unmonitored Area Analysis Projected Basin-maximum annual PM2.5 design values

Simulation	Maximum Annual PM2.5 Concentration in the Basin
2021 Baseline	13.0
2021 PM Control Strategy	12.7
2023 O3 Control Strategy	11.7
2025 Baseline	12.8
2025 with non-182(e)(5) Measures	12.3

Base-year (2012) spatially interpolated design values are also presented for comparison with the future year projections (Figure V-6-56). The interpolated 2012 grid center design values and projected design values determined from the unmonitored area analysis lined up closely with the station design values. This analysis demonstrates that the relative response to the control program is more effective in the Eastern Basin while portions of the western Basin do not exhibit the equivalent response to the implementation of the proposed control strategy, but they remain in attainment.

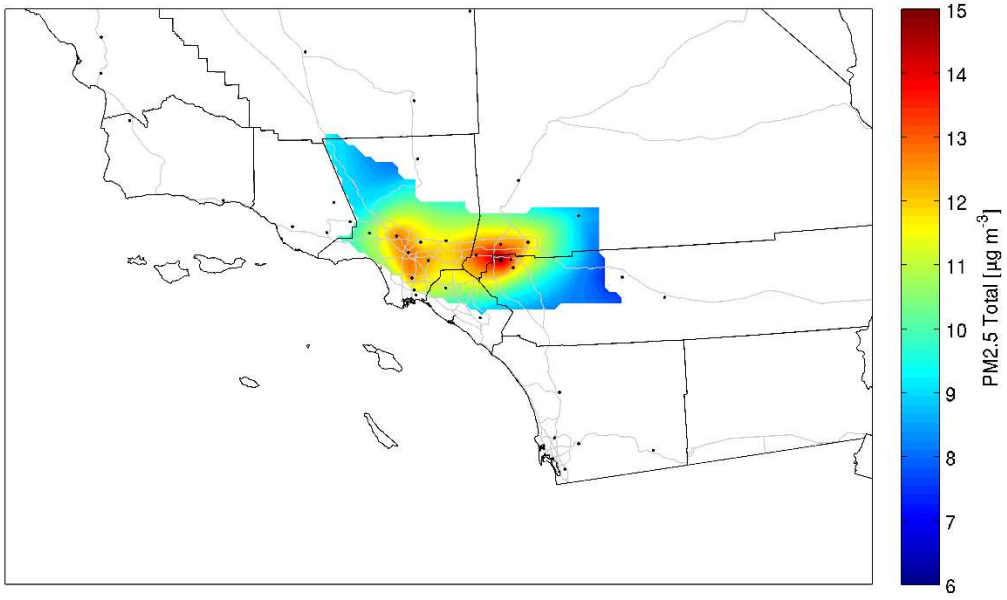

FIGURE V-6-56

2012 Baseline PM2.5 design values

Summary and Control Strategy Choices

PM2.5 has five major precursors that contribute to the mass of the ambient aerosol including ammonia, NOx, SOx, VOC, and directly emitted PM2.5. Various combinations of reductions in these pollutants could all provide a path to clean air. The annual 24-hour PM2.5 attainment strategy presented in this 2016 AQMP relies partially on the control strategy to attain the 1997 8-hour ozone standard in 2023. When all the NOx reductions needed to meet the 8-hour ozone standard in 2023 were incorporated, the annual PM2.5 concentration was projected to be well below the 12 µg/m3 standard, suggesting no further PM control is needed to meet the standard. Due to the limitation of not being able to apply emission reductions associated with CAA Section 182(e)(5) toward PM2.5 attainment, NOx reductions resulted from only non-182(e)(5) measures were simulated as well. This scenario that includes approximately 37 TPD of NOx reduction leads to annual PM2.5 attainment in the Basin in 2025.

The 2016 AQMP includes measures to reduce directly emitted PM emissions. Among them, the measures that have quantified emission reductions are BCM-01, Further Emission Reductions from Commercial Cooking and BCM-10, Emission Reductions from greenwaste composting. The PM emission reductions estimated from the two measures were expected to lead to attainment of the annual PM2.5 standard in 2025, indicating the PM control measures can be used as contingency measures to ensure attainment of the PM2.5 standard in case the NOx reductions from the ozone attainment strategy would not provide sufficient air PM2.5 improvement.

References

Baker, K. R., A. G. Carlton, T. E. Kleindienst, J. H. Offenberg, M. R. Beaver, D. R. Gentner, A. H. Goldstein, P. L. Hayes, J. L. Jimenez, J. B. Gilman, J. A. de Gouw, M. C. Woody, H. O. T. Pye, J. T. Kelly, M. Lewandowski, M. Jaoui, P. S. Stevens, W. H. Brune, Y. H. Lin, C. L. Rubitschun and J. D. Surratt (2015). "Gas and aerosol carbon in California: comparison of measurements and model predictions in Pasadena and Bakersfield." Atmos. Chem. Phys. 15(9): 5243-5258.

Frank, N. H. (2006). “Retained nitrate, hydrated sulfates, and carbonaceous mass in Federal Reference Method fine particulate matter for six eastern U.S. Cities.” Journal of the Air and Waste Management Association 56(4): 500-511.

Hayes, P. L., A. G. Carlton, K. R. Baker, R. Ahmadov, R. A. Washenfelder, S. Alvarez, B. Rappenglück, J. B. Gilman, W. C. Kuster, J. A. de Gouw, P. Zotter, A. S. H. Prévôt, S. Szidat, T. E. Kleindienst, J. H. Offenberg, P. K. Ma and J. L. Jimenez (2015). "Modeling the formation and aging of secondary organic aerosols in Los Angeles during CalNex 2010." Atmospheric Chemistry and Physics 15(10): 5773-5801.

Hayes, P. L., A. M. Ortega, M. J. Cubison, K. D. Froyd, Y. Zhao, S. S. Cliff, W. W. Hu, D. W. Toohey, J. H. Flynn, B. L. Lefer, N. Grossberg, S. Alvarez, B. Rappenglück, J. W. Taylor, J. D. Allan, J. S. Holloway, J. B. Gilman, W. C. Kuster, J. A. de Gouw, P. Massoli, X. Zhang, J. Liu, R. J. Weber, A. L. Corrigan, L. M. Russell, G. Isaacman, D. R. Worton, N. M. Kreisberg, A. H. Goldstein, R. Thalman, E. M. Waxman, R. Volkamer, Y. H. Lin, J. D. Surratt, T. E. Kleindienst, J. H. Offenberg, S. Dusanter, S. Griffith, P. S. Stevens, J. Brioude, W. M. Angevine and J. L. Jimenez (2013). "Organic aerosol composition and sources in Pasadena, California, during the 2010 CalNex campaign." Journal of Geophysical Research: Atmospheres 118(16): 9233-9257.

Jathar, S. H., T. D. Gordon, C. J. Hennigan, H. O. T. Pye, G. Pouliot, P. J. Adams, N. M. Donahue and A. L. Robinson (2014). "Unspeciated organic emissions from combustion sources and their influence on the secondary organic aerosol budget in the United States." Proceedings of the National Academy of Sciences 111(29): 10473-10478.

Parrish, D. (2014). Synthesis of Policy Relevant Findings from the CalNex 2010 Field Study: Final Report to the Research Division of CARB. Boulder, CO, NOAA/ESRL/Chemical Sciences Division.

Zhao, Y., C. J. Hennigan, A. A. May, D. S. Tkacik, J. A. de Gouw, J. B. Gilman, W. C. Kuster, A. Borbon and A. L. Robinson (2014). "Intermediate-Volatility Organic Compounds: A Large Source of Secondary Organic Aerosol." Environmental Science & Technology 48(23): 13743-13750.

CHAPTER 7

24-HOUR PM2.5 ATTAINMENT DEMONSTRATION

Introduction

This chapter demonstrates attainment of the federal 24-hour PM2.5 standard. The annual PM2.5 attainment demonstration provided in the 2007 AQMP was approved by U.S. EPA on September 30, 2011. The 2012 AQMP updated Annual PM2.5 attainment with supplemental submission on Feb 2015. U.S. EPA approved the reasonably available control measure (RACM), RFP, and impracticability demonstrations in the 2012 PM2.5 Plan. The 2016 AQMP provides newly designated "serious" non-attainment area attainment demonstration. The plan employs the most recent emissions inventory and state-of-the-science numerical modeling tools. An update of the model simulation results for the annual PM2.5 standard is presented in Chapter 6.

The initial sections of this chapter describe the PM2.5 Federal Reference Method (FRM) monitoring data and sampling network, the historical trend of 24-hour PM2.5 design values, revisions to the speciated monitoring attainment test (SMAT) and SANDWICH data analyses, and the CMAQ modeling methodology. The subsequent sections of this chapter provide the 24-hour PM2.5 attainment demonstration, the unmonitored area analysis, and a supporting weight-of-evidence analyses.

24-Hour PM2.5 Sampling

In 2014, the U.S. EPA released the "*Draft Modeling Guidance for Demonstrating Attainment of Air Quality Goals for Ozone, PM2.5 and Regional Haze*." The new guidance recommends using the 8 highest days of FRM data per quarter for each year for each FRM site to calculate the daily design values to ensure that the 98th percentile concentration day for the year is included in the analysis. This resulted in 32 days of FRM data for each year for each site. Tables V-7-1 through V-7-4 list the 2012 FRM data subset included as a component of the 24-hour PM NAAQS attainment analysis. Data from 2010, 2011, 2012, 2013 and 2014 complete the data requirement for the revised attainment test. Except for the Fontana site, which has a FRM sampling schedule of 1-in-3 days, FRM mass samples are collected daily at the other four FRM sampling sites (average sampling days = 341 days per year). The third highest yearly daily maximum represents the design value in Fontana, while the 8th highest is the design value for the rest of the FRM sites. Table V-7-5 provides the 5-year weighted 24-hour PM2.5 design vales for the five sites, which are the four SASS sites plus Mira Loma, the site with the highest concentration in the Basin. The 5-year weighted averages were calculated as the average of the three, three-year design values. The three-year design value periods were 2010-2012, 2011-2013 and 2012-2014. The 5-year weighted average base design value carries one digit to the right of the decimal point for 24-hour PM2.5, per EPA guidance. SASS sampling occurs on an every 6th day frequency.

In many cases, the FRM and SASS monitoring locations do not overlap. The FRM network has 21 stations where the SASS network size has varied in time, being limited to 4 sites in 2012. Four of the SASS sites are co-located with the FRM sites. In Mira Loma, the FRM design site is located in the upwind adjacent grid cell to the Rubidoux SASS sampler. The PM2.5 guidance document recommends estimating speciated

concentrations from a nearby speciation monitor when an FRM site does not have speciation data. Therefore, the Mira Loma FRM data is speciated using the Rubidoux SASS data.

TABLE V-7-1

2012 Eight Highest PM2.5 FRM Data for Each Quarter at Anaheim

	Q1	Q2	Q3	Q4
Highest	42.9	24.1	16.5	50.1
2nd Highest	25.7	19.8	15.4	43.1
3rd Highest	24.9	16.5	15.1	42.5
4th Highest	24.6	15.7	14.7	28.0
5th Highest	23.0	14.3	14.7	25.0
6th Highest	21.6	14.2	14.5	23.1
7th Highest	21.1	14.1	14.2	22.3
8th Highest	**20.0**	**14.0**	**14.0**	**21.9**

TABLE V-7-2

2012 Eight Highest PM2.5 FRM Data for Each Quarter at Central Los Angeles

	Q1	Q2	Q3	Q4
Highest	32.2	31.7	25.0	58.7
2nd Highest	32.0	25.9	21.6	44.0
3rd Highest	28.2	23.6	18.1	39.1
4th Highest	25.6	21.9	18.0	36.4
5th Highest	25.5	21.9	17.7	32.6
6th Highest	23.9	20.6	16.8	31.8
7th Highest	23.7	20.3	16.2	29.8
8th Highest	**23.3**	**20.2**	**16.0**	**29.1**

TABLE V-7-3

2012 Eight Highest PM2.5 FRM Data for Each Quarter at Fontana. Note that Fontana is sampled every third day, and thus the 98th percentile is the 3rd highest day.

	Q1	Q2	Q3	Q4
Highest	28.6	21.1	39.9	36.0
2nd Highest	26.3	20.8	20.0	35.6
3rd Highest	**22.8**	**19.1**	**18.5**	**25.6**
4th Highest	22.5	17.1	17.6	25.3
5th Highest	22.1	16.3	17.3	18.3
6th Highest	17.9	16.1	16.1	17.6
7th Highest	16.8	16.1	14.7	16.4
8th Highest	15.3	15.5	14.4	15.7

TABLE V-7-4

2012 Eight Highest PM2.5 FRM Data for Each Quarter at Mira Loma

	Q1	Q2	Q3	Q4
Highest	35.8	33.2	30.7	39.3
2nd Highest	35.1	29.3	20.8	37.9
3rd Highest	34.5	27.4	20.5	36.8
4th Highest	32.2	25.8	19.3	36.5
5th Highest	31.5	25.6	18.0	35.9
6th Highest	27.0	23.9	17.8	35.9
7th Highest	26.7	23.0	17.1	34.6
8th Highest	**26.5**	**22.7**	**17.0**	**34.1**

TABLE V-7-5

2012 Eight Highest PM2.5 FRM Data for Each Quarter at Rubidoux

	Q1	Q2	Q3	Q4
Highest	37.5	31.0	30.4	38.1
2nd Highest	33.7	30.8	18.9	37.3
3rd Highest	32.3	25.2	18.8	36.9
4th Highest	31.5	24.9	17.5	36.5
5th Highest	27.1	24.1	17.5	36.2
6th Highest	23.9	23.2	17.1	35.9
7th Highest	22.6	22.4	17.1	32.5
8th Highest	**22.6**	**21.8**	**16.9**	**31.6**

TABLE V-7-5

5-year Weighted Design Values for 24-Hour PM2.5 (µg/m^3)

Monitoring Site	24-Hour PM2.5 Design
Anaheim	25.8
Los Angeles	30.5
Fontana	32.7
Mira Loma	36.5
Rubidoux	33.1

The revised guidance updates the quarterly species fractions on "high" days, which are required for the 24-hour modeled attainment test. The new guidance recommends using the top 10% of days in each quarter as the "high" days, resulting in two days per quarter for the 1-in-6 day 2012 SASS data. Figures V-7-2 through V-7-5 depict the PM2.5 chemical species breakdown from the average of the top two PM2.5 concentration days for each quarter for the four SASS sites in the Basin. The data show the unadjusted direct measurements of the chemical species at each site. In general, concentrations in the first or fourth quarter are higher than those in the other quarters and secondary ammonium, nitrate and sulfate can comprise more than half of the total PM2.5 concentrations. Organic carbon (OC) is another significant component, which may contribute close to half of the total mass concentration in some quarters and sites.

OC as measured by a SASS sampler is believed to be highly uncertain with a mostly-positive sampling artifact. The flow rate of the SASS sampler (6.7 LPM) used to collect OC is approximately 2.5 times lower than that of the FRM sampling system (16.7 LPM), which provides the official PM2.5 mass measurement. The slower flow rate in the SASS sampler reduces the pressure drop across the filter and increases the adsorption of organic vapor on the quartz filter medium. The FRM uses a Teflon filter for mass measurements which is much less subject to organic vapor adsorption. Therefore, for the same air mass, more OC can be collected by the SASS sampler than the FRM sampler, often leading to an overbalance in the sum of the PM2.5 species relative to FRM mass. There are uncertainties in the measurements and the speciation analyses for all species; however, the greatest uncertainty in species concentration is generally associated with the measurement and analysis of OC.

U.S. EPA recommends estimating uncertain OC concentrations through an adjustment that is discussed as part of the "**S**ulfate, **A**djusted **N**itrate, **D**erived **W**ater, **I**nferred **C**arbon **H**ybrid (SANDWICH)" material balance method in the 2007 AQMP and U.S. EPA's PM2.5 modeling guidance document (Frank, 2007). According to the SANDWICH method, OC is estimated from the difference between the measured mass and the sum of all chemical species, water and a filter blank of 0.5 $\mu g/m^3$. The new species fractions for each quarter for each site are calculated by estimating OC, which are then applied to the 32 highest days of FRM mass data. Figures V-7-6 through V-7-9 depict the 2012 species fractional splits for the 6 primary components and water vapor for the four SASS sites after SANDWICH was applied.

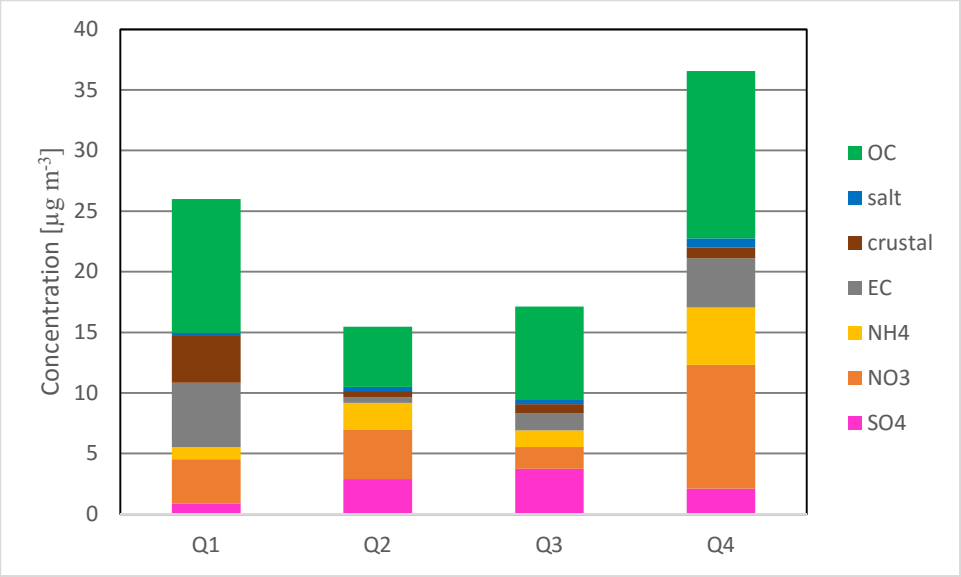

FIGURE V-7-2

Anaheim Top Two day Averaged 24-Hr PM2.5 Concentrations per Quarter in 2012

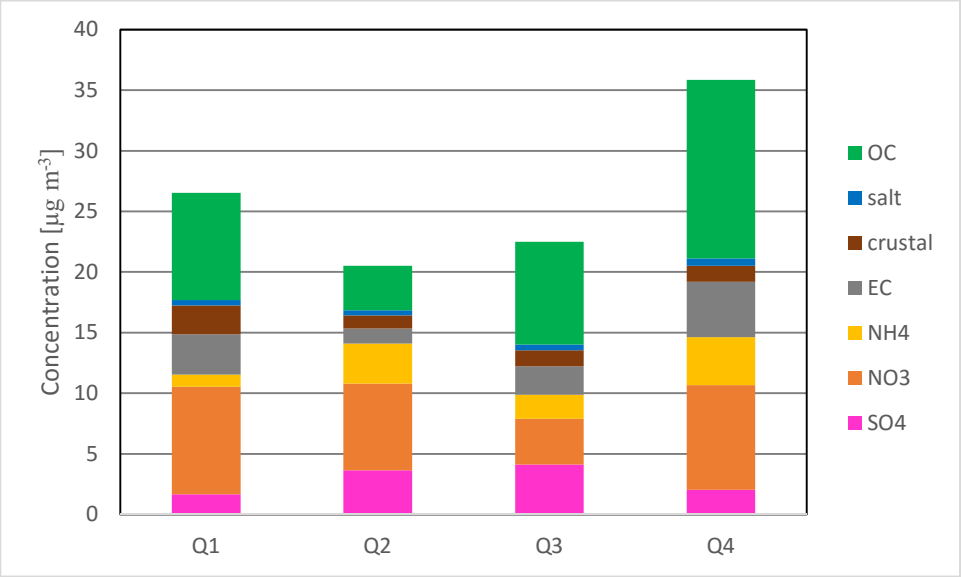

FIGURE V-7-3

Los Angeles Top Two day Averaged 24-Hr PM2.5 Concentrations per Quarter in 2012

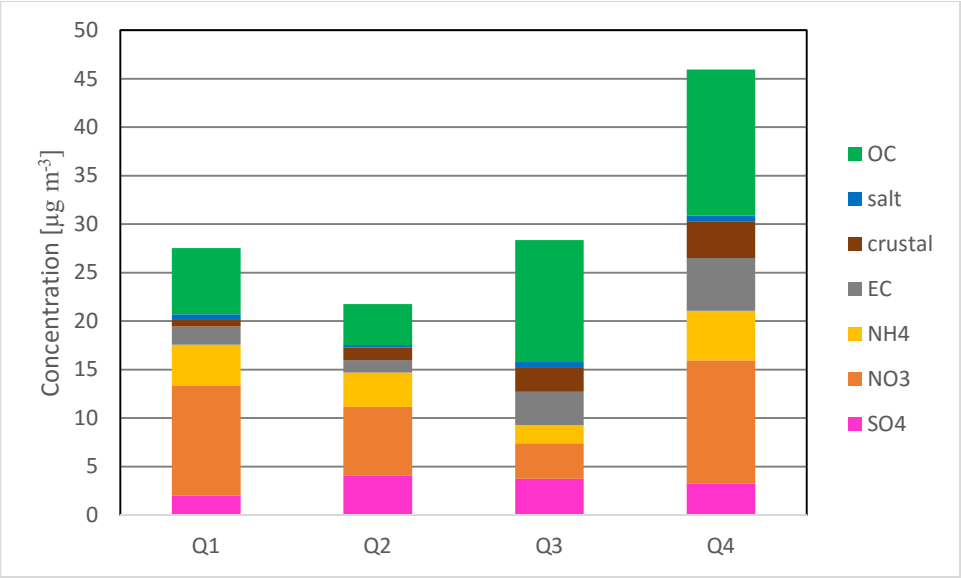

FIGURE V-7-4

Fontana Top Two day Averaged 24-Hr PM2.5 Concentrations per Quarter in 2012

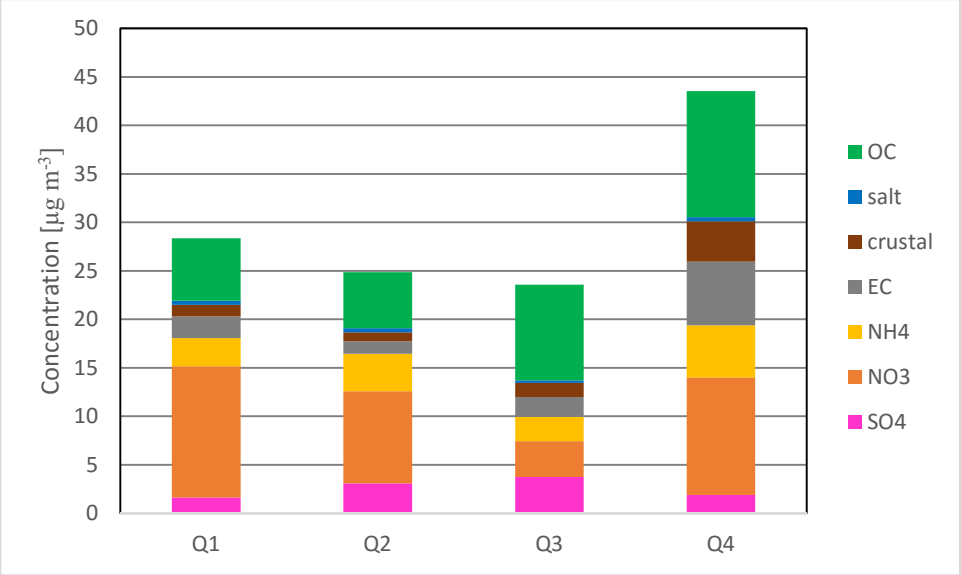

FIGURE V-7-5

Rubidoux Top Two day Averaged 24-Hr PM2.5 Concentrations per Quarter in 2012

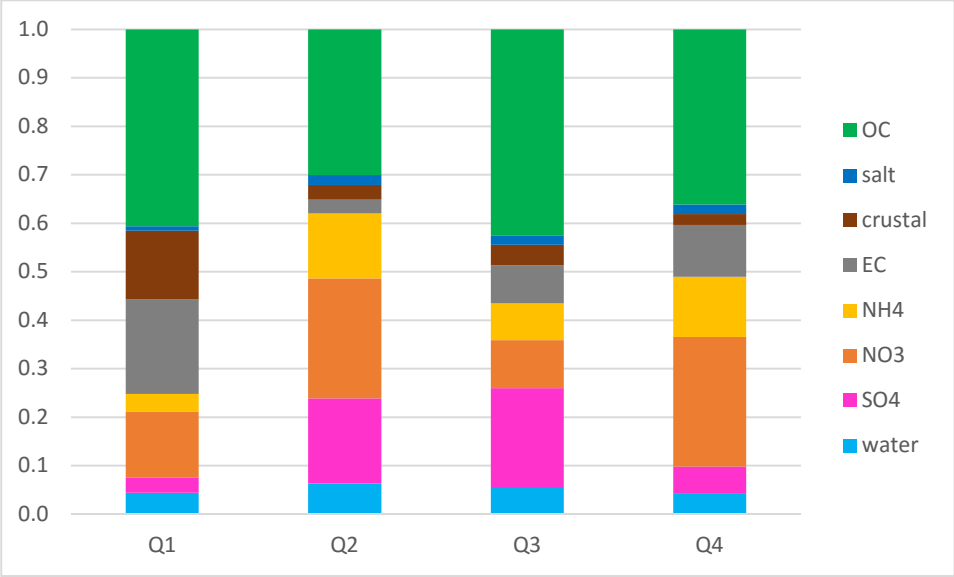

FIGURE V-7-6

2012 Anaheim Top Two day Averaged PM2.5 species fraction after SANDWICH

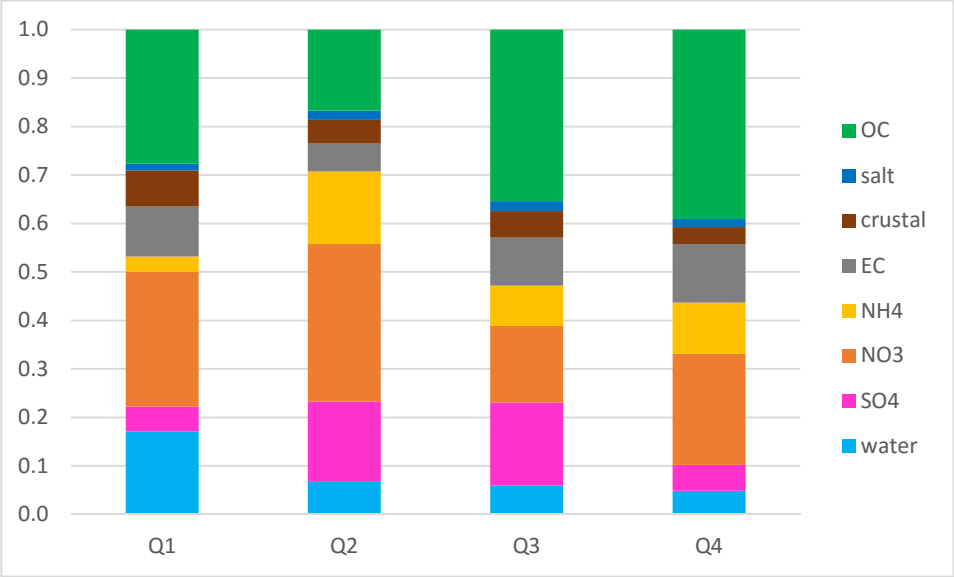

FIGURE V-7-7

2012 Los Angeles Top Two day Averaged PM2.5 species fraction after SANDWICH

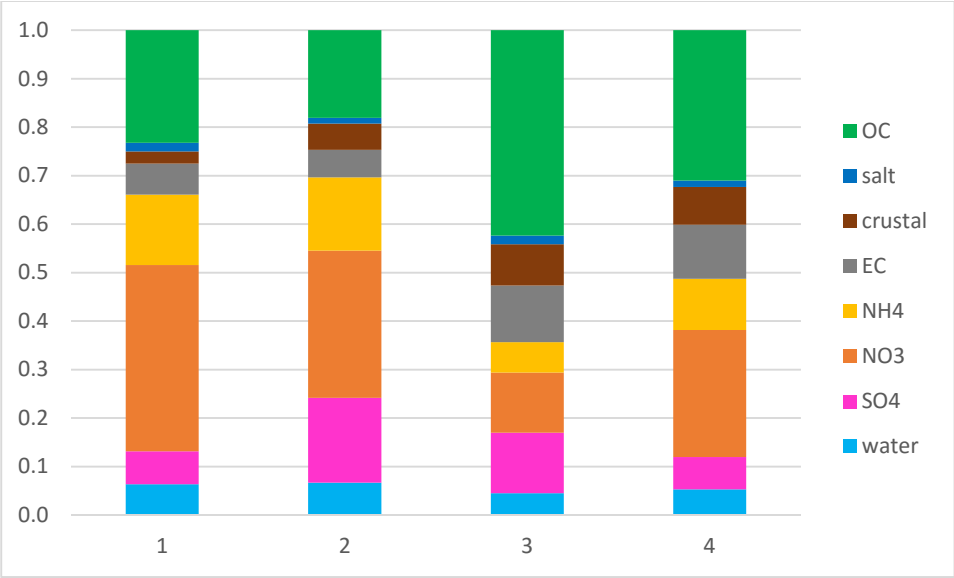

FIGURE V-7-8

2012 Fontana Top Two day Averaged PM2.5 species fraction after SANDWICH

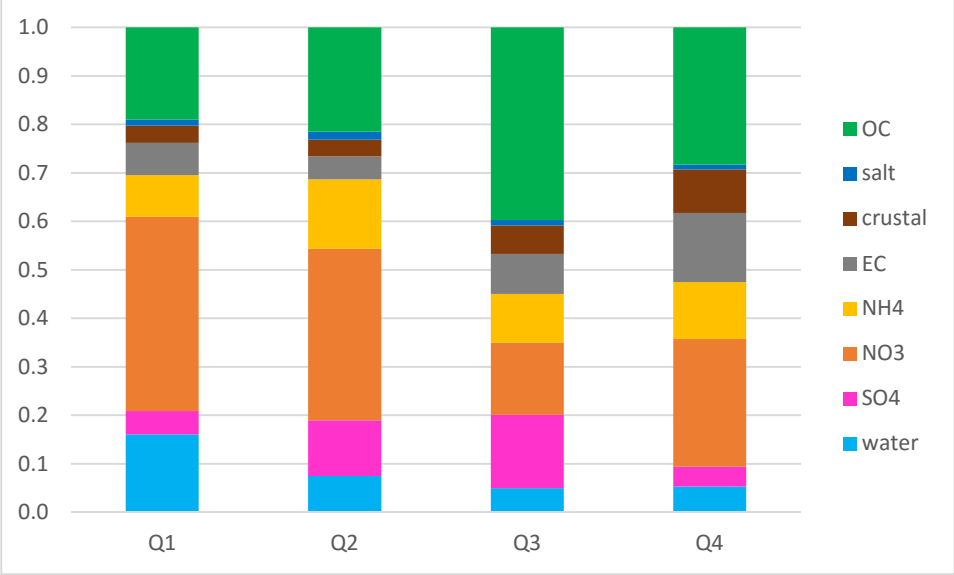

FIGURE V-7-9

2012 Rubidoux Top Two day Averaged PM2.5 species fraction after SANDWICH

24-Hour PM2.5 Modeling Approach

CMAQ simulations were conducted for each day in 2012. The simulations included 8784 consecutive hours (366 days x 24 hours) from which daily 24-hour average PM2.5 concentrations (0000-2300 hours) were calculated. A set of species-specific RRFs were generated for each future year simulation from the top 10% of modelled PM2.5 days. RRFs were generated for the ammonium ion (NH4), nitrate ion (NO3), sulfate ion (SO4), organic carbon (OC), elemental carbon (EC), sea salt (Salt) and a combined grouping of other primary PM2.5 material (Other). A total of 7 RRFs were generated for each quarter of the future year simulation. Future year concentrations of the seven component species were calculated by applying the model generated quarterly RRFs to the speciated 24-hour PM2.5 (FRM) data sorted by quarter for each of the five years used in the design value calculation. The speciation fractions used to generate 24-hour speciated PM2.5 values were determined from the "high" days. Particle bound water was determined using U.S. EPAs regression model approximation of the AIM model based on simulated concentrations of the ammonium, nitrate and sulfate ions (EPA, 2006). A blank mass of 0.5 $\mu g/m^3$ was added to each base and future year simulation. The 32 days in each year (8 per quarter) were then re-ranked based on the sum of all predicted PM species to establish a new 98^{th} percentile concentration. A weighted average of the resulting future year 98^{th} percentile concentrations for each of the five years was used to calculate future design values for the attainment demonstration. The 98^{th} percentile value was determined based on the FRM sampling frequency. All the SASS sites except Fontana have a daily FRM sampling, which gives the 8^{th} highest day as the 98^{th} percentile. Fontana has every-three-day sampling, thus the 3^{rd} highest day becomes the 98^{th} percentile.

Future year PM2.5 24-hour average design values are projected for 2019, the attainment deadline for the 2006 standard of 35 $\mu g/m^3$.

Future Air Quality

The 2012 AQMP demonstrated attainment of the federal PM2.5 air quality standards by December 2014. However, due to the unforeseen drought conditions that prevailed from 2012 to 2014, and into the first quarter of 2015, 24-hour PM2.5 concentrations did not fall to the degree predicted by the model. The District was granted a voluntary bump-up to serious non-attainment status by U.S. EPA, which extended the attainment deadline by 4-years to 2019.

A simulation of 2019 baseline emissions (no controls) was conducted to assess future 24-hour PM2.5 levels in the Basin. The simulation used the projected emissions from 2012 which include all adopted control measures that will be implemented by December 31, 2019.

Simulation of the 2019 baseline emissions indicates that the Basin will attain the federal 24-hour PM2.5 standard in 2019 without additional controls. This is consistent with the findings of the 2012 AQMP, which showed attainment by 2019 with no additional controls. The projected 2019 design value is 32.1 $\mu g/m^3$ at Mira Loma.

Figure V-7-10 depicts future 24-hour PM2.5 air quality projections at the Basin design site (Mira Loma) and the four other PM2.5 monitoring sites equipped with comprehensive particulate species characterization. Shown in the figure are the baseline design values for 2012 along with projections for 2019. All of the sites will meet the 24-hour PM2.5 standard by 2019 without additional reductions beyond already adopted control measures.

Table V-7-6 provides the RRFs developed from the 2012 and 2019 baseline simulations. Table V-7-7 provides the 24-hour PM2.5 design values by component species for 2012. Table V-7-8 provides the projected future year 24-hour PM2.5 design values by component species for 2019.

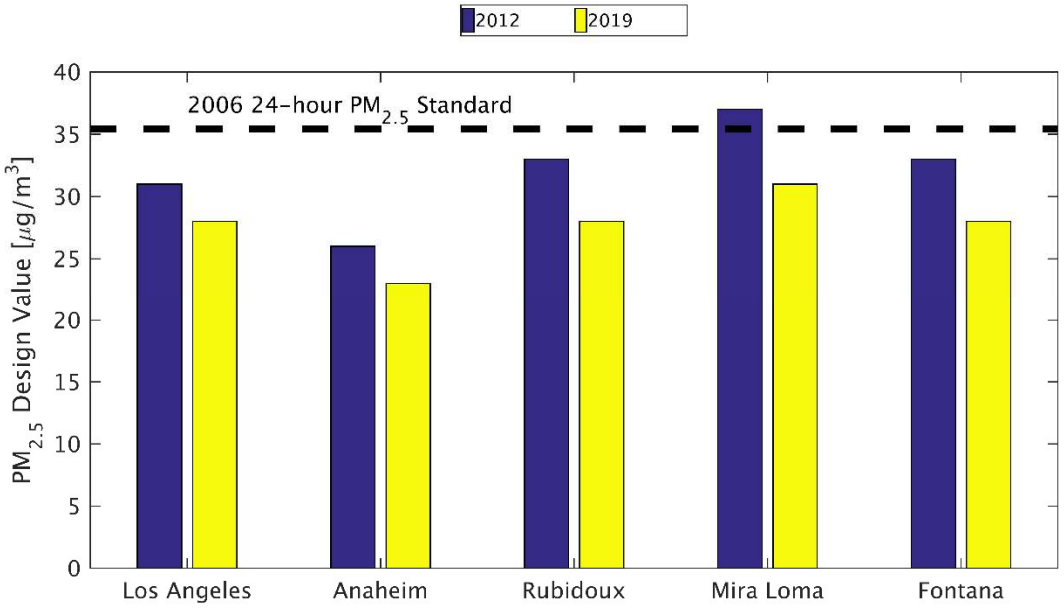

FIGURE V-7-10

Maximum 24-Hour Average PM2.5 Design Concentrations:
2012 and 2019 Baseline.

TABLE V-7-6

CMAQ predicted RRFs per species and quarter at the four SASS sites

Station	Quarter	SO4	NO3	NH4	OC	EC	Salt	Other
Anaheim	Q1	0.931	0.816	0.806	0.995	0.742	0.879	1.099
	Q2	0.936	0.714	0.718	0.993	0.756	0.903	1.09
	Q3	0.889	0.713	0.723	0.999	0.72	0.875	1.082
	Q4	0.938	0.884	0.874	0.991	0.723	0.911	1.095
Los Angeles	Q1	0.975	0.934	0.92	0.978	0.704	0.904	1.075
	Q2	0.921	0.826	0.818	0.981	0.702	0.896	1.071
	Q3	0.884	0.815	0.8	0.993	0.695	0.902	1.07
	Q4	0.979	0.908	0.905	0.982	0.694	0.887	1.076
Fontana	Q1	0.985	0.824	0.82	0.973	0.681	0.938	1.091
	Q2	0.961	0.675	0.69	0.966	0.668	0.915	1.078
	Q3	0.943	0.682	0.707	0.967	0.651	0.971	1.072
	Q4	0.966	0.748	0.752	0.972	0.677	0.924	1.086
Rubidoux	Q1	0.981	0.816	0.81	0.985	0.675	0.926	1.114
	Q2	0.92	0.676	0.667	0.976	0.645	0.948	1.093
	Q3	0.925	0.673	0.683	0.979	0.632	0.983	1.09
	Q4	0.969	0.795	0.793	0.988	0.668	0.942	1.115

TABLE V-7-7

24-hour PM2.5 chemical species and total mass for Base Year, 2012 (µg/m^3)

Locations	NH4	NO3	SO4	OC	EC	Salt	Other	Water	Blank	Mass
Anaheim	1.90	4.88	1.06	9.79	3.96	0.35	2.28	1.11	0.50	25.82
Fontana	3.43	8.48	2.52	10.14	3.29	0.49	2.17	1.73	0.50	32.74
Los Angeles	3.22	6.89	2.38	10.94	3.36	0.51	1.16	1.56	0.50	30.52
Mira Loma	3.34	13.34	1.67	7.58	3.01	0.43	1.70	4.94	0.50	36.52
Rubidoux	3.30	12.29	1.99	6.70	2.32	0.43	1.33	4.30	0.50	33.16

TABLE V-7-8

24-hour PM2.5 chemical component and total mass projected for 2019 (µg/m^3)

Locations	NH4	NO3	SO4	OC	EC	Salt	Other	Water	Blank	Mass
Anaheim	2.21	5.06	1.17	9.30	2.35	0.39	1.44	1.07	0.50	23.49
Fontana	2.57	6.34	2.41	9.75	2.17	0.46	2.33	1.48	0.50	28.01
Los Angeles	2.29	6.07	1.94	10.61	2.35	0.43	1.46	1.96	0.50	27.60
Mira Loma	2.94	9.40	1.54	8.46	2.67	0.37	2.58	2.90	0.50	31.36
Rubidoux	2.37	8.88	1.80	7.37	1.83	0.36	1.76	3.40	0.50	28.27

Spatial Projections of PM2.5 Design Values

Figure V-7-11 provides a Basin-wide perspective of the spatial extent of 24-hour PM2.5 levels in the base year 2012 resulting from the interpolation of design values at the five stations included in the attainment demonstration. Figure V-7-12 shows an interpolated spatial representation of future model-predicted 24-hour design values in 2019. Several areas around the northwestern portion of Riverside and southwestern portion of San Bernardino Counties depict grid cells with weighted PM2.5 24-hour design values exceeding 35 µg/m^3 in 2012. By 2019, Mira Loma, the PM2.5 24-hour design station, will attain the federal standard. The entire South Coast air basin, determined by the interpolated design values from the five speciation sites show attainment by 2019.

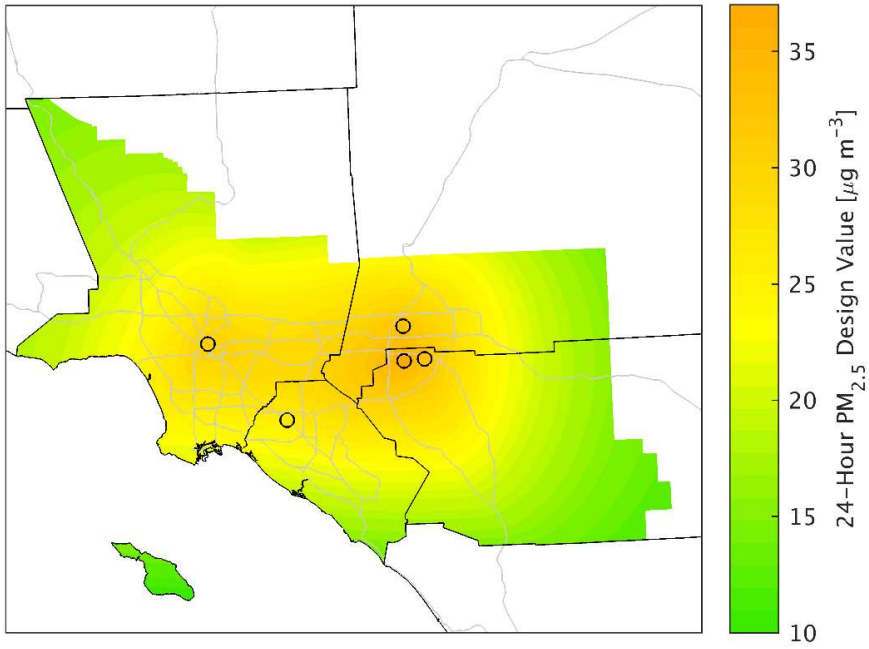

FIGURE V-7-11

2012 24-Hour PM2.5 Design Values interpolated to the South Coast Air Basin (µg/m^3). Colors Correspond to the AQI.

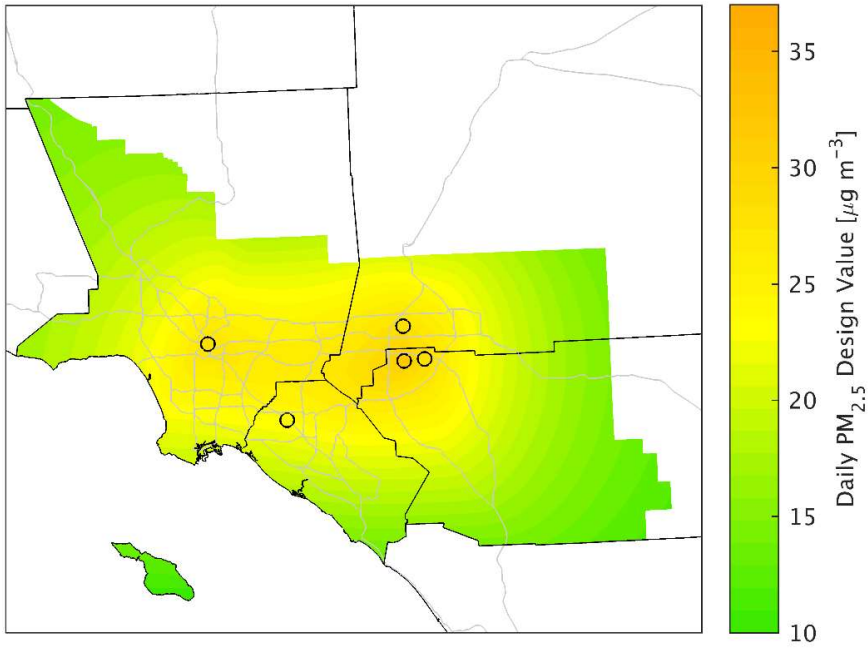

FIGURE V-7-12

2019 projected 24-Hour PM2.5 concentrations interpolated to the South Coast Air Basin (µg/m^3). Colors Correspond to the AQI.

Unmonitored Area Analysis

U.S. EPA modeling guidance requires that the attainment demonstration include an analysis that confirms that all grid cells in the modeling domain meet the federal standard. This "unmonitored area analysis" is essential since speciation monitoring is conducted at a limited number of sites in the modeling domain. Variance in the species profiles at selected locations coupled with the differing responses to emissions control scenarios are expected to result in spatially variable impacts to PM2.5 air quality in any grid cell. As described earlier in this chapter, speciation profiles from SASS sites in adjacent or collocated grid cells are used in the formal attainment demonstration for Mira Loma. With interpolation of the SASS speciation profiles, attainment demonstrations can be directly conducted for the remaining grid cells where FRM mass data has been collected over the 5-year period (2010–2014). The unmonitored area attainment test requires assessing the impacts for 32 days per year, for five years, at each unmonitored grid cell.

The methodology used to assess the unmonitored grid cell impact is as follows. The speciation fractions throughout the Basin for each relevant species, except particle bound water, were estimated with a natural neighbor interpolation for each quarter of 2012. While the four SASS speciation stations encompass all areas of high PM concentrations in the Basin, it was necessary to create "pseudo stations" at the corners of the modelling domain to aid in extrapolation. The speciation fractions at these pseudo stations were assigned as the average speciation fraction measured at all four stations. The speciation

fractions in areas of the Basin which are expected to have high PM concentrations were not appreciably affected by the choice of "pseudo station" speciation as the areas of interest are much closer to the SASS stations than the "pseudo stations." A natural neighbor interpolation based on a Voronoi tessellation has been shown to reproduce ozone concentration profiles in the Basin more accurately than an inverse distance weighting, inverse distance weight squared, nearest neighbor, or linear interpolation scheme (see Appendix 5, Chapter 5.). Figure V-7-13 details the interpolated nitrate species fractions in quarters 1-4. The interpolated species fractions for all relevant species are presented in Attachment 8.

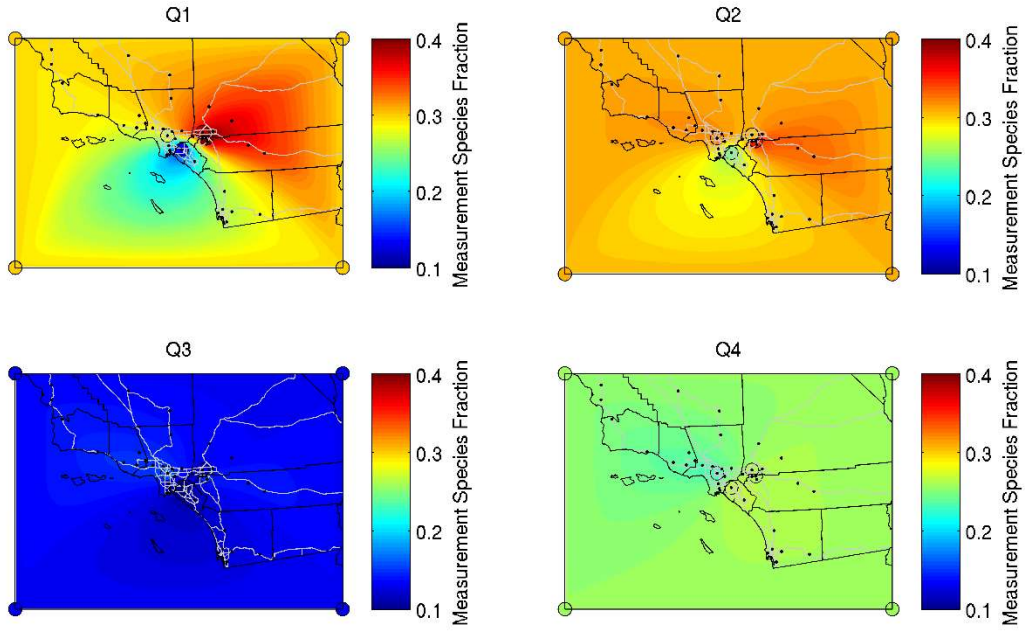

FIGURE V-7-13

2012 Interpolated Measurement Species Fractions for Nitrate. FRM locations are illustrated with black dots. SASS speciation stations and "pseudo stations" are illustrated with circles.

FRM data from 38 monitoring sites within the modeling domain were extracted from the U.S. EPA's AQS database for each year of the 5-year period. Data from stations without daily sampling were adjusted to simulate a daily sampling rate by filling in missing days with nearest measured value. Therefore, the 8th highest value in each year represented the 98th percentile measurement for each station, regardless of the sampling frequency. The highest eight concentrations sampled in each quarter in each of the five years were selected to generate the data set. This resulted in 8 x 4 x 5 = 160 days of data for each of the 38 FRM stations. Data for each of the 38 speciation stations were aggregated so that the highest concentration day measured at a station in a specific quarter and year corresponded the highest concentration day measured at all other stations in the same quarter and year. The interpolated speciation fractions were then applied to the 160 days selected depending on quarter and location. The

species concentrations on each of the 160 selected days were interpolated using a natural neighbor technique.

RRFs were calculated from the model output at each cell in the Basin using the same strategy employed for the station-specific analysis. However, the absence of measurement data between the stations did not allow for the use of selection criteria to filter out days where model performance is inadequate. Quarterly specific RRFs for nitrate are presented in Figure V-7-14. RRFs for all other species are presented in Attachment 8. The interpolated FRM data were then multiplied by the seasonally sorted, RRF-interpolated species fractions to project the future year 24-hr PM2.5 species distribution for each of the five years.

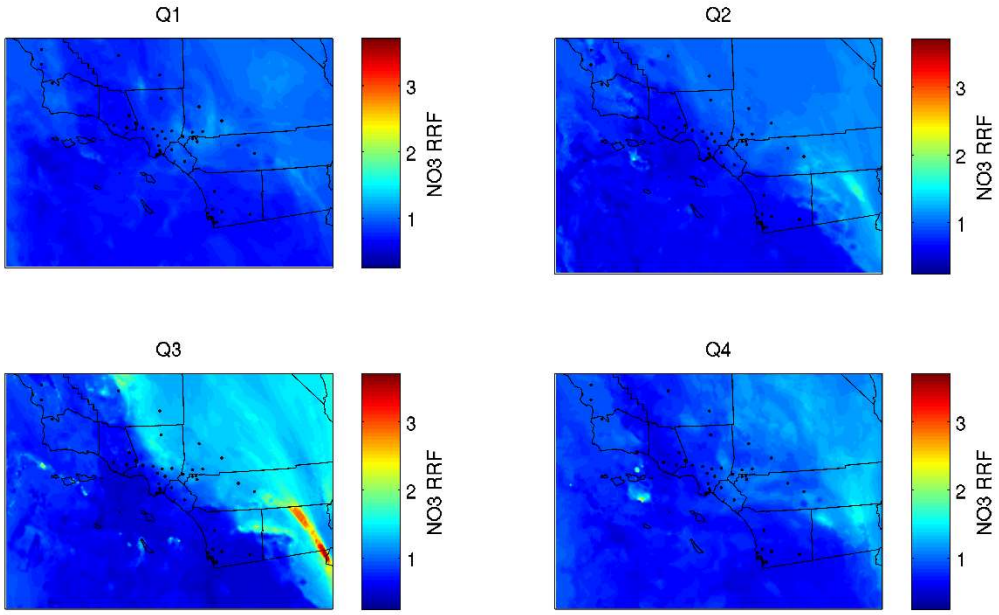

FIGURE V-7-14

2019 Spatial RRFs for Nitrate

Particle-bound water was calculated and then summed along with "blank" and all species concentrations to generate total PM2.5 mass for each of the 160 days. The eighth-highest value at each grid cell was then selected for each year and a 5-year weighted-average was applied to generate a projected 24-hour design value at each grid-cell within the Basin. The projected 24-hour design value for 2019 is presented in Figure V-7-15. All regions of the Basin are expected to attain the 24-hour standard by 2019 with a projected Basin Maximum of 32 µg m^{-3}. Figure V-7-16 presents the 2012 base-year design values for comparison.

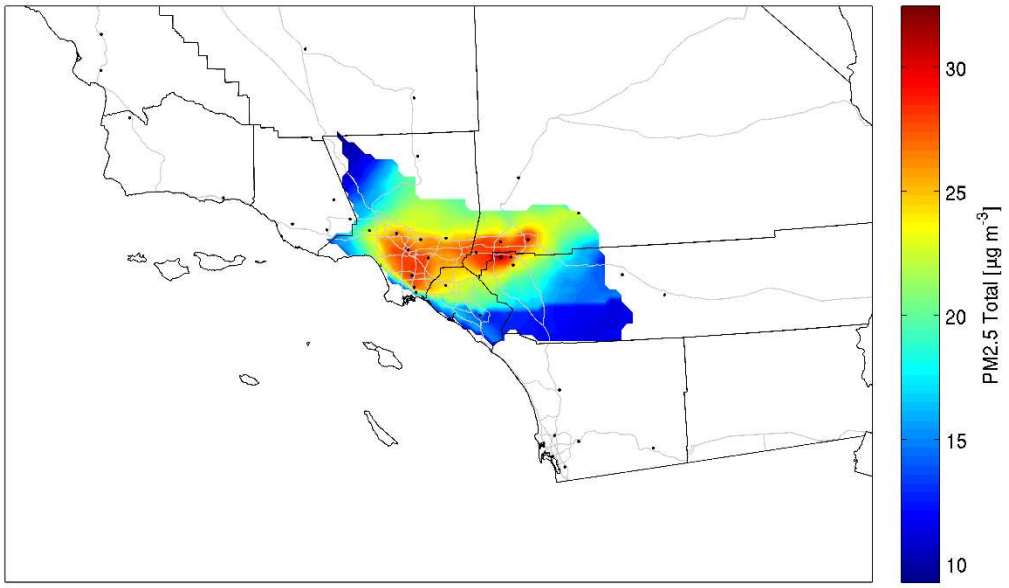

FIGURE V-7-15

2019 Projected 24-hour Design Values.

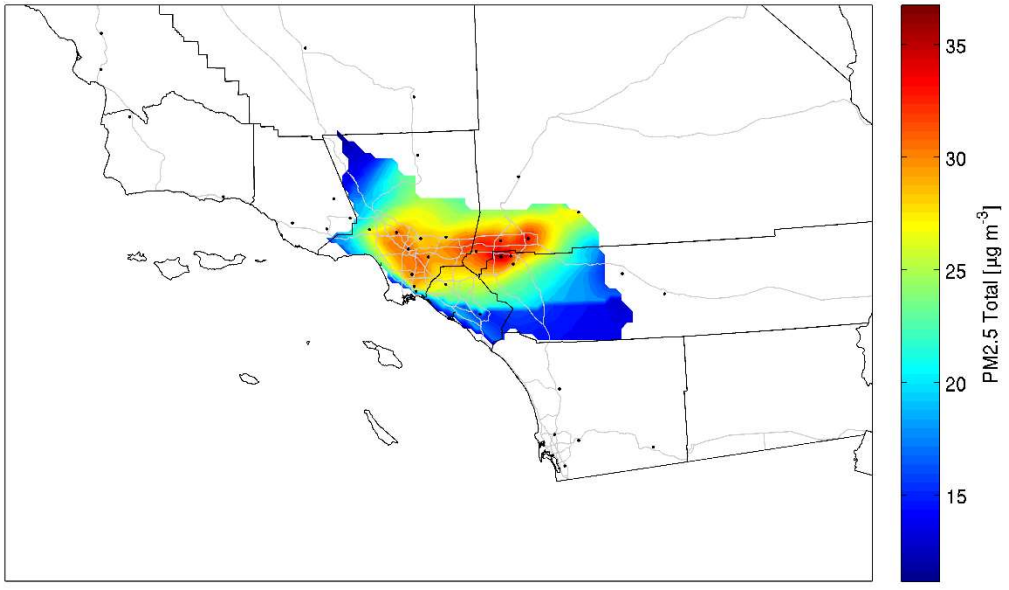

FIGURE V-7-16

2012 Baseline 24-hour Design Values.

The interpolated 2012 design values and 2019 projected design values determined from the unmonitored area analysis line up closely with the station design values. The 2019 maximum projected 24-hour PM2.5 design of 33 µg/m^3 occurred in the Mira Loma grid cell

This analysis demonstrates that the relative response to the control program is more effective in the Eastern Basin while portions of the western Basin do not exhibit the equivalent response to the implementation of the proposed control strategy but remain in attainment of the 24-hour PM2.5 NAAQS.

Effects of the Drought

In the 2012 AQMP, the 24-hour PM2.5 design value was projected to be 34.3 µg/m^3 in 2014 for Mira Loma, which would have met the standard. However, projections were not met and the measured design value ended up being 38 µg/m^3. The five year period used for the design calculation for the 2012 AQMP covered a meteorological period that was typical compared to the long term (50+ year) statistics. As a consequence, the 2014 projected 24-hour PM2.5 design value for Mira Loma assumed a similar window of average precipitation events and rainfall totals with the concurrent natural pollution dispersion potential associated with unstable weather. However, the lack of rainfall and drought conditions in the South Coast Air Basin for the past three years has impacted PM2.5 ambient levels. According to a recent study by Griffin and Anchukaitis (2014) which analyzed tree ring samples, reduced precipitation during these last years is not unprecedented, but its combination with higher temperatures due to climate change is making the drought the most severe in 1,200 years. Limited rain means there is less crusting and wetting of soil and road surfaces. Thus, more road dust and fugitive dust emissions are generated. A reduced frequency of storms translates to fewer days of enhanced pollution dispersion. Without such dispersion, there is no deep mixing of the atmosphere, particulate matter captured by raindrops or wind to transport the pollution away from the region. Further discussion on the effects of the drought can be found in Chapter 2 of the AQMP.

Figure V-7-17 depicts the trends in emissions of PM2.5 and precursors projected to 2019. In addition to the direct contribution from PM2.5 emissions, VOC contribute to the formation of organic carbon, whereas NOx and SOx contribute to the formation of aerosol nitrates and sulfates. Previous simulations for 2014 showed the relative contribution of PM2.5 precursors to total 24-hour PM2.5 concentrations, which provided a basis to aggregate emissions weighted based on their potential to form PM2.5, as equivalent PM2.5 emissions. The relative weight of each precursor was found to be the following: 0.3 for VOC, 1 for NOx, 7.8 for SOx and 14.8 for PM2.5. Figure V-7-18 shows the trend in Equivalent PM2.5 Emissions projected to 2019, which shows a steady decline throughout that time span. Figure V-7-18 also shows the trend in annual 98th percentile 24-Hour PM2.5 concentrations and their corresponding 3-Year design values, overlaid by the number of rain days for Quarters 1 (January–March) and 4 (October–December). With constant meteorological conditions, one would expect the 24-Hour PM2.5 3-Year Design Values to continue to decline following the decline in PM2.5 precursor emissions. However, dry and stable conditions persistent during the past years have offset the benefits of emission reductions and have reversed the decreasing trend in PM2.5. Considering the years 2007 and 2014, which experienced similar low precipitation, the Annual 98th percentile 24-Hour PM2.5 decreased by 42%, in parallel with a 38%

decrease in equivalent PM2.5 emissions. This suggests that despite the effects of the drought, PM2.5 concentrations should continue their decline due to the steady decrease in emissions of PM2.5 precursors. It is uncertain, however, given uncertainties in future weather patterns, how fast the decline in 24-hour PM2.5 will be. Therefore, considering the uncertainties associated with future weather conditions, 2019 remains the attainment target year for the 24-hour PM2.5 standard.

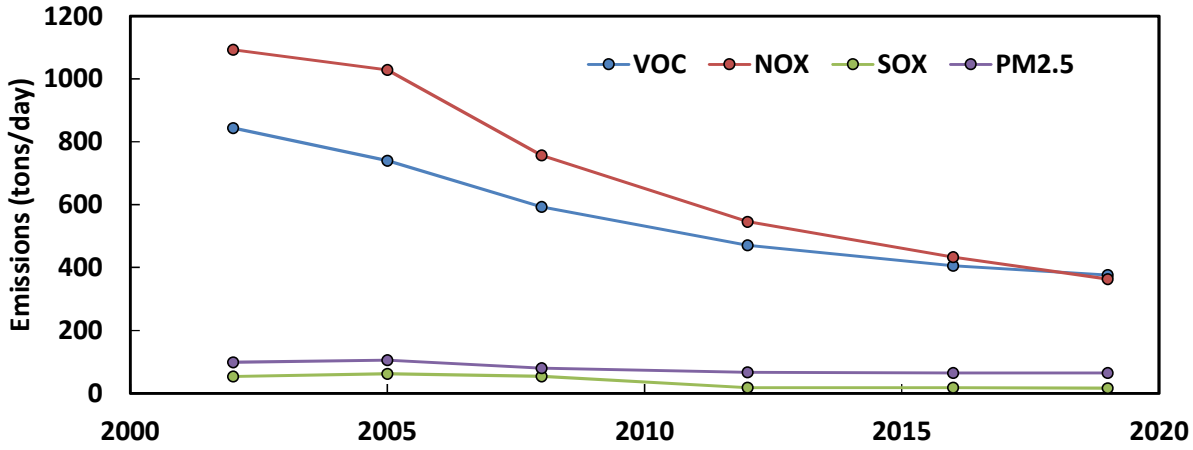

FIGURE V-7-17

Trend of PM2.5 precursor emissions from 2002 to 2019

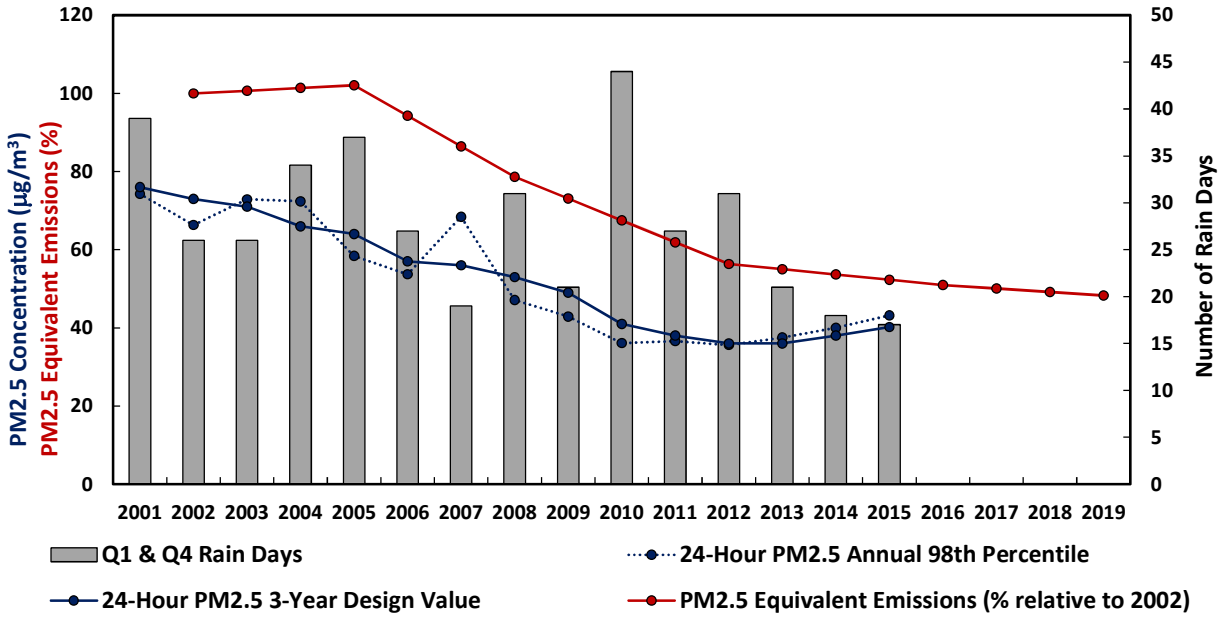

FIGURE V-7-18

Trend of South Coast Air Basin Maximum 24-Hour PM2.5 3-Year Design Values and Corresponding Annual 98th Percentile Concentration, with Number of Rain Days for Quarters 1 (Jan.–Mar.) and 4 (Oct.–Dec.) and Annual Trends of PM2.5 Equivalent Emissions Relative to 2002
(PM2.5 from Riverside-Rubidoux air monitoring station through 2006, then Mira Loma after that station was installed; 2015 PM2.5 data is preliminary)

References

Griffin D., Anchukaitis K.J., 2014. How unusual is the 2012-2014 California drought? *Geophysical Research Letters*, 41, 9017-9023

CHAPTER 8

1-HOUR OZONE ATTAINMENT DEMONSTRATION

Introduction

On February 6th, 2013, in response to a California Ninth Circuit Court of Appeals remand, U.S. EPA published a final rule to require California to provide a new 1-hour ozone attainment demonstration for the South Coast Air Basin (U.S. EPA, 2013). EPA disapproved the attainment demonstration in the 2003 SIP revision because it relied in large part on control measures that had been withdrawn by CARB following revocation of the 1-hour standard. A comprehensive plan for 1-hour ozone attainment was submitted as a part of the 2012 AQMP. A detailed background discussion on the reasoning for the required revision to the 1-hour ozone SIP was provided in the 2012 AQMP.

The U.S. EPA rule requires that attainment is achieved as expeditiously as practicable, but no later than five years, with a total of up to ten years for attainment of the now revoked 1-hour standard, if the state shows that ten years are needed. This required a demonstration of attainment of the 0.12 ppm standard by 2023, with emissions reductions in place by the end of 2022.

This section updates the attainment demonstration based on most recent emissions inventory and modeling configuration.

Background

Modeling platforms, meteorological models and chemistry packages have undergone significant enhancements since the 1997 AQMP attainment demonstration when the Urban Airshed Model (UAM) with CB-IV chemistry was the primary tool for projecting air quality. During development of the 2003 AQMP, the District convened a panel of seven experts to independently review the regional air quality modeling for ozone. The consensus of the panel was for the District to move to more current state-of-the-art dispersion platforms and chemistry modules. At that time, the model selected for the 2007 AQMP ozone attainment demonstrations was the Comprehensive Air Quality Model with Extensions (CAMx) (Environ, 2002), using SAPRC99 chemistry. The 2012 AQMP continued to move forward in the incorporation of current state-of-the-art modeling platforms to conduct regional modeling analyses. The 2012 AQMP PM2.5 attainment demonstration and ozone implementation update was developed using the U.S. EPA supported Community Multiscale Air Quality (CMAQ) (version 4.7.1) air quality modeling platform with SAPRC99 chemistry, and the Weather Research and Forecasting Model (WRF) (version 3.3) meteorological fields. The 2016 relies on a similar platform with incremental upgrades: CMAQ version 5.0.2 with SAPRC07 chemistry and WRF version 3.6. Appendix V, Chapter 2 provides an expanded discussion of the current modeling platform.

Ozone Representativeness

The 1997 AQMP and 2003 AQMP 1-hour ozone attainment demonstrations relied on direct output from model simulations to project future year air quality and design values. This “deterministic” approach was based on the premise that future year projected baseline inventories were accurate and the impacts of

implementing the control program were well-simulated. In addition, the form of the 1-hour ozone standard was directed at the fourth highest concentration in a three year period for a given air monitoring station. In essence, the analysis looked at the 2nd highest concentration in a given year, typically occurring during the worst-case meteorological scenario.

On the other hand, the 8-hour ozone attainment demonstrations included in the 2007 AQMP and 2012 AQMP have relied on the use of relative response factors (RRF) determined from the ratio of future to base year simulation projections to estimate future year design values. Since shifting to the 8-hour ozone standard, the RRF estimated from multiple meteorological episodes has been the primary methodology to estimate future design values. Both approaches, (deterministic or RRF), have their limitations: the deterministic method relies on accurate modeling and the proper selection of a meteorological episode while the RRF approach tends to place less reliance on individual day model performance since the factor is based on an average of several events having similar meteorological profiles. However, basing the RRF on multiple days may mask the meteorological profile characteristics of an extreme event such as an annual second maximum concentration.

The 1-hour ozone portion of the 2012 AQMP relied on a deterministic approach with the RRF approach included as part of the weight of evidence discussion. The RRF approach employed in the 2012 AQMP as the weight of evidence analysis is deemed the 'tiered approach', which tiered the concentration threshold for accepting a simulation station day based on three criteria for evaluation: (1) the base year daily maximum concentration absolute prediction error (calculated for a station per episode day) must be 20 percent or less; (2) the observed station concentration must be within 25 percent of the design value; and (3) a minimum of four station specific days simulated must meet the error at the set concentration threshold for the RRF to be calculated. If there are less than four days to meet the selection criteria, the threshold was lowered by 5 ppb increments until the RRF included a minimum four days. The first two categories were identical to the 8-hour criteria.

No specific modeling guidance applies to this current analysis since the 1-hour standard has been revoked. For the current AQMP, a RRF method was used as a primary tool to project future design values in order to ensure consistency with the 8-hour analysis.

The approach used in the current AQMP to project 1-hour ozone is similar to the RRF approach established in the U.S. EPA guidance (U.S. EPA, 2014) for 8-hour ozone. The new 8-hour guidance requires 10 days to be included in the RRF. If any of the top 10 days are predicted to be lower than 60 ppb, they are excluded in the RRF calculation, but a minimum of 6 days are required. In the 1-hour analysis, 90 ppb was used as a threshold, which was found to be the optimal value for the 1-hour RRF calculation in the San Joaquin Valley Air Basin (Kulkarni 2014). The 8-hour ozone standards takes the 4th highest reading in a year and averages over a three-year period. However, the 1-hour standard allows on average one exceedance per year, therefore, the 4th highest value over a three-year period is the design value. In other words, the 1-hour standard focuses on the 1st or 2nd highest days of the year, while the 8-hour standard accounts for the 4th highest. In this context, the 10-day RRF approach used in the 8-hour attainment demonstration may be inappropriate for the 1-hour demonstration and may mask the characteristics of the extreme events. Therefore, additional analysis was included using fewer days to estimate future design values.

Calculations with three, five, and ten days included in the RRF were conducted to determine the RRF methodology that represents the 1-hour standard appropriately.

In the 2012 AQMP, the maximum modelled grid cell in the 3x3 grid centered at each station was retrieved from the base and future simulations. In the current AQMP, the maximum modelled value in the 3x3 grid surrounding each station is compared to the corresponding grid position in the future year.

This update to the future year ozone projection focuses on 153 days of ozone air quality observed from May 1st through September 30th of 2012. During this period, several well defined multiday ozone episodes occurred in the Basin with 16 total days having daily Basin-wide maximum concentrations of 120 ppb or higher.

Figure V-8-1 depicts the time series of the daily Basin maximum and the Fontana, Upland, and Redlands daily maximum 1-hour ozone air quality during the ozone season in 2012 (May through September). The design site for 1-hour ozone is Fontana (138 ppb), while the 8-hour ozone design site is Redlands. Several locations in the San Bernardino and Riverside Valleys exhibit similar transport and daily patterns of ozone formation as Fontana. The Basin max for 1-hour ozone in year 2012 was observed at Glendora on August 11th, with a value of 147 ppb.

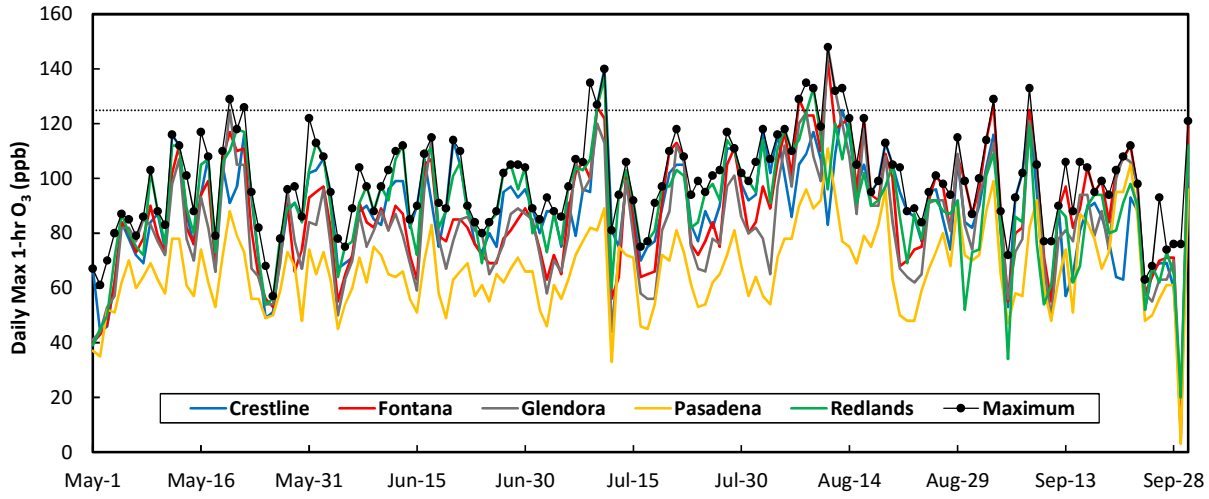

FIGURE V-8-1

Observed Basin, Fontana, Upland, and Redlands Daily Maximum 1-Hr Average Ozone Concentrations: May 1 through Sept 30, 2012.

One-hour ozone design values were calculated for the 2010 to 2014 period for the attainment analysis. At each station, the fourth highest value over each three year period between 2010 and 2014 was averaged, representing the five year average design value. The same data completeness requirement used in the 8-hour design value was adopted for the 1-hour standard as well. In that, even if a year did

not meet the 75% of data completeness test, it was only retained if the resulting design value was greater than the standard.

Table V-8-1 lists the 2010 to 2014 5-year weighted design values used in the future year ozone projections. Stations are color coded according to their performance evaluation zone defined in the Model Performance Evaluation section below.

TABLE V-8-1

2010–2014 Weighted 1-hr Ozone Design Values.

Station	2010–2014 1-hr Design Value	Performance Evaluation Zone
Costa Mesa	86.7	Coastal
LAX	81.3	Coastal
Long Beach	--*	Coastal
Mission Viejo	97.3	Coastal
West Los Angeles	93.7	Coastal
Burbank	--*	SanFernando
Reseda	125.0	SanFernando
Santa Clarita	132.7	SanFernando
Azusa	112.7	Foothills
Glendora	132.3	Foothills
Pasadena	--*	Foothills
Anaheim	86.0	UrbanSource
Central Los Angeles	89.3	UrbanSource
La Habra	98.3	UrbanSource
Pico Rivera	100.0	UrbanSource
Pomona	117.0	UrbanSource
Banning	--*	UrbanReceptor
Crestline	132.7	UrbanReceptor
Fontana	138.3	UrbanReceptor
Lake Elsinore	108.3	UrbanReceptor
Perris	114.7	UrbanReceptor
Redlands	133.3	UrbanReceptor
Rubidoux	124.3	UrbanReceptor
San Bernardino	123.7	UrbanReceptor
Upland	135.0	UrbanReceptor
Indio	97.3	CoachellaValley
Palm Springs	112.0	CoachellaValley

* did not meet the U.S. EPA's data completeness requirement and therefore no Design Value is available

Ozone Modeling Configuration

In the 2007 AQMP, the Comprehensive Air Quality Model with extensions (CAMx) was used as the primary chemical transport modeling platform. CAMx, including its predecessor, the Urban Airshed Model (UAM) (EPA, 1990) has been applied to many air pollution episodes in California and has demonstrated its capability as a valid tool for attainment demonstrations. While the District has a long history and significant expertise with the use of CAMx, the Community Multi-scale Air Quality (CMAQ) model provides two distinct advantages: CMAQ has been widely applied to various locations and episodes and is actively updated by a large users' community, including the U.S. EPA. Therefore, the 2012 AQMP used CMAQ as the primary modeling tool and CAMx to provide weight of evidence. The CMAQ version 5.0.2 used in the current AQMP has an updated aerosol chemical mechanism, updated numerical solvers for mass-consistent advection schemes, updated in-line plume rise calculation, updated in-line photolysis calculation, and an updated adjustment for nocturnal diffusion parameters when compared to version 4.7.1 used in the 2012 AQMP. SAPRC07 with version "c" toluene updates, Euler Backward Iterative (EBI) chemical solver, aero6 aerosol module, Yamo horizontal advection scheme, WRF vertical advection, and Asymmetric Convective Model version-2 (ACM2) vertical diffusion scheme were used in CMAQ. See Chapter 2 of Appendix 5 for the details of the modeling protocol associated with the chemical transport modeling.

The inner-most modelling domain of the WRF meteorological simulations overlaps the CMAQ modeling domain, with the exception of an extra 3 grid cells along the western, southern, and eastern boundary and an extra 9 grid cells along the northern boundary in the WRF domain. The CMAQ domain contains 156 cells in the east/west direction and 102 cells in the N-S direction. The vertical coordinate and each computational layer definition are identical to those of the WRF domain. However, layers in the middle and upper troposphere are combined to maximize computational efficiency, resulting in fewer layers. Impacts of vertical layer collapsing and the configuration employed to minimize artificial errors associated with this approximation have been evaluated intensively during the 2012 AQMP; therefore, the configuration developed in the previous AQMP was employed in the current simulations. In total, 18 layers were included in the CMAQ simulations with approximately 14 layers located below 2000 m above the ground level.

Base-year Ozone Model Performance Evaluation

For the CMAQ performance evaluation, the modeling domain is separated into several sub-regions or zones. Figure V-8-2 depicts the sub-regional zones used for the base-year simulation performance. The different zones present unique air quality profiles. Different performance evaluation zones were used in previous ozone modeling attainment demonstrations. Past evaluations included nine zones that represented the Basin and portions of Ventura County, the Mojave Desert and the Coachella Valley.

For the current analysis, the Basin has been re-categorized into six zones to make the analysis more concise and illustrative: A "Coastal" zone representing source receptor areas (SRA) 2-4 and 18-21, a "San Fernando" zone representing SRA 6,7, and 13 within the San Fernando Valley, a "Foothills" zone representing SRA 8 and 9, an "Urban Source" zone representing SRA 1, 5, 10-12, 16, and 17, an "Urban Receptor" zone representing SRA 22-29 and 33-38, and a "Coachella Valley" zone representing SRA 30 and 31. Of the six zones, the "Urban Receptor" region represents the Basin maximum ozone concentrations and the primary downwind impact zone. Table V-8-2 contains additional information regarding each station used in the analysis.

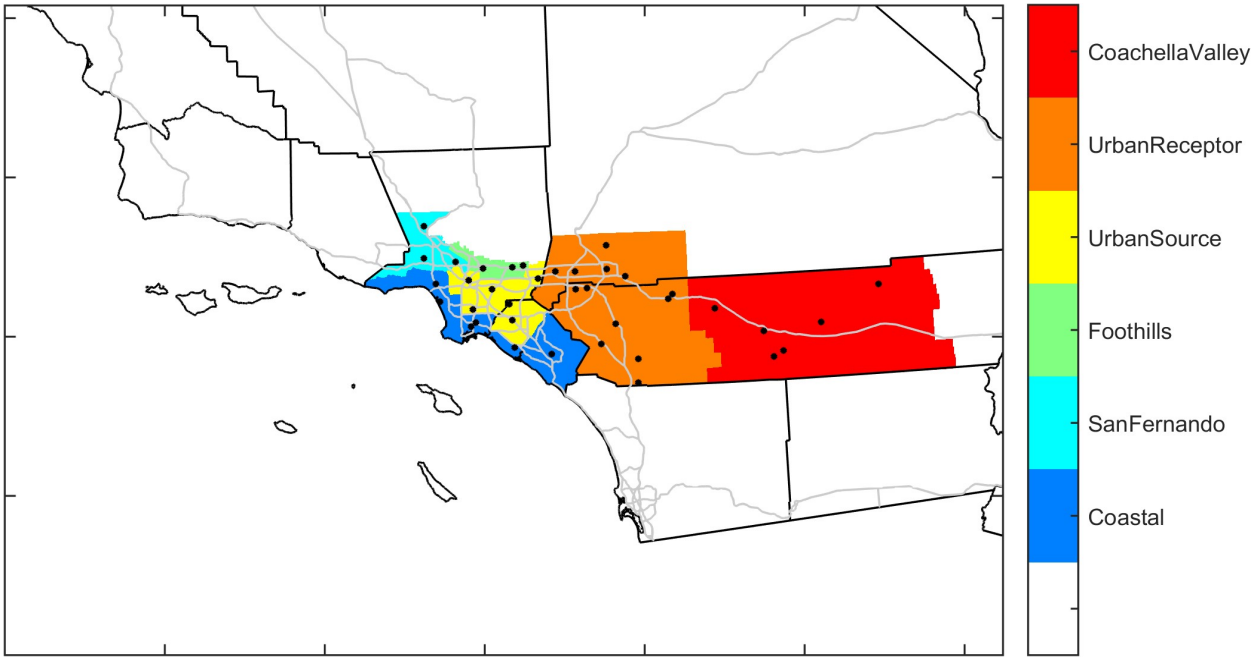

FIGURE V-8-2

Performance Evaluation Zones

TABLE V-8-2

Station Information

Location	Abbrev.	County	EPA Site Number	Source Receptor Area	Performance Evaluation Zone
Costa Mesa	CSTA	Orange	1003	18	Coastal
LAX	LAXH	Los Angeles	5005	3	Coastal
Long Beach	LGBH	Los Angeles	4002	4	Coastal
Long Beach Hudson	HDSN	Los Angeles	4006	4	Coastal
Mission Viejo	MSVJ	Orange	2022	19	Coastal
West Los Angeles	WSLA	Los Angeles	113	2	Coastal
Burbank	BURK	Los Angeles	1002	7	SanFernando
Reseda	RESE	Los Angeles	1201	6	SanFernando
Santa Clarita	SCLR	Los Angeles	6012	13	SanFernando
Azusa	AZUS	Los Angeles	2	9	Foothills
Glendora	GLEN	Los Angeles	16	9	Foothills
Pasadena	PASA	Los Angeles	2005	8	Foothills
Anaheim	ANAH	Orange	7	17	UrbanSource
Central Los Angeles	CELA	Los Angeles	1103	1	UrbanSource
Compton	CMPT	Los Angeles	1302	12	UrbanSource
La Habra	LAHB	Orange	5001	16	UrbanSource
Pico Rivera	PICO	Los Angeles	1602	11	UrbanSource
Pomona	POMA	Los Angeles	1701	10	UrbanSource
Banning	BNAP	Riverside	12/1016	29	UrbanReceptor
Crestline	CRES	San Bernardino	5	37	UrbanReceptor
Fontana	FONT	San Bernardino	2002	34	UrbanReceptor
Lake Elsinore	ELSI	Riverside	9001	25	UrbanReceptor
Mira Loma	MRLM	Riverside	8005	23	UrbanReceptor
Perris	PERI	Riverside	6001	24	UrbanReceptor
Redlands	RDLD	San Bernardino	4003	35	UrbanReceptor
Riverside	RIVR	Riverside	8001	23	UrbanReceptor
San Bernardino	SNBO	San Bernardino	9004	34	UrbanReceptor
Temecula	TMCA	Riverside	9	26	UrbanReceptor
Upland	UPLA	San Bernardino	1004	32	UrbanReceptor
Indio	INDI	Riverside	1999/2002	30	CoachellaValley
Palm Springs	PLSP	Riverside	5001	30	CoachellaValley

Statistical Evaluation

The statistics used to evaluate 1-hour average CMAQ ozone performance include the following:

Statistic for O_3	Definition
Daily-Max Bias Error Unpaired	Average of the differences in observed and predicted daily maximum values. Negative values indicate under-prediction. $BiasError = \frac{1}{N}\sum(Obs - Pred)$
Daily-Max Bias Error Paired	Average of the differences in daily maximum observed value and the corresponding predicted concentration at the hour that the observational maximum was reached. Negative values indicate under-prediction. $BiasError = \frac{1}{N}\sum(Obs - Pred)$
Daily-Max Gross Error Unpaired	Average of the absolute differences in observed and predicted daily maximum values $GrossError = \frac{1}{N}\sum\lvert Obs - Pred\rvert$
Daily-Max Gross Error Paired	Average of the absolute differences in daily maximum observed value and the corresponding predicted concentration at the hour that the observational maximum was reached. $GrossError = \frac{1}{N}\sum\lvert Obs - Pred\rvert$
Normalized Daily-Max Bias Error Unpaired	Average of the quantity: difference in observed and predicted daily maximum values normalized by the observed daily maximum values. Negative values indicate under-prediction. $NormBiasError = \frac{1}{N}\sum\left(\frac{Obs-Pred}{Obs}\right)\cdot 100$

Normalized Daily-Max Bias Error Paired	Average of the quantity: difference in daily maximum observed value and the corresponding predicted concentration at the hour that the observational maximum was reached normalized by the observed daily maximum concentration. Negative values indicate under-prediction. $NormBiasError = \frac{1}{N}\sum\left(\frac{Obs-Pred}{Obs}\right)\cdot 100$
Normalized Daily-Max Gross Error Unpaired	Average of the quantity: absolute difference in observed and predicted daily maximum values normalized by the observed daily maximum concentration $NormGrossError = \frac{1}{N}\sum\left\|\frac{Obs-Pred}{Obs}\right\|\cdot 100$
Normalized Daily-Max Gross Error Paired	Average of the quantity: absolute difference in daily maximum observed value and the corresponding predicted concentration at the hour that the observational maximum was reached normalized by the observed daily maximum concentration $NormGrossError = \frac{1}{N}\sum\left\|\frac{Obs-Pred}{Obs}\right\|\cdot 100$
Peak Prediction Accuracy Unpaired	Difference in the maximum of the observed daily maximum and the maximum of the predicted daily maximum normalized by the maximum of the observed daily maximum $PPA = \frac{(maximum(Pred)-\text{maximum}(Obs))}{\text{maximum}(Pred)}$

Predicted concentrations are extracted from model output in the grid cell that each monitoring station resides.

The base year average regional model performance for May through September 2012 for each of the five zones are presented in Tables V-8-3 to V-8-8 for days when Basin maximum 8-hour ozone levels were at least 60 ppb. Only stations with more than 75percent of the hourly measurements during each month of the ozone season were included in the analysis.

In general, the model over-predicts 8-hr daily-maximum ozone concentrations in the “Coastal” and “Urban Source” regions. Conversely, the model under-predicts 8-hr daily-maximum ozone concentrations in the “San Fernando”, “Foothills”, and “Urban Receptor” regions.

Model performance can be evaluated graphically with density scatter plots. Figure V-8-3 compares the measured and modelled 1-hr ozone concentrations for every hour in each region. Figure V-8-4 compares the measured and modelled maximum 1-hr ozone concentrations for 2012.

TABLE V-8-3

2012 Base Year 1-Hour Average Ozone Performance for Days When Regional 1-Hour Maximum ≥ 100 ppb in the "Coastal" region

Region	Coastal													
Month	Mean Pred. [ppb]	Mean Obs. [ppb]	Daily-Max Mean Pred. Unpaired [ppb]	Daily-Max Mean Pred. Paired [ppb]	Daily-Max Mean Obs. [ppb]	Daily-Max Bias Err. Unpaired [ppb]	Daily-Max Bias Err. Paired [ppb]	Daily-Max Gross Err. Unpaired [ppb]	Daily-Max Gross Err. Paired [ppb]	Norm Daily-Max Bias Err. Unpaired [%]	Norm Daily-Max Bias Err. Paired [%]	Norm Daily-Max Gross Err. Unpaired [%]	Norm Daily-Max Gross Err. Paired [%]	Peak Prediction Accuracy Unpaired [ppb]
May	41.8	38.8	65.5	59.5	58.5	7	1	10.1	9.8	9.2	-3.5	15.4	19.5	5.6
Jun	37.3	36.8	60.7	52.5	51	9.7	1.5	11.4	8.4	14.4	-5.5	18.6	22.1	7.5
Jul	31.9	32.5	54.8	50.2	51.9	2.9	-1.8	7.5	8.2	3.1	-8.6	13.4	19	13
Aug	36	29.9	62.6	57.6	49.8	12.8	7.7	14.5	12.2	17.6	9.1	21.5	19.9	9.9
Sep	38.2	33	65.3	58.9	61	4.3	-2.1	11.7	12.9	4.2	-10	18.1	25.8	-4.7

TABLE V-8-4

2012 Base Year 1-Hour Average Ozone Performance for Days When Regional 1-Hour Maximum ≥ 100 ppb in the "San Fernando" region

Region	San Fernando													
Month	Mean Pred. [ppb]	Mean Obs. [ppb]	Daily-Max Mean Pred. Unpaired [ppb]	Daily-Max Mean Pred. Paired [ppb]	Daily-Max Mean Obs. [ppb]	Daily-Max Bias Err. Unpaired [ppb]	Daily-Max Bias Err. Paired [ppb]	Daily-Max Gross Err. Unpaired [ppb]	Daily-Max Gross Err. Paired [ppb]	Norm Daily-Max Bias Err. Unpaired [%]	Norm Daily-Max Bias Err. Paired [%]	Norm Daily-Max Gross Err. Unpaired [%]	Norm Daily-Max Gross Err. Paired [%]	Peak Prediction Accuracy Unpaired [ppb]
May	47.6	42.1	73.6	70.9	83.6	-10.1	-12.7	12.2	14.7	-15.2	-20.1	17.8	22.5	-28.7
Jun	44.8	41.8	75.6	70.4	79.5	-4	-9.2	8.7	12	-6	-14.4	11.7	18.1	2
Jul	39	42.6	72	67.2	86.5	-14.5	-19.2	16.3	19.9	-20.6	-29.6	23	30.5	-33
Aug	46.3	41.7	80.6	74.9	92.9	-12.4	-18	15.1	19.1	-16.2	-25.7	19.5	27.1	-30.3
Sep	42.3	38.2	70.2	61.6	86.6	-16.5	-25	17.5	25.1	-28.1	-49.2	29.4	49.3	-38.9

TABLE V-8-5

2012 Base Year 1-Hour Average Ozone Performance for Days When Regional 1-Hour Maximum ≥ 100 ppb in the "Foothills" region

Region	Foothills													
Month	Mean Pred. [ppb]	Mean Obs. [ppb]	Daily-Max Mean Pred. Unpaired [ppb]	Daily-Max Mean Pred. Paired [ppb]	Daily-Max Mean Obs. [ppb]	Daily-Max Bias Err. Unpaired [ppb]	Daily-Max Bias Err. Paired [ppb]	Daily-Max Gross Err. Unpaired [ppb]	Daily-Max Gross Err. Paired [ppb]	Norm Daily-Max Bias Err. Unpaired [%]	Norm Daily-Max Bias Err. Paired [%]	Norm Daily-Max Gross Err. Unpaired [%]	Norm Daily-Max Gross Err. Paired [%]	Peak Prediction Accuracy Unpaired [ppb]
May	47.4	37.5	74.8	69.4	79.2	-4.4	-9.8	10.3	12.7	-6.5	-15.3	13.8	18.8	-27.2
Jun	43.3	37.4	72.4	65.1	74.1	-1.7	-9	8.9	11.5	-2.9	-14.4	12.1	17.8	-27
Jul	36.8	36.6	68.8	61.8	83	-14.2	-21.2	15.8	21.6	-22.8	-37	24.7	37.5	-20.2
Aug	44.1	35.8	78.6	72.7	90.4	-11.8	-17.8	15.7	19.8	-17.3	-27.7	21.9	30.3	-27.1
Sep	42.8	39.3	68.2	64	91.5	-23.3	-27.5	24.1	27.6	-42.1	-51.5	43	51.6	-25.2

TABLE V-8-6

2012 Base Year 1-Hour Average Ozone Performance for Days When Regional 1-Hour Maximum ≥ 100 ppb in the "Urban Source" region

Region	Urban Source													
Month	Mean Pred. [ppb]	Mean Obs. [ppb]	Daily-Max Mean Pred. Unpaired [ppb]	Daily-Max Mean Pred. Paired [ppb]	Daily-Max Mean Obs. [ppb]	Daily-Max Bias Err. Unpaired [ppb]	Daily-Max Bias Err. Paired [ppb]	Daily-Max Gross Err. Unpaired [ppb]	Daily-Max Gross Err. Paired [ppb]	Norm Daily-Max Bias Err. Unpaired [%]	Norm Daily-Max Bias Err. Paired [%]	Norm Daily-Max Gross Err. Unpaired [%]	Norm Daily-Max Gross Err. Paired [%]	Peak Prediction Accuracy Unpaired [ppb]
May	42.2	35.8	70.8	65.6	64.2	6.6	1.5	9.9	8.2	8.8	0.8	13.7	12.8	1.6
Jun	38.2	34.9	67.5	61.5	59	8.6	2.6	10.6	8.4	12.2	2.7	15.3	13.7	0.6
Jul	32.4	31.4	62.5	55.1	61.5	0	-6	9.2	11.1	-1	-12.8	14.5	20.4	1.3
Aug	37.5	29.2	72.6	66.8	64.5	8.1	2.4	13.4	12.7	9.5	0.7	18.2	19.6	7.9
Sep	37.7	31.2	66.3	60.6	72.8	-6.4	-12.2	14.3	16	-13.1	-25.8	24.2	31.6	-28.3

TABLE V-8-7

2012 Base Year 1-Hour Average Ozone Performance for Days When Regional 1-Hour Maximum ≥ 100 ppb in the "Urban Receptor" region

Region	Urban Receptor													
Month	Mean Pred. [ppb]	Mean Obs. [ppb]	Daily-Max Mean Pred. Unpaired [ppb]	Daily-Max Mean Pred. Paired [ppb]	Daily-Max Mean Obs. [ppb]	Daily-Max Bias Err. Unpaired [ppb]	Daily-Max Bias Err. Paired [ppb]	Daily-Max Gross Err. Unpaired [ppb]	Daily-Max Gross Err. Paired [ppb]	Norm Daily-Max Bias Err. Unpaired [%]	Norm Daily-Max Bias Err. Paired [%]	Norm Daily-Max Gross Err. Unpaired [%]	Norm Daily-Max Gross Err. Paired [%]	Peak Prediction Accuracy Unpaired [ppb]
May	58.2	52.4	88.7	81.1	92.4	-3.8	-9.8	10.8	14.1	-4.8	-13.2	12.4	17.8	-5.7
Jun	53.8	48.4	85	80.4	87.4	-2.4	-7	9.9	10.7	-3.9	-10.2	12	14.5	-5.8
Jul	48.1	49.5	81.9	75.9	93.2	-11.1	-16.9	15.1	18.2	-15.5	-25.3	20	26.8	-17.3
Aug	54	49.1	91.4	84.2	97	-5.6	-12.7	14.5	18.1	-8.6	-19.5	17.4	25	-8
Sep	46.2	42.9	70.7	62.9	86.4	-15.6	-23.5	20.7	26.2	-26.5	-47.4	32.1	50.4	-13.4

TABLE V-8-8

2012 Base Year 1-Hour Average Ozone Performance for Days When Regional 1-Hour Maximum ≥ 100 ppb in the "Coachella Valley" region

Region	Coachella Valley													
Month	Mean Pred. [ppb]	Mean Obs. [ppb]	Daily-Max Mean Pred. Unpaired [ppb]	Daily-Max Mean Pred. Paired [ppb]	Daily-Max Mean Obs. [ppb]	Daily-Max Bias Err. Unpaired [ppb]	Daily-Max Bias Err. Paired [ppb]	Daily-Max Gross Err. Unpaired [ppb]	Daily-Max Gross Err. Paired [ppb]	Norm Daily-Max Bias Err. Unpaired [%]	Norm Daily-Max Bias Err. Paired [%]	Norm Daily-Max Gross Err. Unpaired [%]	Norm Daily-Max Gross Err. Paired [%]	Peak Prediction Accuracy Unpaired [ppb]
May	64.7	64.7	76.5	70.3	82.6	-6.1	-12.3	10.3	14.6	-8.5	-18.9	13.5	21.7	-23.6
Jun	56.5	58.4	69.8	62.6	76.9	-7.1	-14.3	9.6	15.5	-11.5	-26.4	14.8	28	-3.8
Jul	48.8	49.4	64	55	66.9	-2.7	-11.7	7.7	13.1	-4.6	-22.9	12.3	25.1	-9.8
Aug	51.8	48.4	66.5	57.6	67.2	-0.7	-9.6	9.5	12.3	-0.9	-18	14.3	22.4	-20.7
Sep	45.4	38.6	56.3	50.2	58.4	-2.1	-8.2	8.6	12.1	-4.3	-20	15.1	27.1	-24.8

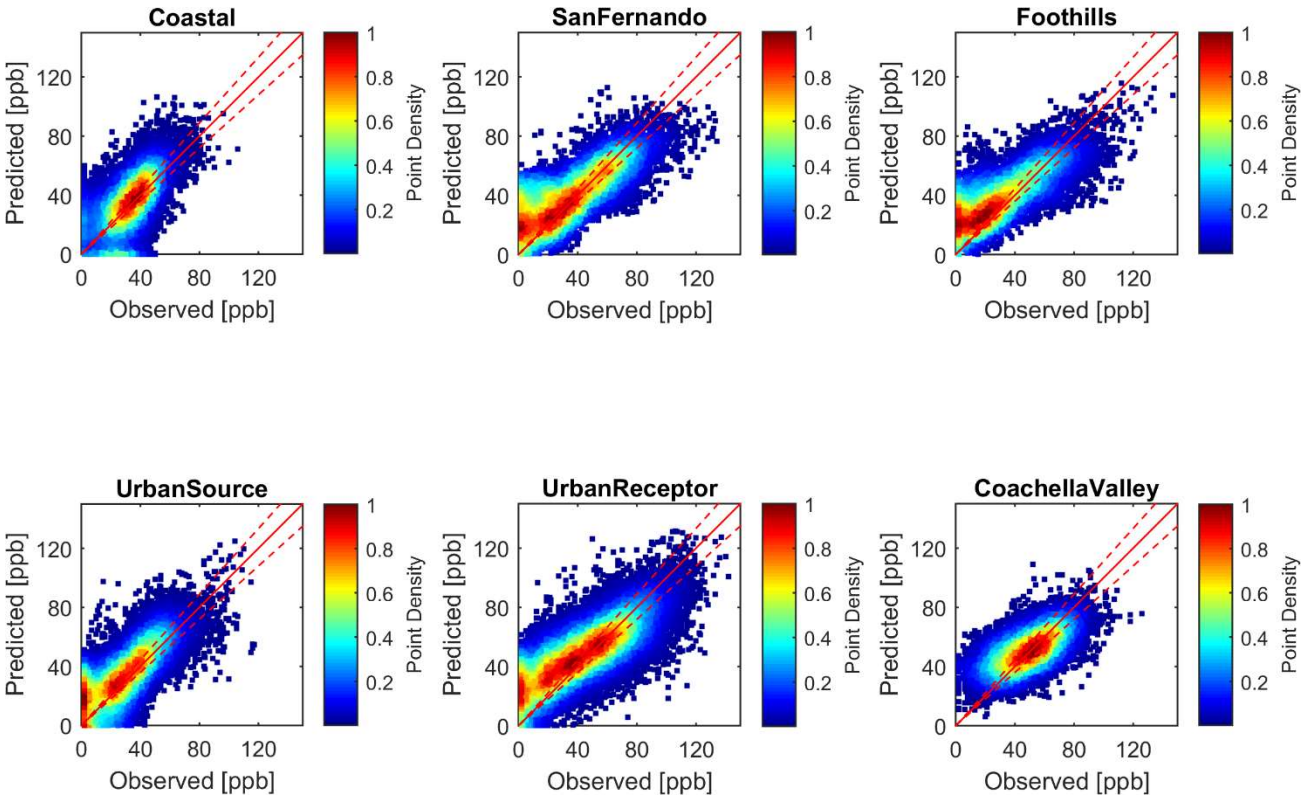

FIGURE V-8-3

Density scatter plot of Observed Vs. Predicted 1-Hour regional ozone hourly values. Dashed lines indicate 10 percent error bounds.

The density scatter plots further illustrate the over-prediction of high 1-hour ozone values in coastal regions. Ozone is also over-predicted at low concentrations at "Urban Receptor", "San Fernando", and "Foothills" stations, which may be due to the uncertainties associated with nocturnal chemistry. However, predictions significantly lower than the 120 ppb standard are unlikely to affect the attainment demonstration. In other words, model performance of the daily maximum is more relevant to the attainment demonstration. Figure V-8-4 presents the density scatter plots of 1-hour daily maximum regional ozone values. A focus on the daily maximum also reveals an over-prediction in "Coastal" and "Urban Source" regions on days with relatively high daily maximum concentrations. In general, the "Urban Receptor" region is slightly under-predicted. Other regions are represented well. While all the analysis zones exhibit varying degrees of bias, the RRF approach assumes that the model biases that exist in the base year are carried over to future year. Thus, the RRF approach, instead of direct model predictions, is expected to minimize errors caused by systematic model biases.

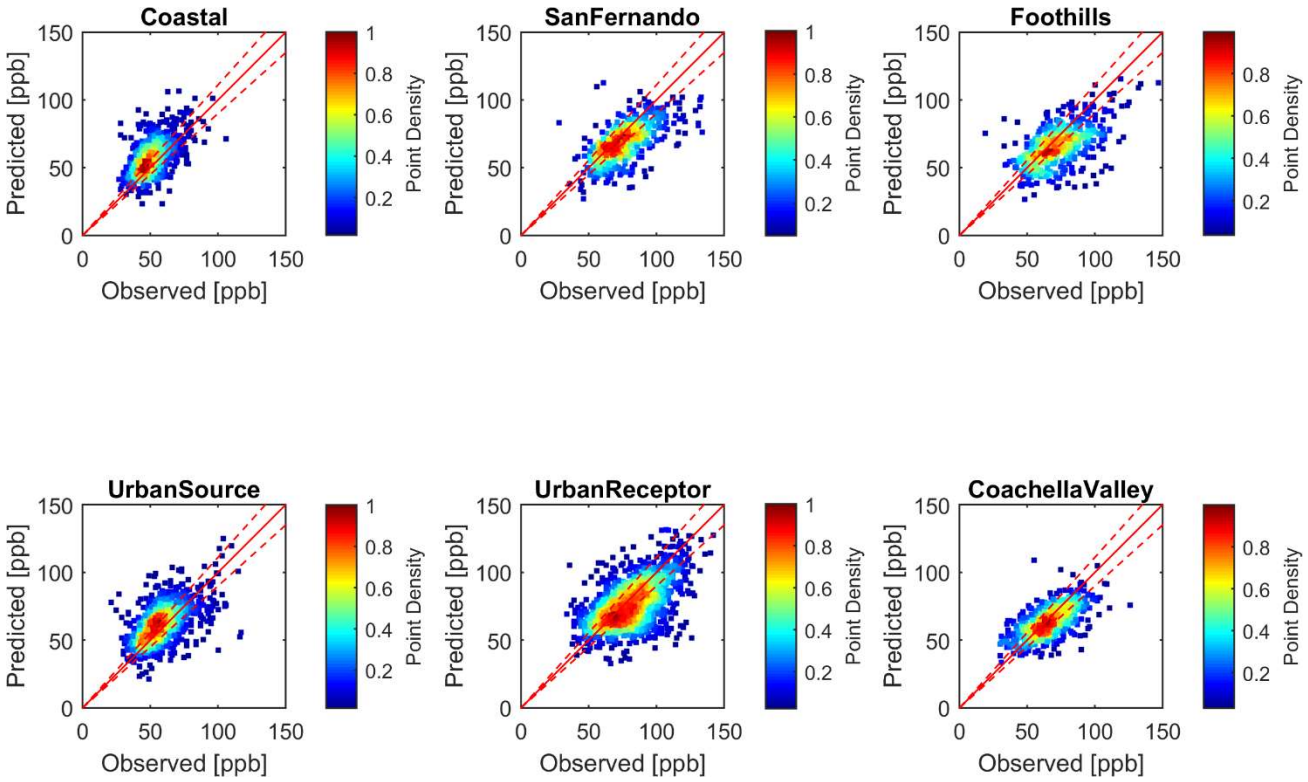

FIGURE V-8-4

Density scatter plot of Observed Vs. Predicted 1-Hour regional ozone daily-maximum values. Dashed lines indicate 10percent error bounds.

Diurnal Trends in 1-hour Ozone

Figures V-8-5 through V-8-10 show the diurnal trends of observed and predicted 1-hour ozone for each day from June 1 through August 31, 2012 for six stations following a transport route from the coastal area of the Basin to inland Crestline and Banning. Supplemental diurnal observed and predicted 1-hour ozone for all remaining air quality sites are provided as Attachment 2 to this appendix. In West Los Angeles, the model over-predicts 1-hr ozone concentrations over several periods during June, July, and August. Conversely, there are periods where the model predicts concentrations in the "Coastal" region well, capturing daily maxima and diurnal trends accurately. In central Los Angeles, the model slightly under-predicts the daily maxima, but captures the diurnal variation well. Daily maximum ozone concentrations are under-predicted in Glendora and Fontana during some periods while daily minimum ozone concentrations are over-predicted. Daily maximum ozone concentrations in Crestline were well-simulated with the exception of nocturnal low ozone. Nighttime NOx scavenging is generally not well represented in the simulations, which is typical in regional photochemical models. Ozone predictions at Banning, the easternmost site in the Basin, track the peak concentrations reasonably well with a slight bias towards over prediction.

Overall, it is important to note that the effects of prediction biases or errors are mitigated by the use of relative response factors for the attainment analysis.

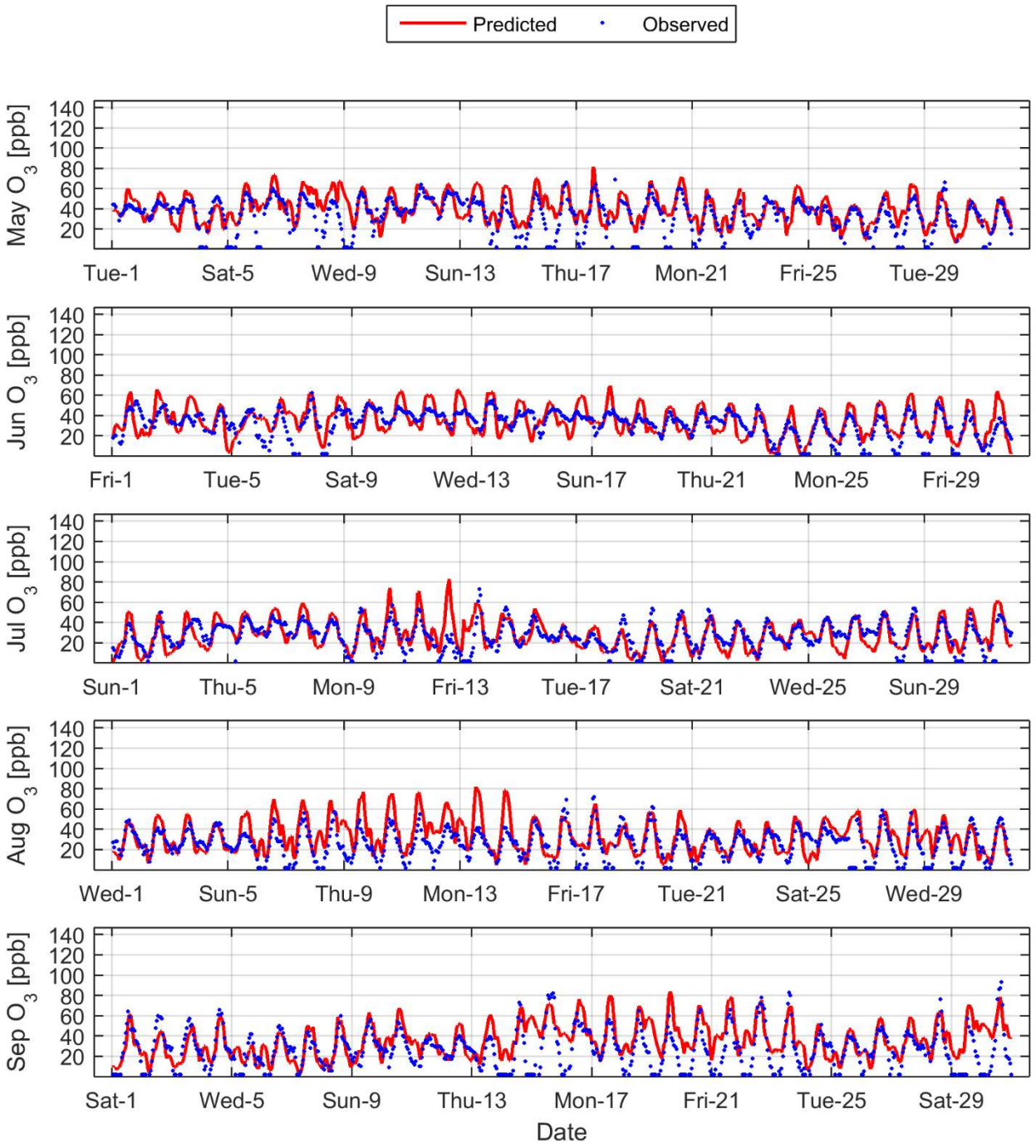

FIGURE V-8-5

Time Series of Observed Vs. Predicted 1-Hour West Los Angeles Ozone

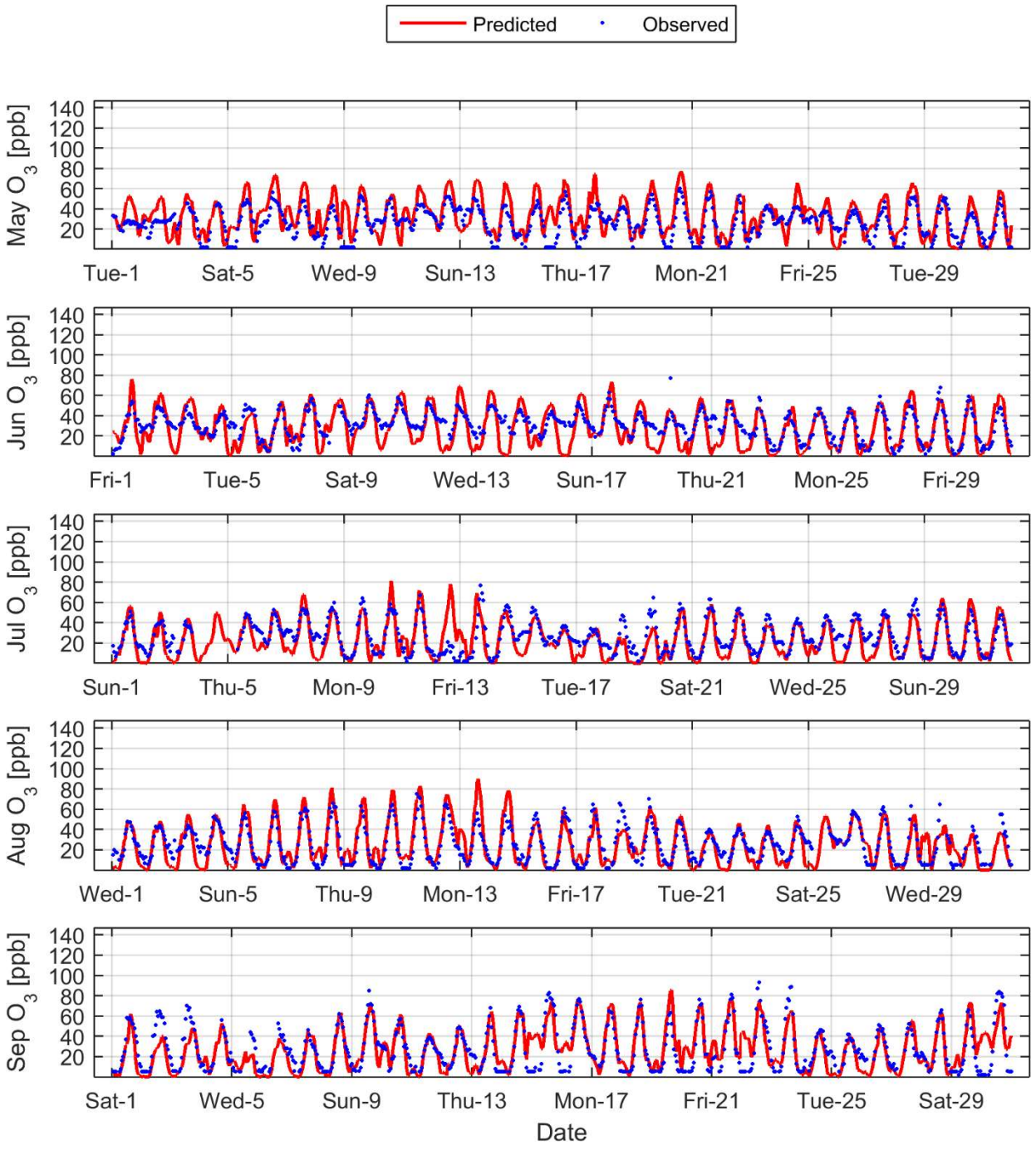

FIGURE V-8-6

Time Series of Observed Vs. Predicted 1-Hour Central Los Angeles Ozone

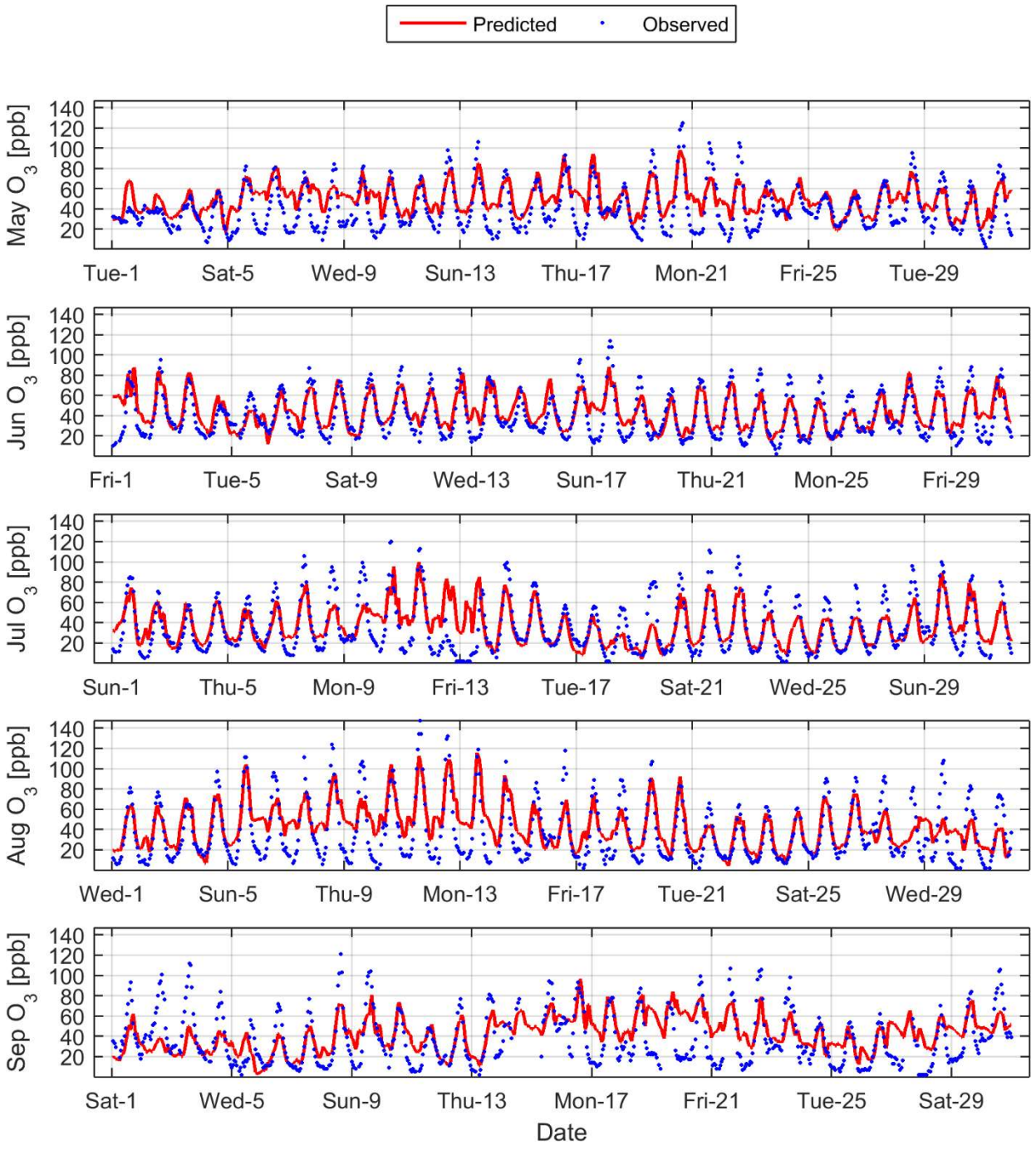

FIGURE V-8-7

Time Series of Observed Vs. Predicted 1-Hour Glendora Ozone

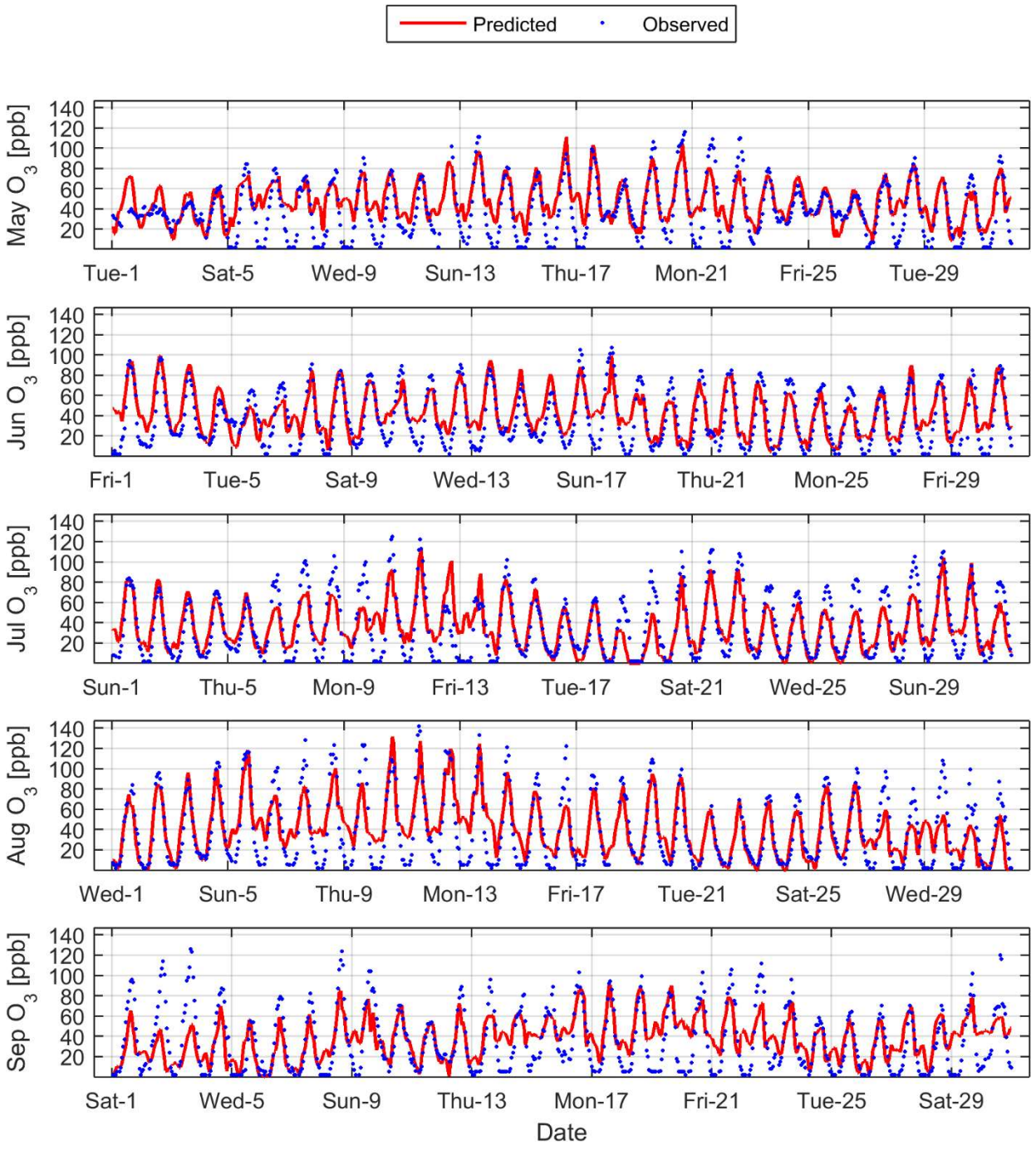

FIGURE V-8-8

Time Series of Observed Vs. Predicted 1-Hour Fontana Ozone

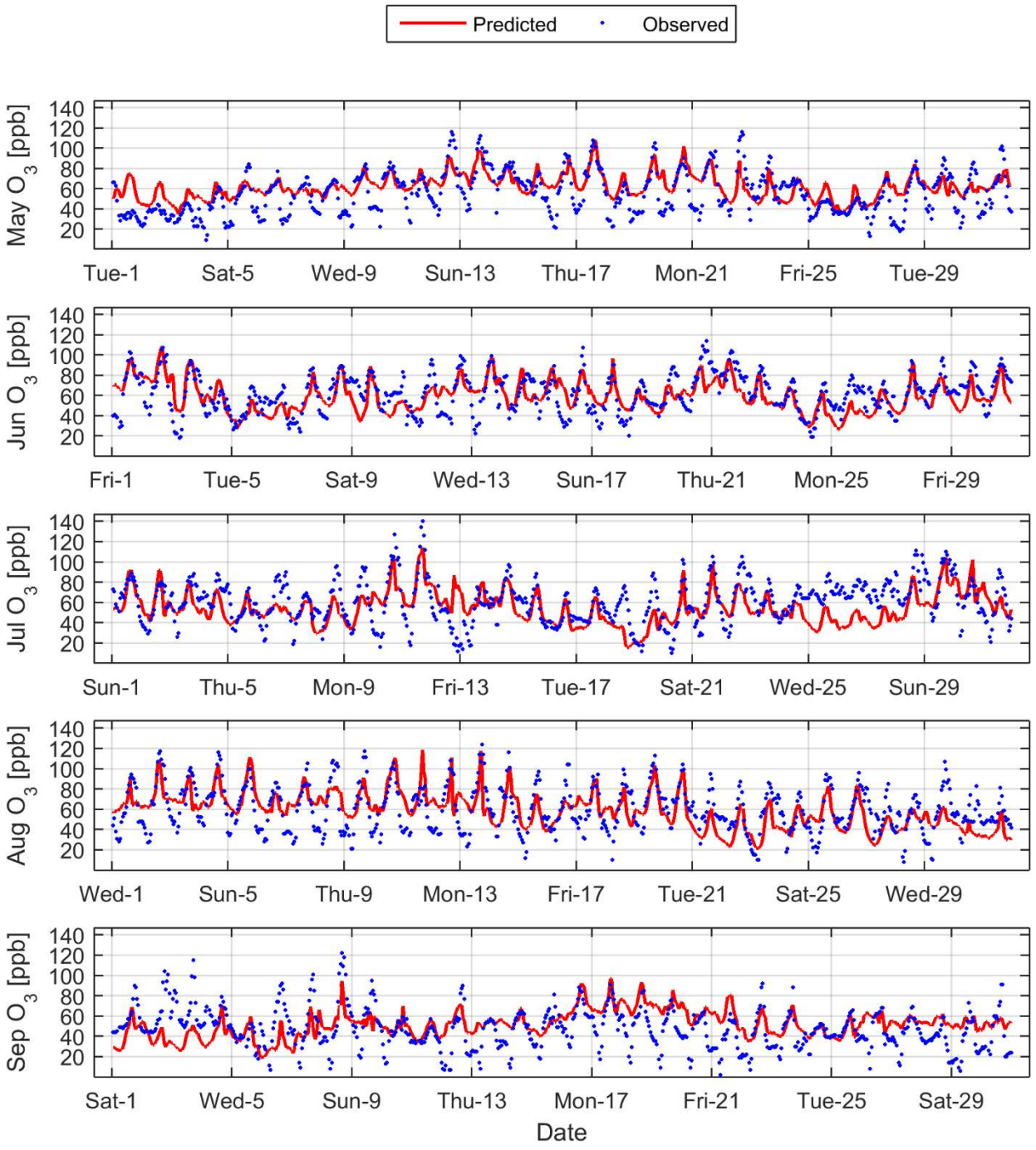

FIGURE V-8-9

Time Series of Observed Vs. Predicted 1-Hour Crestline Ozone

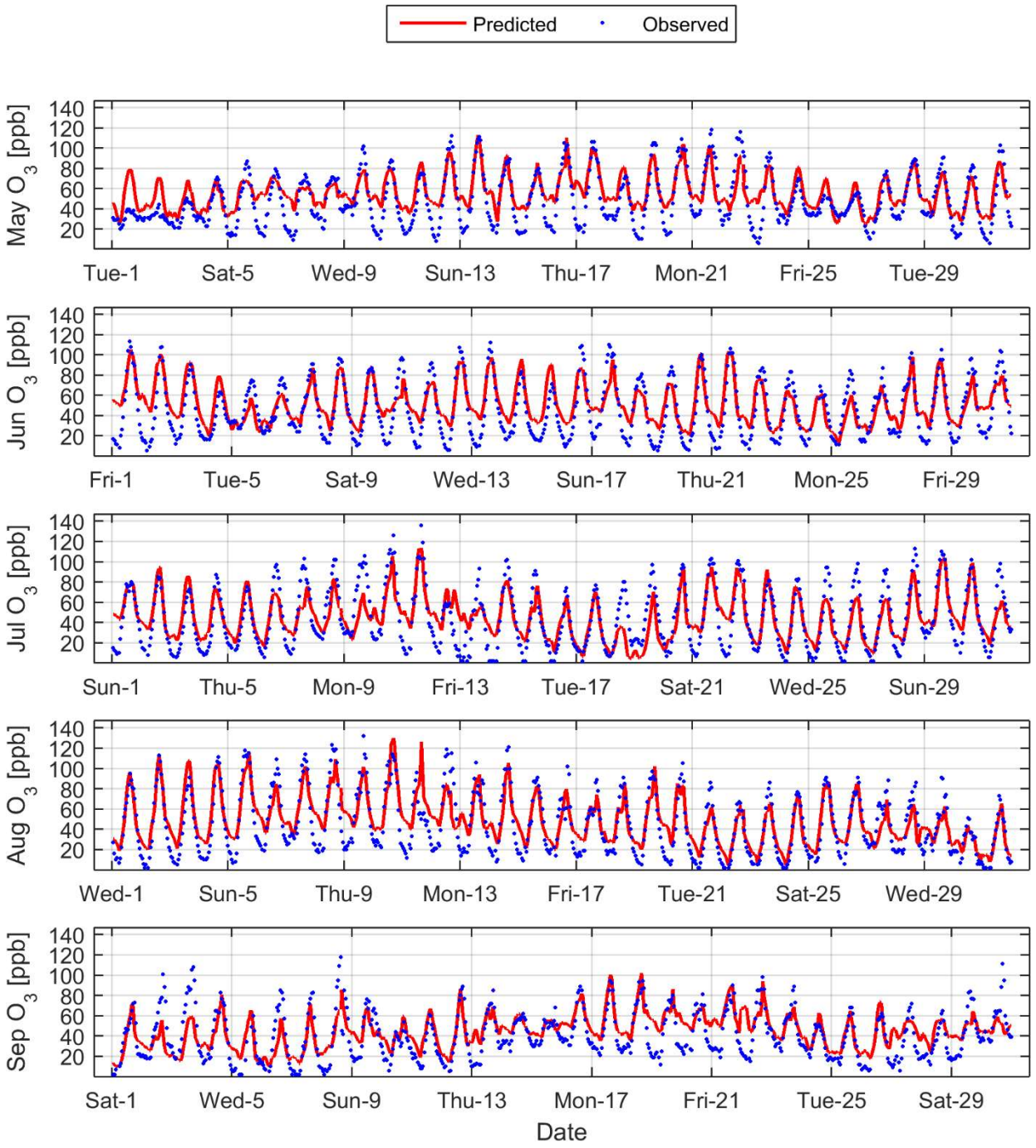

FIGURE V-8-10

Time Series of Observed Vs. Predicted 1-Hour Redlands Ozone

Future-Year Ozone Modeling Approach

The set of 153 days from May 1st through September 30th, 2012 were simulated and analyzed to determine daily 1-hour ozone for the base year (2012) and future attainment year (2022). A set of simulations with incremental VOC and NOx emissions reductions from 2022 baseline emissions was generated to create ozone isopleths for each station in the Basin. The ozone isopleths provide updated guidance for the formulation of future control strategies.

The top three days were chosen for the RRF calculation. While the adjustment was made based on the definition of the design value, a thorough analysis was performed to ensure coherence of the 1-hour and 8-hour attainment demonstrations. (See Weight of Evidence discussion).

The remainder of the attainment demonstration methodology was identical to that of the 8-hour analysis. RRFs were based on a 3x3 cell array of model data centered on the cell that each station resides. The max prediction from the 3x3 array was chosen for the base year simulation and the grid cell location was carried to future year simulations. The number of grids in the array and the comparison of the grid cell location from the base year simulation with the same grid cell in the future year have been established in the 2014 guidance. 20percent peak prediction criteria was applied in the 1-hour as well, except that the threshold for inclusion in the RRFs was set to 90 ppb, consistent with the 60 ppb suggested for the 8-hour analysis.

1-hour Ozone episode

Two episodes during the 2012 ozone season were selected for an in-depth analysis of model performance: July 8-11 and August 9-14. The two episodes included hourly measurements that exceeded the 1-hour ozone standard. Both episodes were characterized by the typical southern California climate conditions that are conducive to ozone episodes, i.e. stagnant flow, strong subsidence induced by synoptic scale high pressure, and subsequently limited vertical mixing and spatial dispersion. High pressure affecting Utah, Colorado and Wyoming and low pressure off the coast of the Basin caused a subsidence inversion and reduced vertical mixing. These conditions brought temperatures greater than 100 oF to many areas of the basin.

During the episode in early July, ozone concentrations remained elevated until July 11, when peak ozone reached 140 ppb in Crestline. This period was followed by slight precipitation on July 12th that broke the stagnation, reduced temperatures and consequently improved ozone air quality.

During the episode in August, ozone concentrations at several stations exceeded the 1-hour standard over a six-day period. The absolute maximum 1-hour ozone concentration in the Basin for 2012 was reached in Glendora, with an ozone concentration of 148 ppb on August 11.

Figure V-8-11 displays maximum 1-hour ozone concentrations at various locations. The air quality model performed well during the August episode, with an overall normalized unpaired bias and normalized unpaired gross error of 2.2percent and 13.8percent, respectively. Model simulations agreed reasonably well during the July episode, with normalized unpaired bias and normalized unpaired gross error of 3.5percent and 30.4percent. The reduced model performance during the July episode is in part attributable to the presence of rain, which is typically more difficult to model than dry conditions.

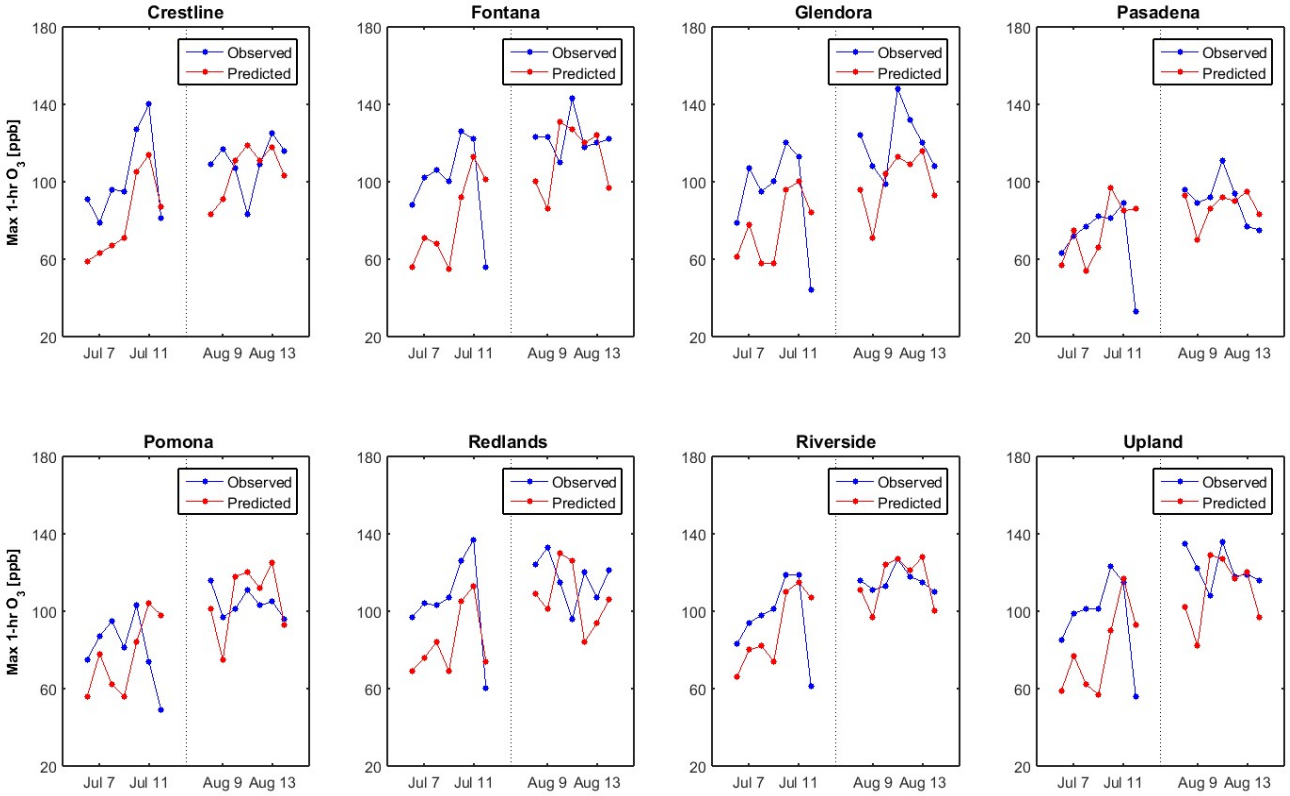

FIGURE V-8-11

Observed Vs. Predicted 1-Hour Max Ozone at selected monitoring stations during the two episodes

Future Ozone Air Quality

The 2016 AQMP addresses the 1979 1-hour ozone standard of 0.12 ppm with an attainment date of February 6, 2023, which requires all the required emission reductions to meet the standard need to be in placed by December 31, 2022. Table V-8-9 summarizes the results of the updated ozone simulations. Included in the table are the 2022 ozone baseline and controlled ozone projections from the 2012 AQMP ozone attainment demonstration. The 2012 AQMP concluded that the carrying capacity to meet 1-hour standard was 150 TPD of NOx, which was approximately a 56 percent additional reduction from 2022 baseline.

The 2016 AQMP baseline ozone simulations reflect the changes made to the 2022 baseline inventories. The 2016 AQMP summer planning inventory for 2022 has the same VOC/NOx emissions ratio of 1.29 as the inventory developed under the 2012 AQMP, although total tonnages of both precursor emissions are lower than the 2012 AQMP. Reduced 2022 baseline VOC and NOx emissions in the 2016 AQMP relative to the 2012 AQMP reflect the rules and regulations updated after the 2012 AQMP, updates in emission estimate methodologies, and updated growth projections.

The current analysis shows that the 2022 baseline emissions with no additional reduction beyond already adopted measures do not lead to attainment, indicating additional emission reductions are necessary to meet the standard. The carrying capacity was estimated to be approximately 250 TPD of NOx if no VOC control is introduced. However, as shown in the ozone isopleths plot (Figure V-8-12), VOC is as effective as or even more effective than NOx reductions in the high ozone regime near the upper right corner of the figure. This indicates the 47 TPD of needed reduction can be achieved either in VOC, NOx, or a combination of both. While the 8-hour ozone strategy relies on NOx reduction, 1-hour ozone can benefit from both NOx and VOC controls.

The revised carrying capacity—250 TPD of NOx, or higher with additional VOC control—is significantly higher than the estimates presented in the 2012 AQMP. As discussed in the earlier 8-hour attainment demonstration, several factors contributed to this change: improved air quality, a revised attainment demonstration methodology, and a revised baseline emissions inventory.

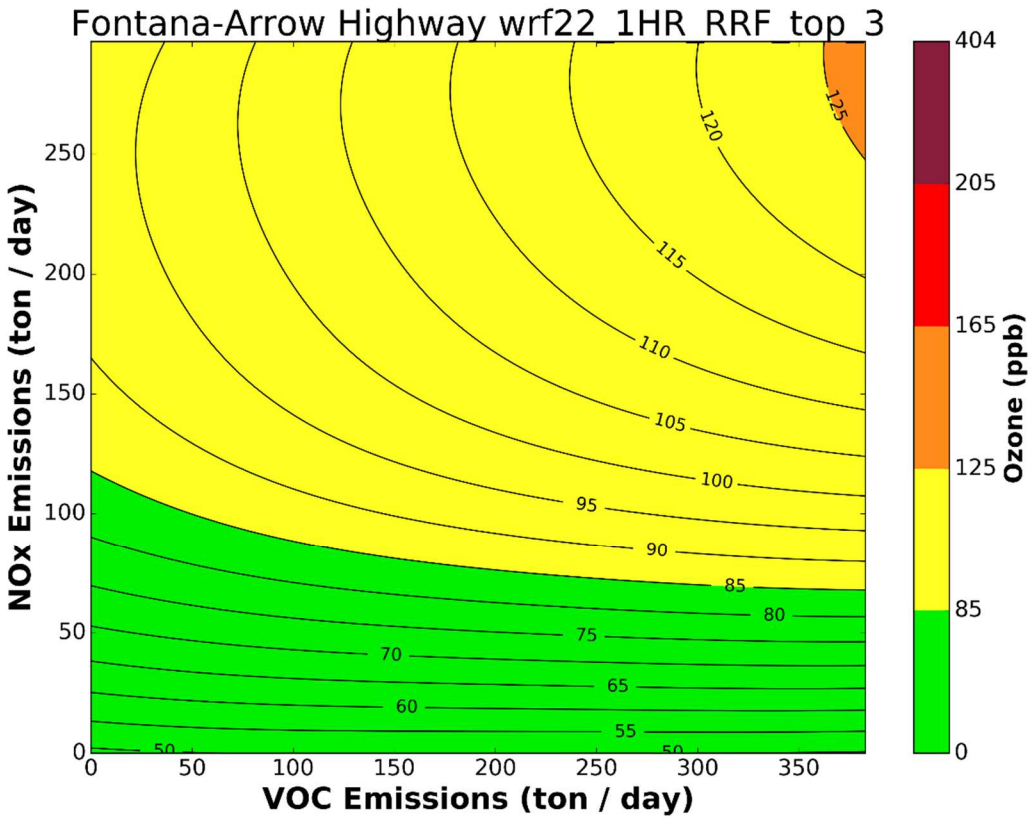

FIGURE V-8-12

1-hour Ozone Isopleths for Fontana

The progress toward to the 2023 target level to meet the 8-hour standard is expected to ensure attainment of the 1-hour standard in 2022. Given the possible approval of emission reductions associated with CAA Section 182(e)(5) measures, a set of future reductions from only defined measures were simulated to test attainment of the 1-hour standard. This scenario consists of reductions of 35 TPD of NOx and 10 TPD of VOC. Refer to CEPA reports presented in Attachment 3 for details. With the proposed defined controls in place, all stations in the Basin will meet the federal one-hour ozone standard by 2022.

The Coachella Valley is expected to meet the 1-hour ozone standard in 2022 with no additional controls beyond already adopted rules and regulations.

TABLE V-8-9

Model-Predicted 1-Hour Ozone Design Values (ppb)

Station	2012 5-year Weighted Design Value	2012 AQMP		2016 AQMP	
		2022 Baseline	2022 Controlled	2022 Baseline	2022 Controlled
Azusa	112.7	139.9	131.0	104	101
Burbank	--	123.0	111.6	--	--
Reseda	125.0	112.4	101.0	105	103
Pomona	117.0	124.5	108.8	103	101
Pasadena	--	141.6	134.6	--	--
Santa Clarita	132.7	119.7	105.3	110	108
Glendora	132.3	143.3	133.5	121	119
Riverside	124.3	116.9	103.8	109	106
Perris	114.7	111.5	94.5	108	106
Lake Elsinore	108.3	108.8	90.9	93	91
Banning	--	119.7	102.5	--	--
Upland	135.0	135.9	121.1	122	119
Crestline	132.7	134.9	116.4	120	118
Fontana	138.3	128.3	110.8	125	122
San Bernardino	123.7	127.7	110.9	107	104
Redlands	133.3	127.2	109.6	120	118

NOTE: Burbank, Pasadena, and Banning do not have 2012 base-year design values due incomplete measurement data in one or multiple years between 2010 and 2014. A design value of 124.9 ppb or lower is needed for attainment

Spatial Projections of 1-Hour Ozone Design Values

The spatial distribution of ozone design values for the 2012 base year is shown in Figure V-8-13. Future year ozone air quality projections for 2022 with and without implementation of non-182(e)(5) control measures are presented in Figures V-8-14 and V-8-15. The predicted ozone concentrations will be significantly reduced in the future years in all parts of the Basin with the implementation of proposed control measures in the South Coast Air Basin. Future design values are predicted from model RRFs and measured base-year design values. Future design values are then interpolated using a natural neighbor interpolation to generate the interpolated fields.

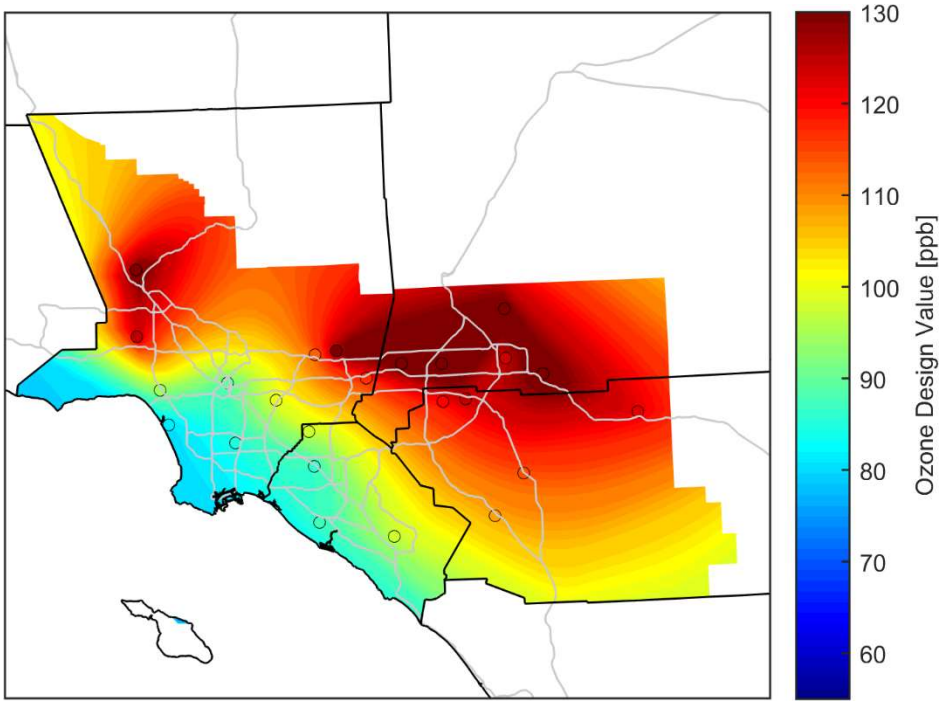

FIGURE V-8-13

2012 Model-Predicted Baseline 1-Hour Ozone Design Concentrations (ppb). The circles indicate the location of air monitoring stations.

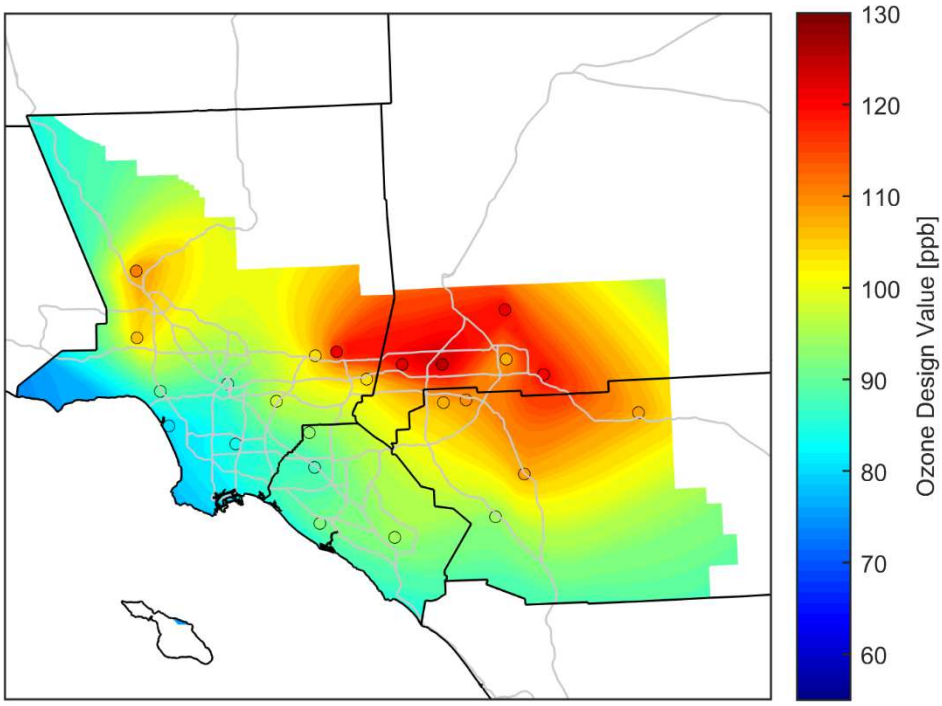

FIGURE V-8-14

Model-Predicted 2022 baseline 1-Hour Ozone Concentrations (ppb)

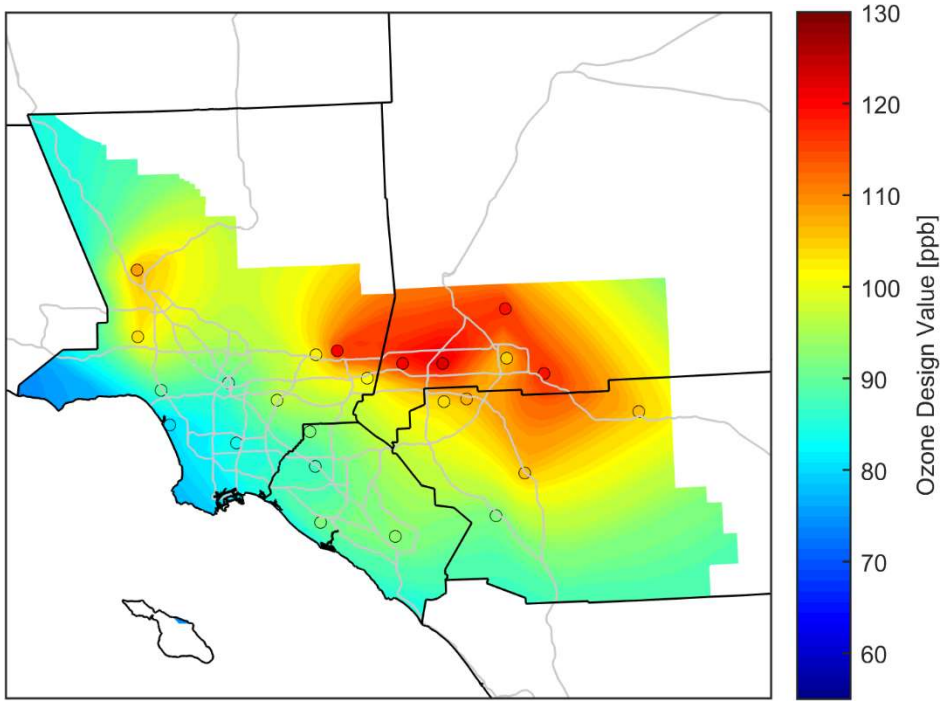

FIGURE V-8-15

Model-Predicted 2022 Controlled 1-Hour Ozone Concentrations (ppb)

Weight of Evidence

The number of days used to represent the RRF can change future predicted ozone design values. To maintain consistency with recommendations for the 8-hour ozone attainment demonstration, only the top three days at each site were used to determine the RRF. The 8-hour standard is based on the fourth highest day of the year and requires ten days in the RRF calculation. The 1-hour standard is based on the fourth highest day in a three year period, which on average, falls between the first and second highest value in a single year (1.33rd highest value). Using the top three days in the RRF calculation results in a similar ratio between the number of days used for the RRF and the standard as the 8-hour guidance requires. (10 RRF days/4th highest day = 2.5 for 8-hour standard; 3 RRF days/1.33rd highest day = 2.3 for 1-hour standard). Calculating the RRF with only the top three days would more accurately predict concentrations in the high end of the ozone distribution, when the exceedances occur. Using too many days for the RRF calculation can mask the impacts of meteorology or chemistry on extreme ozone days. 2012 base year design values along with 2022 baseline concentrations with several RRF methodologies are presented in Table V-8-10. 2022 projected concentrations at Fontana, the 1-hour ozone design station, attain the standard when only using the top two, three or five days, as opposed to using the top ten days. Glendora is more sensitive to the RRF methodology, but like Fontana, attainment is reached when using the top two, three, or five days as opposed to ten days in the RRF calculation.

TABLE V-8-10

RRF Adjusted Future Design Values as a Function of Number of Days Selected for the RRF Calculation

	DV (ppm)	RRF Adjusted 2022 Concentrations (ppm) [non-(e)(5) measures]			
Station	2012 Base Year	2nd highest day	Top 3 days	Top 5 days	Top 10 days
Anaheim	86	84	86	89	87
Azusa	112	98	101	107	109
Central Los Angeles	89	89	88	88	87
Compton	84	83	83	85	85
Crestline	132	114	118	117	115
Costa Mesa	86	90	91	88	85
Lake Elsinore	108	90	91	91	92
Fontana	138	118	122	121	123
Glendora	132	121	119	124	129
Indio	97	85	87	87	87
La Habra	98	91	92	97	100
LAX	81	80	80	79	79
Mira Loma	119	105	104	105	110
Mission Viejo	97	93	93	91	91
Perris	114	107	106	104	100
Pico Rivera	100	97	96	98	101
Palm Springs	112	97	97	98	98
Pomona	117	101	101	107	109
Redlands	133	114	118	118	120
Reseda	125	103	103	106	107
Riverside	124	107	106	108	115
Santa Clarita	132	107	108	113	113
San Bernardino	123	104	104	109	113
Upland	135	120	119	118	121
West Los Angeles	93	89	89	92	91

References

United States EPA, Finding of Substantial Inadequacy of Implementation Plan: Call for California State Implementation Plan Revision; South Coast, February 2013, EPA-R09-OAR-2012-0721

Sarika Kulkarni, Ajith P. Kaduwela, Jeremy C. Avise, John A. DaMassa and Daniel Chau (2014) An extended approach to calculate the ozone relative response factors used in the attainment demonstration for the National Ambient Air Quality Standards, Journal of the Air & Waste Management Association, 64:10, 1204-1213, DOI: 10.1080/10962247.2014.936984

CHAPTER 9

SUMMARY AND CONCLUSIONS

Comparison to State and Federal Standards

Comparison to State and Federal Standards

Figure V-9-1 shows the Basin-wide maximum 8-hour ozone concentrations in the base year (2012) along with projected design values for the attainment deadline of the 1997 standard of 80 ppb (2023) and for the 2008 standard of 75 ppb (2031). Figure V-9-2 shows the same projected design values relative to the California standards. With the controls proposed in the 2016 AQMP, the future year ozone concentrations are expected to meet the federal standards. NOx reductions of approximately 45 percent and 55 percent from the baseline levels are needed in 2023 and 2031, respectively (Figure V-9-3). Approximately 50 TPD of NOx and VOC combined reductions from the 2022 baseline is needed to meet the 1-hour ozone standard by 2022, confirming that the 8-hour standard is more stringent than the 1-hour standard. The strategies developed for attainment of the 2023 and 2031 8-hour standards will ensure attainment of the 1-hour standard by 2022 (Table V-9-1).

The California standard for 8-hour ozone is 70 ppb, the same level as the 2015 revised federal standard. This State standard will not be achieved by 2031. Preliminary analysis suggests additional emission reductions beyond the level required in 2031 are needed to meet the 70 ppb standard. Challenges in achieving the 70 ppb standard are discussed in Chapter 8.

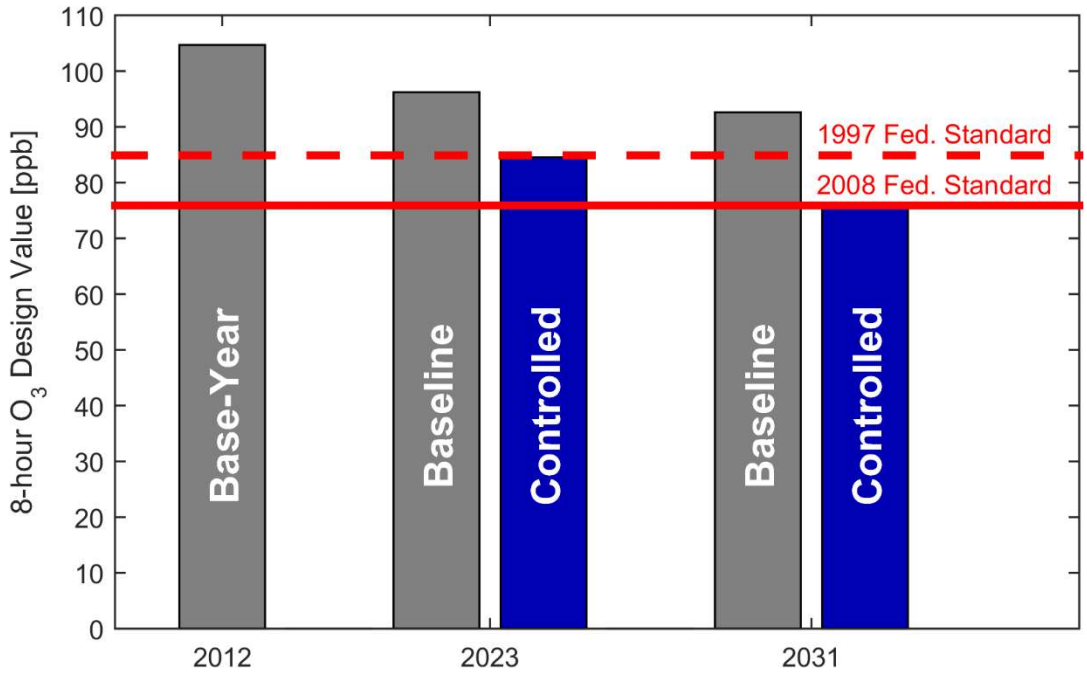

FIGURE V-9-1

Projection of future 8-hour ozone air quality in the Basin
in comparison to federal standards

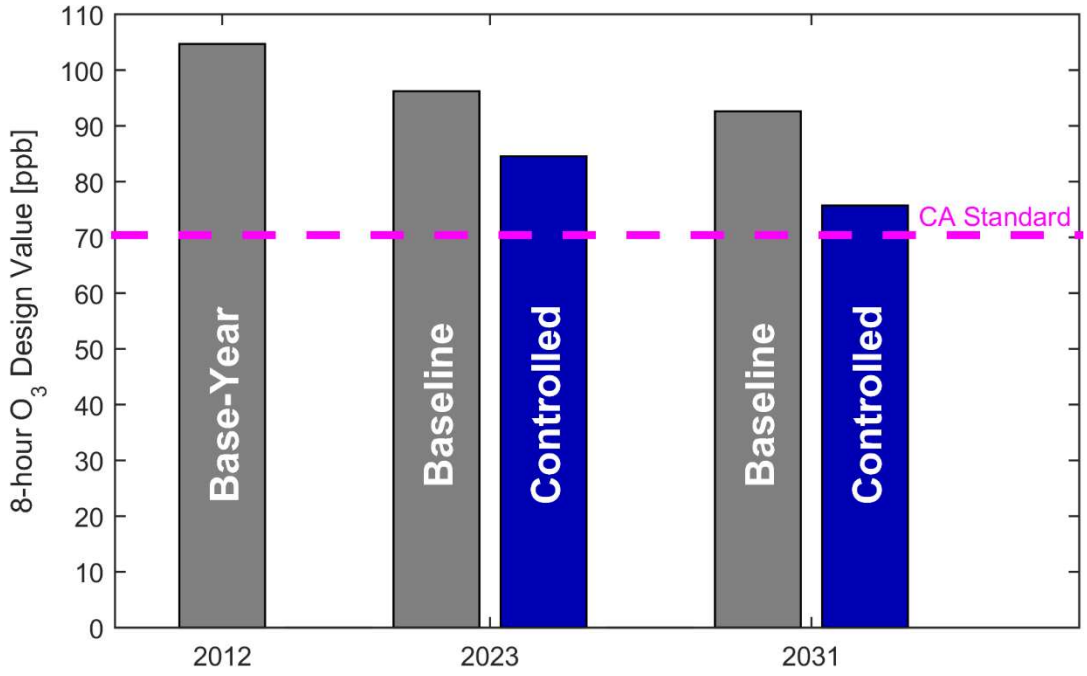

FIGURE V-9-2

Projection of future 8-hour ozone air quality in the Basin in comparison to California standards

TABLE V-9-1

Basin NOx Carrying Capacity for Ozone Attainment

Attainment Year	2022	2023	2031
Federal Standard	1-hr Ozone (120 ppb)	8-hr Ozone (80 ppb)	8-hr Ozone (75 ppb)
NOx Carrying Capacity (TPD)	245	141	96

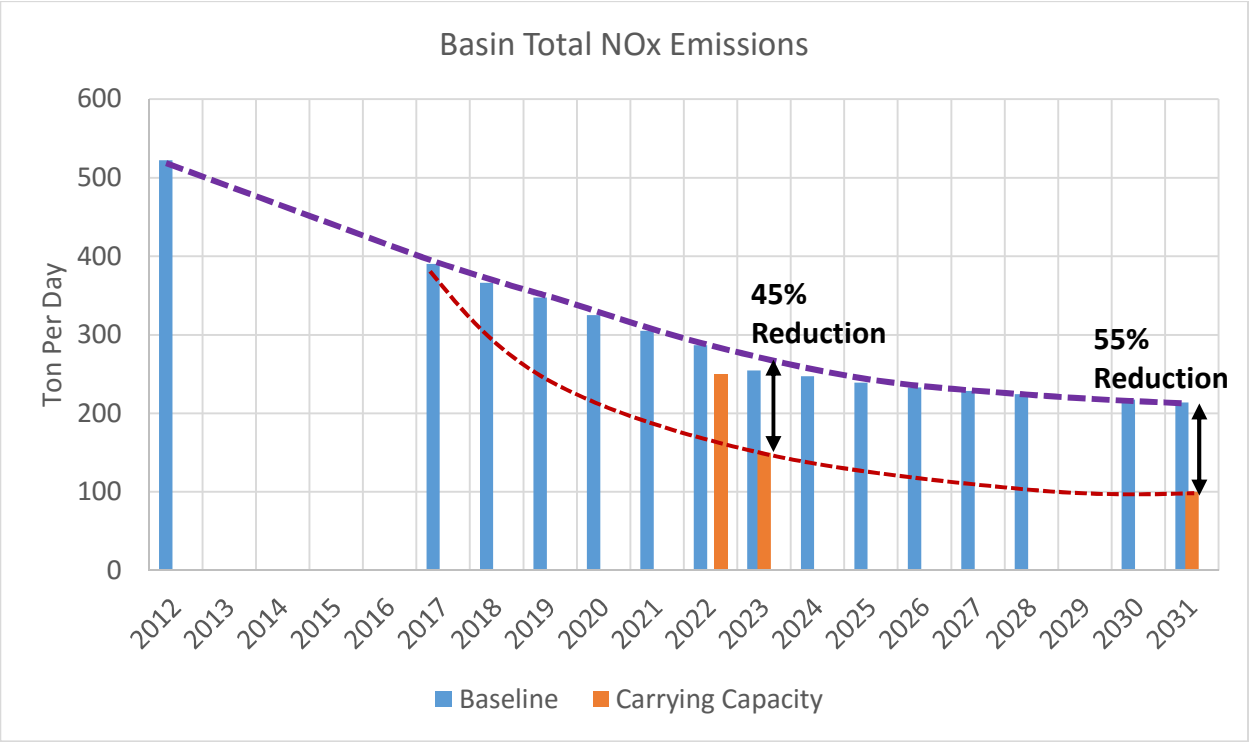

FIGURE V-9-3

Summer planning baseline emissions and ozone carrying capacity

Figure V-9-4 shows the 2012 observed base-year design value along with the 2021, 2023 and 2025 model-predicted future design values of annual PM2.5. The federal annual PM2.5 standards are predicted to be achieved in 2023 with implementation of the proposed ozone strategy. However, the federal CAA does not allow 182(e)(5) measures in the attainment demonstration of PM2.5; therefore, an additional scenario using only non-182(e)(5) measures was developed for 2025 to comply with the CAA requirements. With only the non-182(e)(5) measure reductions, the annual PM2.5 standard is expected to be met in 2025. The California annual PM2.5 standard will not be attained in 2021.

Table V-9-2 presents the future Basin annual PM2.5 design values under each control scenario. Table V-9-2 also contains the predicted 2025 design value resulting from the ozone control strategy in the absence of 182(e)(5) measures. Attainment is achieved in 2025 under this scenario.

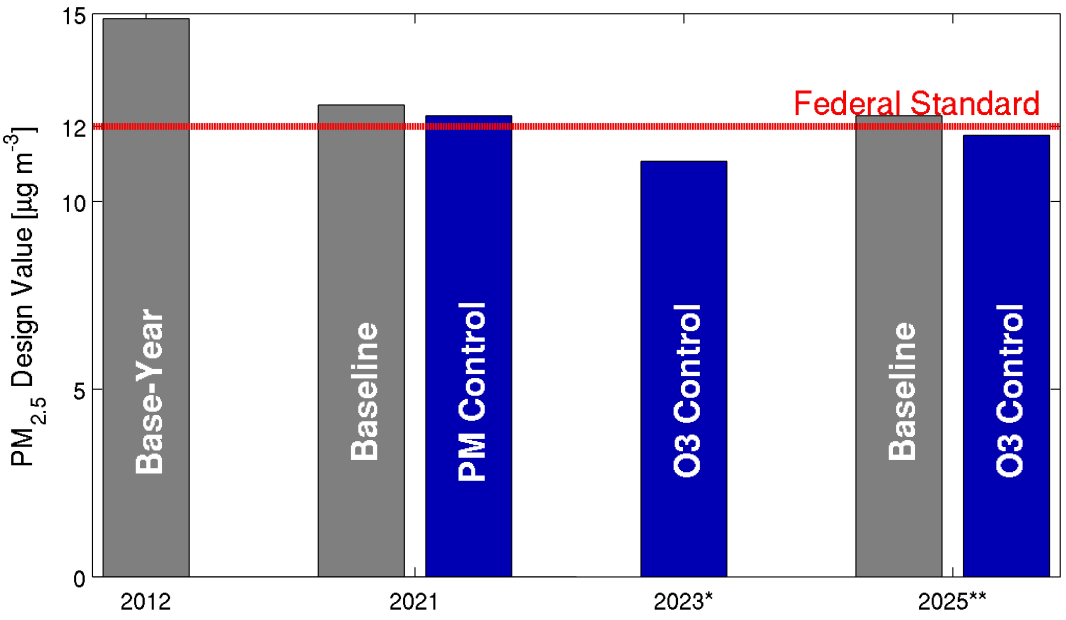

FIGURE V-9-4

Projection of future annual PM2.5 air quality in the Basin in comparison with Federal Standards

*INCLUDES 182(E)(5) MEASURES
**DOES NOT INCLUDE 182(E)(5) MEASURES

TABLE V-9-2

Future Design Values of Annual Average PM2.5 at Mira Loma in µg/m^3

Station	Baseline	Controlled	Control Strategy
2021	12.6	12.3	Directly emitted PM reduction
2023	12.1	11.1	Ozone co-benefit including 182(e)(5) measures
2025	12.3	11.8	Ozone co-benefit without 182(e)(5) measures

The 24-hour PM2.5 standard is expected to attain in 2019 without emission reductions beyond already adopted controls and measures. The 2019 baseline design value was predicted to be 31.4 µg/m^3 at Mira Loma.

Attachment 1

WRF MODEL PERFORMANCE TIME SERIES

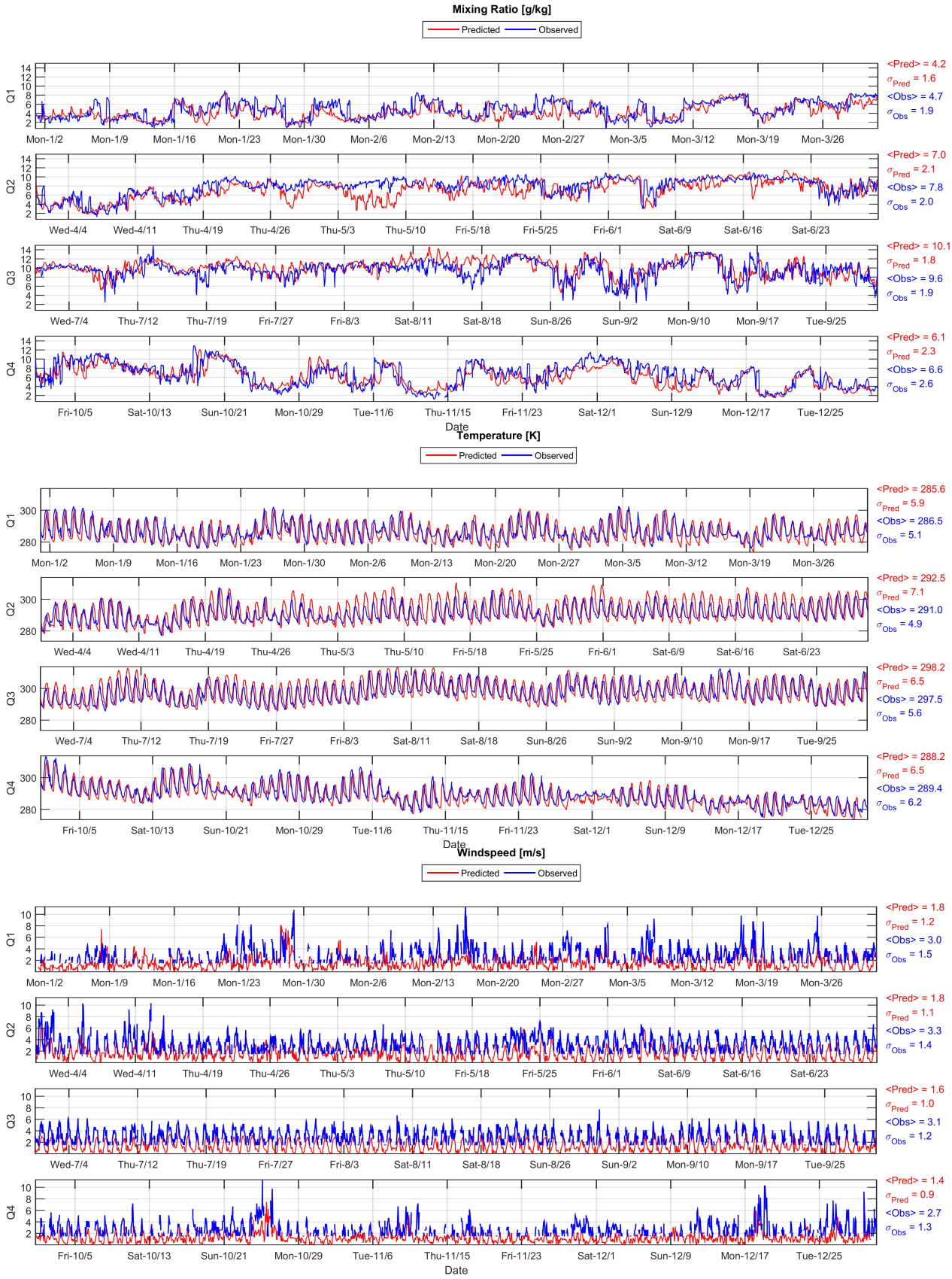

Figure 1: Time Series of Measured and WRF Simulated Mixing Ratio (Top), Temperature (Middle), and Wind Speed (Bottom) for the Period of Jan 1 to Dec 31, 2012 at Burbank International Airport

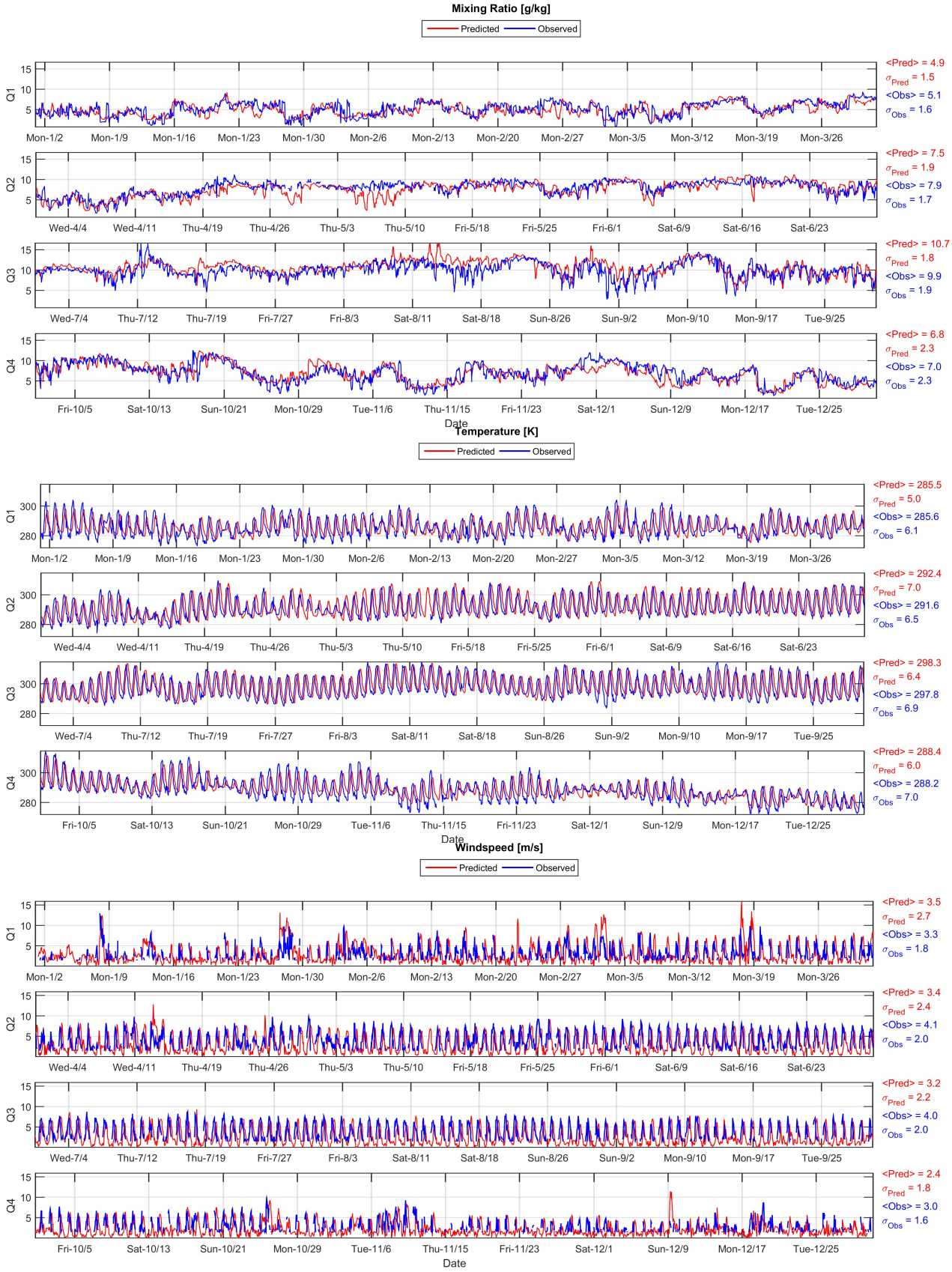

Figure 2: Time Series of Measured and WRF Simulated Mixing Ratio (Top), Temperature (Middle), and Wind Speed (Bottom) for the Period of Jan 1 to Dec 31, 2012 at Chino Airport

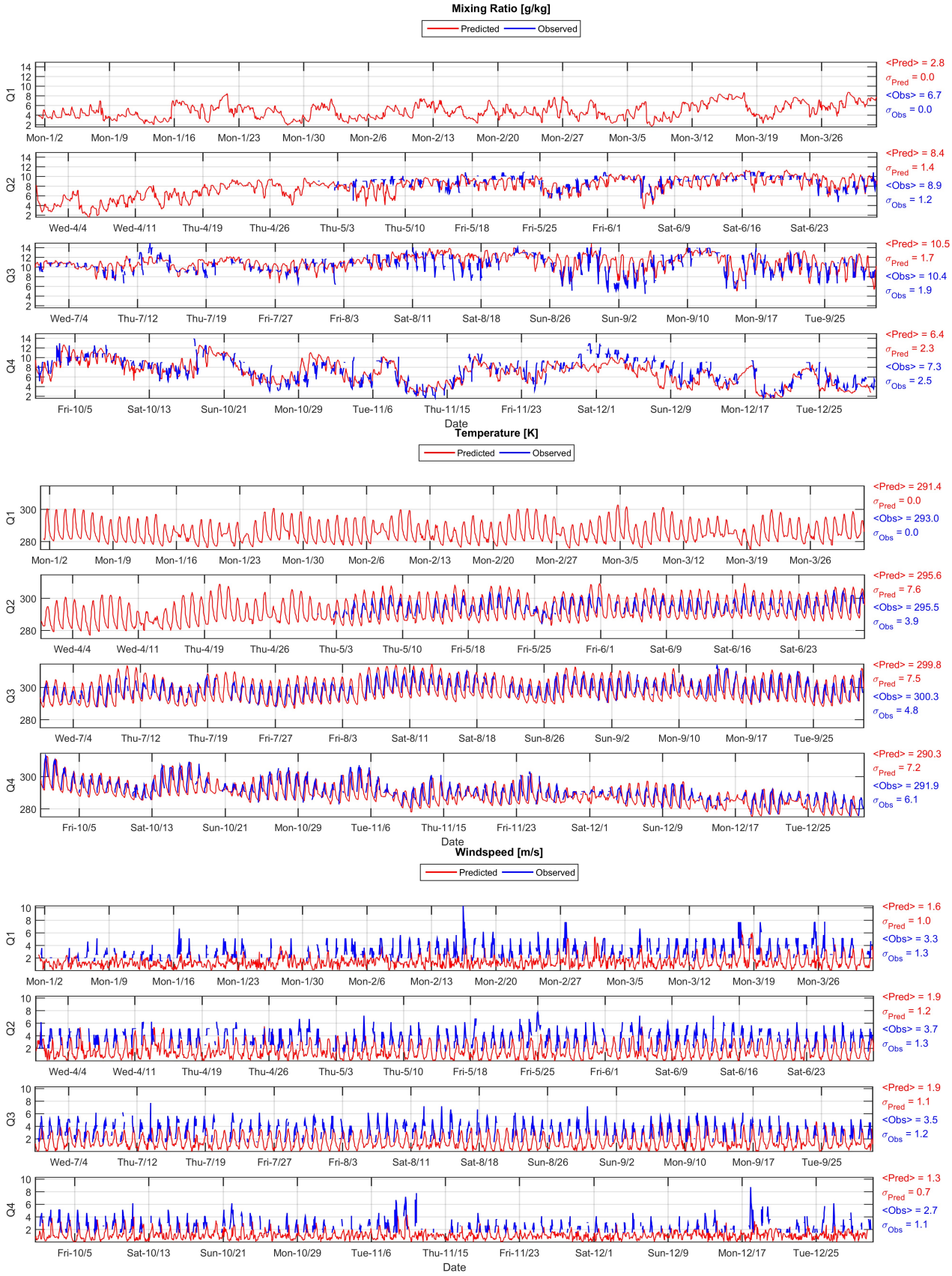

Figure 3: Time Series of Measured and WRF Simulated Mixing Ratio (Top), Temperature (Middle), and Wind Speed (Bottom) for the Period of Jan 1 to Dec 31, 2012 at El Monte Airport

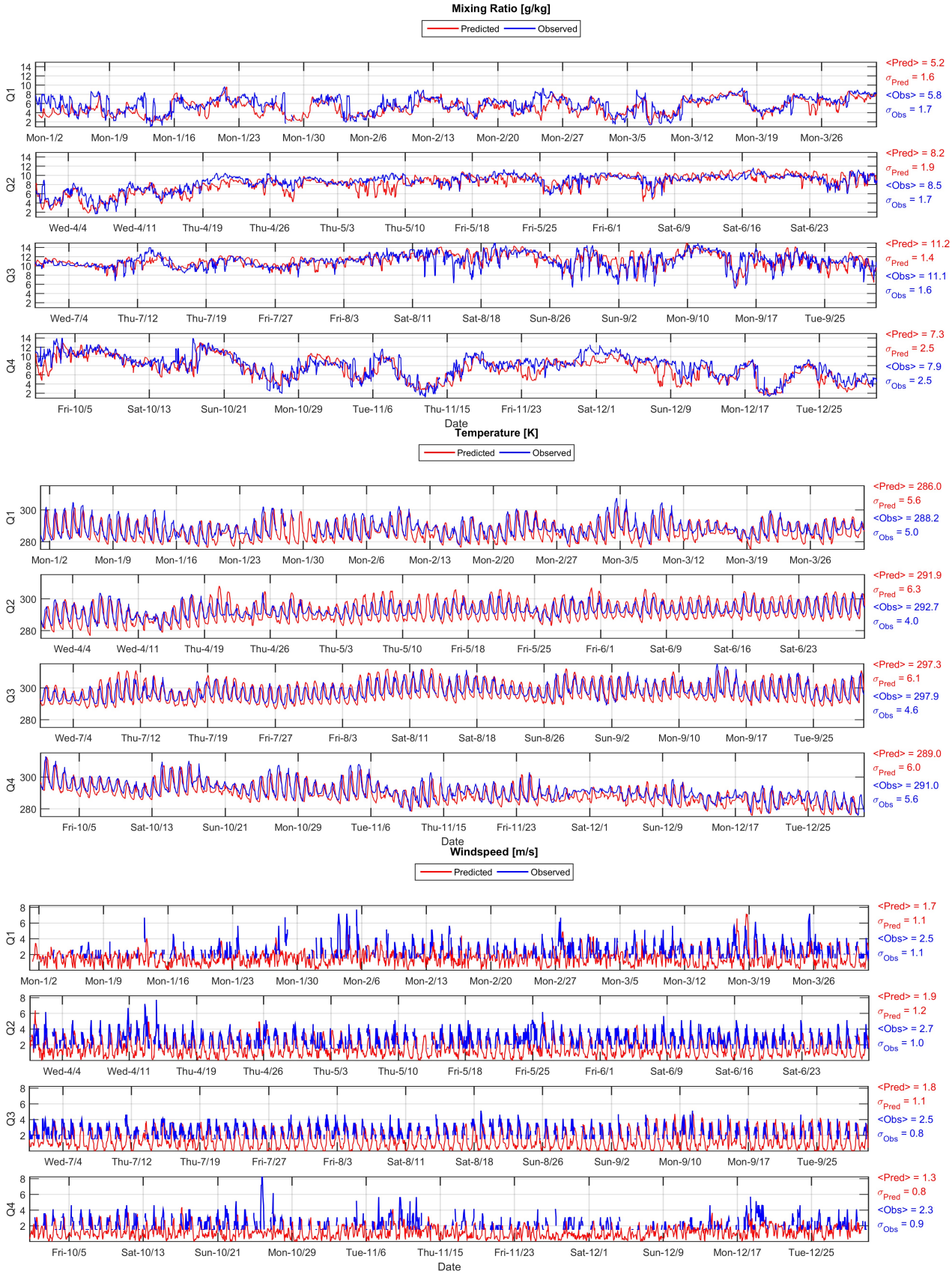

Figure 4: Time Series of Measured and WRF Simulated Mixing Ratio (Top), Temperature (Middle), and Wind Speed (Bottom) for the Period of Jan 1 to Dec 31, 2012 at Fullerton Municipal Airport

Figure 5: Time Series of Measured and WRF Simulated Mixing Ratio (Top), Temperature (Middle), and Wind Speed (Bottom) for the Period of Jan 1 to Dec 31, 2012 at Hawthorne Airport

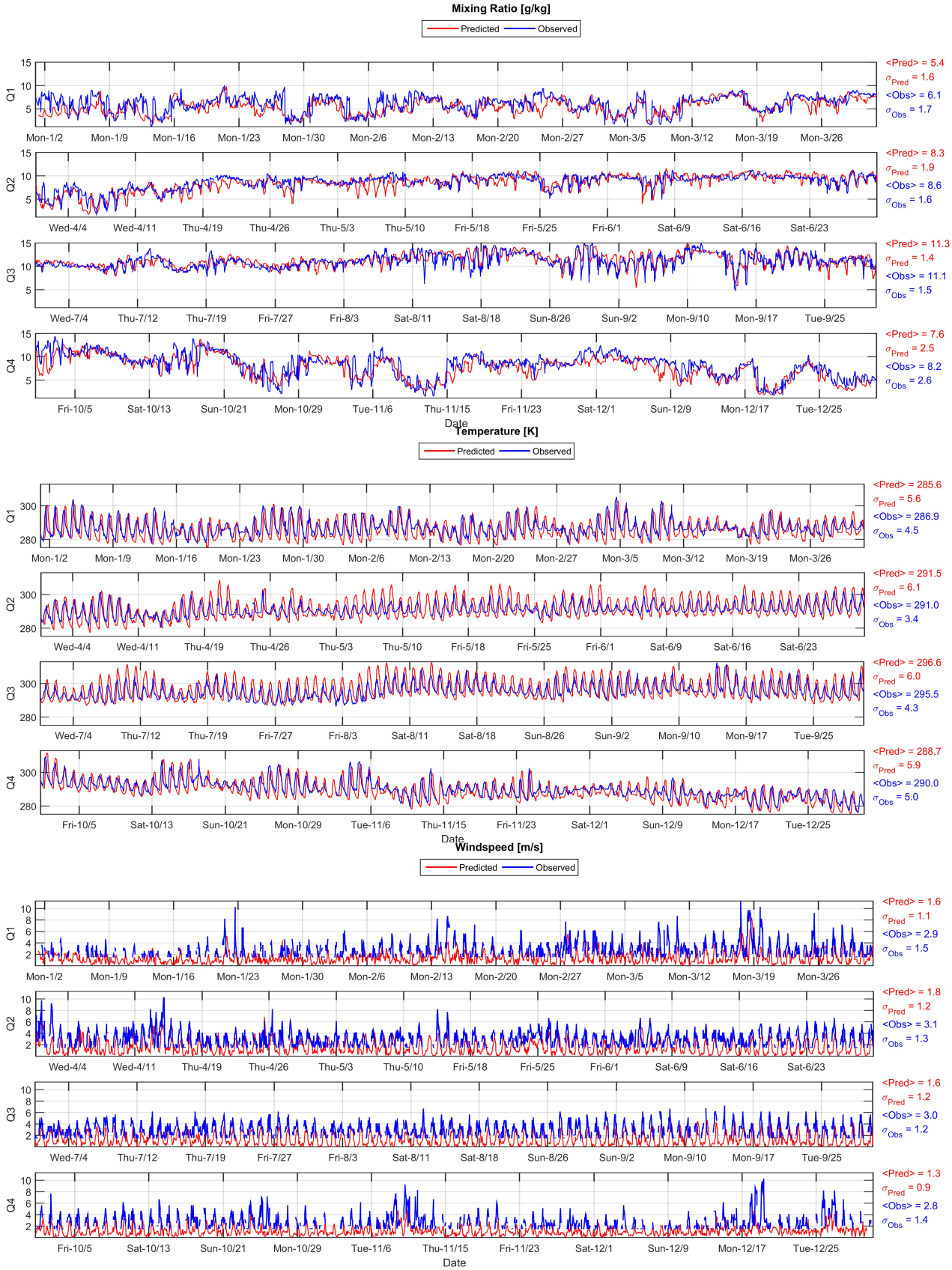

Figure 6: Time Series of Measured and WRF Simulated Mixing Ratio (Top), Temperature (Middle), and Wind Speed (Bottom) for the Period of Jan 1 to Dec 31, 2012 at Long Beach Airport

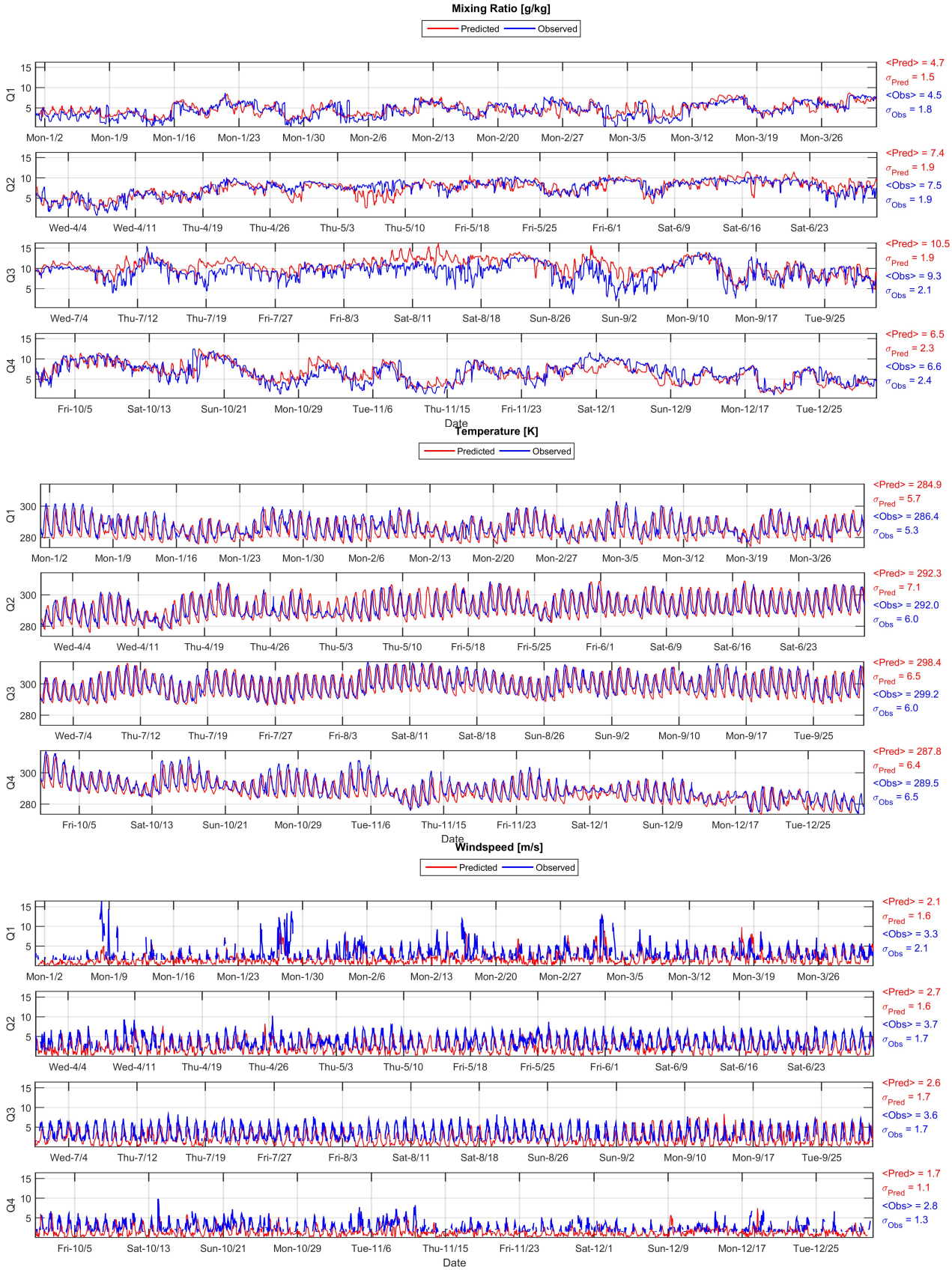

Figure 7: Time Series of Measured and WRF Simulated Mixing Ratio (Top), Temperature (Middle), and Wind Speed (Bottom) for the Period of Jan 1 to Dec 31, 2012 at Ontario International Airport

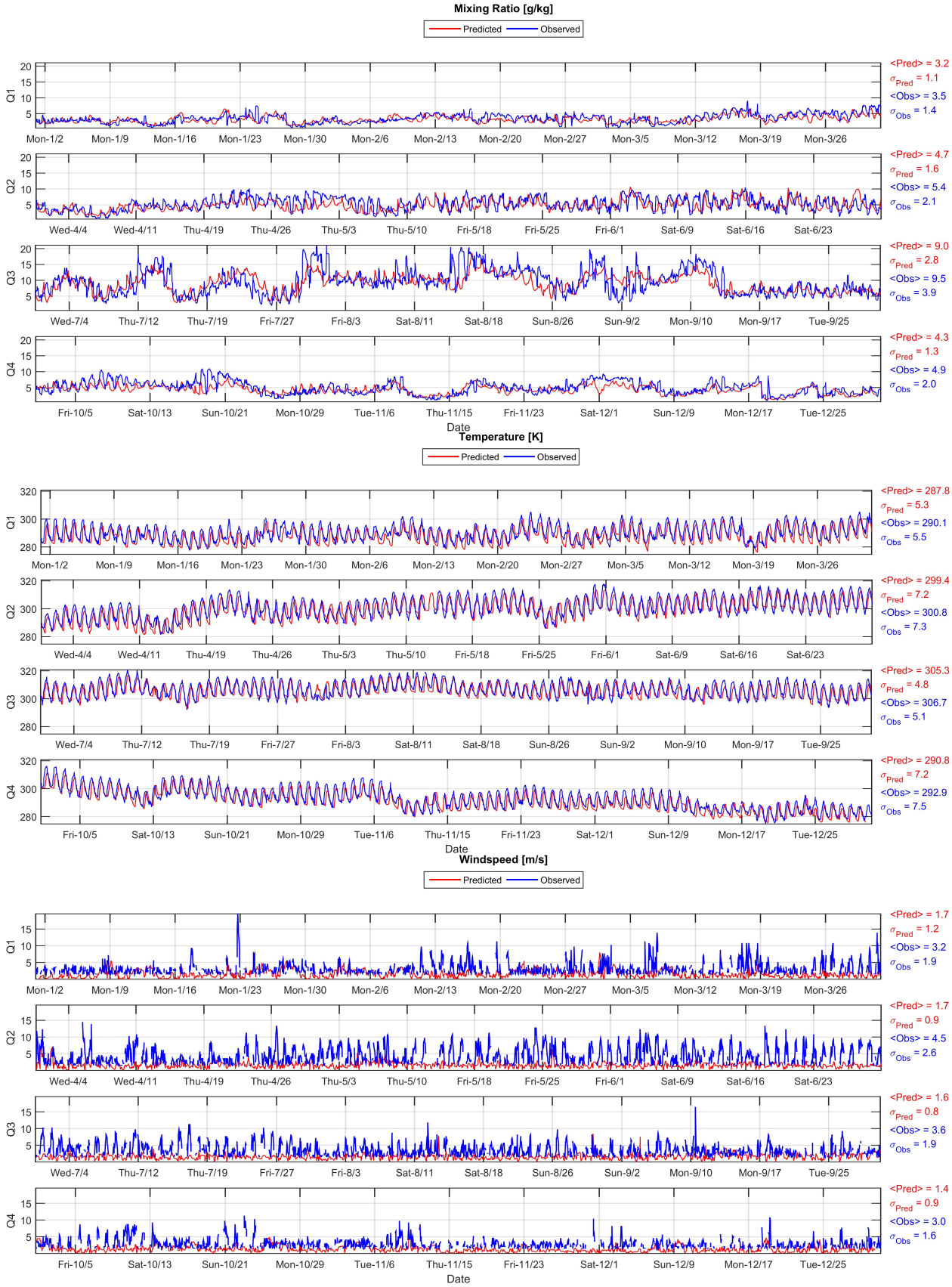

Figure 8: Time Series of Measured and WRF Simulated Mixing Ratio (Top), Temperature (Middle), and Wind Speed (Bottom) for the Period of Jan 1 to Dec 31, 2012 at Palm Springs International Airport

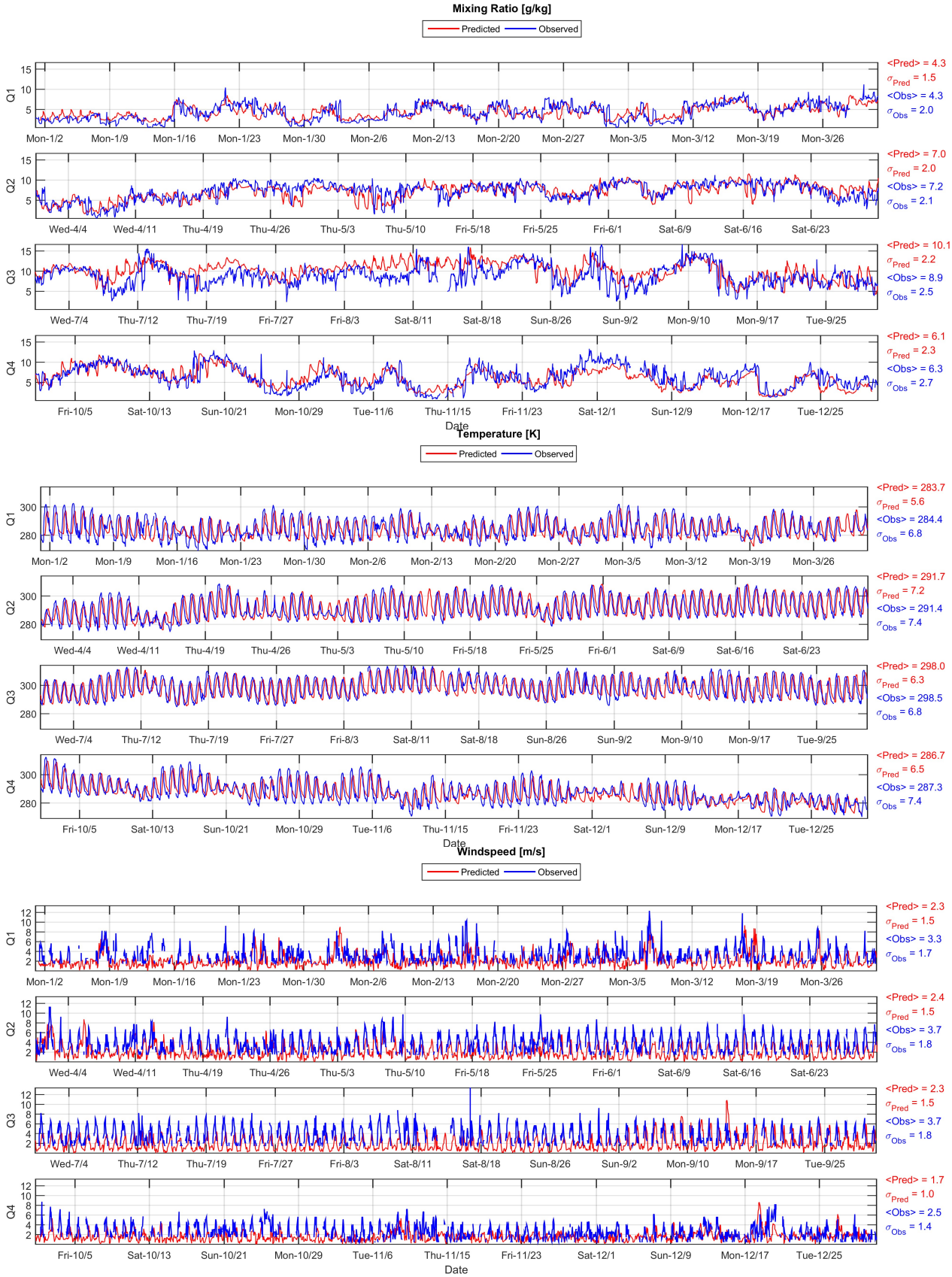

Figure 9: Time Series of Measured and WRF Simulated Mixing Ratio (Top), Temperature (Middle), and Wind Speed (Bottom) for the Period of Jan 1 to Dec 31, 2012 at Riverside Municipal Airport

Figure 10: Time Series of Measured and WRF Simulated Mixing Ratio (Top), Temperature (Middle), and Wind Speed (Bottom) for the Period of Jan 1 to Dec 31, 2012 at San Bernardino International Airport

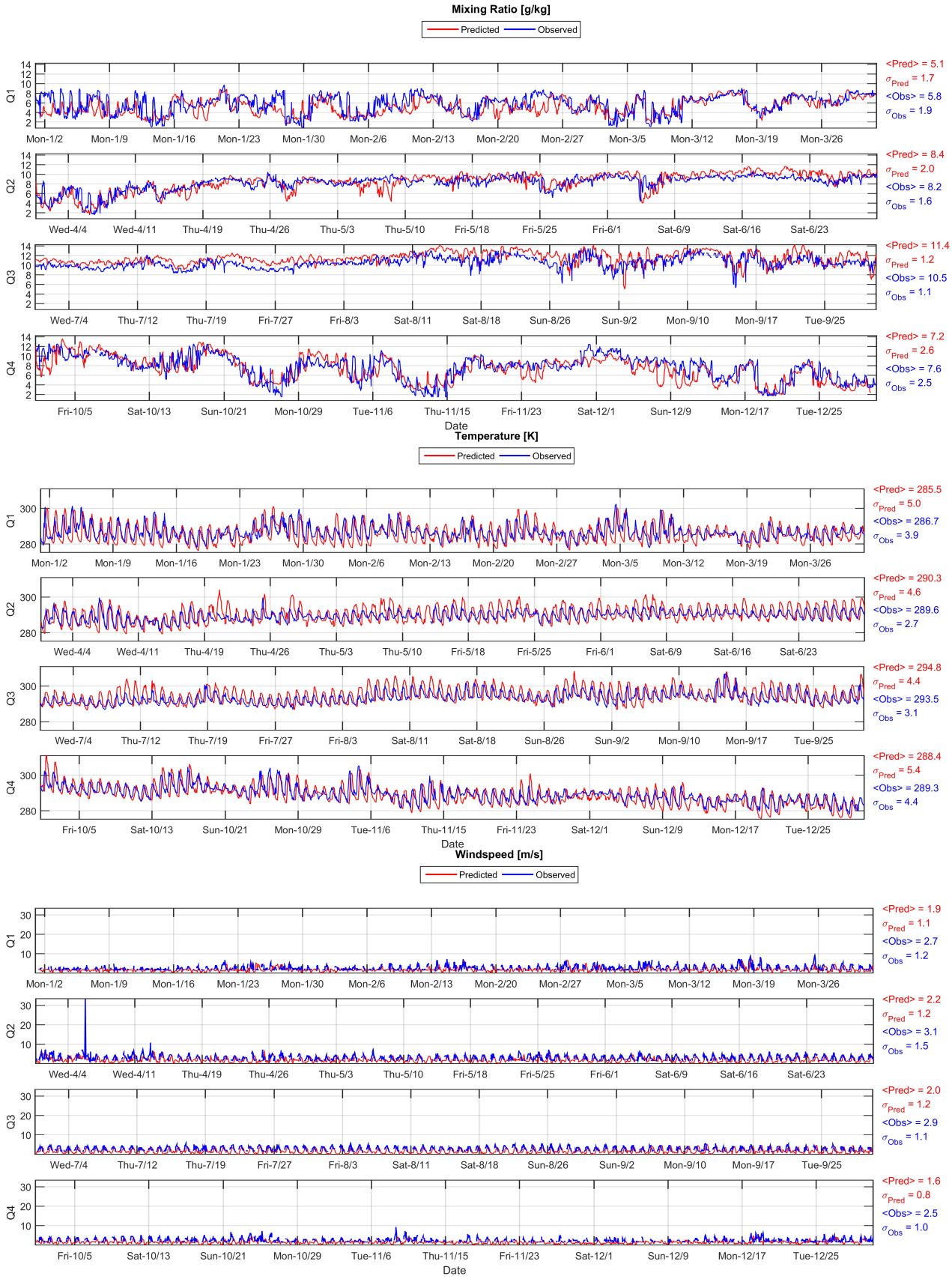

Figure 11: Time Series of Measured and WRF Simulated Mixing Ratio (Top), Temperature (Middle), and Wind Speed (Bottom) for the Period of Jan 1 to Dec 31, 2012 at Santa Monica Airport

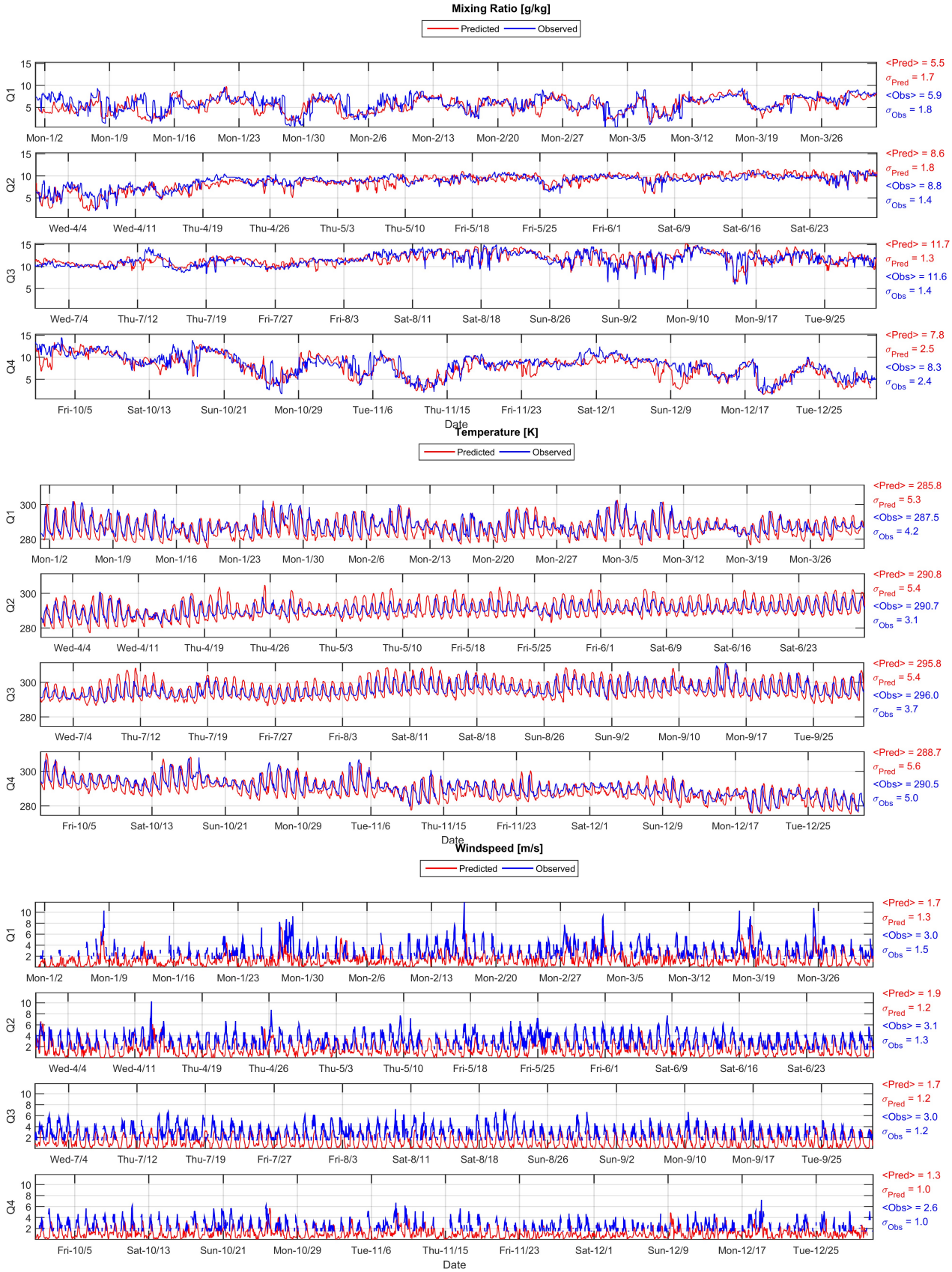

Figure 12: Time Series of Measured and WRF Simulated Mixing Ratio (Top), Temperature (Middle), and Wind Speed (Bottom) for the Period of Jan 1 to Dec 31, 2012 at John Wayne-Orange County Airport

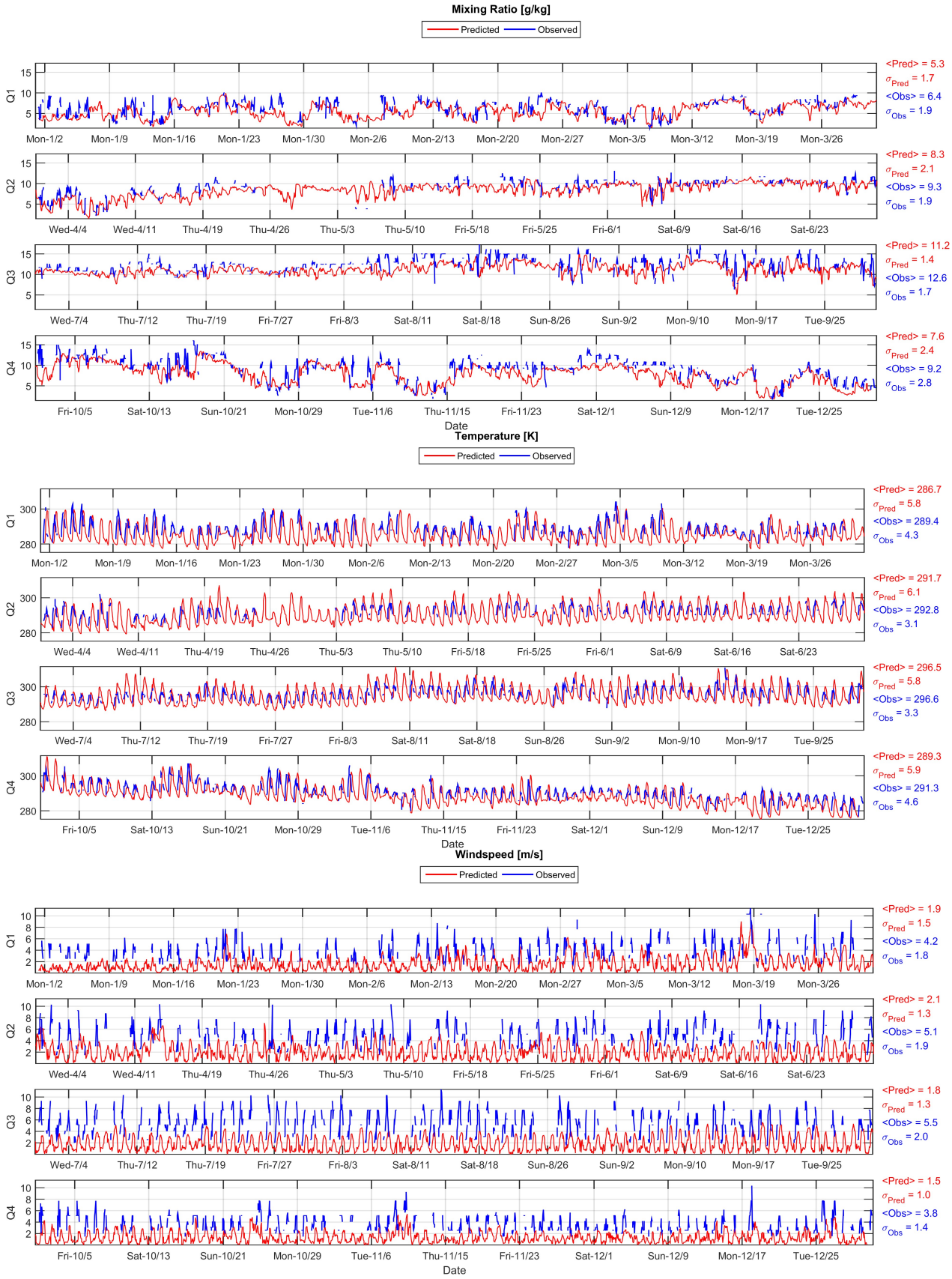

Figure 13: Time Series of Measured and WRF Simulated Mixing Ratio (Top), Temperature (Middle), and Wind Speed (Bottom) for the Period of Jan 1 to Dec 31, 2012 at Torrance Airport

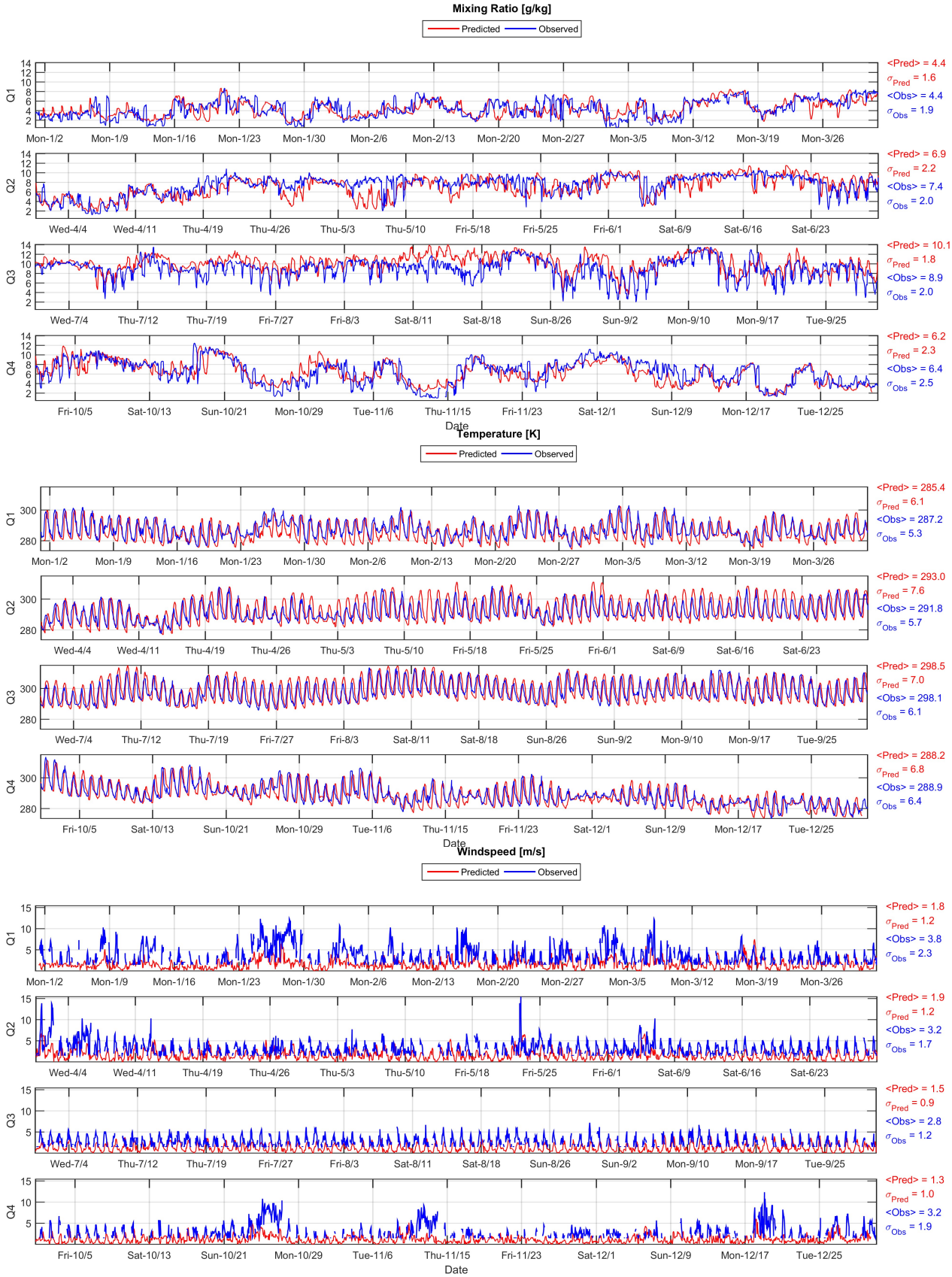

Figure 14: Time Series of Measured and WRF Simulated Mixing Ratio (Top), Temperature (Middle), and Wind Speed (Bottom) for the Period of Jan 1 to Dec 31, 2012 at Van Nuys Airport

Attachment 2

CMAQ MODEL PERFORMANCE TIME SERIES

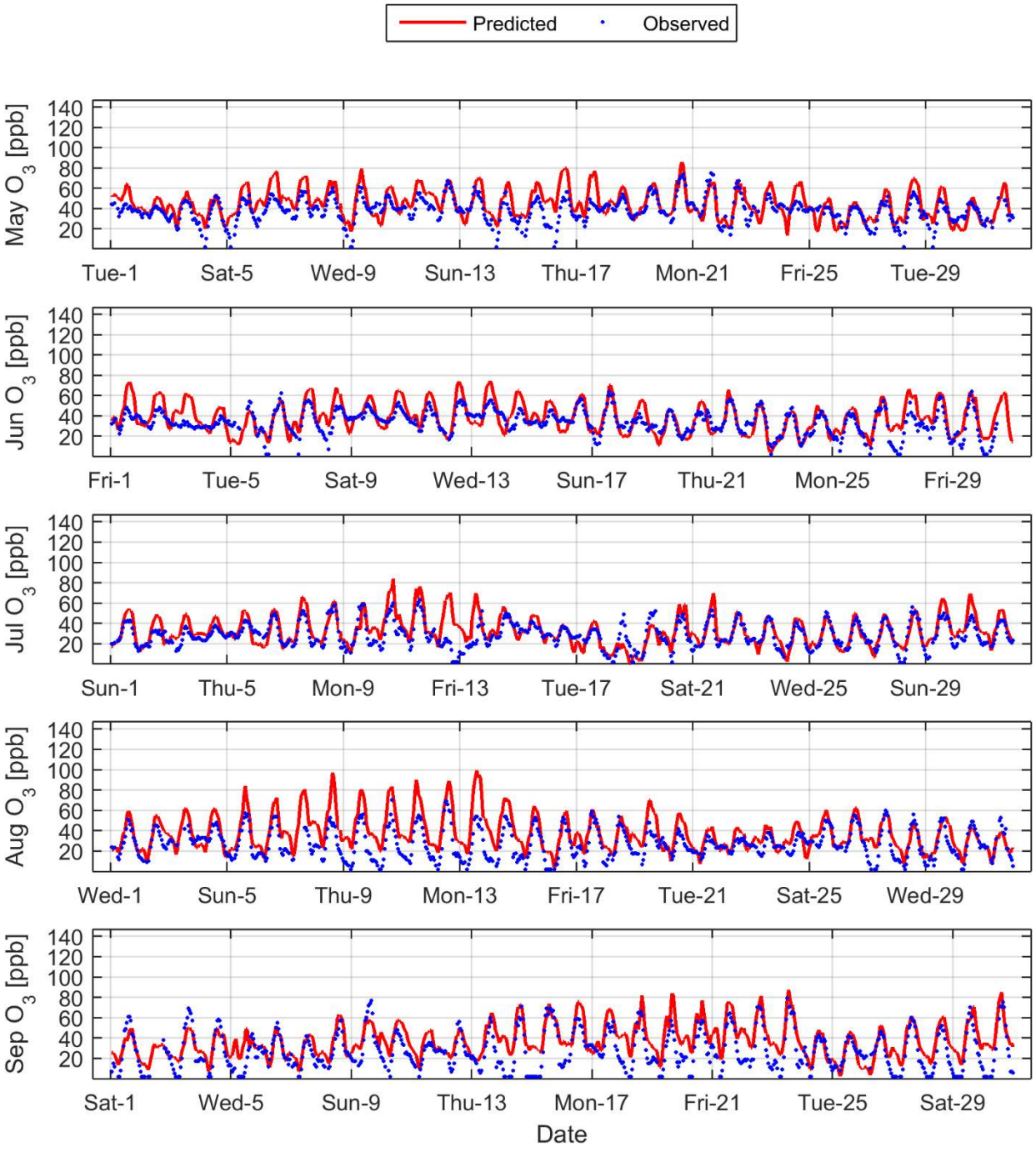

Figure 1: 2012 1-hour Ozone model prediction and measurement comparison at Anaheim

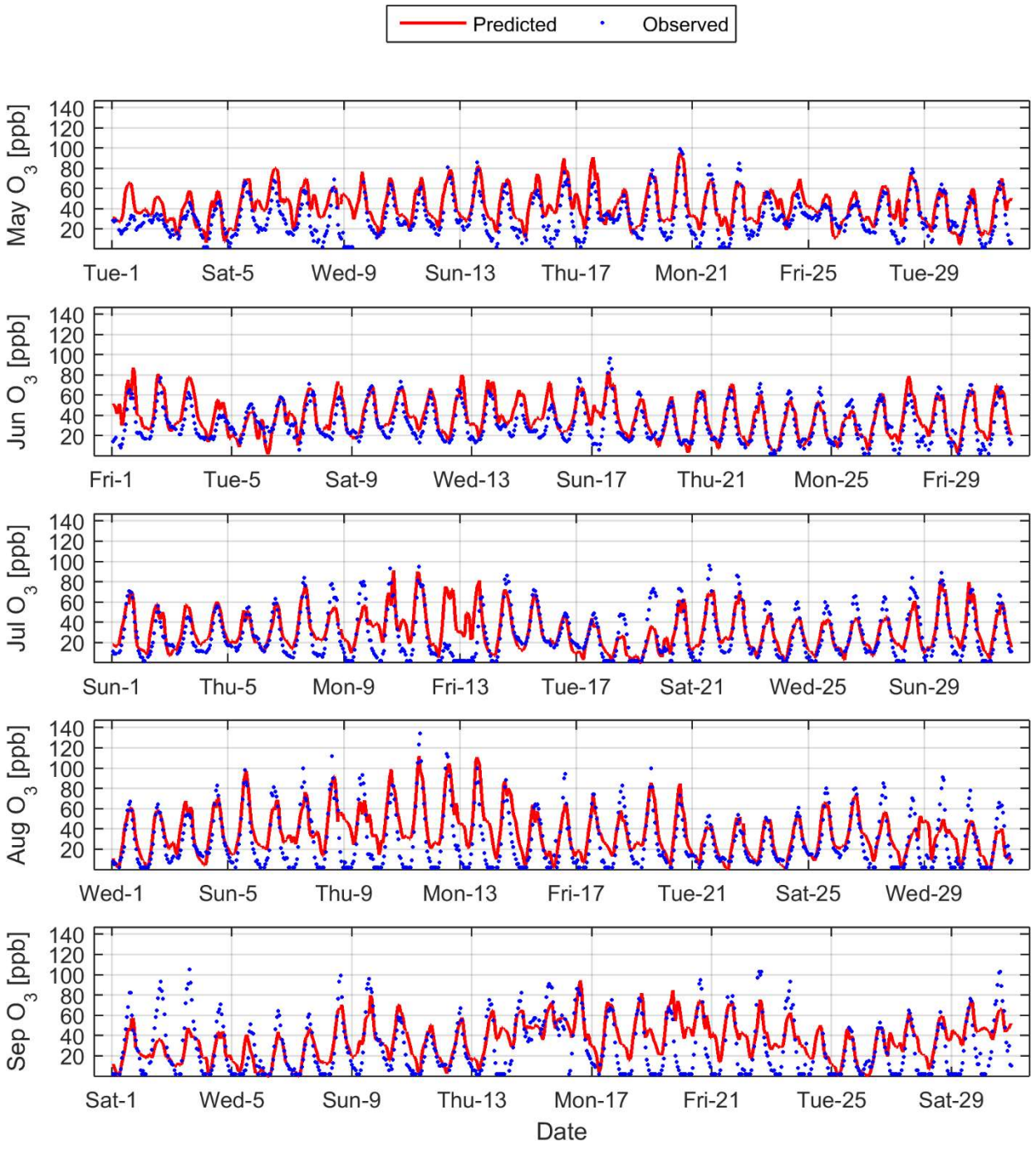

Figure 2: 2012 1-hour Ozone model prediction and measurement comparison at Azusa

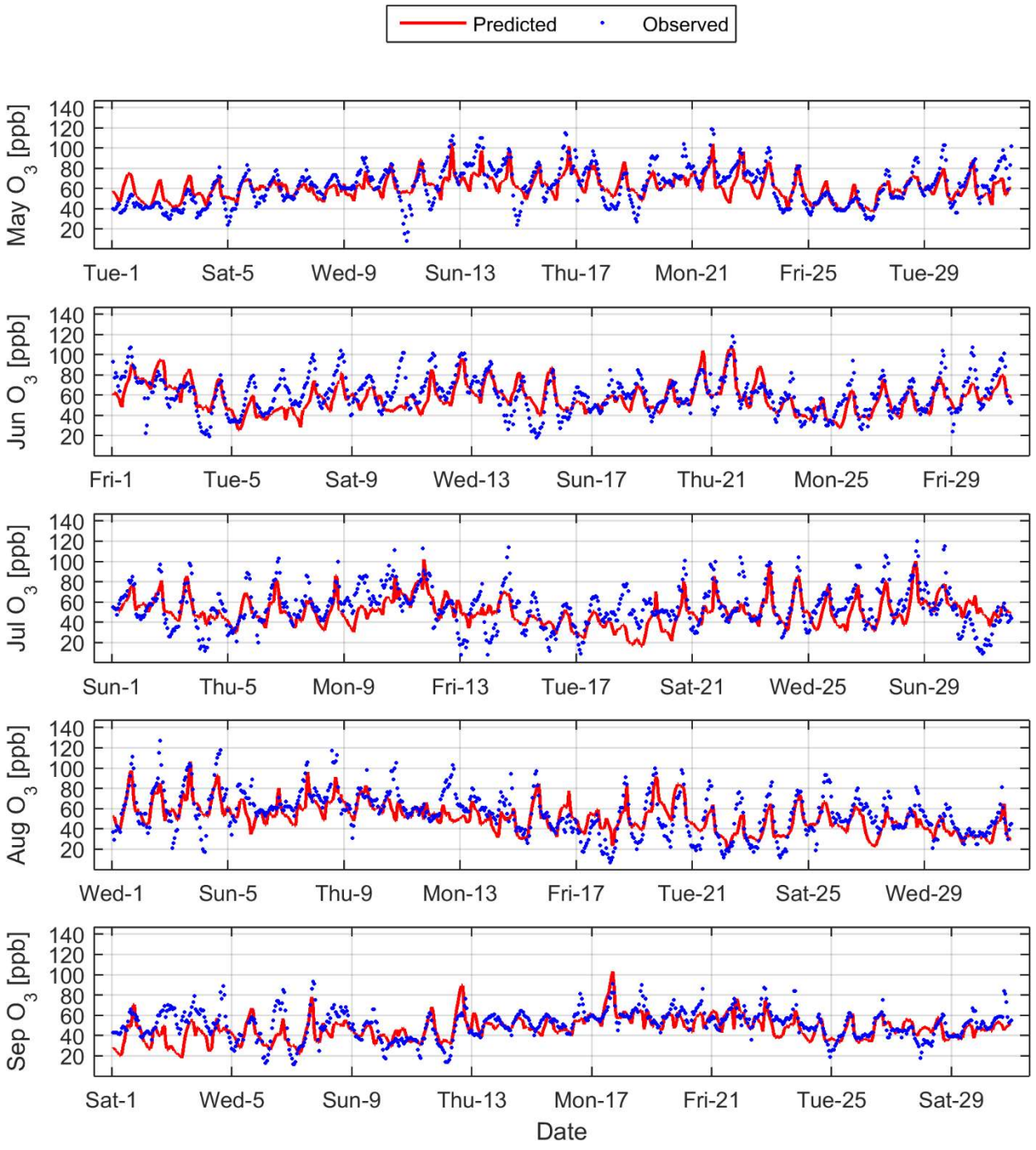

Figure 3: 2012 1-hour Ozone model prediction and measurement comparison at Banning

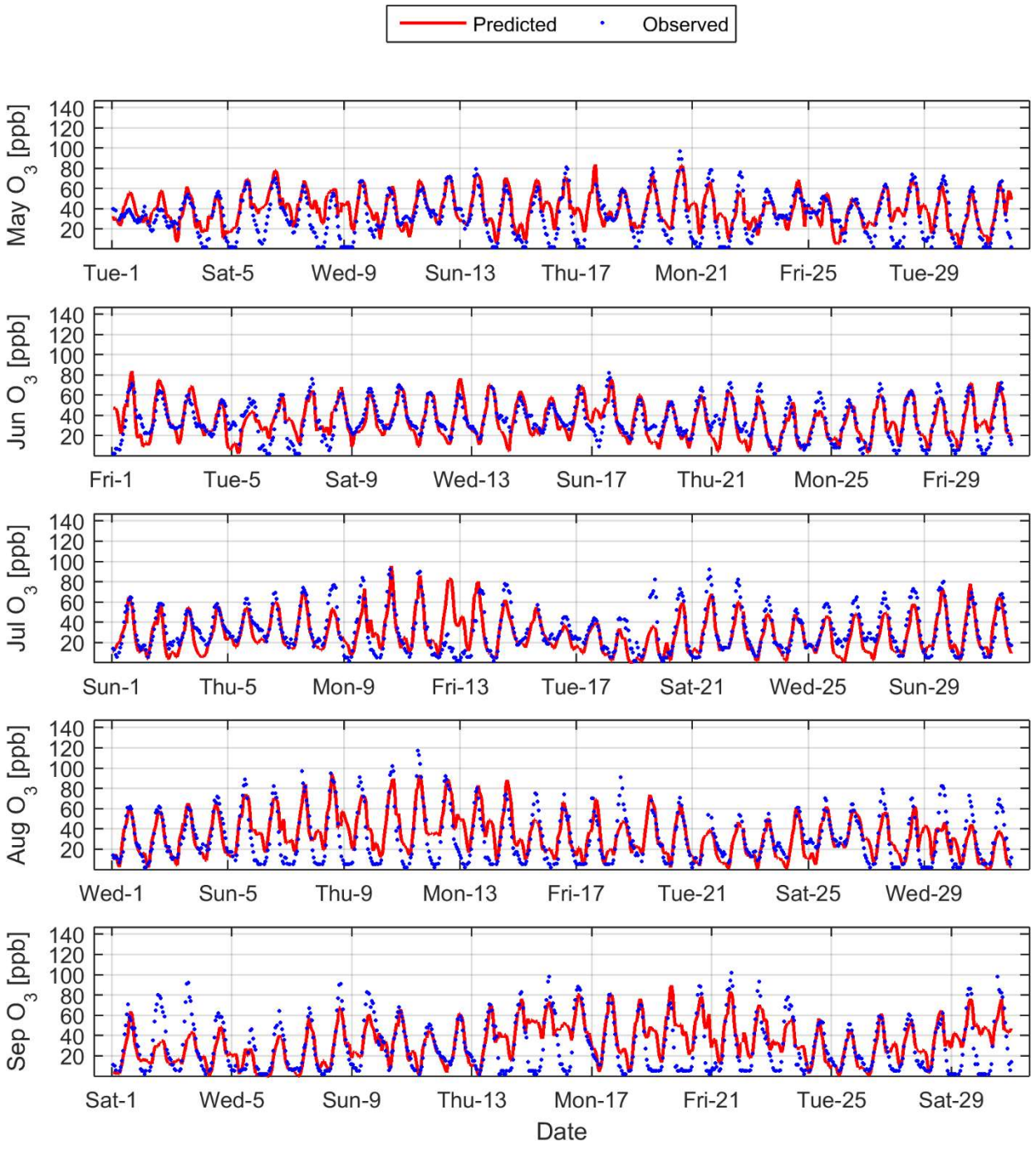

Figure 4: 2012 1-hour Ozone model prediction and measurement comparison at Burbank

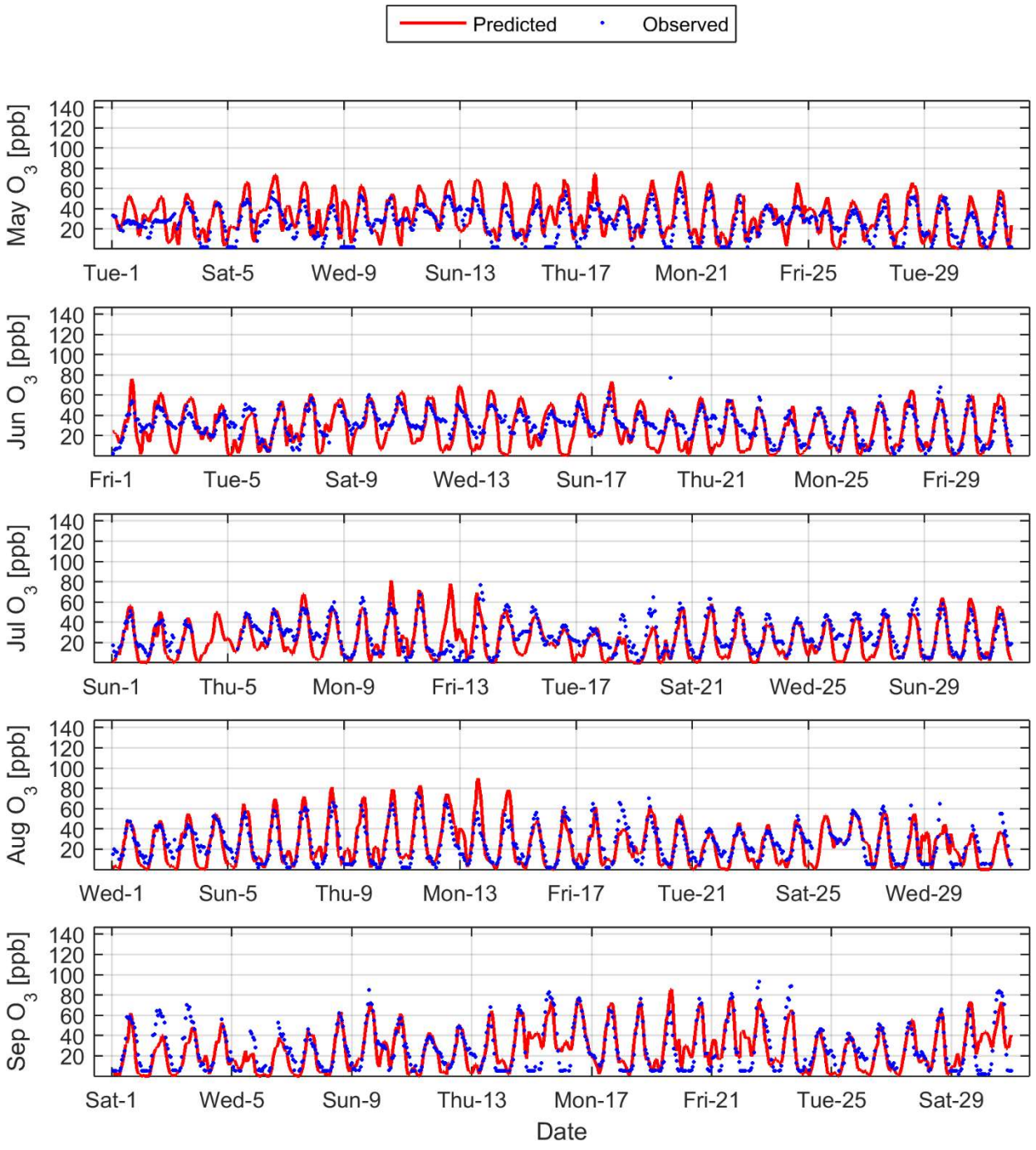

Figure 5: 2012 1-hour Ozone model prediction and measurement comparison at Central Los Angeles

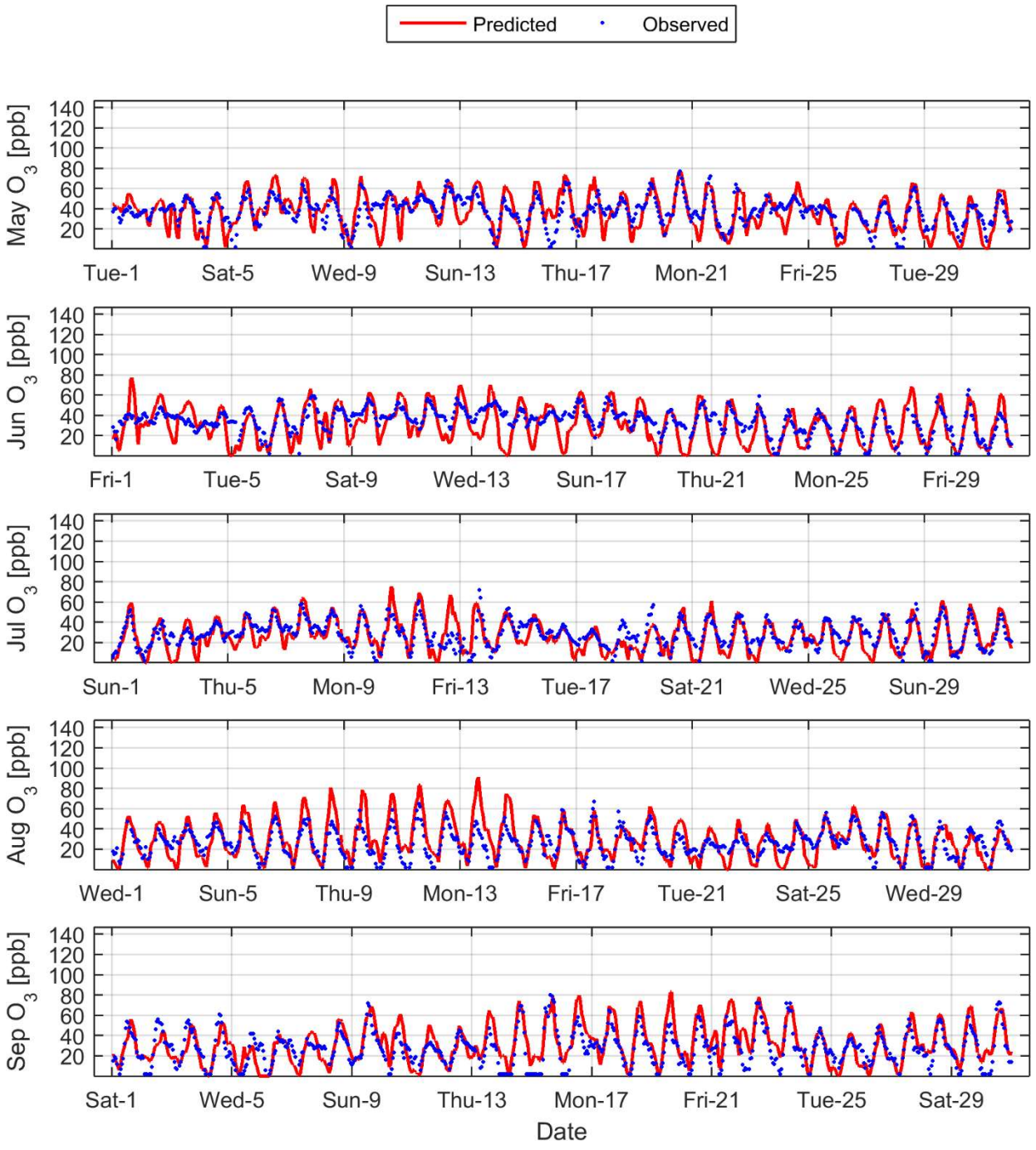

Figure 6: 2012 1-hour Ozone model prediction and measurement comparison at Compton

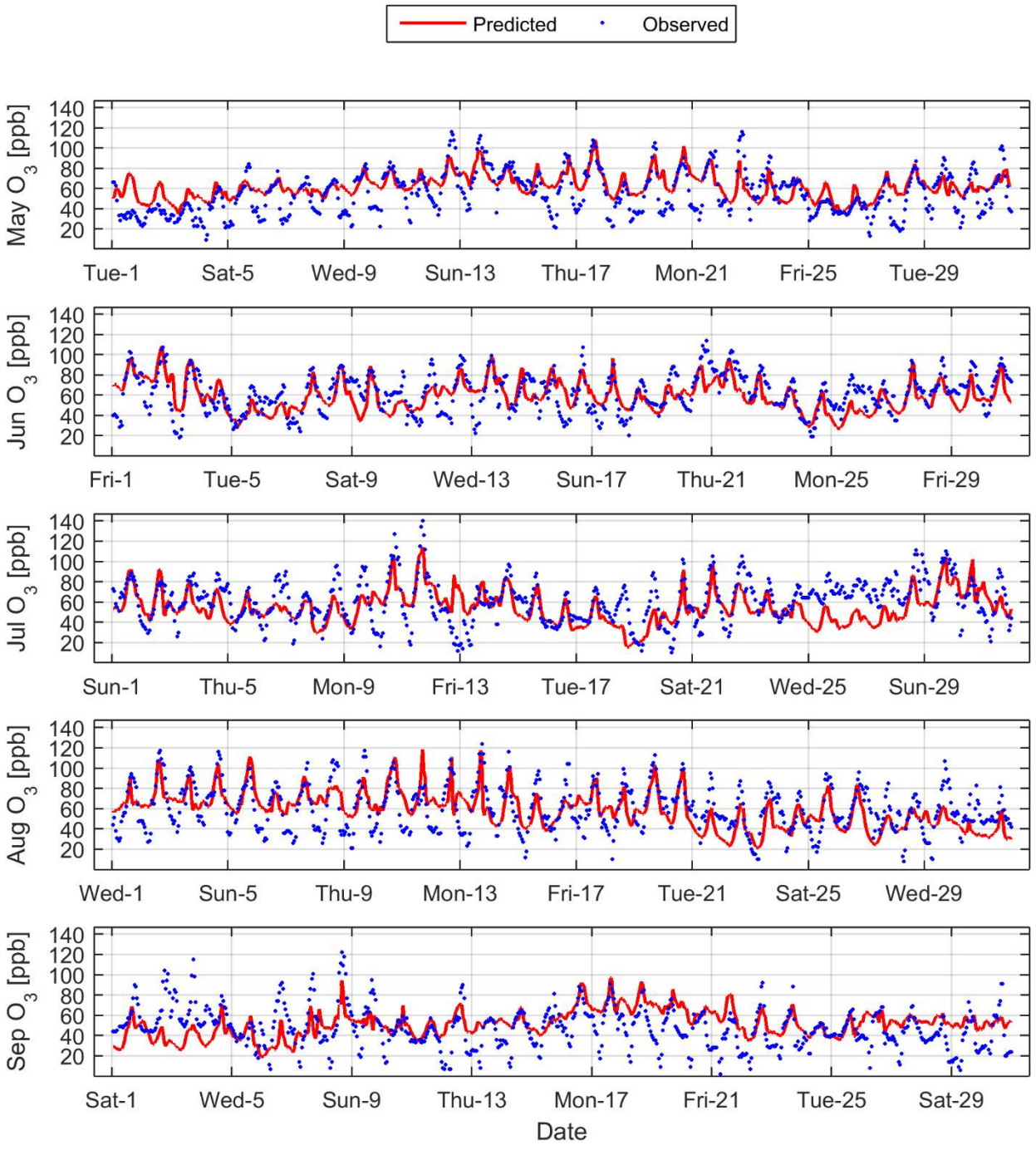

Figure 7: 2012 1-hour Ozone model prediction and measurement comparison at Crestline

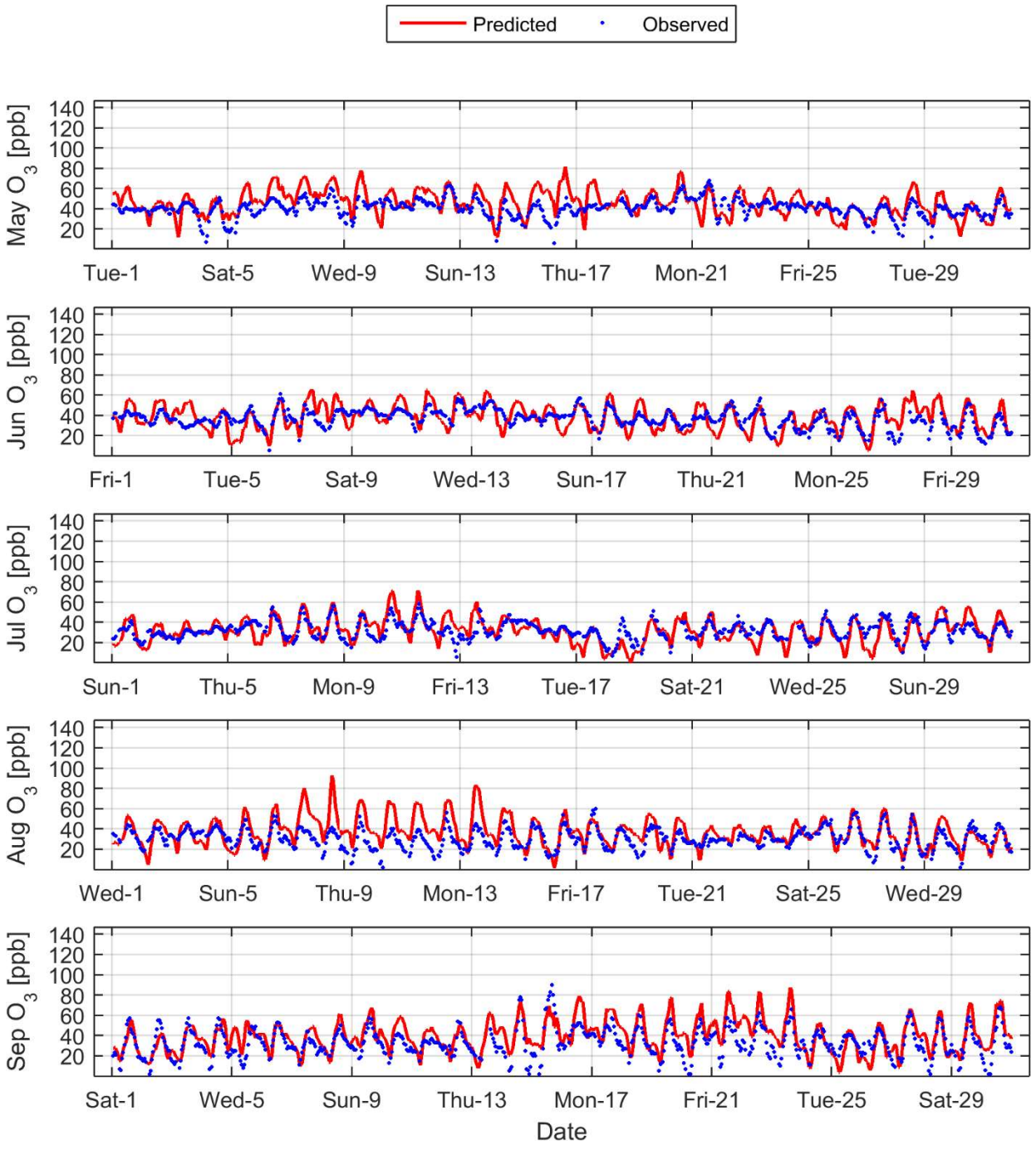

Figure 8: 2012 1-hour Ozone model prediction and measurement comparison at Costa Mesa

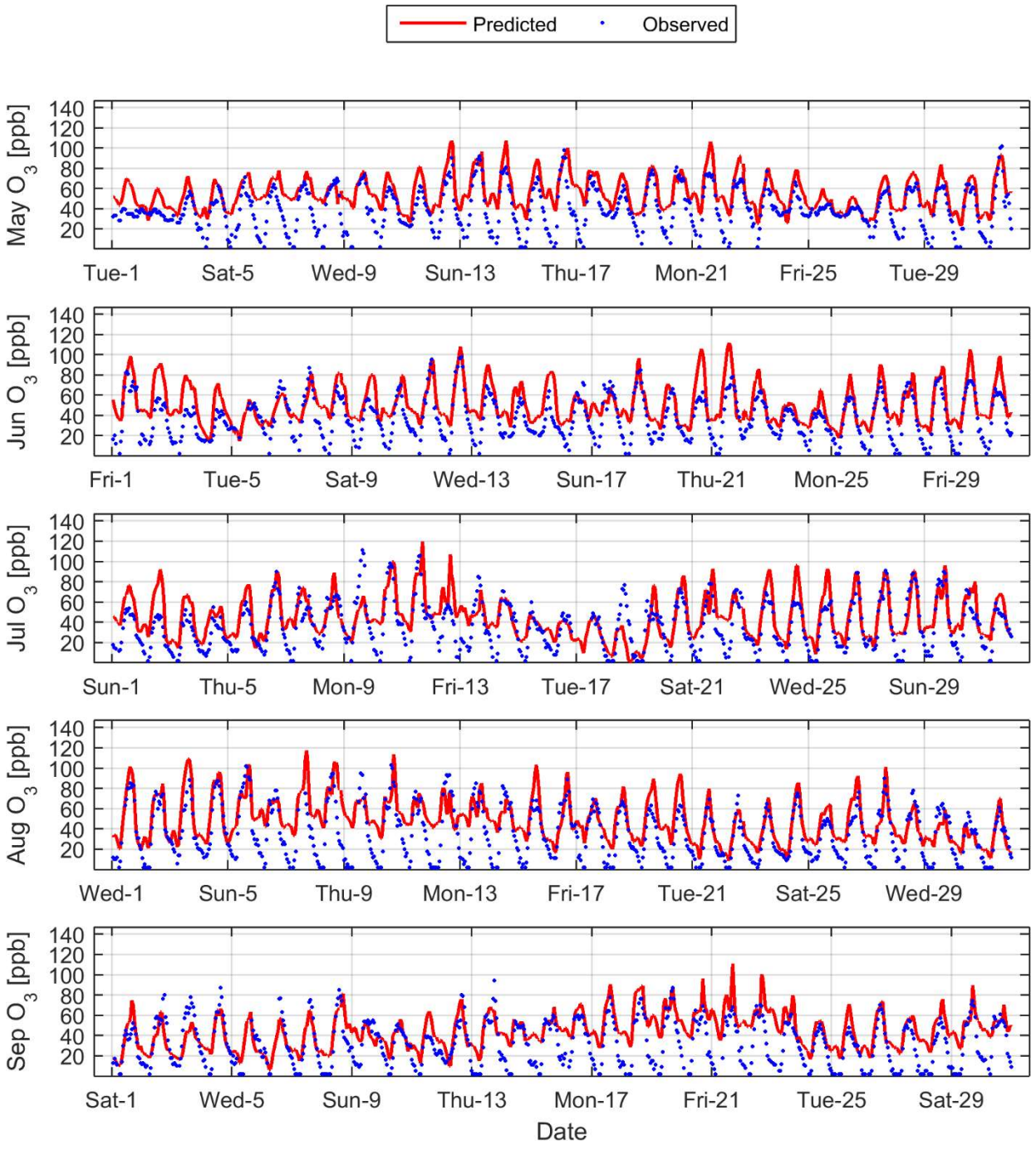

Figure 9: 2012 1-hour Ozone model prediction and measurement comparison at Lake Elsinore

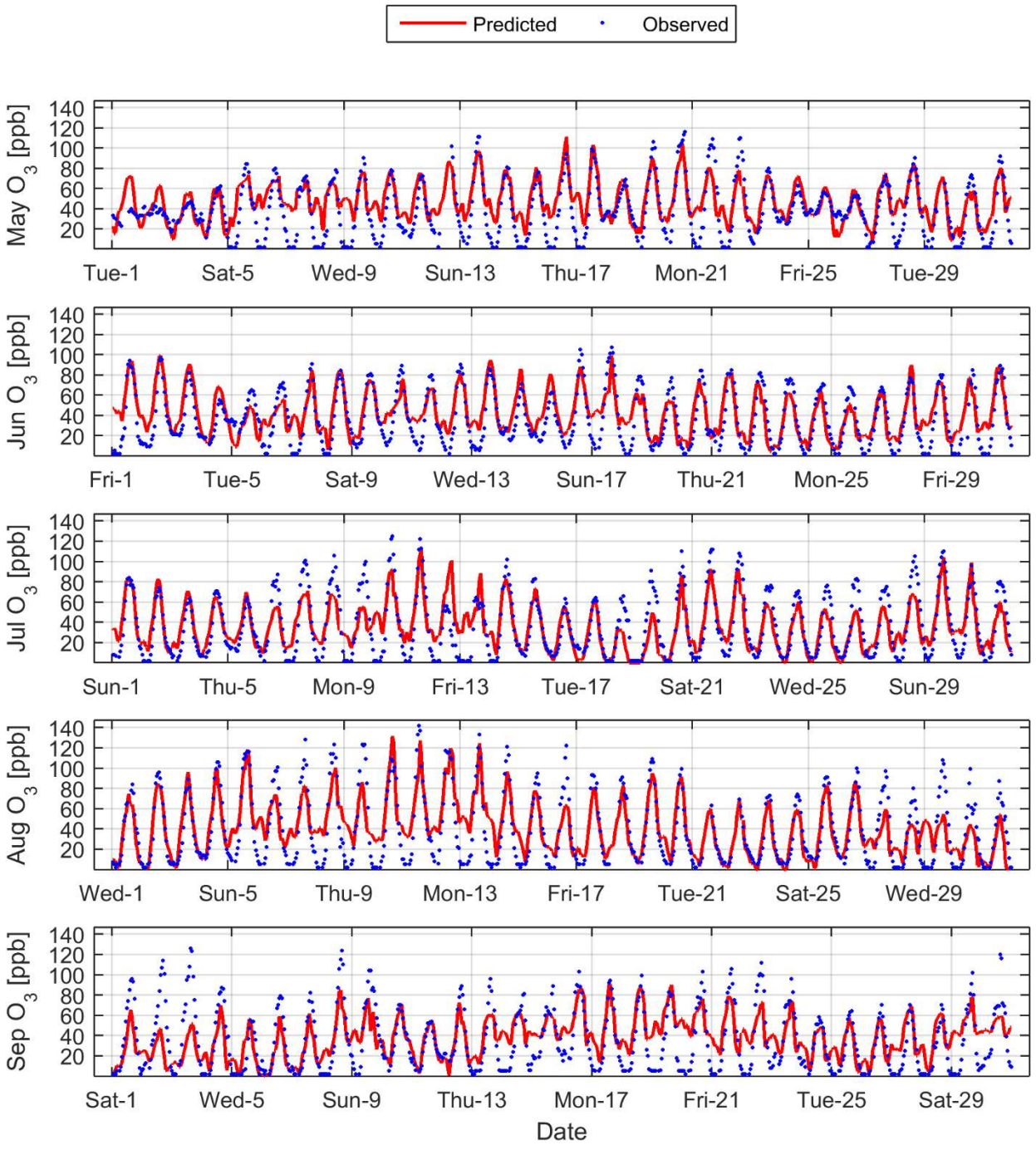

Figure 10: 2012 1-hour Ozone model prediction and measurement comparison at Fontana

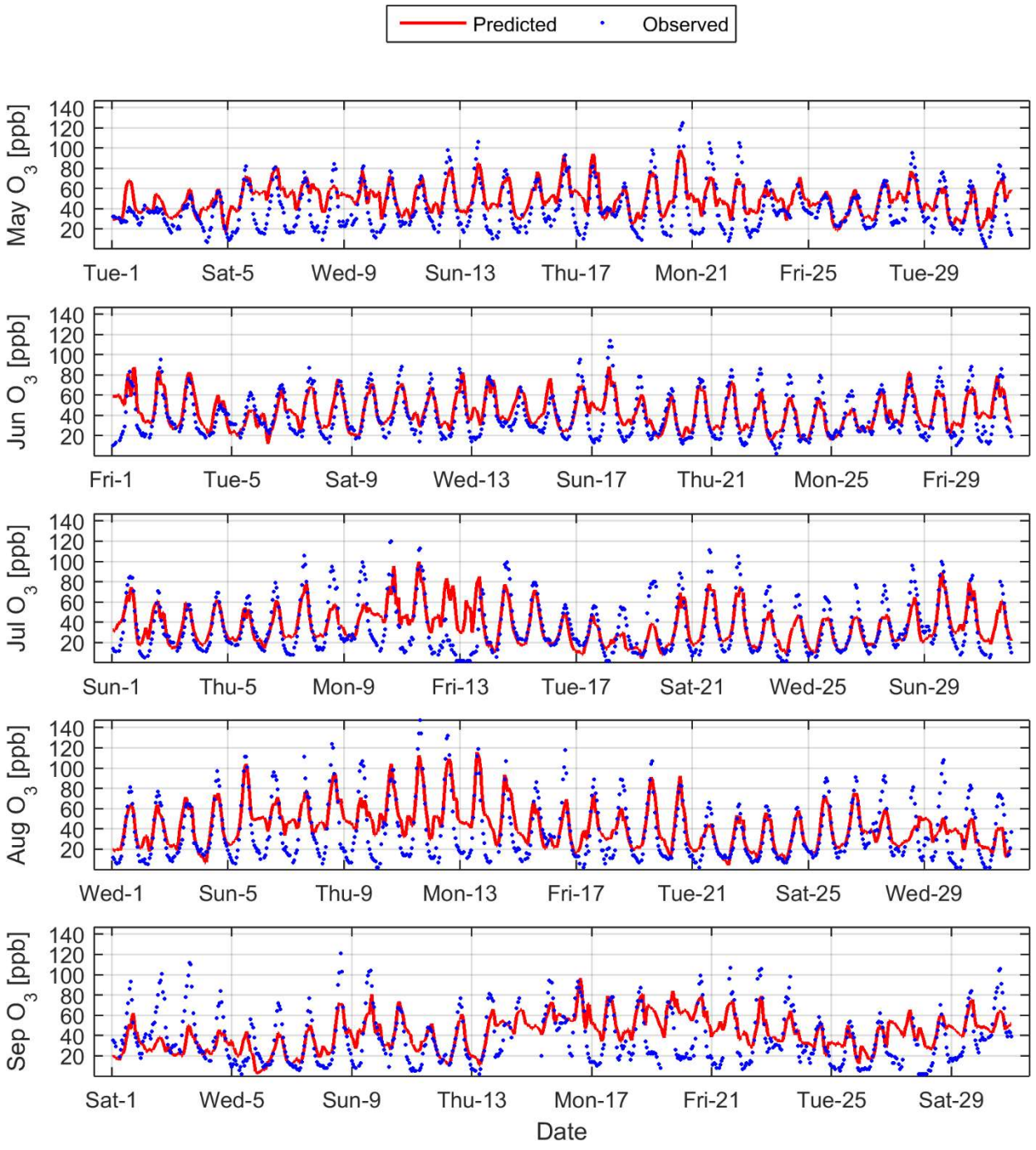

Figure 11: 2012 1-hour Ozone model prediction and measurement comparison at Glendora

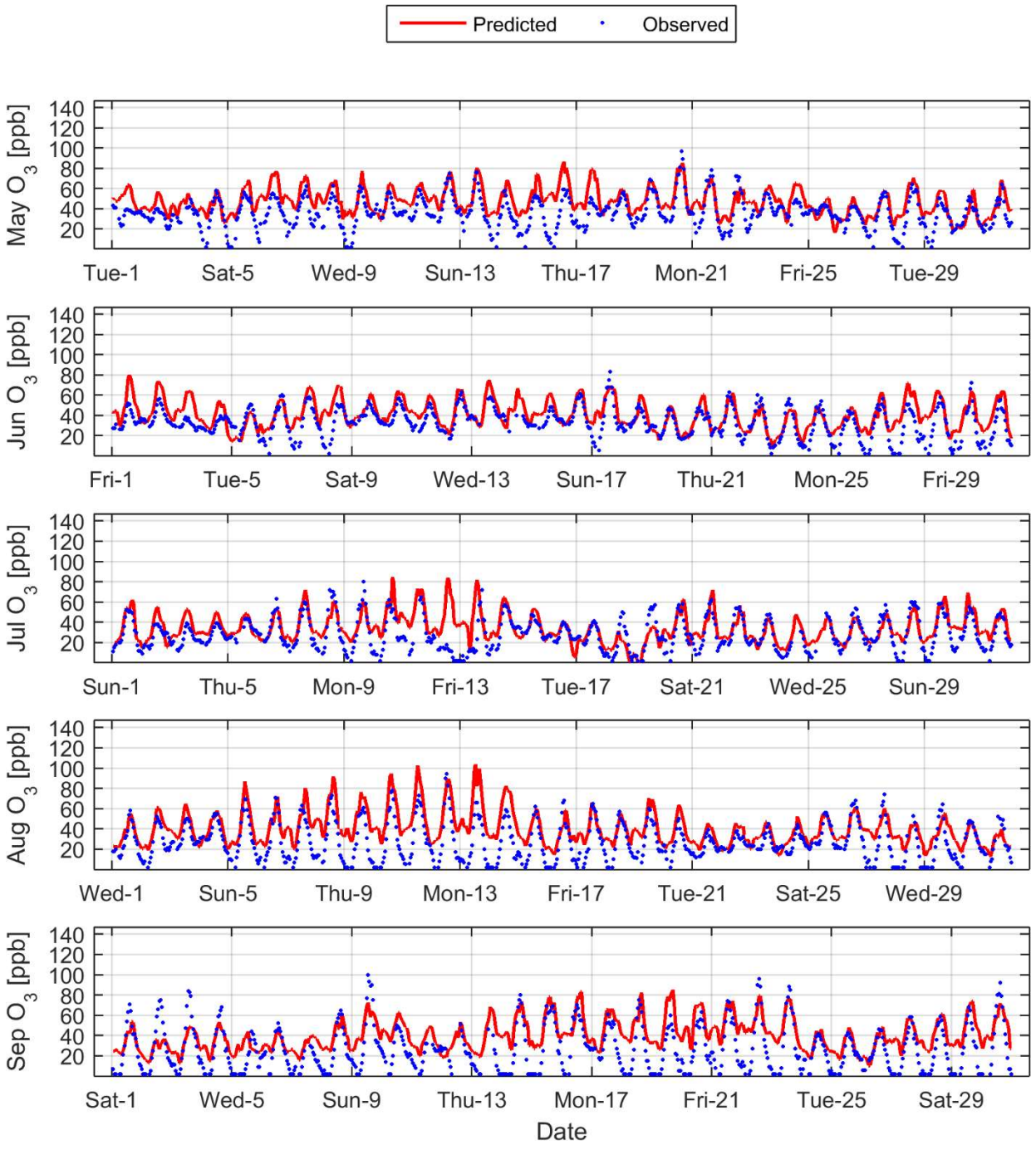

Figure 12: 2012 1-hour Ozone model prediction and measurement comparison at La Habra

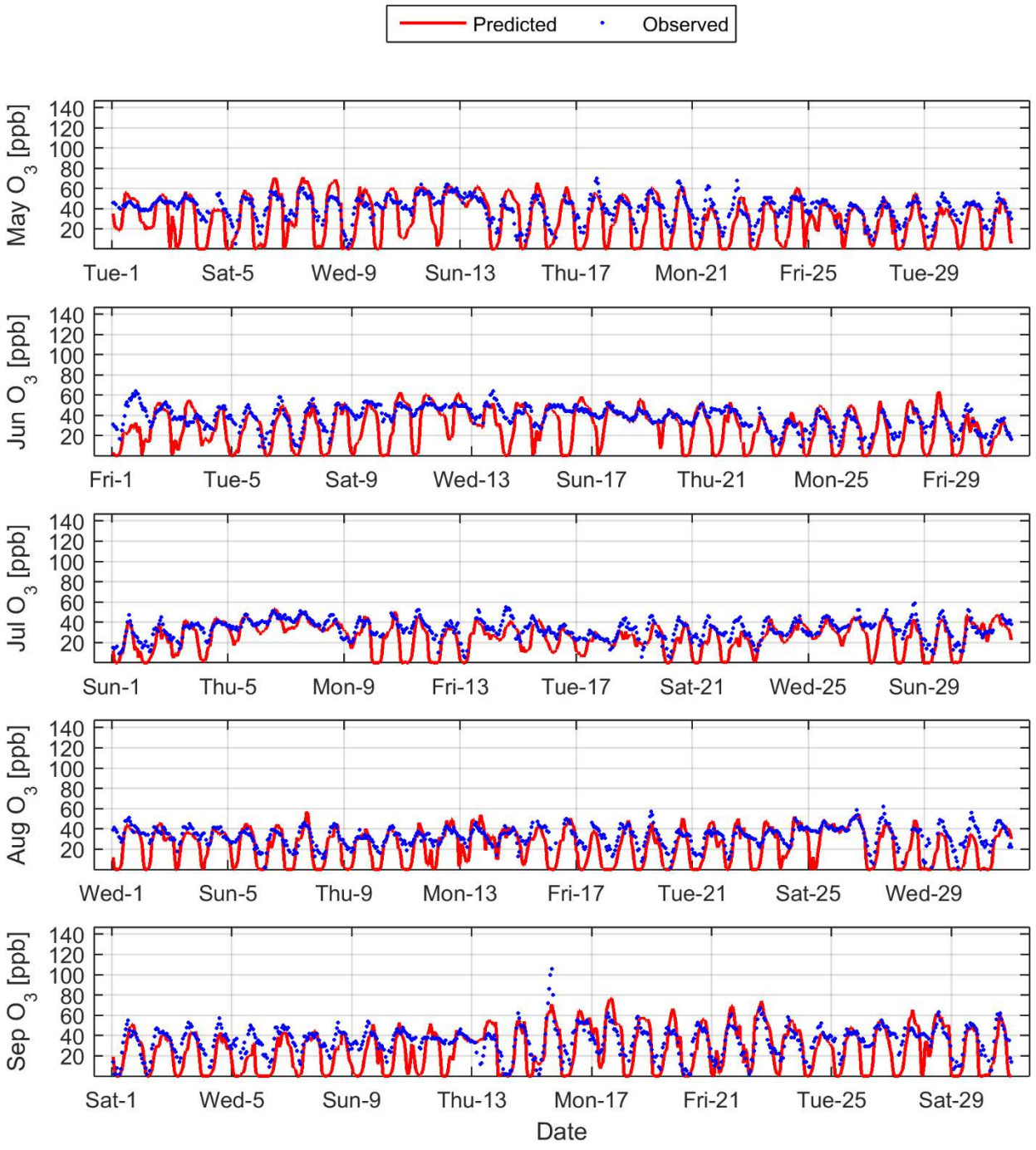

Figure 13: 2012 1-hour Ozone model prediction and measurement comparison at LAX

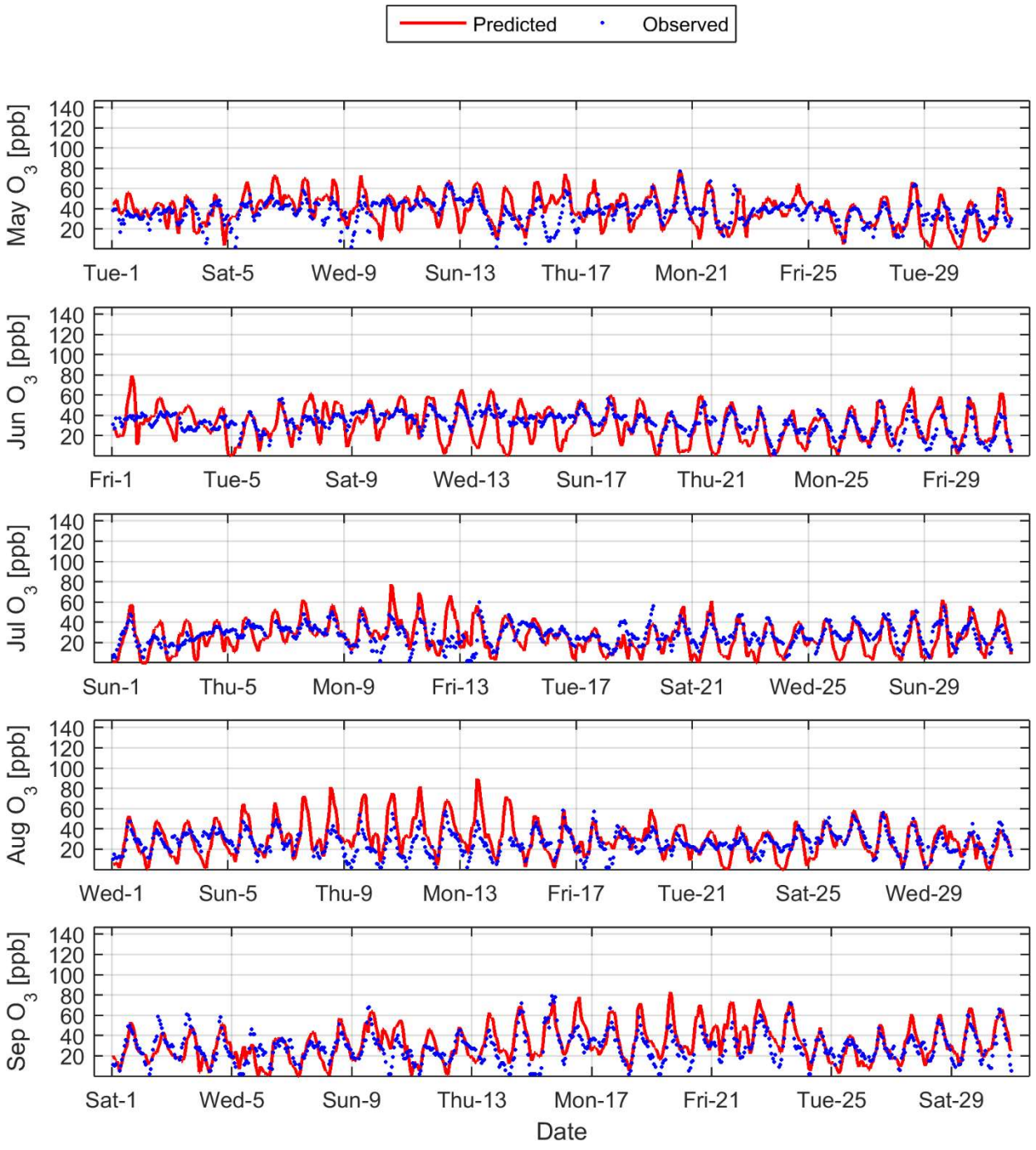

Figure 14: 2012 1-hour Ozone model prediction and measurement comparison at Long Beach

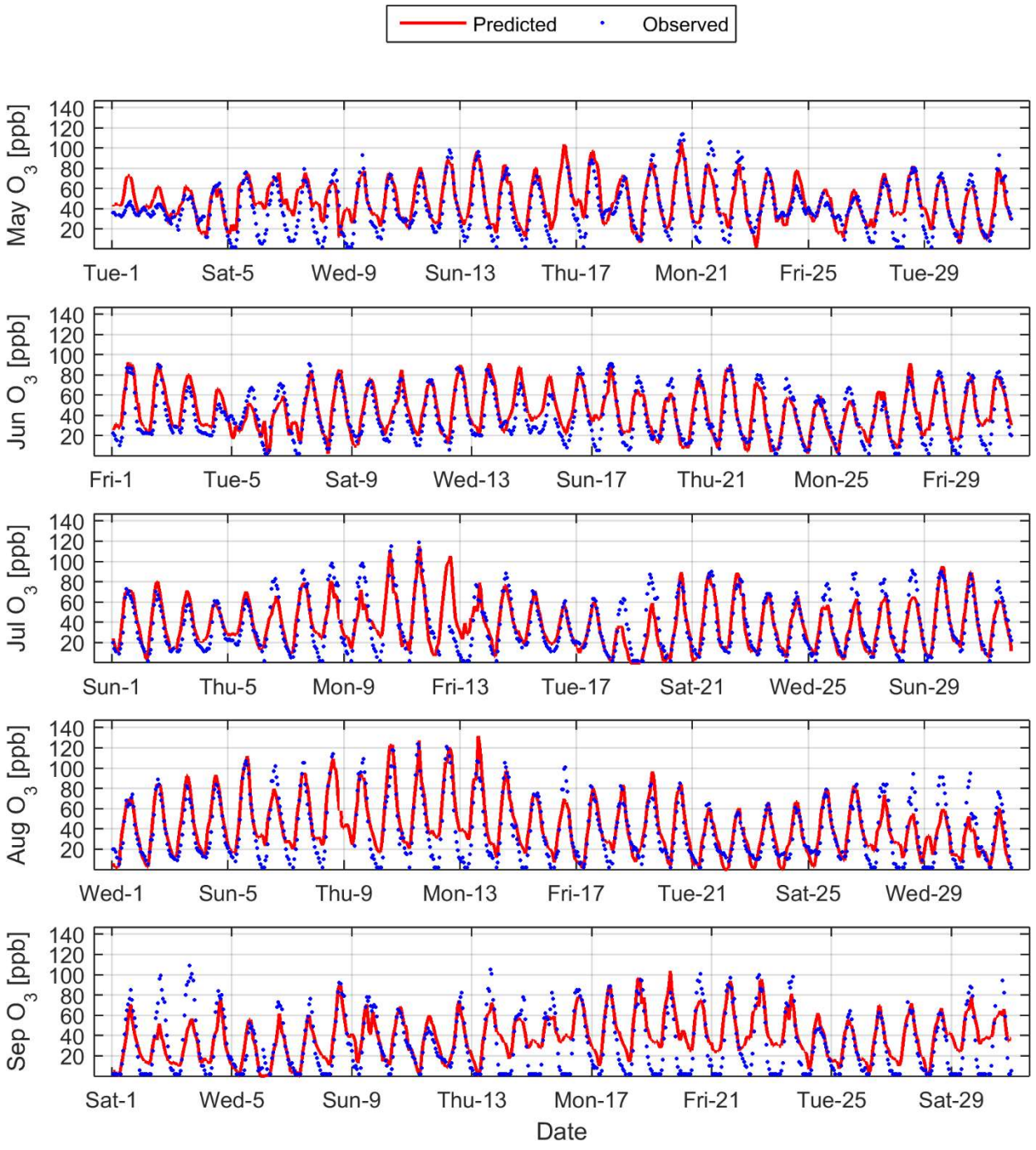

Figure 15: 2012 1-hour Ozone model prediction and measurement comparison at Mira Loma

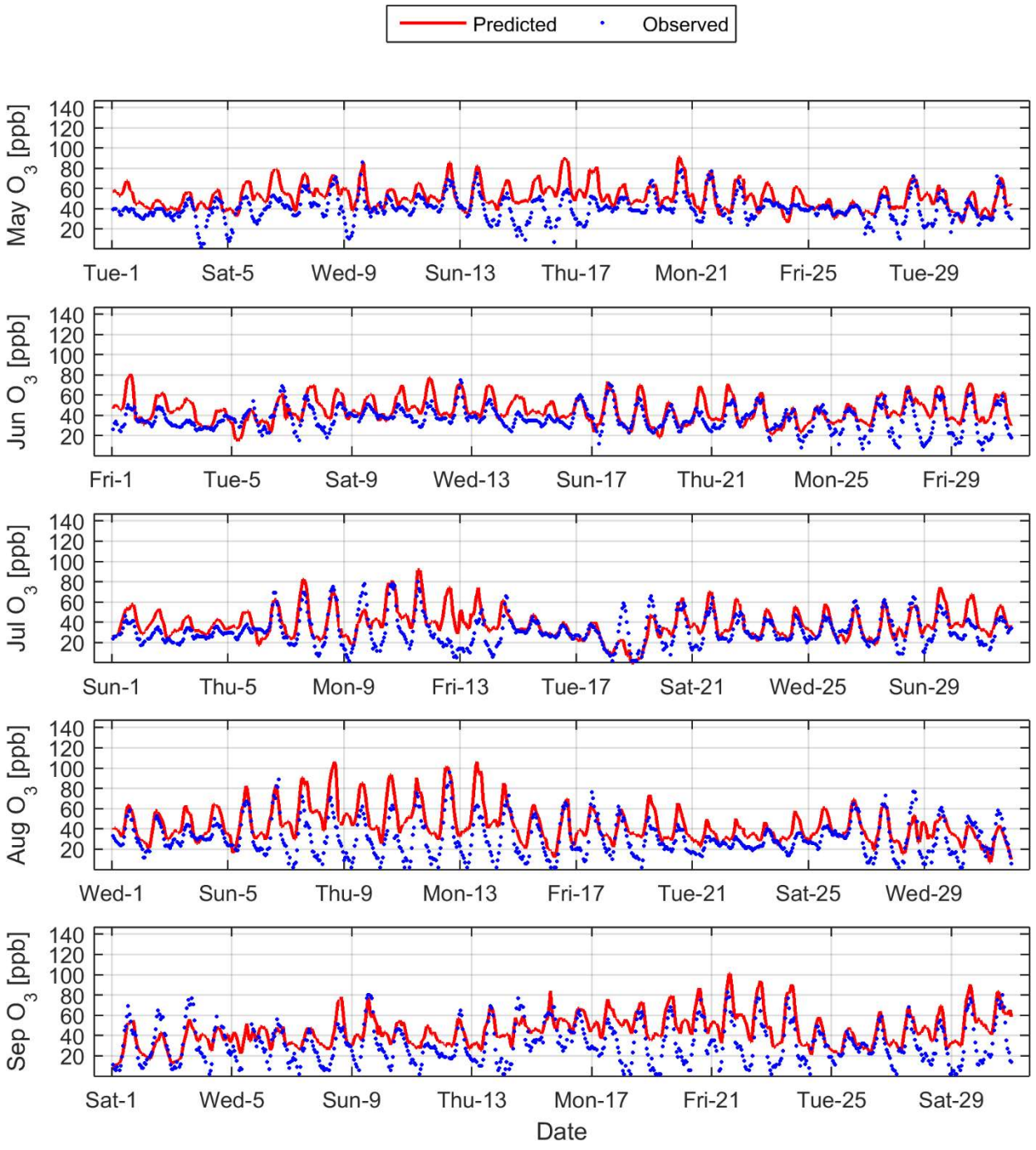

Figure 16: 2012 1-hour Ozone model prediction and measurement comparison at Mission Viejo

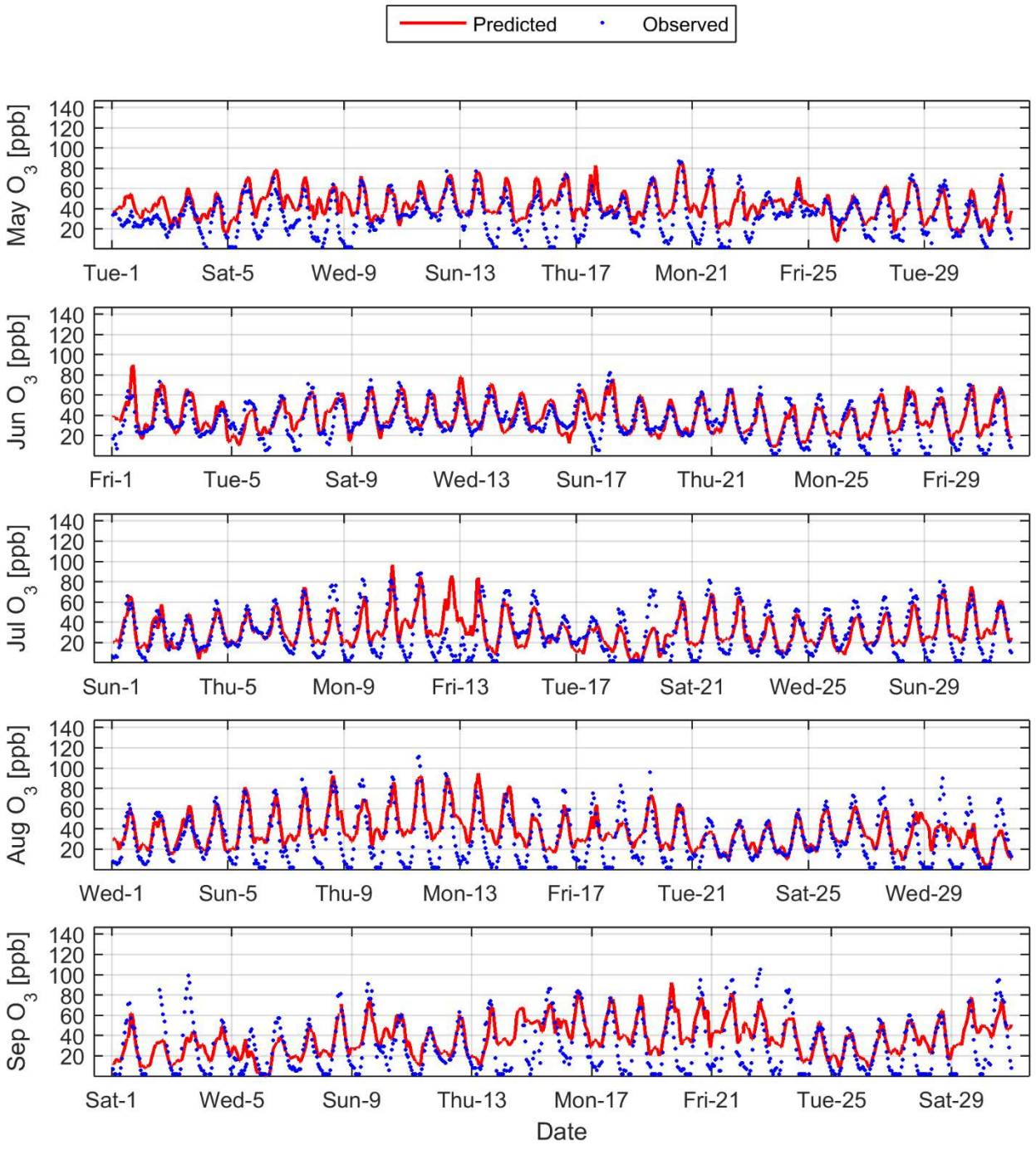

Figure 17: 2012 1-hour Ozone model prediction and measurement comparison at Pasadena

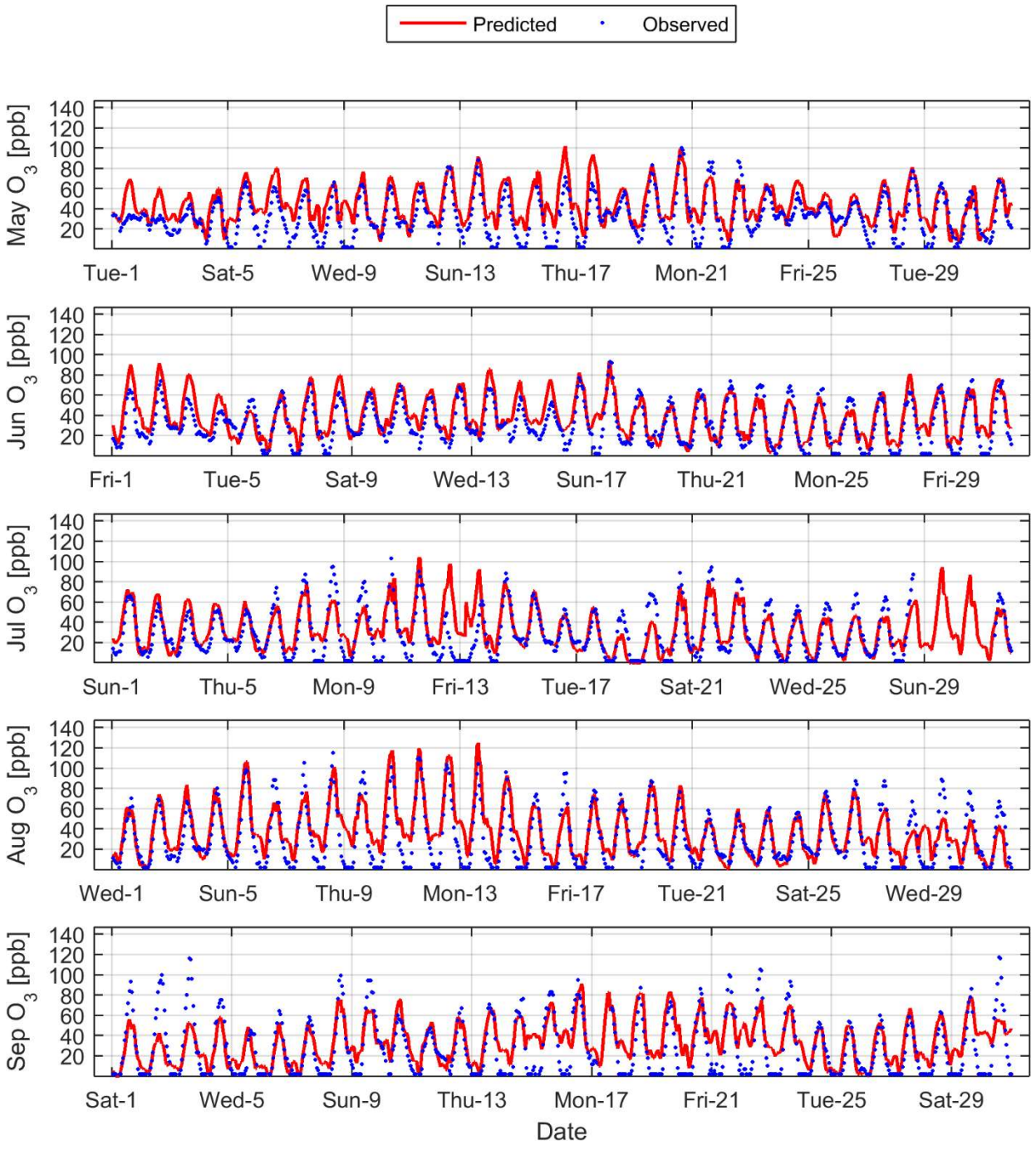

Figure 18: 2012 1-hour Ozone model prediction and measurement comparison at Pomona

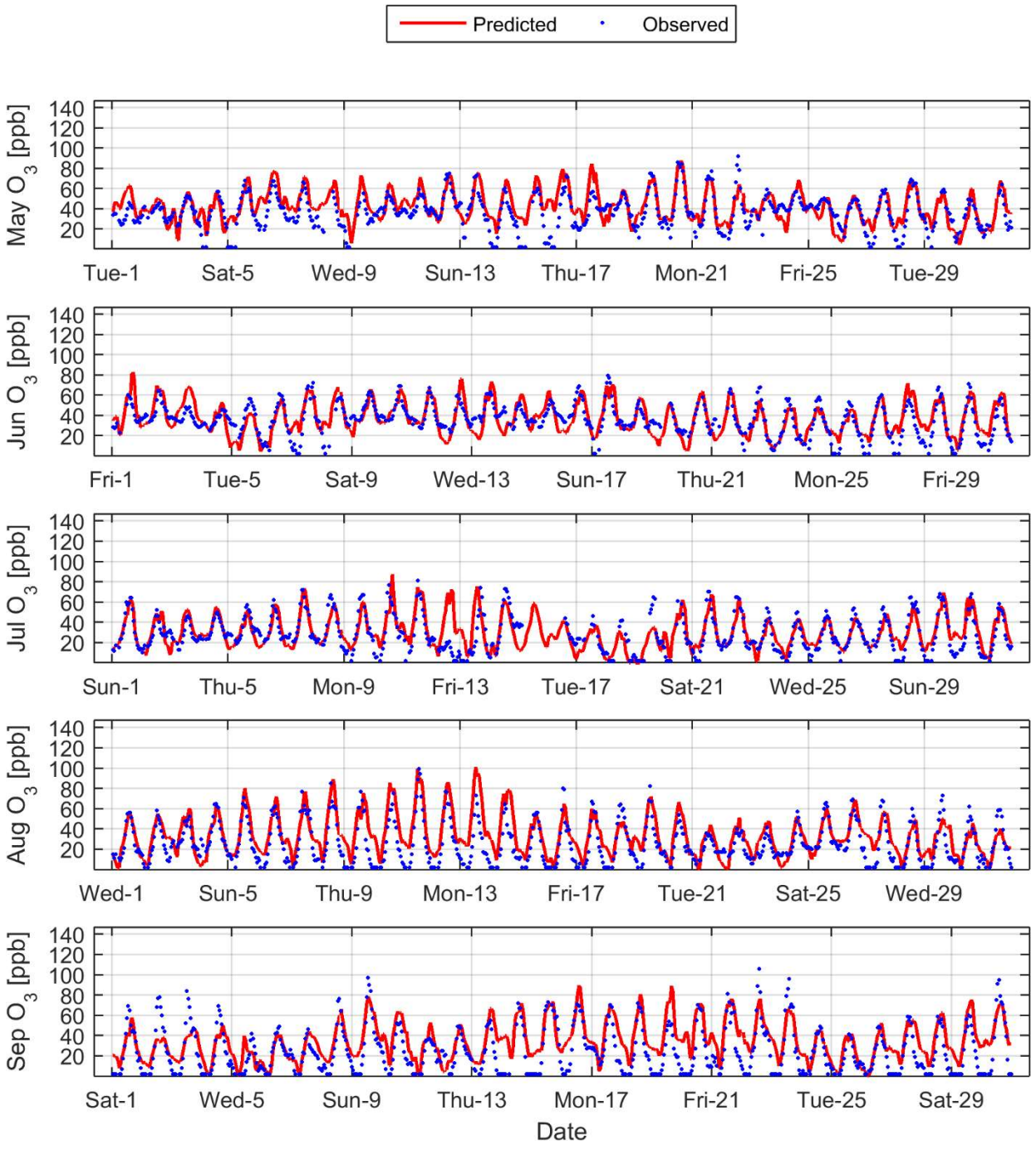

Figure 19: 2012 1-hour Ozone model prediction and measurement comparison at Pico Rivera

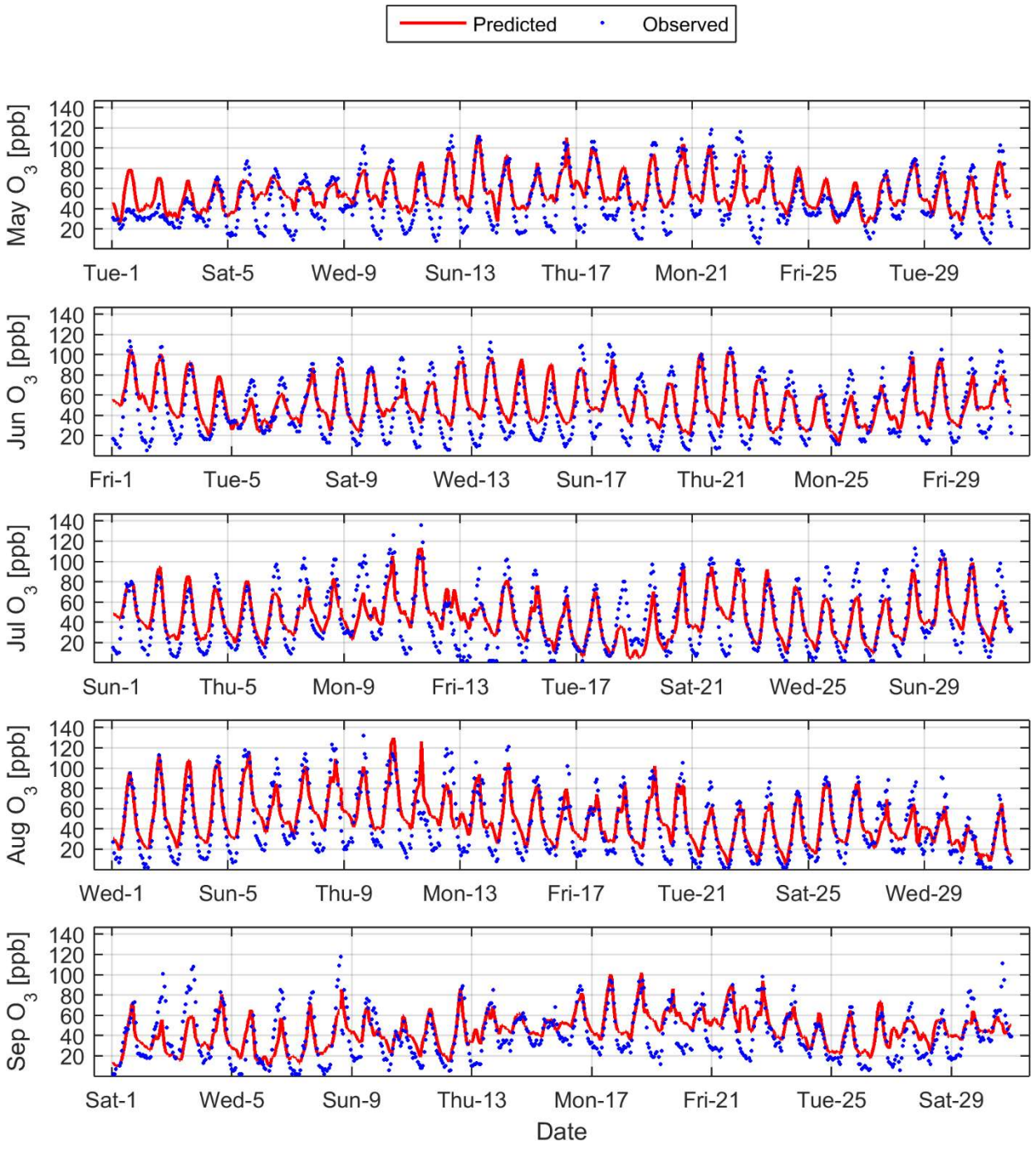

Figure 20: 2012 1-hour Ozone model prediction and measurement comparison at Redlands

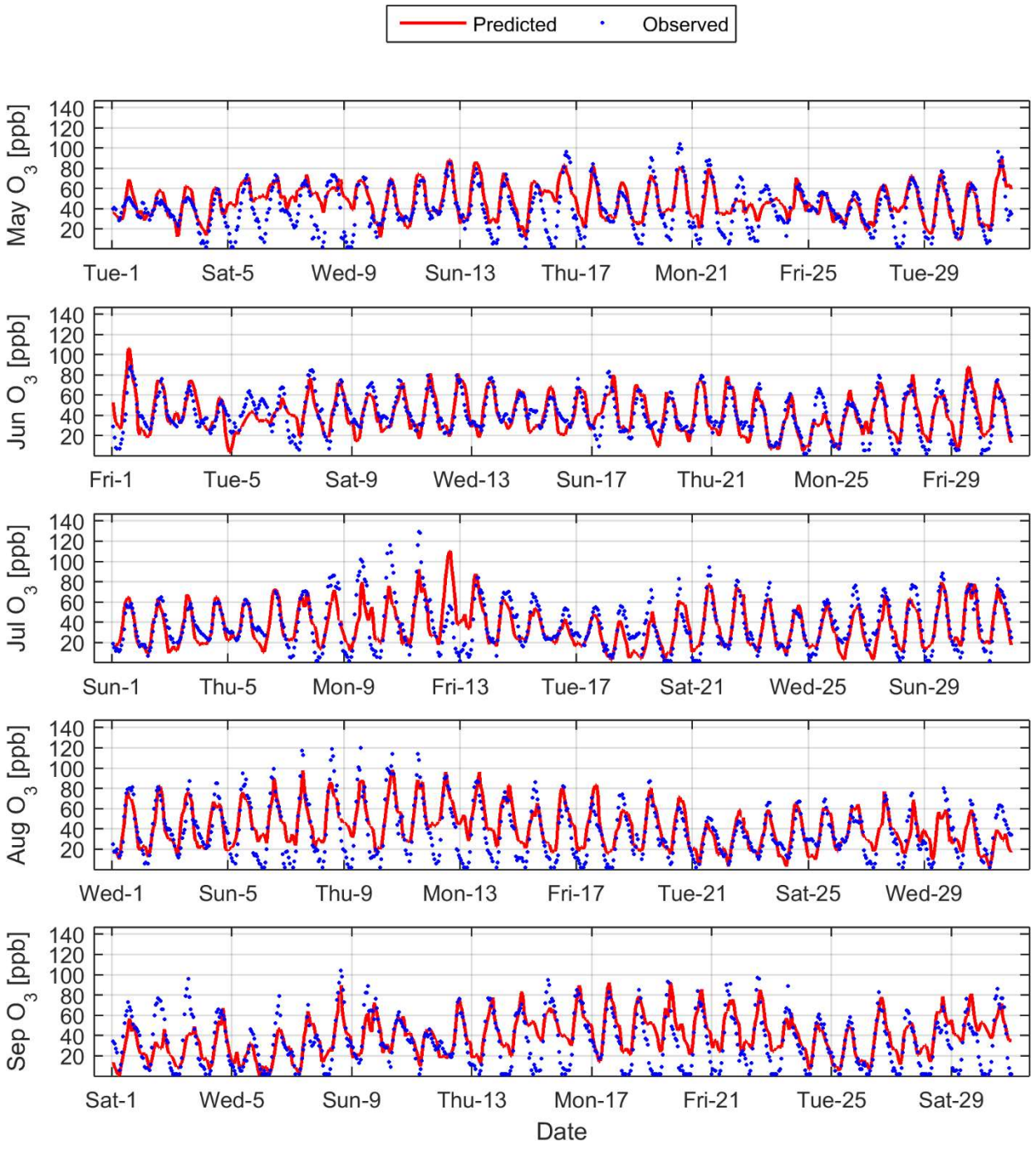

Figure 21: 2012 1-hour Ozone model prediction and measurement comparison at Reseda

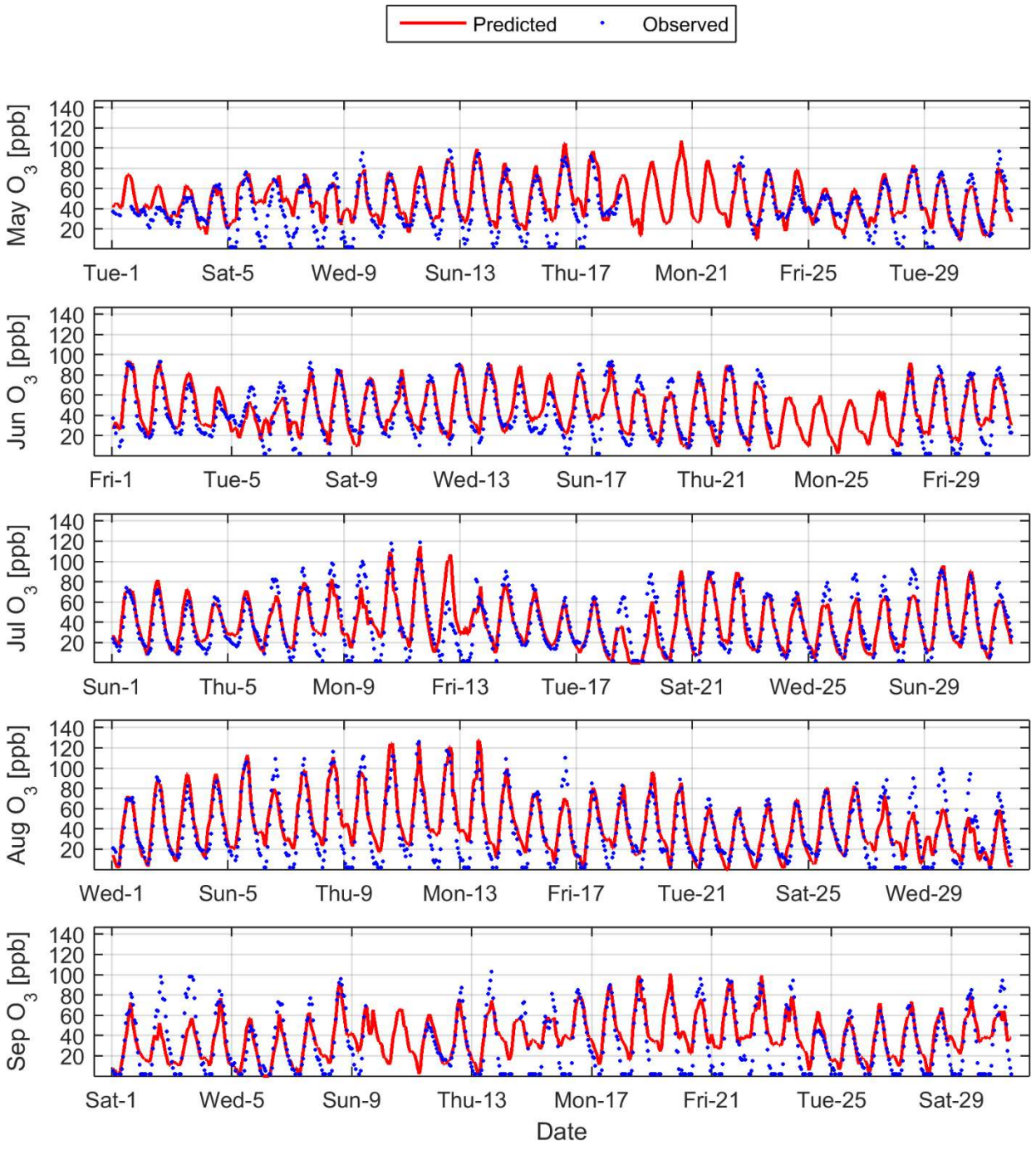

Figure 22: 2012 1-hour Ozone model prediction and measurement comparison at Riverside

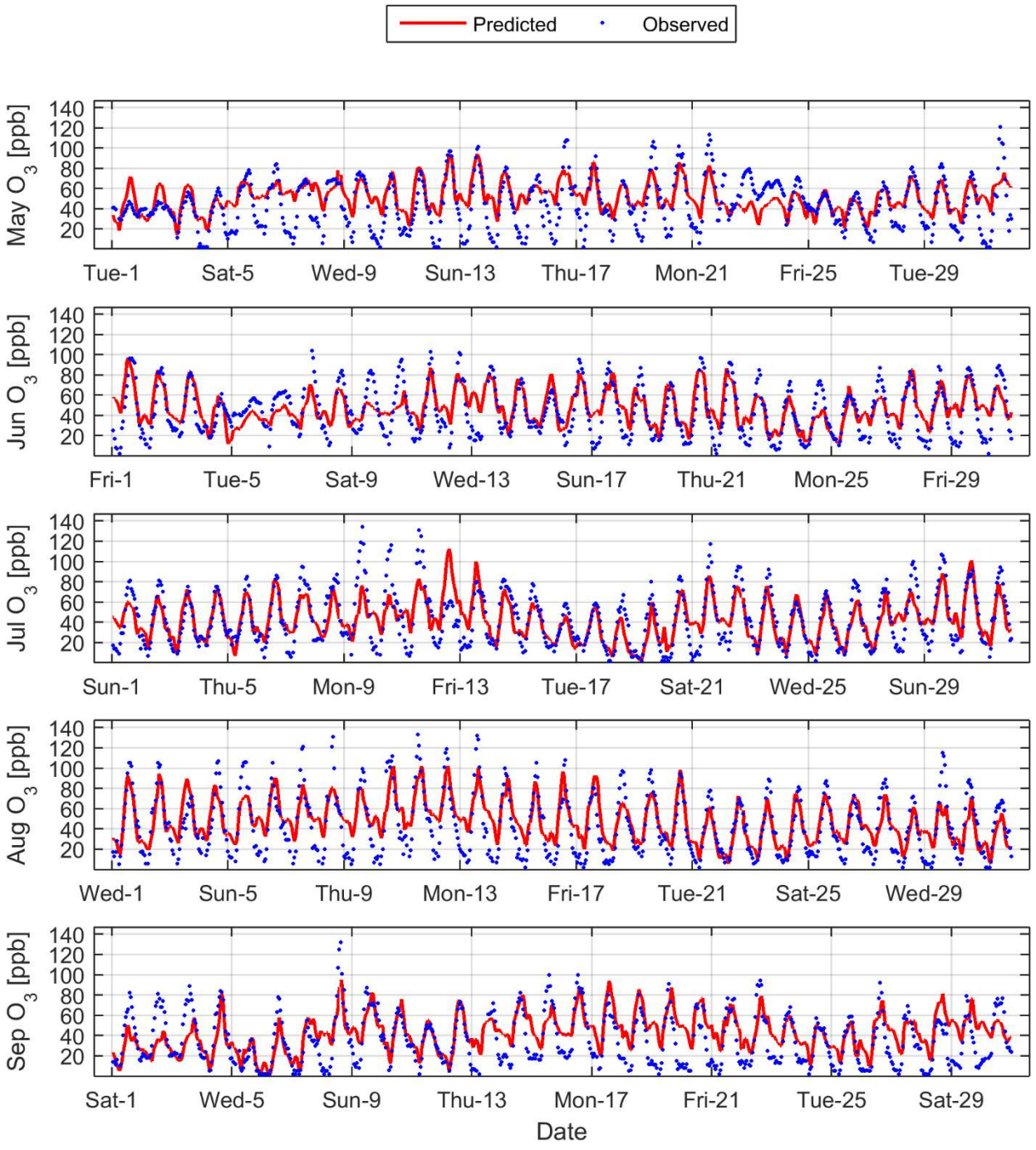

Figure 23: 2012 1-hour Ozone model prediction and measurement comparison at Santa Clarita

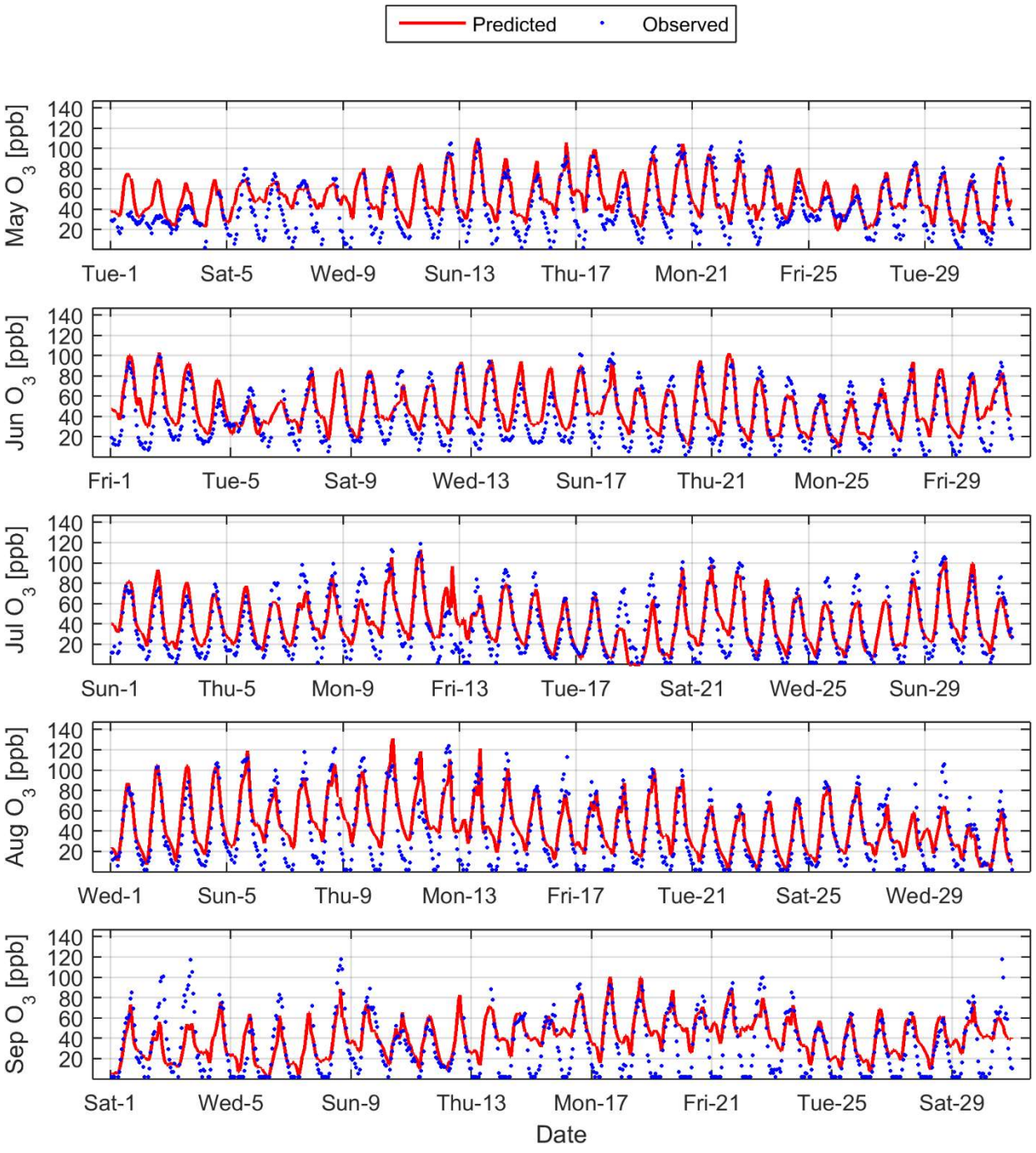

Figure 24: 2012 1-hour Ozone model prediction and measurement comparison at San Bernardino

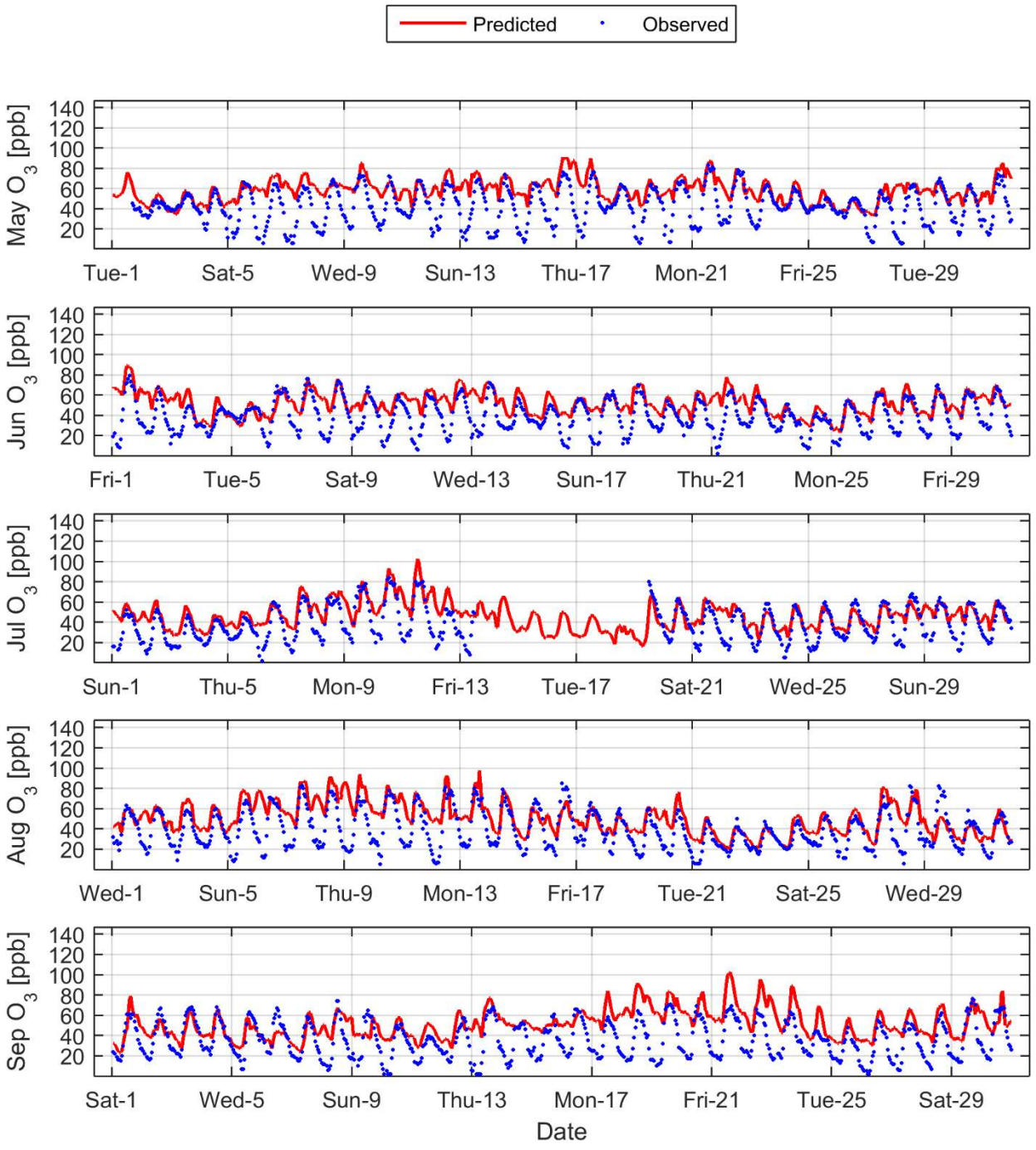

Figure 25: 2012 1-hour Ozone model prediction and measurement comparison at Temecula

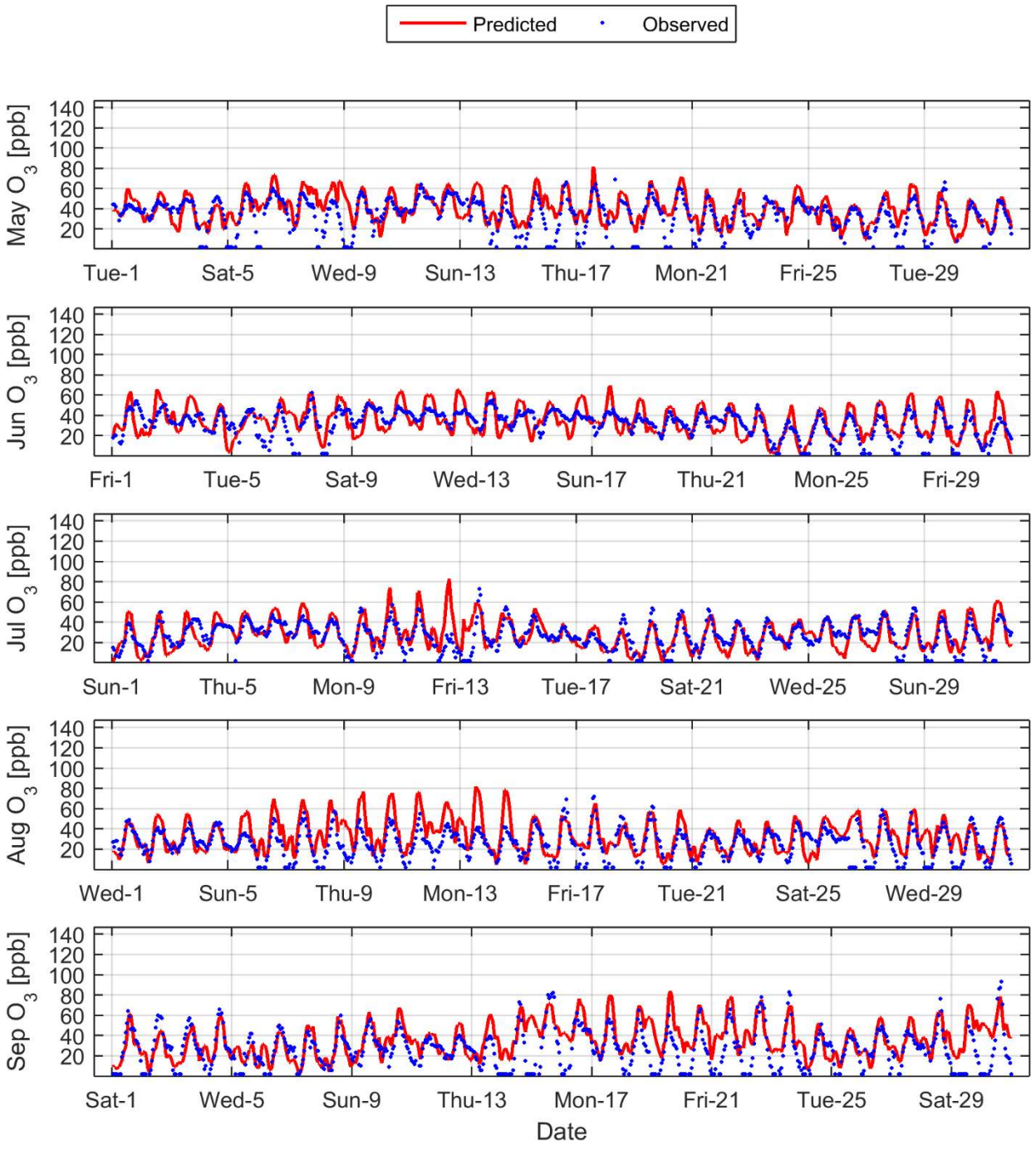

Figure 26: 2012 1-hour Ozone model prediction and measurement comparison at West Los Angeles

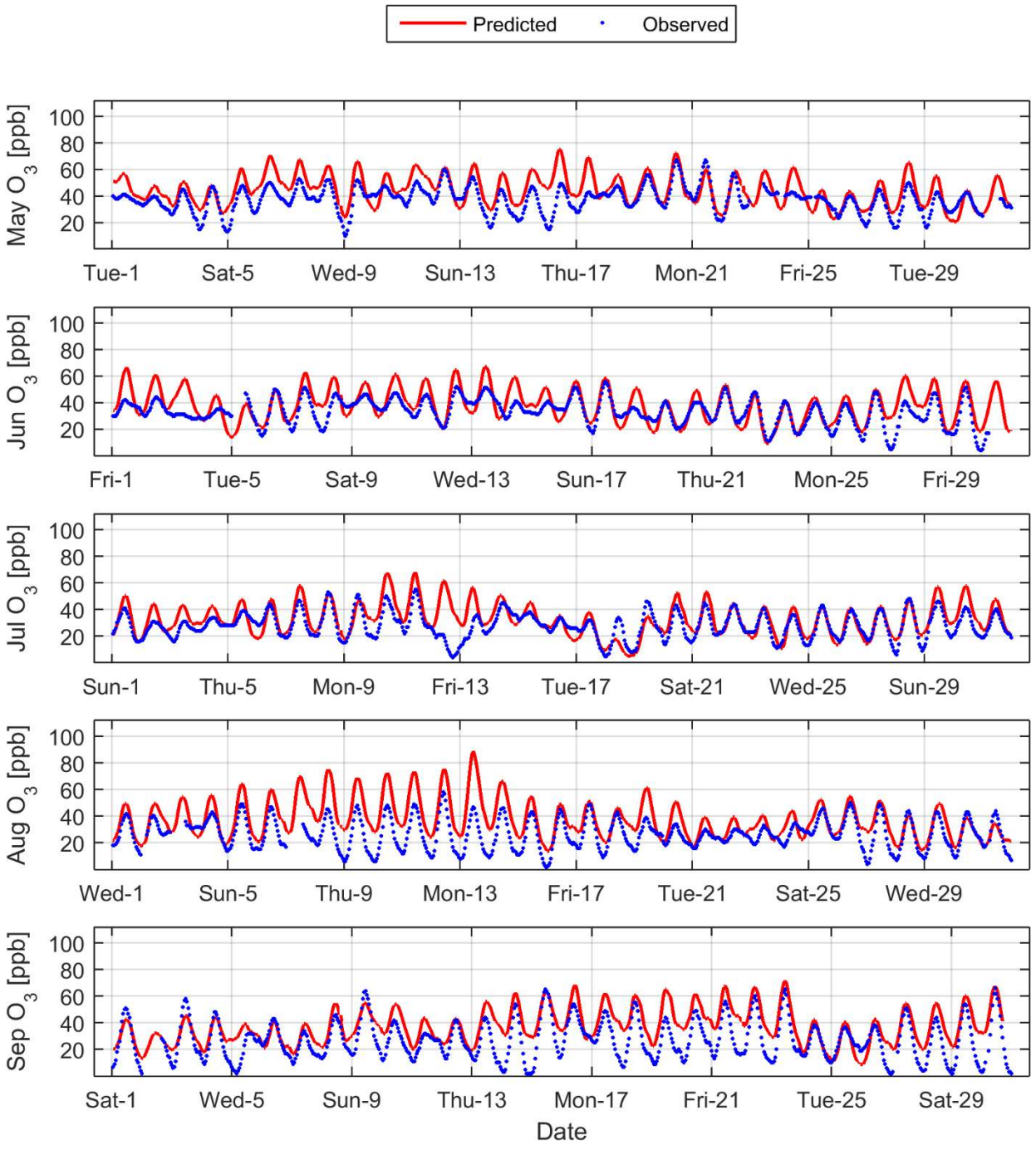

Figure 27: 2012 8-hour Ozone model prediction and measurement comparison at Anaheim

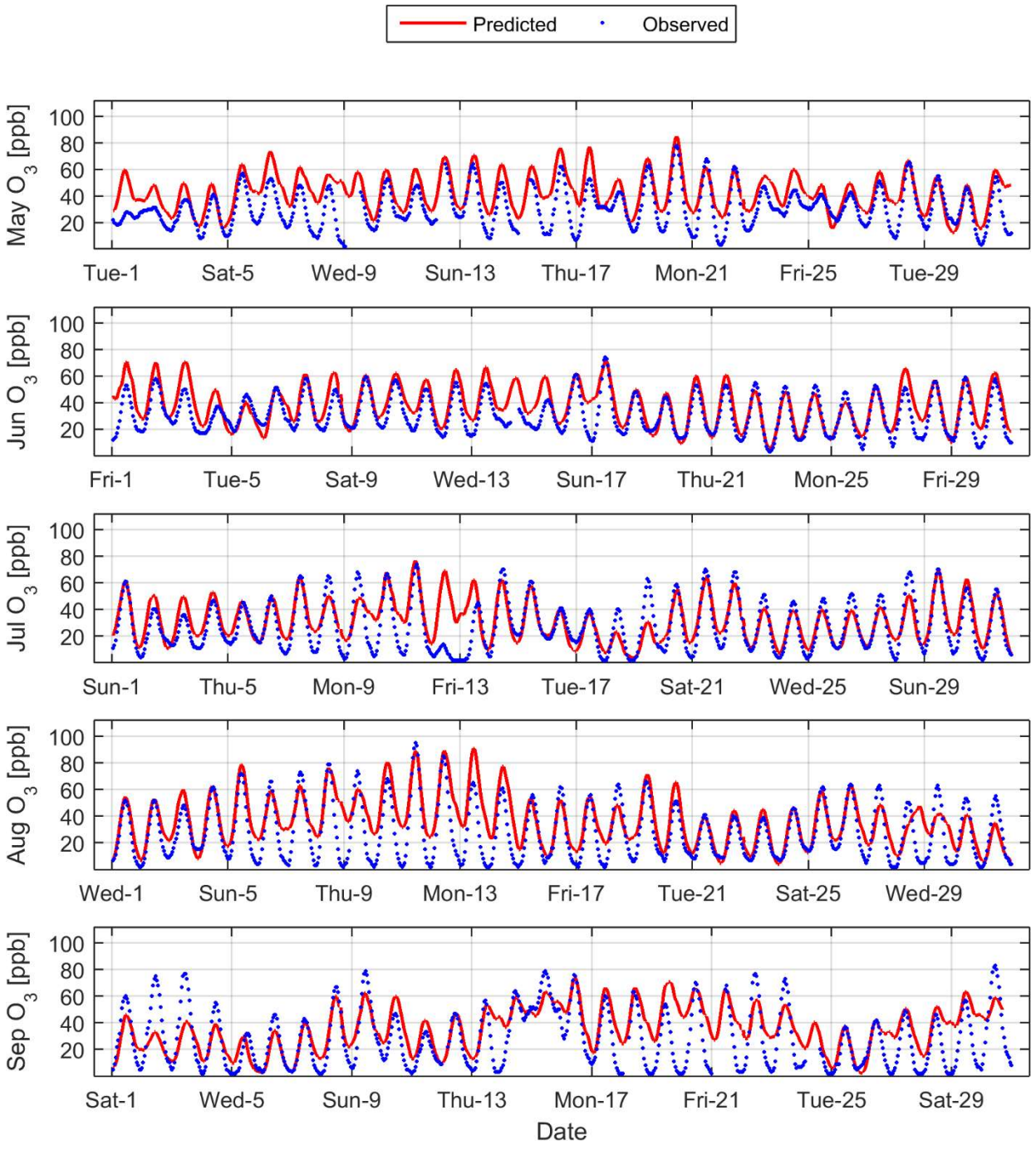

Figure 28: 2012 8-hour Ozone model prediction and measurement comparison at Azusa

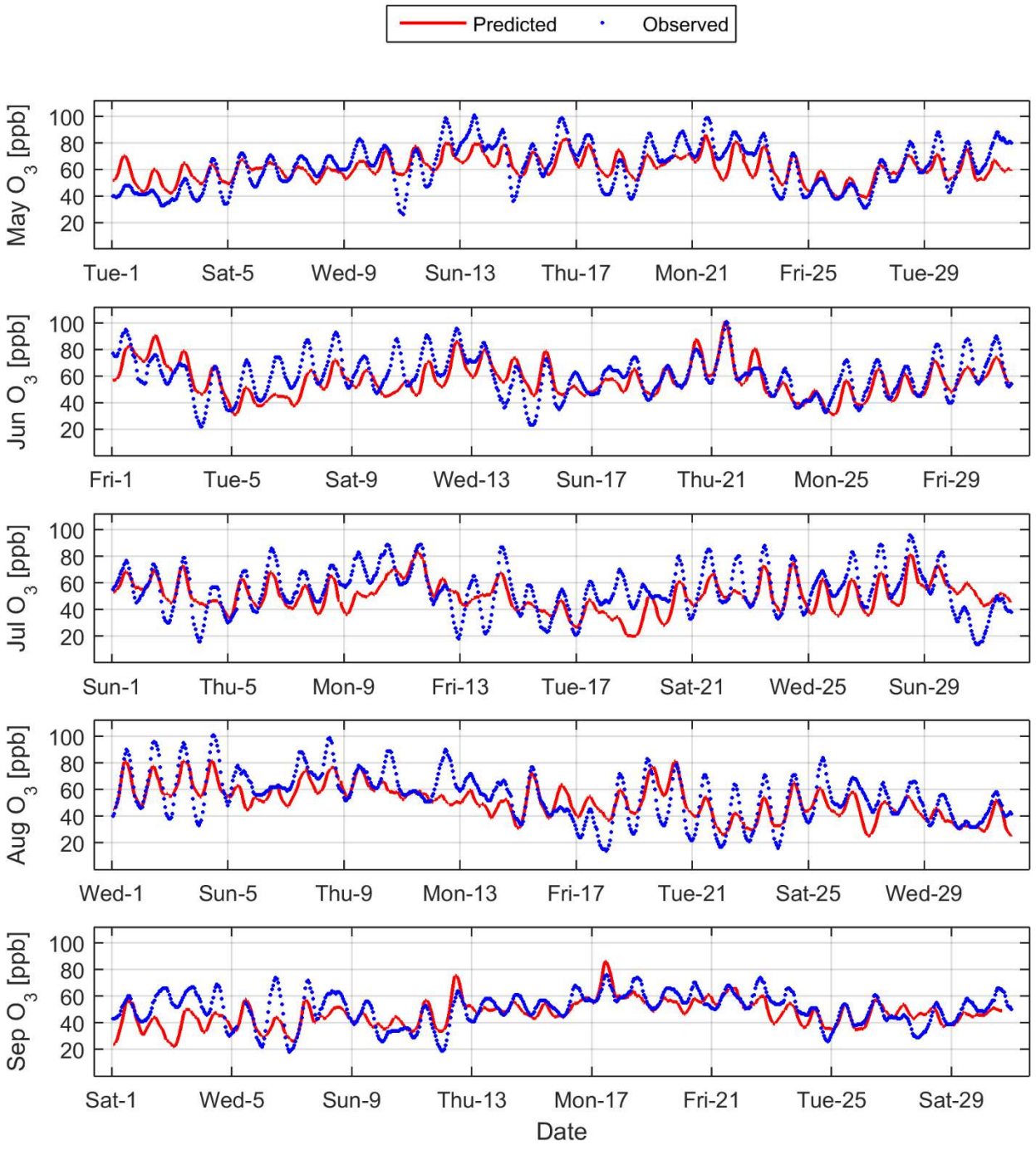

Figure 29: 2012 8-hour Ozone model prediction and measurement comparison at Banning

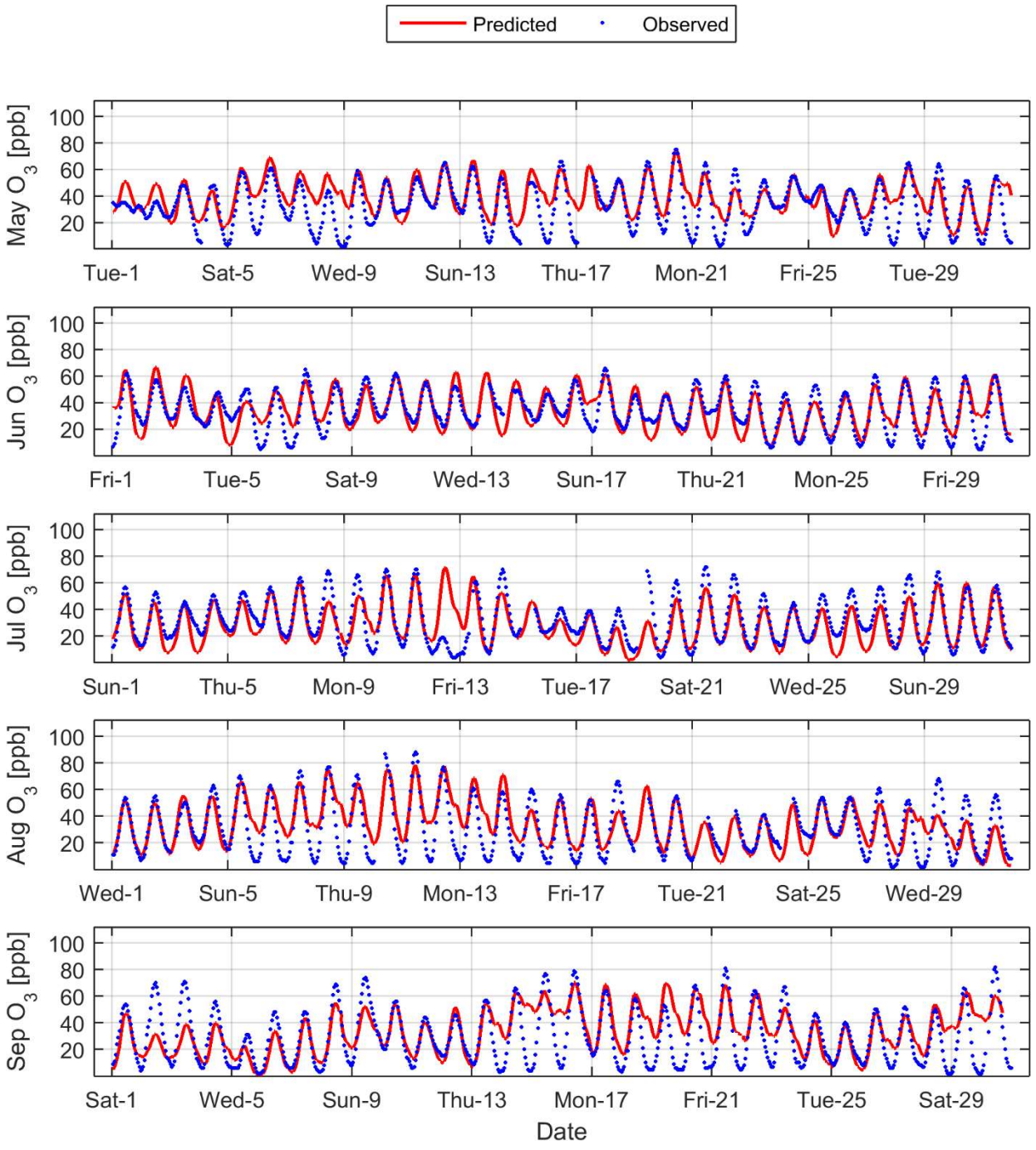

Figure 30: 2012 8-hour Ozone model prediction and measurement comparison at Burbank

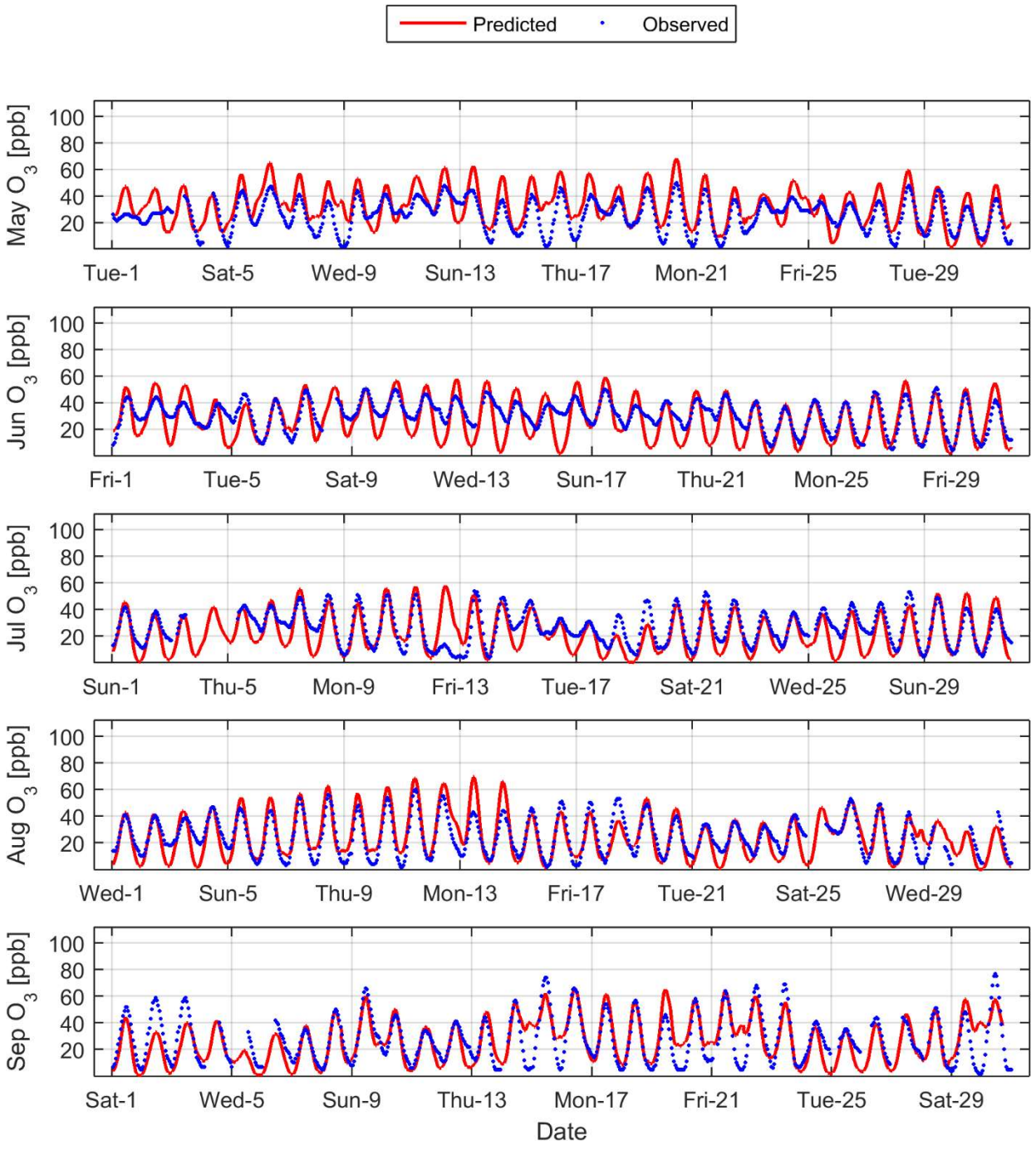

Figure 31: 2012 8-hour Ozone model prediction and measurement comparison at Central Los Angeles

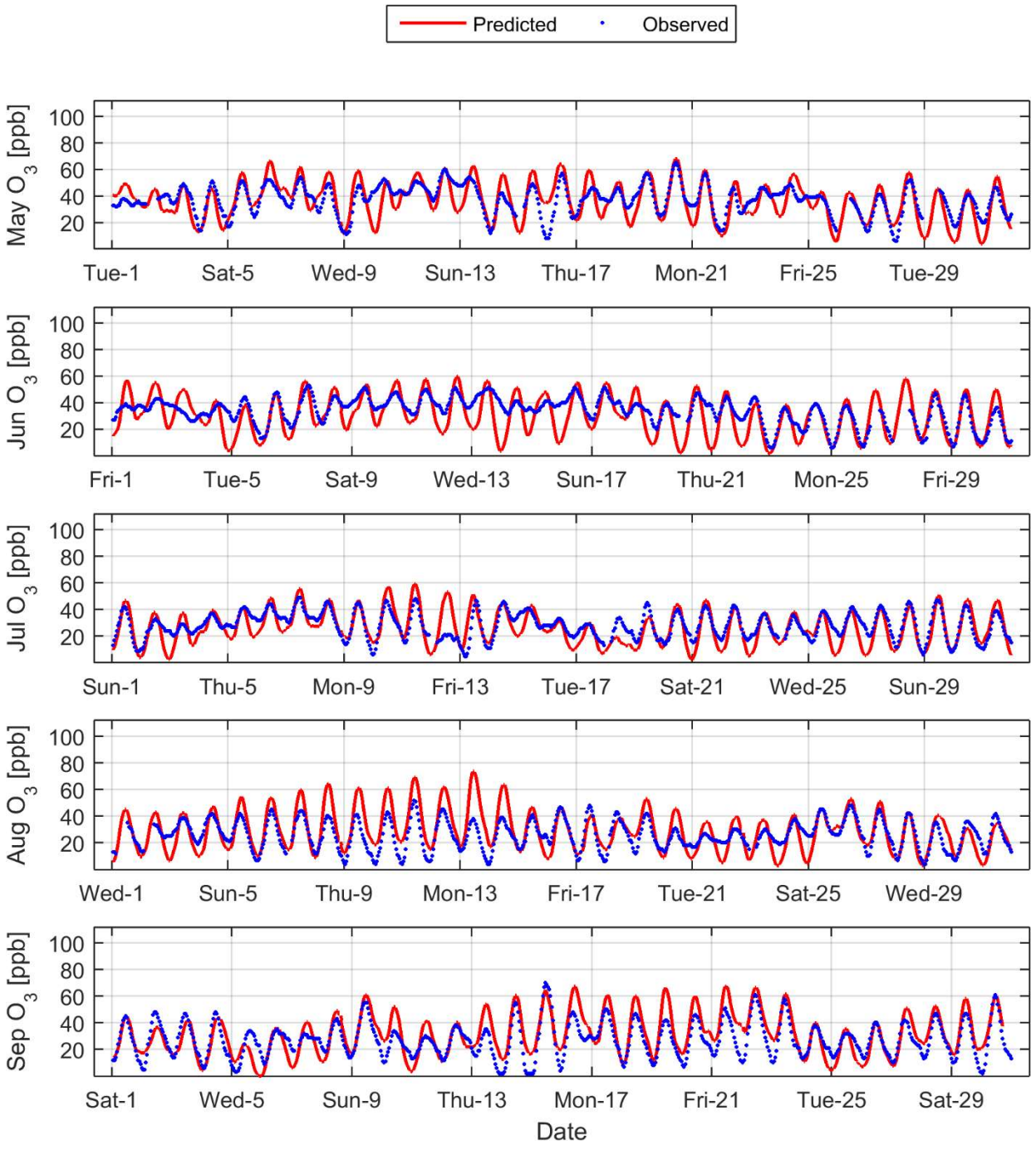

Figure 32: 2012 8-hour Ozone model prediction and measurement comparison at Compton

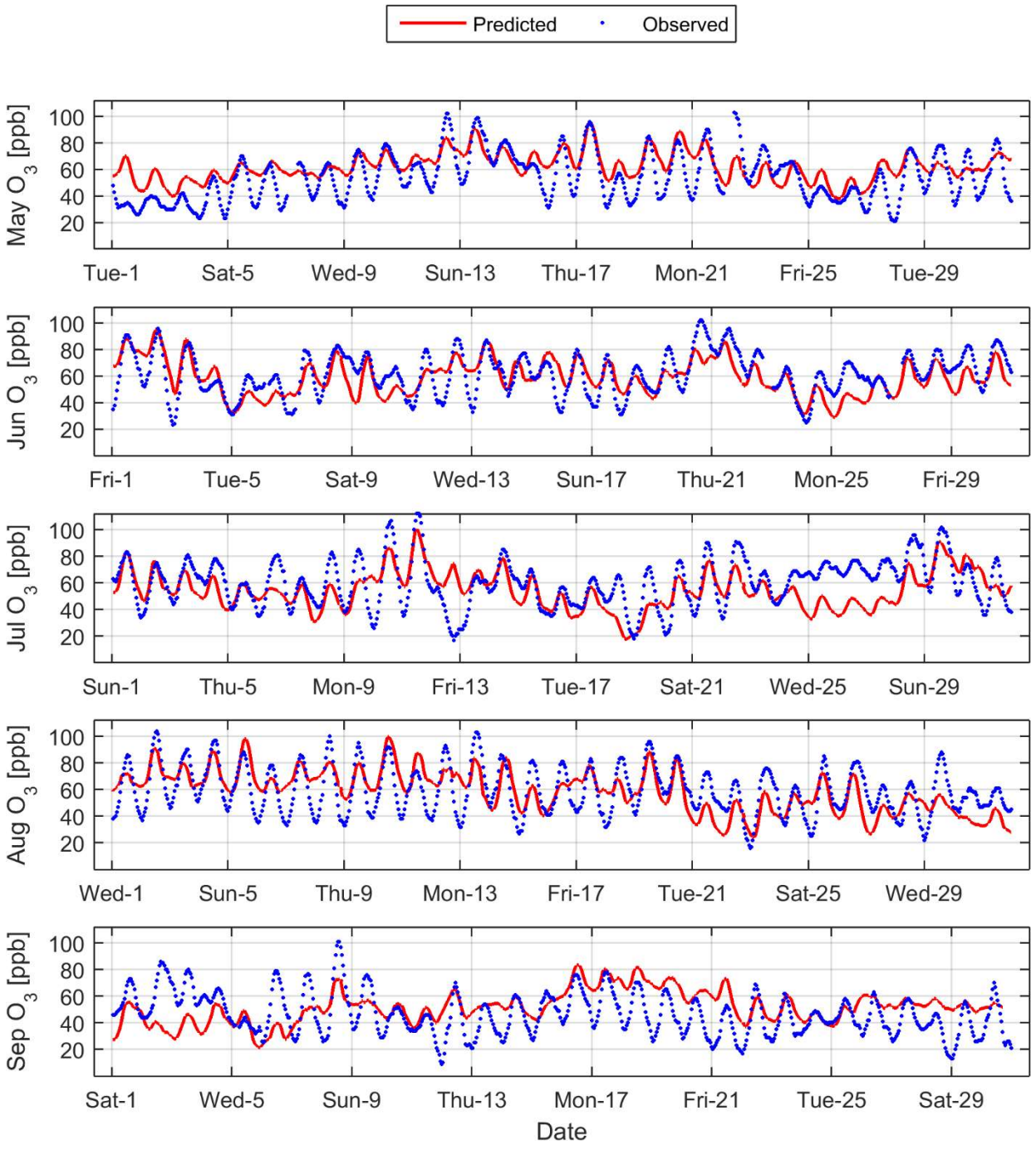

Figure 33: 2012 8-hour Ozone model prediction and measurement comparison at Crestline

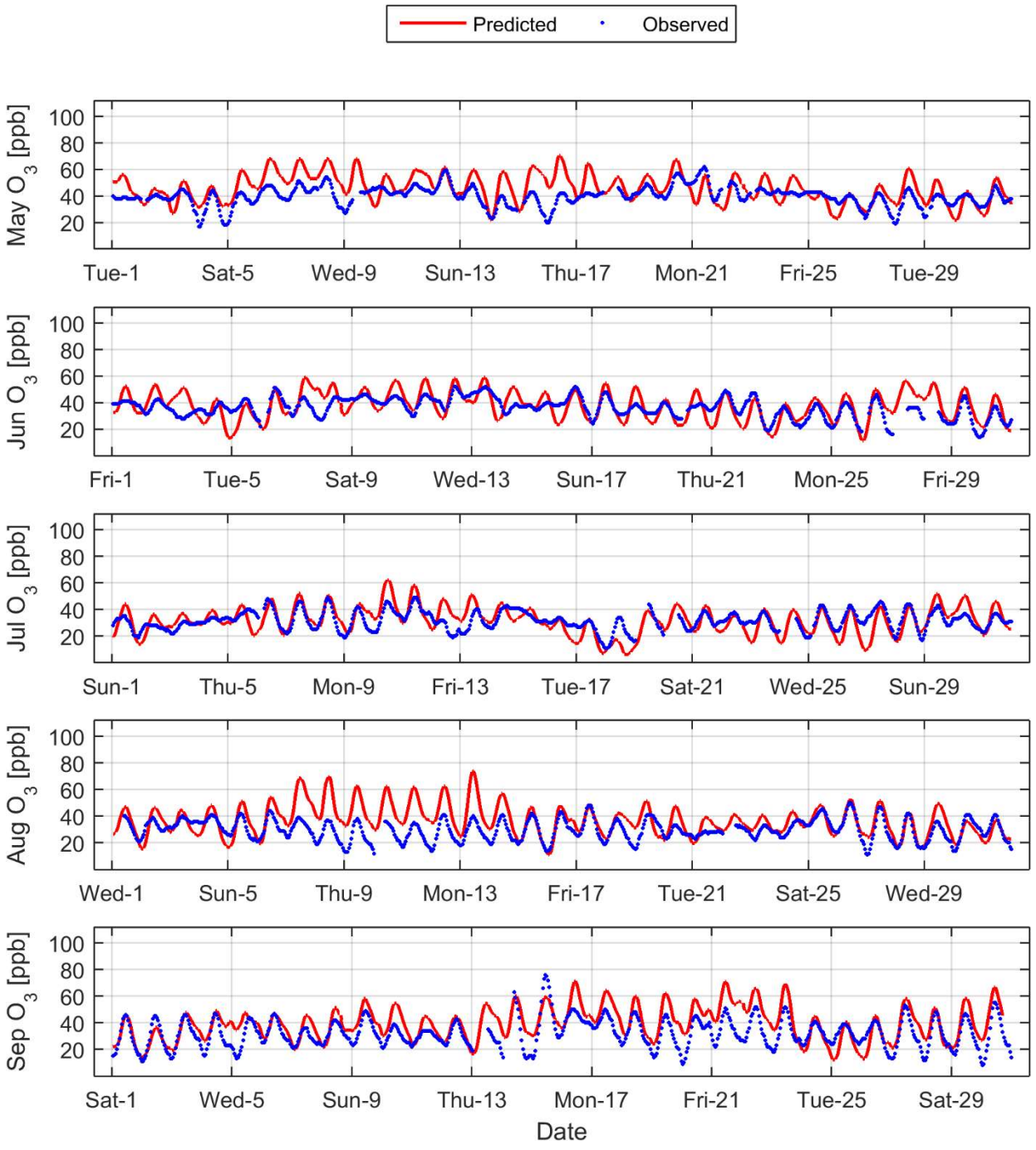

Figure 34: 2012 8-hour Ozone model prediction and measurement comparison at Costa Mesa

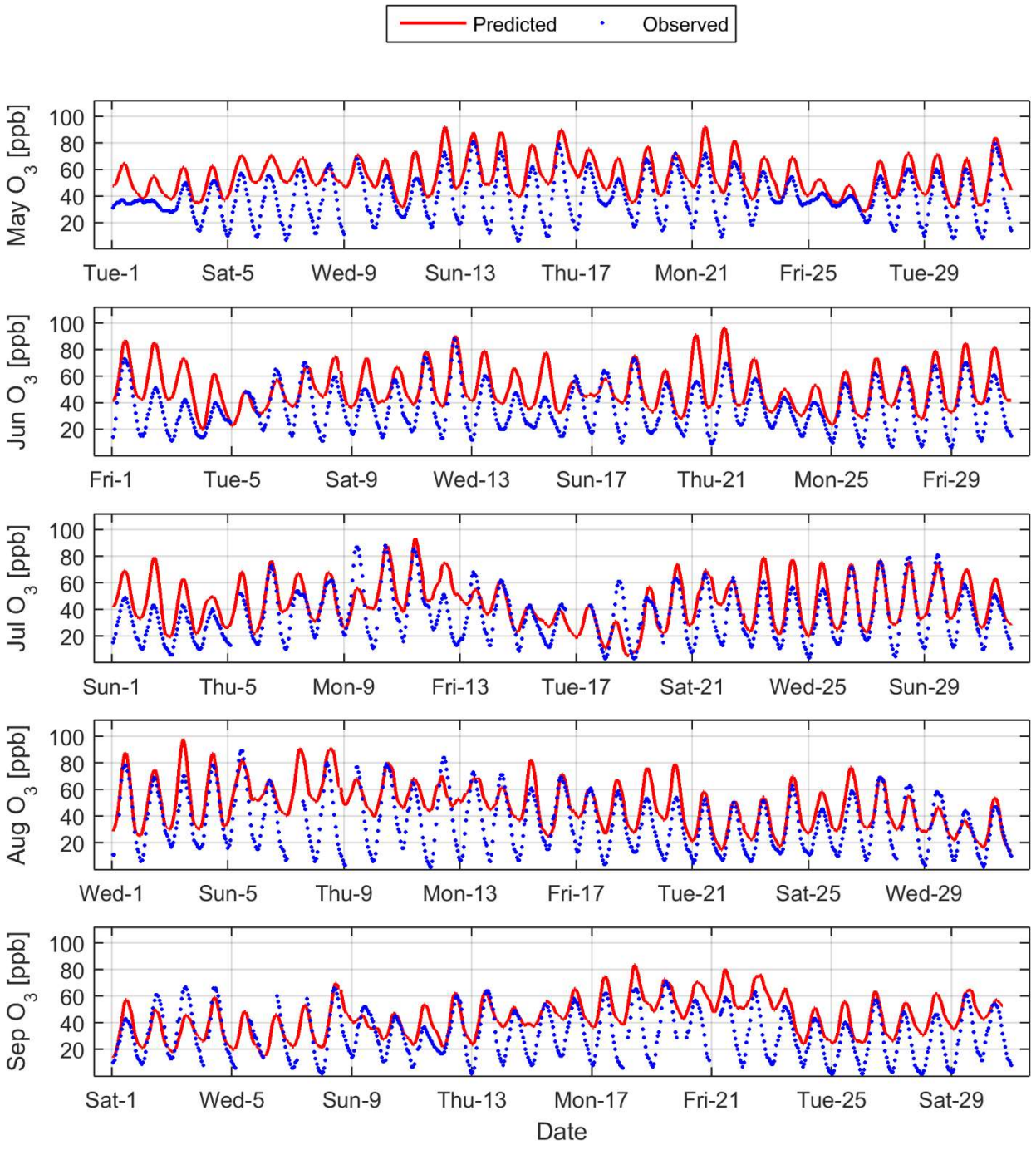

Figure 35: 2012 8-hour Ozone model prediction and measurement comparison at Lake Elsinore

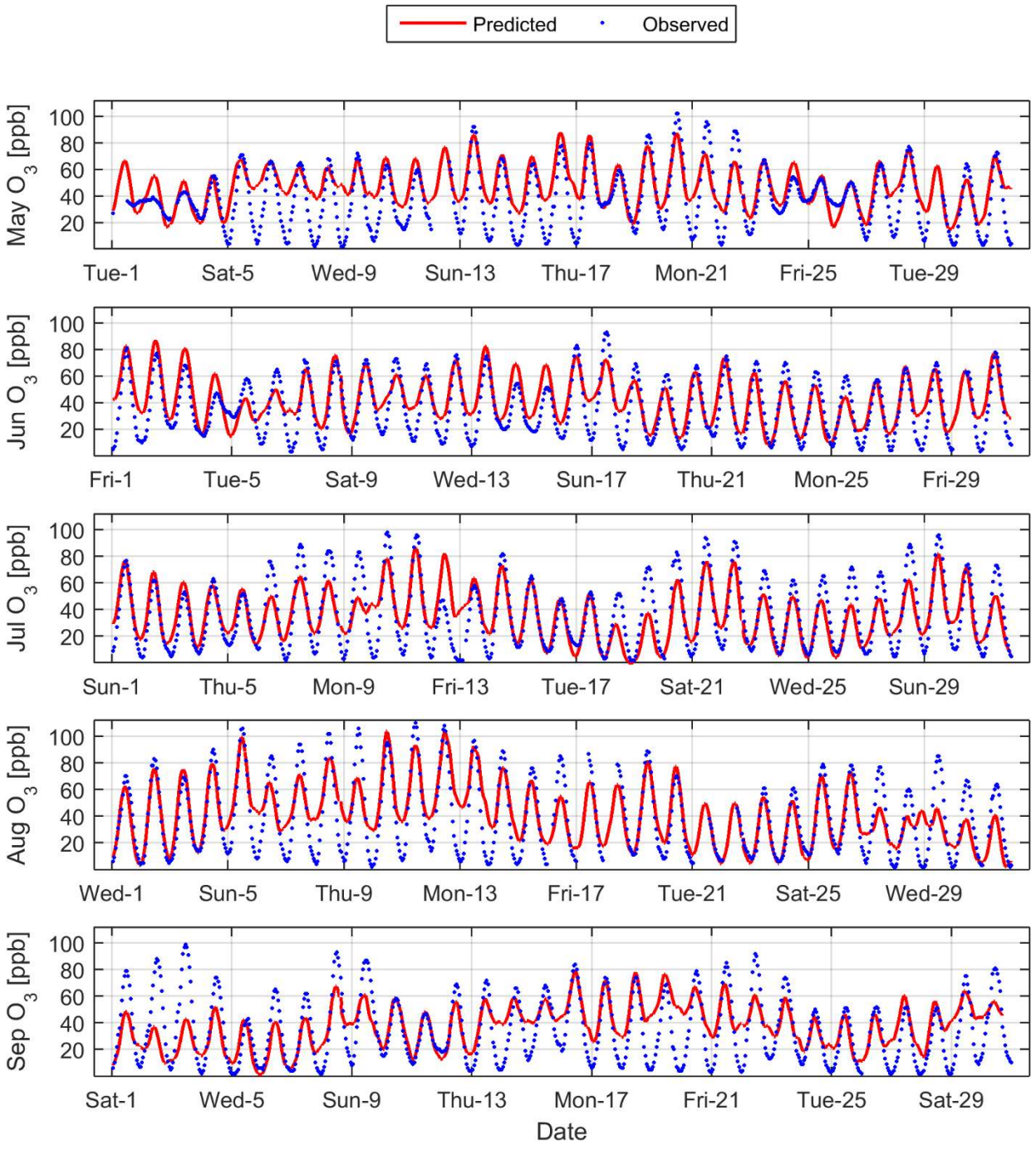

Figure 36: 2012 8-hour Ozone model prediction and measurement comparison at Fontana

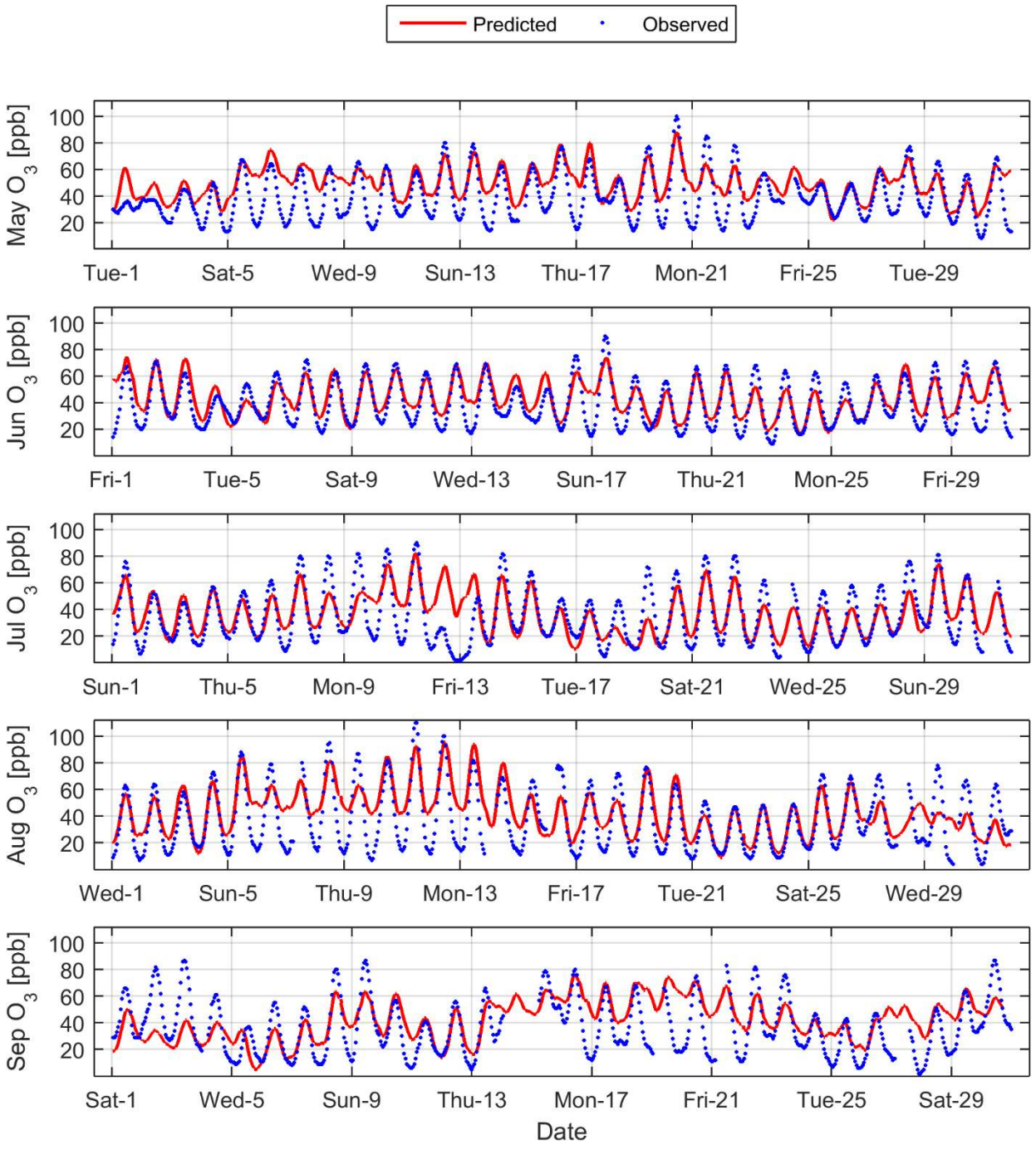

Figure 37: 2012 8-hour Ozone model prediction and measurement comparison at Glendora

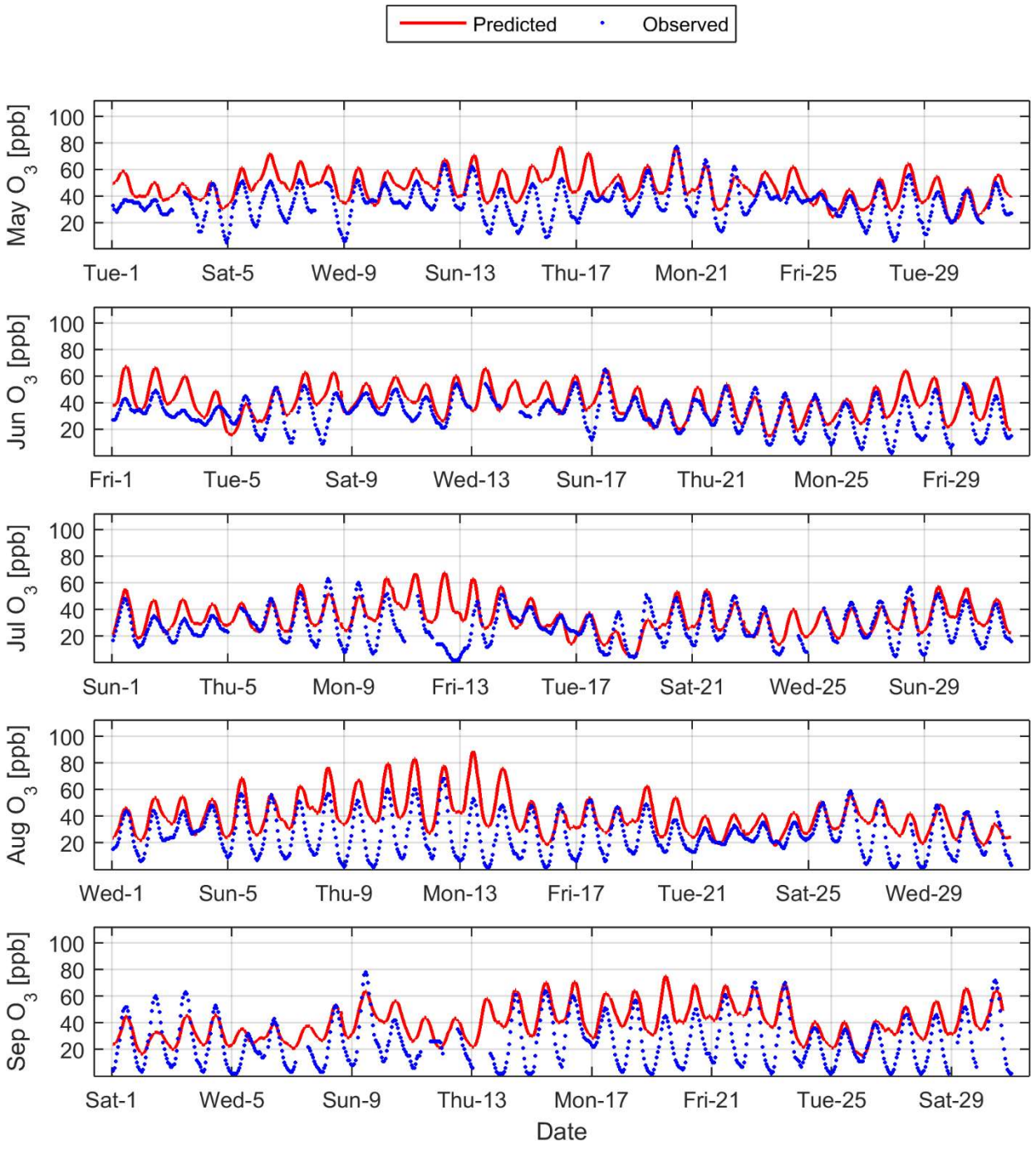

Figure 38: 2012 8-hour Ozone model prediction and measurement comparison at La Habra

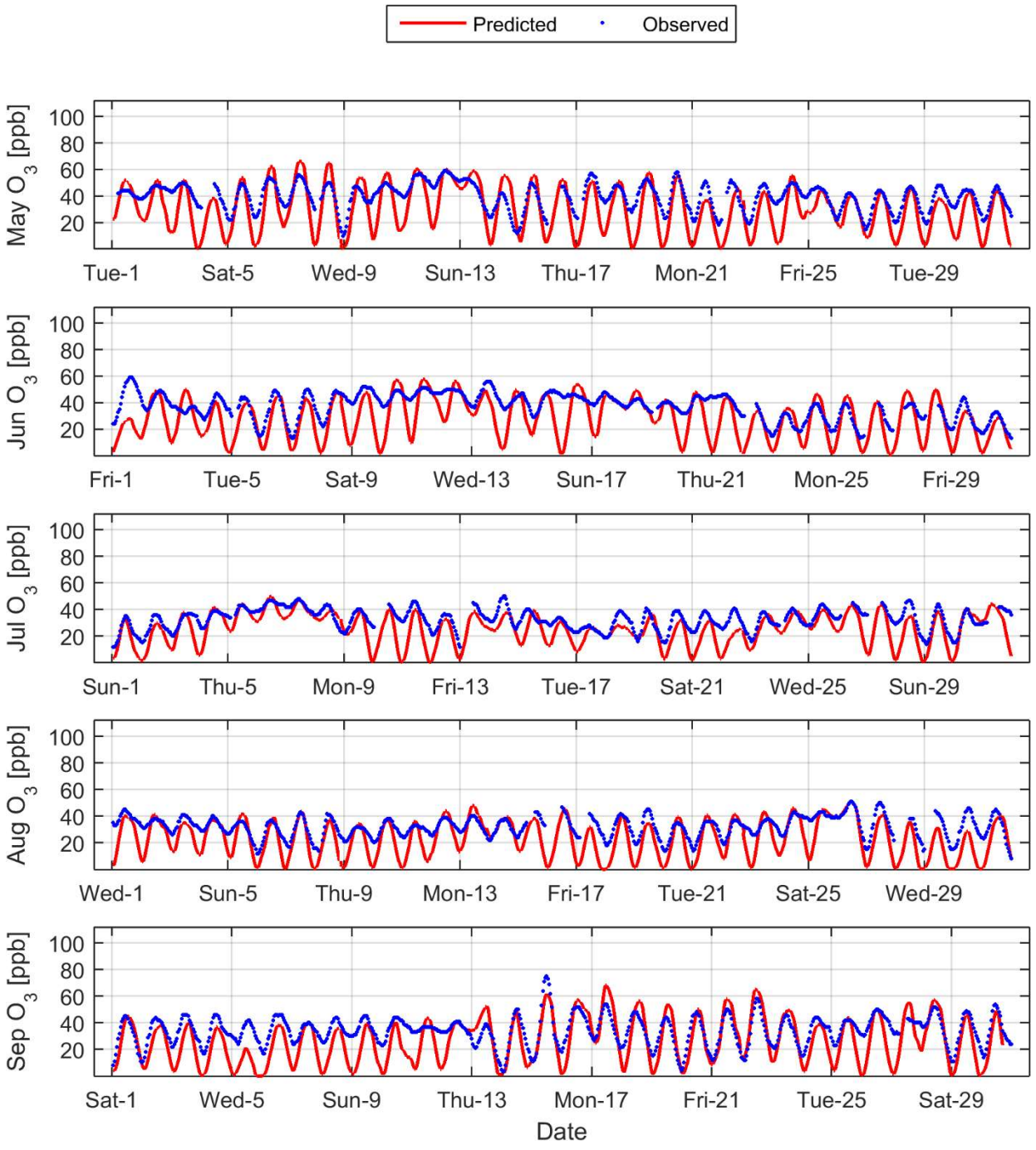

Figure 39: 2012 8-hour Ozone model prediction and measurement comparison at LAX

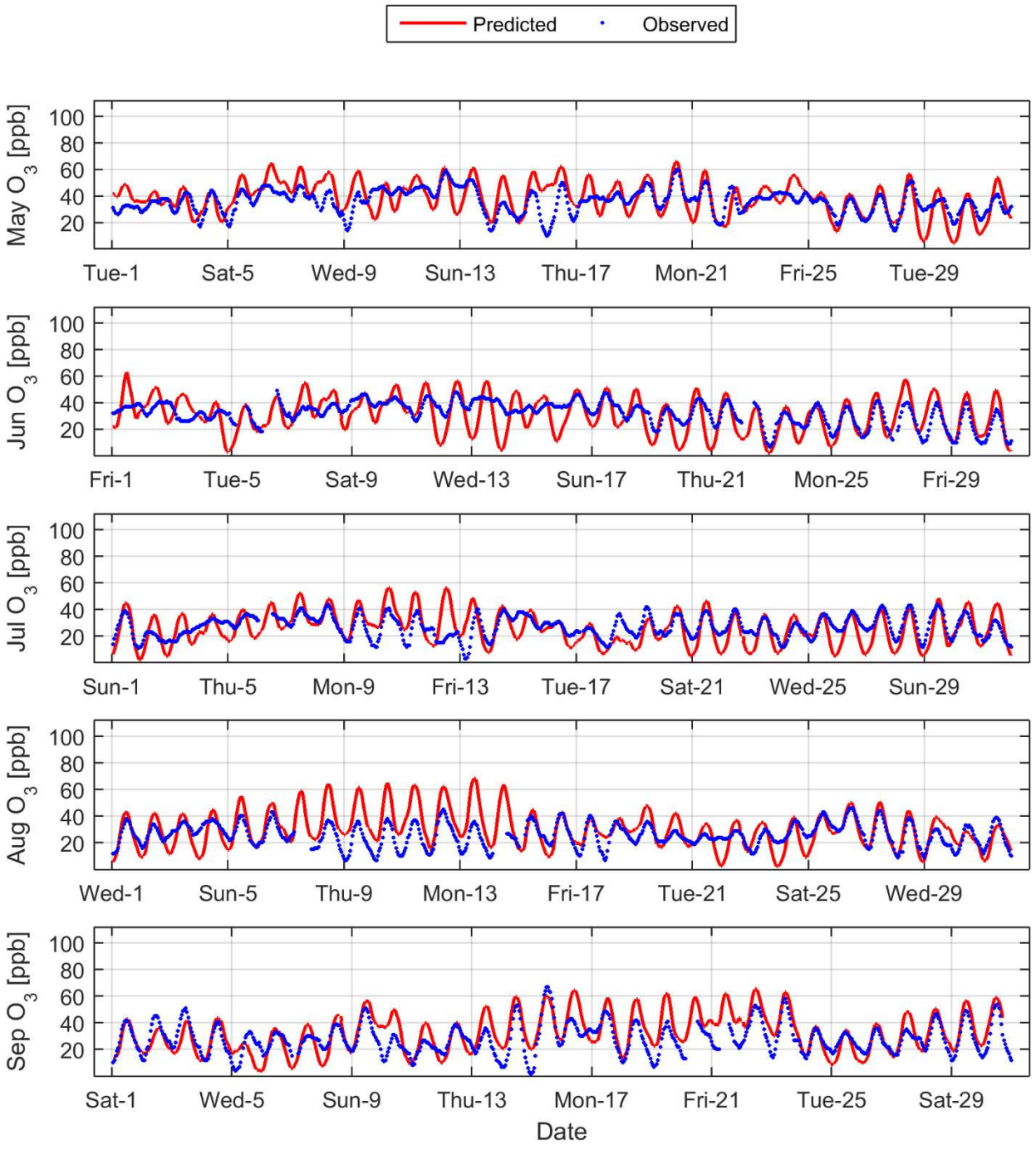

Figure 40: 2012 8-hour Ozone model prediction and measurement comparison at Long Beach

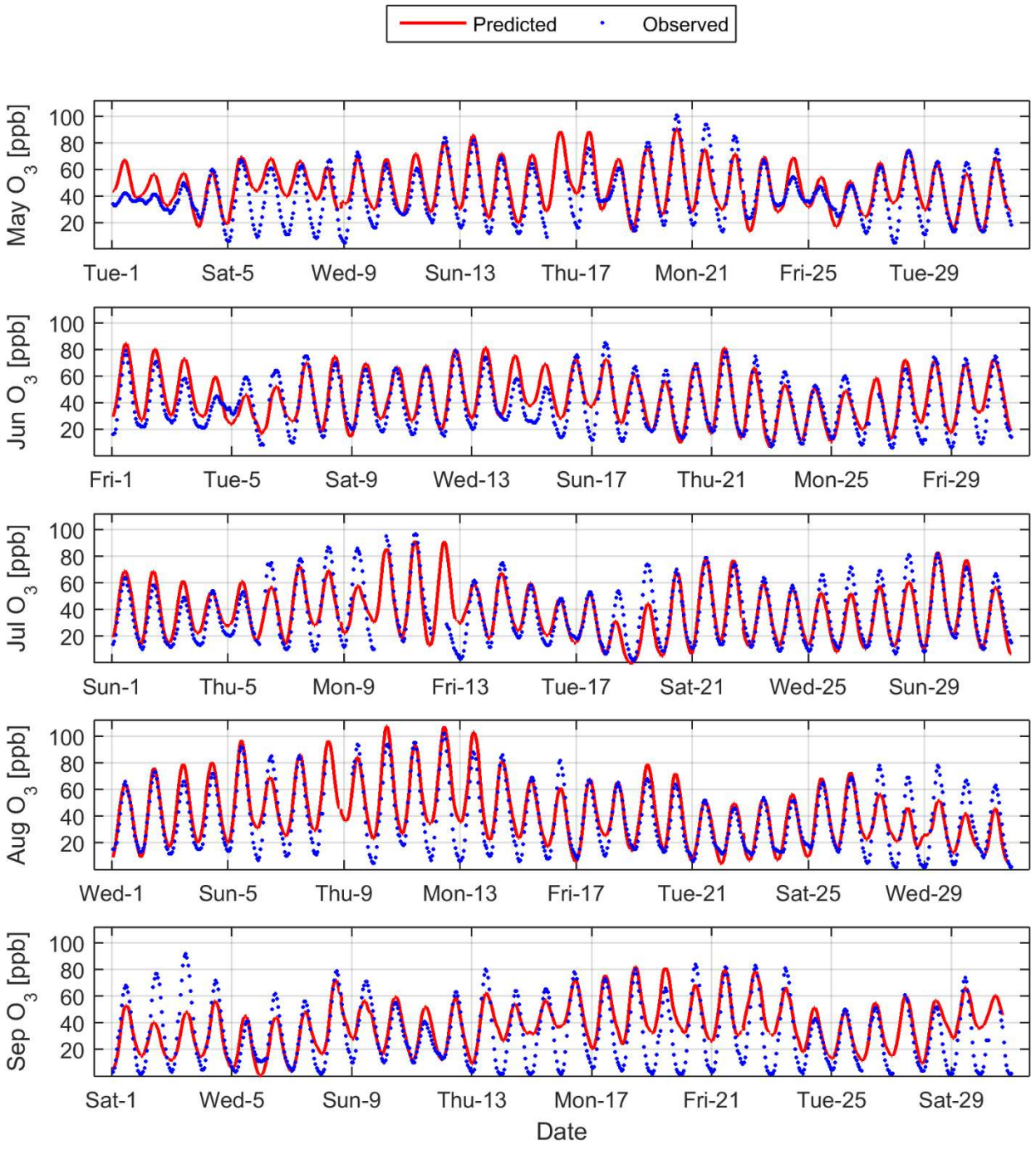

Figure 41: 2012 8-hour Ozone model prediction and measurement comparison at Mira Loma

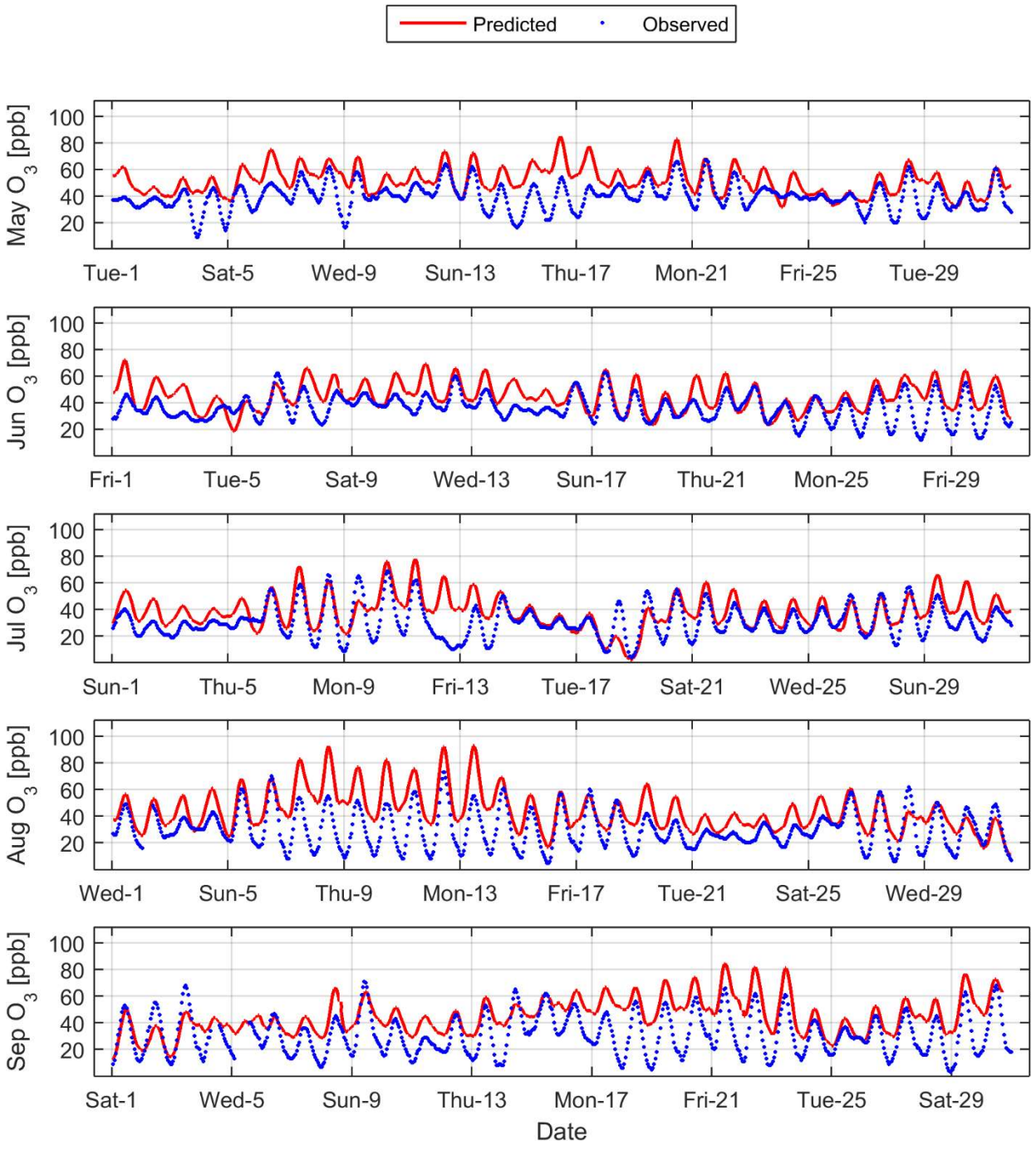

Figure 42: 2012 8-hour Ozone model prediction and measurement comparison at Mission Viejo

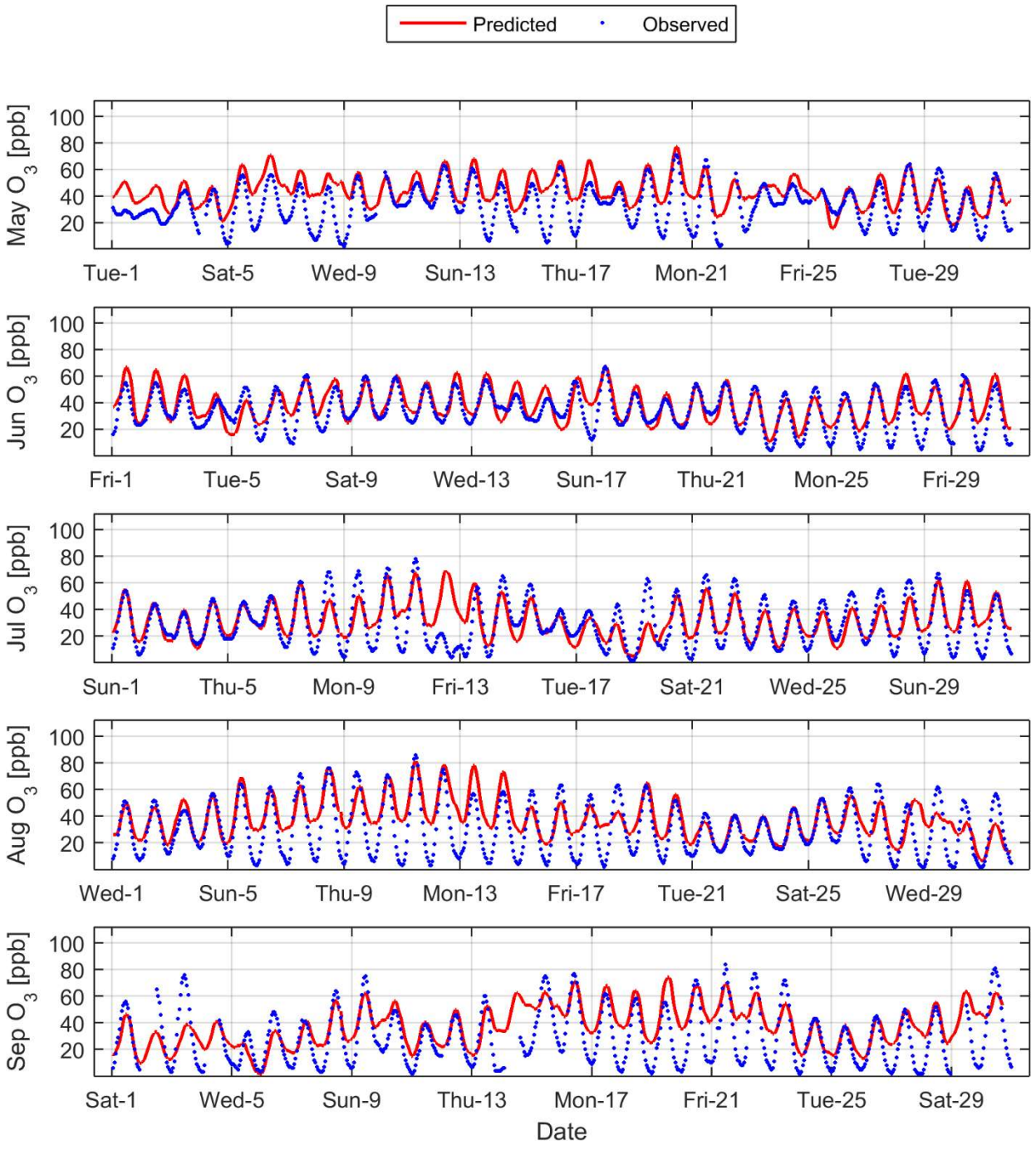

Figure 43: 2012 8-hour Ozone model prediction and measurement comparison at Pasadena

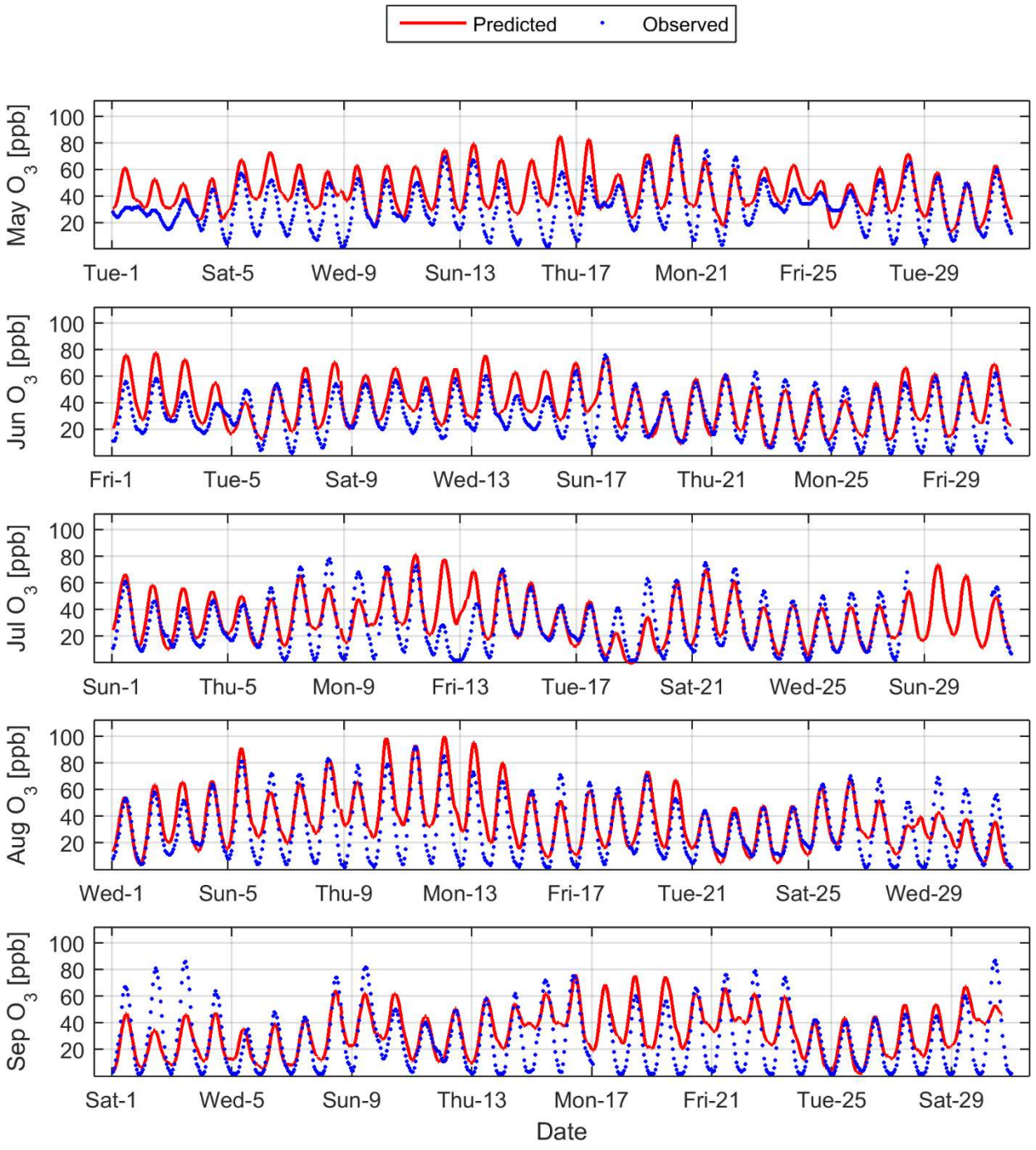

Figure 44: 2012 8-hour Ozone model prediction and measurement comparison at Pomona

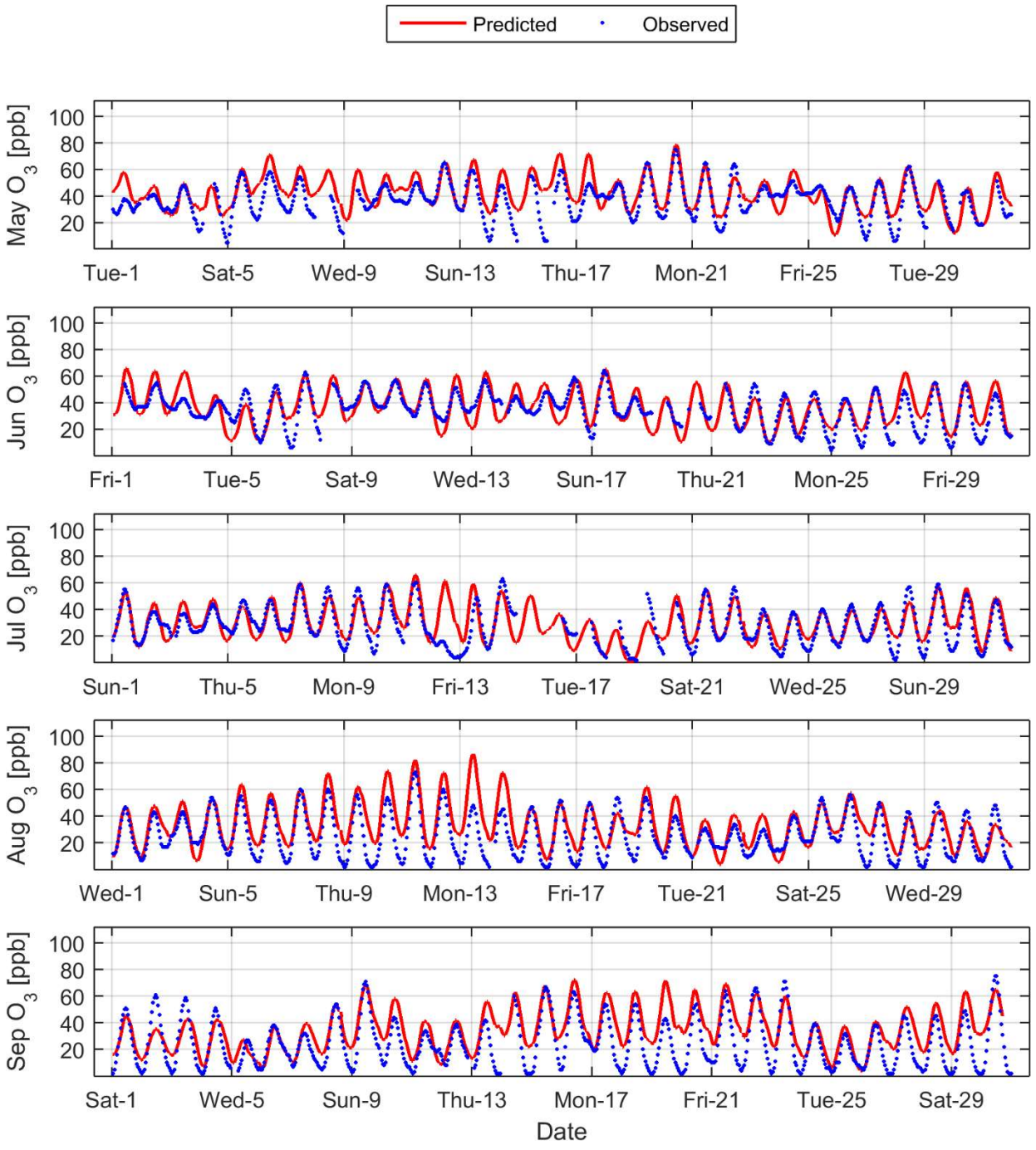

Figure 45: 2012 8-hour Ozone model prediction and measurement comparison at Pico Rivera

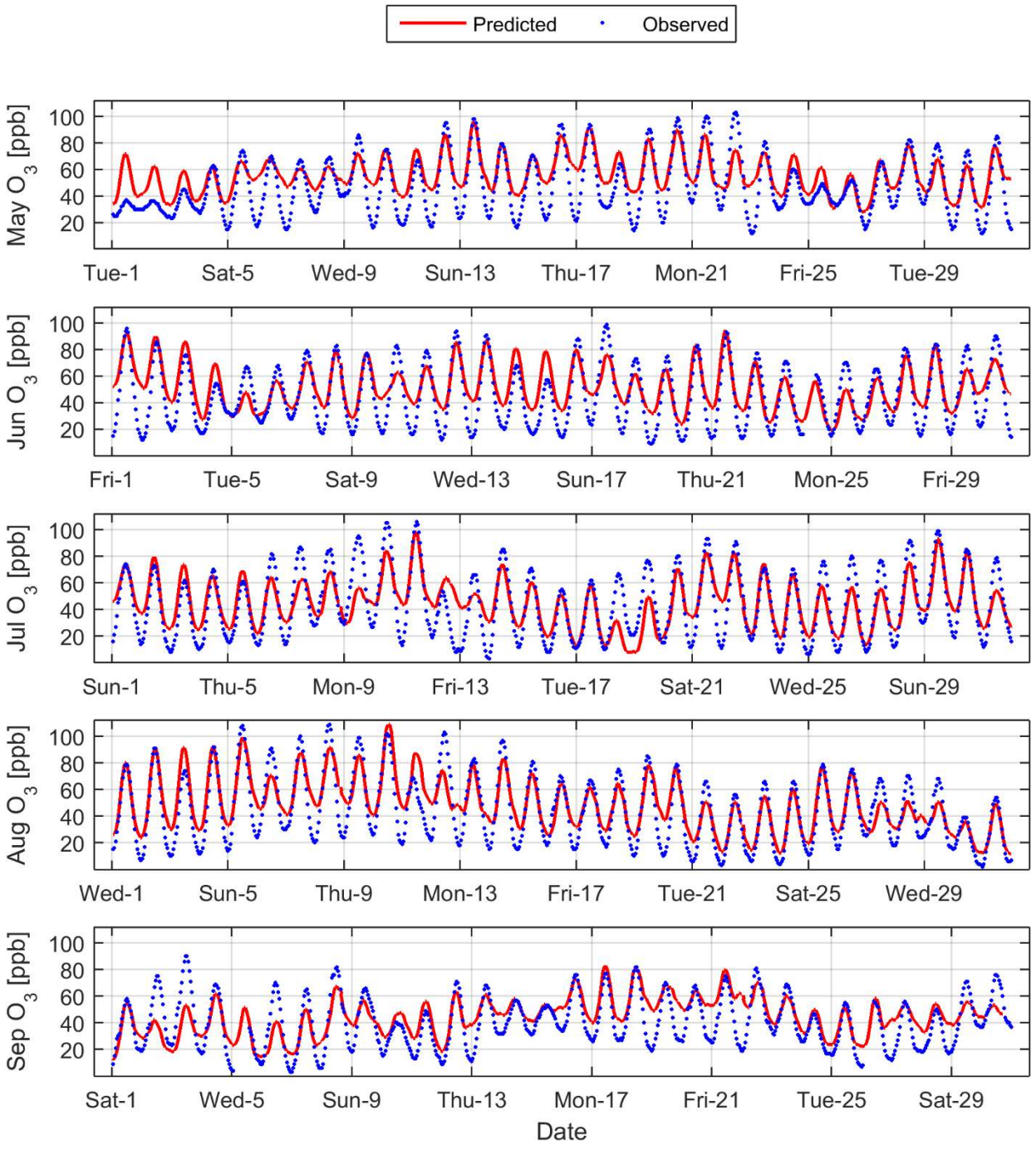

Figure 46: 2012 8-hour Ozone model prediction and measurement comparison at Redlands

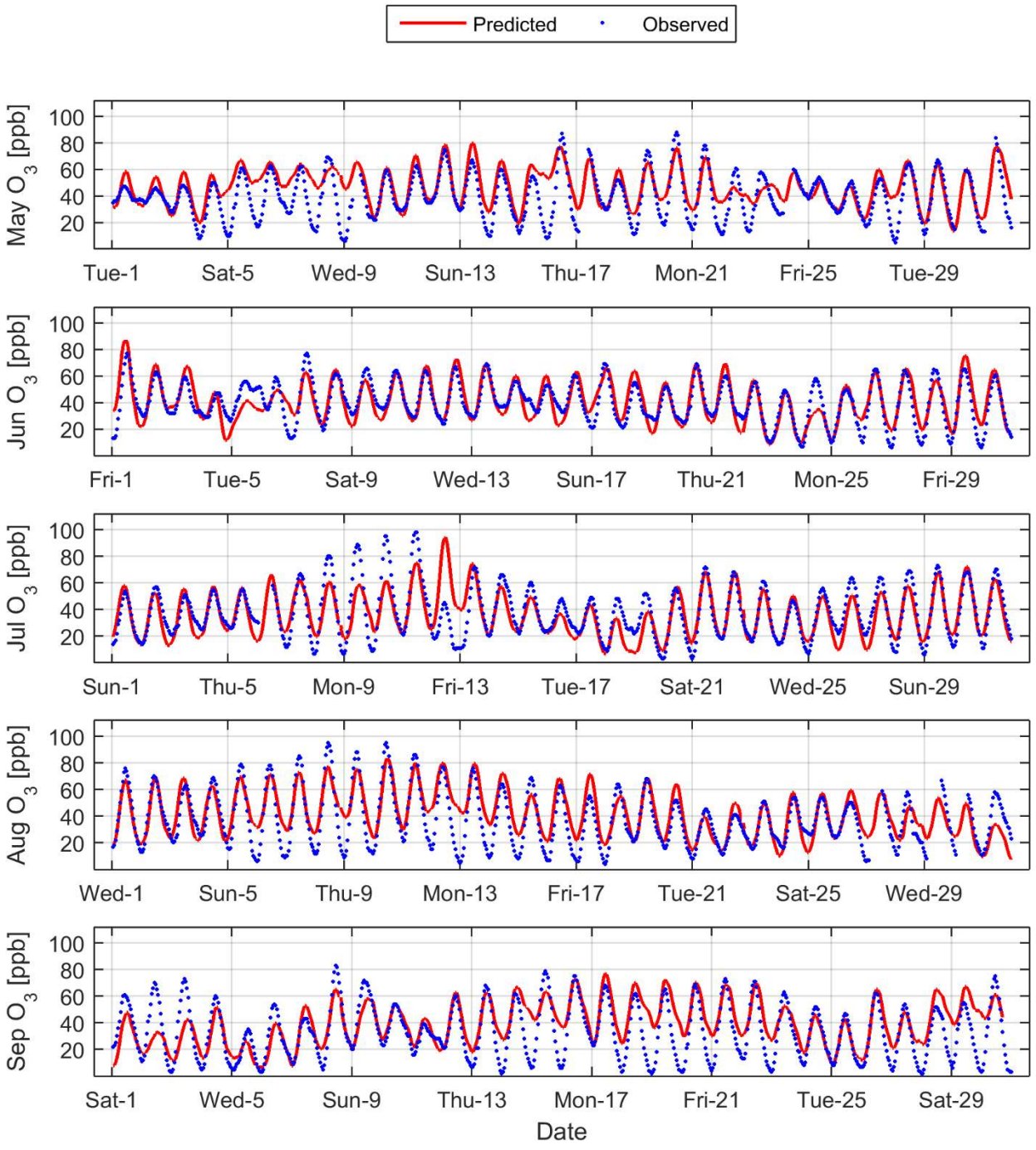

Figure 47: 2012 8-hour Ozone model prediction and measurement comparison at Reseda

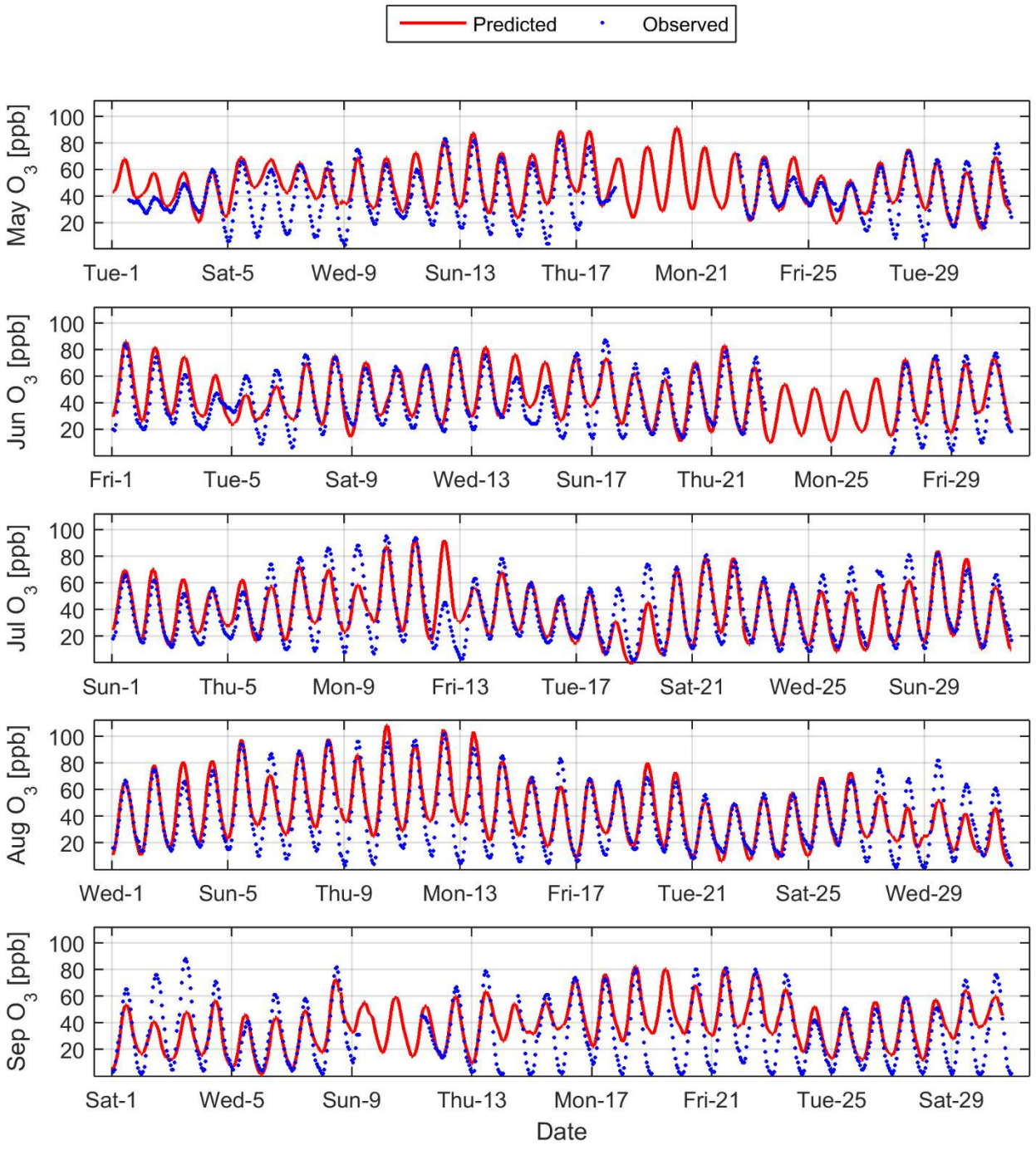

Figure 48: 2012 8-hour Ozone model prediction and measurement comparison at Riverside

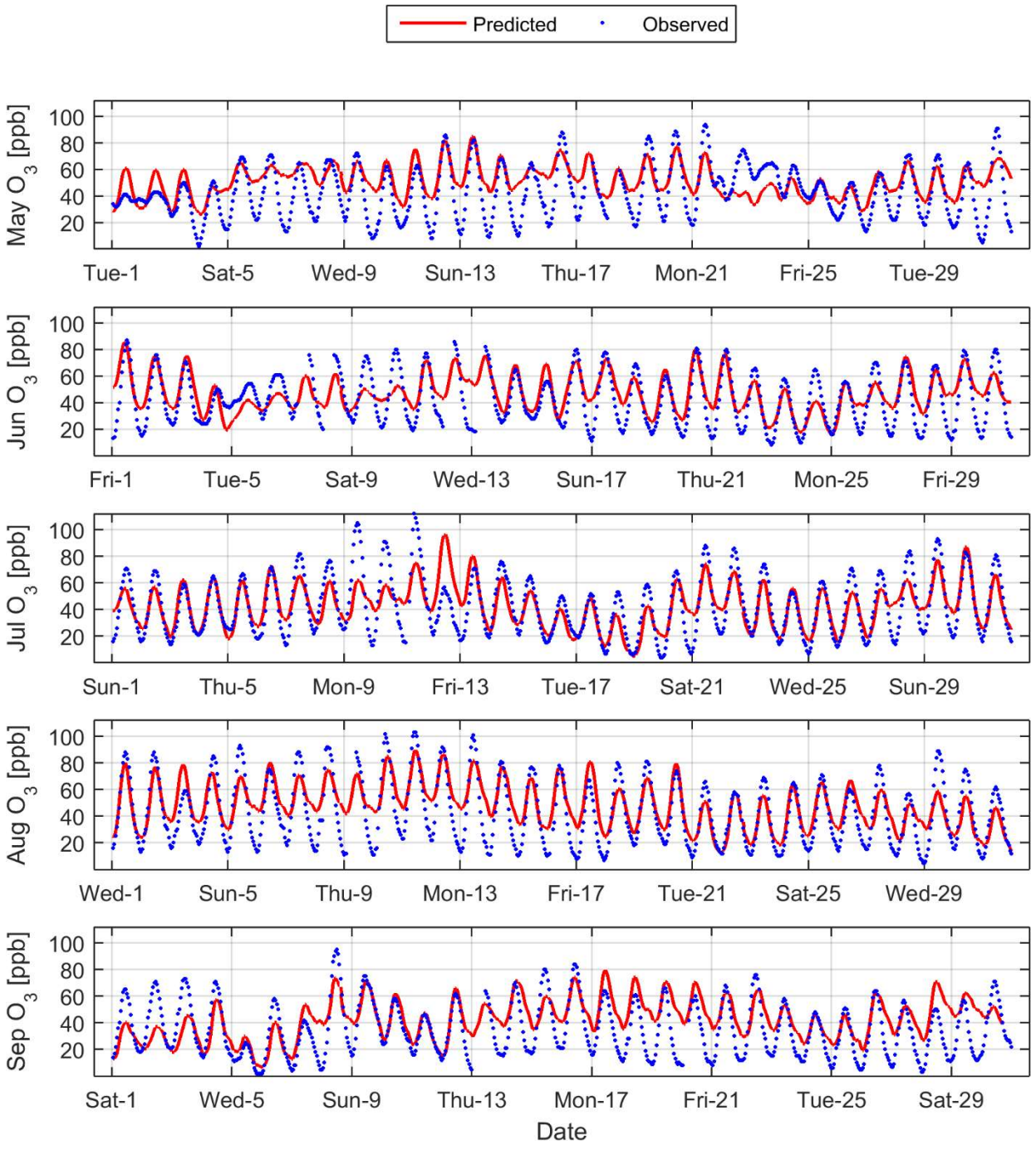

Figure 49: 2012 8-hour Ozone model prediction and measurement comparison at Santa Clarita

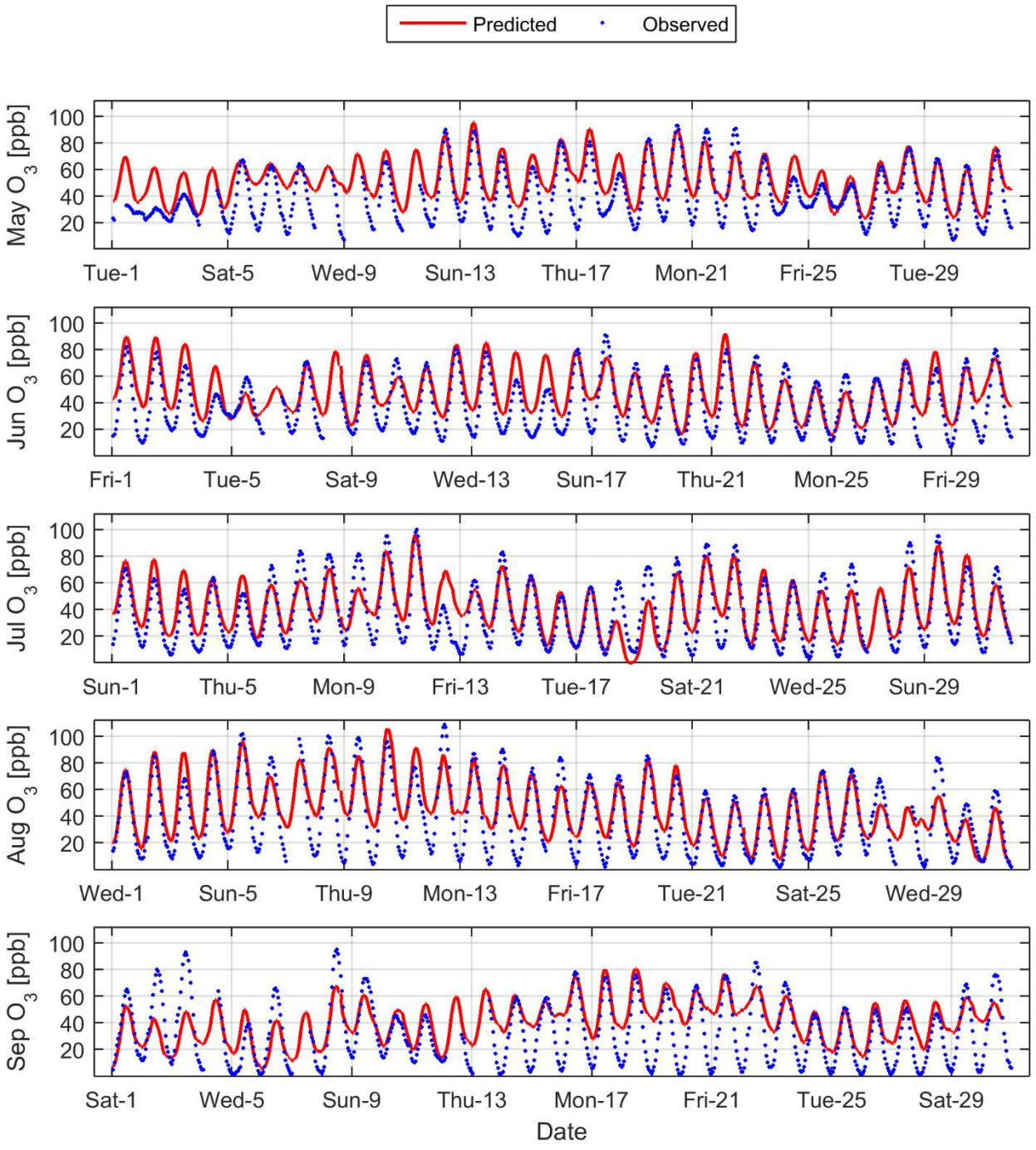

Figure 50: 2012 8-hour Ozone model prediction and measurement comparison at San Bernardino

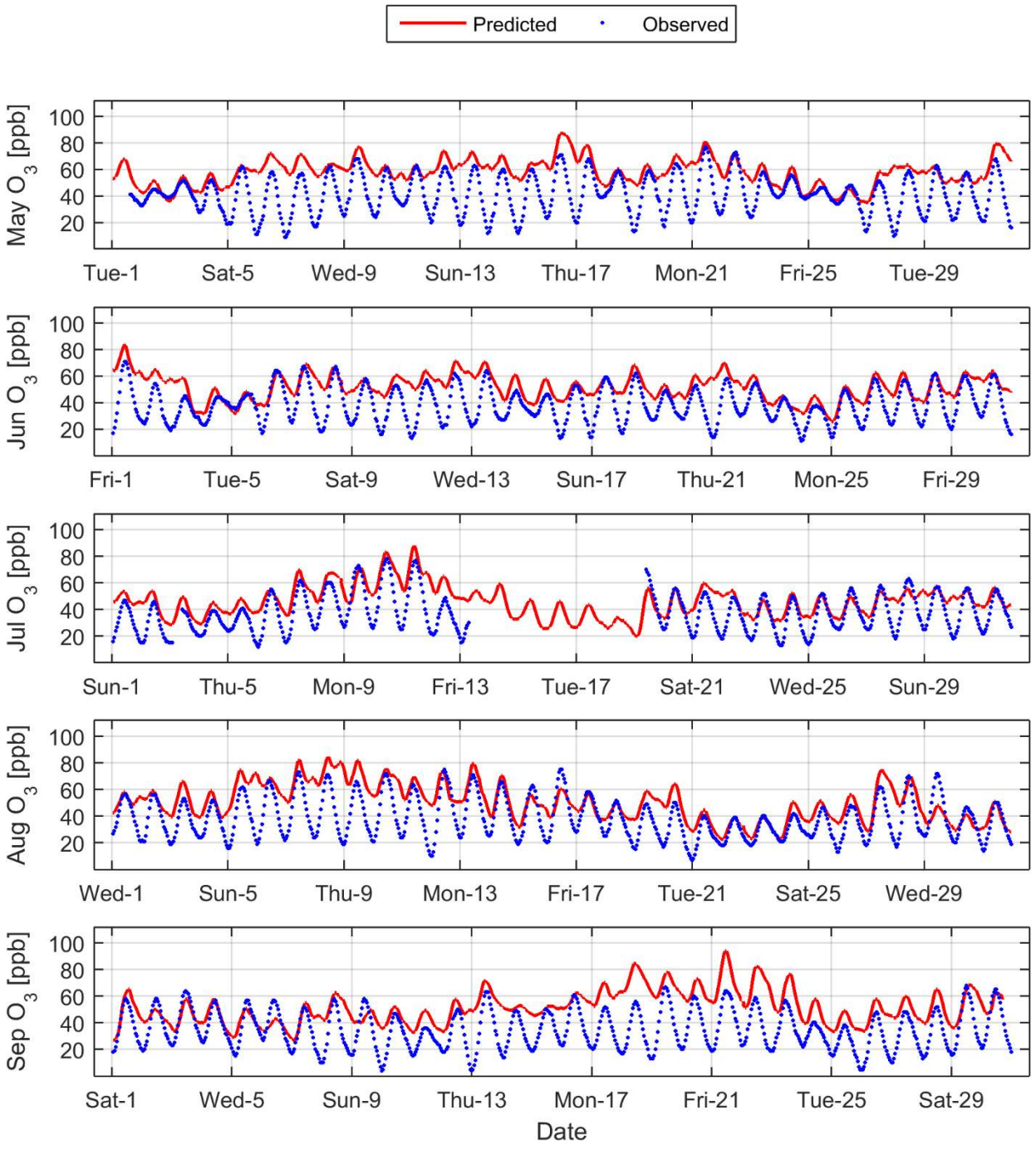

Figure 51: 2012 8-hour Ozone model prediction and measurement comparison at Temecula

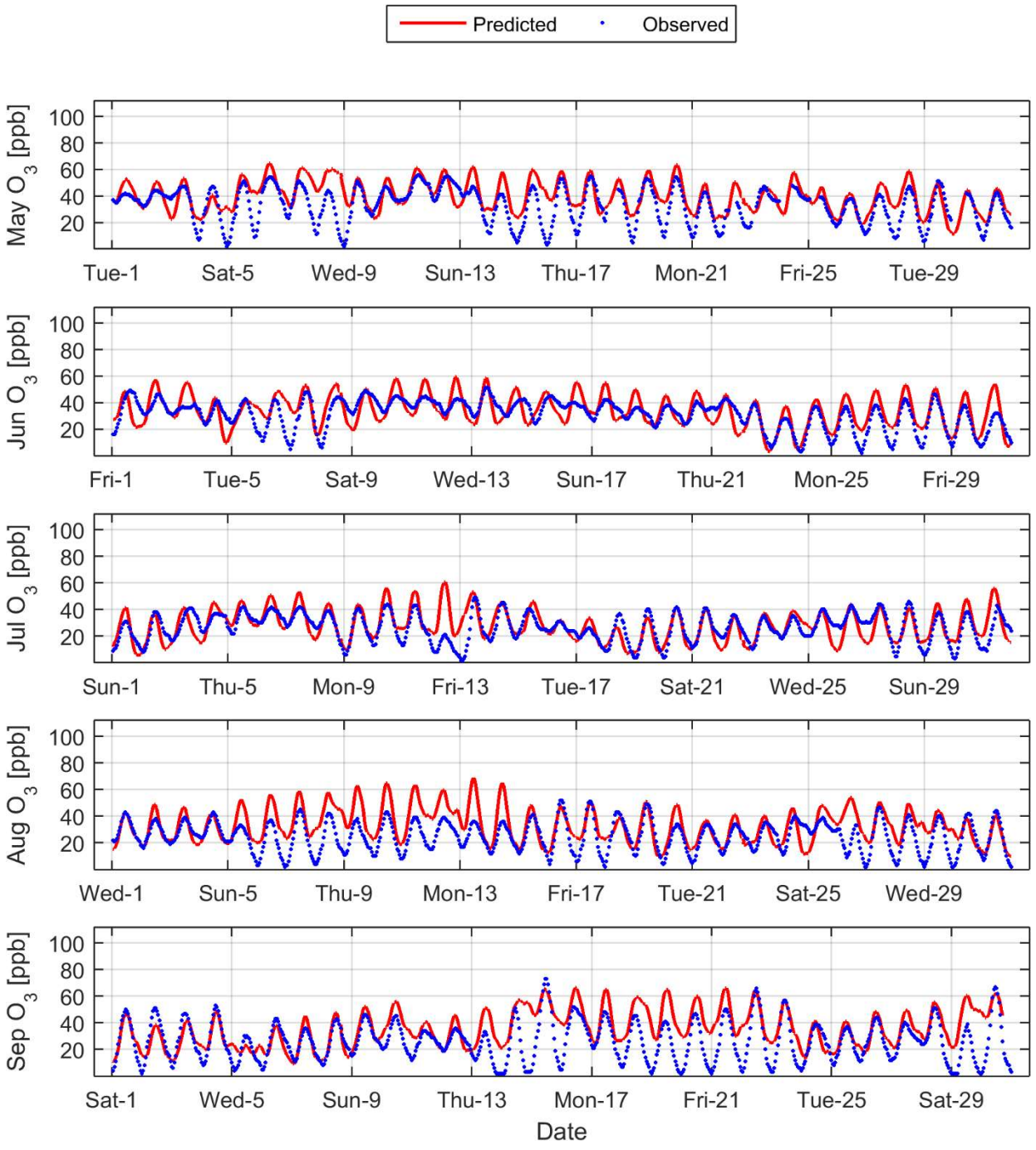

Figure 52: 2012 8-hour Ozone model prediction and measurement comparison at West Los Angeles

Attachment 3

DRAFT CEPA SOURCE LEVEL EMISSIONS REDUCTION SUMMARY

1. 2031 8-hour Ozone Attainment Scenario

2. 2023 8-hour Ozone Attainment Scenario

3. 2022 1-hour Ozone Attainment Scenario

1. 2031 8-hour Ozone Attainment Scenario

Run Date: 12/2/2016 6:11:08 PM

(P2016sy CepaV02 SIC / Nov 2014)
M:\SYan\2016AQMP\CM\D16P_s6f_31b_2\cf2031b_2_D16P_s6f.txt
M:\SYan\2016AQMP\CM\D16P_s6f_31b_2\master.txt
M:\SYan\2016AQMP\ARBdump0616r2\sc\ems31sc.txt
M:\SYan\2016AQMP\CM\D16P_s6f_31b_2\scen6f.txt
M:\SYan\2016AQMP\CM\D16P_s6f_31b_2\impact_rule.txt
M:\SYan\2016AQMP\CM\D16P_s6f_31b_2\lineitem_p16_aa_shaved.prn
M:\SYan\2016AQMP\CM\D16P_s6f_31b_2\lineitem_p16_pl_shaved.prn

Year 2031 Emission Reductions Excluding Natural Sources by Control Measure in the South Coast Air Basin (Planning Inventory - Tons/Day)

(A) Reductions Without Overlapping/Double-Counting With Other Control Measures (1)

		(Reductions - Tons/Day)			
Measure	Name	VOC	NOx	CO	NO2
BA-01	MOB-14 (Existing Projects) - School Buses - Diesel	0.00	0.07	0.01	0.07
BA-04	MOB-14 (Existing Projects) - Freight Locomotives (Prop1B/Moyer)	0.06	1.22	0.25	1.22
BA-06	MOB-14 (Existing Projects) - Offroad Equipment - Construction/Min	0.55	2.40	7.43	1.53
BA-07	MOB-14 (Existing Projects) - Harborcraft (Fishing Vessels)	0.00	0.00	0.00	0.00
ECC-02	Co-Benefits from Energy Efficiency Measures - Res/Comm Bldg	0.29	1.15	9.00	1.74
ECC-03	Additional Enhancement of Building Energy Efficiency	0.31	2.11	9.79	3.29
CMB-01	Zero and Near-Zero Emission Technologies at Stationary Sources	2.80	5.96	10.83	5.82
CMB-02	Commercial and Multi-Residential Space & Water Heating	0.36	2.80	3.14	3.89
CMB-03	Emission Reductions From Non-Refinery Flares	0.40	1.50	1.07	1.50
CMB-04	Emission Reductions From Restaurant Burners and Residential Cooki	0.12	1.60	0.73	1.60
FUG-01	Improved Leak Detection and Repair	2.00	0.00	0.00	0.00
CTS-01	Further Reduction from Coatings, Solvents, Adhesives & Lubricants	2.00	0.00	0.00	0.00
BCM-01	Further Emission Reductions from Commercial Cooking	0.00	0.00	0.00	0.00
BCM-10	Emission Reduction from Greenwaste Composting	1.80	0.00	0.00	0.00
ARB-LDV	On-Road Light Duty Vehicles	13.17	5.61	83.73	6.11
ARB-HDV	On-Road Heavy Duty Vehicles	2.43	27.02	19.08	27.63
ARB-OFRD	Offroad Equipment (All except Airc/Loco/OGV)	32.12	21.00	274.88	16.70
CP	Consumer Products	4.99	0.00	0.00	0.00
FIS-AIRC	Federal/International - Aircrafts	2.90	13.00	29.92	13.00
FIS-LOCO	Federal/International - Locomotives	0.33	6.10	1.66	6.10
FIS-OGV	Federal/International - Ocean Going Vessels	2.68	14.98	4.85	14.98
MOB-10	Extension of the SOON Provision	0.25	1.91	2.14	1.33
MOB-11	Extended Exchange Program	1.86	1.00	17.16	0.86
MOB-14a	MOB-14 (Future Project Funding) - School Buses	0.01	0.32	0.03	0.32
MOB-14c	MOB-14 (Future Project Funding) - Cargo Handling Equipment	0.06	0.25	6.23	0.24
MOB-14d	MOB-14 (Future Project Funding) - Freight Locomotives - Road Haul	0.01	0.15	0.17	0.15
MOB-14e	MOB-14 (Future Project Funding) - Heavy Duty Diesel Trucks (>1400	0.12	3.41	1.14	3.47
Grand Total (Net)		71.59	113.55	483.25	111.57

Year 2031 Emission Reductions Excluding Natural Sources by Control Measure in the South Coast Air Basin (Planning Inventory - Tons/Day)

(B) Reductions With Overlapping/Double-Counting With Other Control Measures (2)

		(Reductions - Tons/Day)			
Measure	Name	VOC	NOx	CO	NO2
BA-01	MOB-14 (Existing Projects) - School Buses - Diesel	0.00	0.07	0.01	0.07
BA-04	MOB-14 (Existing Projects) - Freight Locomotives (Prop1B/Moyer)	0.06	1.22	0.25	1.22
BA-06	MOB-14 (Existing Projects) - Offroad Equipment - Construction/Min	0.55	2.40	7.43	1.53
BA-07	MOB-14 (Existing Projects) - Harborcraft (Fishing Vessels)	0.00	0.00	0.00	0.00
ECC-02	Co-Benefits from Energy Efficiency Measures - Res/Comm Bldg	0.29	1.15	9.00	1.74
ECC-03	Additional Enhancement of Building Energy Efficiency	0.35	2.37	11.02	3.70
CMB-01	Zero and Near-Zero Emission Technologies at Stationary Sources	2.80	5.96	10.83	5.82
CMB-02	Commercial and Multi-Residential Space & Water Heating	0.50	4.08	4.78	5.77
CMB-03	Emission Reductions From Non-Refinery Flares	0.40	1.50	1.07	1.50
CMB-04	Emission Reductions From Restaurant Burners and Residential Cooki	0.18	2.21	1.04	2.21
FUG-01	Improved Leak Detection and Repair	2.00	0.00	0.00	0.00
CTS-01	Further Reduction from Coatings, Solvents, Adhesives & Lubricants	2.00	0.00	0.00	0.00
BCM-01	Further Emission Reductions from Commercial Cooking	0.00	0.00	0.00	0.00
BCM-10	Emission Reduction from Greenwaste Composting	1.80	0.00	0.00	0.00
ARB-LDV	On-Road Light Duty Vehicles	13.17	5.61	83.73	6.11
ARB-HDV	On-Road Heavy Duty Vehicles	2.43	27.02	19.08	27.63
ARB-OFRD	Offroad Equipment (All except Airc/Loco/OGV)	32.12	21.00	274.88	16.70
CP	Consumer Products	4.99	0.00	0.00	0.00
FIS-AIRC	Federal/International - Aircrafts	2.90	13.00	29.92	13.00
FIS-LOCO	Federal/International - Locomotives	0.33	6.10	1.66	6.10
FIS-OGV	Federal/International - Ocean Going Vessels	2.68	14.98	4.85	14.98
MOB-10	Extension of the SOON Provision	0.45	3.47	3.89	2.42
MOB-11	Extended Exchange Program	3.38	1.81	31.15	1.55
MOB-14a	MOB-14 (Future Project Funding) - School Buses	0.01	0.32	0.03	0.32
MOB-14c	MOB-14 (Future Project Funding) - Cargo Handling Equipment	0.11	0.52	11.42	0.50
MOB-14d	MOB-14 (Future Project Funding) - Freight Locomotives - Road Haul	0.01	0.21	0.25	0.21
MOB-14e	MOB-14 (Future Project Funding) - Heavy Duty Diesel Trucks (>1400	0.29	8.12	2.71	8.26
Grand Total (with potential overlapping)		73.78	123.12	508.99	121.37

EMISSION SUMMARY FOR
(POINT, AREA, MOBILE SOURCE, AND OFF-ROAD MV)

BASELINE EMISSIONS

	VOC	NOx	CO	NO2
Point source	33.63	7.67	35.18	7.67
Area source	197.76	26.54	118.82	31.66
RECLAIM	0.00	14.90	0.00	14.90
Total Stationary	231.39	49.10	154.00	54.23
On-road	49.48	65.00	304.36	67.70
Off-road	76.14	79.41	630.55	68.98
Aircraft	4.50	20.19	46.47	20.19
TOTAL	361.51	213.70	1135.37	211.10

EMISSION REDUCTIONS

Point source	0.91	2.72	4.89	2.72
Area source	14.15	12.40	29.68	15.12
RECLAIM	0.00	5.14	0.00	5.14
Total Stationary	15.06	20.26	34.56	22.98
On-road	15.73	36.42	103.99	37.61
Off-road	37.91	49.01	314.78	43.12
Aircraft	2.90	13.00	29.92	13.00
TOTAL	71.59	118.69	483.25	116.71

REMAINING EMISSIONS

Point source	32.72	4.95	30.29	4.95
Area source	183.61	14.14	89.14	16.54
RECLAIM	0.00	9.76	0.00	9.76
Total Stationary	216.33	28.85	119.43	31.25
On-road	33.74	28.58	200.37	30.09
Off-road	38.24	30.40	315.77	25.86
Aircraft	1.60	7.19	16.54	7.19
TOTAL	289.91	95.01	652.12	94.39
NSR/Set-Aside	4.42	1.03	0.00	1.03
Public Funding	0.00	0.00	0.00	0.00
GRAND TOTAL (T/D)	294.33	96.04	652.12	95.42
Mobility Adjustments (3)	0.00	0.00	0.00	0.00

(1) Emission reductions for individual measures were estimated based on the sequence of listing contained here. When the sequence changes, reductions from each measure could be affected, but the net total remain the same. The purpose of this table is to estimate total emission reductions without overlapping or double-counting between measures.
(2) Emission reductions for individual measures were estimated in the absence of other measures. Therefore, the sequence of listing does not affect the reduction estimates. The purpose of this table is to provide emission reduction estimates for Appendix IV control measure summary tables as well as cost effectiveness analysis.
(3) Mobility Adjustment includes TCM-01, ATT-01, ATT-02, ATT-05 and adjustments are reflected in the CEPA baseline beyond year 2000.

EMISSION SUMMARY BY AGENCY FOR
EPA, ARB AND SCAQMD

BASELINE EMISSIONS BASE EMISSIONS	VOC	NOx	CO	NO2
EPA	19.08	63.99	216.42	63.36
ARB	211.53	102.82	765.52	95.27
SCAQMD (1)	130.90	46.89	153.44	52.46
TOTAL (2)	361.51	213.70	1135.38	211.09
EMISSION REDUCTIONS				
EPA	11.15	43.77	112.57	43.47
ARB	51.47	55.38	336.28	50.82
SCAQMD	8.98	19.55	34.41	22.42
TOTAL	71.60	118.70	483.26	116.71
REMAINING EMISSIONS				
EPA	7.93	20.22	103.85	19.89
ARB	160.06	47.44	429.24	44.45
SCAQMD (1)	121.92	27.34	119.03	30.04
TOTAL (2)	289.91	95.00	652.12	94.38

(1) SCAQMD figures include RECLAIM
(2) Totals do not include the line items

2. 2023 8-hour Attainment Scenario

Run Date: 12/6/2016 12:19:06 PM

(P2016sy CepaV02 SIC / Nov 2014)
M:\SYan\2016AQMP\CM\D16P_s6f_23d\cf2023d_D16P_s6f.txt
M:\SYan\2016AQMP\CM\D16P_s6f_23d\master.txt
M:\SYan\2016AQMP\ARBdump0616r2\sc\ems23sc.txt
M:\SYan\2016AQMP\CM\D16P_s6f_23d\scen6f.txt
M:\SYan\2016AQMP\CM\D16P_s6f_23d\impact_rule.txt
M:\SYan\2016AQMP\CM\D16P_s6f_23d\lineitem_p16_aa_shaved.prn
M:\SYan\2016AQMP\CM\D16P_s6f_23d\lineitem_p16_pl_shaved.prn

Year 2023 Emission Reductions Excluding Natural Sources by Control Measure in the South Coast Air Basin (Planning Inventory - Tons/Day)

(A) Reductions Without Overlapping/Double-Counting With Other Control Measures (1)

		(Reductions - Tons/Day)			
Measure	Name	VOC	NOx	CO	NO2
BA-01	MOB-14 (Existing Projects) - School Buses - Diesel	0.00	0.17	0.01	0.17
BA-04	MOB-14 (Existing Projects) - Freight Locomotives (Prop1B/Moyer)	0.07	1.17	0.21	1.17
BA-06	MOB-14 (Existing Projects) - Offroad Equipment - Construction/Min	0.32	1.98	3.68	1.26
BA-07	MOB-14 (Existing Projects) - Harborcraft (Fishing Vessels)	0.22	2.28	0.91	1.95
ECC-02	Co-Benefits from Energy Efficiency Measures - Res/Comm Bldg	0.07	0.30	2.19	0.51
ECC-03	Additional Enhancement of Building Energy Efficiency	0.16	1.19	5.05	2.19
CMB-01	Zero and Near-Zero Emission Technologies at Stationary Sources	1.15	2.48	4.39	2.41
CMB-02	Commercial and Multi-Residential Space & Water Heating	0.13	1.12	1.22	1.79
CMB-03	Emission Reductions From Non-Refinery Flares	0.37	1.40	1.01	1.40
CMB-04	Emission Reductions From Restaurant Burners and Residential Cooki	0.06	0.80	0.37	0.80
FUG-01	Improved Leak Detection and Repair	2.00	0.00	0.00	0.00
CTS-01	Further Reduction from Coatings, Solvents, Adhesives & Lubricants	1.02	0.00	0.00	0.00
BCM-01	Further Emission Reductions from Commercial Cooking	0.00	0.00	0.00	0.00
BCM-10	Emission Reduction from Greenwaste Composting	1.50	0.00	0.00	0.00
ARB-LDV	On-Road Light Duty Vehicles	12.37	7.01	88.03	7.66
ARB-HDV	On-Road Heavy Duty Vehicles	4.03	37.41	28.54	38.48
ARB-OFRD	Offroad Equipment (All except Airc/Loco/OGV)	31.50	22.00	222.22	16.94
CP	Consumer Products	0.00	0.00	0.00	0.00
FIS-AIRC	Federal/International - Aircrafts	2.55	11.01	26.28	11.01
FIS-LOCO	Federal/International - Locomotives	0.18	3.09	0.36	3.09
FIS-OGV	Federal/International - Ocean Going Vessels	1.47	13.00	2.71	13.00
MOB-10	Extension of the SOON Provision	0.20	1.91	1.28	1.30
MOB-11	Extended Exchange Program	5.73	2.89	51.58	2.48
MOB-14a	MOB-14 (Future Project Funding) - School Buses	0.00	0.24	0.02	0.25
MOB-14c	MOB-14 (Future Project Funding) - Cargo Handling Equipment	0.04	0.18	2.85	0.18
MOB-14d	MOB-14 (Future Project Funding) - Freight Locomotives - Road Haul	0.01	0.25	0.10	0.25
MOB-14e	MOB-14 (Future Project Funding) - Heavy Duty Diesel Trucks (>1400	0.16	4.76	1.32	4.85
Grand Total (Net)		65.30	116.62	444.33	113.14

Year 2023 Emission Reductions Excluding Natural Sources by Control Measure in the South Coast Air Basin (Planning Inventory - Tons/Day)

(B) Reductions With Overlapping/Double-Counting With Other Control Measures (2)

		(Reductions - Tons/Day)			
Measure	Name	VOC	NOx	CO	NO2
BA-01	MOB-14 (Existing Projects) - School Buses - Diesel	0.00	0.17	0.01	0.17
BA-04	MOB-14 (Existing Projects) - Freight Locomotives (Prop1B/Moyer)	0.07	1.17	0.21	1.17
BA-06	MOB-14 (Existing Projects) - Offroad Equipment - Construction/Min	0.32	1.98	3.68	1.26
BA-07	MOB-14 (Existing Projects) - Harborcraft (Fishing Vessels)	0.22	2.28	0.91	1.95
ECC-02	Co-Benefits from Energy Efficiency Measures - Res/Comm Bldg	0.07	0.30	2.19	0.51
ECC-03	Additional Enhancement of Building Energy Efficiency	0.17	1.23	5.19	2.25
CMB-01	Zero and Near-Zero Emission Technologies at Stationary Sources	1.15	2.48	4.39	2.41
CMB-02	Commercial and Multi-Residential Space & Water Heating	0.15	1.29	1.43	2.09
CMB-03	Emission Reductions From Non-Refinery Flares	0.37	1.40	1.01	1.40
CMB-04	Emission Reductions From Restaurant Burners and Residential Cooki	0.07	0.87	0.41	0.87
FUG-01	Improved Leak Detection and Repair	2.00	0.00	0.00	0.00
CTS-01	Further Reduction from Coatings, Solvents, Adhesives & Lubricants	1.02	0.00	0.00	0.00
BCM-01	Further Emission Reductions from Commercial Cooking	0.00	0.00	0.00	0.00
BCM-10	Emission Reduction from Greenwaste Composting	1.50	0.00	0.00	0.00
ARB-LDV	On-Road Light Duty Vehicles	12.37	7.01	88.03	7.66
ARB-HDV	On-Road Heavy Duty Vehicles	4.03	37.41	28.54	38.48
ARB-OFRD	Offroad Equipment (All except Airc/Loco/OGV)	31.50	22.00	222.22	16.94
CP	Consumer Products	0.00	0.00	0.00	0.00
FIS-AIRC	Federal/International - Aircrafts	2.55	11.01	26.28	11.01
FIS-LOCO	Federal/International - Locomotives	0.18	3.09	0.36	3.09
FIS-OGV	Federal/International - Ocean Going Vessels	1.47	13.00	2.71	13.00
MOB-10	Extension of the SOON Provision	0.32	3.09	2.08	2.11
MOB-11	Extended Exchange Program	9.31	4.70	83.73	4.03
MOB-14a	MOB-14 (Future Project Funding) - School Buses	0.00	0.24	0.02	0.25
MOB-14c	MOB-14 (Future Project Funding) - Cargo Handling Equipment	0.06	0.32	4.64	0.31
MOB-14d	MOB-14 (Future Project Funding) - Freight Locomotives - Road Haul	0.01	0.25	0.10	0.25
MOB-14e	MOB-14 (Future Project Funding) - Heavy Duty Diesel Trucks (>1400	0.50	15.20	4.22	15.50
Grand Total (with potential overlapping)		69.40	130.47	482.36	126.71

EMISSION SUMMARY FOR
(POINT, AREA, MOBILE SOURCE, AND OFF-ROAD MV)

BASELINE EMISSIONS

	VOC	NOx	CO	NO2
Point source	31.85	7.24	33.82	7.24
Area source	189.26	27.39	118.86	35.07
RECLAIM	0.00	14.90	0.00	14.90
Total Stationary	221.10	49.53	152.69	57.21
On-road	67.68	88.01	458.44	92.58
Off-road	85.86	99.79	592.29	85.58
Aircraft	4.01	17.31	41.31	17.31
TOTAL	378.65	254.63	1244.73	252.67

EMISSION REDUCTIONS

Point source	0.57	1.88	2.49	1.88
Area source	5.90	5.40	11.75	7.22
RECLAIM	0.00	0.00	0.00	0.00
Total Stationary	6.46	7.28	14.24	9.10
On-road	16.57	49.59	117.92	51.41
Off-road	39.72	48.74	285.90	41.62
Aircraft	2.55	11.01	26.28	11.01
TOTAL	65.30	116.62	444.33	113.14

REMAINING EMISSIONS

Point source	31.28	5.36	31.33	5.36
Area source	183.36	21.99	107.12	27.85
RECLAIM	0.00	14.90	0.00	14.90
Total Stationary	214.64	42.25	138.45	48.10
On-road	51.12	38.41	340.52	41.18
Off-road	46.13	51.05	306.39	43.95
Aircraft	1.46	6.30	15.04	6.30
TOTAL	313.35	138.01	800.40	139.53
NSR/Set-Aside	4.52	3.08	0.00	3.08
Public Funding	0.00	0.00	0.00	0.00

GRAND TOTAL (T/D)	317.87	141.09	800.40	142.61
Mobility Adjustments (3)	0.00	0.00	0.00	0.00

(1) Emission reductions for individual measures were estimated based on the sequence of listing contained here. When the sequence changes, reductions from each measure could be affected, but the net total remain the same. The purpose of this table is to estimate total emission reductions without overlapping or double-counting between measures.
(2) Emission reductions for individual measures were estimated in the absence of other measures. Therefore, the sequence of listing does not affect the reduction estimates. The purpose of this table is to provide emission reduction estimates for Appendix IV control measure summary tables as well as cost effectiveness analysis.
(3) Mobility Adjustment includes TCM-01, ATT-01, ATT-02, ATT-05 and adjustments are reflected in the CEPA baseline beyond year 2000.

EMISSION SUMMARY BY AGENCY FOR
EPA, ARB AND SCAQMD

BASELINE EMISSIONS BASE EMISSIONS	VOC	NOx	CO	NO2
EPA	17.69	68.62	205.40	68.00
ARB	237.36	138.69	887.20	129.23
SCAQMD (1)	123.61	47.32	152.12	55.44
TOTAL (2)	378.66	254.63	1244.72	252.67
EMISSION REDUCTIONS				
EPA	9.17	37.53	93.48	37.34
ARB	50.91	72.10	336.67	66.93
SCAQMD	5.23	6.98	14.17	8.87
TOTAL	65.31	116.61	444.32	113.14
REMAINING EMISSIONS				
EPA	8.52	31.09	111.92	30.66
ARB	186.45	66.59	550.53	62.30
SCAQMD (1)	118.38	40.34	137.95	46.57
TOTAL (2)	313.35	138.02	800.40	139.53

(1) SCAQMD figures include RECLAIM
(2) Totals do not include the line items

3. 2022 1-hour Attainment Scenario

Run Date: 10/19/2016 11:11:16 AM
(P2016sy CepaV02 SIC / Nov 2014)
M:\SYan\2016AQMP\CM\D16P_s11rb_2022\cf2022_D16P_s11rb.txt
M:\SYan\2016AQMP\CM\D16P_s11rb_2022\master.txt
M:\SYan\2016AQMP\dump0616r\sc\ems22sc.txt
M:\SYan\2016AQMP\CM\D16P_s11rb_2022\scen11.txt
M:\SYan\2016AQMP\CM\D16P_s11rb_2022\impact_rule.txt
M:\SYan\2016AQMP\lineitem_p16_aa_shaved.prn
M:\SYan\2016AQMP\lineitem_p16_pl_shaved.prn

Year 2022 Emission Reductions Excluding Natural Sources by Control Measure in the South Coast Air Basin (Planning Inventory - Tons/Day)

(A) Reductions Without Overlapping/Double-Counting With Other Control Measures (1)

		(Reductions - Tons/Day)			
Measure	Name	VOC	NOx	CO	NO2
BA-01	MOB-14 (Existing Projects) - School Buses - Diesel	0.00	0.15	0.01	0.15
BA-04	MOB-14 (Existing Projects) - Freight Locomotives (Prop1B/Moyer)	0.06	1.01	0.18	1.01
BA-06	MOB-14 (Existing Projects) - Offroad Equipment - Construction/Min	0.27	1.72	2.95	1.10
BA-07	MOB-14 (Existing Projects) - Harborcraft (Fishing Vessels)	0.18	1.96	0.74	1.68
ECC-02	Co-Benefits from Energy Efficiency Measures - Res Bldg	0.06	0.26	1.87	0.45
ECC-03	Additional Enhancement of Building Energy Efficiency	0.14	1.03	4.31	1.92
CMB-01	Zero and Near-Zero Emission Technologies at Stationary Sources	1.00	2.14	3.78	2.09
CMB-02	Commercial and Multi-Residential Space & Water Heating	0.11	0.98	1.07	1.60
CMB-03	Emission Reductions From Non-Refinery Flares	0.37	1.40	1.01	1.40
CMB-04	Emission Reductions From Restaurant Burners and Residential Cooki	0.06	0.80	0.37	0.80
FUG-01	Improved Leak Detection and Repair	2.00	0.00	0.00	0.00
CTS-01	Further Reduction from Coatings, Solvents, Adhesives & Lubricants	1.01	0.00	0.00	0.00
BCM-01	Further Emission Reductions from Commercial Cooking	0.00	0.00	0.00	0.00
BCM-10	Emission Reduction from Greenwaste Composting	1.50	0.00	0.00	0.00
ARB-LDV	On-Road Light Duty Vehicles	0.00	0.00	0.00	0.00
ARB-HDV	On-Road Heavy Duty Vehicles (transit buses)	0.11	1.96	1.64	2.03
ARB-OFF1	Offroad Equipment (lawn & garden)	3.50	0.35	14.49	0.30
CP	Consumer Products	0.00	0.00	0.00	0.00
FIS-AIRC	Federal/International - Aircrafts	0.00	0.00	0.00	0.00
FIS-LOCO	Federal/International - Locomotives (Road Haul)	0.45	10.00	2.73	10.00
FIS-OGV	Federal/International - Ocean Going Vessels (at berth)	0.16	2.00	0.37	2.00
MOB-10	Extension of the SOON Provision	0.00	0.00	0.00	0.00
MOB-11	Extended Exchange Program (lawn & garden)	4.99	2.48	44.70	2.13
MOB-14a	MOB-14 (Future Project Funding) - School Buses	0.00	0.17	0.01	0.17
MOB-14c	MOB-14 (Future Project Funding) - Cargo Handling Equipment	0.03	0.17	2.24	0.16
MOB-14d	MOB-14 (Future Project Funding) - Freight Locomotives - Road Haul	0.00	0.05	0.01	0.05
MOB-14e	MOB-14 (Future Project Funding) - Heavy Duty Diesel Trucks (>1400	0.13	4.24	0.78	4.35
Grand Total (Net)		16.13	32.86	83.26	33.38

Year 2022 Emission Reductions Excluding Natural Sources by Control Measure in the South Coast Air Basin (Planning Inventory - Tons/Day)

(B) Reductions With Overlapping/Double-Counting With Other Control Measures (2)

		(Reductions - Tons/Day)			
Measure	Name	VOC	NOx	CO	NO2
BA-01	MOB-14 (Existing Projects) - School Buses - Diesel	0.00	0.15	0.01	0.15
BA-04	MOB-14 (Existing Projects) - Freight Locomotives (Prop1B/Moyer)	0.06	1.01	0.18	1.01
BA-06	MOB-14 (Existing Projects) - Offroad Equipment - Construction/Min	0.27	1.72	2.95	1.10
BA-07	MOB-14 (Existing Projects) - Harborcraft (Fishing Vessels)	0.18	1.96	0.74	1.68
ECC-02	Co-Benefits from Energy Efficiency Measures - Res Bldg	0.06	0.26	1.87	0.45
ECC-03	Additional Enhancement of Building Energy Efficiency	0.14	1.06	4.41	1.97
CMB-01	Zero and Near-Zero Emission Technologies at Stationary Sources	1.00	2.14	3.78	2.09
CMB-02	Commercial and Multi-Residential Space & Water Heating	0.12	1.11	1.22	1.82
CMB-03	Emission Reductions From Non-Refinery Flares	0.37	1.40	1.01	1.40
CMB-04	Emission Reductions From Restaurant Burners and Residential Cooki	0.07	0.86	0.40	0.86
FUG-01	Improved Leak Detection and Repair	2.00	0.00	0.00	0.00
CTS-01	Further Reduction from Coatings, Solvents, Adhesives & Lubricants	1.01	0.00	0.00	0.00
BCM-01	Further Emission Reductions from Commercial Cooking	0.00	0.00	0.00	0.00
BCM-10	Emission Reduction from Greenwaste Composting	1.50	0.00	0.00	0.00
ARB-LDV	On-Road Light Duty Vehicles	0.00	0.00	0.00	0.00
ARB-HDV	On-Road Heavy Duty Vehicles (transit buses)	0.11	1.96	1.64	2.03
ARB-OFF1	Offroad Equipment (lawn & garden)	3.50	0.35	14.49	0.30
CP	Consumer Products	0.00	0.00	0.00	0.00
FIS-AIRC	Federal/International - Aircrafts	0.00	0.00	0.00	0.00
FIS-LOCO	Federal/International - Locomotives (Road Haul)	0.45	10.00	2.73	10.00
FIS-OGV	Federal/International - Ocean Going Vessels (at berth)	0.16	2.00	0.37	2.00
MOB-10	Extension of the SOON Provision	0.00	0.00	0.00	0.00
MOB-11	Extended Exchange Program (lawn & garden)	5.52	2.64	47.45	2.26
MOB-14a	MOB-14 (Future Project Funding) - School Buses	0.00	0.22	0.01	0.23
MOB-14c	MOB-14 (Future Project Funding) - Cargo Handling Equipment	0.03	0.17	2.24	0.16
MOB-14d	MOB-14 (Future Project Funding) - Freight Locomotives - Road Haul	0.01	0.14	0.04	0.14
MOB-14e	MOB-14 (Future Project Funding) - Heavy Duty Diesel Trucks (>1400	0.13	4.24	0.78	4.35
Grand Total (with potential overlapping)		16.69	33.37	86.33	33.99

EMISSION SUMMARY FOR
(POINT, AREA, MOBILE SOURCE, AND OFF-ROAD MV)

BASELINE EMISSIONS

	VOC	NOx	CO	NO2
Point source	31.65	7.19	33.54	7.19
Area source	188.07	27.63	119.03	35.65
RECLAIM	0.00	14.90	0.00	14.90
Total Stationary	219.73	49.72	152.57	57.74
On-road	71.40	116.78	490.38	122.57
Off-road	88.02	110.92	588.68	95.96
Aircraft	3.92	16.91	40.52	16.91
TOTAL	383.07	294.33	1272.16	293.18

EMISSION REDUCTIONS

Point source	0.54	1.81	2.27	1.81
Area source	5.71	4.79	10.13	6.44
RECLAIM	0.00	0.00	0.00	0.00
Total Stationary	6.24	6.61	12.41	8.25
On-road	0.24	6.52	2.44	6.71
Off-road	9.64	19.73	68.42	18.43
Aircraft	0.00	0.00	0.00	0.00
TOTAL	16.13	32.86	83.26	33.38

REMAINING EMISSIONS

Point source	31.11	5.38	31.26	5.38
Area source	182.37	22.84	108.90	29.21
RECLAIM	0.00	14.90	0.00	14.90
Total Stationary	213.48	43.11	140.16	49.49
On-road	71.16	110.26	487.94	115.86
Off-road	78.39	91.18	520.26	77.53
Aircraft	3.92	16.91	40.52	16.91
TOTAL	366.95	261.47	1188.89	259.80
NSR/Set-Aside	4.52	3.08	0.00	3.08
Public Funding	0.00	0.00	0.00	0.00
GRAND TOTAL (T/D)	371.47	264.55	1188.89	262.88
Mobility Adjustments (3)	0.00	0.00	0.00	0.00

(1) Emission reductions for individual measures were estimated based on the sequence of listing contained here. When the sequence changes, reductions from each measure could be affected, but the net total remain the same. The purpose of this table is to estimate total emission reductions without overlapping or double-counting between measures.
(2) Emission reductions for individual measures were estimated in the absence of other measures. Therefore, the sequence of listing does not affect the reduction estimates. The purpose of this table is to provide emission reduction estimates for Appendix IV control measure summary tables as well as cost effectiveness analysis.
(3) Mobility Adjustment includes TCM-01, ATT-01, ATT-02, ATT-05 and adjustments are reflected in the CEPA baseline beyond year 2000.

EMISSION SUMMARY BY AGENCY FOR
EPA, ARB AND SCAQMD

BASELINE EMISSIONS BASE EMISSIONS	VOC	NOx	CO	NO2
EPA	18.18	83.56	205.63	83.17
ARB	242.26	163.26	914.52	154.03
SCAQMD (1)	122.63	47.51	152.01	55.97
TOTAL (2)	383.07	294.33	1272.16	293.17
EMISSION REDUCTIONS				
EPA	1.84	14.33	7.15	14.32
ARB	9.30	12.18	63.76	11.01
SCAQMD	4.99	6.35	12.35	8.04
TOTAL	16.13	32.86	83.26	33.37
REMAINING EMISSIONS				
EPA	16.34	69.23	198.48	68.85
ARB	232.96	151.08	850.76	143.02
SCAQMD (1)	117.64	41.16	139.66	47.93
TOTAL (2)	366.94	261.47	1188.90	259.80

(1) SCAQMD figures include RECLAIM
(2) Totals do not include the line items

Attachment 4

2031 8-HOUR OZONE ISOPLETHS

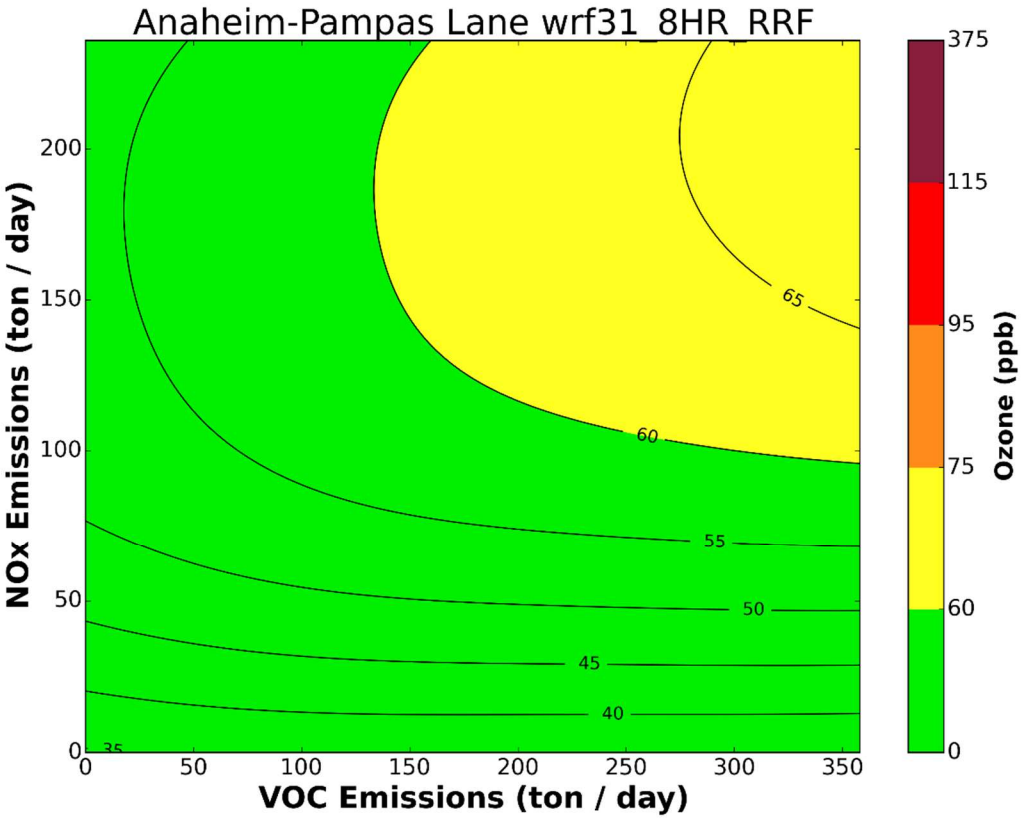
Anaheim-Pampas Lane wrf31_8HR_RRF
NOx Emissions (ton / day)
VOC Emissions (ton / day)
Ozone (ppb)
0
50
100
150
200
250
300
350
375
115
95
75
60
65
60
55
50
45
40
35

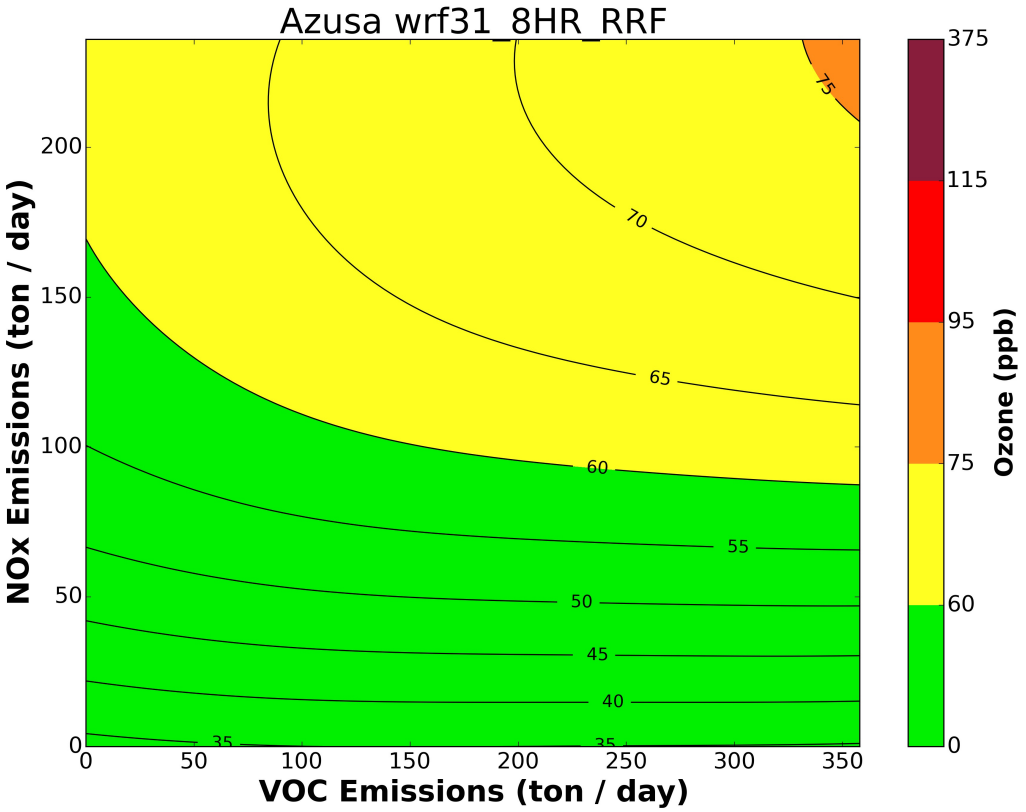
Azusa wrf31_8HR_RRF
NOx Emissions (ton / day)
VOC Emissions (ton / day)
Ozone (ppb)
0
50
100
150
200
250
300
350
375
115
95
75
60
0
75
70
65
60
55
50
45
40
35

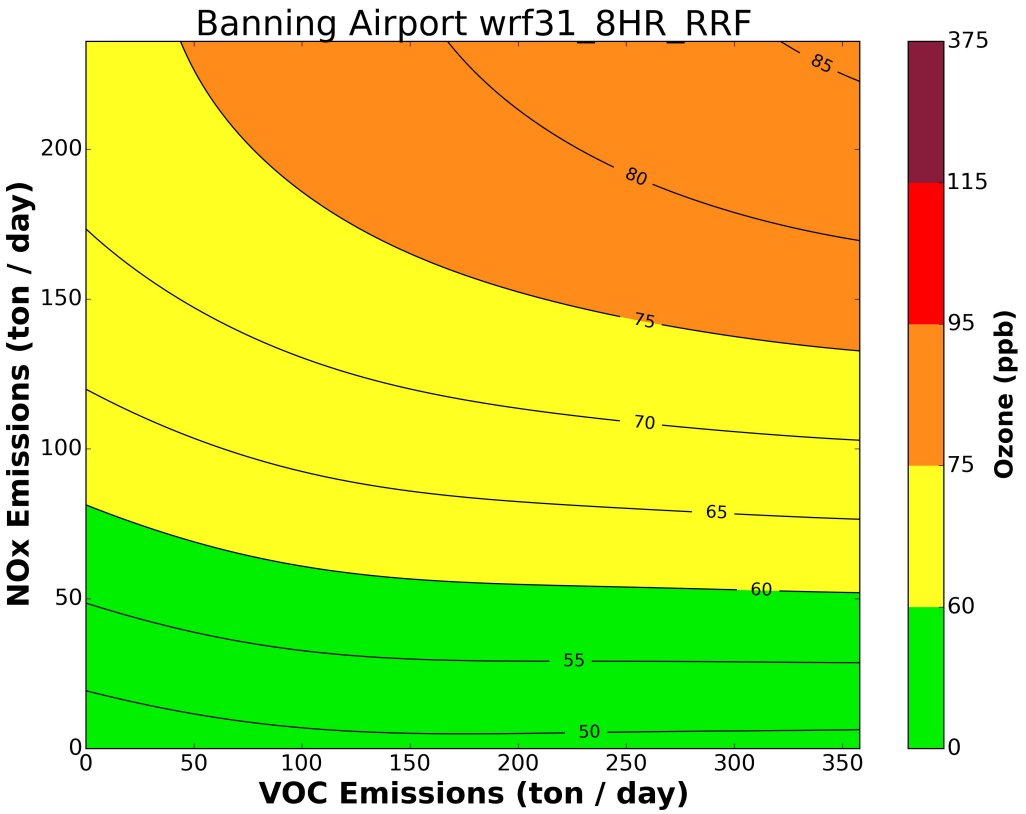
Banning Airport wrf31_8HR_RRF
NOx Emissions (ton / day)
VOC Emissions (ton / day)
Ozone (ppb)
0
50
100
150
200
250
300
350
375
115
95
75
60
85
80
75
70
65
60
55
50

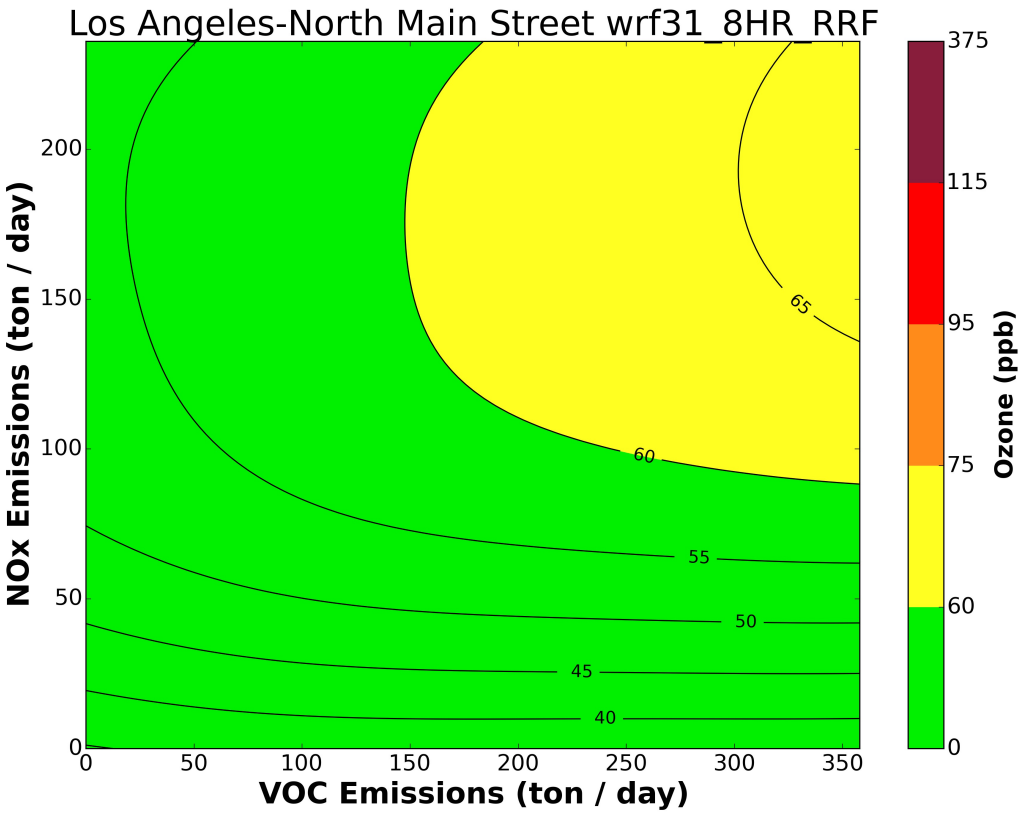
Los Angeles-North Main Street wrf31_8HR_RRF
NOx Emissions (ton / day)
VOC Emissions (ton / day)
Ozone (ppb)
0
50
100
150
200
250
300
350
375
115
95
75
60
65
60
55
50
45
40

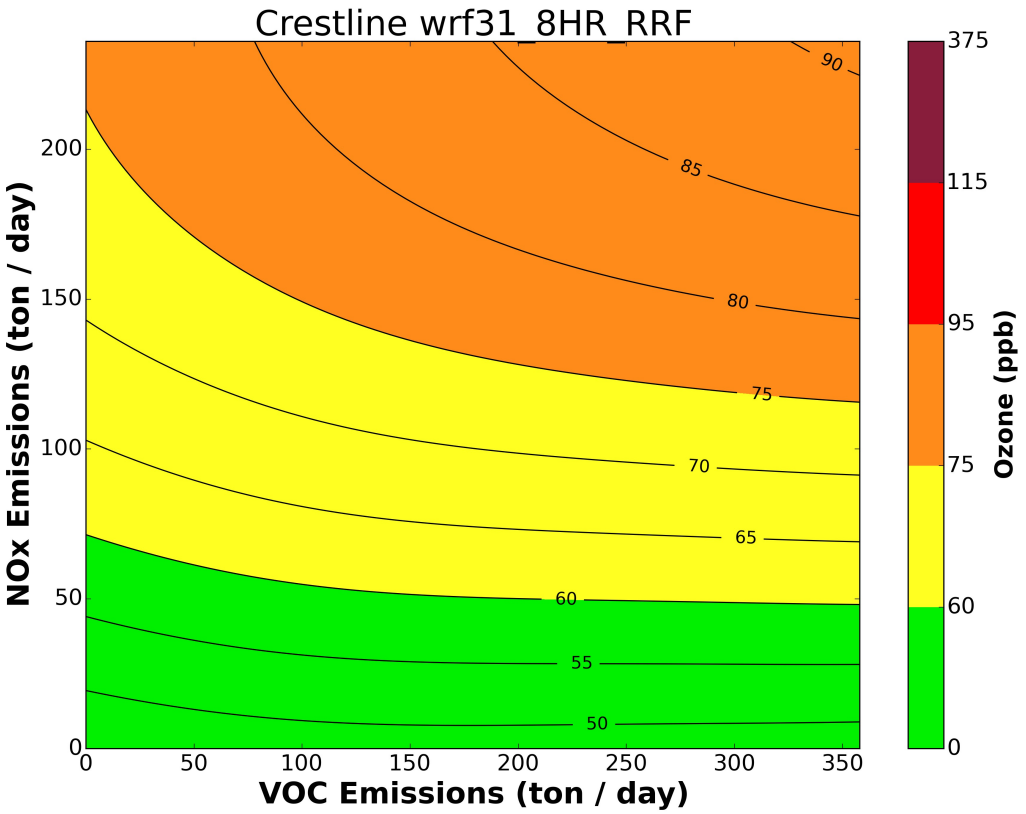
Crestline wrf31_8HR_RRF
NOx Emissions (ton / day)
VOC Emissions (ton / day)
Ozone (ppb)
0
50
100
150
200
250
300
350
90
85
80
75
70
65
60
55
50
375
115
95
75
60
0

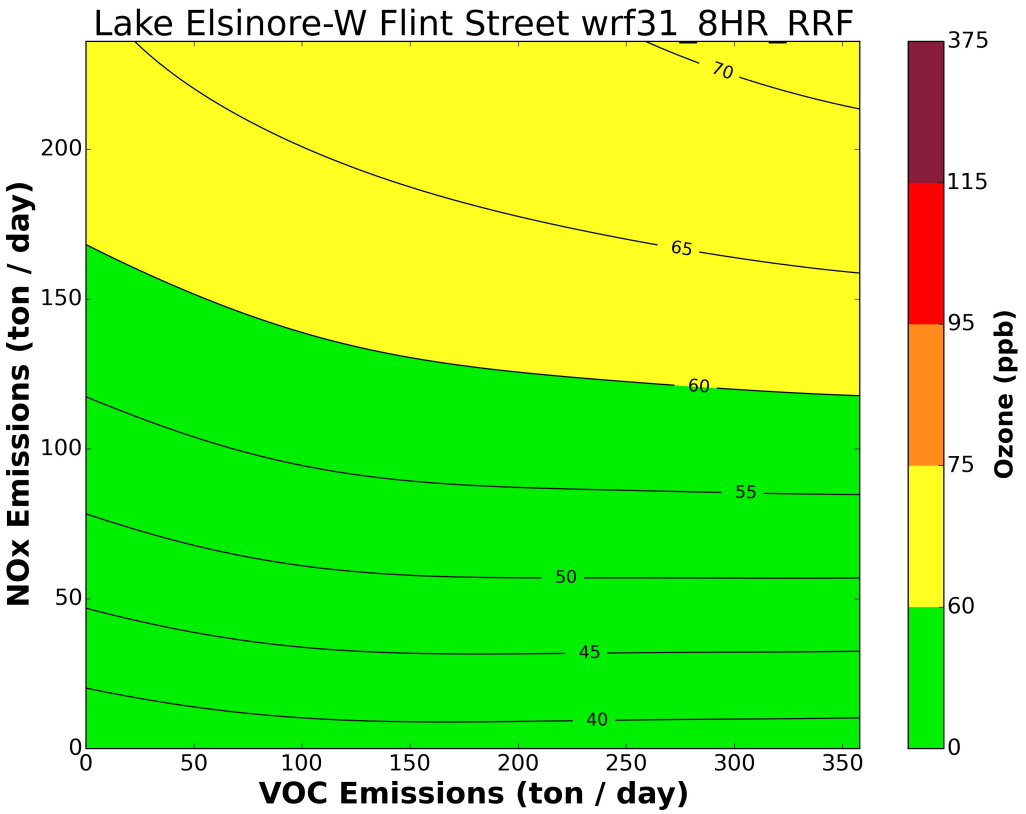
Lake Elsinore-W Flint Street wrf31_8HR_RRF
NOx Emissions (ton / day)
VOC Emissions (ton / day)
Ozone (ppb)
70
65
60
55
50
45
40
0
50
100
150
200
250
300
350
375
115
95
75
60
0

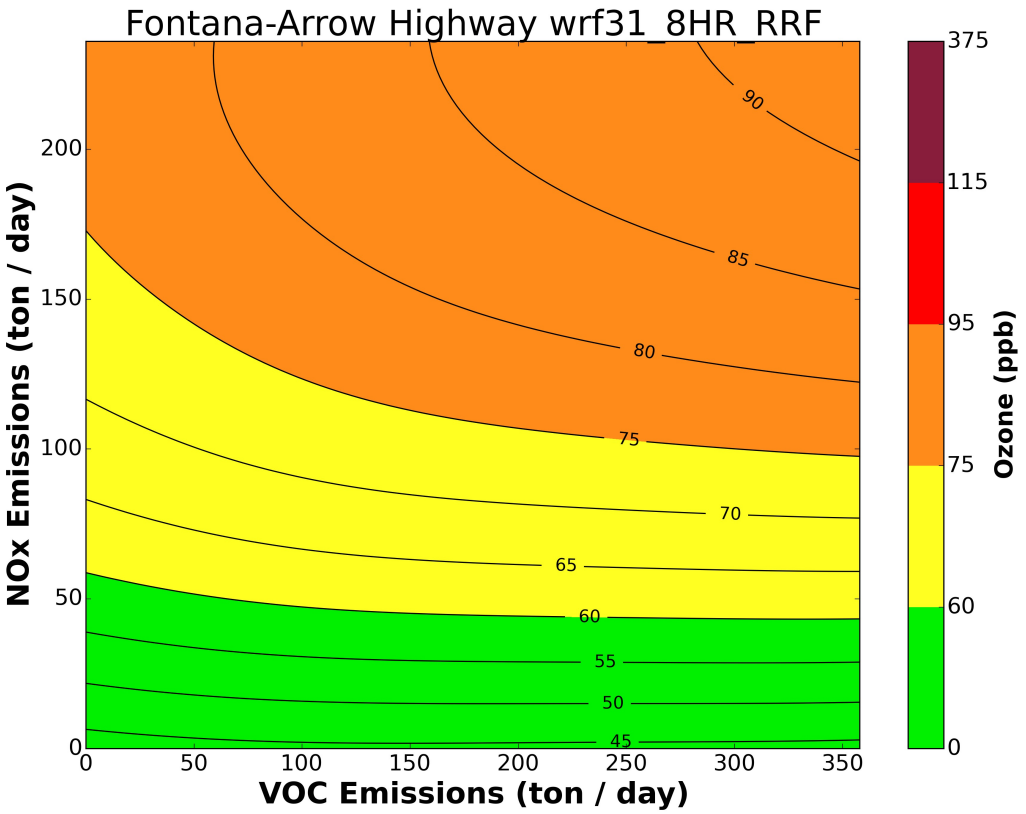
Fontana-Arrow Highway wrf31_8HR_RRF
NOx Emissions (ton / day)
VOC Emissions (ton / day)
Ozone (ppb)
0
50
100
150
200
250
300
350
375
115
95
75
60
90
85
80
75
70
65
60
55
50
45

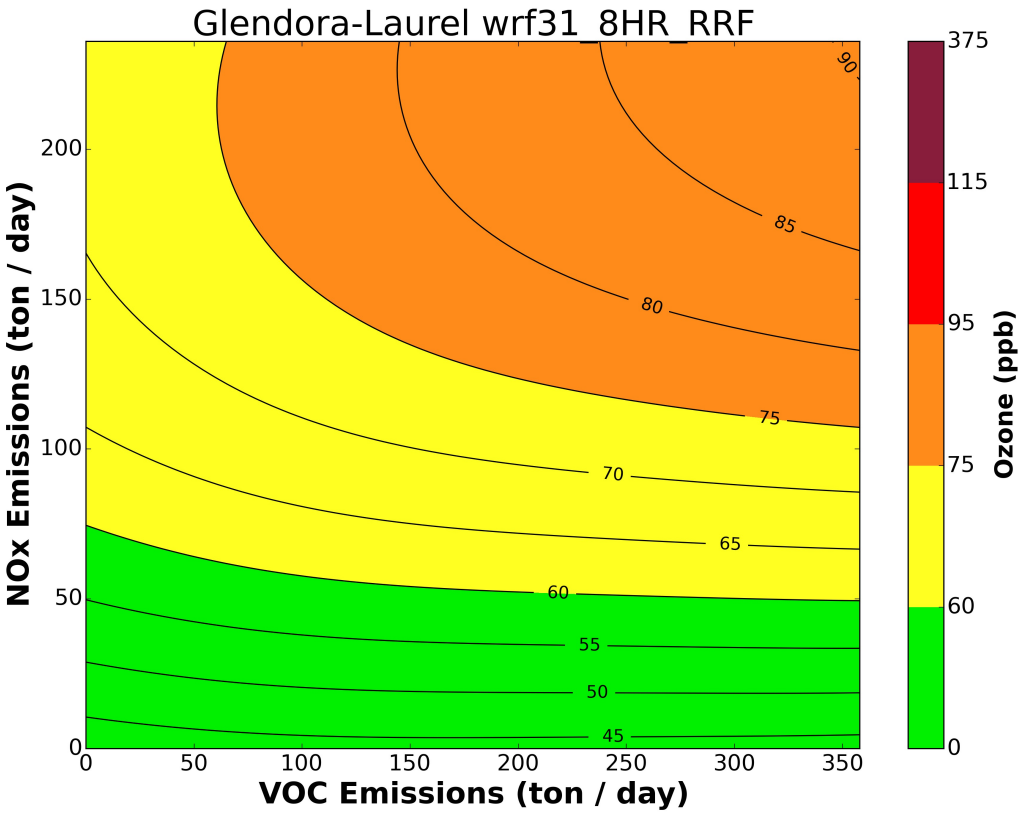
Glendora-Laurel wrf31_8HR_RRF
NOx Emissions (ton / day)
VOC Emissions (ton / day)
Ozone (ppb)
0
50
100
150
200
250
300
350
45
50
55
60
65
70
75
80
85
90
0
60
75
95
115
375

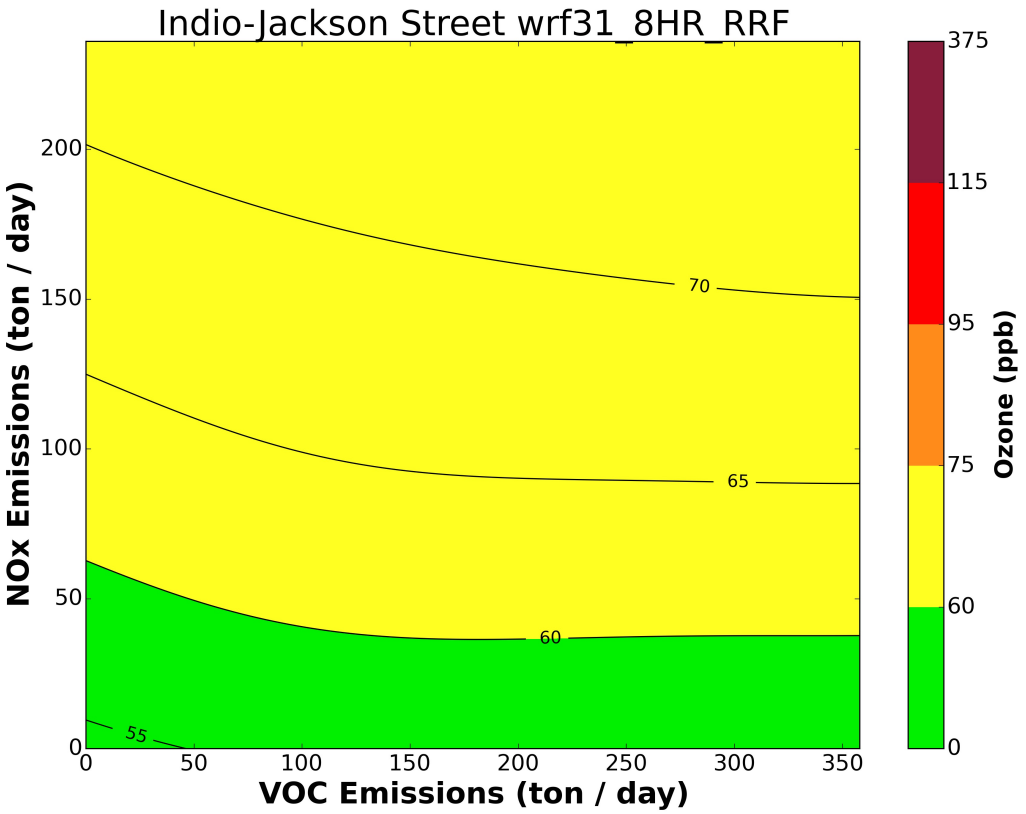
Indio-Jackson Street wrf31_8HR_RRF
NOx Emissions (ton / day)
VOC Emissions (ton / day)
Ozone (ppb)
0
50
100
150
200
250
300
350
375
115
95
75
60
70
65
60
55

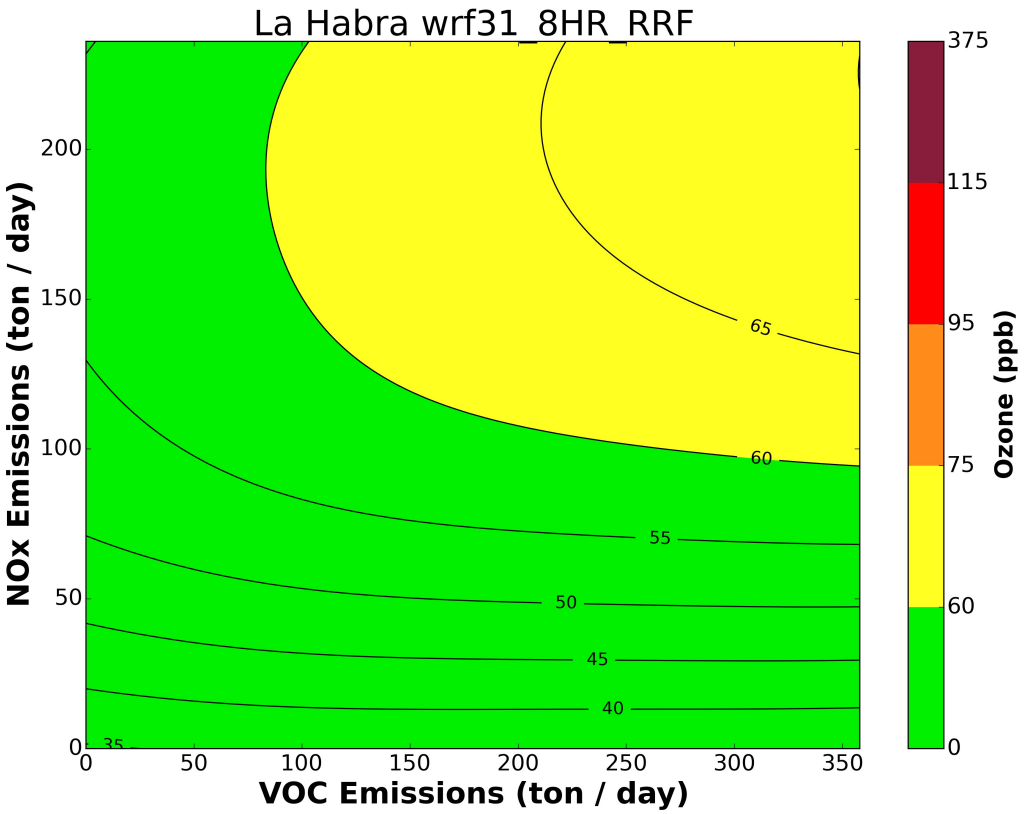
La Habra wrf31_8HR_RRF
NOx Emissions (ton / day)
VOC Emissions (ton / day)
Ozone (ppb)
0
50
100
150
200
250
300
350
375
115
95
75
60
65
60
55
50
45
40
35

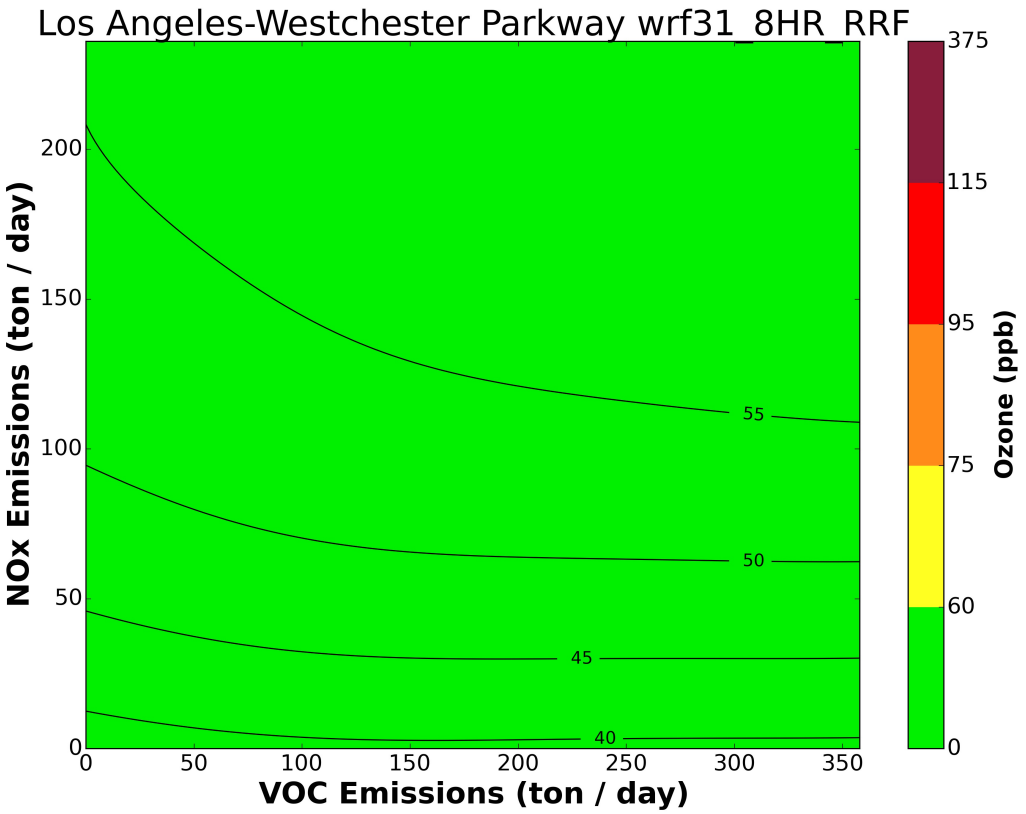
Los Angeles-Westchester Parkway wrf31_8HR_RRF
NOx Emissions (ton / day)
VOC Emissions (ton / day)
Ozone (ppb)
0
50
100
150
200
250
300
350
55
50
45
40
375
115
95
75
60
0

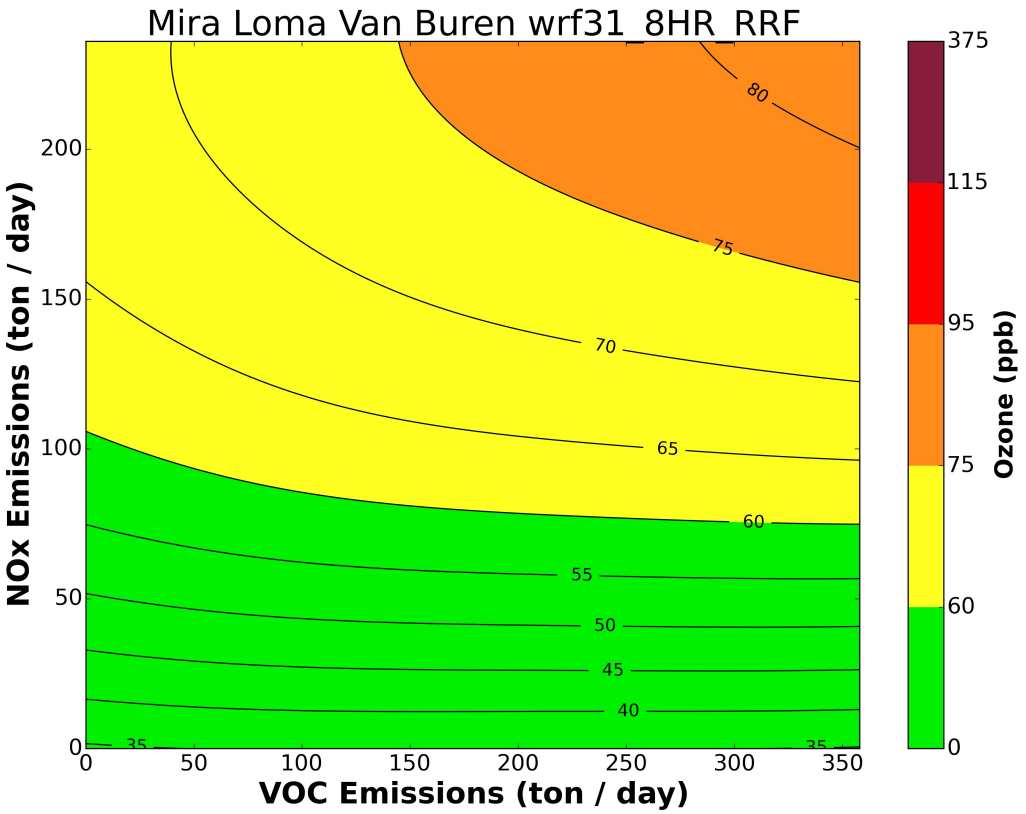
Mira Loma Van Buren wrf31_8HR_RRF
NOx Emissions (ton / day)
VOC Emissions (ton / day)
Ozone (ppb)
0
50
100
150
200
250
300
350
375
115
95
75
60
80
70
65
55
50
45
40
35

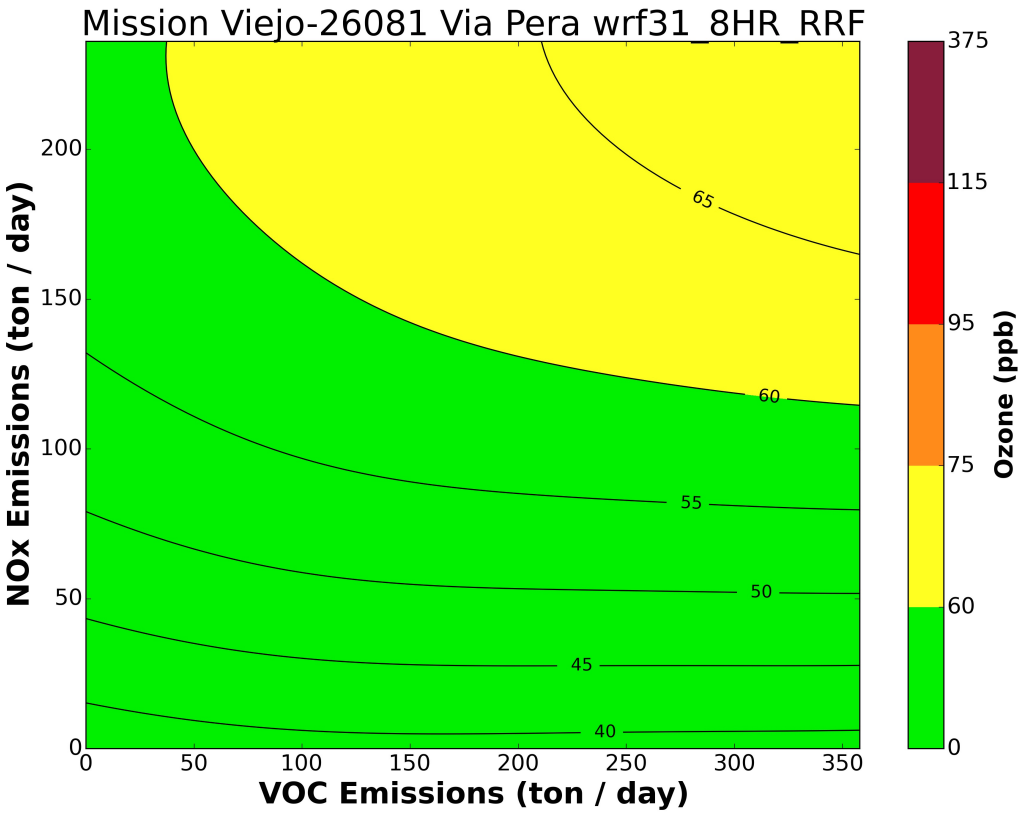
Mission Viejo-26081 Via Pera wrf31_8HR_RRF
NOx Emissions (ton / day)
VOC Emissions (ton / day)
Ozone (ppb)
0
50
100
150
200
250
300
350
65
60
55
50
45
40
375
115
95
75
60
0

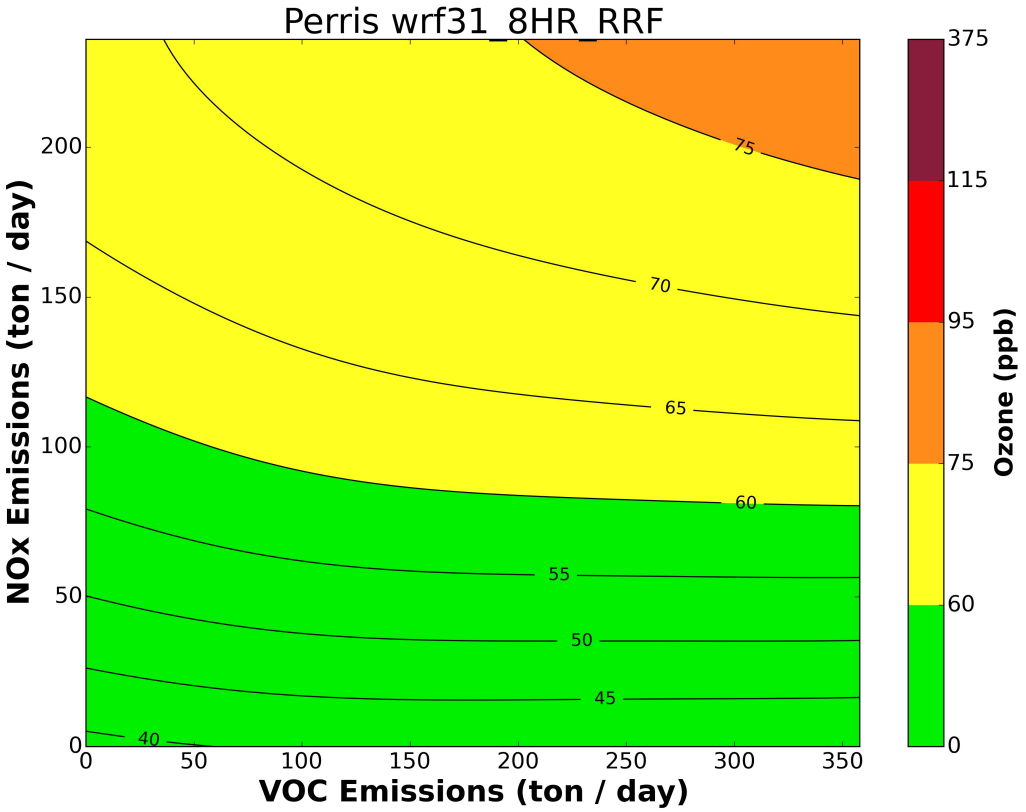
Perris wrf31_8HR_RRF
NOx Emissions (ton / day)
VOC Emissions (ton / day)
Ozone (ppb)
0
50
100
150
200
250
300
350
375
115
95
75
60
40
45
50
55
60
65
70
75

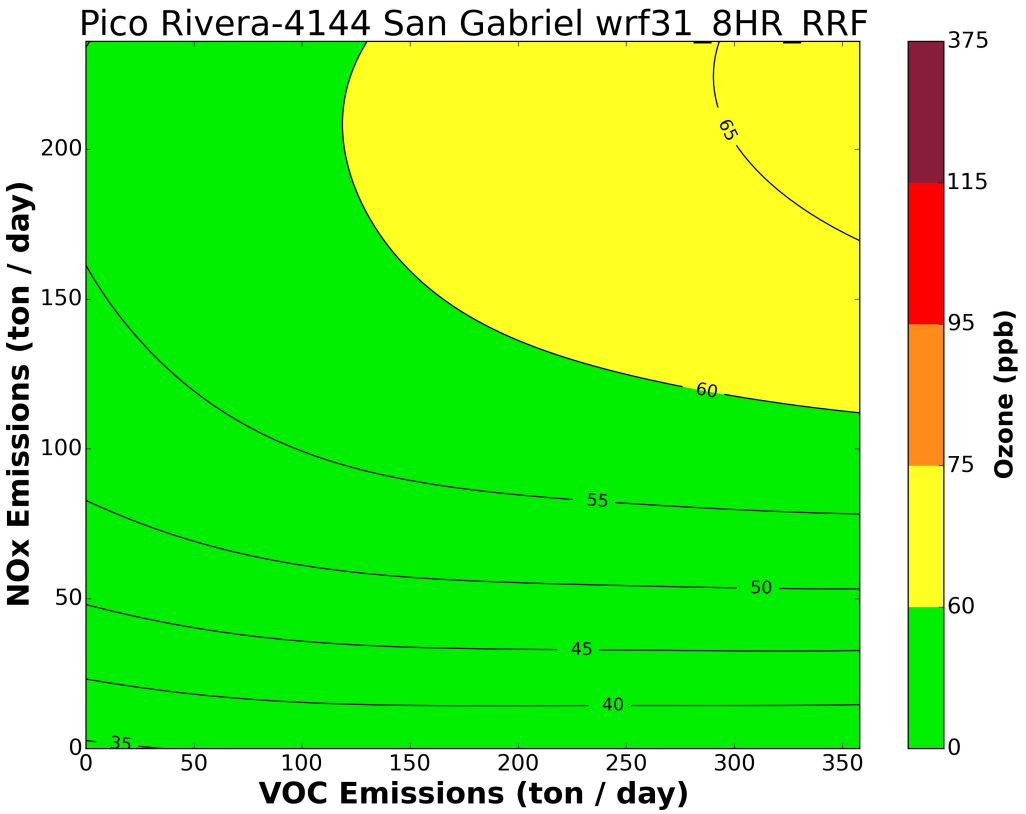
Pico Rivera-4144 San Gabriel wrf31_8HR_RRF
NOx Emissions (ton / day)
VOC Emissions (ton / day)
Ozone (ppb)
0
50
100
150
200
250
300
350
375
115
95
75
60
65
60
55
50
45
40
35

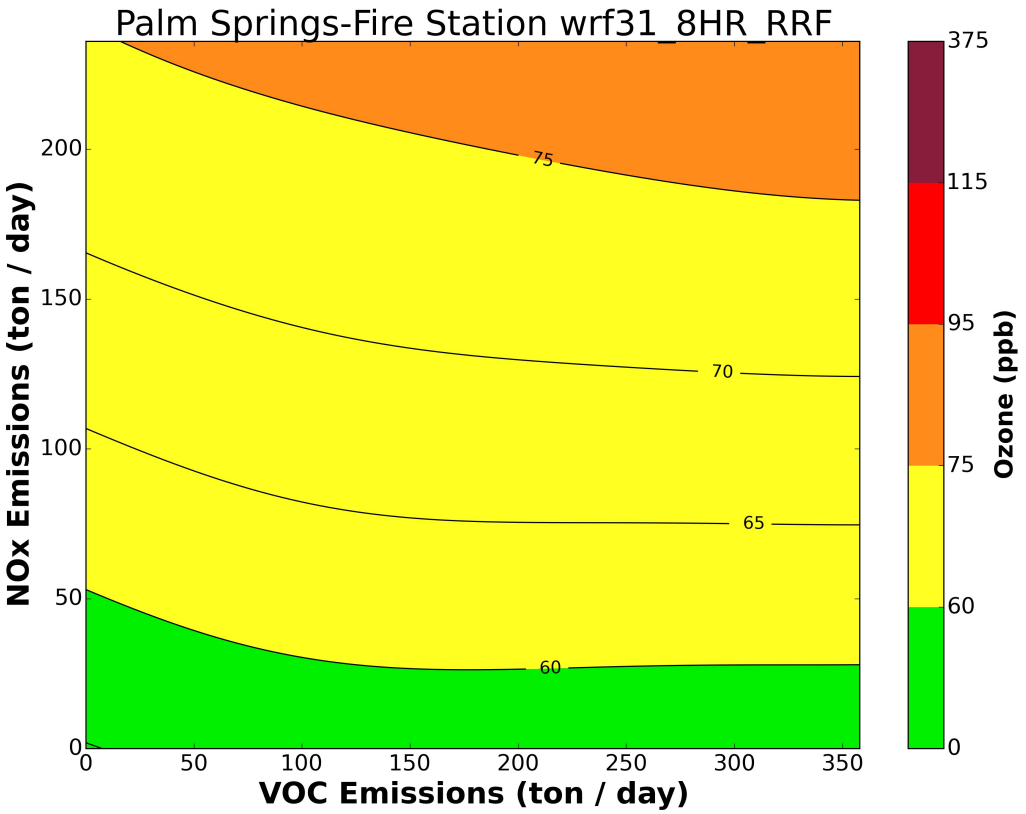
Palm Springs-Fire Station wrf31_8HR_RRF
NOx Emissions (ton / day)
VOC Emissions (ton / day)
Ozone (ppb)
0
50
100
150
200
250
300
350
375
115
95
75
60
75
70
65
60

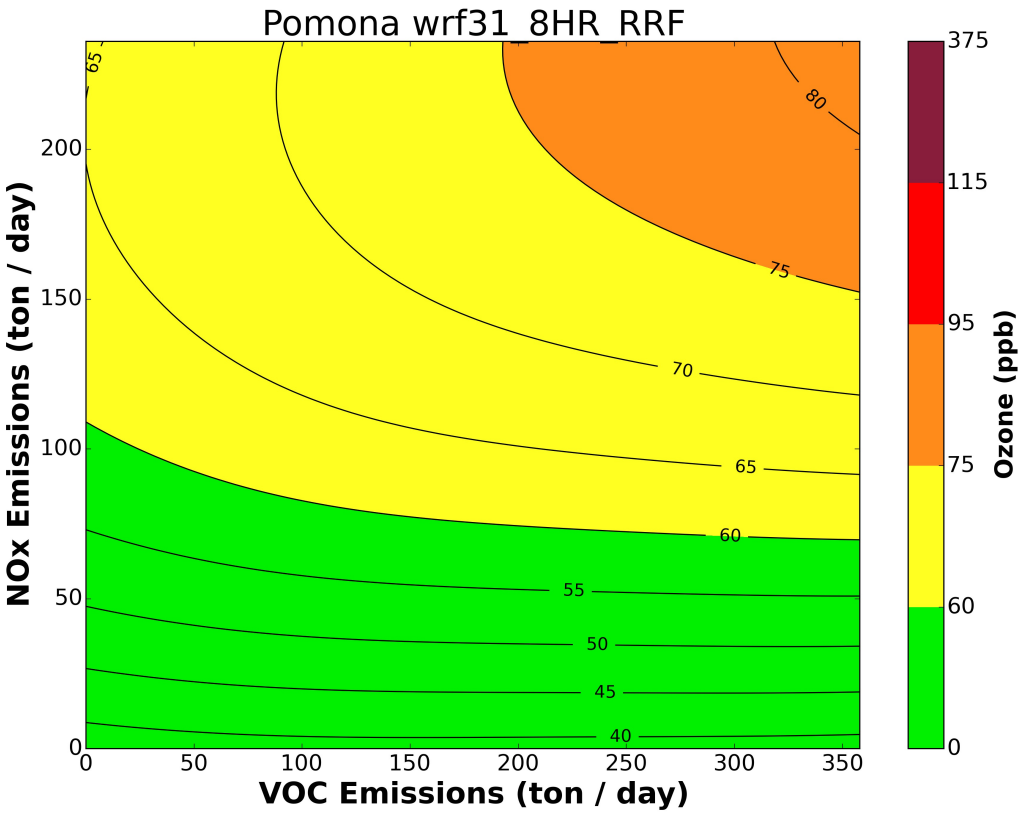
Pomona wrf31_8HR_RRF
NOx Emissions (ton / day)
VOC Emissions (ton / day)
Ozone (ppb)
0
50
100
150
200
250
300
350
375
115
95
75
60
65
70
80
55
45
40

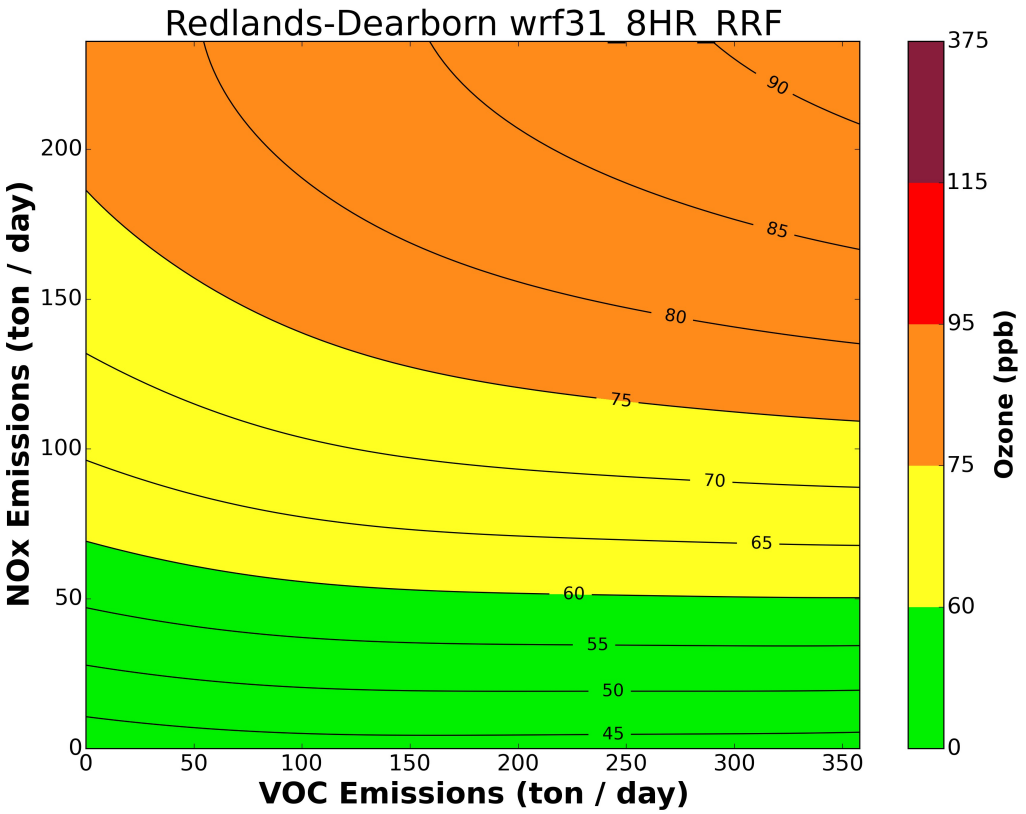
Redlands-Dearborn wrf31_8HR_RRF
NOx Emissions (ton / day)
VOC Emissions (ton / day)
Ozone (ppb)
0
50
100
150
200
250
300
350
375
115
95
75
60
90
85
80
75
70
65
60
55
50
45

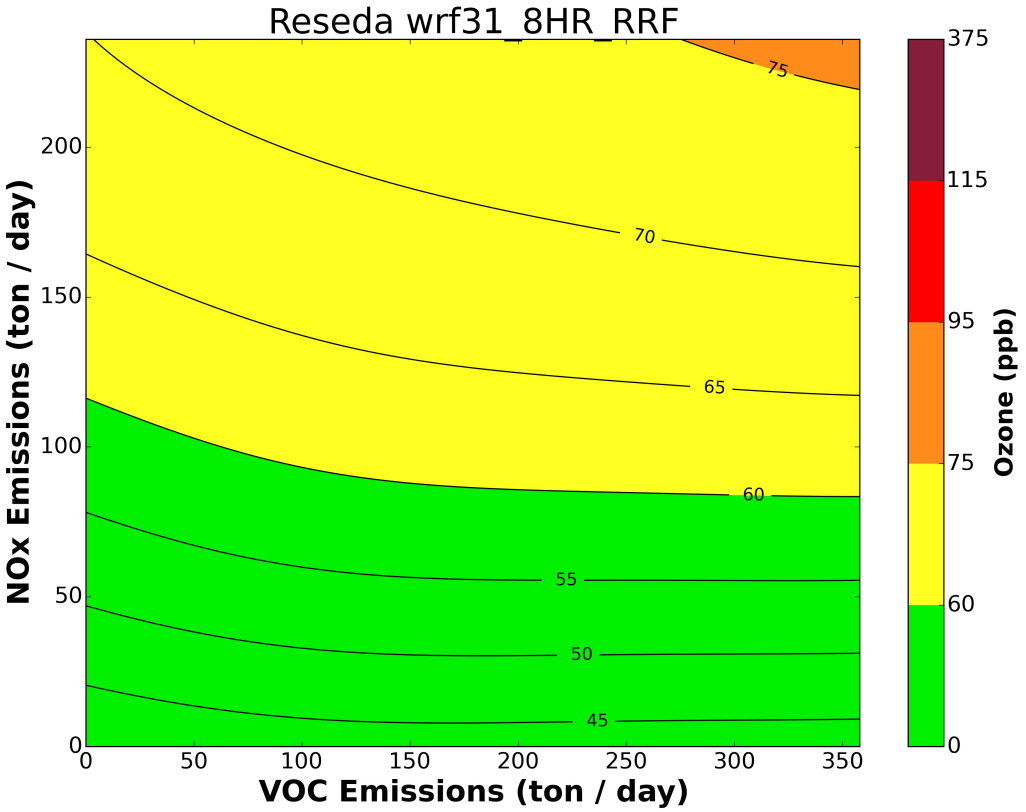
Reseda wrf31_8HR_RRF
NOx Emissions (ton / day)
VOC Emissions (ton / day)
Ozone (ppb)
0
50
100
150
200
250
300
350
375
115
95
75
60
45
55
65
70

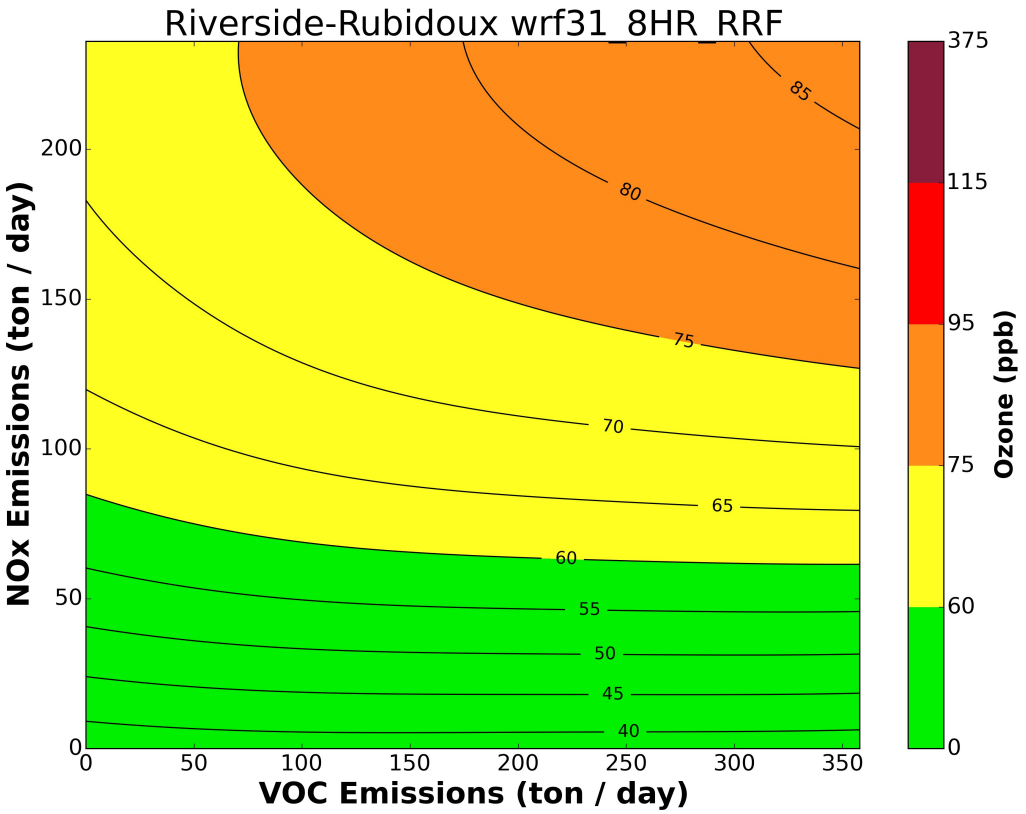
Riverside-Rubidoux wrf31_8HR_RRF
NOx Emissions (ton / day)
VOC Emissions (ton / day)
Ozone (ppb)
0
50
100
150
200
250
300
350
375
115
95
75
60
85
80
75
70
65
60
55
50
45
40

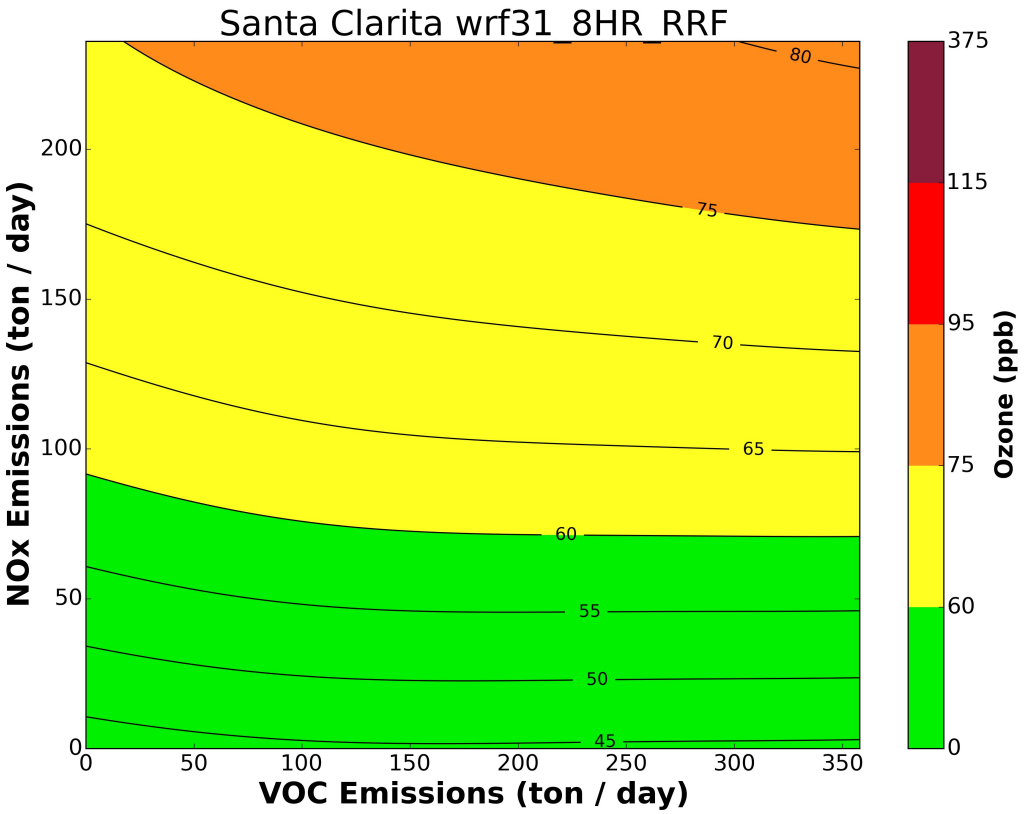
Santa Clarita wrf31_8HR_RRF
NOx Emissions (ton / day)
VOC Emissions (ton / day)
Ozone (ppb)
80
75
70
65
60
55
50
45
0
50
100
150
200
250
300
350
375
115
95
75
60
0

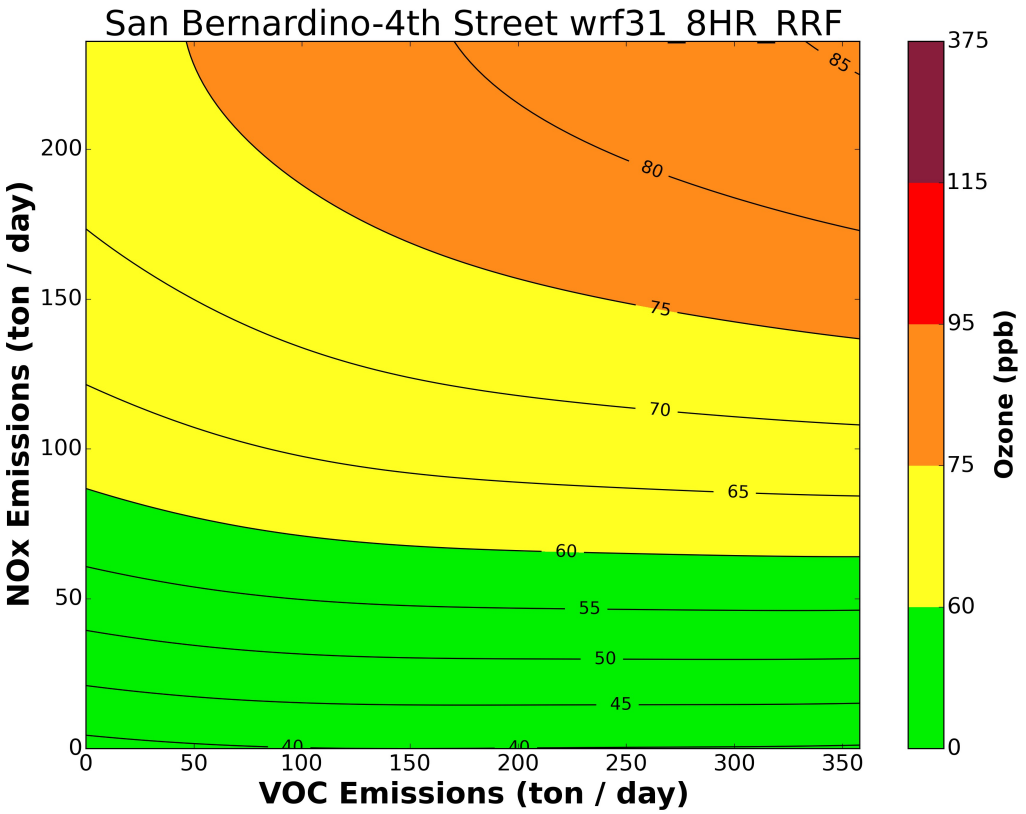
San Bernardino-4th Street wrf31_8HR_RRF
NOx Emissions (ton / day)
VOC Emissions (ton / day)
Ozone (ppb)
0
50
100
150
200
250
300
350
375
115
95
75
60
85
80
75
70
65
60
55
50
45
40

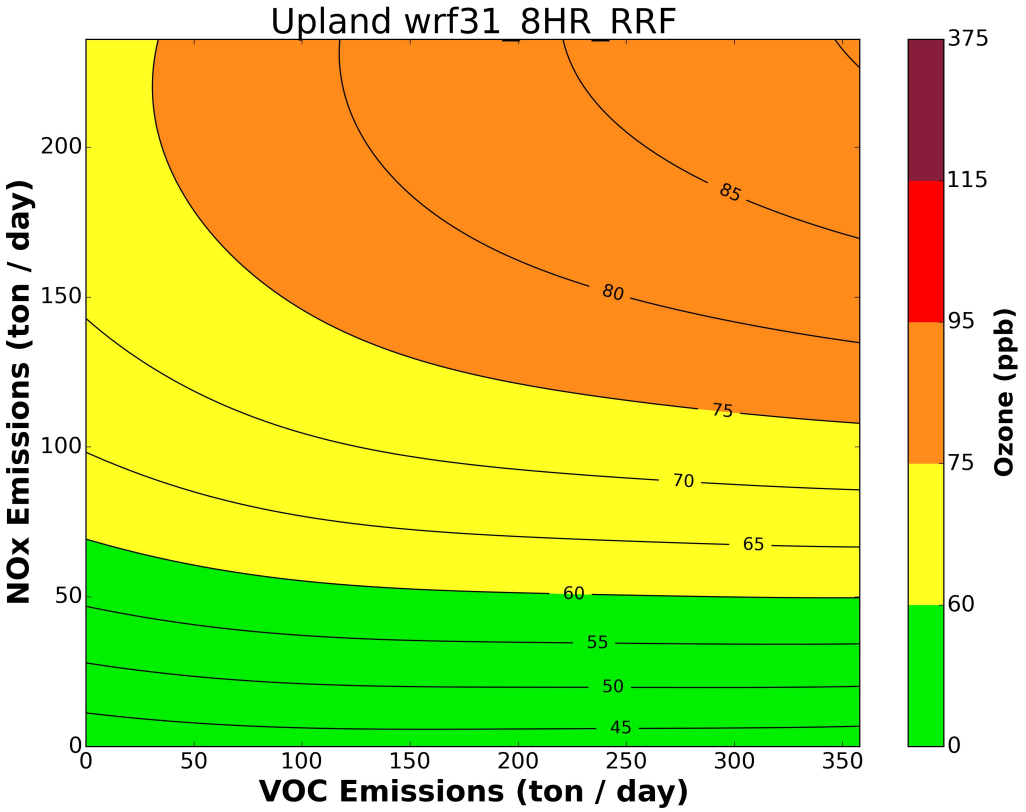
Upland wrf31_8HR_RRF
NOx Emissions (ton / day)
VOC Emissions (ton / day)
Ozone (ppb)
0
50
100
150
200
250
300
350
375
115
95
75
60
85
80
75
70
65
60
55
50
45

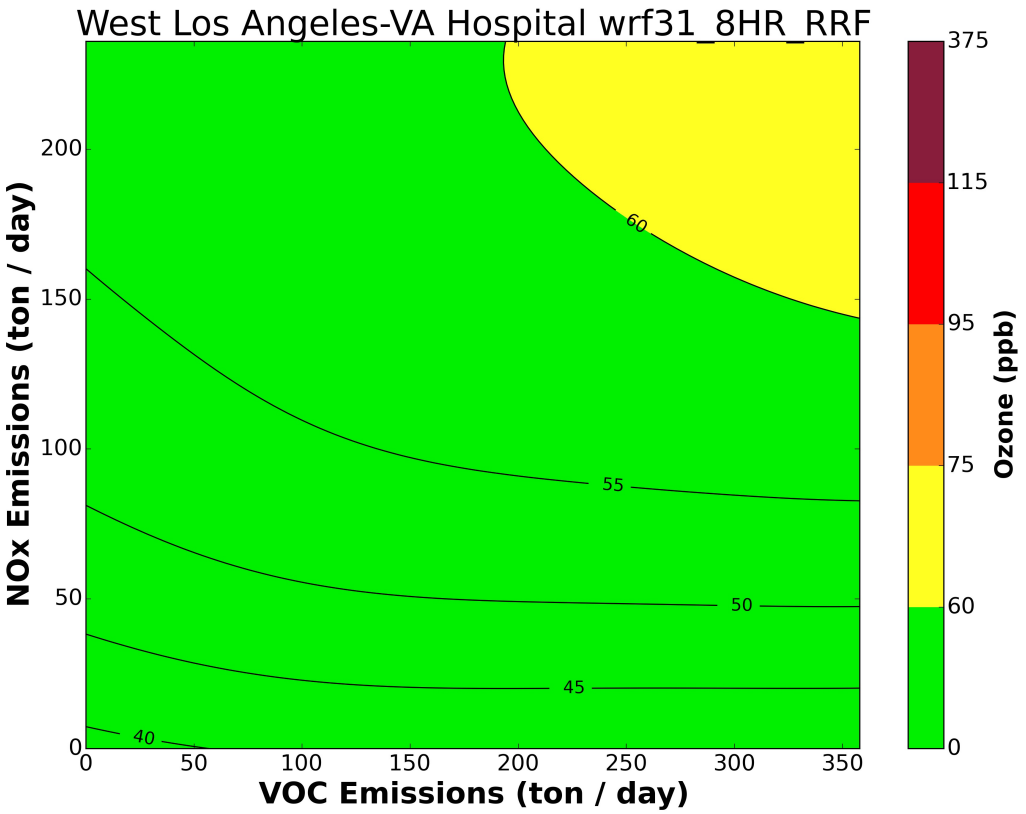
West Los Angeles-VA Hospital wrf31_8HR_RRF
NOx Emissions (ton / day)
VOC Emissions (ton / day)
Ozone (ppb)
0
50
100
150
200
250
300
350
375
115
95
75
60
40
45
55
60

Attachment 5

2023 8-HOUR OZONE ISOPLETHS

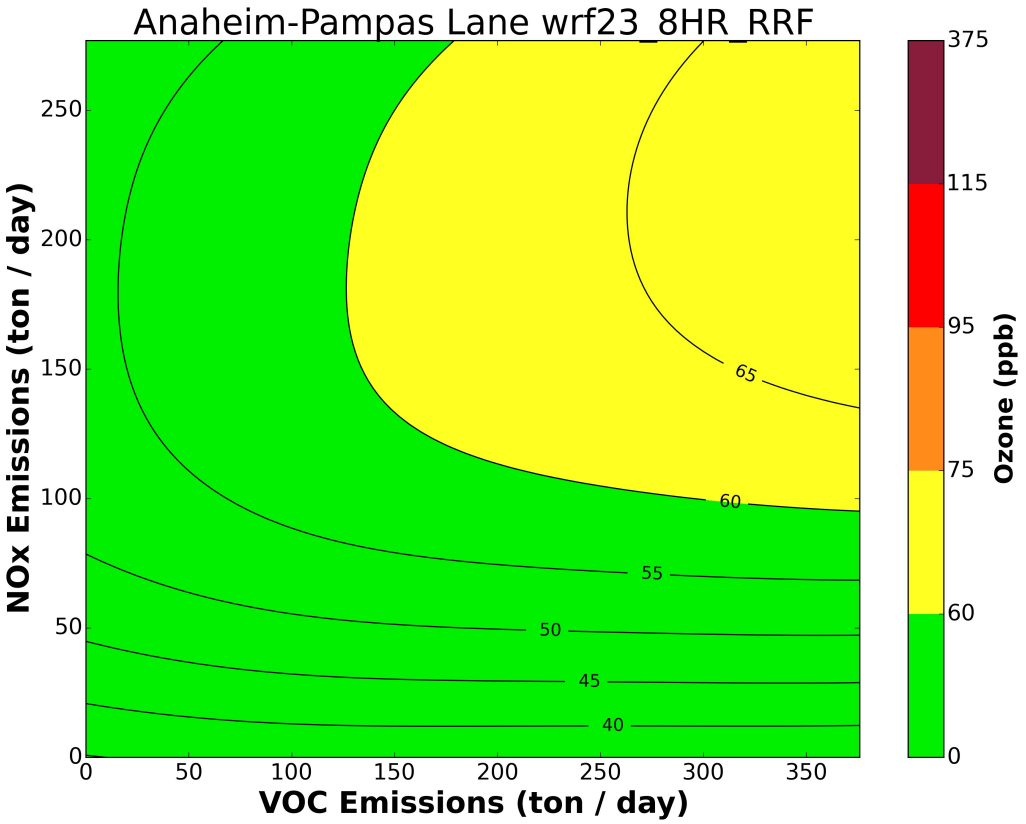
Anaheim-Pampas Lane wrf23_8HR_RRF
NOx Emissions (ton / day)
VOC Emissions (ton / day)
Ozone (ppb)
0
50
100
150
200
250
300
350
375
115
95
75
60
65
60
55
50
45
40

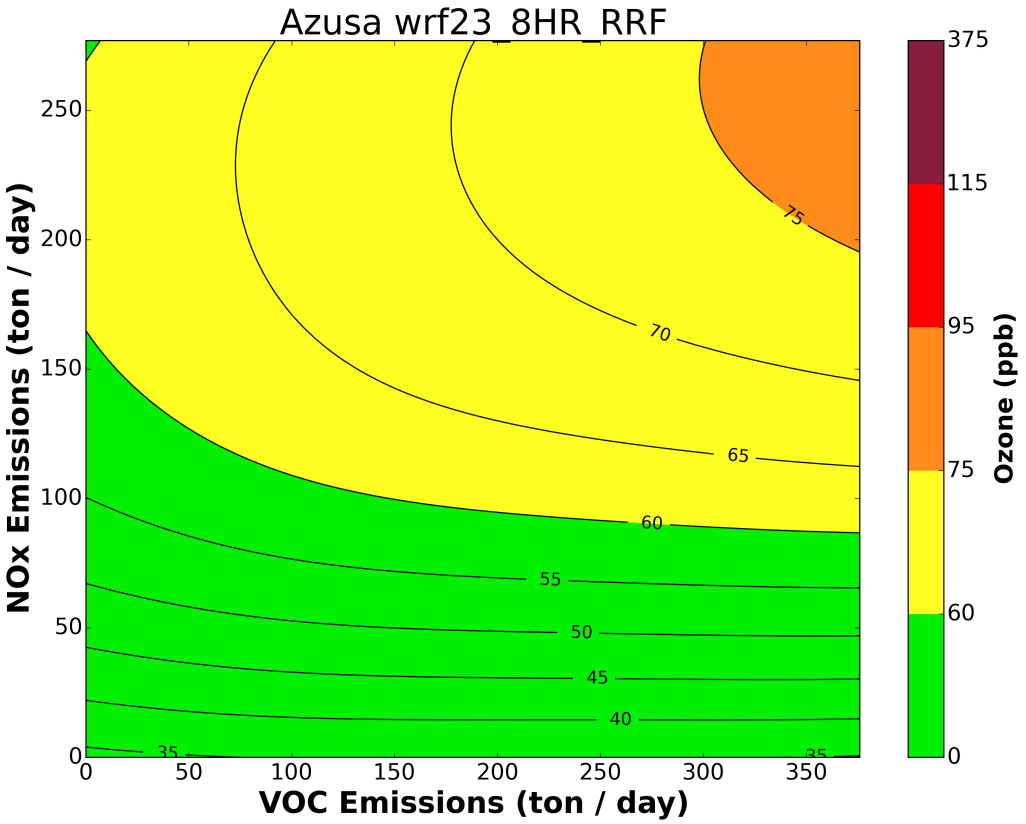
Azusa wrf23_8HR_RRF
NOx Emissions (ton / day)
VOC Emissions (ton / day)
Ozone (ppb)
0
50
100
150
200
250
300
350
375
115
95
75
60
0
75
70
65
60
55
50
45
40
35

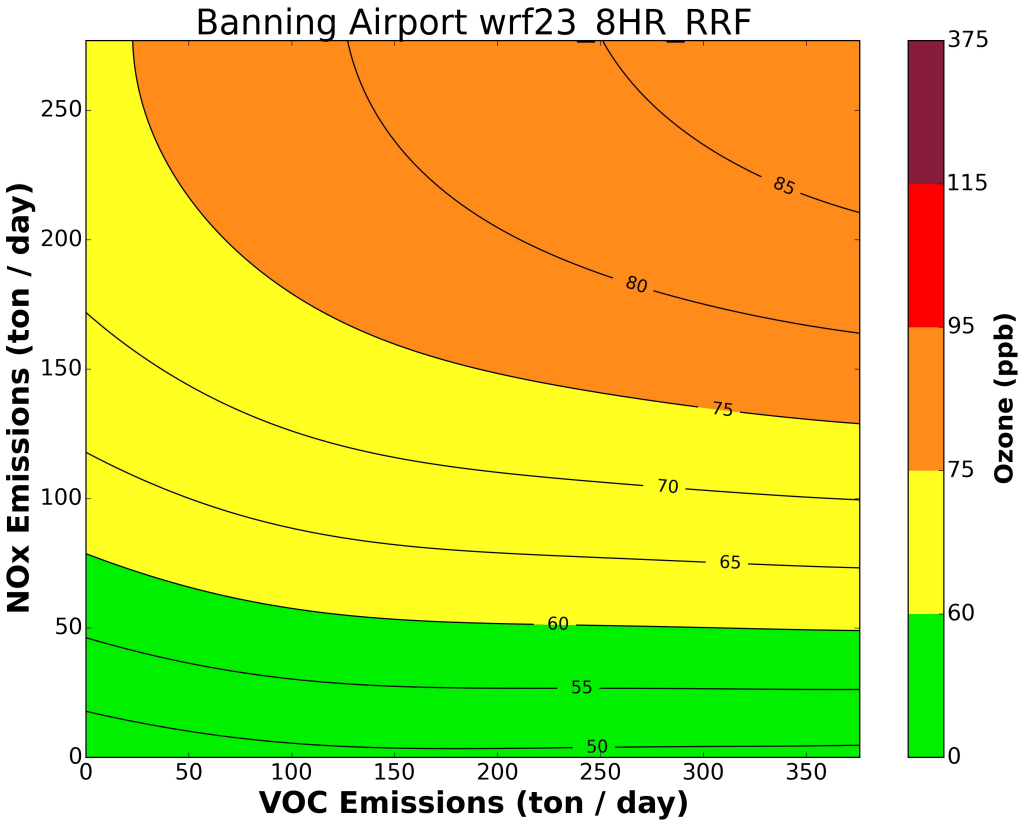
Banning Airport wrf23_8HR_RRF
NOx Emissions (ton / day)
VOC Emissions (ton / day)
Ozone (ppb)
0
50
100
150
200
250
300
350
375
115
95
75
60
85
80
75
70
65
60
55
50

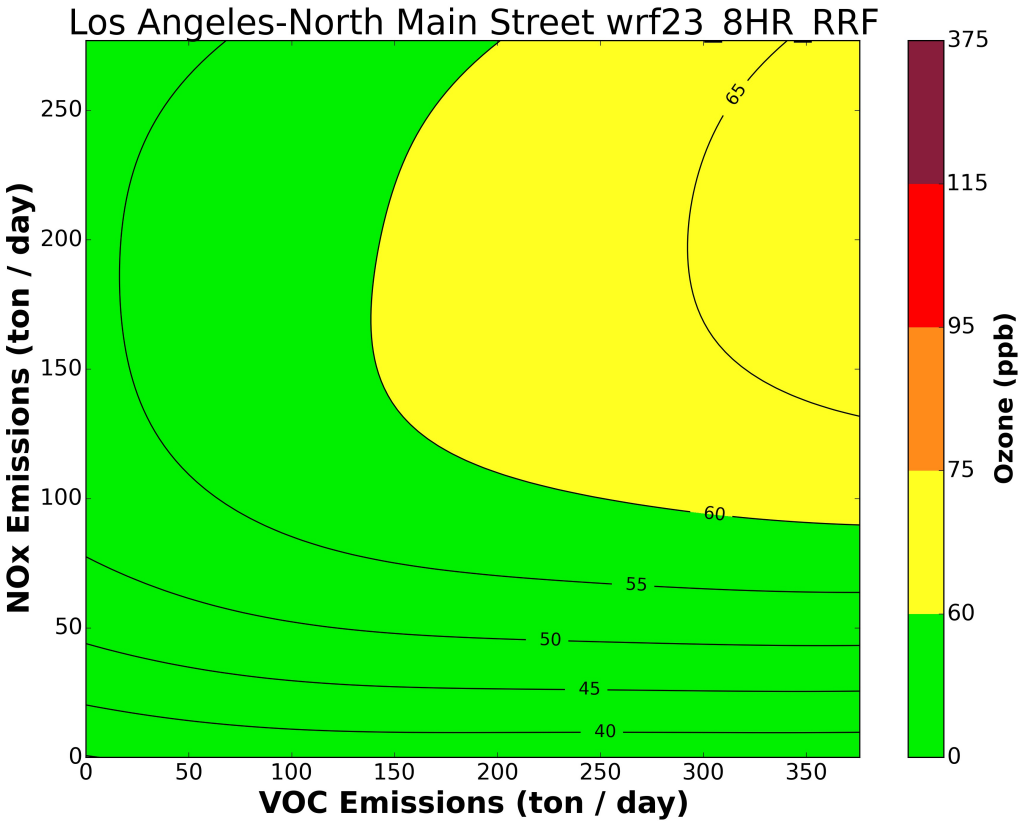
Los Angeles-North Main Street wrf23_8HR_RRF
NOx Emissions (ton / day)
VOC Emissions (ton / day)
Ozone (ppb)
0
50
100
150
200
250
300
350
375
115
95
75
60
65
60
55
50
45
40

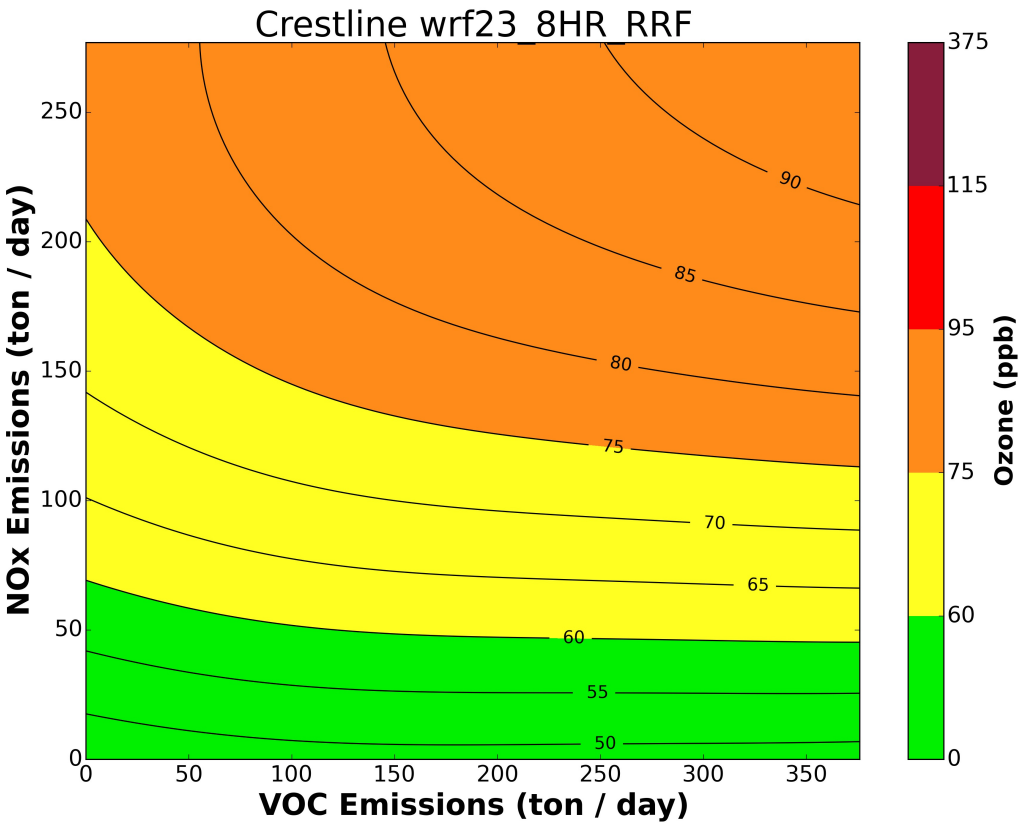
Crestline wrf23_8HR_RRF
NOx Emissions (ton / day)
VOC Emissions (ton / day)
Ozone (ppb)
0
50
100
150
200
250
300
350
375
115
95
75
60
90
85
80
75
70
65
60
55
50

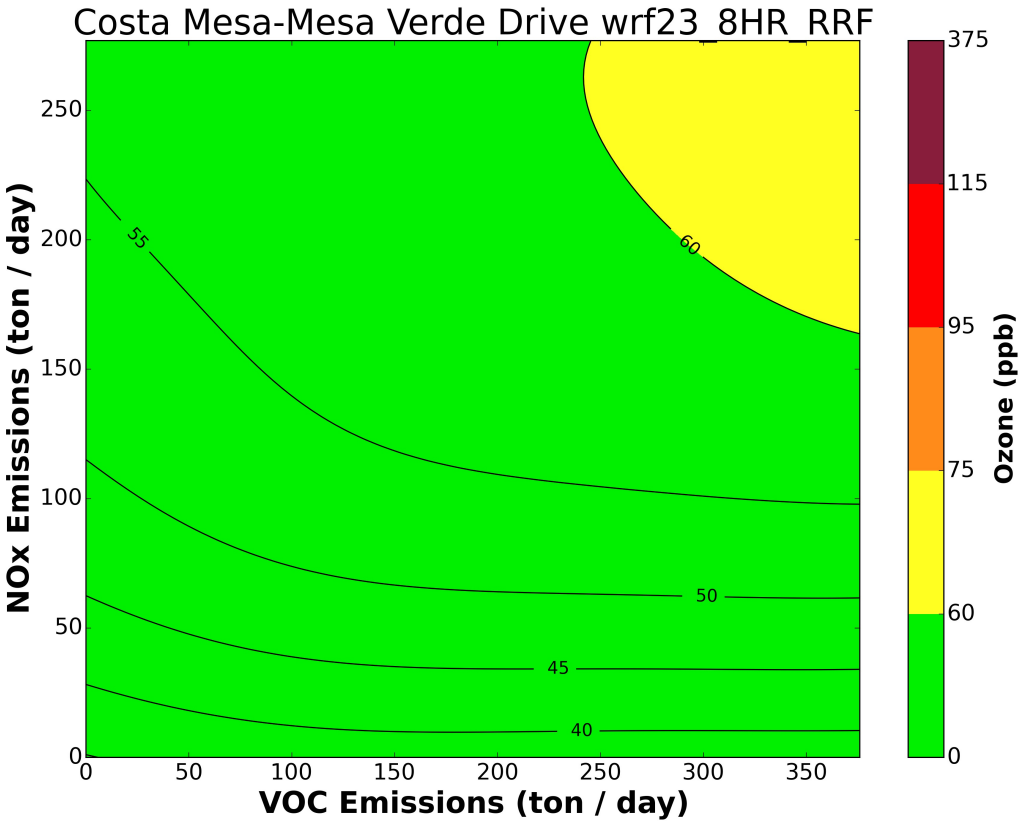
Costa Mesa-Mesa Verde Drive wrf23_8HR_RRF
NOx Emissions (ton / day)
VOC Emissions (ton / day)
Ozone (ppb)
0
50
100
150
200
250
300
350
375
115
95
75
60
55
50
45
40

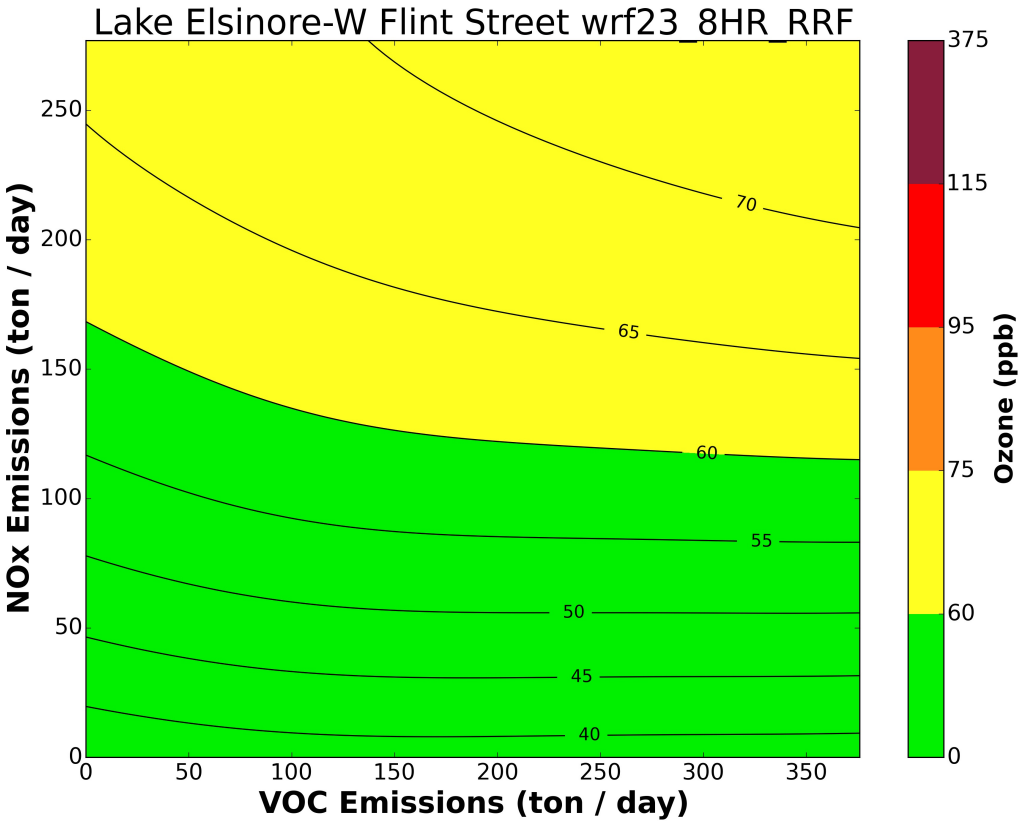
Lake Elsinore-W Flint Street wrf23_8HR_RRF
NOx Emissions (ton / day)
VOC Emissions (ton / day)
Ozone (ppb)
0
50
100
150
200
250
300
350
375
115
95
75
60
70
65
60
55
50
45
40

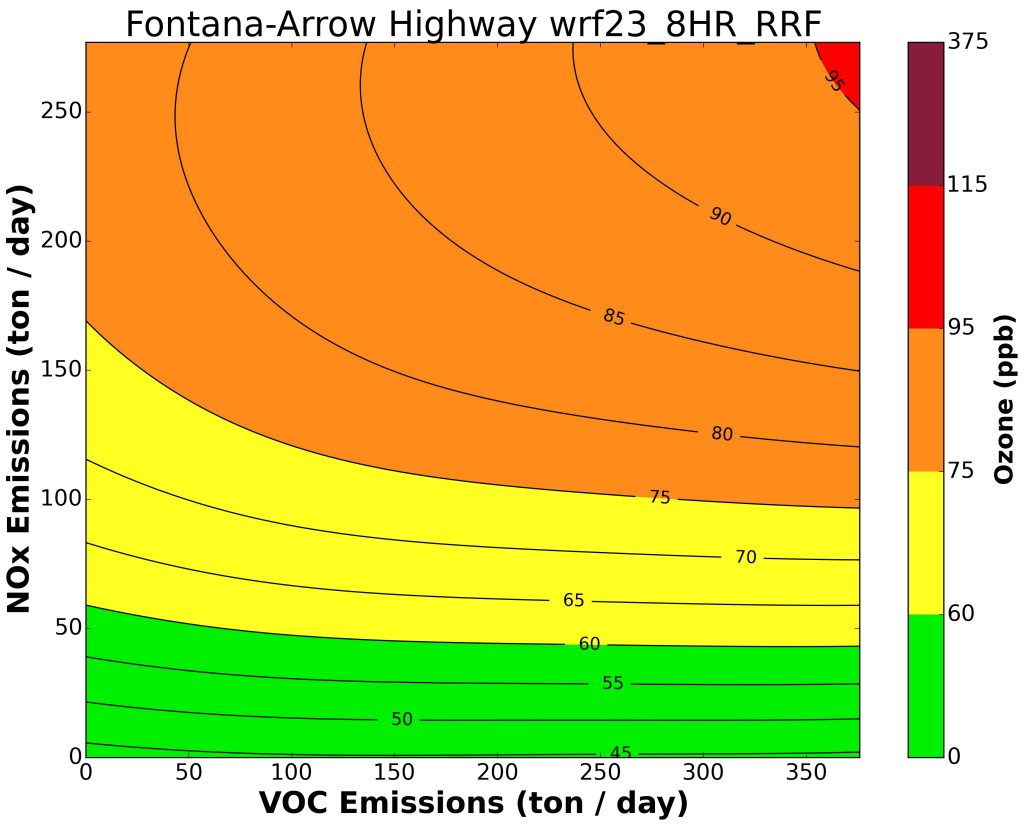
Fontana-Arrow Highway wrf23_8HR_RRF
NOx Emissions (ton / day)
VOC Emissions (ton / day)
Ozone (ppb)
0
50
100
150
200
250
300
350
375
115
95
75
60
95
90
85
80
75
70
65
60
55
50
45

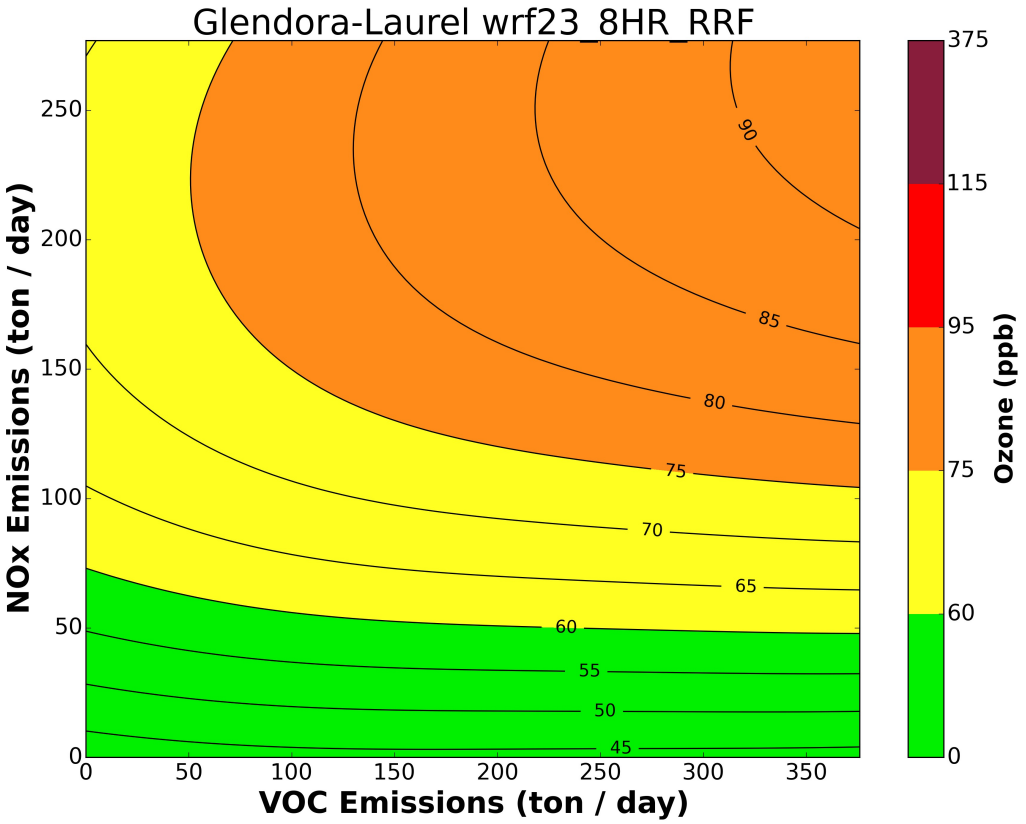
Glendora-Laurel wrf23_8HR_RRF
NOx Emissions (ton / day)
VOC Emissions (ton / day)
Ozone (ppb)
0
50
100
150
200
250
300
350
375
115
95
75
60
90
85
80
75
70
65
60
55
50
45

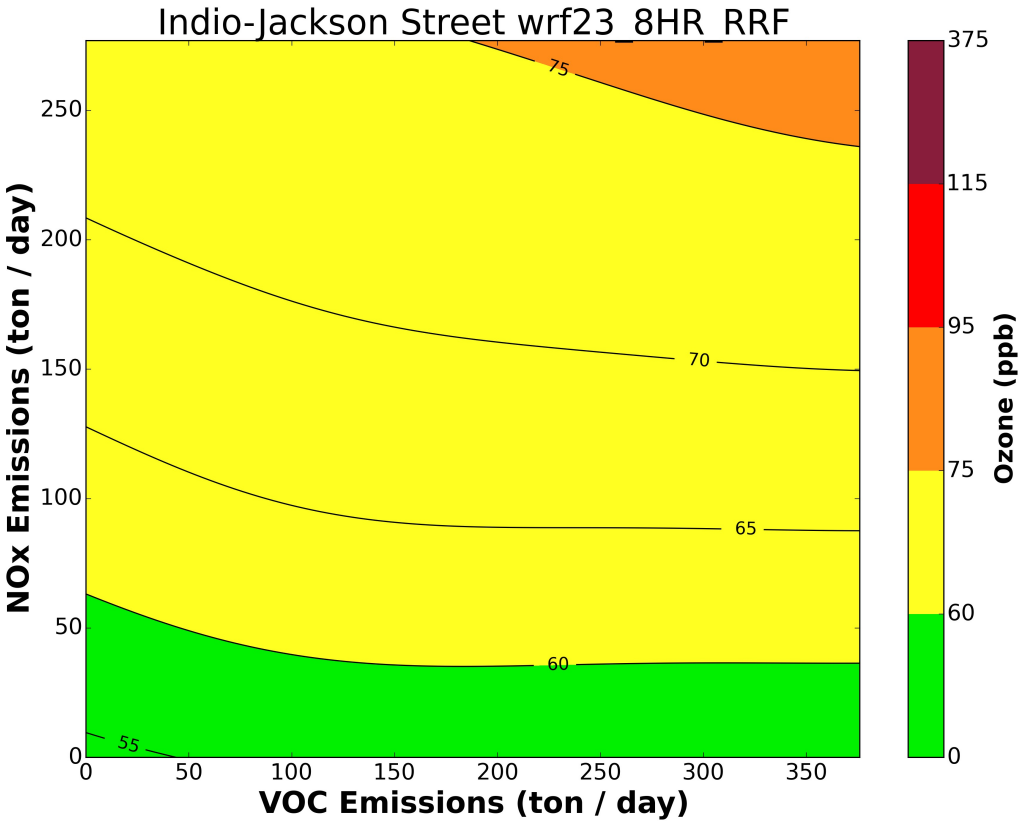
Indio-Jackson Street wrf23_8HR_RRF
NOx Emissions (ton / day)
VOC Emissions (ton / day)
Ozone (ppb)
0
50
100
150
200
250
300
350
375
115
95
75
60
0
55
60
65
70
75

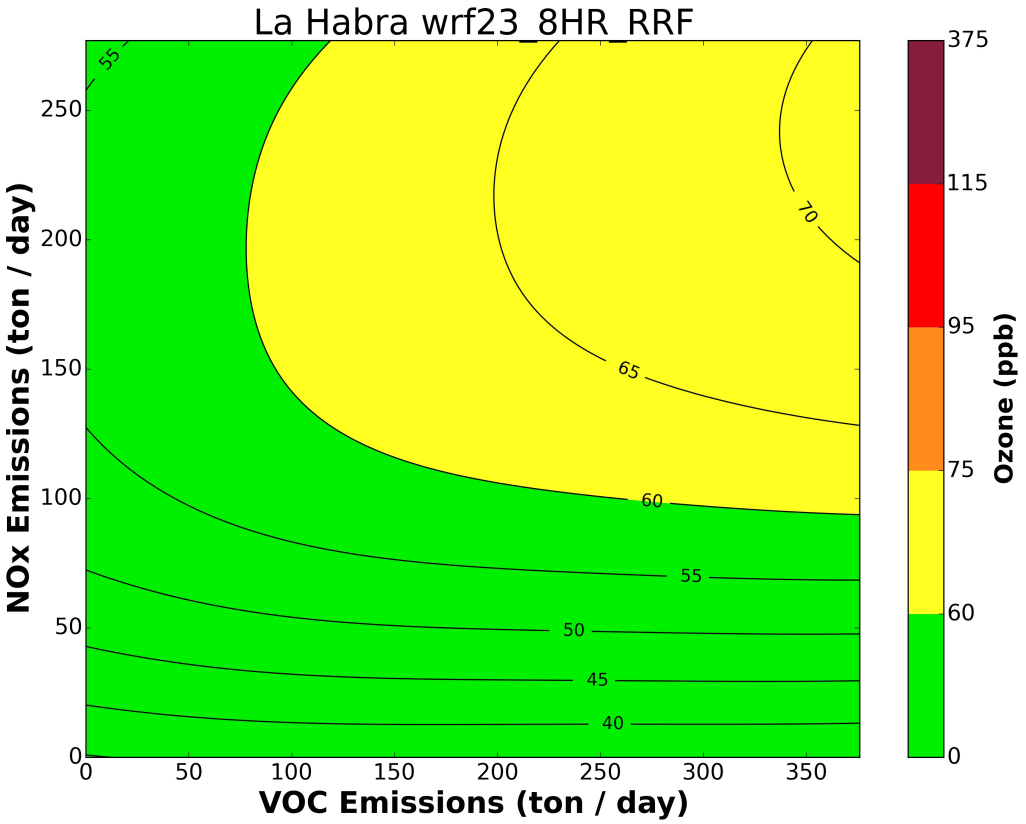
La Habra wrf23_8HR_RRF
NOx Emissions (ton / day)
VOC Emissions (ton / day)
Ozone (ppb)
0
50
100
150
200
250
300
350
375
115
95
75
60
55
70
65
60
55
50
45
40

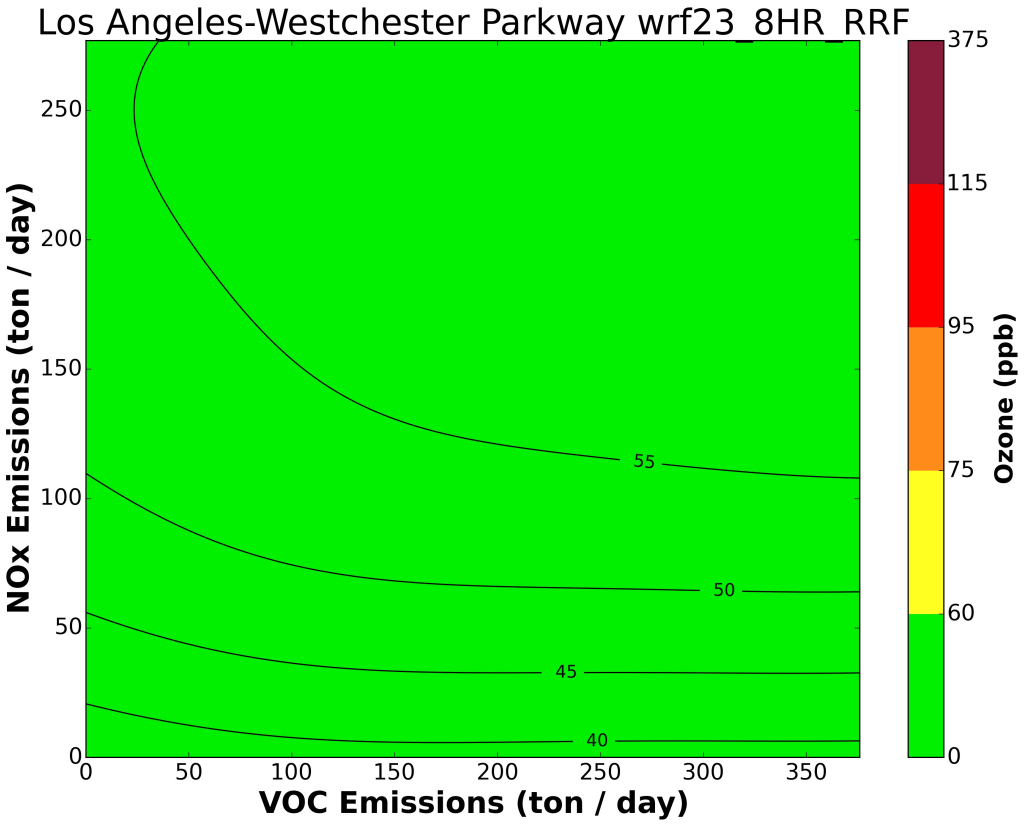
Los Angeles-Westchester Parkway wrf23_8HR_RRF
NOx Emissions (ton / day)
VOC Emissions (ton / day)
Ozone (ppb)
0
50
100
150
200
250
300
350
375
115
95
75
60
55
50
45
40

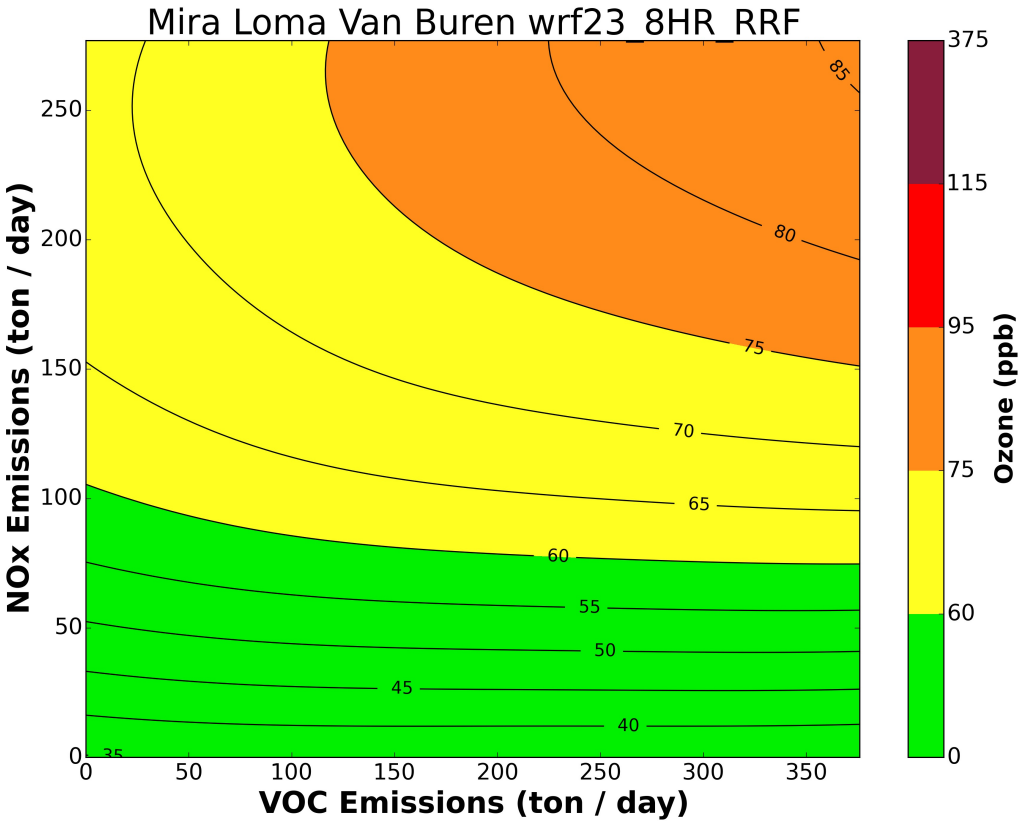
Mira Loma Van Buren wrf23_8HR_RRF
NOx Emissions (ton / day)
VOC Emissions (ton / day)
Ozone (ppb)
0
50
100
150
200
250
300
350
375
115
95
75
60
85
80
75
70
65
60
55
50
45
40
35

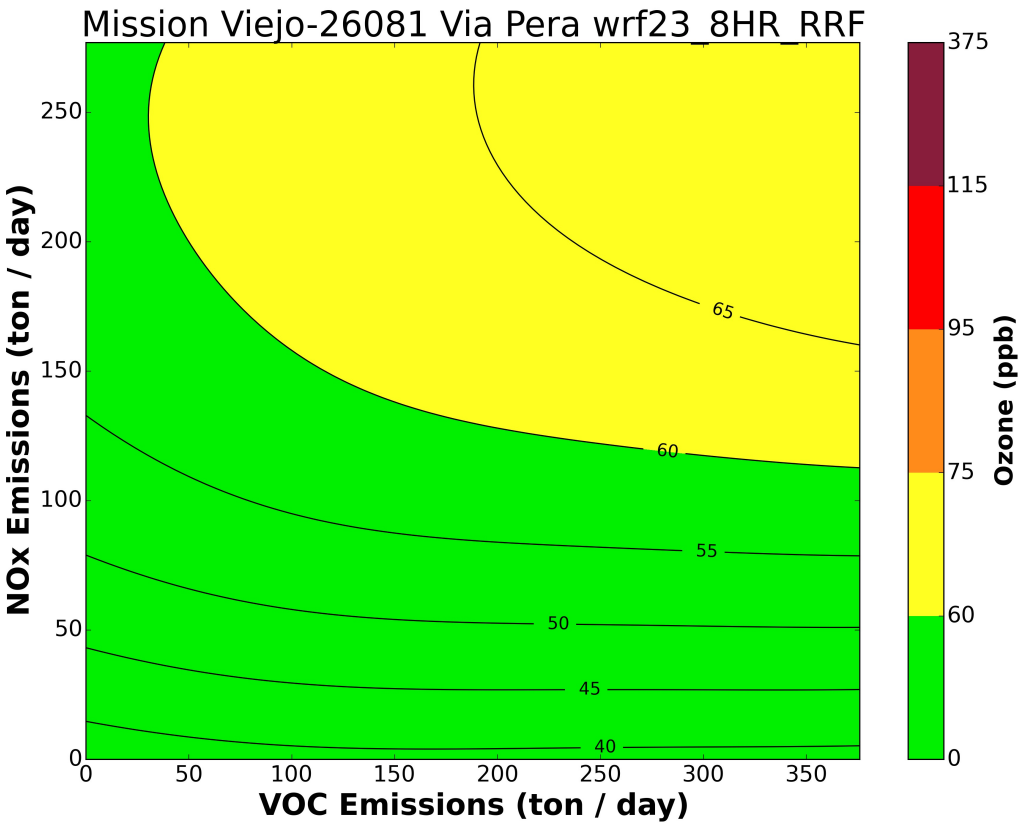
Mission Viejo-26081 Via Pera wrf23_8HR_RRF
NOx Emissions (ton / day)
VOC Emissions (ton / day)
Ozone (ppb)
0
50
100
150
200
250
300
350
65
60
55
50
45
40
375
115
95
75
60
0

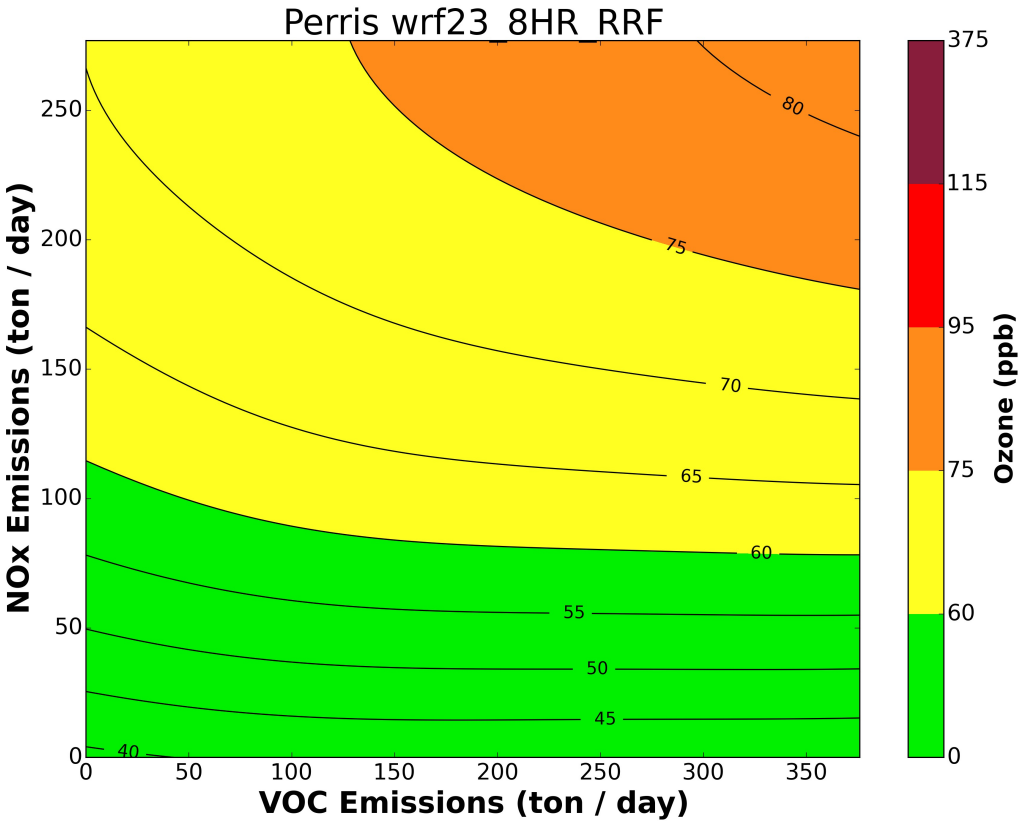
Perris wrf23_8HR_RRF
NOx Emissions (ton / day)
VOC Emissions (ton / day)
Ozone (ppb)
0
50
100
150
200
250
300
350
375
115
95
75
60
80
70
65
55
50
45
40

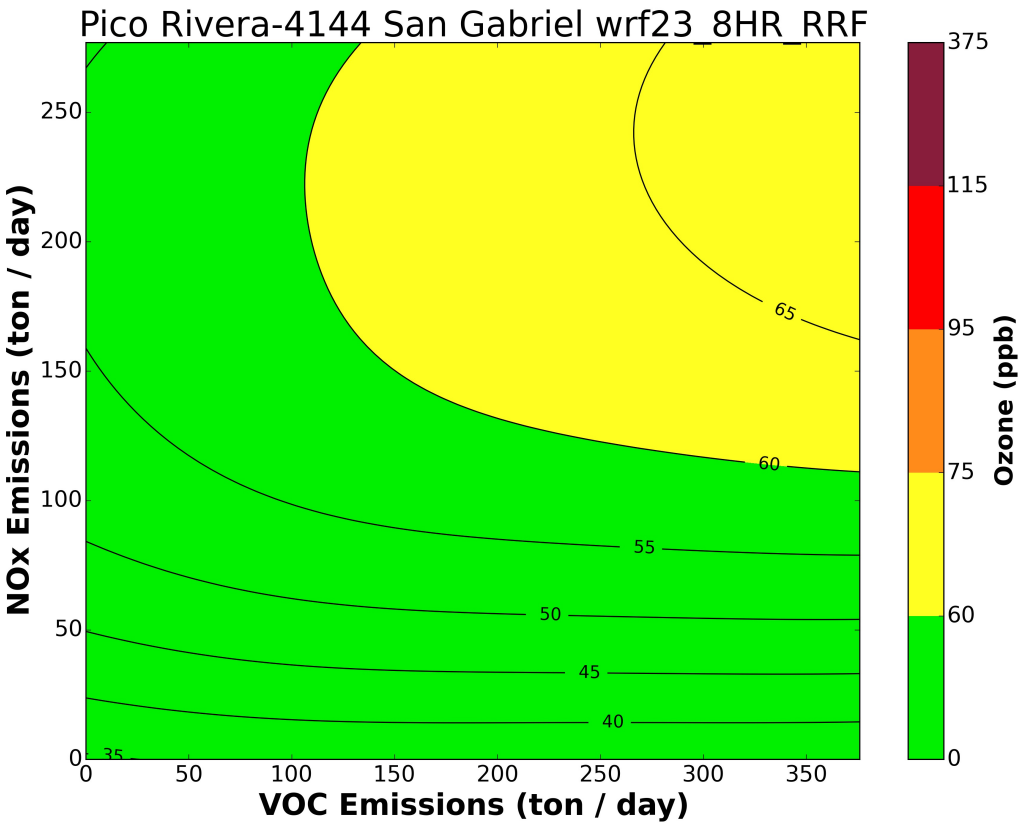
Pico Rivera-4144 San Gabriel wrf23_8HR_RRF
NOx Emissions (ton / day)
VOC Emissions (ton / day)
Ozone (ppb)
0
50
100
150
200
250
300
350
375
115
95
75
60
65
60
55
50
45
40
35

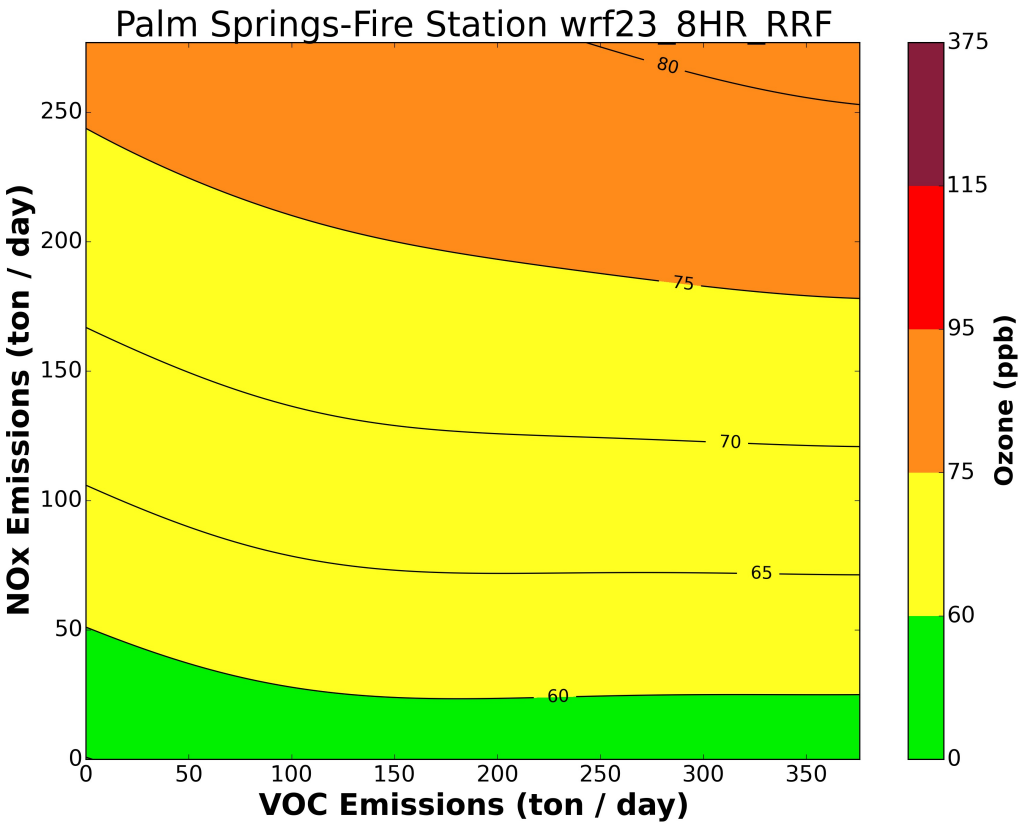
Palm Springs-Fire Station wrf23_8HR_RRF
NOx Emissions (ton / day)
VOC Emissions (ton / day)
Ozone (ppb)
80
75
70
65
60
0
50
100
150
200
250
300
350
375
115
95

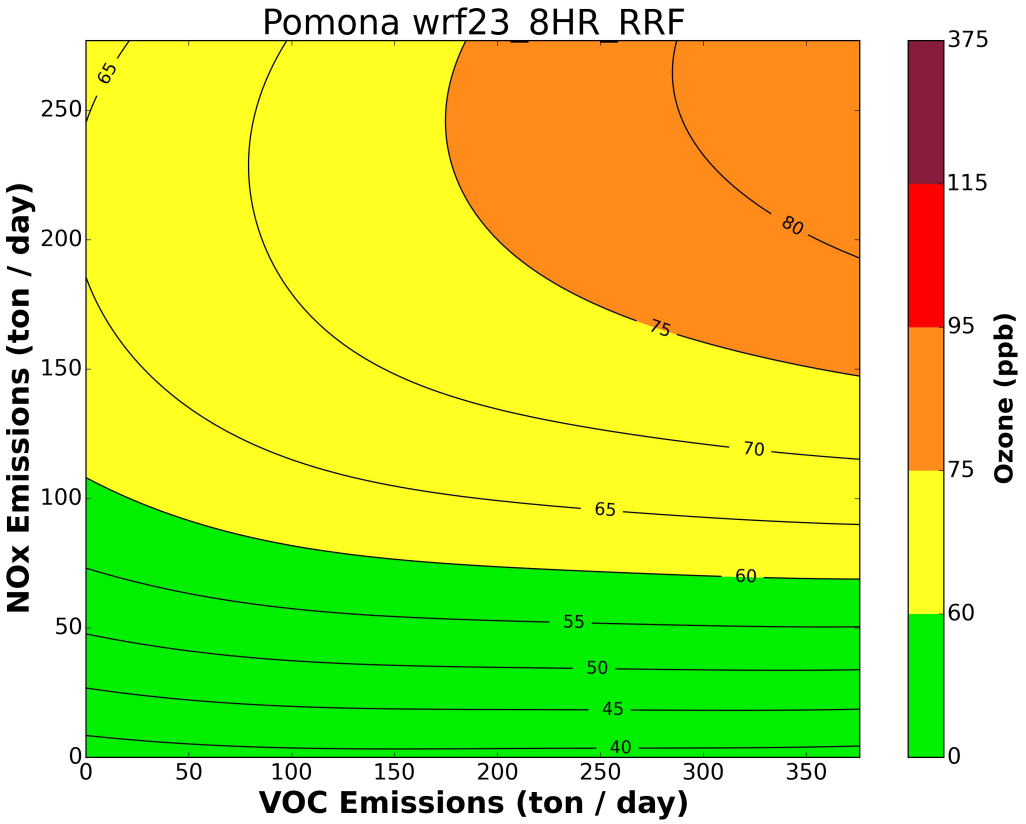
Pomona wrf23_8HR_RRF
NOx Emissions (ton / day)
VOC Emissions (ton / day)
Ozone (ppb)
0
50
100
150
200
250
300
350
375
115
95
75
60
40
45
50
55
60
65
70
75
80

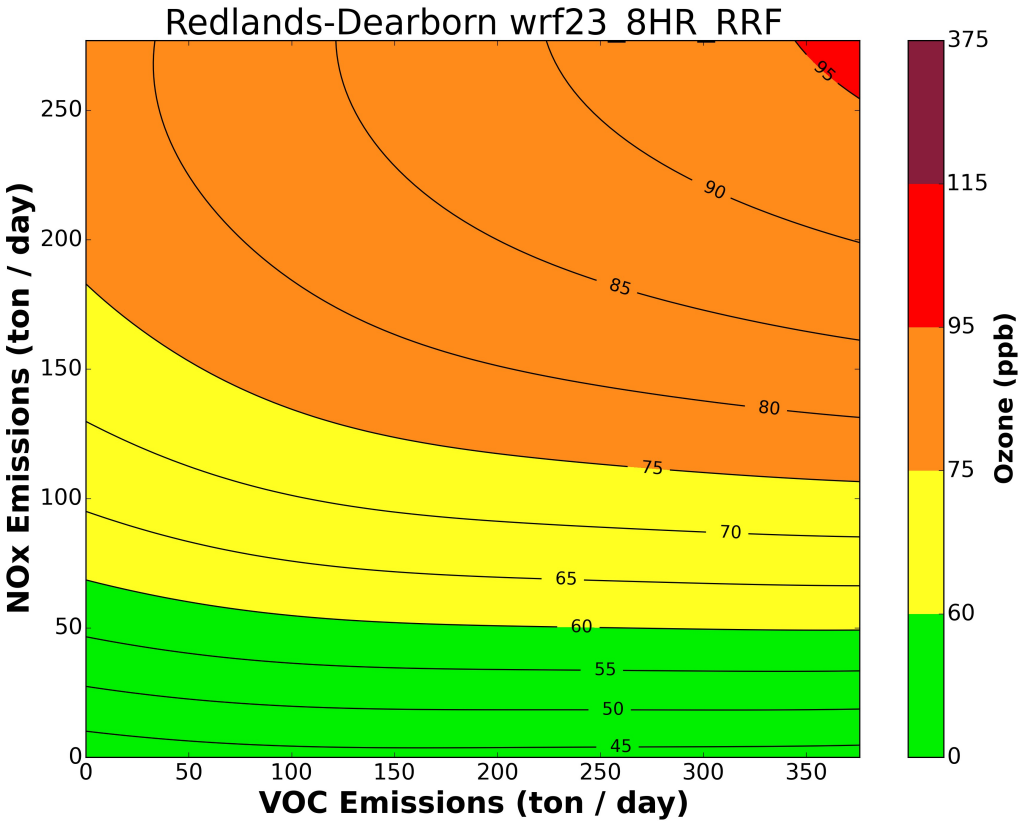
Redlands-Dearborn wrf23_8HR_RRF
NOx Emissions (ton / day)
VOC Emissions (ton / day)
Ozone (ppb)
0
50
100
150
200
250
300
350
375
115
95
75
60
0
95
90
85
80
75
70
65
60
55
50
45

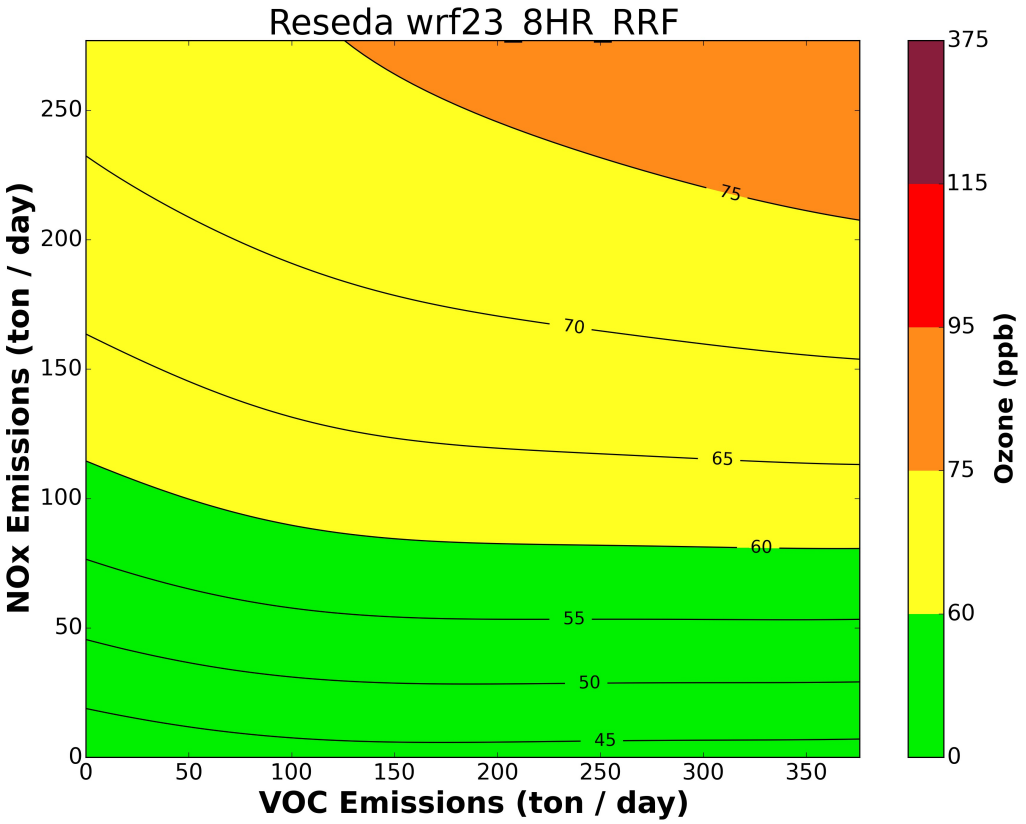
Reseda wrf23_8HR_RRF
NOx Emissions (ton / day)
VOC Emissions (ton / day)
Ozone (ppb)
0
50
100
150
200
250
300
350
375
115
95
75
60
0
45
50
55
60
65
70
75

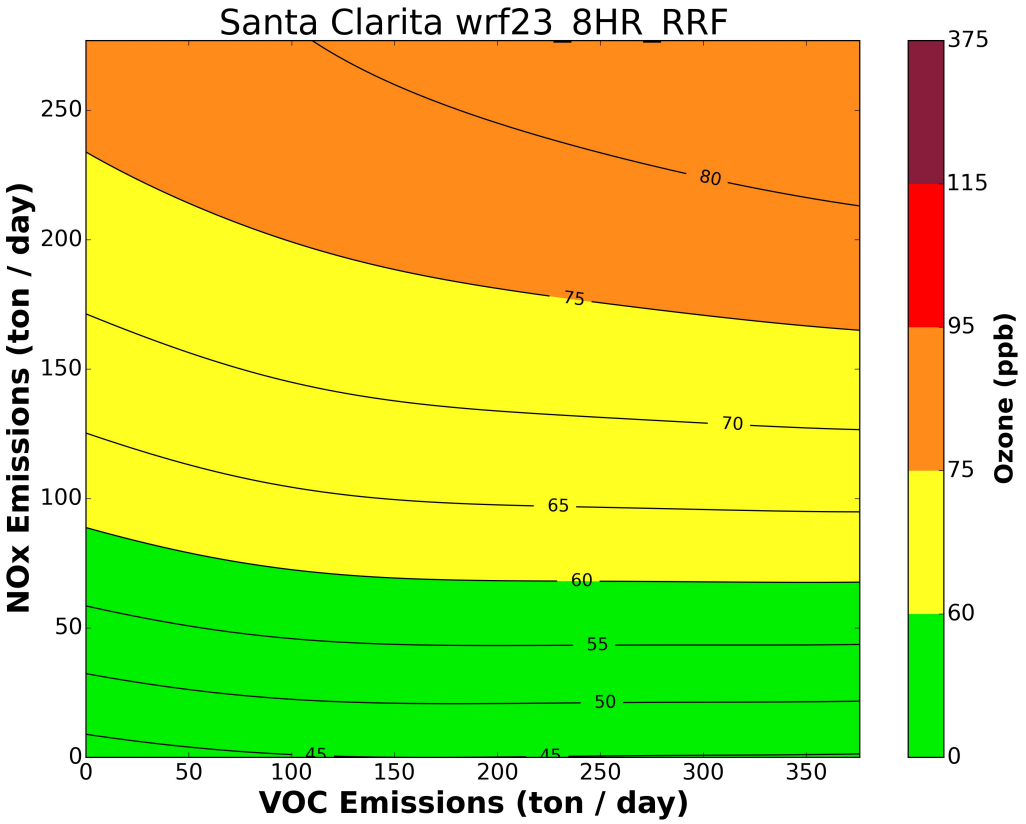
Santa Clarita wrf23_8HR_RRF
NOx Emissions (ton / day)
VOC Emissions (ton / day)
Ozone (ppb)
0
50
100
150
200
250
300
350
80
75
70
65
60
55
50
45
375
115
95
75
60
0

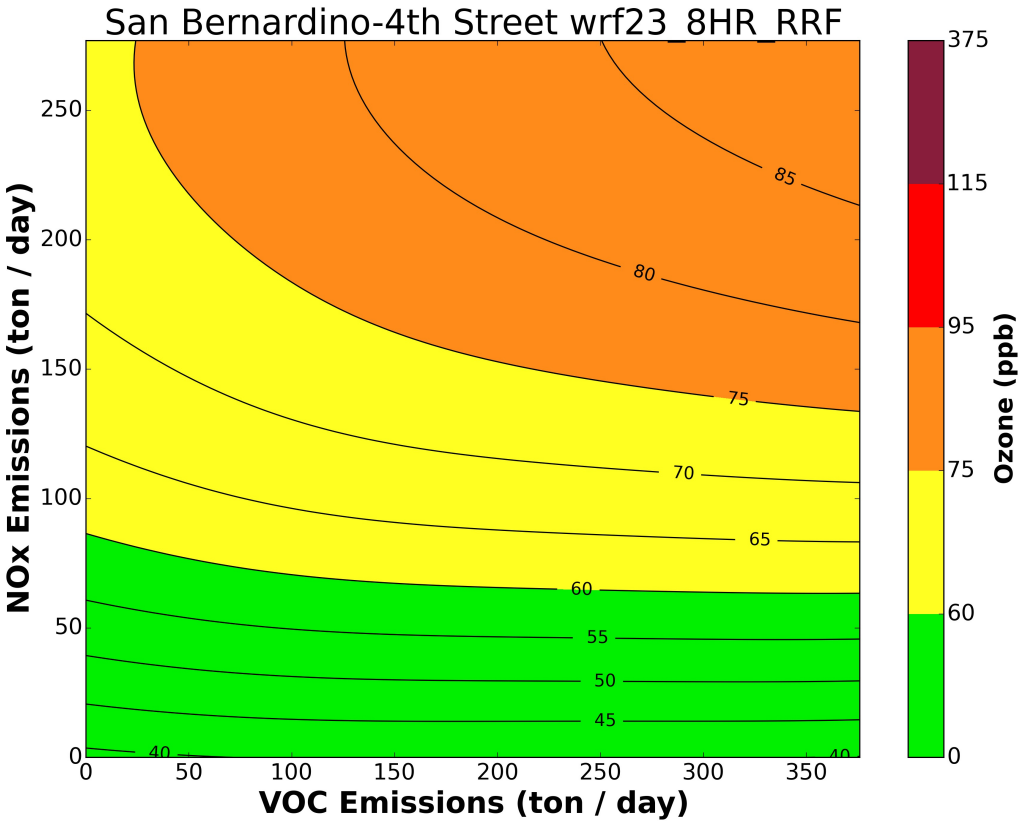
San Bernardino-4th Street wrf23_8HR_RRF
NOx Emissions (ton / day)
VOC Emissions (ton / day)
Ozone (ppb)
0
50
100
150
200
250
300
350
375
115
95
75
60
85
80
75
70
65
60
55
50
45
40

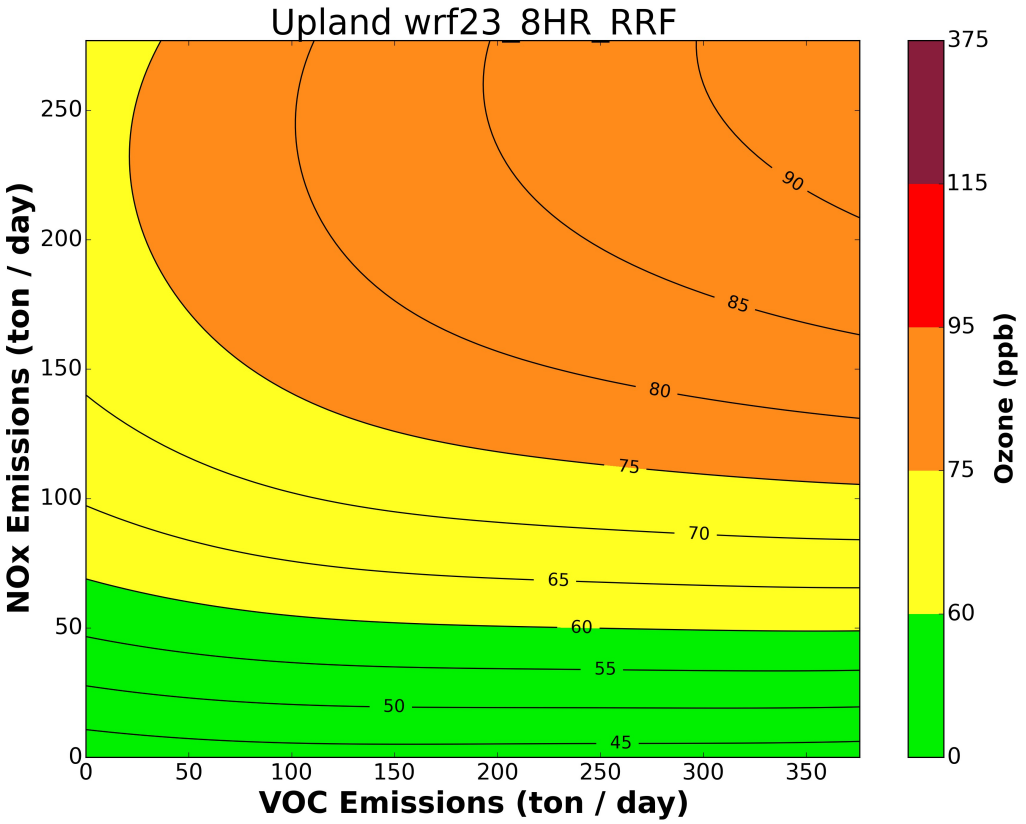
Upland wrf23_8HR_RRF
NOx Emissions (ton / day)
VOC Emissions (ton / day)
Ozone (ppb)
0
50
100
150
200
250
300
350
375
115
95
75
60
90
85
80
75
70
65
60
55
50
45

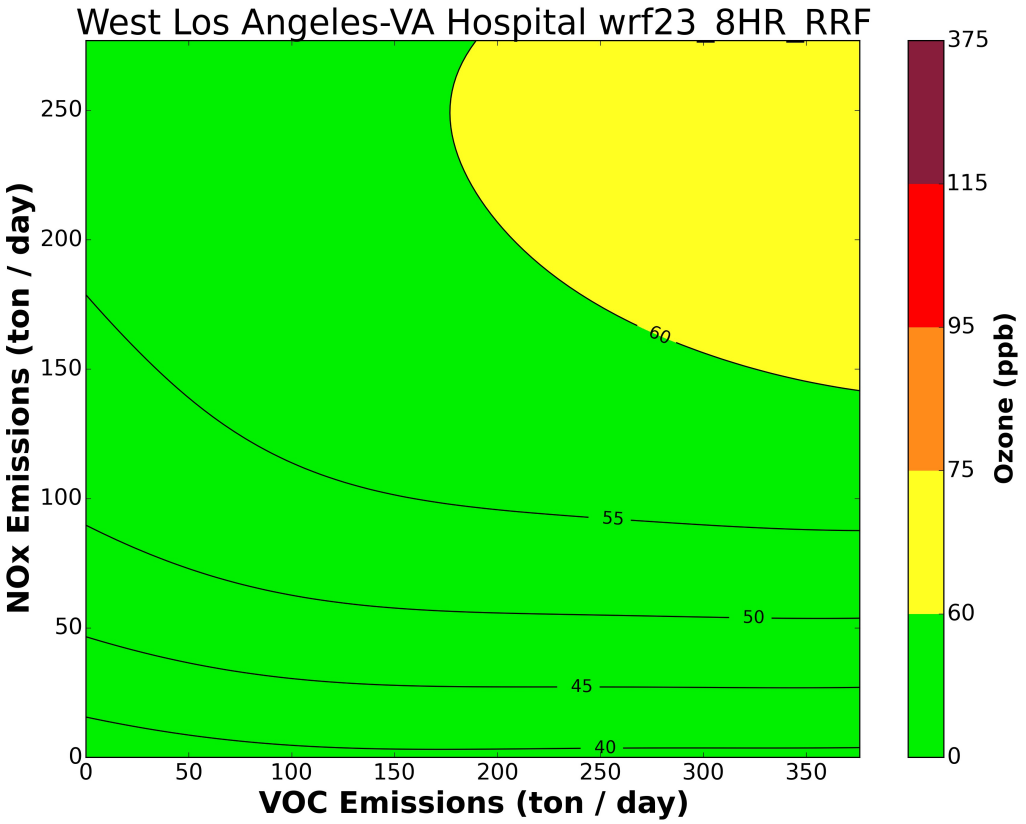
West Los Angeles-VA Hospital wrf23_8HR_RRF
NOx Emissions (ton / day)
VOC Emissions (ton / day)
Ozone (ppb)
0
50
100
150
200
250
300
350
375
115
95
75
60
55
50
45
40

Attachment 6

2022 1-HOUR OZONE ISOPLETHS

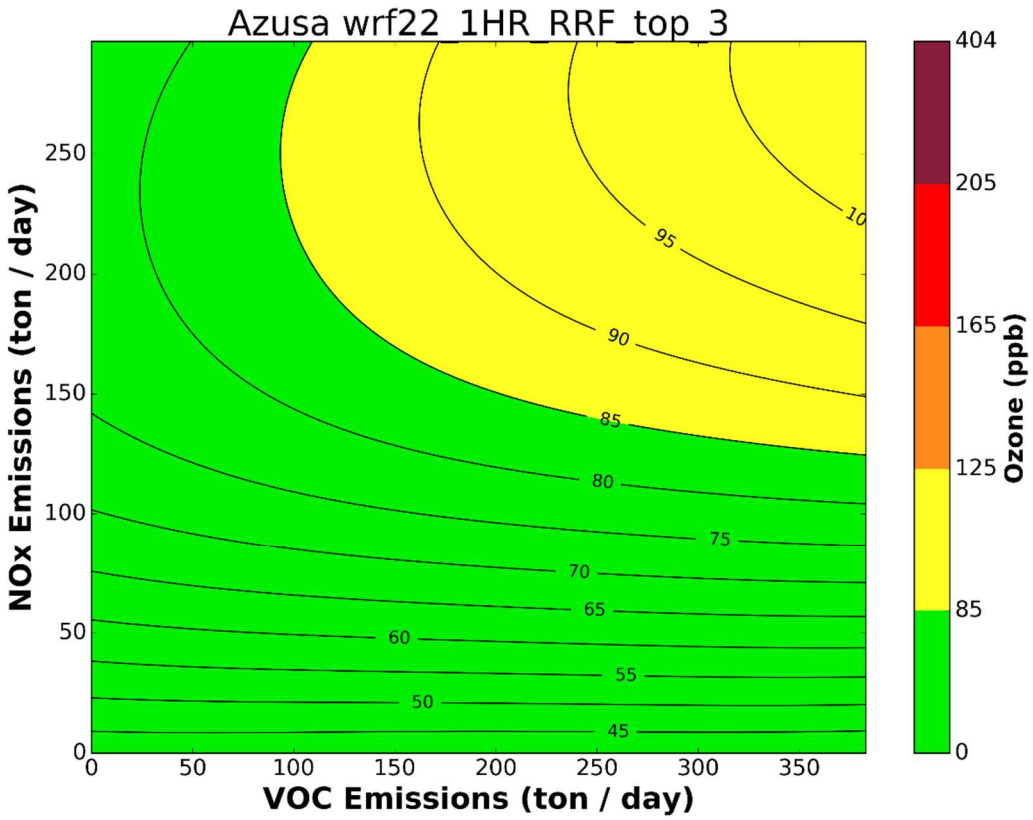
Azusa wrf22_1HR_RRF_top_3
NOx Emissions (ton / day)
VOC Emissions (ton / day)
Ozone (ppb)
0
50
100
150
200
250
300
350
404
205
165
125
85
0
95
90
85
80
75
70
65
60
55
50
45

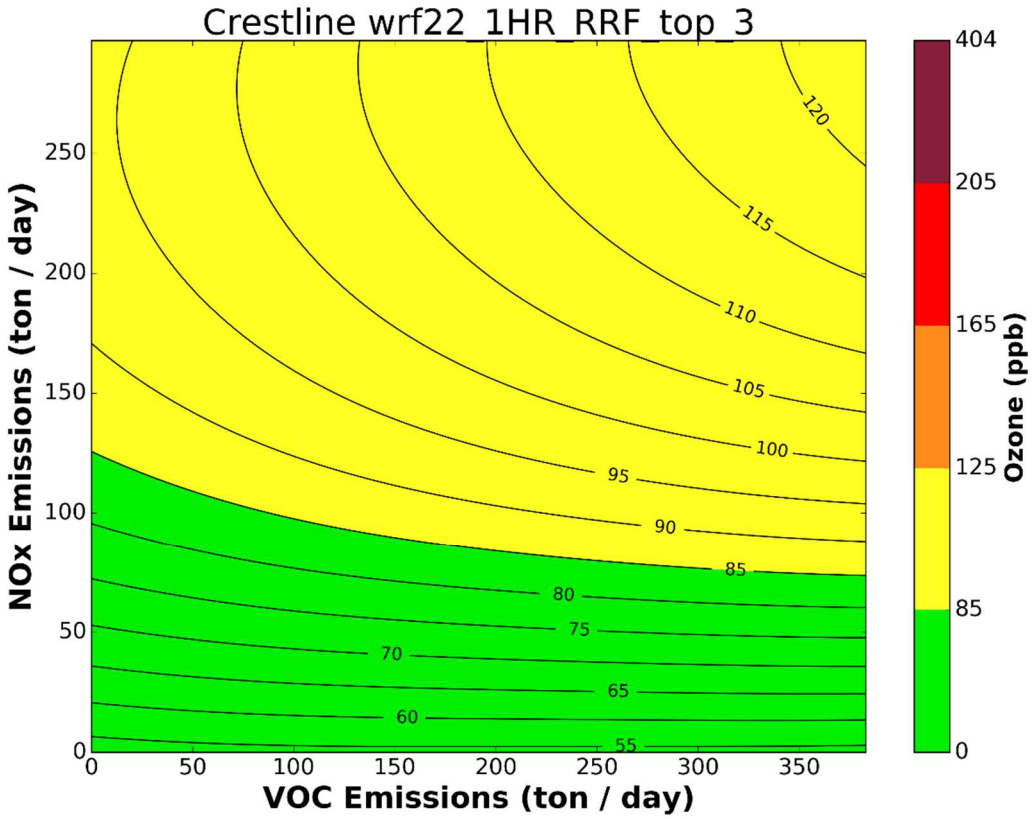
Crestline wrf22_1HR_RRF_top_3
NOx Emissions (ton / day)
VOC Emissions (ton / day)
Ozone (ppb)
0
50
100
150
200
250
300
350
404
205
165
125
85
0
120
115
110
105
100
95
90
85
80
75
70
65
60
55

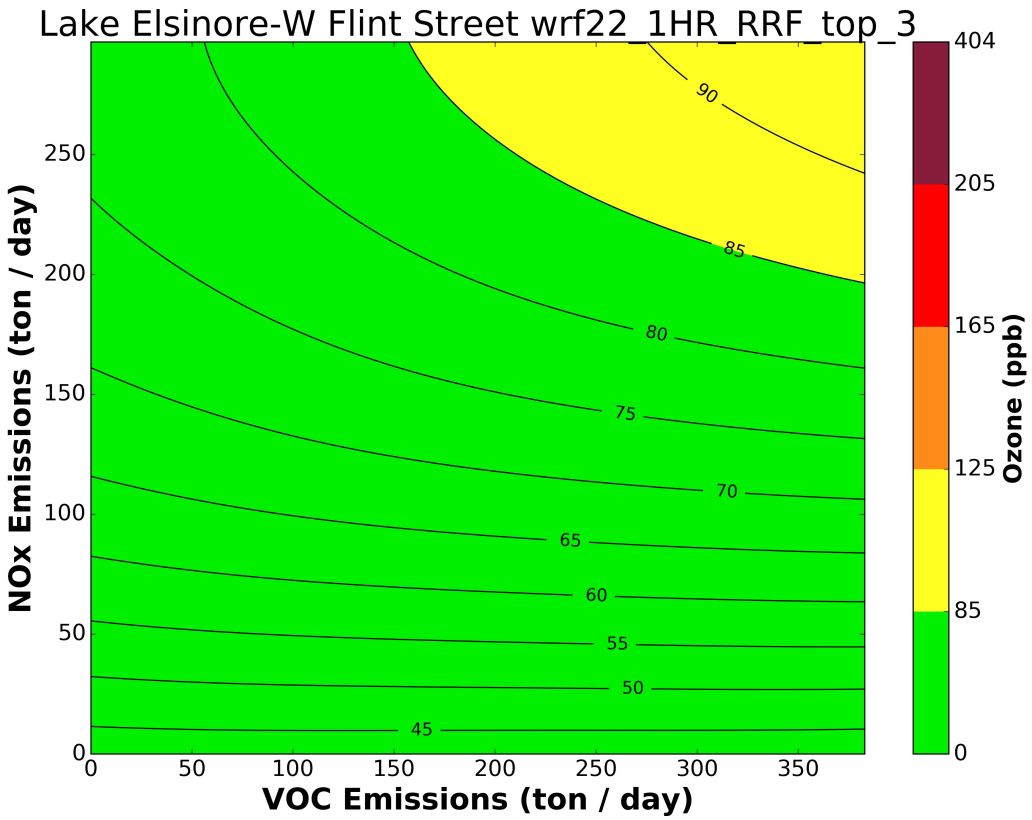
Lake Elsinore-W Flint Street wrf22_1HR_RRF_top_3
NOx Emissions (ton / day)
VOC Emissions (ton / day)
Ozone (ppb)
0
50
100
150
200
250
300
350
404
205
165
125
85
0
90
85
80
75
70
65
60
55
50
45

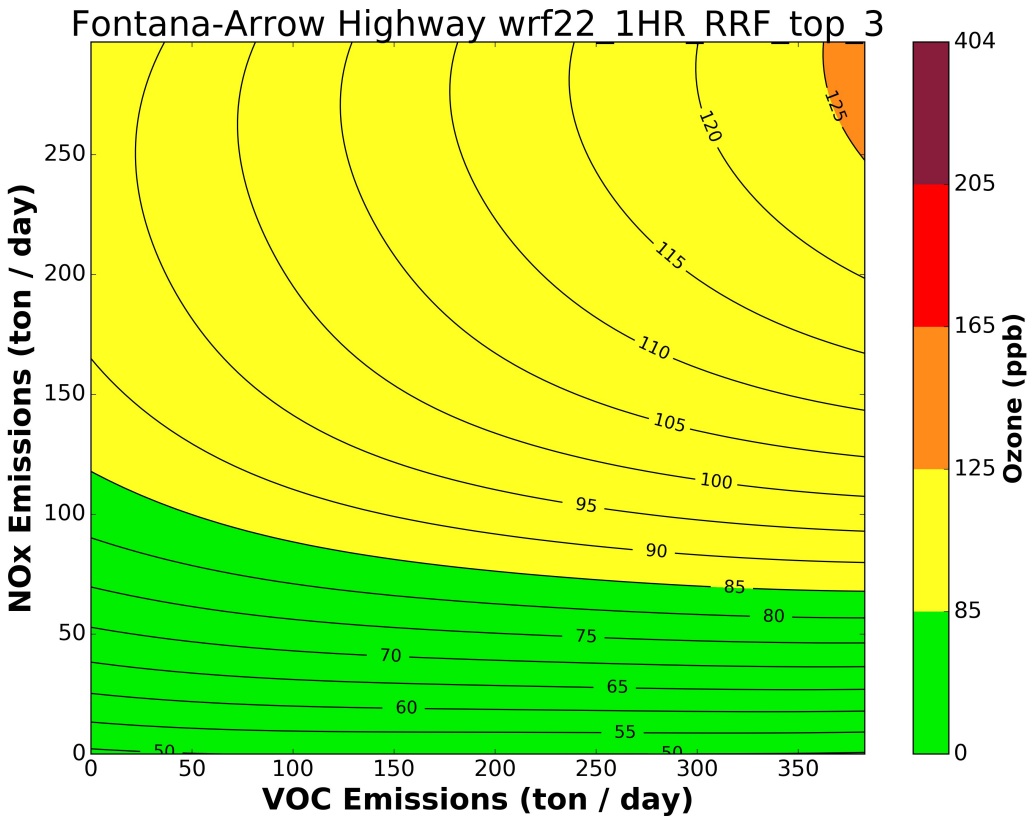
Fontana-Arrow Highway wrf22_1HR_RRF_top_3
NOx Emissions (ton / day)
VOC Emissions (ton / day)
Ozone (ppb)
0
50
100
150
200
250
300
350
404
205
165
125
85
0
125
120
115
110
105
100
95
90
85
80
75
70
65
60
55
50

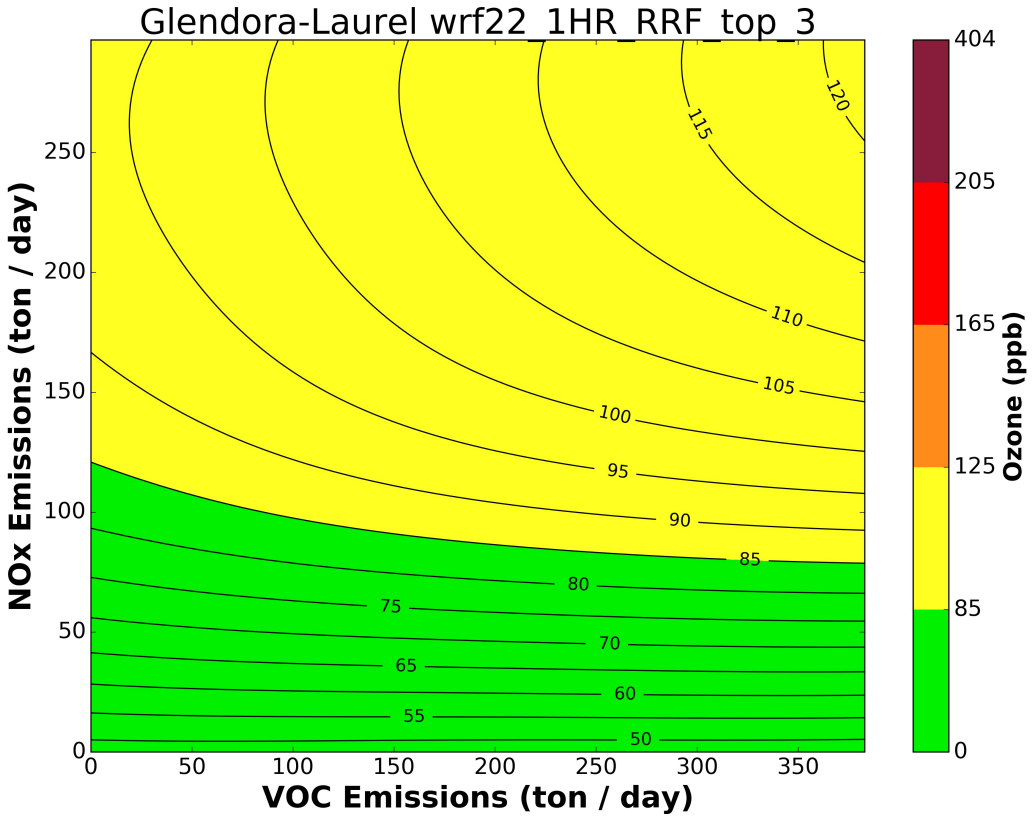
Glendora-Laurel wrf22_1HR_RRF_top_3
NOx Emissions (ton / day)
VOC Emissions (ton / day)
Ozone (ppb)
0
50
100
150
200
250
300
350
404
205
165
125
85
0
120
115
110
105
100
95
90
85
80
75
70
65
60
55
50

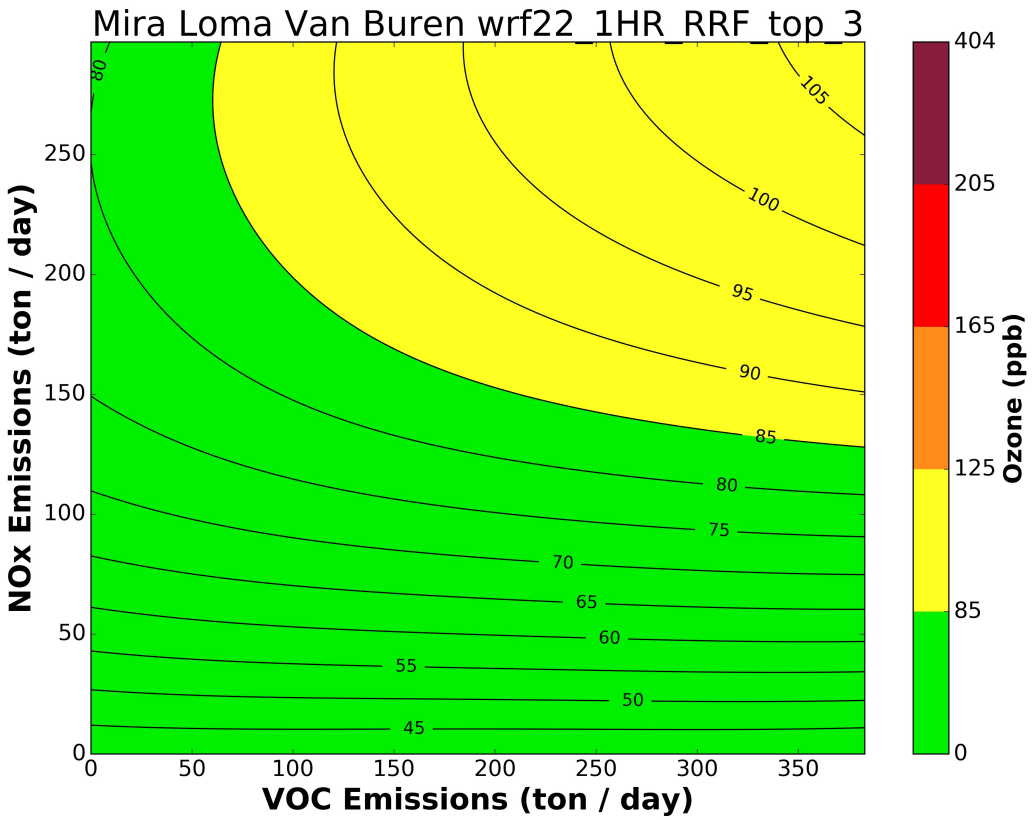
Mira Loma Van Buren wrf22_1HR_RRF_top_3
NOx Emissions (ton / day)
VOC Emissions (ton / day)
Ozone (ppb)
0
50
100
150
200
250
300
350
404
205
165
125
85
0
105
100
95
90
85
80
75
70
65
60
55
50
45

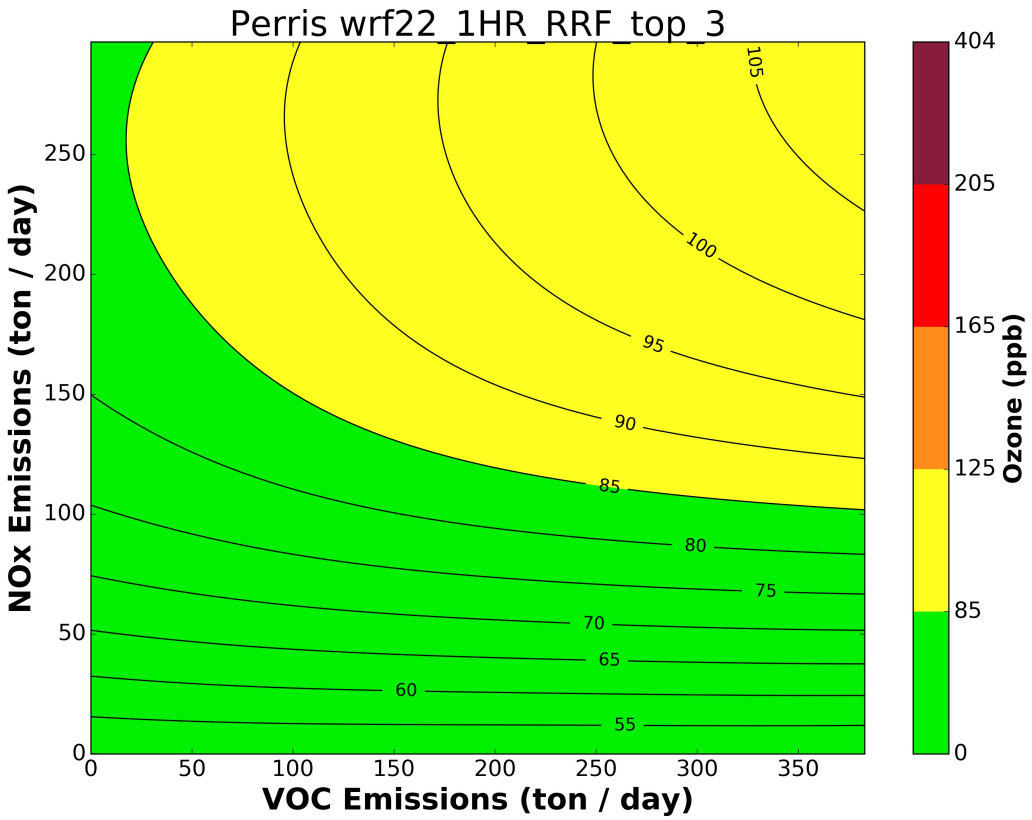
Perris wrf22_1HR_RRF_top_3
NOx Emissions (ton / day)
VOC Emissions (ton / day)
Ozone (ppb)
0
50
100
150
200
250
300
350
404
205
165
125
85
0
105
100
95
90
85
80
75
70
65
60
55

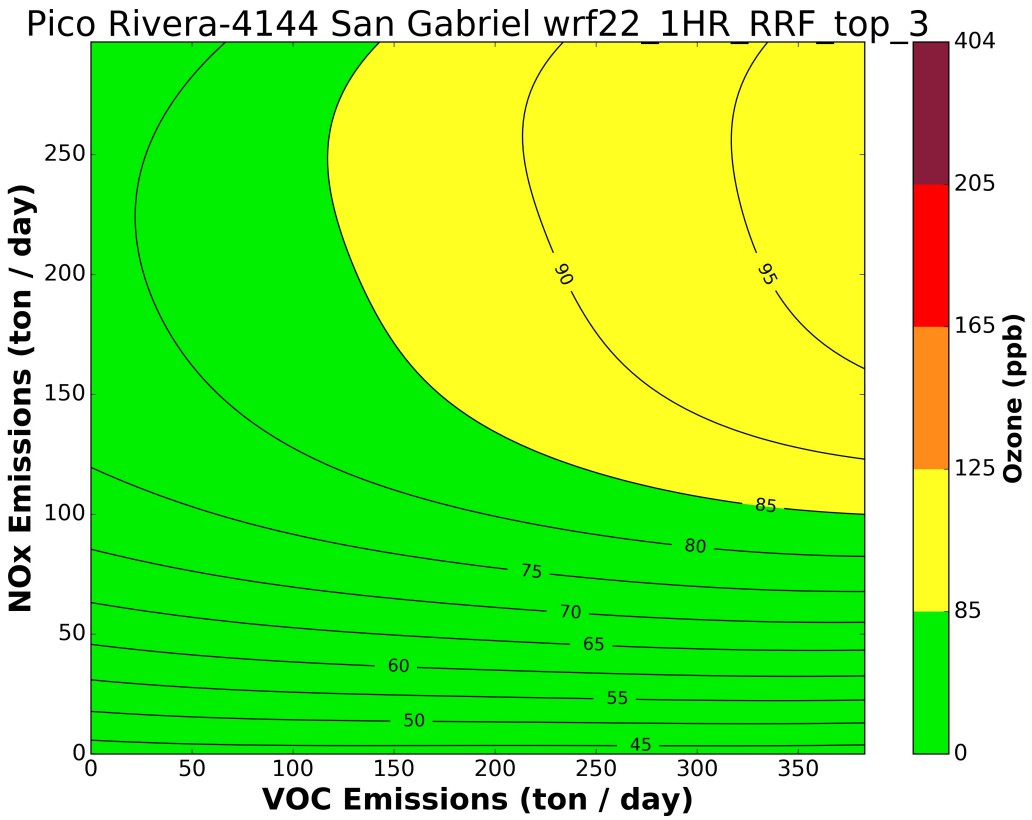
Pico Rivera-4144 San Gabriel wrf22_1HR_RRF_top_3
NOx Emissions (ton / day)
VOC Emissions (ton / day)
Ozone (ppb)
0
50
100
150
200
250
300
350
404
205
165
125
85
0
90
95
85
80
75
70
65
60
55
50
45

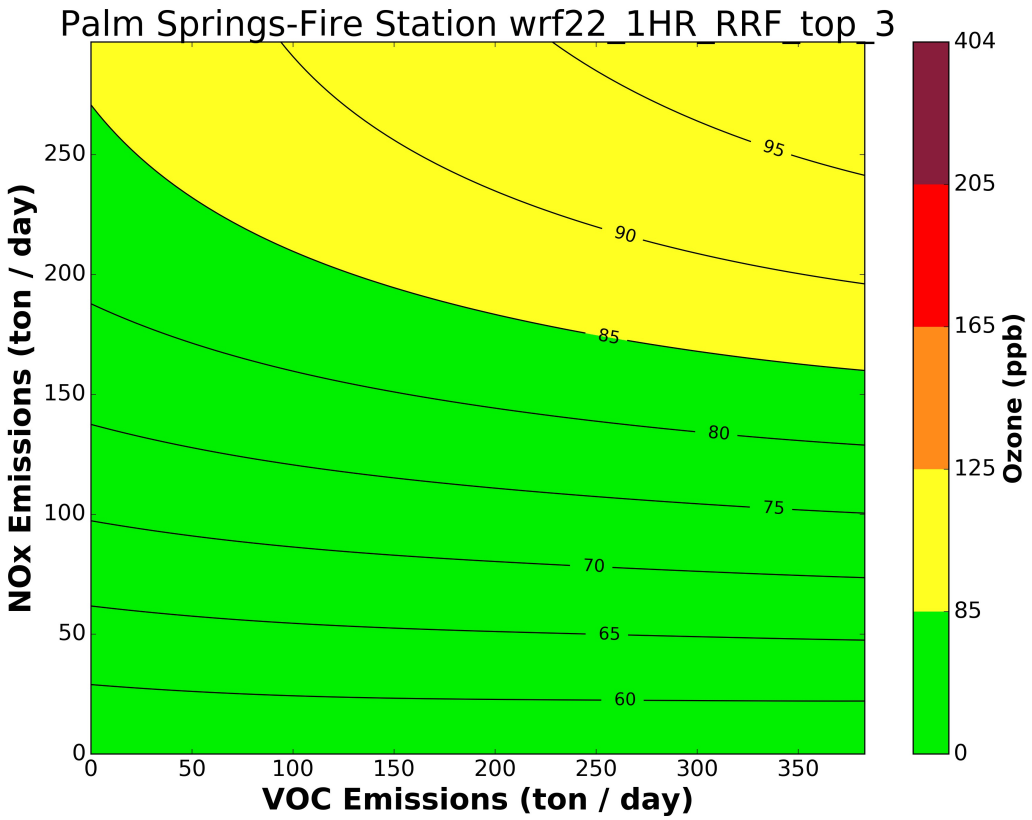
Palm Springs-Fire Station wrf22_1HR_RRF_top_3
NOx Emissions (ton / day)
VOC Emissions (ton / day)
Ozone (ppb)
0
50
100
150
200
250
300
350
95
90
85
80
75
70
65
60
404
205
165
125
85
0

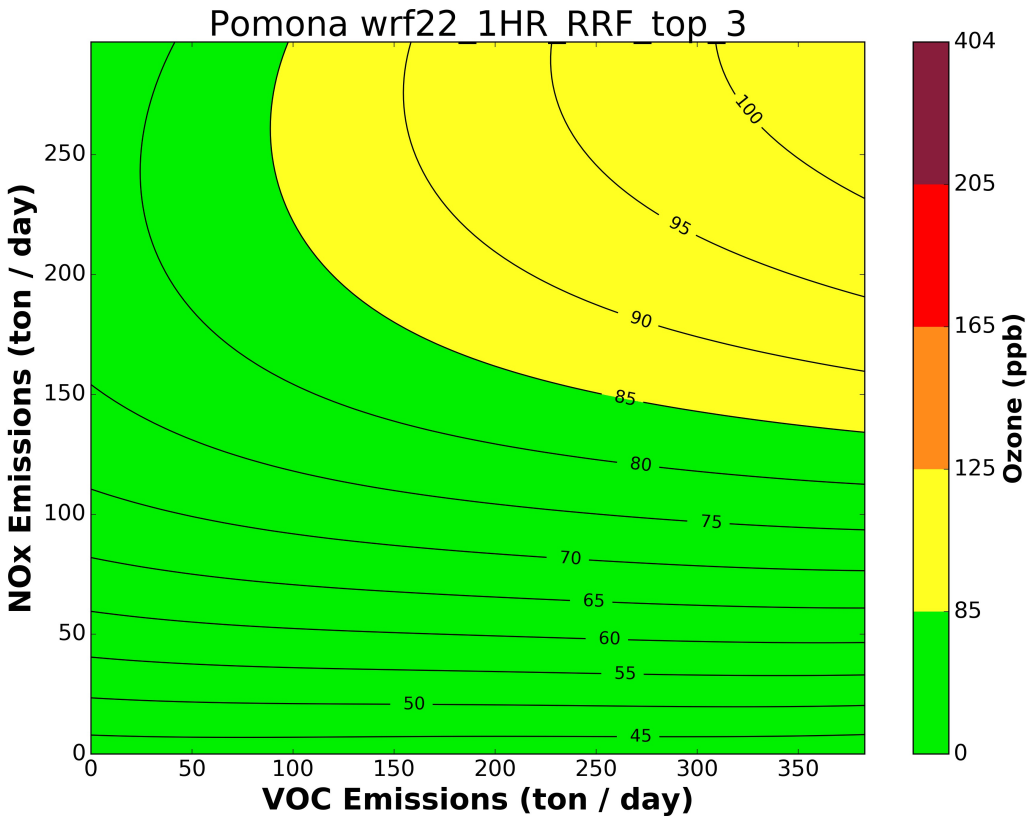
Pomona wrf22_1HR_RRF_top_3
NOx Emissions (ton / day)
VOC Emissions (ton / day)
Ozone (ppb)
0
50
100
150
200
250
300
350
404
205
165
125
85
0
100
95
90
85
80
75
70
65
60
55
50
45

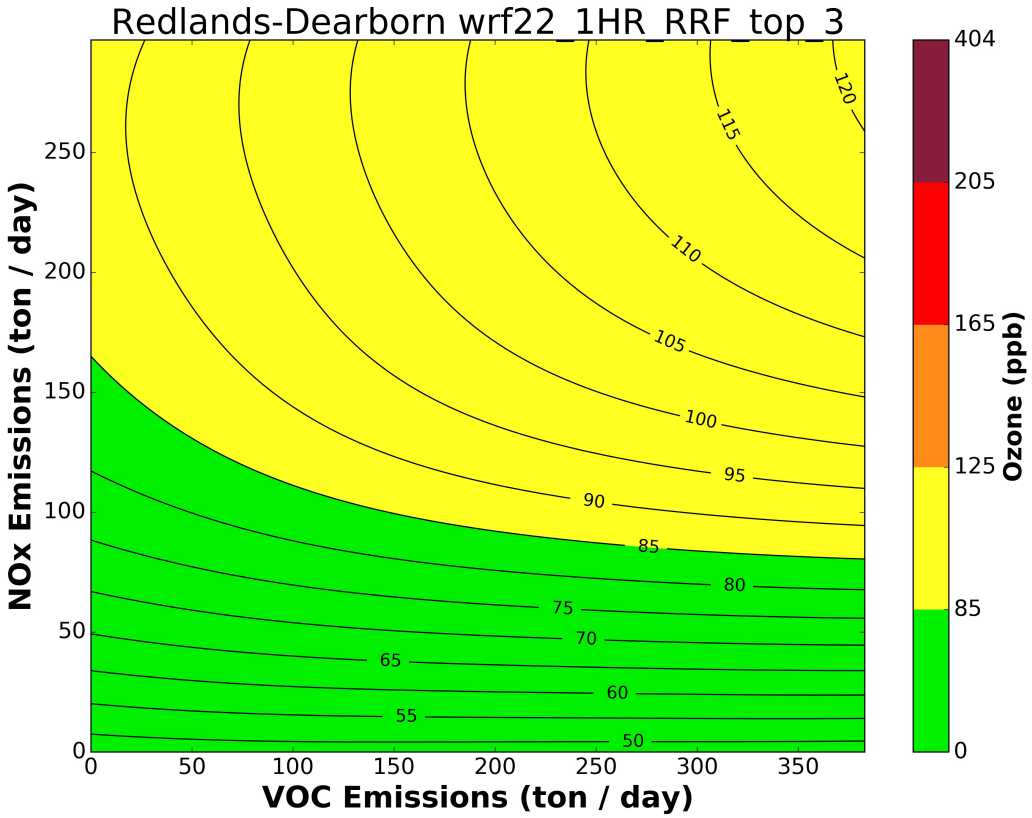
Redlands-Dearborn wrf22_1HR_RRF_top_3
NOx Emissions (ton / day)
VOC Emissions (ton / day)
Ozone (ppb)
0
50
100
150
200
250
300
350
404
205
165
125
85
0
120
115
110
105
100
95
90
85
80
75
70
65
60
55
50

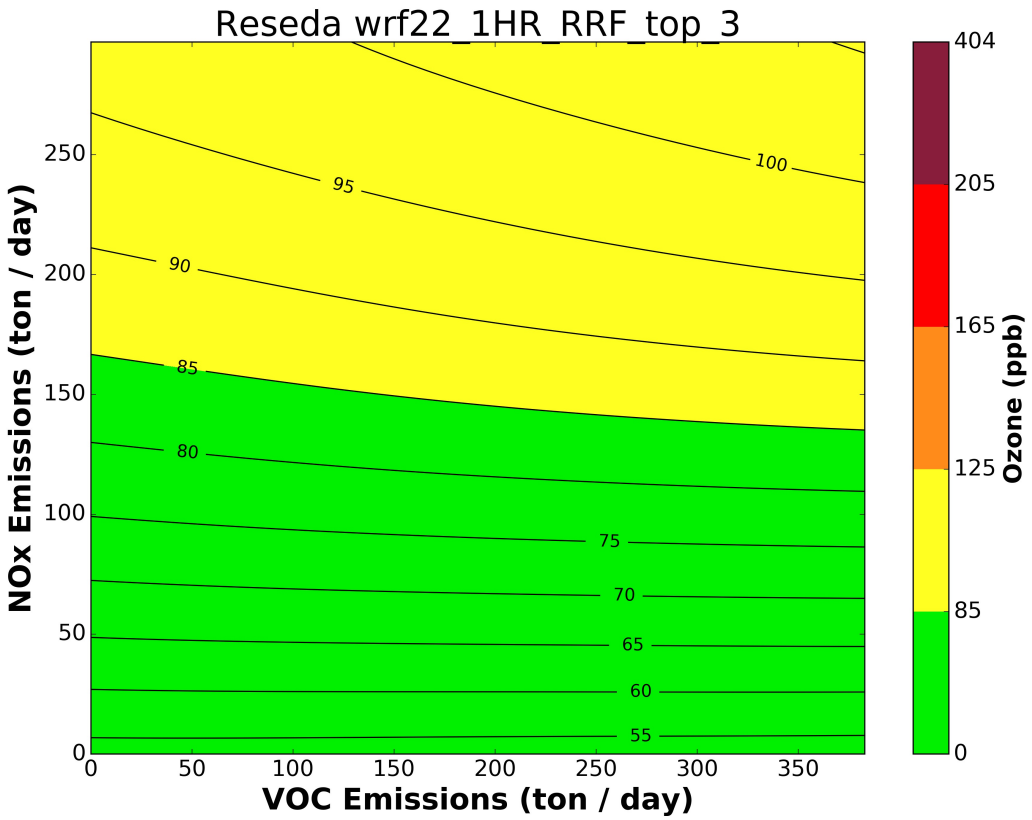
Reseda wrf22_1HR_RRF_top_3
NOx Emissions (ton / day)
VOC Emissions (ton / day)
Ozone (ppb)
0
50
100
150
200
250
300
350
404
205
165
125
85
0
100
95
90
85
80
75
70
65
60
55

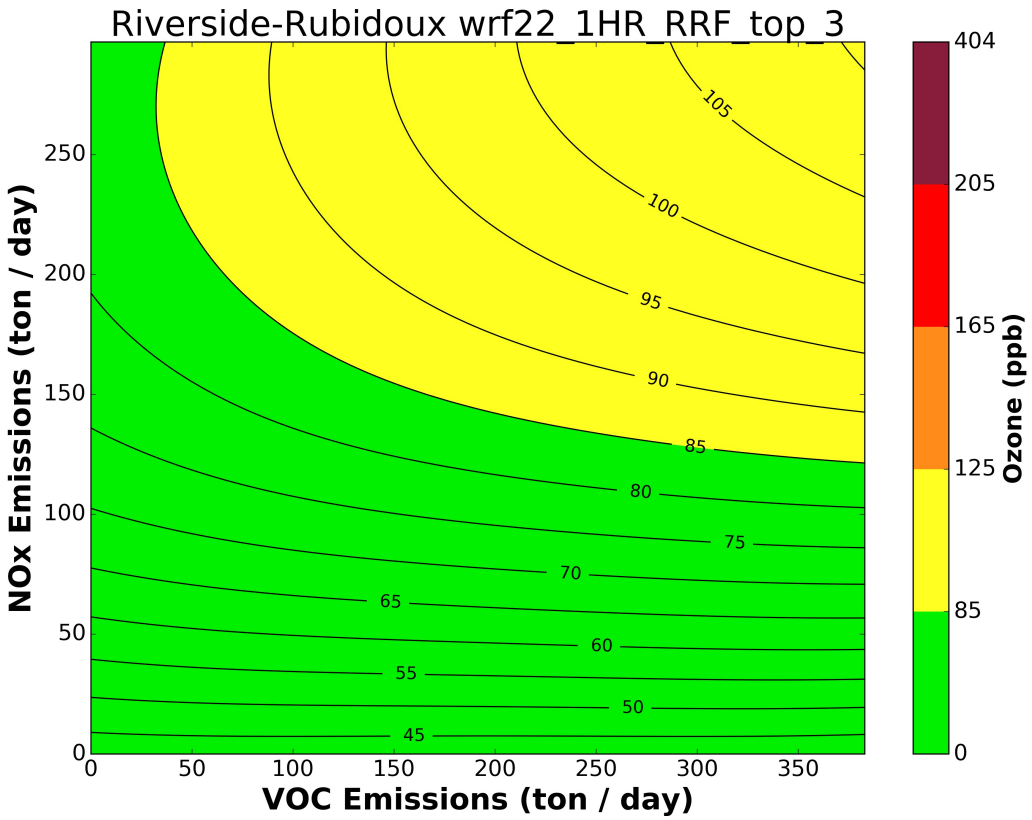
Riverside-Rubidoux wrf22_1HR_RRF_top_3
NOx Emissions (ton / day)
VOC Emissions (ton / day)
Ozone (ppb)
0
50
100
150
200
250
300
350
105
100
95
90
85
80
75
70
65
60
55
50
45
404
205
165
125
85
0

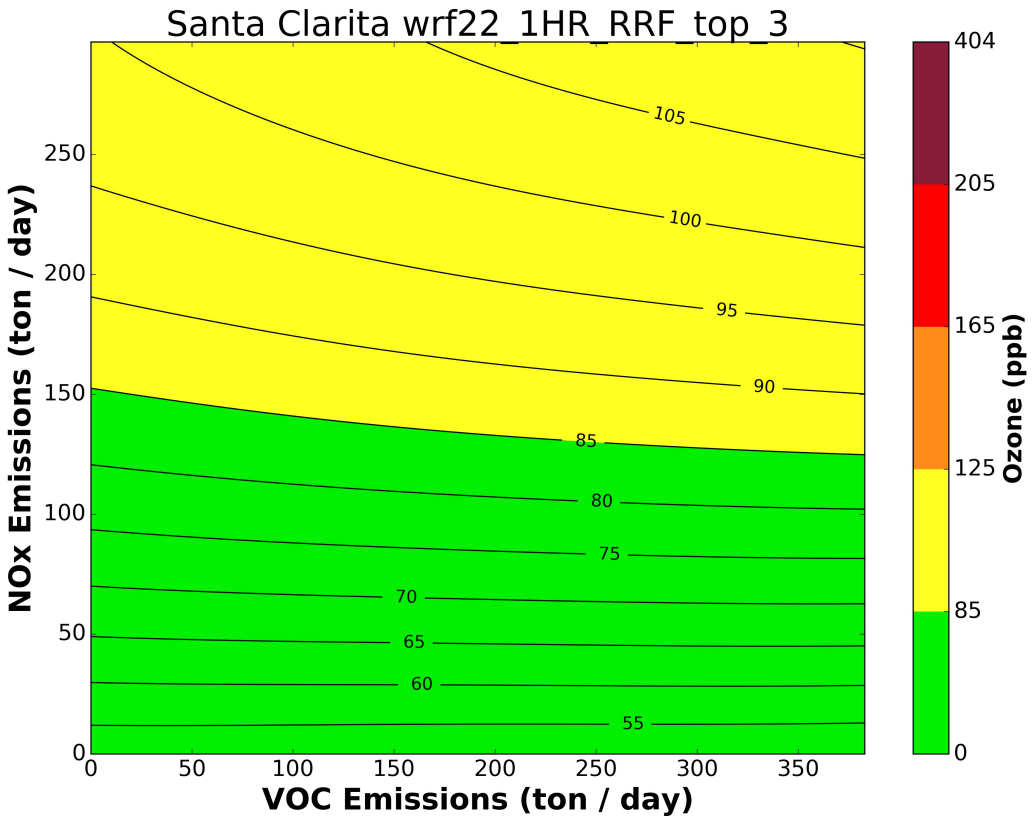
Santa Clarita wrf22_1HR_RRF_top_3
NOx Emissions (ton / day)
VOC Emissions (ton / day)
Ozone (ppb)
105
100
95
90
85
80
75
70
65
60
55
0
50
100
150
200
250
300
350
404
205
165
125
85
0

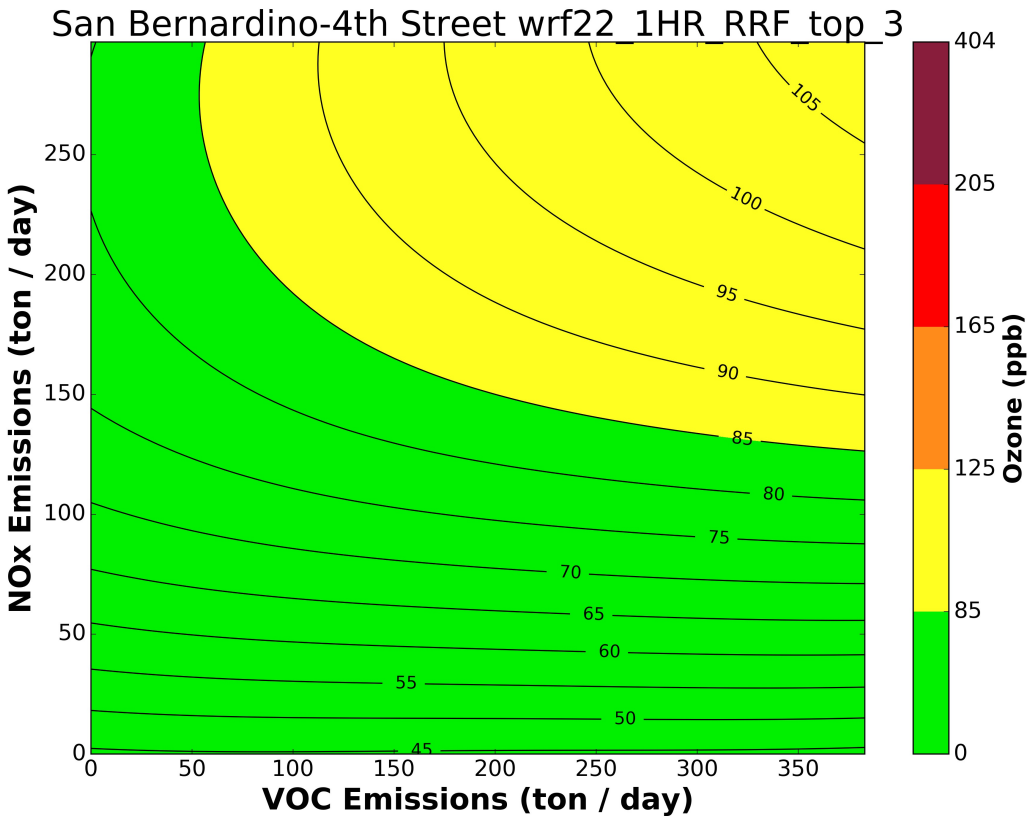
San Bernardino-4th Street wrf22_1HR_RRF_top_3
NOx Emissions (ton / day)
VOC Emissions (ton / day)
Ozone (ppb)
0
50
100
150
200
250
300
350
105
100
95
90
85
80
75
70
65
60
55
50
45
404
205
165
125
85
0

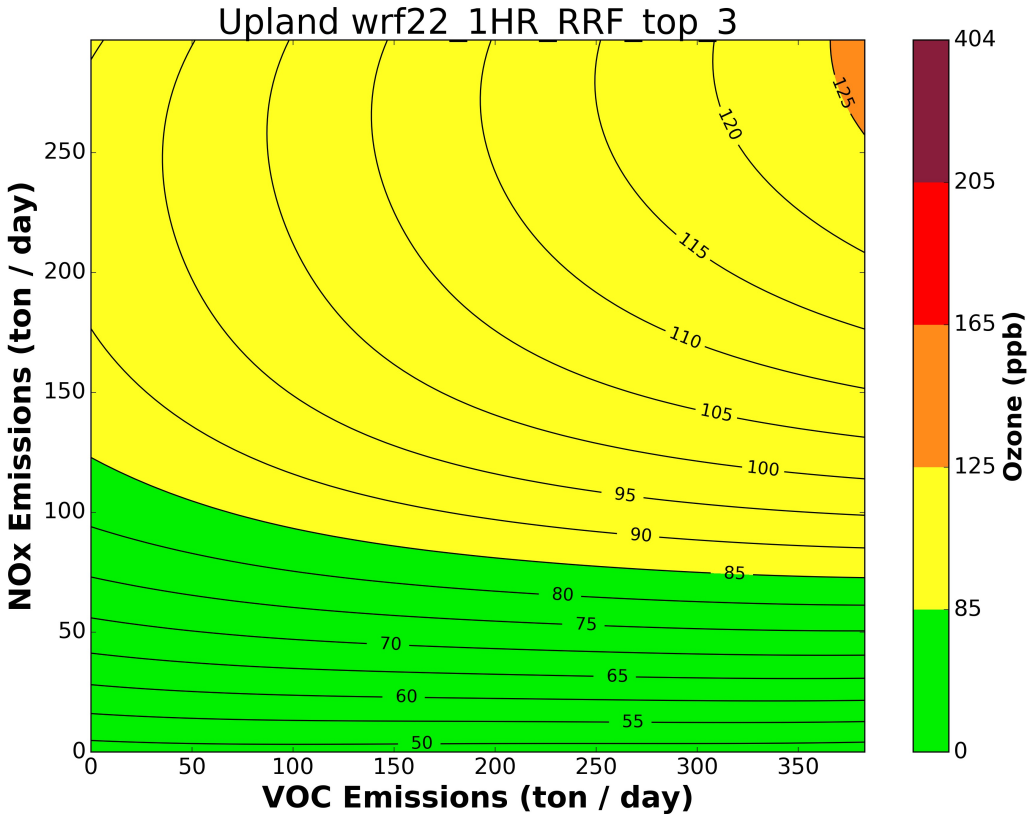
Upland wrf22_1HR_RRF_top_3
NOx Emissions (ton / day)
VOC Emissions (ton / day)
Ozone (ppb)
0
50
100
150
200
250
300
350
404
205
165
125
85
0
125
120
115
110
105
100
95
90
85
80
75
70
65
60
55
50

Attachment 7

ANNUAL UNMONITORED AREA ANALYSIS SUPPLEMENT

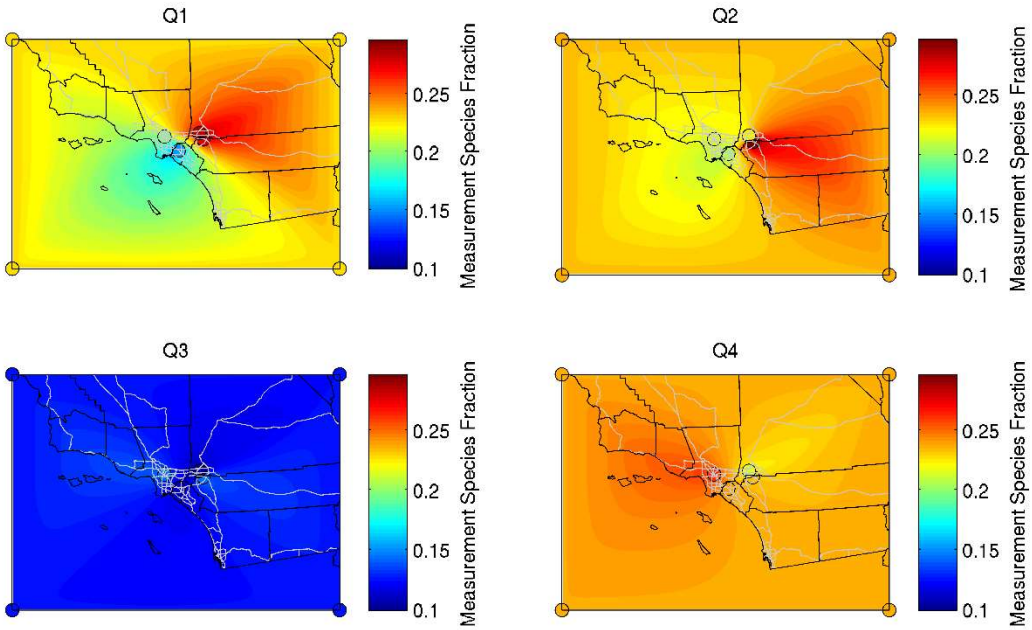

FIGURE 1

2012 Interpolated Measurement Species Fractions for Nitrate. FRM locations are illustrated with black dots. SASS speciation stations and "pseudo stations" are illustrated with black circles.

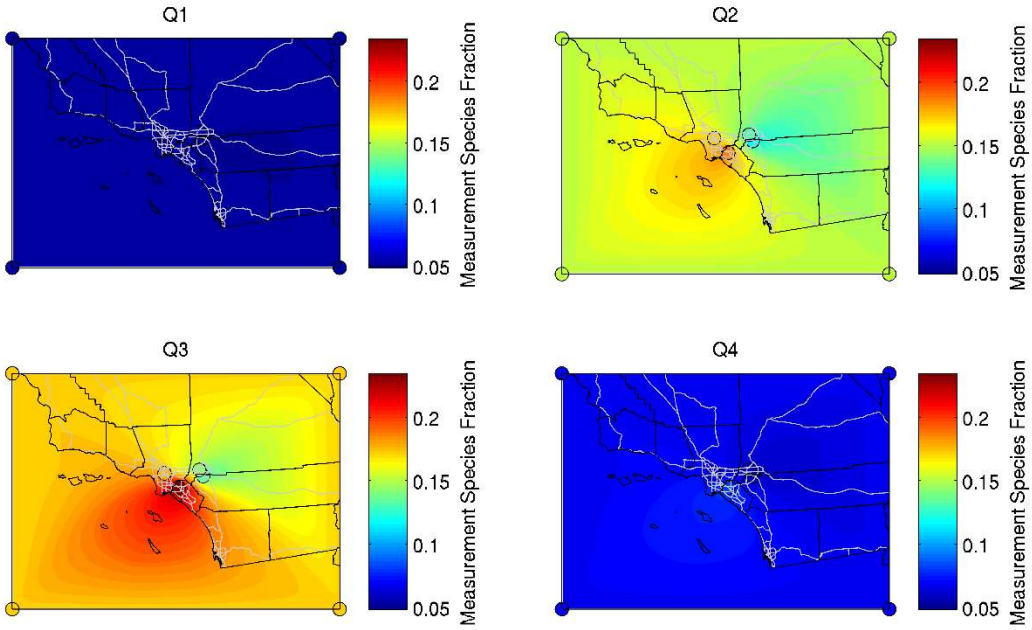

FIGURE 2

2012 Interpolated Measurement Species Fractions for Sulfate. FRM locations are illustrated with black dots. SASS speciation stations and "pseudo stations" are illustrated with black circles.

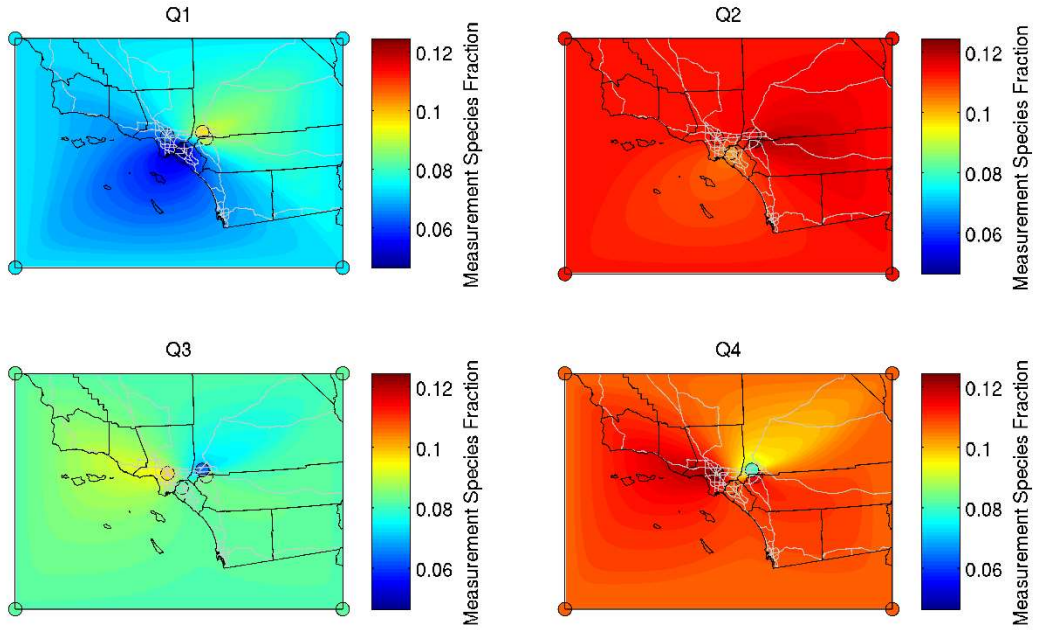

FIGURE 3

2012 Interpolated Measurement Species Fractions for Ammonium. FRM locations are illustrated with black dots. SASS speciation stations and "pseudo stations" are illustrated with black circles.

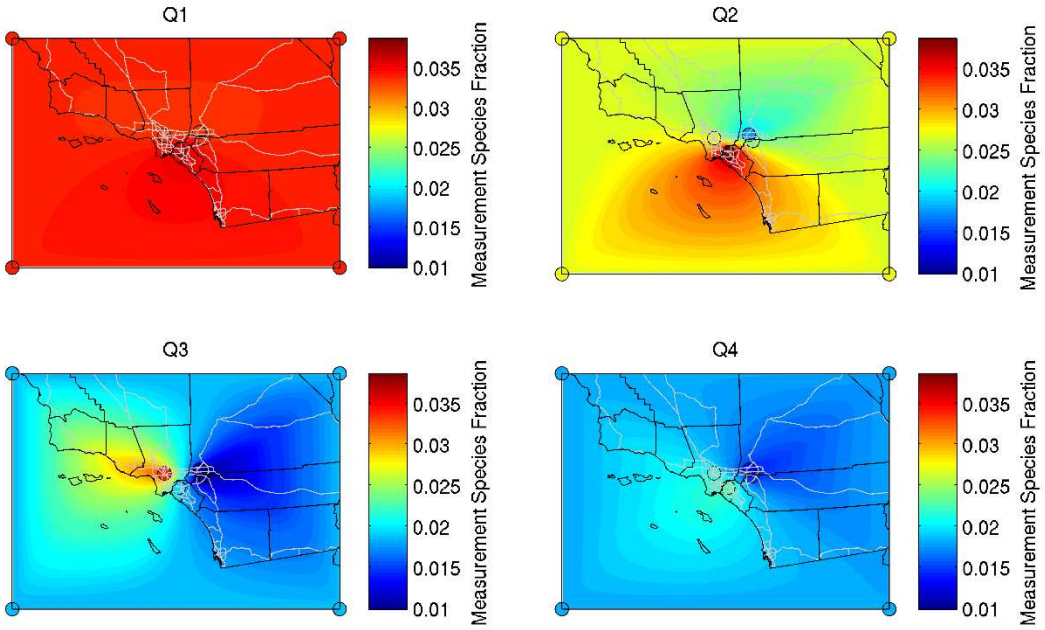

FIGURE 4

2012 Interpolated Measurement Species Fractions for Salt. FRM locations are illustrated with black dots. SASS speciation stations and "pseudo stations" are illustrated with black circles.

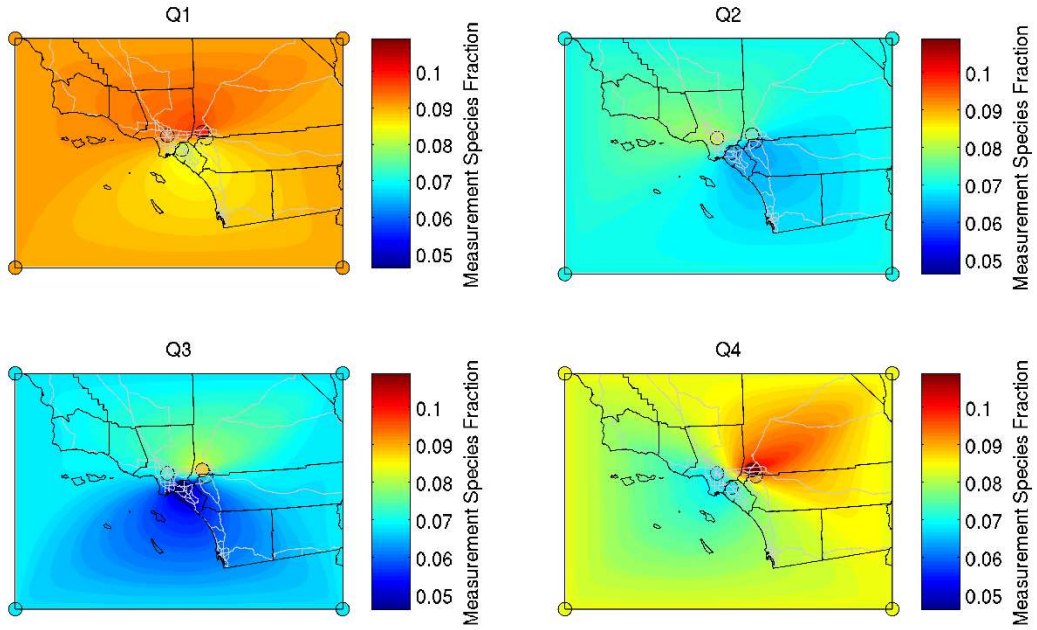

FIGURE 5

2012 Interpolated Measurement Species Fractions for Crustal. FRM locations are illustrated with black dots. SASS speciation stations and "pseudo stations" are illustrated with black circles.

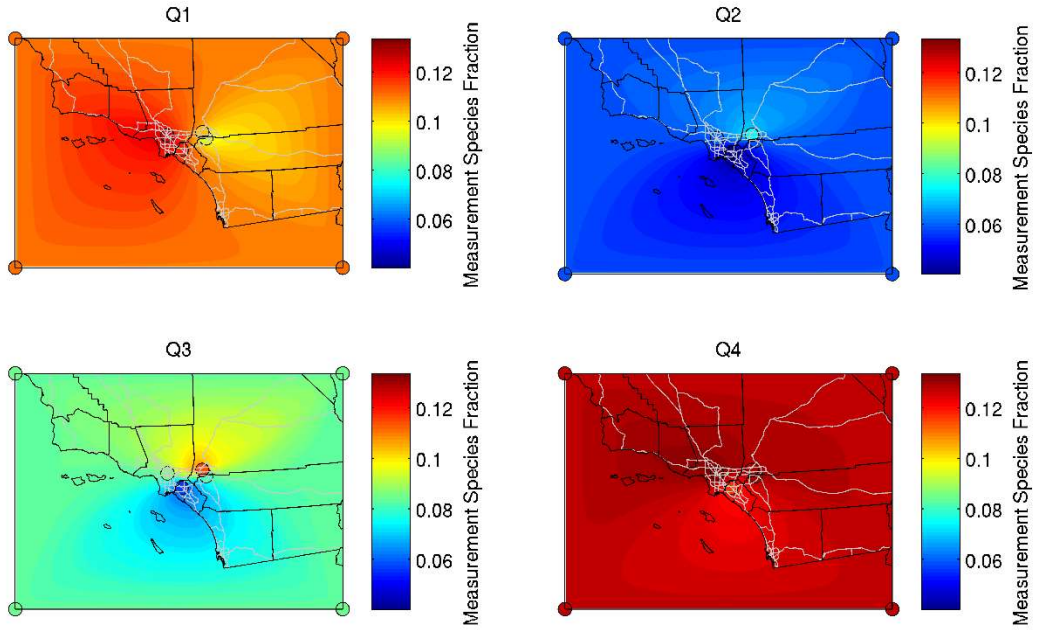

FIGURE 6

2012 Interpolated Measurement Species Fractions for Elemental Carbon. FRM locations are illustrated with black dots. SASS speciation stations and "pseudo stations" are illustrated with black circles.

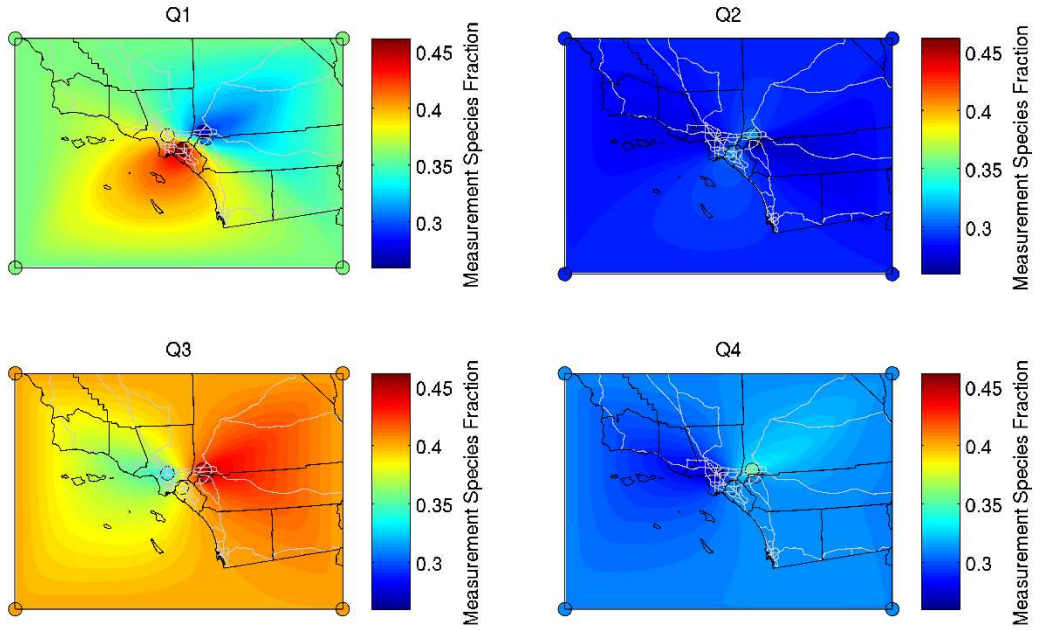

FIGURE 7

2012 Interpolated Measurement Species Fractions for Organic Carbon. FRM locations are illustrated with black dots. SASS speciation stations and "pseudo stations" are illustrated with black circles.

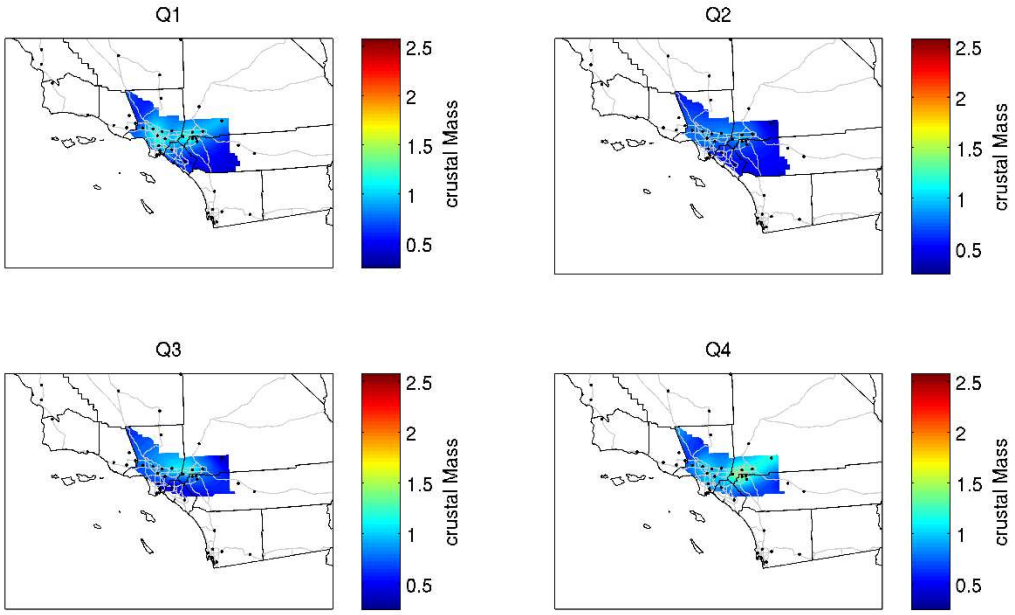

FIGURE 8

Annual quarterly-averaged crustal mass

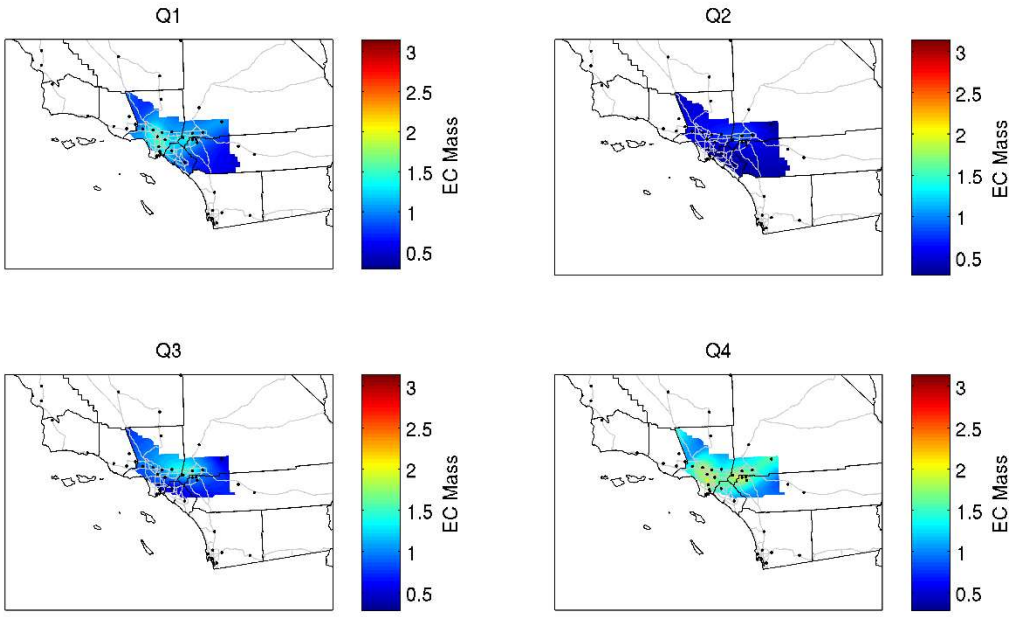

FIGURE 9

Annual quarterly-averaged elemental carbon mass

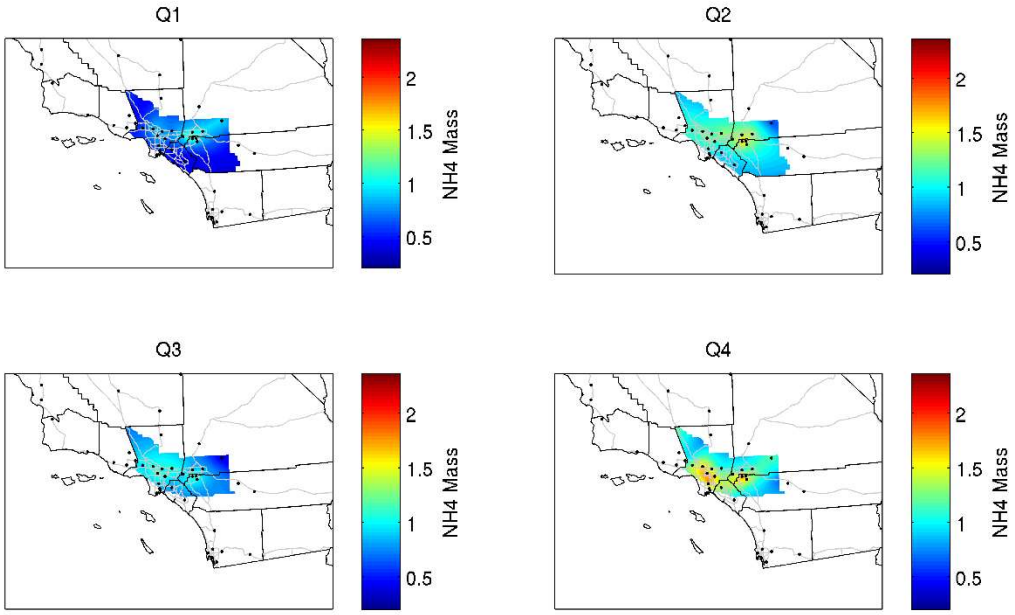

FIGURE 10

Annual quarterly-averaged ammonium mass

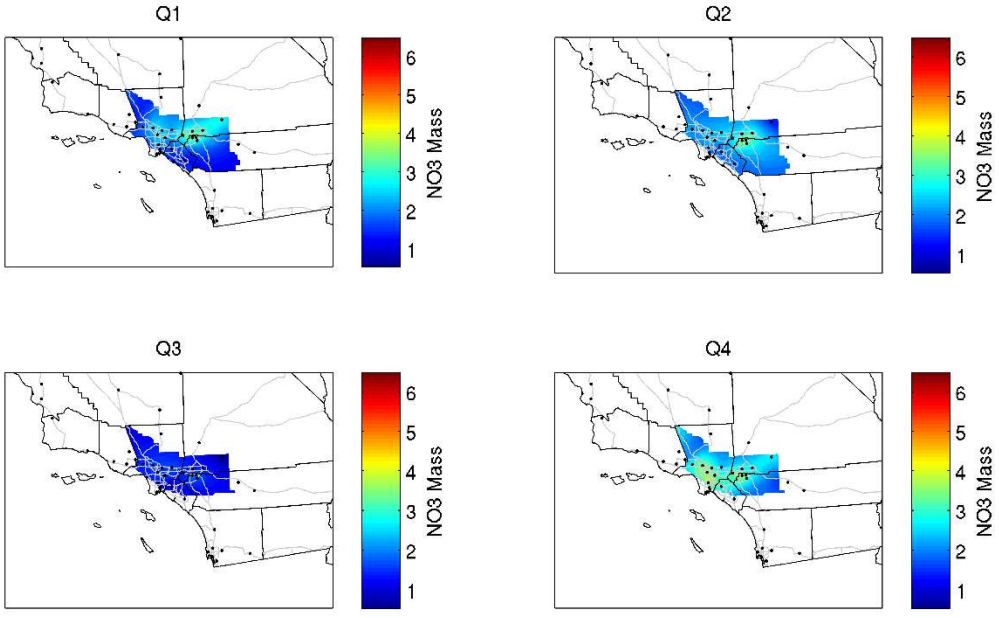

FIGURE 11

Annual quarterly-averaged nitrate mass

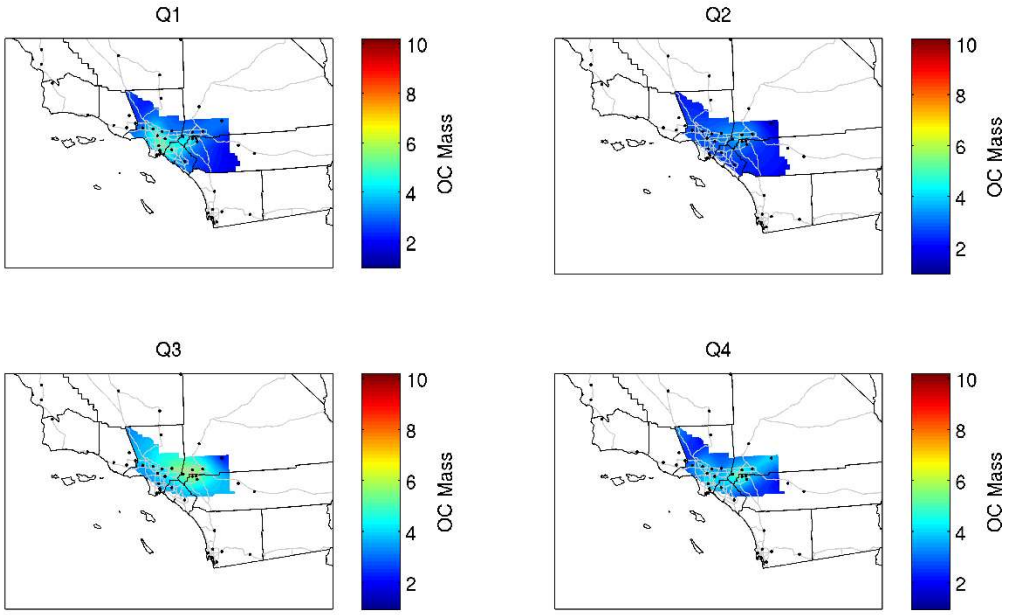

FIGURE 12

Annual quarterly-averaged organic carbon mass

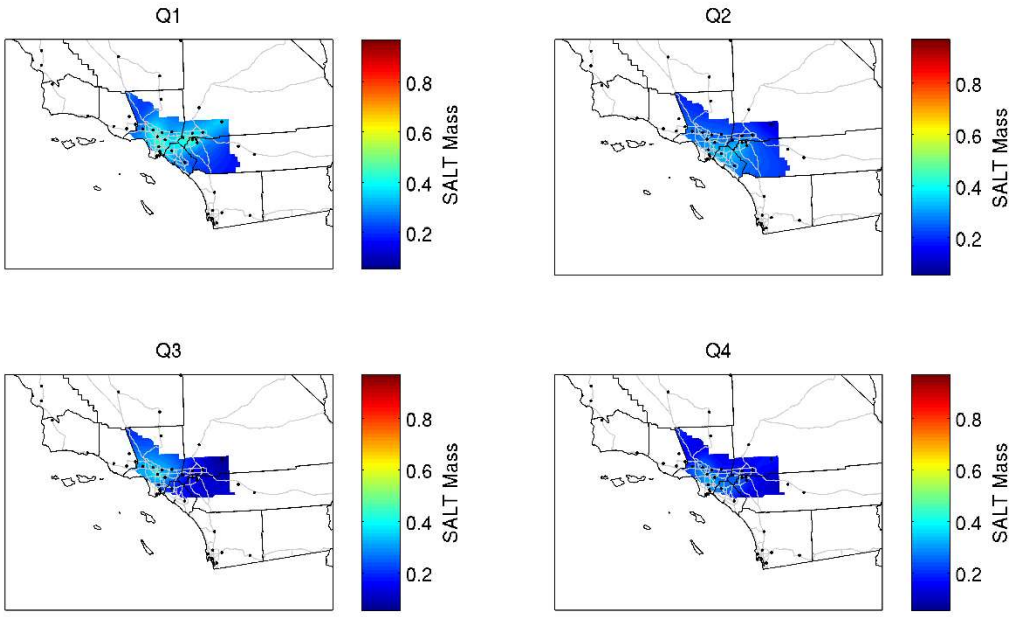

FIGURE 13

Annual quarterly-averaged sea salt mass

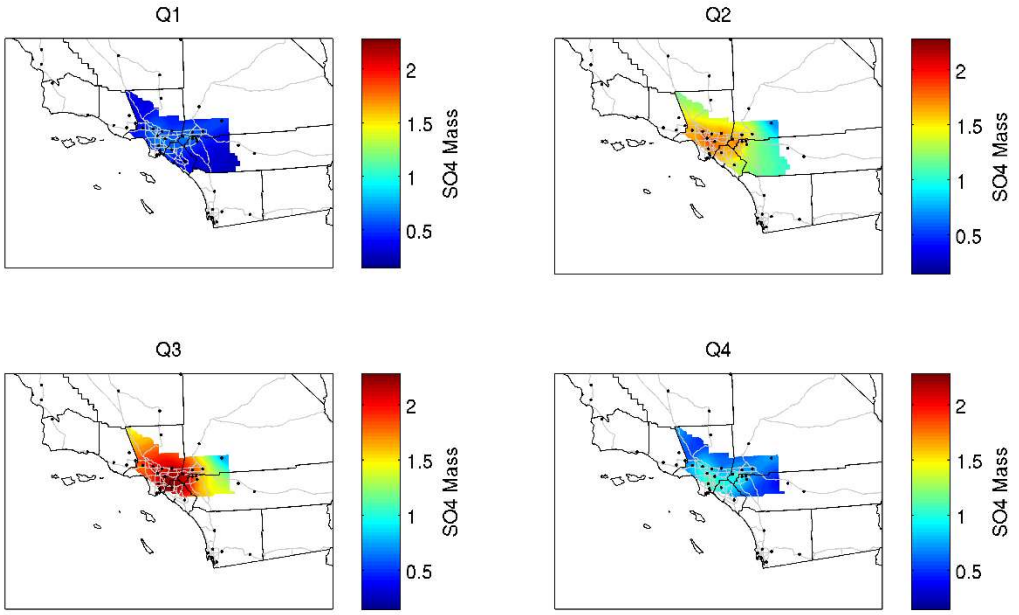

FIGURE 14

Annual quarterly-averaged sulfate mass

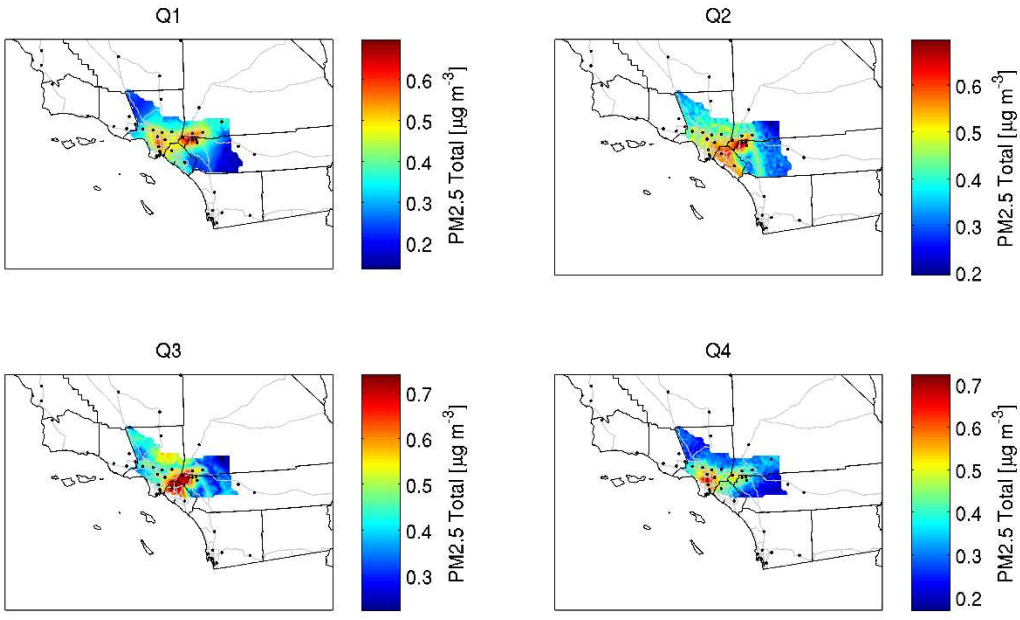

FIGURE 15

Annual quarterly-averaged 2021 uncontrolled projected design values

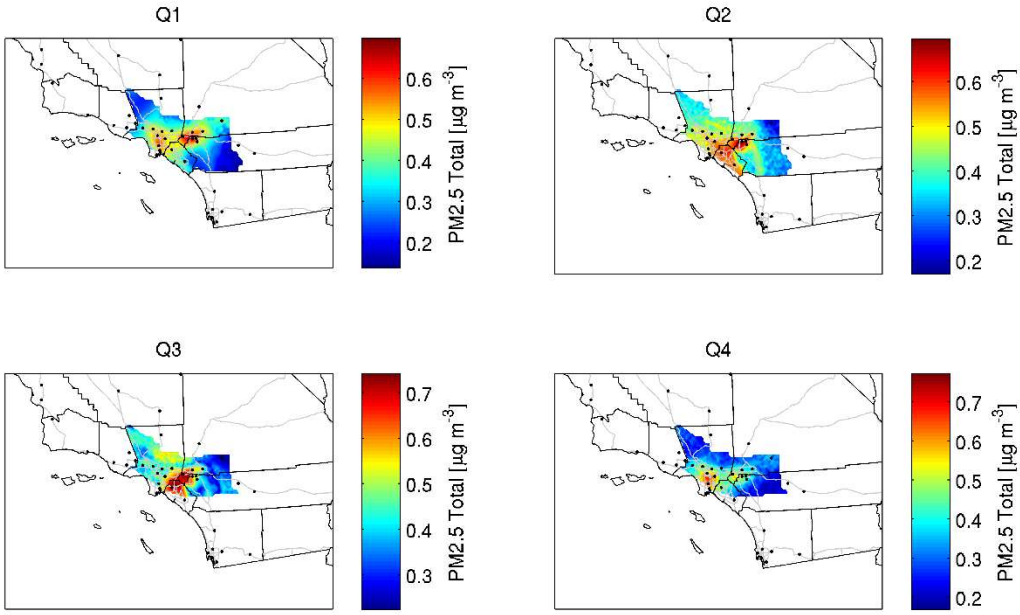

FIGURE 16

Annual quarterly-averaged 2021 controlled projected design values

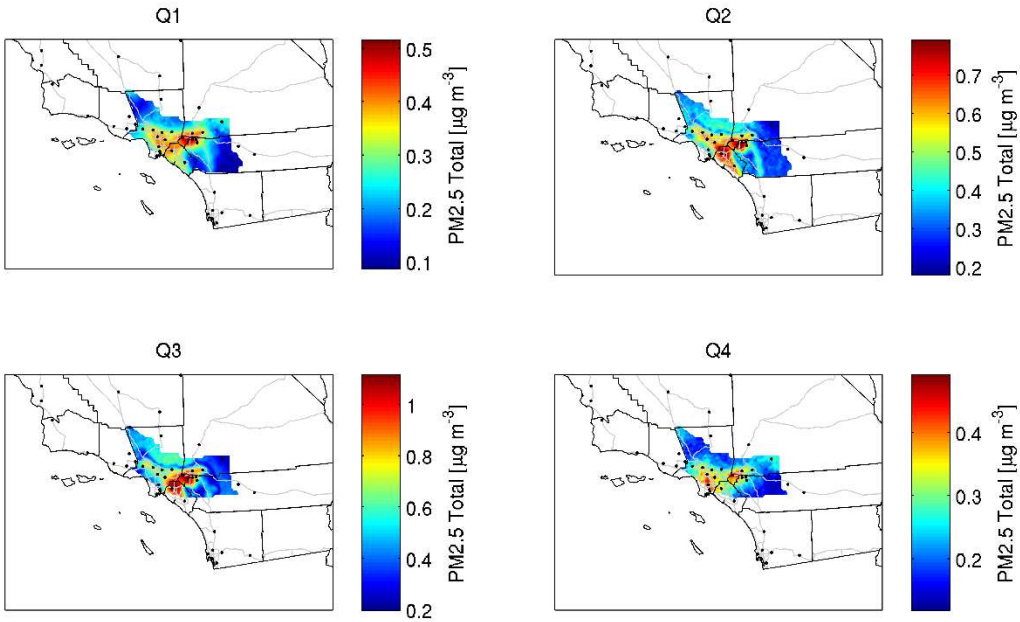

FIGURE 17

Annual quarterly-averaged 2023 ozone control projected design values

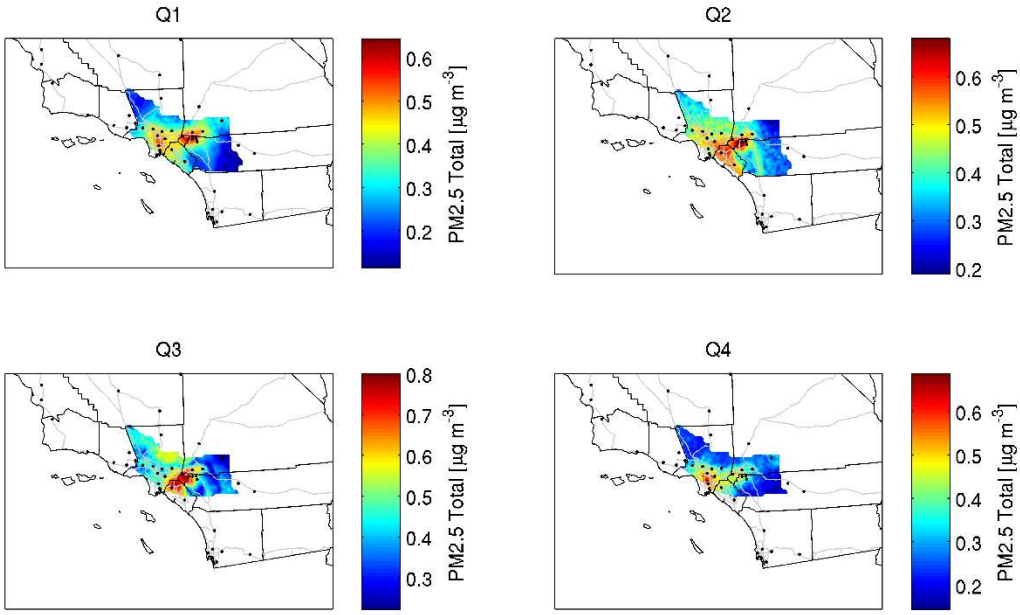

FIGURE 18

Annual quarterly-averaged 2025 uncontrolled projected design values

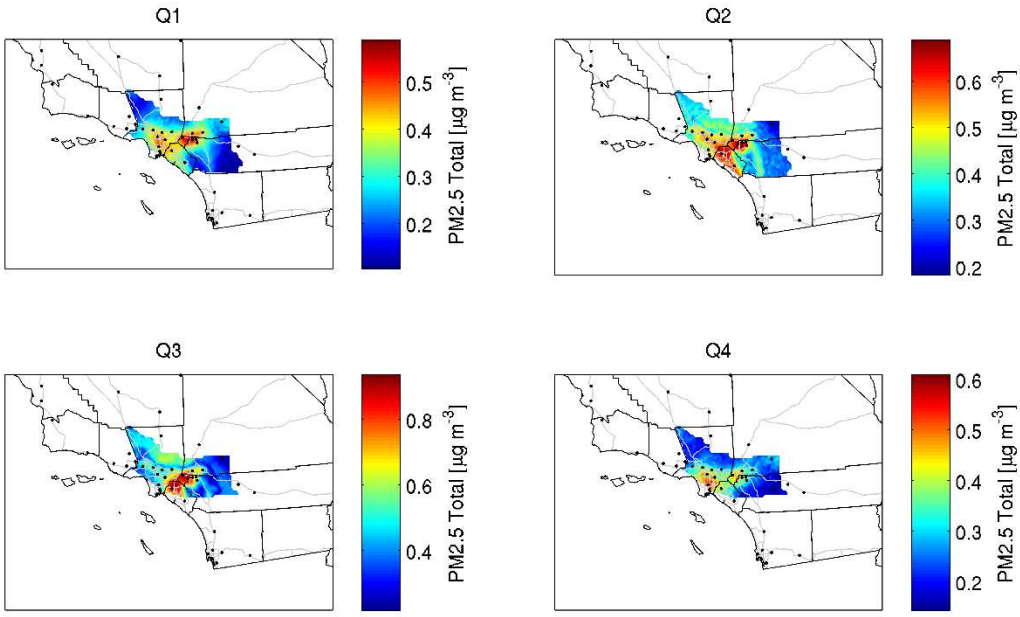

FIGURE 19

Annual quarterly-averaged 2025 controlled projected design values

Attachment 8

24-HOUR UNMONITORED AREA ANALYSIS SUPPLEMENT

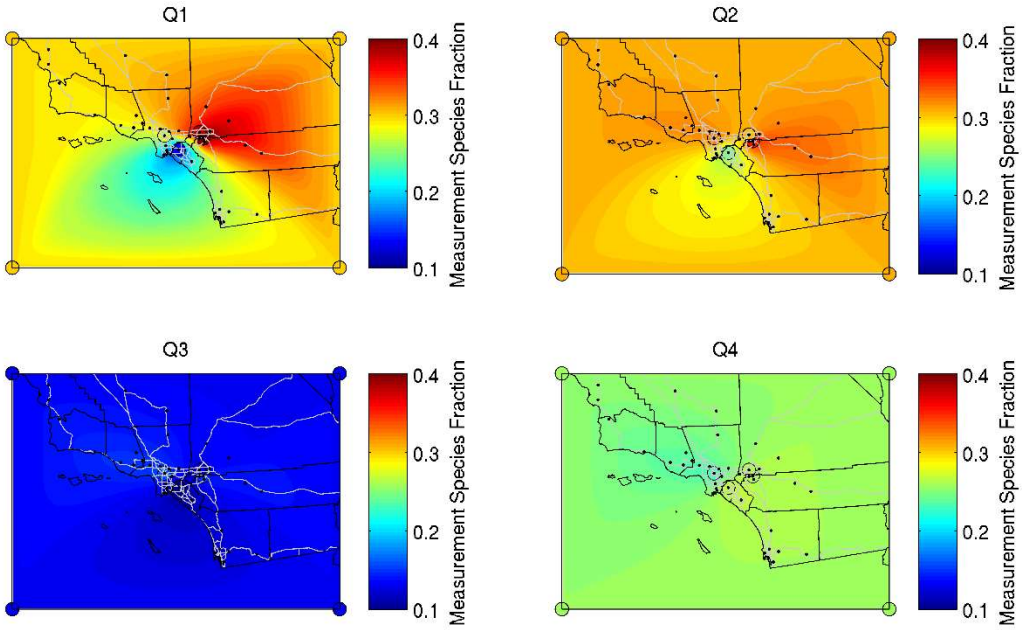

FIGURE 1

2012 Interpolated Measurement Species Fractions for Nitrate. FRM locations are illustrated with black dots. SASS speciation stations and "pseudo stations" are illustrated with black circles.

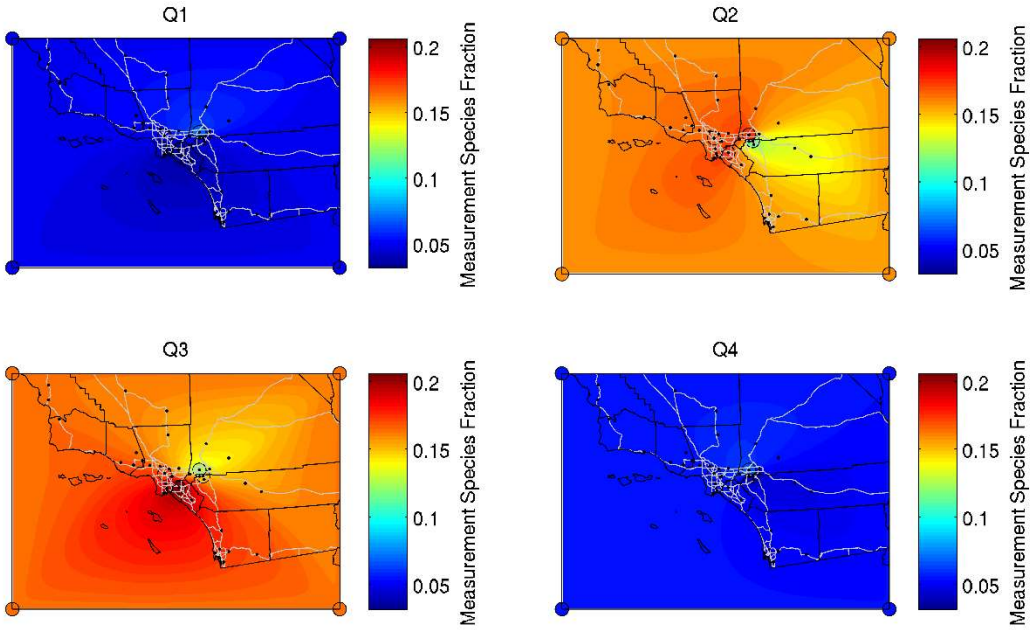

FIGURE 2

2012 Interpolated Measurement Species Fractions for Sulfate. FRM locations are illustrated with black dots. SASS speciation stations and "pseudo stations" are illustrated with black circles.

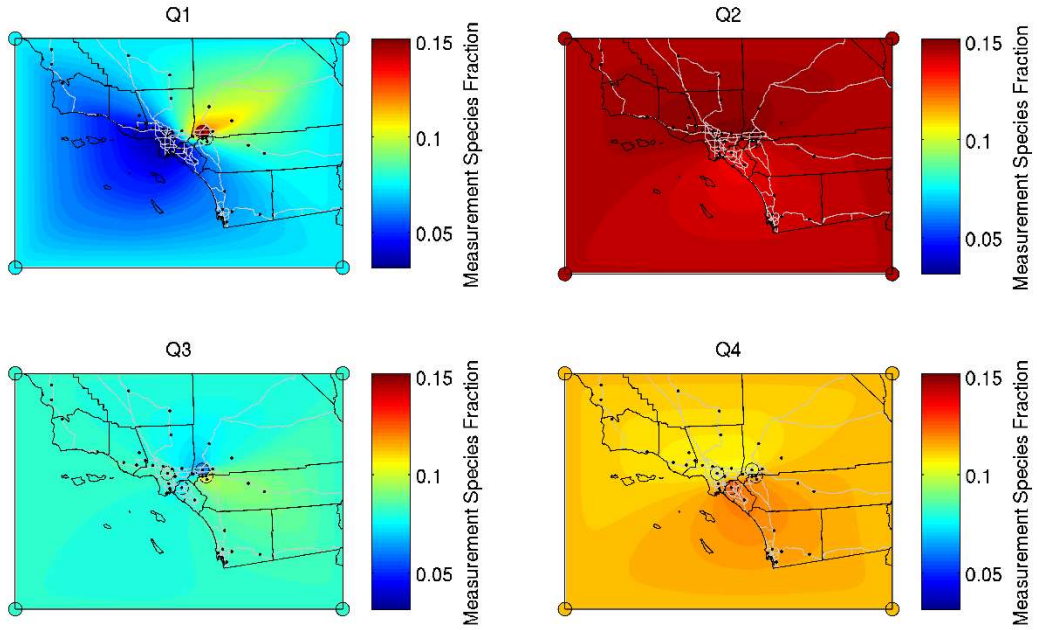

FIGURE 3

2012 Interpolated Measurement Species Fractions for Ammonium. FRM locations are illustrated with black dots. SASS speciation stations and "pseudo stations" are illustrated with black circles.

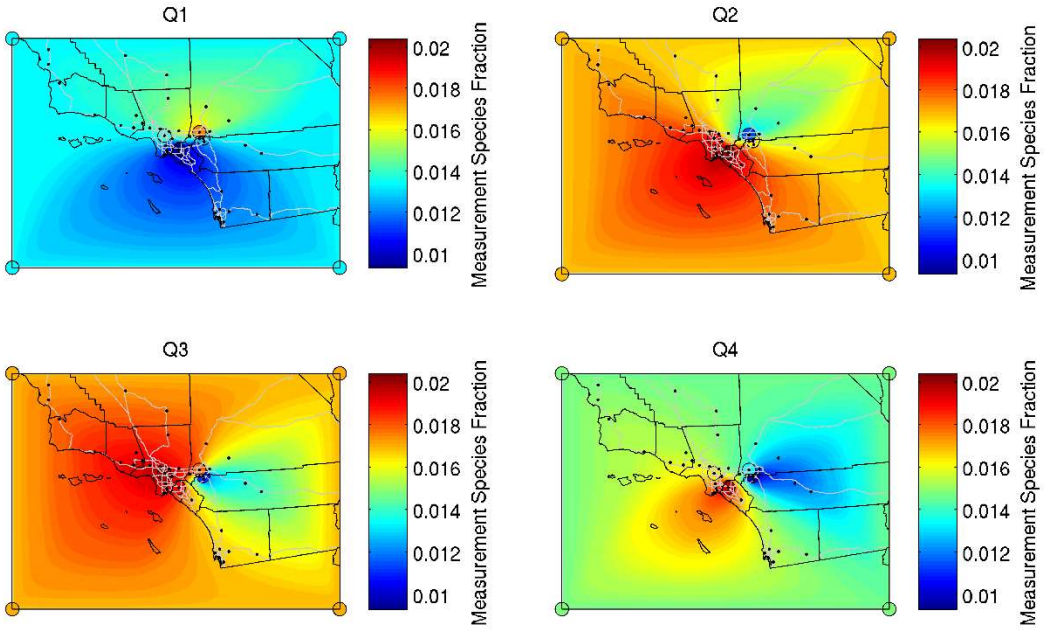

FIGURE 4

2012 Interpolated Measurement Species Fractions for Salt. FRM locations are illustrated with black dots. SASS speciation stations and "pseudo stations" are illustrated with black circles.

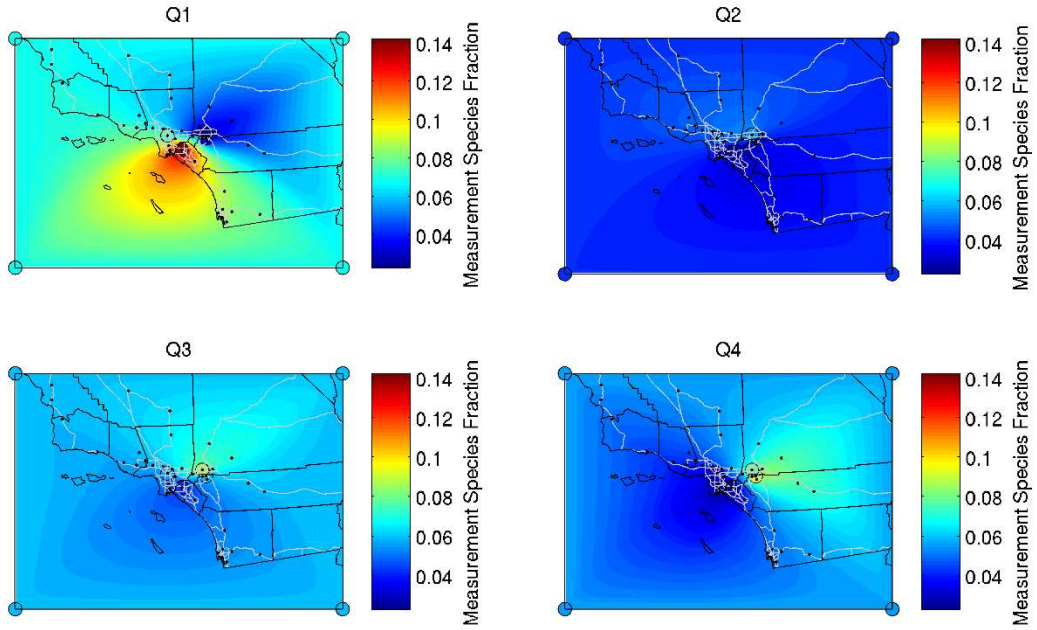

FIGURE 5

2012 Interpolated Measurement Species Fractions for Crustal. FRM locations are illustrated with black dots. SASS speciation stations and "pseudo stations" are illustrated with black circles.

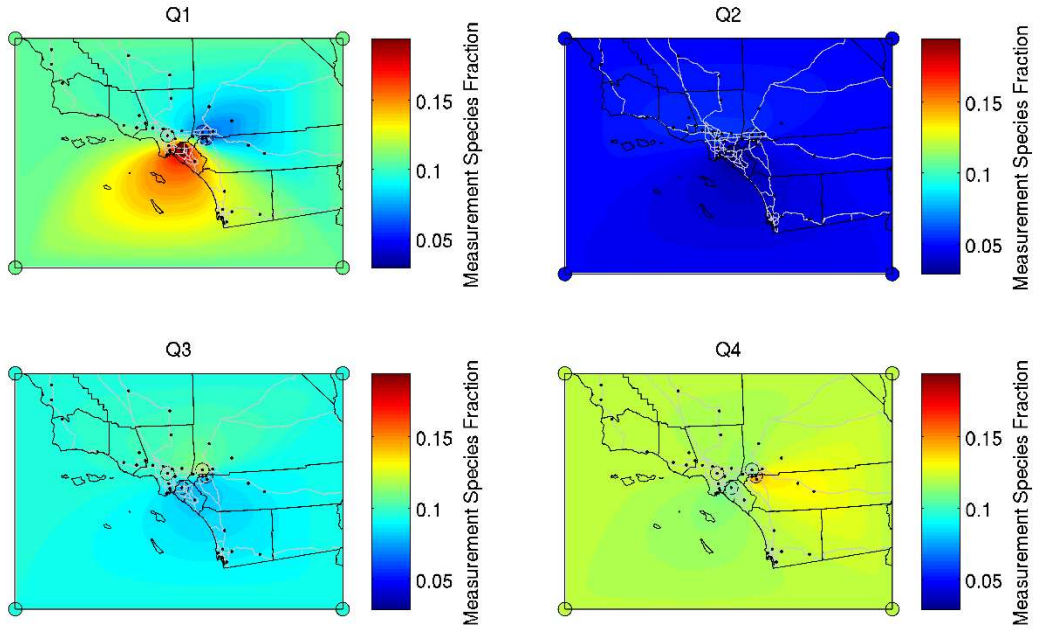

FIGURE 6

2012 Interpolated Measurement Species Fractions for Elemental Carbon. FRM locations are illustrated with black dots. SASS speciation stations and "pseudo stations" are illustrated with black circles.

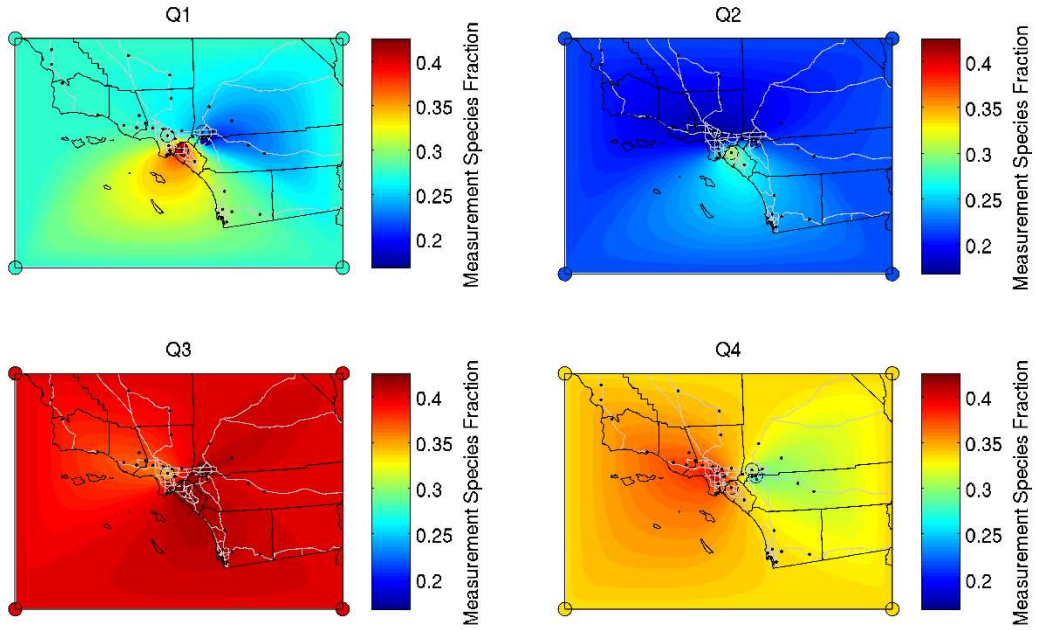

FIGURE 7

2012 Interpolated Measurement Species Fractions for Organic Carbon. FRM locations are illustrated with black dots. SASS speciation stations and "pseudo stations" are illustrated with black circles.

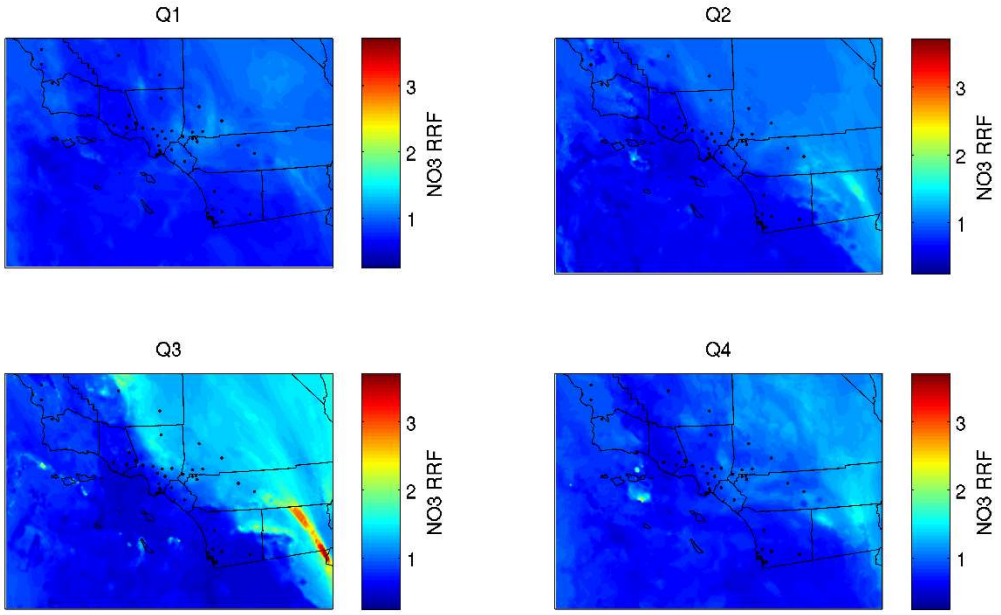

FIGURE 8

2019 Spatial RRFs for Nitrate

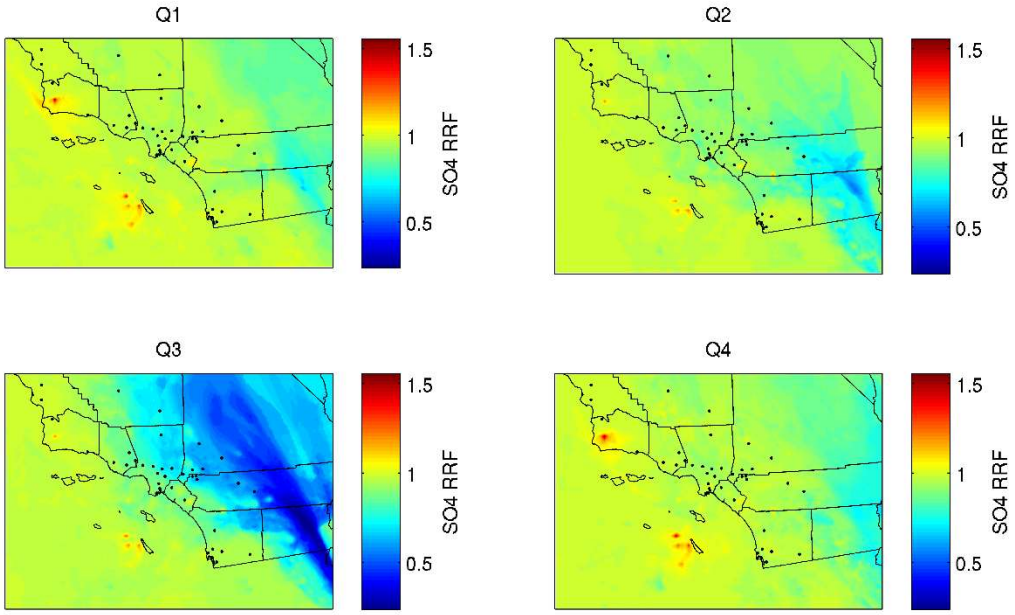

FIGURE 9

2019 Spatial RRFs for Sulfate

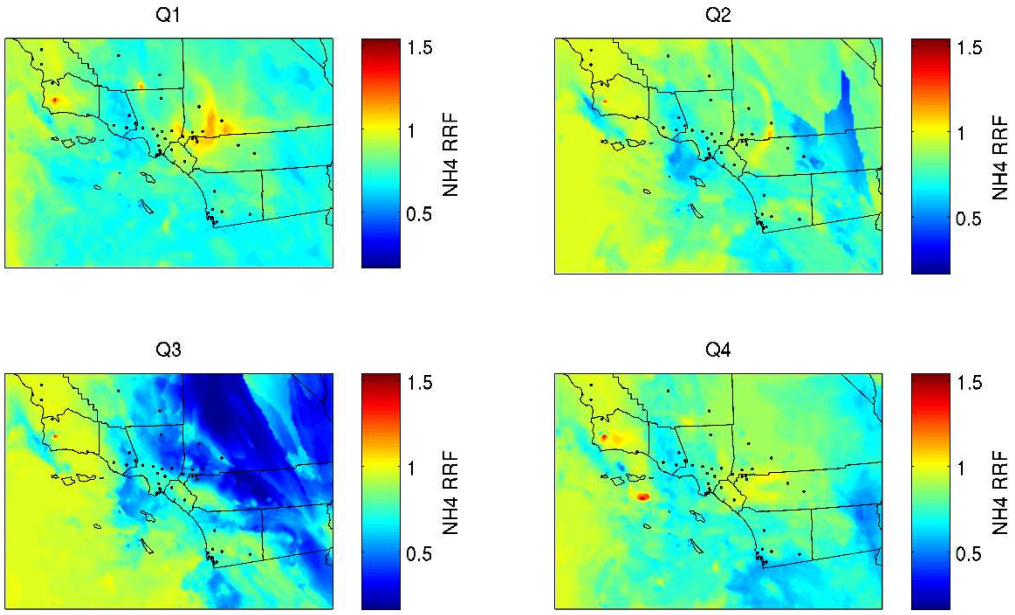

FIGURE 10

2019 Spatial RRFs for Ammonium

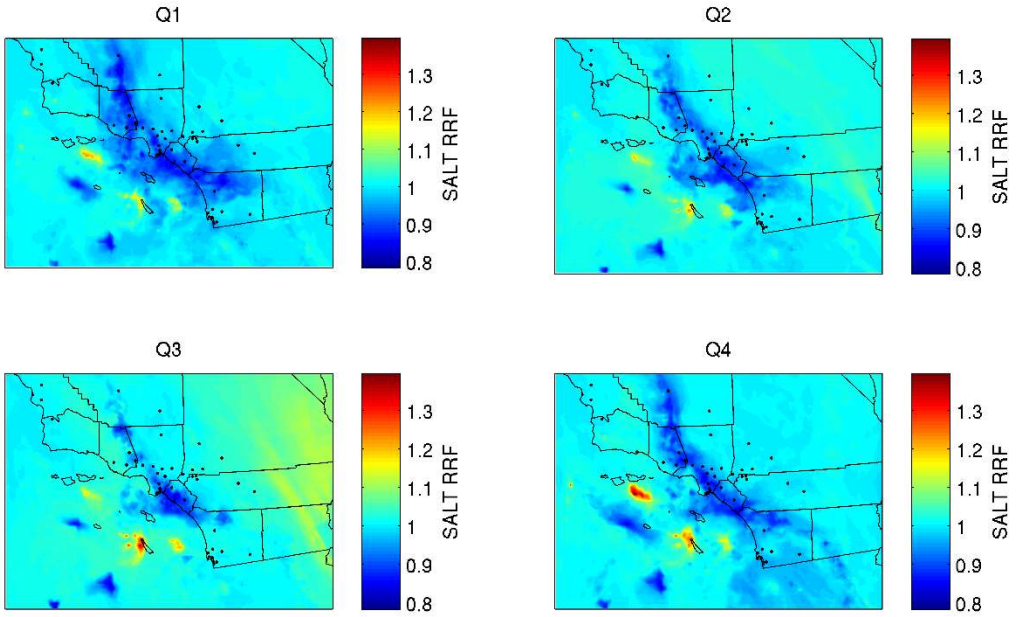

FIGURE 11

2019 Spatial RRFs for Salt

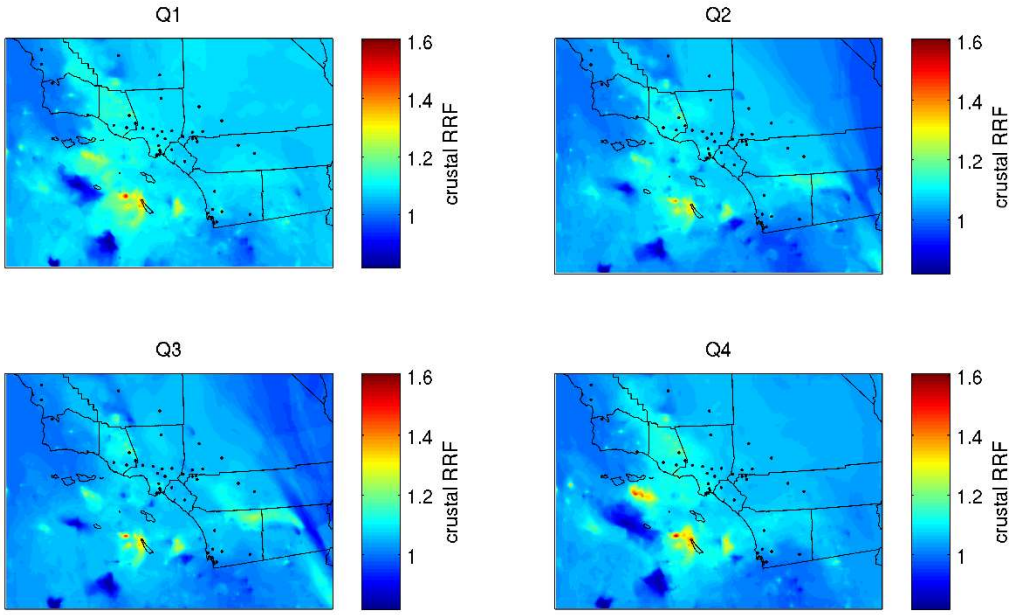

FIGURE 12

2019 Spatial RRFs for Crustal

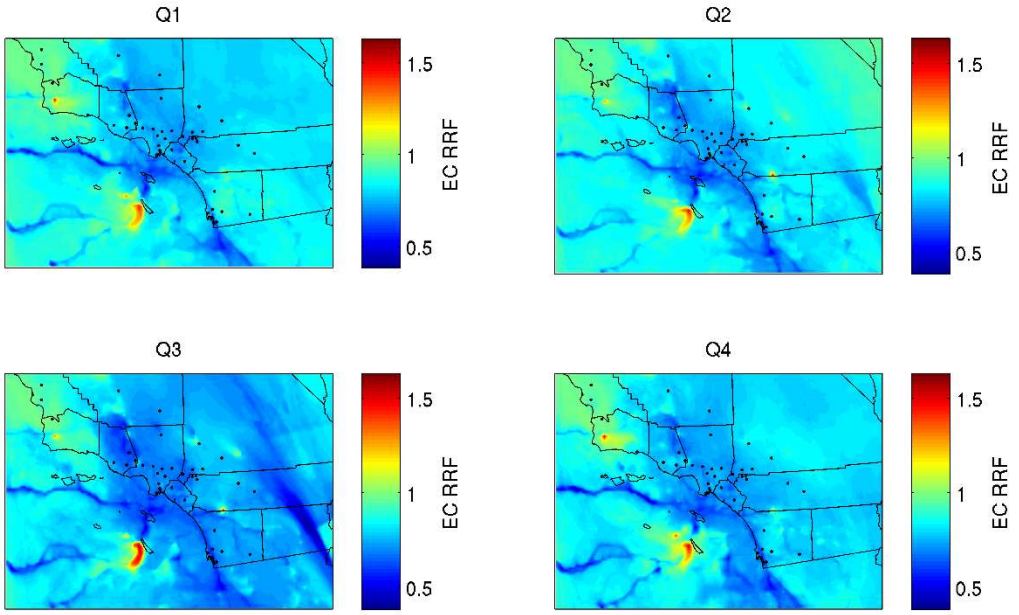

FIGURE 13

2019 Spatial RRFs for Elemental Carbon

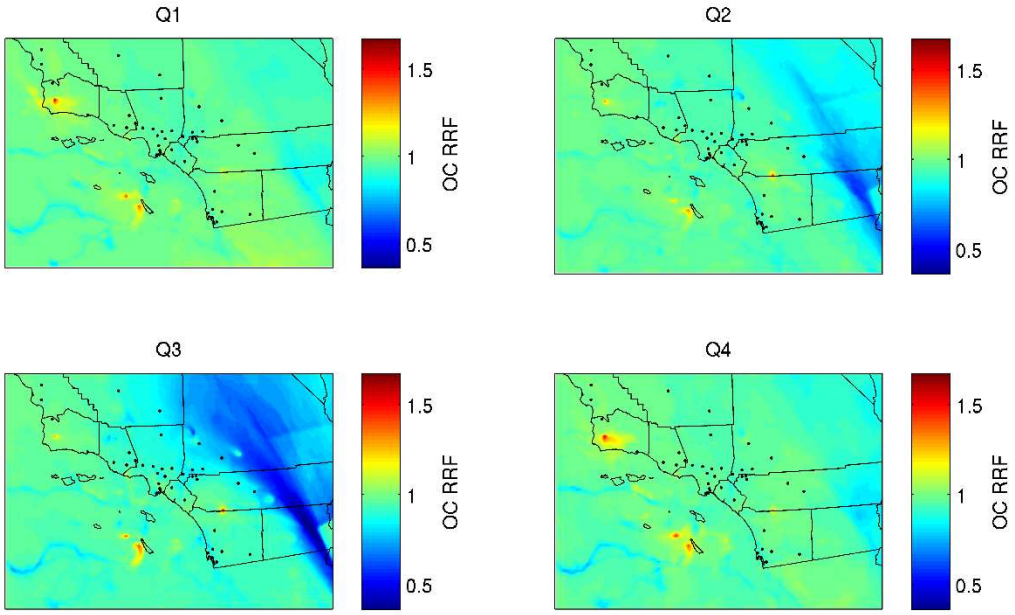

FIGURE 14

2019 Spatial RRFs for Organic Carbon